Geologiska Föreningen 1871 2021 150 ÅR

SPECIALPUBLIKATION 1

GEOLOGICAL SOCIETY OF SWEDEN 150 YEAR ANNIVERSARY MEETING

Uppsala, August 17–19, 2022

Abstract volume

Jeanette Bergman Weihed, Åke Johansson & Emma Rehnström (Eds.)

Errata list

Page 34: An author (Lars E. Holmer) has been added.

Page 226: A sentence has been added under the heading "Mobile Metal Ions in different sample media": In addition, research is going on in new EU-funded project Sustainable exploration for orthomagmatic (critical) raw materials in the EU: Charting the road to the green energy transition (SEMACRET).

Suggested citation for entire volume:
Bergman Weihed, J., Johansson, Å. & Rehnström, E. (Eds.) 2022: Geological Society of Sweden, 150 year anniversary meeting, Uppsala, August 17–19 2022, Abstract volume. *Geologiska Föreningen Specialpublikation 1*, 452 pp.

Suggested citation for an individual paper:
Johansson, Å., 2022: Cleaning up the record – Revised U-Pb zircon ages and new Hf isotope data from southern Sweden. *In:* Bergman Weihed, J., Johansson, Å. & Rehnström, E. (Eds.): Geological Society of Sweden, 150 year anniversary meeting, Uppsala, August 17–19 2022, Abstract volume. *Geologiska Föreningen Specialpublikation 1*, 242–243.

This volume can be downloaded from
geologiskaforeningen.se

Cover photograph: Staircase in bedrock, Stångehuvud, Lysekil.
Foto: Carina Andreasson / Mostphotos.

ISBN 978-91-987833-0-8

Layout: Jeanette Bergman Weihed, Tellurit AB

Welcome

Welcome to the 150 year anniversary of the Geological Society of Sweden!

This anniversary took place in 2021, but due to the travel restrictions and the implementation of social distancing due to the Covid-19 pandemic, all celebration of the occasion was postponed.

We therefore decided to celebrate the anniversary with a jubilee meeting in 2022 instead. Our hope and aim has been to bring together the geoscientific community in Sweden, to have the opportunity to learn more about ongoing research in Swedish geology and to connect and reconnect with colleagues and coworkers.

It is therefore truly a pleasure to see the great interest in this meeting, with participants from academia as well as industry, from both Sweden and abroad.

From the organizing committee and the board of the society we would like to direct our gratitude towards our sponsors for their generosity and to the scientific committee for their professional work.

From me personally, I also send my deepest gratitude to the organizing committee that has been pivotal for the success of this meeting and without whose commitment it would not have possible at all.

With that I welcome you all to celebrate the first one and a half century with the Geological Society – a mere blink in geological time but quite impressive for a geological society. I sincerely hope that the years to come will be equally successful and that this meeting will be the start of a new tradition of biannual Swedish geological meetings.

My warmest welcome!

Emma Rehnström

Chairman of the Geological Society of Sweden,
on behalf of the Geological Society of Sweden and the
150 year Anniversary Meeting Organizing Committee

The meeting is a co-arrangement between the Geological Society of Sweden, Geosektionen, Uppsala University and the Geological Survey of Sweden.

Organising committee

(in alphabetical order)

Stefan Andersson
Uppsala University

Therese Bejgarn
Geological Survey of Sweden

Jeanette Bergman Weihed
Tellurit AB

Paul Evins
WSP

Magnus Hellqvist
Geoveta

Karin Högdahl
Uppsala University

Nils Jansson
Luleå University of Technology

Magnus Johansson
Geosektionen, Naturvetarna

Åke Johansson
Swedish Museum of Natural History

Hannes Mattsson
Uppsala University

Katarina Persson Nilsson
Svemin

Emma Rehnström
Geological Society of Sweden

Pär Weihed
Luleå University of Technology

Scientific committee

(in alphabetical order)

Jenny Andersson
Geological Survey of Sweden

Ulf B. Andersson
LKAB

Tobias Bauer
Luleå University of Technology

Mikael Calner
Lund University

Sarah Conrad
Luleå University of Technology

Karin Eliaeson
Geological Survey of Sweden

Paul Evins
WSP

Magnus Hellqvist
Geoveta AB

Roger Herbert
Uppsala University

Lars Holmer
Uppsala University

Dan Holtstam
Swedish Museum of Natural History

Karin Högdahl
Uppsala University

Erika Ingvald
Geological Survey of Sweden

Martin Jakobsson
Stockholm University

Åke Johansson
Swedish Museum of Natural History

Mark Johnson
University of Gothenburg

Erik Jonsson
Geological Survey of Sweden

Christopher Juhlin
Uppsala University

Anna Ladenberger
Geological Survey of Sweden

Jörgen Langhof
Swedish Museum of Natural History

Geoffrey Lemdahl
Linnaeus University

Stefan Luth
Geological Survey of Sweden

Hannes Mattsson
Uppsala University

Renaud Merle
Uppsala University

Anna Neubeck
Uppsala University

Bo Olofsson
KTH

Lena Persson
Geological Survey of Sweden

Katarina Persson Nilsson
Svemin

Iain Pitcairn
Stockholm University

Thorkild Maack Rasmussen
Luleå University of Technology

Emma Rehnström
Geological Society of Sweden

Anders Scherstén
Lund University

Ian Snowball
Uppsala University

Michael B. Stephens
Uppsala

Vivi Vajda
Swedish Museum of Natural History

Christina Wanhainen
Luleå University of Technology

Pär Weihed
Luleå University of Technology

Martin Whitehouse
Swedish Museum of Natural History

Lovisa Zillén Snowball
Geological Survey of Sweden

Contents

Thematic Session 1
Applied geosciences

Thematic Session 2
Economic geology

Thematic Session 3
Environmental geosciences

Thematic Session 4
Hydrogeology

Thematic Session 5
Geochemistry

Thematic Session 6
Geochronology and isotope geology

Thematic Session 7
Geophysics

Thematic Session 8
Marine geosciences

Thematic Session 9
Sedimentology & palaeontology

Thematic Session 11
Quaternary geology

Thematic Session 12
Structural geology & tectonics

General Session 1
3 billion years of geological evolution – The build-up of Sweden

Session Chairs:
Åke Johansson (ake.johansson@nrm.se)
Vivi Vajda (vivi.vajda@nrm.se)
Michael Stephens (michael@stephens.se)

Geodynamic models for the Sveconorwegian orogeny

Bernard Bingen[a], Giulio Viola[b], Charlotte Möller[c], Jaqueline Vander Auwera[d], Antonin Laurent[e], Espen Torgersen[f]

[a]Geological Survey of Norway, Trondheim, Norway, bernard.bingen@ngu.no; [b]Department of Biological, Geological and Environmental Sciences, University of Bologna, Bologna, Italy, giulio.viola3@unibo.it; [c]Department of Geology, Lund University, Lund, Sweden, charlotte.moller@geol.lu.se; [d]Department of Geology, University of Liège, 4000 Liège, Belgium, jvdauwera@uliege.be; [e]Department of Geology, University of Lyon, UJM-Saint-Etienne, Saint-Etienne, France, antonin.laurent@univ-st-etienne.fr; [f]Geological Survey of Norway, Trondheim, Norway & Department of Geoscience and Petroleum, Norwegian University of Science and Technology, Trondheim, Norway, espen.torgersen@ngu.no.

Summary. The paradigm of Rodinia supercontinent assembly carries the idea that late Mesoproterozoic to early Neoproterozoic orogenic belts formed by collision between the cratons welded into Rodinia. The geological record inside these orogens is key to test Rodinia assembly models. The Sveconorwegian orogen is one of these orogenic belts, located along the western margin of Fennoscandia / Proto-Baltica. New data on the Sveconorwegian orogen have resulted in a significant improvement in the definition and sequencing of regional events. However, this also has resulted in a diversification of tectonic evolutionary models, leading to more rather than less speculative Rodinia assembly models. In this contribution, we discuss the merits and demerits of three recent geodynamic models for the Sveconorwegian orogeny, #1 collision model with Proto-Baltica in upper plate position, #2 collision model with Proto-Baltica in lower plate position, and #3 accretionary orogeny.

The 550 km wide Sveconorwegian orogen in S Norway and SW Sweden is a portion of a large and hot orogenic belt, structured during the long-duration Sveconorwegian orogeny between 1150 and 900 Ma. It consists of five lithotectonic units, from east to west, the Eastern Segment and the Idefjorden, Kongsberg, Bamble and Telemarkia lithotectonic units (Bingen et al., 2021; Möller and Andersson, 2018; Slagstad et al., 2020; Stephens & Wahlgren, 2020). The western parts of the Sveconorwegian orogen carry evidence for high-grade metamorphism between c. 1150 and 920 Ma, and voluminous pre-to syn-orogenic magmatism between c. 1280 and 900 Ma. The Eastern Segment experienced high-PT metamorphism first at c. 990 Ma, and underwent volumetrically significantly less magmatism.

Prior to the Sveconorwegian orogeny, lithosphere inside the orogen was generated from east to west in accretionary settings, between c. 1800 and 1480 Ma. In the western part of the orogen, quartzite deposition records post-accretion thermal subsidence (1480–1370 Ma). In the Eastern Segment, the Hallandian magmatic and orogenic event may record renewed accretionary setting between 1470 and 1380 Ma. Between 1280 and 1145 Ma, bimodal magmatism in the Telemarkia lithotectonic unit overlaps with demonstrably extensional intramontane basin sedimentation between c. 1210 and 1050 Ma. Convergence-related Sveconorwegian metamorphism shows increasingly high-pressure signature eastwards with time, i.e. towards the (cratonic) Fennoscandia foreland. Peak P-T-t conditions of 1.15 GPa - 850 °C - 1145–1130 Ma are recorded in the Bamble-Kongsberg lithotectonic units, 1.5 GPa - 740 °C - 1046 Ma in the Idefjorden lithotectonic unit, and 1.8 GPa - 870 °C - 990 Ma in the Eastern Segment.

In the Eastern Segment, eclogite bodies with prograde-zoned garnet are well described. Peak metamorphism was followed by isothermal decompression and partial melting and an eclogite-bearing nappe was exhumed at 980 Ma by extrusion during convergence. Westwards, towards the hinterland, Sveconorwegian syn-orogenic magmatism is increasing in volume. The 1066–1020 Ma high-K calc-alkaline Sirdal-Feda plutonic suite is interpreted as voluminous melting of the crust, coeval with (mantle-derived) mafic underplating. This magmatism was followed by two ferroan plutonic suites, the hydrous hornblende-biotite granite (HBG) suite between 990 and 925 Ma and the anhydrous anorthosite-mangerite-charnockite (AMC) suite between 935 and 915 Ma. Anorthosite plutons contain 1040 Ma-old high-alumina orthopyroxene megacrysts, and are interpreted as product of remelting (at 1.1 GPa) of 1040 Ma mafic underplates. The crust was affected by prolonged granulite-facies metamorphism peaking twice in ultra-high temperature conditions, at 0.6 GPa - 920 °C - 1029–1006 Ma and 0.4 GPa - 920 °C - 930 Ma, overlapping in time with the magmatism. The extreme temperatures in the crust imply asthenosphere directly under the crust between 1030 and 925 Ma. After c. 930 Ma, removal of a c. 16 km thick overburden required a combination of erosion and extensional tectonics. The recently mapped Nisser detachment zone in Telemark attests to extension between the superstructure and infrastructure of the orogen at the end of orogeny. The N-S trending Blekinge-Dalarna dolerites attest to relaxation in the foreland of the orogen between 980 and 940 Ma.

Three main geodynamic models have been proposed recently for the Sveconorwegian orogeny. (1) Long-duration collision between Proto-Baltica in upper-plate position and another major continent, orthogonal or transpressional, with all lithotectonic units of the orogen endemic to Fennoscandia, and ocean closure(s) west of the exposed orogen (Bingen et al., 2021; Cawood & Pisarevsky, 2017; Stephens & Wahlgren, 2020). (2) Collision between Proto-Baltica in lower-plate position and a continental mass consisting of the four western lithotectonic units of the orogen (Sveconorwegia), possibly attached to another major continent (Möller and Andersson, 2018). In this model, the intervening ocean closed at c. 990 Ma along the Mylonite Zone, between the Eastern Segment and the Idefjorden lithotectonic unit. (3) A long-duration (non-collisional) accretionary (Andean) orogeny, continuing into the Neoproterozoic, with a subduction trench west of the exposed orogen (Slagstad et al., 2020). Geodynamic interpretation is complicated by the fact that the mantle potential temperature in the Mesoproterozoic was probably c. 100 °C higher than today's. Therefore, analogies with Phanerozoic orogenies require caution.

In model #1, the main continental collision is best estimated to start at c. 1065 Ma, together with widespread high-grade metamorphism and magmatism. Before 1065 Ma, the orogenic zone was restricted to the western part of the orogen, possibly as a back-arc Cordillera-style orogenic plateau. After 1065 Ma, the orogenic zone grew stepwise eastwards, as a collisional Tibetan-style orogenic plateau. Formation of the orogenic plateau is paired with retro-delamination and foundering of the heavy continental lithospheric mantle towards the foreland. Foundering took place in three steps, at c. 1130, 1050 and 990 Ma, as recorded by high-pressure metamorphism.

Model #2 explains the formation and exhumation of the eclogite-bearing nappe in the lower-plate Eastern Segment at and after c. 990 Ma, the syn- and post-tectonic magmatism in the upper plate, and is compatible with the contrast in geological records between the Eastern Segment and the western part of the orogen. It is supported by recent models of the Himalaya-Tibet collision, featuring underthrusting of Indian lithosphere under the Tibetan orogenic plateau (Klemperer et al., 2022).

Model #3 cannot be validated after c. 1000 Ma, as it is not compatible with the characteristically dry nature of anorthosite magmatism and associated granulite facies metamorphism at c. 930 Ma, with the ferroan signature of the post-1000 Ma plutonism, nor with the magmatic quiescence after 900 Ma.

References

Bingen, B., Viola, G., Möller, C., Vander Auwera, J., Laurent, A. T., & Yi, K., 2021: The Sveconorwegian orogeny. *Gondwana Research 90,* 273–313.

Cawood, P. A. & Pisarevsky, S. A., 2017: Laurentia-Baltica-Amazonia relations during Rodinia assembly. *Precambrian Research 292,* 386–397.

Hoffman, P. F., 1991: Did the breakout of Laurentia turn Gondwanaland inside-out? *Science 252,* 1409–1412.

Klemperer, S. L., Zhao, P., Whyte, C. J., Darrah, T. H., Crossey, L. J., Karlstrom, K. E., Liu, T., Winn, C., Hilton, D. R., & Ding, L., 2022: Limited underthrusting of India below Tibet: $^3He/^4He$ analysis of thermal springs locates the mantle suture in continental collision. *Proceedings of the National Academy of Sciences 119,* e2113877119.

Möller, C. & Andersson, J., 2018: Metamorphic zoning and behaviour of an underthrusting continental plate. *Journal of Metamorphic Geology 36,* 567–589.

Slagstad, T., Marker, M., Roberts, N. M. W., Saalmann, K., Kirkland, C. L., Kulakov, E., Ganerød, M., Røhr, T. S., Møkkelgjerd, S. H. H., Granseth, A., & Sørensen, B. E., 2020: The Sveconorwegian orogeny – Reamalgamation of the fragmented southwestern margin of Fennoscandia. *Precambrian Research 350,* 105877.

Stephens, M. B. & Wahlgren, C. H., 2020: Accretionary orogens reworked in an overriding plate setting during protracted continent–continent collision, Sveconorwegian orogen, southwestern Sweden. In: Stephens, M.B. & Bergman Weihed, J. (eds) Sweden: *Lithotectonic Framework, Tectonic Evolution and Mineral Resources.* Geological Society, London, Memoirs 50, 435–448.

Marine Baltic records over the later part of the Quaternary − a biological proxy perspective

Helena L. Filipsson

Department of Geology, Lund University, Lund, Sweden, e-mail; helena.filipsson@geol.lu.se

Summary. In this presentation, I will discuss environmental changes occurring in the Baltic Sea land-sea aquatic continuum over the last two millennia. The global Industrial Revolution (~1850 CE) resulted in an intensification and expansion of anthropogenic impacts on terrestrial and aquatic environments through land-use changes, industrialization, and urbanization. We have dramatically altered the land- and the seascape and concurrently, the climate is changing. Available marine and terrestrial biological proxy records will be used to put these potential changes into perspective.

Coastal environments in the Baltic Sea have experienced large ecological changes as a result of human activities over the last 100–200 years. To understand the severity and potential consequences of such changes, paleoenvironmental records provide important contextual information. The Baltic Sea coastal zone is naturally a vulnerable system and subject to significant human-induced impacts. To put the recent environmental degradation in the Baltic coastal zone into a long-term perspective, and to assess the natural and anthropogenic drivers of environmental change, we present sedimentary records covering the last 2000 years obtained from several coastal inlets and lakes in Sweden, two of them being the inlet Gåsfjärden, close to Västervik on the Swedish east coast, and the lake Storsjön located in the Gåsfjärden catchment area. We investigate the links between a pollen-based land cover reconstruction from Lake Storsjön and paleoenvironmental variables from Gåsfjärden itself, including a range of variables such as diatom assemblages, organic carbon (C) and nitrogen (N) contents, stable C and N isotopic ratios, and biogenic silica contents (Ning et al., 2018).

The Lake Storsjön record shows that regional land use was characterized by small-scale agricultural activity between 900 and 1400 CE, which slightly intensified between 1400 and 1800 CE. Substantial expansion of cropland was observed between 1800 and 1950 CE, before afforestation between 1950 and 2010 CE. From the Gåsfjärden record, prior to 1800 CE, relatively minor changes in the diatom and geochemical proxies were found. The onset of cultural eutrophication in Gåsfjärden can be traced to the 1800s and intensified land use is identified as the main driver. Anthropogenic activities in the 20th century have caused unprecedented ecosystem changes in the coastal inlet, as reflected in the diatom composition and geochemical proxies. Furthermore, we will discuss these documented biological changes in relation to other biological proxy records from the coastal Baltic Sea, covering the last 2000 years.

References

Ning, W., Nielsen, A. B., Ivarsson, L. N., Jilbert, T., Akesson, C. M., Slomp, C. P., Andren, E., Brostrom, A., & Filipsson, H. L.,2018: Anthropogenic and climatic impacts on a coastal environment in the Baltic Sea over the last 1000 years. *Anthropocene*, *21*, 66-79.

Return to ice ages and the relevance of Quaternary geology in the modern world

Dan Hammarlund

Department of Geology, Lund Universty, Lund, Sweden, dan.hammarlund@geol.lu.se

Summary. Quaternary geology has strong traditions in Sweden. Insight into glacial processes and Quaternary deposits developed over the last 150 years has provided solutions or mitigation to several problems of societal importance. At the same time, Swedish Quaternary geologists have contributed substantially to the academic progress of the subject. Some examples will be provided as part of a brief overview of the history of Quaternary research, and an outlook for the future will be delivered. In addition, the importance of Quaternary geology within the emerging field of geosystem services will be discussed.

Status of Quaternary research in Sweden

The Quaternary Period is represented by a wealth of highly resolved and relatively well-dated records preserved in a range of natural archives. Such empirical data are of immense value for comparison with recent variations and projected future changes in environment and climate as depicted by monitoring and modelling. Since the advent of the glacial theory, which broadly coincided with the foundation of the Geological Society of Sweden, Quaternary research has developed strongly and remained prosperous, not least in Scandinavia. Interestingly, the stature and traditions of this resarch contributed to the survival of the Quaternary as a formal chronstratigraphic term, contrary to the Primary, Secondary and Tertiary, when the International Commission on Stratigraphy let the scientific community vote on its rank in 2009 (Gibbard & Head 2010).

Swedish scholars have made important and long-lasting contributions to Quaternary research. The pioneering work by Torell (1872) on the application of the glacial theory in Scandinavia, de Geer's (1912) establishment of the clay varve chronology (The Swedish Time Series), and von Post's (1918) invention of pollen analysis are worth mentioning, as well as more recent work on regional and global stratigraphy and chronology (Mangerud 1974, Björck et al. 1998, Walker et al. 2012). Swedish Quaternary geology has developed, diversified and remained prosperous during recent decades. Objective bibliometric analyses are difficult to obtain but a simple time series of articles involving authors with Swedish affiliations published in one of the leading journals in the field, *Quaternary Science Reviews*, gives an indication of the status of Quaternary research in Sweden (Fig. 1).

Interestingly, *GFF*, the scientific journal of the Geological Sociey of Sweden, has published 97 articles between 1994 and 2022 yielding hits when searching for "Quaternary or Pleistocene or Weichselian or Holocene" in Web of Science.

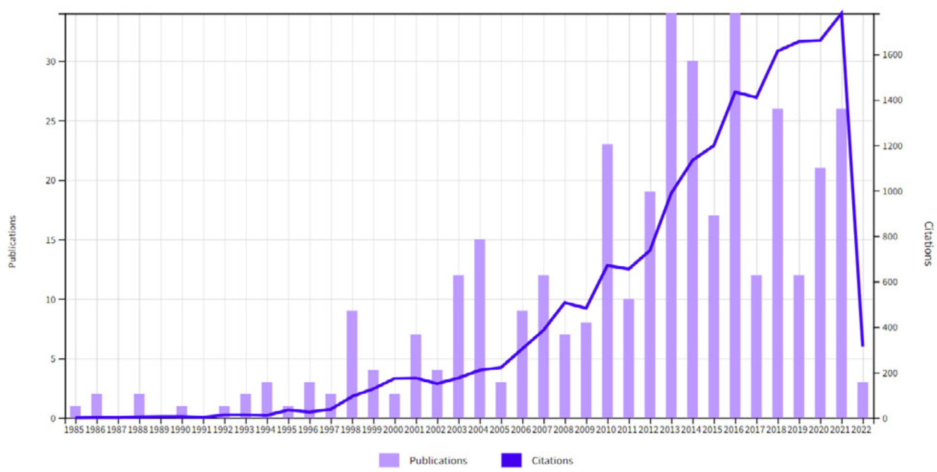

Figure 1. Bibliometric analysis of articles involving authors with Swedish affiliations published in *Quaternary Science Reviews* from the journal's establishment in 1985 to today (n = 377). Source: Web of Science.

Novel applications, future prospects and challenges

By focussing on the overburden where the majority of societal activity takes place, as well as ongoing processes, not least climate change, Quaternary geology is highly relevant within a range of public management contexts. The subject also offers links to many other disciplines, such as ecosystem and atmospheric sciences, as well as applied research within the environment and energy sectors, thereby providing access to funding from sources other than those traditionally explored by geologists. The increasing focus on sustainable development and the emerging awareness of the value of the subsurface as a provider of geosystem services and geodiversity to modern society will likely strenghten this development (van Ree & van Beukering 2016, Gray 2018). Global change processes of the "Anthropocene" need to be assessed against baseline conditions and natural variability, and a Quaternary or Holocene time perspective is often appropriate for such comparisons. At least, proxy records extending beyond monitoring series are needed, as demonstrated by numerous studies based on natural archives (e.g. Bragée et al. 2015, Fredh et al. 2017, Yang et al. 2021, Björnerås et al. 2022).

Therefore, the demand for geoscientists, not least with a solid training in Quaternary geology, will likely increase in the near future, and educational systems at different levels need to adapt to this demand. However, in many parts of the world higher education policies tend to disfavour this development, as expressed in a recent *Nature* editorial (https://www.nature.com/articles/s43017-021-00216-1.pdf). This is highly worrying, particularly in Sweden where geology is poorly represented in the school curriculum, which suppresses the awareness of career paths among young people and leads to insufficient application pressure for higher education programmes. Swedish universities that still offer geology or earth science programmes must stand united against this trend of downgrading the organisational status of our subject. The Geological Society of Sweden has an important role to play in this perspective, preferably with the support of various stakeholders.

References

Björck, S., Walker, M.J.C., Cwynar, L.C., Johnsen, S., Knudsen, K.L., Lowe, J.J. & Wohlfarth, B. 1998: An event stratigraphy for the Last Termination in the North Atlantic region based on the Greenland ice-core record: a proposal by the INTIMATE group. *Journal of Quaternary Science 13*, 283–292.

Björnerås, C., Weyhenmeyer, G.A., Hammarlund, D., Persson, P., & Kritzberg, E.S. 2022: Sediment records shed light on drivers of decadal iron concentration increase in a Boreal Lake. *Journal of Geophysical Research: Biogeosciences, 127*, e2021JG006670.

Bragée, P., Mazier, F., Nielsen, A.B., Rosén, P., Fredh, D., Broström, A., Granéli, W. & Hammarlund, D. 2015: Historical TOC concentration minima during peak sulfur deposition in two Swedish lakes. *Biogeosciences 12*, 307–322.

De Geer, G. 1912: Geochronologie der letzten 12,000 Jahre: *Geologische Rundschau, Zeitschrift fur allegemeine Geologie 3*, 457–471.

Fredh, D., Mazier, F., Bragée, P., Lagerås, P., Rundgren, M., Hammarlund, D. & Broström, A. 2017: The effect of local land-use changes on floristic diversity during the past 1000 years in southern Sweden. *The Holocene 27*, 694–711.

Gibbard, P.L. & Head, M.J. 2010: The newly-ratified definition of the Quaternary System/Period and redefinition of the Pleistocene Series/Epoch, and comparison of proposals advanced prior to formal ratification. *Episodes 33*, 152–158.

Gray, M. 2018: The confused position of the geosciences within the "natural capital" and "ecosystem services" approaches. *Ecosystem Services 34*, 106–112.

Mangerud, J., Andersen, S.T., Berglund, B.E. & Donner, J.J. 1974: Quaternary stratigraphy of Norden, a proposal for terminology and classification. *Boreas 3*, 109–128.

Torell, O. 1872: Undrsökningar öfver istiden. *Proceedings of the Royal Swedish Academy of Sciences*.

van Ree, C.C.D.F. & van Beukering, P.J.H. 2016: Geosystem services: A concept in support of sustainable development of the subsurface. *Ecosystem Services 20*, 30–36.

von Post, L. 1918: Skogsträdpollen i sydsvenska torvmosselagerföljder. *Forhandlinger ved de Skandinaviske Naturforskeres 16. Møte i Kristiania den 10-15 juli 1916*, 432–468.

Walker, M.J.C., Berkelhammer, M., Björck, S., Cwynar, L.C., Fisher, D.A., Long, A.J., Lowe, J.J, Newnham, R.M., Rasmussen, S.O. & Weiss, H. 2012: Formal subdivision of the Holocene Series/Epoch: a discussion paper by a working group of INTIMATE (Integration of ice-core, marine and terrestrial records) and the Subcommission on Quaternary Stratigraphy (International Commission on Stratigraphy). *Journal of Quaternary Science 27*, 649–659.

Yang, B., Nielsen, A.B., Ljung, K., Fahlgren, E., Hormes, A. & Hammarlund, D. 2021: Quantitative landscape reconstruction and erosion history during the past 1,100 years in the Skogaryd Research Catchment, southern Sweden. *Vegetation History and Archaeobotany 29*, 657–670.

Early animal life and its quest for entering the oxic world

Emma U. Hammarlund[a], Kasper Hancke[b]

[a]Department of Laboratory Medicine, Lund University, Lund, Sweden, emma.hammarlund@med.lu.se
[b]Norsk Institut for Water Research (NIVA), Oslo, Norge.

Summary. The Cambrian explosion broadly mirrors an expansion in marine shelf area, but the mechanism linking this environmental change to organismal ecology remains tenuous. With a biogeochemical model, we constrain diurnal oxygen dynamics at the sunlit sediment-water interface and find that variability changed from modest to severe. If organisms with efficient oxygen sensing mechanisms were favored by this environmental shift, it links greenhouse climate, continental flooding and expansion of shelf area to ecophysiology and selective diversification during the Cambrian.

From stress to an adaptive radiation

The delay between the origin of animals in the Neoproterozoic and their later Cambrian diversification remains perplexing (Mills & Canfield 2014 for review; see also Budd & Jensen 2000). While the Cambrian explosion would have been preceded by permissive both extrinsic factors (e.g. temperature or oxygen) and intrinsic potential (e.g. developmental programs, fitness generating behaviors, or stemness control), current hypotheses do not account for its particular timing to the early Cambrian. For example, the attainment of non-limiting global oxygen concentrations can be argued conducive but does not address how long or short thereafter radiation could proceed (Marshall 2006). In addition, what we generally assumed to be permissive oxic conditions requires reexamination as we learn how tissue homeostasis is oxygen sensitive.

Fluctuations in oxygen concentrations can be argued a stressor for animal tissues, since it can require cell metabolism to switch at the same pace. Thereto, eukaryotic organisms are challenged by exposure to sulfide ions and scarcity of ferrous iron when intervals of oxygen depression (i.e. consumption) reach anoxia. These risks associated with fluctuating oxygen concentrations affect tissue homeostasis. In parallel, we know that benthic microalgae drive oxygen fluctuations on a daily basis at the sediment-water interface (Gattuso 2006). We also regard the Cambrian explosion as a benthic affair (Sperling 2015). Therefore, it is valid to explore patterns of oxygen fluctuations at the sediment-water interface before and during the Cambrian explosion.

We investigated oxygen dynamics at the sunlit sandy sediment-water interface in an icehouse scenario (~720 Ma) and a greenhouse scenario (~520 Ma), using a biogeochemical model. We identified that daily fluctuations went from modest (oxic-hypoxic) in the Cryogenian to severe (oxic-anoxic) in the Cambrian. The severe and rapid fluctuations from oxic (defined as >65 uM) to anoxic (<0.03 uM) conditions were presumed to affect the entire marine sandy shelf niche that increased dramatically in the Cambrian, for example in Scandinavia and the Baltic Sea area. Thus, we hypothesized that these stressors created needs that drove the adaptive radiation of animals with efficient oxygen-sensing mechanisms to cope with these fluctuations. These findings have implications for advancing our understanding of the driver behind and timing of the Cambrian explosion.

References

Budd G.E. & Jensen S. 2000. A critical reappraisal of the fossil record of the bilaterian phyla. *Biol Rev Camb Philos Soc*. 75, 253-295.

Gattuso, J-P. 2006. Light availability in the coastal ocean: impact on the distribution of benthic photosynthetic organisms and their contribution to primary production. *Biogeosciences*, 3, 489–513, 2006

Marshall, C.R., 2006. Explaining the Cambrian 'Explosion' of animals. *Annual Review of Earth and Planetary Sciences* 34:1, 355-384.

Mills, D.B. & Canfield, D.E. 2014. Oxygen and animal evolution: did a rise of atmospheric oxygen "trigger" the origin of animals? *Bioessays 36*, 1145-1155.

Sperling, E.A., Knoll, A.H. & Girguis, P.R., 2015. The ecological physiology of Earth's second oxygen revolution. *Annual Review of Ecology, Evolution, and Systematics* 46:1, 215-235.

Mineral deposits in the Fennoscandian Shield, Sweden, with focus on syn-orogenic 1.9−1.8 Ga ore provinces

Nils F. Jansson, Tobias E. Bauer

Division of Geosciences and Environmental Engineering, Luleå University of Technology, Luleå, Sweden, e-mail niljan@ltu.se

Summary. The Svecokarelian orogen in Sweden is endowed in metallic mineral deposits, including early syngenetic base metal and iron oxide deposits, and epigenetic deposits formed during later syn-orogenic magmatism, deformation and metamorphism. We discuss the spatial and temporal framework for various deposit types with emphasis on polymetallic sulphide, iron oxide, gold and tungsten deposits.

Introduction

Metallic mineral deposits in the Fennoscandian Shield of Sweden occur predominantly in Palaeoproterozoic rocks in the 2.0−1.8 Ga Svecokarelian orogen, bordering poorly endowed Archaean rocks inside this orogen to the northeast, and poorly endowed late Palaeoproterozoic and Mesoproterozoic rocks in the 1.1−0.9 Ga Sveconorwegian orogen to the southwest. The deposits mainly occur in four lithotectonic units inside the 2.0−1.8 Ga orogen; 1) The Norrbotten and Överkalix lithotectonic units (NLU-ÖLU), 2) the Bothnia-Skellefte lithotectonic unit (BSLU) and 3) the Bergslagen lithotectonic unit (BLU). This review mainly builds on Bergman and Weihed (2020), Skyttä et al. (2020), Stephens and Jansson (2020) and Stephens (2020), and references therein. Additional references are only provided for specific key concepts or recent work not covered in these papers.

Deposits formed prior to 1.87 Ga

Banded iron formations, iron skarn deposits, and stratiform and stratabound Cu-Fe and subordinate Zn sulphide deposits occur in a c. 2.3−2.0 Ga succession of basalt, komatiite and associated sedimentary rocks in the NLU-ÖLU, deposited in conjunction with rifting of the Archaean craton and the development of failed rifts and a passive margin environment. The most significant sulphide and iron deposits are however associated with syn-orogenic 1.91−1.88 Ga felsic-intermediate arc and back-arc volcanic rocks, and associated plutonic rocks with a subduction signature. In the Skellefte district of the northern BSLU, more than 85 Zn-Cu-Au-Ag-dominated VMS deposits formed in an volcanic arc undergoing strong extension and differential intra-arc basin development. Involvement of juvenile magmas and possibly reworking of accreted 1.96−1.94 Ga immature mafic arc volcanic rocks and 2.2−2.0 Ga oceanic crust in the petrogenesis of the Skellefte district rocks has been proposed based on Lu-Hf (Guitreau et al. 2014) and primitive ore Pb (Blichert-Toft et al. 2016) data. VMS mineralization in 1.96 Ga volcanic rocks in the BSLU indicate a potential role of recycling of base metals and gold during formation of the Skellefte deposits. In this context, a major understudied district comprise the so called ‘nickel line’ south of the Skelleft district, for which little information exists.

In the BLU, thousands of iron oxide deposits including banded iron formations, iron skarn deposits and iron oxide apatite deposits formed in conjunction with a prolific phase of predominantly rhyolitic syn-orogenic volcanism at 1.91−1.89 Ga. Key differences to the Skellefte district include 1) predominance of shallow marine environments and 2) recyling of sedimentary detritus from c. 2.1 Ga and Archaean continental crust. These differences from the BSLU are echoed by 1) a generally minor Cu- and Au-endowment and higher Pb endowment in the mineral deposits, 2) a more evolved character of Bergslagen ore Pb (Blichert-Toft et al. 2016), 3) shallow marine former limestone strata as traps to stratabound sulphide deposits and 4) involvement of highly saline, probably evaporitic brines in the formation of stratiform sulphide deposits.

Porphyry-style Cu-Au deposits formed in the northern part of the BSLU at c. 1.88−1.87 Ga, temporally related to the latest stages of arc/back-arc extension at the transition to transpression, uplift, erosion and concurrent magmatism. Further north in the NLU, this timing overlaps with the formation of the iron oxide apatite deposits at c. 1.88 Ga (e.g. Kiruna) and more poorly constrained porphyry-style Cu-Au in the age range 1.89−1.87 Ga (e.g. Aitik). In the BLU, a syn-metamorphic stage of REE mineralization has been inferred around 1.87−1.86 Ga but, otherwise, few deposits of this age are known.

Deposits formed after c. 1.87 Ga

All lithotectonic units contain W±Sn and Mo deposits related to crustal melts formed at 1.8 Ga. In the BLU, W skarns and intrusion-hosted Mo deposits formed in the time range 1.82−1.78 Ga, overlapping temporally with the emplacement of spatially associated, anatectic, crustally derived granite and pegmatite inboard of an active continental margin represented by the coeval magmatic rocks in the Transscandinavian Igneous Belt. Albeit subordinate to 1.91−1.87 Ga Fe oxide and sulphide deposits, many of the younger deposits formed at up to 15 kilometers depth inside the orogen, followed by uplift and erosion to the present level of exposure. Hence, in particular the shallow part of individual deposits or mineralized systems formed at 1.82−1.78 Ga had a low preservation potential in comparison to the 1.91−1.87 Ga syngenetic deposits, where even the shallow parts of deposits could be preserved with their supracrustal hosts in synclines.

Controversy exists regarding the timing of orogenic Au mineralization in the BSLU, including the so called 'gold line'; some authors favor a syn-D_1 or -D_2 origin at c. 1.88−1.87 Ga, others favor a later timing at 1.8 Ga related to N–S trending, D_3 structures that were (re-) activated during late-orogenic E–W compression. Spatial coincidence between Au and W mineralization in the BSLU lend support to the latter alternative. In the NLU-ÖLU iron oxide-copper gold (IOCG) deposits formed during the latest stages of the early-orogenic compression at c. 1.86−1.85 Ga (e.g. Rakurijärvi) as well as at the end of the late-orogenic compression at c. 1.80−1.78 Ga (e.g. Nautanen).

References

Bergman, S., Weihed, P., 2020. Archean (>2.6 Ga) and Paleoproterozoic (2.5–1.8 Ga), pre- and syn-orogenic magmatism, sedimentation and mineralization in the Norrbotten and Överkalix lithotectonic units, Svecokarelian orogen. In: Stephens, M.B., Bergman Weihed, J., (eds), 2020. *Sweden: Lithotectonic Framework, Tectonic Evolution and Mineral Resources. Geological Society, London, Memoirs, 50*, 27–81.

Blicher-Toft, J., Delile, H., Lee, C-T., Stos-Gale, Z., Billström, K., Andersen, T., Huhma, H., Albarède, F, 2016: Large-scale tectonic cycles in Europe revealed by distinct Pb isotope provinces. *Geochem. Geophys. Geosyst.,17*, 3854–3864.

Guitreau, M., Blicher-Toft, J., Billström, K., 2014: Hafnium isotope evidence for early-Proterozoic volcanic arc reworking in the Skellefte district (northern Sweden) and implications for the Svecofennian orogen. *Precambrian Research*, 252, 39–52.

Skyttä, P., Weihed, P., Högdahl, K., Bergman, S., Stephens, M.B., 2020. Paleoproterozoic (2.0–1.8 Ga) syn-orogenic sedimentation, magmatism and mineralization in the Bothnia–Skellefteå lithotectonic unit, Svecokarelian orogen. In: Stephens, M.B., Bergman Weihed, J., (eds), 2020. *Sweden: Lithotectonic Framework, Tectonic Evolution and Mineral Resources. Geological Society, London, Memoirs, 50*, 27–81.

Stephens, M.B, Jansson, N.F., 2020: Paleoproterozoic (1.9–1.8 Ga) syn-orogenic magmatism, sedimentation and mineralization in the Bergslagen lithotectonic unit, Svecokarelian orogen. In: Stephens, M.B., Bergman Weihed, J., (eds), 2020. *Sweden: Lithotectonic Framework, Tectonic Evolution and Mineral Resources. Geological Society, London, Memoirs, 50*, 237–250.

Stephens, M.B, 2020: Outboard-migrating accretionary orogeny at 1.9–1.8 Ga (Svecokarelian) along a margin to the continent Fennoscandia. In: Stephens, M.B., Bergman Weihed, J., (eds), 2020. *Sweden: Lithotectonic Framework, Tectonic Evolution and Mineral Resources. Geological Society, London, Memoirs, 50*, 237–250.

Position of Fennoscandia (Baltica) within Columbia and Rodinia, and models for the intervening break-up and collision

Åke Johansson

Department of Geosciences, Swedish Museum of Natural History, Stockholm, Sweden. ake.johansson@nrm.se

Summary. Baltica formed by the amalgamation of Fennoscandia, Volgo-Uralia and Sarmatia at c. 2.0 to 1.8 Ga. Subsequently, Baltica enjoyed a protracted but stormy relationship with Laurentia, with repeated break-ups and collisions in new configurations within Columbia, Rodinia and Pangea. The relation with Amazonia and West Africa along its soutwestern and southern margins presumably remained stable throughout Columbia and Rodinia. Although most authors agree that the Grenville-Sveconorwegian-Sunsas orogeny was caused by Laurentia-Baltica-Amazonia collision, several models exist for how this collision occurred.

Baltica in Columbia (Nuna)

The continental lithosphere in Baltica (a.k.a. East European Craton; Gorbatschev & Bogdanova 1993, Johansson 2009) amalgamated firstly at c. 2.0 Ga by collision of the Volgo-Uralia and Sarmatia cratons, and subsequently during the Svecofennian (a.k.a. Svecokarelian) orogeny by their oblique collision with Fennoscandia at c. 1.8 Ga (e.g. Bogdanova et al. 2015). Alternative orogenic models for the 2.0–1.8 Ga orogeny in Fennoscandia comprise subduction-related accretion followed by continent-continent collision in the west at 1.9–1.8 Ga (e.g. Lahtinen et al. 2009) or solely accetionary orogeny (e.g. Stephens 2020). The assembly of Baltica was part of the formation of the Columbia (a.k.a. Nuna) supercontinent. In Columbia, the present-day northern margin of Baltica was attached to the east Greenland margin of Laurentia, according to consistent paleomagnetic evidence (Pesonen et al. 2012, Salminen et al. 2021, and references therein). Johansson (2009; SAMBA model) suggested that the southwestern margin along the Trans-European Suture Zone was attached to northwest Amazonia, and the southern (Black Sea–Caspian Sea) margin to West Africa, and that Baltica, Amazonia and West Africa formed a coherent block from 1.8 to at least 0.8 Ga, both in Columbia and Rodinia. The situation in the east (present-day Ural margin) remains unclear, while the western margin formed the oceanic side of Columbia and remained intermittently active from 1.8 to 0.9 Ga.

Baltica in Rodinia

Break-up between Baltica (northern Fennoscandia) and Laurentia (Greenland), presumably around 1.25 Ga, was followed by clockwise rotation of Baltica relative to Laurentia (Cawood et al. 2010), the Grenville-Sveconorwegian-Sunsas orogeny and the formation of Rodinia. However, even though most authors agree that this orogeny was caused by Laurentia-Baltica-Amazonia interaction and collision, there are several conflicting geodynamic models on how it occurred.

Some early authors (e.g. Karlstrom et al. 2001) suggested that Baltica remained fixed relative to Laurentia, and jointly collided with Amazonia (or some other southerly craton/s). In such a model, the Sveconorwegian orogen forms a continuation of the Grenville orogen of eastern Canada, with the Sunsas belt possibly being the opposite margin. The Li et al. (2008) tectonic model for Rodinia also assumes a collision between Amazonia on the one hand, and Laurentia and Baltica on the other, with the Grenvillian Oaxaquia terrane of Mexico sandwiched between Amazonia and Baltica (cf. Bingen et al. 2021). Other models have assumed collision of Amazonia with southern Laurentia (Llano segment in Texas), followed by rotation of Amazonia along the Laurentian Grenville margin from south to north (Tohver et al. 2002, 2004), collision of Baltica and the Greenland part of Laurentia along their future Caledonian margins (Lorenz et al. 2012, Gee et al. 2015), or no collision at all when it comes to the Sveconorwegian margin of Baltica (continued accretion; Slagstad et al. 2013, 2017, 2020). The preferred model here would involve clockwise rotation of Baltica away from the Greenland margin, followed by collision further south along the Laurentian Grenville margin of Baltica and Amazonia, but no collision between these two, no Oaxaquia block sandwiched between them, and the Grenville and Sveconorwegian-Sunsas orogens forming opposite margins of the collisional orogenic belt.

Baltica in Pangea

Following break-up and separation of Baltica from both Amazonia, West Africa and Laurentia in the Neoproterozoic, Baltica became a continent on its own for about 200 million years, from 600 to 400 Ma, travelling north until it collided with Laurentia again along its northwestern Caledonian margin, with microcontinents such as Avalonia and Cadomia along its southwestern margin, and with Siberia along its eastern margin, thereby becoming totally embedded into Pangea. The latest step in this epic plate tectonic journey is the break-up between Scandinavia and Greenland which created the present-day North Atlantic Ocean, leading to renewed separation between Baltica (Eurasia) and Laurentia.

References

Bingen, B., Viola, G., Möller, C., Vander Auwera, J., Laurent, A., Yi, K., 2021: The Sveconorwegian orogeny. *Gondwana Research 90*, 273–313.

Bogdanova, S.V, Gorbatschev, R., Skridlaite, G., Soesoo, A., Taran, L., Kurlovich, D., 2015. Trans-Baltic Palaeoproterozoic correlations towards the reconstruction of supercontinent Columbia/Nuna. *Precambrian Research 259*, 5–33.

Cawood, P.A., Strachan, R., Cutts, K., Kinny, P.D., Hand, M. & Pisarevsky, S., 2010: Neoproterozoic orogeny along the margin of Rodinia: Valhalla orogen, North Atlantic. *Geology 38*, 99–102.

Gee, D.G., Andréasson, P.-G., Lorenz, H., Frei, D. & Majka, J., 2015: Detrital zircon signatures of the Baltoscandian margin along the Arctic Circle Caledonides in Sweden: The Sveconorwegian connection. *Precambrian Research 265*, 40–56.

Gorbatschev, R. & Bogdanova, S., 1993. Frontiers in the Baltic Shield. *Precambrian Research 64*, 3–21.

Johansson, Å., 2009: Baltica, Amazonia and the SAMBA connection – 1000 million years of neighbourhood during the Proterozoic? *Precambrian Research 175*, 221–234.

Karlstrom, K.E., Åhäll, K.-I., Harlan, S.S., Williams, M.L., McLelland, J. & Geissman, J.W., 2001: Long-lived (1.8–1.0 Ga) convergent orogen in southern Laurentia, its extension to Australia and Baltica, and implications for refining Rodinia. *Precambrian Research 111*, 5–30.

Lahtinen, R., Korja, A., Nironen, M. & Heikkinen, P. 2009: Palaeoproterozoic accretionary processes in Fennoscandia. In Cawood, P.A. & Kröner, A. (eds): *Earth Accretionary Systems in Space and Time.* Geological Society, London, Special Publications 318, 237–256.

Li, Z.X., Bogdanova, S.V., Collins, A.S., Davidson, A., De Waele, B., Ernst, R.E., Fitzsimons, I.C.W., Fuck, R.A., Gladkochub, D.P., Jacobs, J., Karlstrom, K.E., Lu, S., Natapov, L.M., Pease, V., Pisarevsky, S.A., Thrane, K. & Vernikovsky, V., 2008: Assembly, configuration, and break-up history of Rodinia: a synthesis. *Precambrian Research 160*, 179–210.

Lorenz, H., Gee, D.G., Larionov, A. & Majka, J., 2012: The Grenville-Sveconorwegian orogen in the High Arctic. *Geological Magazine 149*, 875–891.

Pesonen, L.J., Mertanen, S., Veikkolainen, T., 2012: Paleo-Mesoproterozoic supercontinents – a paleomagnetic view. *Geophysica 48*, 5–48.

Salminen, J., Lehtonen, E., Mertanen, S., Pesonen, L.P., Elming, S.-Å. & Luoto, T, 2021: The Precambrian drift history and paleogeography of Baltica. In Pesonen et al. (eds.): *Ancient Supercontinents and the Paleogeography of Earth*. Elsevier, 155–205.

Slagstad, T., Roberts, N.M.W., Marker, M., Røhr, T.S. & Schiellerup, H., 2013: A non-collisional, accretionary Sveconorwegian orogen. *Terra Nova 25*, 30–37.

Slagstad, T., Roberts, N.M.W. & Kulakov, E., 2017: Linking orogenesis across a supercontinent; the Grenvillian and Sveconorwegian margins on Rodinia. *Gondwana Research 44*, 109–115.

Slagstad, T., Marker, M., Roberts, N.M.W., Saalmann, K., Kirkland, C.L., Kulakov, E., Ganerød, M., Røhr, T.S., Møkkelgjerd, S.H.H., Granseth, A., Sørensen, B.E., 2020: The Sveconorwegian orogeny – Reamalgamation of the fragmented southwestern margin of Fennoscandia. *Precambrian Research 350*, 105877.

Stephens, M.B. 2020: Outboard-migrating accretionary orogeny at 1.9–1.8 Ga (Svecokarelian) along a margin to the continent Fennoscandia. In Stephens, M.B. & Bergman Weihed, J. (eds): Sweden: *Lithotectonic Framework, Tectonic Evolution and Mineral Resources*. Geological Society, London, Memoirs 50, 237–250.

Tohver, E., van der Pluijm, B.A., Van der Voo, R., Rizzotto, G. & Scandolara, J.E., 2002: Paleogeography of the Amazon craton at 1.2 Ga: early Grenville collision with the Llano segment of Laurentia. *Earth and Planetary Science Letters 199*, 185– 200.

Tohver, E., Bettencourt, J.S., Tosdal, R., Mezger, K., Leite, W.B. & Payolla, B.L., 2004: Terrane transfer during the Grenville orogeny: tracing the Amazonian ancestry of southern Appalachian basement through Pb and Nd isotopes. *Earth and Planetary Science Letters 228*, 161–176.

Glacial rebound and the triggering of large earthquakes

Björn Lund[a], Colby Smith[b], Henrik Mikko[c], Raymond Munier[d], Lars O. Ericsson[e], Peter Schmidt[f]

[a]Department of Earth Sciences, Uppsala University, Uppsala, Sweden, bjorn.lund@geo.uu.se; [b]Geological Survey of Sweden, Uppsala, Sweden, colby.smith@sgu.se; [c]Geological Survey of Sweden, Uppsala, Sweden, henrik.mikko@sgu.se; [d]Terra Mobile Consultants AB, Stockholm, Sweden, raymond@terramobile.se; [e]Department of Architecture and Civil Engineering, Division of Geology and Geotechnics, Chalmers University of Technology, Gothenburg, Sweden, lars.o.ericsson@chalmers.se; [f]Department of Earth Sciences, Uppsala University, Uppsala, Sweden, peter.schmidt@geo.uu.se

Summary. The association of prominent fault scarps in northern Fennoscandia with large earthquakes triggered by deglaciation changed the understanding of seismic hazard in Sweden and initiated a whole new field of research in seismology. Here we review the development of investigations and point to important further research directions.

Introduction

Late-glacial, post-glacial, end-glacial, early Holocene, glacio-isostatic, glacially induced (GIF) or glacially triggered (GTF)? The large fault scarps in northern Sweden, Finland and Norway have been called many names since their association with deglaciation in the 1960s and 1970s. Recent attempts to agree on GIF or GTF (Steffen et al. 2022) are once again challenged, now by new dating of large ruptures on the Stuoragurra fault as late as 600 years ago (Olesen et al. 2022), when induced glacial stresses had relaxed significantly.

Glacially induced faults

The Pärvie fault, long known to the Sami population in the area, was the first fault scarp in Sweden to be associated with earthquake rupture during deglaciation (Lundqvist & Lagerbäck 1976). Using aerial photography and trenching in the next two decades, R. Lagerbäck and co-workers identified more than a dozen GIFs in Sweden. Disturbed glacial landforms, sediments and landslides were used to infer that the GIFs had hosted large earthquakes during or shortly after the Late Weichselian deglaciation (Lagerbäck & Sundh 2008). Due to the implications for long-term bedrock stability, the Swedish Nuclear Fuel and Waste Management Company (SKB), conducted numerous investigation campaigns at a number of GIF sites (e.g. Bäckblom & Stanfors 1989; Stanfors & Ericsson 1993) and are still supporting research in this area.

Stratigraphic investigations of some faults indicated that the fault scarps reached their full length and height as a result of single ruptures shortly after deglaciation. The single rupture hypothesis was applied to the scarps, implying that the glacially triggered earthquakes would have reached magnitudes of 7 to 8 (e.g. Steffen et al 2022). Interest in the GIFs was renewed in the 2000s, with the installation of the modern Swedish national seismic network, seismic reflection and other geophysical investigations and, not least, the availability of high-resolution digital elevation models based on LiDAR data (Mikko et al. 2015). The latter refined the catalog of scarps by both adding and removing features, see Figure 1. Examination of geomorphic relationships in LiDAR imagery has also demonstrated that not all segments of the same fault ruptured at the same time, and that some segments had ruptured more than once (Smith et al. 2022). Bearing in mind the recent dating results from the Stuoragurra fault, this indicates that the GIFs still need more investigation in order to be fully understood.

Figure 1: Locations and names of glacially induced fault scarps in Sweden. (map from Smith et al. 2022).

Mechanics of glacially triggered earthquakes

Why did the earthquakes occur in response to deglaciation? Glacial isostatic adjustment (GIA) models of how the waxing and waning of the Weichselian ice sheet affected the crustal stress field in Fennoscandia (e.g. Wu et al. 1999; Lund et al. 2009) show that fault stability depends critically not only on the size and evolution of the ice sheet but also on the pre-existing stress field. The elastic and viscous properties of the Earth mainly affect induced stress magnitudes and to some extent their temporal development. As the ice sheet grows, the Earth below the ice subsides and compressive flexural horizontal stresses develop in the crust. Away from the ice margin the crust is instead uplifted in the fore-bulge, where tensional horizontal stresses develop. Combined with a pre-existing stress field that is either strike-slip or reverse, as in Sweden, the induced glacial stresses tend to stabilize faults under the ice sheet. Deglaciation removes the ice load much faster than the Earth can respond with rebound, which produces a significant stress difference between horizontal and vertical stresses. Combined with a reverse pre-existing stress field, this induced stress imbalance can destabilize faults and thus trigger earthquakes. Tectonic strain accumulated during the stabilized phase of the glaciation likely adds to this destabilization.

Outstanding questions

Although much knowledge has been gained in the last decade, there are still important questions remaining about the GIFs, both from a scientific and a seismic hazard perspective. Why are the large scarps mostly in northern Fennoscandia? How did other processes, such as permafrost or pore pressure variations, contribute to the ruptures? Many of the GIFs host significant seismicity today. Is that aftershock-related or evidence of current stress accumulation? How is the evidence of recent ruptures on the faults associated with deglaciation, if at all? Furthermore, how do the indications of repeated ruptures agree with models of strain accumulation in the Fennoscandian Shield?

Smith et al (2022) indicate repeated ruptures on the Pärvie fault that may “only” have had about 2 m of surface offset. This indicates smaller earthquakes than a magnitude 8 Pärvie event, but still on the order of magnitude 7. Repeated earthquakes and the Olesen et al (2022) finding of a magnitude 7 earthquake only 600 years ago is cause for re-evaluation of seismic hazard along the GIFs, for both mines and hydropower dams in their vicinity.

References

Bäckblom, G., Stanfors, R., 1989: Interdisciplinary study of post-glacial faulting in the Lansjärv area Northern Sweden 1986 – 1988. *TR-89-31, Swedish Nuclear Fuel and Waste Management Co. (SKB),* Stockholm, Sweden.

Stanfors, R., Ericsson, L.O. (eds.), 1993: Post-glacial faulting in the Lansjärv area, Northern Sweden. Comments from the expert group on a field visit at the Molberget post-glacial fault area, 1991. *TR-93-11, Swedish Nuclear Fuel and Waste Management Co. (SKB),* Stockholm, Sweden.

Lund, B., Schmidt, P., Hieronymus, C., 2009: Stress evolution and fault stability during the Weichselian glacial cycle. *TR-09-15, Swedish Nuclear Fuel and Waste Management Co. (SKB),* Stockholm, Sweden, 106pp.

Lagerbäck, R., Sundh, M., 2008: Early Holocene faulting and paleoseismicity in northern Sweden: Research Paper C 836. Geological Survey of Sweden.

Lundqvist, J. & Lagerbäck, R., 1976: The Pärve Fault: A late-glacial fault in the Precambrian of Swedish Lapland. *Geologiska Föreningen i Stockholm Förhandlingar 98:1*, 45-51. doi:10.1080/11035897609454337.

Mikko, H., Smith, C.A., Lund, B., Ask, M.V.S., Munier, R., 2015: LiDAR-derived inventory of post-glacial fault scarps in Sweden Article LiDAR-derived inventory of post-glacial fault scarps in Sweden. GFF 137, 334–338.

Olesen, O., Olsen, L., Gibbons, S.J., Ruud, B.O., Høgaas, F., Johansen, T.A., Kvaerna, T., 2022: Postglacial faulting in Norway, Large magnitude earthquakes of the late Holocene age. In: Steffen, H., Olesen, O., Sutinen, R., *Glacially Triggered Faulting,* Cambridge University Press, Cambridge, U.K. doi:10.1017/9781108779906.

Smith, C.A., Mikko, H., Grigull, S., 2022: Glacially Induced Faults in Sweden, The rise and reassessment of the single-rupture hypothesis. In: Steffen, H., Olesen, O., Sutinen, R., *Glacially Triggered Faulting,* Cambridge University Press, Cambridge, U.K. doi:10.1017/9781108779906.

Steffen, H., Olesen, O., Sutinen, R., 2022: *Glacially Triggered Faulting,* Cambridge University Press, Cambridge, U.K.

Wu, P., Johnston, P., Lambeck, K., 1999: Postglacial rebound and fault instability in Fennoscandia. *Geophys.J.Int. 139,* 657 – 670.

Tectonic evolution and crustal growth of Sweden at 2.7–1.4 Ga as part of the global supercontinent cycle

Stefan Luth, Edward P. Lynch

Department of Mineral Resources, Geological Survey of Sweden, Uppsala, Sweden, stefan.luth@sgu.se, edward.lynch@sgu.se

Summary. Much of the geological record in Sweden relates to the growth of continental crust from 2.7 to 1.4 Ga that led to the assembly of the supercontinent Columbia. More broadly, the geology of Fennoscandia records Mesoarchean–Neoarchean cratonization, Siderian–Rhyacian rift-to-drift crustal thinning and possible ocean growth, and Orosirian–Calymmian continental convergence and growth via episodic accretionary and, according to some studies, collisional orogenesis. Using available information, we present a "bigger picture" assessment of the tectonic evolution of Sweden from 2.7 to 1.4 Ga within the broader context of Fennoscandia and the global supercontinent cycle.

Supercontinent cycles record the tectonic amalgamation, break-up, dispersal, and re-amalgamation of Earth's paleocontinents over geological time. On a global scale, four supercontinents are proposed since the Mesoproterozoic (Columbia/Nuna, Rodinia, Pannotia, Pangea), while the merger of proto-continental fragments in the Neoarchean is thought to have formed several less coherent supercratons at that time (e.g. Superia/Kenorland). Aside from determining the configuration of the continents and oceans, supercontinent- or "Wilson"-cycle tectonics provides a fundamental first-order control on the distribution of magmatic-metamorphic belts, sedimentary basins, mineral deposits, and global sea-level and climate variations.

Within this geodynamic framework, the oldest rocks in Sweden (northern Norrbotten) record tonalite-trondhjemite-granodiorite (TTG)-type calc-alkalic magmatism at c. 2.72–2.62 Ga, marking continental growth along the western margin of Karelia - the cratonic core of Archean proto-Fennoscandia and a part of Superia by c. 2.5 Ga. After a period of stability, plume-initiated rifting at c. 2.45 Ga and a switch to divergent tectonics resulted in ultramafic-mafic magmatism, crustal thinning, and the possible detachment of Norrbotten from western Karelia. By at least c. 1.96 Ga and following passive margin foundering, a switch to convergence and subduction is recorded by arc magmatism in northern Sweden (Knaften) and ophiolitic rocks in Finland. Possible earlier subduction from c. 2.1 Ga is supported by detrital zircon and isotopic data suggesting that juvenile continental crust locally formed a substrate to younger syn-orogenic rocks (Svecofennian) exposed at the present surface (Fig. 1).

Most magmatic rocks in Sweden formed between c. 1.96 and 1.76 Ga during active margin subduction producing continental arc magmatism, the opening and closure of intra-arc basins, and the accretion of supra-subduction material to the older continental foreland (Svecokarelian orogeny). Whether subduction was continuously northward as part of a long-lived retreating-advancing plate boundary, or if several subduction zones – possibly with opposing polarities – (co-)existed between different arcs or microcontinents (e.g. Bergslagen) remains a matter of debate. The recognition, however, of four key magmatic pulses (P1–P4) punctuated by three metamorphic episodes (M1–M3) are interpreted as interlinked and repeating tectonothermal events, each lasting c. 25–50 million years during ongoing orogenesis and global-scale plate reconfiguration (Fig. 1). We suggest these orogenic phases likely reflect changes in relative plate motions and subduction zone dynamics along an evolving hemispheric-scale plate boundary referred to by Condie (2013) as the "Great Proterozoic Accretionary Orogen". By about 1.8 Ga, postulated collision of Fennoscandia with the Volgo-Sarmatia craton formed the larger paleocontinent Baltica marking the terminal Svecokarelian-cycle orogenic phase.

After 1.7 Ga, when the bulk of Sweden was cratonized, orogenic activity continued via continental arc magmatism (TIB 2; Eastern Segment) at c. 1.71–1.66 Ga and accretionary processes at c. 1.66–1.52 Ga (Gothian orogeny) in southwestern Sweden (Idefjorden terrane). A new phase of magmatism and orogenesis occurred again at c. 1.47–1.38 Ga in southern Sweden (Hallandian orogeny) followed by rift-type magmatism after 1.4 Ga that potentially marks the break-up of the Columbia supercontinent.

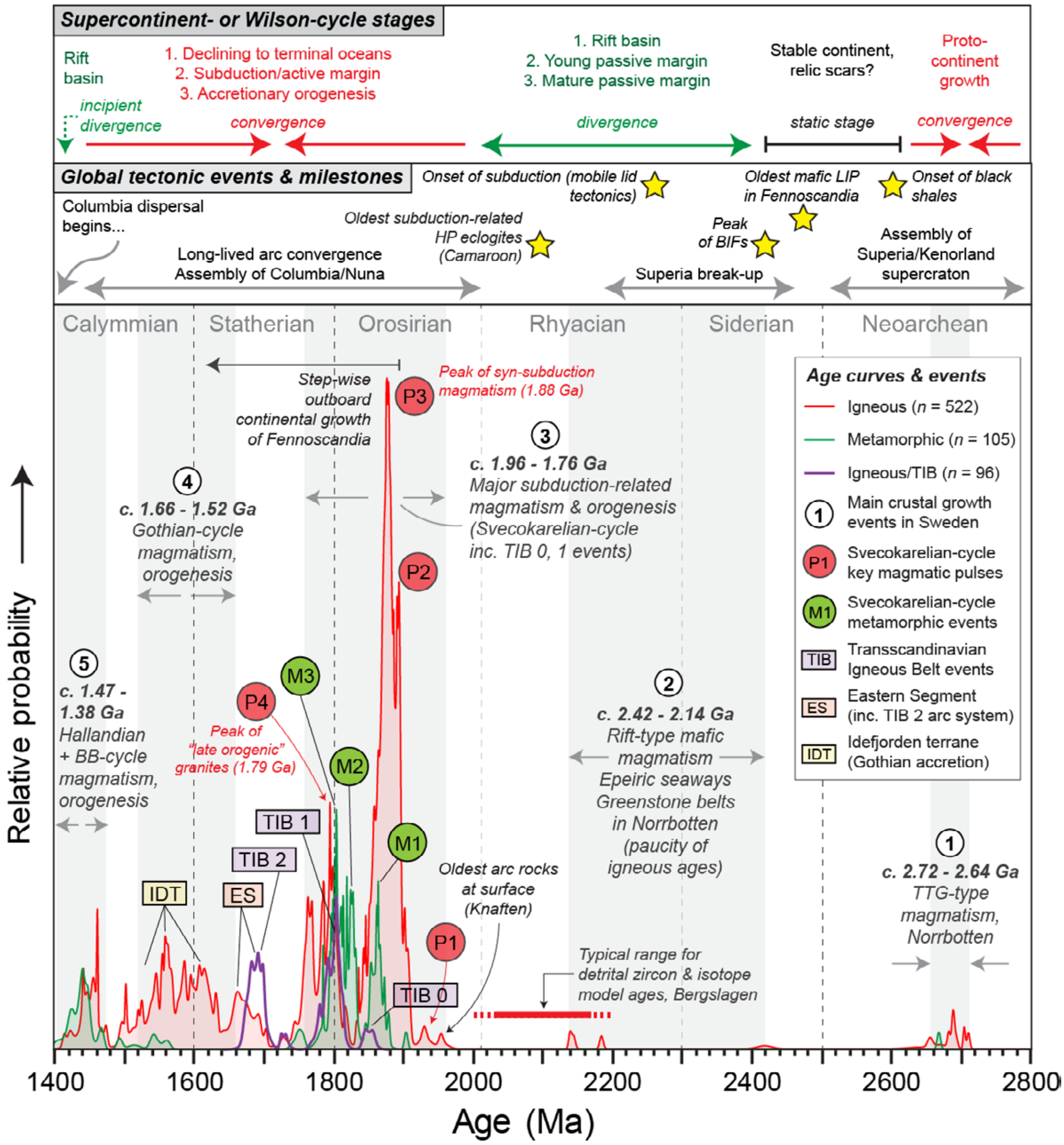

Figure 1. Probability curves for c. 2.7–1.4 Ga igneous and metamorphic ages in Sweden (based on age compilations in Stephens & Bergman Weihed 2020, and references therein). Main tectonothermal events in Sweden are also highlighted. Probability peaks for metamorphic and Transscandinavian Igneous Belt (TIB) ages are plotted relative to the total number of igneous ages (red curve, n = 522). Corresponding major global tectonic events and supercontinent cycle stages are shown at the top. BB = Blekinge-Bornholm, BIF = banded iron formation, HP = high pressure, LIP = large igneous province, TTG = tonalite-trondhjemite-granodiorite.

References

Condie, K. (2013). Preservation and Recycling of Crust during Accretionary and Collisional Phases of Proterozoic Orogens: A Bumpy Road from Nuna to Rodinia. *Geosciences*, 3, 240 – 261.

Stephens, M.B., Bergman Weihed J. (2020). *Sweden: Lithotectonic Framework, Tectonic Evolution and Mineral Resources*. Geological Society Memoir no. 50. 631 pp.

Subduction of a Baltica margin followed by Baltica-Laurentia collision as part of the assembly of Pangea

Jarosław Majka

Department of Earth Sciences, Uppsala University, Uppsala, Sweden, jaroslaw.majka@geo.uu.se; and Faculty of Geology, Geophysics and Environmental Protection, AGH University of Science and Technology, Kraków, Poland

Summary. The Scandinavian Caledonides is a Himalaya-type orogen, which bears a record of at least 100 million year long Iapetus Ocean closure and subsequent collision between Baltica and Laurentia. In this orogen, the convergent plate tectonic process resulted in a production of arc-basin systems including ophiolites, and high (or ultra-high) pressure rocks known from different tectonostratigraphic levels. A brief summary of subduction-collision processes in the orogen as part of the northern Iapetus realm is given below.

Subduction and convergence between paleocontinents Laurentia and Baltica within the northern Iapetus Ocean lasted for at least 100 million years. These processes are best recorded by (ultra-)high pressure ((U)HP) rocks of the formerly downgoing plate, and arc-basin systems including ophiolites of the formerly overriding plate. In the Scandinavian Caledonides, (U)HP rocks occur within the Middle, Upper and possibly Uppermost allochthons, and in the basal parautochthonous units of the Western Gneiss Region (e.g. Cuthbert et al. 2000, Brueckner & van Roermund 2004, Janák et al. 2012, Gee et al. 2013). In contrast, arc-basin systems including ophiolites are present within the Upper Allochthon (Stephens et al. 1985, Dunning & Pedersen 1988).

The earliest record of a deep subduction of a continent-ocean transition zone, including the outermost margin of Baltica, is known from the Seve Nappe Complex of the Middle Allochthon in Norrbotten, Sweden, where late Cambrian to Early Ordovician eclogitized blueschists and eclogites occur (e.g. Andréasson et al. 1985, Kullerud et al. 1990, Mørk et al. 1988, Bukała et al. 2018, Barnes et al. 2019). Walczak et al. (2022) also recently reported an Early Ordovician age for (U)HP metamorphism recorded by a diamond-bearing gneiss in the Seve farther south in Jämtland. The upper plate to these oldest (U)HP rocks has been hypothesized to be an island arc developed within the Iapetus Ocean (Dallmeyer & Gee 1986). Indeed the lower thrust sheets of the Upper Allochthon bear a record of a Cambrian to Ordovician arc-basin system including ophiolite (Stephens 2020 and references therein).

Middle to Late Ordovician deep subduction of the Baltica margin is best recorded within the Seve Nappe Complex of northern Jämtland. It is manifested by a multitude of orogenic peridotites, eclogites and (U)HP gneisses (e.g. Brueckner & van Roermund 2007, Janák et al. 2013, Fassmer et al. 2017). Additionally, diamond-bearing Seve gneisses in southern Västerbotten and west-central Jämtland attest to the deep subduction of the Baltica crust (e.g. Majka et al. 2014, Klonowska et al. 2017), but the exact age and tectonic significance of this (U)HP event is currently a matter of debate. Mafic magmatic activity recorded in the Upper and Uppermost allochthons along the entire orogen, locally including ophiolite formation (e.g. Stephens et al. 1985, Slagstad & Kirkland 2018), and migmatization in the Seve Nappe Complex in Jämtland (Ladenberger et al. 2014) prevailed during the early Silurian (c. 443 to 434 Ma) prior to Scandian crustal shortening and thickening.

Ongoing convergence between Baltica and Laurentia resulted in the Silurian to Early Devonian vanishing of Iapetus, contemporary deep underthrusting of Baltica beneath Laurentia, and formation of one of the largest and most spectacular (U)HP terranes in the world, namely the Western Gneiss Region. Shortening and thickening continued until the Early Carboniferous, as indicated by the youngest Caledonian (U)HP rocks occurring in the East Greenland Caledonides belonging to the formerly overriding Laurentia plate (e.g. Gilotti et al. 2004).

References

Andréasson, P.G., Gee, D.G., Sukotji, S., 1985: Seve eclogites in the Norrbotten Caledonides, Sweden. In: Gee, D.G. & Sturt, B.A. (eds) *The Caledonide Orogen—Scandinavia and Related Areas*. John Wiley and Sons, Chichester, UK, 887–902.

Barnes, C.J., Majka J., Schneider, D. et al., 2019: High-spatial resolution dating of monazite and zircon reveals the timing of subduction–exhumation of the Vaimok Lens in the Seve Nappe Complex (Scandinavian Caledonides). *Contributions to Mineralogy and Petrology 174: 5*.

Brueckner, H.K. & van Roermund, H.L.M., 2004: Dunk tectonics: a multiple subduction/eduction model for the evolution of the Scandinavian Caledonides. *Tectonics 23*, 1–20.

Brueckner, H.K. & van Roermund, H.L.M., 2007: Concurrent HP metamorphism on both margins of Iapetus: Ordovician ages for eclogites and garnet pyroxenites from the Seve Nappe Complex, Swedish Caledonides. *Journal of the Geological Society London 164,* 117–128.

Bukała, M., Klonowska, I., Barnes, C., et al., 2018: UHP metamorphism recorded by phengite eclogite from the Caledonides of northern Sweden: P–T path and tectonic implications. *Journal of Metamorphic Geology 36,* 547–566.

Cuthbert, S.J., Carswell, D.A., Krogh-Ravna, E.J., Wain, A., 2000: Eclogites and eclogites in the Western Gneiss Region, Norwegian Caledonides. *Lithos 52*, 165–195.

Dallmeyer, R.D. & Gee, D.G. 1986: $^{40}Ar/^{39}Ar$ mineral dates from retrogressed eclogites within the Baltoscandian miogeocline: Implications for a polyphase Caledonian orogenic evolution. *Geological Society of America Bulletin 97*, 6–34.

Dunning, G. & Pedersen, R.-B., 1988: U/Pb ages of ophiolites and arc-related plutons of the Norwegian Caledonides: Implications for the development of Iapetus. *Contributions to Mineralogy and Petrology 98*, 13–23.

Fassmer, K., Klonowska, I., Walczak, K., et al., 2017: Middle Ordovician subduction of continental crust in the Scandinavian Caledonides: an example from Tjeliken, Seve Nappe Complex, Sweden. *Contributions to Mineralogy and Petrology 172,* 1–21.

Gee, D.G., Janák, M., Majka, J., et al., 2013: Subduction along and within the Baltoscandian margin during closing of the Iapetus Ocean and Baltica–Laurentia collision. *Lithosphere 5,* 169–178.

Gilotti, J.A., Nutman, A.P., Brueckner, H.K., 2004: Devonian to Carboniferous collision in the Greenland Caledonides: U-Pb zircon and Sm-Nd ages of high-pressure and ultrahigh-pressure metamorphism. *Contributions to Mineralogy and Petrology 148,* 216–235.

Janák, M., Ravna, E.J.K., Kullerud, K., 2012: Constraining peak P–T conditions in UHP eclogites: calculated phase equilibria in kyanite- and phengite-bearing eclogite of the Tromsø Nappe, Norway. *Journal of Metamorphic Geology 30,* 377–396.

Janák, M., van Roermund, H., Majka, J., Gee, D., 2013: UHP metamorphism recorded by kyanite-bearing eclogite in the Seve Nappe Complex of northern Jämtland, Swedish Caledonides. *Gondwana Research 23,* 865–879.

Klonowska, I., Janák, M., Majka, J., et al., 2017: Microdiamond on Åreskutan confirms regional UHP metamorphism in the Seve Nappe Complex of the Scandinavian Caledonides. *Journal of Metamorphic Geology 35,* 541–564.

Kullerud, K., Stephens, M.B., Zachrisson, E., 1990: Pillow lavas as protoliths for eclogites: evidence from a late Precambrian-Cambrian continental margin, Seve Nappes, Scandinavian Caledonides. *Contributions to Mineralogy and Petrology 105,* 1–10.

Ladenberger, A., Be'eri-Shevin, Y., Claesson, S., Gee, D.G., et al., 2014: Tectonometamorphic evolution of the Åreskutan Nappe – Caledonian history revealed by SIMS U–Pb zircon geochronology. In: Corfu, F., Gasser, D. & Chew, D.M. (eds) *New Perspectives on the Caledonides of Scandinavia and Related Areas*. Geological Society London Special Publications 390, 337–368.

Majka, J., Rosén, Å., Janák, M., et al., 2014: Microdiamond discovered in the Seve Nappe (Scandinavian Caledonides) and its exhumation by the "vacuum-cleaner" mechanism. *Geology 42,* 1107–1110.

Mørk, M.B.E., Kullerud, K., Stabel, A., 1988: Sm–Nd dating of Seve eclogites, Norrbotten, Sweden—evidence for early Caledonian (505 Ma) subduction. *Contributions to Mineralogy and Petrology 99,* 344–351.

Slagstad T. & Kirkland, C.L., 2018: Timing of collision initiation and location of the Scandian orogenic suture in the Scandinavian Caledonides. *Terra Nova 30*, 179–188.

Stephens, M.B., Furnes, H., Robins, B., Sturt, B.A., 1985: Igneous activity within the Scandinavian Caledonides. In: Gee, D.G. & Sturt, B.A. (eds) *The Caledonide Orogen – Scandinavia and Related Areas*. John Wiley and Sons, Chichester, UK, 623–656.

Stephens, M.B., 2020: Upper and uppermost thrust sheets in the Caledonide orogen, Sweden: outboard oceanic and exotic continental terranes. In: Stephens, M.B. & Bergman Weihed, A. (eds) *Sweden: Lithotectonic Framework, Tectonic Evolution and Mineral Resources.* Geological Society London Memoirs 50, 549–575.

Walczak, K., Barnes, C.J., Majka, J., et al., 2022: Zircon age depth-profiling sheds light on the early Caledonian evolution of the Seve Nappe Complex in west-central Jämtland. *Geoscience Frontiers 13,* 101112.

The Mesozoic of Sweden

Stephen McLoughlin[a], Vivi Vajda[a], Lars E. Holmer[b]

[a]Department of Palaeobiology, Swedish Museum of Natural History, Stockholm, Sweden; steve.mcloughlin@nrm.se, vivi.vajda@nrm.se, [b]Department of Earth Sciences, Palaeobiology, Uppsala University, Uppsala, Sweden; lars.holmer@pal.uu.se

Summary. Triassic–Jurassic rifting and transtensional movements along the Sorgenfrei-Tornquist Zone provided accommodation space for the accumulation of a thick sedimentary succession along Sweden's southern margin. A more passive subsidence regime, accompanied by high sea levels, saw the deposition of extensive shallow marine sediments across Skåne in the Cretaceous. These deposits host a wealth of continental and marine fossils informative of stratal ages, palaeoclimate, and palaeoecology.

Triassic

Induan–Carnian strata deep in the subsurface of the Danish Basin are the oldest Mesozoic deposits in Sweden (Erlström & Sivhed 2012). These reddish to greenish alternating mudrocks and sandstones with minor evaporites and dolomites were deposited in arid continental settings under supermonsoonal climates that developed as Pangea reached its maximum areal extent. The few ostracod, palynomorph, and charophyte fossils in these strata favour correlation with the Buntsandstein–Keuper interval of northern Germany. Initiating in the Late Triassic, and extending into the Jurassic, rifting along Sweden's southern margin, associated with Pangean break-up, was accompanied by deposition of the oldest exposed Mesozoic strata in Sweden: red beds of the Kågeröd Formation, which contain sparse Norian-aged palynomorphs and charophyte oogonia. The succeeding Höganäs Formation incorporates three subunits. The Vallåkra Member (lower Rhaetian), composed of paralic claystone and argillaceous sandstone, contains only sparse palynomorphs. The Bjuv Member (upper Rhaetian) is rich in coals that were exploited for several hundred years until the late 1960s. The unit has yielded over 110 species of fossil plants described over the past 140 years by numerous workers (Pott & McLoughlin 2011 and references therein). These floras are similar to upper Rhaetian assemblages of Greenland and have proven useful in resolving the floristic provincialism of the Late Triassic. The Bjuv Member also hosts fossils of various insects, annelids, fish, amphibians, and numerous dinosaur footprints (Vajda et al. 2013). The extensive macro- and palyno-floras of the Bjuv Member remain the focus of ongoing research, as this unit embraces the horizon marking the end-Triassic extinction event. Across this level, the strata change from coals and dark, organic-rich, mudrocks (Rhaetian), to pale grey and whitish siltstones and sandstones (Hettangian). The palynological transition records a spike in fern-spores, evidence of a subsequent marine incursion and development of post-extinction anachronistic facies including microbial mats (Larsson 2009, Lindström & Erlström 2006).

Jurassic

Lowermost Jurassic (Hettangian) deltaic strata of the Helsingborg Member (uppermost Höganäs Formation) host a rich macroflora and various fossil bivalves, shark egg capsules and dinosaur footprints that track biotic recovery following the end-Triassic extinction. The laterally equivalent, dominantly fluvial, Höör Sandstone represents an important historical source of building stone in Skåne and also hosts a rich macroflora. Other Lower Jurassic strata in Skåne are represented by interdigitating continental to shallow marine siliciclastic facies assigned to various (mostly informal) lithostratigraphic units (Vajda & Wigforss-Lange 2009). Although palynological studies have provided basic age controls on these units, much work remains to resolve the lithostratigraphic and biostratigraphic framework. Sinemurian–Aalenian strata of the 'Rya formation' and its equivalents reflect increasing marine influence on deposition. This alternating mudrock- and sandstone-dominated succession has yielded the remains of fish, diverse invertebrates, sparse macro-plants, and rich palynofloras. Eruptive activity in the central Skåne volcanic province, variously attributed to a local mantle plume or Pangean rifting, peaked around the Pliensbachian and resulted in the emplacement of 100–200 mafic volcanic necks (Bergelin 2009) and several small lahar deposits that host remarkably well permineralized plant remains (Bomfleur et al. 2014). Middle–Upper Jurassic deposits in Skåne reflect a mix of deltaic to shallow marine sedimentation. Rich Bajocian–Bathonian plant assemblages occur in the 'Fuglunda member' of the 'Mariedal formation' (Tralau 1966), whereas overlying Callovian–Tithonian marine strata of the 'Annero formation' contain various microfossils offering scope for improved biostratigraphic resolution (Vajda & Wigforss-Lange 2009).

Cretaceous

Predominantly marine deposition persisted through the Early Cretaceous in Skåne. Strata of this age contain terrestrial and marine palynomorph assemblages offering opportunities for linking continental and marine biozones. Pollen of flowering plants first appears in Sweden at this time, when the region was located in middle latitudes (c. 45°N). Gentle half-graben subsidence and elevated sea levels, attributed to increased global sea-floor spreading rates, saw the incursion of carbonate-producing shallow seas into southern Sweden during the Late Cretaceous. The paralic 'Holma sandstone' and equivalents (Santonian) of the Kristianstad Basin and the 'Köpinge sandstone' (uppermost lower Campanian) in the Vomb Trough both host plant remains but few invertebrate fossils (Halamski et al. 2016, McLoughlin et al. 2021). Mummified and charcoalified angiosperms in un-named Santonian–Campanian clays at Åsen (Kristianstad Basin) are of international importance (Friis et al. 2011) and co-preserved with little-studied but diverse conifer, lycopsid and fungal remains (McLoughlin et al. 2021). This deposit offers great potential for documenting the radiation of angiosperm-dominated vegetation in the Late Cretaceous of northern Europe. Succeeding middle Campanian–Maastrichtian deposits are represented mostly by marine marls and chalks preserving rich invertebrate faunas, various marine vertebrates, and even rare terrestrial vertebrates (Einarsson, 2018). The end-Cretaceous extinction horizon is likely preserved in the southernmost carbonate successions of Sweden but, thus far, no high-resolution palaeontological study of biotic turnover across this level has been carried out.

References

Bergelin, I., 2009: Jurassic volcanism in Skåne, southern Sweden, and its relation to coeval regional and global events. *GFF 131*, 165–175.

Bomfleur, B., McLoughlin, S. & Vajda, V., 2014: Fossilized nuclei and chromosomes reveal 180 million years of genomic stasis in Royal Ferns. *Science 343*, 1376–1377.

Einarsson, E., 2018: Paleoenvironments, palaeoecology and palaeobiogeography of late cretaceous (campanian) faunas from the Kristianstad basin, southern Sweden, with applications for science education. PhD thesis, Lund University, 252 pp.

Erlström, M. & Sivhed, U., 2012: Pre-Rhaetian Triassic strata in Scania and adjacent offshore areas – stratigraphy, petrology and subsurface characteristics. *Sveriges geologiska undersökning, Rapporter och Meddelanden 132*, 1–74.

Friis, E.M., Crane, P.R., Pedersen, K.R., 2011: *Early Flowers and Angiosperm Evolution*. Cambridge University Press, Cambridge, 585 pp.

Halamski, A.T., Kvaček, J., Vajda, V., 2016: Late Cretaceous (Campanian) leaf and palynoflora from southern Skåne, Sweden. In: Kear, B.P., Lindgren, J., Hurum, J.H., Milàn, J., Vajda, V. (Eds.), Mesozoic Biotas of Scandinavia and its Arctic Territories. *Geological Society, London, Special Publications 434*, 207–230.

Larsson, L.M., 2009: Palynostratigraphy of the Triassic–Jurassic transition in southern Sweden. *GFF 131*, 147–163.

Lindström, S. & Erlström, M., 2006: The late Rhaetian transgression in southern Sweden: Regional (and global) recognition and relation to the Triassic–Jurassic boundary. *Palaeogeography, Palaeoclimatology, Palaeoecology 241*, 339–372.

McLoughlin, S., Halamski, A.T., Mays, C. & Kvaček, J. 2021: Neutron tomography, fluorescence and transmitted light microscopy reveal new insect damage, fungi and plant organ associations in the Late Cretaceous floras of Sweden. *GFF 143*, 248–276.

Nathorst, A.G., 1878: *Beiträge zur fossilen Flora Schwedens. Über einige rhätische Pflanzen von Pålsjö in Schonen*. Schweitzerbart'sche Verlagsbuchhandlung, Stuttgart.

Pott, C. & McLoughlin, S., 2011: The Rhaeto-Liassic flora from Rögla, northern Scania, Sweden. *Palaeontology 54*, 1025–1051.

Tralau, H., 1966: Botanical investigations in the fossil flora of Eriksdal in Fyledalen, Scania. *Sveriges Geologiska Undersökning, Serie C 611*, 1–36.

Vajda, V. & Wigforss-Lange, J., 2009: Onshore Jurassic of Scandinavia and related areas. *GFF 131*, 5–23.

Vajda, V, Calner, M. & Ahlberg, A., 2013: Palynostratigraphy of dinosaur footprint-bearing deposits from the Triassic–Jurassic boundary interval of Sweden. *GFF 135*, 120–130.

Ordovician, Silurian and Devonian on Baltica – a tale of tropical reefs, land plant expansion and explosive volcanism

Vivi Vajda, Stephen McLoughlin

Department of Palaeobiology, Swedish Museum of Natural History, PO Box 50007, SE-104 05 Stockholm, Sweden; vivi.vajda@nrm.se

Summary. The paleocontinent Baltica constitutes a large part of northern Europe, bounded by the Scandinavian Caledonides to the northwest, the Uralian orogen to the east and the Trans-European Suture Zone to the southwest (Cocks & Torsvik 2005). Baltica rifted from Rodinia (or its possible successor Pannotia) during the late Neoproterozoic, and formed an isolated continent until the Late Ordovician to Devonian. It then amalgamated with Avalonia and Laurentia during closure of the Tornquist Sea to the southwest (current coordinates) and the Iapetus Ocean to the northwest, respectively. Here we focus on the Ordovician to Devonian paleogeography, depositional setting, and both the marine and land plant biota preserved on the shallow marine Baltica shelf.

Development of Baltica

During convergence of Baltica and Avalonia and subduction, an extensive system of volcanic arcs produced exceptional volumes of volcanic ash by the Middle Ordovician. As Baltica drifted northwards from Gondwana through the Ordovician, the Tornquist Sea was formed alongside the southwestern margin of Baltica, hosting a rich marine invertebrate fauna (Bergström et al. 2013). By the end of the Middle Ordovician, Baltica was positioned around 35°S and the climate was similar to that of modern subtropical belts with extensive formation of reefs in the shallower marine basins. Avalonia collided with Baltica at the end of the Ordovician and a general shallowing is evident from this time onwards, as the Tornquist Sea retreated as a consequence of orogenic uplift (Torsvik & Rehnström, 2003). By the middle Silurian, a shallow marine embayment, extending from the south of Sweden to Gotland and to the Baltic States, was all that remained of this seaway. By the latest Silurian, the docking of Baltica and Avalonia was complete. Baltica then became incorporated into the continent Laurussia (the Old Red Sandstone Continent) that formed as a consequence of the collision of Baltica, Laurentia and Avalonia (Scotese et al., 1985; Torsvik & Rehnström, 2003; Gee 2020). During the late Silurian–Early Devonian, the Caledonian orogeny dramatically influenced sedimentary development towards the west and south. This is manifest as a shift from marine carbonates to more terrestrially influenced sediments, such as commonly reddish sandstones.

Marine Life

The extensive fossil assemblages of the Ordovician and Silurian are rich in graptolites, cephalopods, trilobites and brachiopods, together with cystoids and bryozoans. The most notable examples of Ordovician marine ecosystems of this age are from the island of Öland, where extensive and stratigraphically resolved assemblages from the Lower and Middle Ordovician "Orthoceras limestone" exist. Upper Ordovician reefs of Dalarna in central Sweden also provide a rich source of fossils, including biotic remains from the reefs themselves, from the surrounding inter-reef facies, and also from younger fissure fills inside the reefs. The sedimentary succession reflects a gradual shallowing from deep-water graptolitic shales to shallow marine limestones and sandstones. Following this facies progradation, marine deposition ceased and was replaced by the onset of early Devonian ''Old Red Sandstone'' (Övedskloster Sandstone) deposition.

Plants colonizing land

The origin of land plants was a major macro-evolutionary event having immense consequences for continental and marine ecology, and for the global climate system (Wellman 2010). Land plants triggered an acceleration of weathering processes (Lenton et al. 2012) and the development of structured soils in symbiosis with complex fungal and microbial communities. Empirical studies have also shown that the appearance of land plants boosted CO_2 drawdown, and potentially contributed to Late Ordovician cooling and a rise in atmospheric oxygen pressure (pO_2) (Lenton et al. 2012).

Knowledge of the land plant colonization of Baltica is scarce, with the oldest known records of non-vascular land plant spores coming from the Furudal Limestone (Middle Ordovician: Darriwillian: ~ 460 Ma) from the Kinnekulle drill core (Rubinstein & Vajda 2019). The formation of regolith substrates on land as a consequence of permanent plant cover must in turn have affected the marine biota. Importantly, the earliest global traces of vascular land plants yet recorded were identified in the Late Ordovician (Sandbian: 455 Ma) successions of central Sweden and were preserved while Baltica was an isolated continent. These strata were independently dated by marine microfossils (conodonts) and $^{206}Pb/^{238}U$ dating of volcanic ash deposits. The Silurian was a significant interval for land plant evolution, a period during which the plants became well-established on most continents, markedly increasing in abundance, and with new and more derived forms appearing (Wellman et al. 2010; Mehlqvist et al. 2015). This is clearly reflected in the spore assemblages with more ornamented spores appearing in the upper Silurian sedimentary record. Gotland preserves some of the earliest plant remains, also showing early plant-insect interactions. They occur in nearshore deltaic successions of the Burgsvik Formation, southern Gotland. The rich record of upper Silurian spores from Skåne reveal landscape covered by a thriving vegetation of mosses and small vascular plants – paving the way for the terrestrialisation of animals.

References

Bergström, J., Pärnaste, H. & Zhiyi, Z., 2013: Trilobites and biofacies in the Early−Middle Ordovician of Baltica and a brief comparison with the Yangtze Plate. *Estonian Journal of Earth Sciences 62*, 205–230.

Cocks, L.R.M. & Torsvik, T.H., 2005: Baltica from the late Precambrian to mid-Palaeozoic times: the gain and loss of a terrane's identity. *Earth-Science Reviews 72*, 39–66.

Lenton, T.M., Crouch, M., Johnson, M., Pires, N. & Dolan, L., 2012: First plants cooled the Ordovician. *Nature Geoscience 5*, 86–89.

Mehlqvist, K., Steemans, P. & Vajda, V., 2015: First evidence of Devonian strata in Sweden — a palynological investigation of Övedskloster drillcores 1 and 2, Skåne, Sweden. *Review of Palaeobotany and Palynology 221*, 144–159.

Torsvik, T.H. & Rehnström E.F., 2003: The Tornquist Sea and Baltica – Avalonia docking. *Tectonophysics 362*, 67–82.

Rubinstein, C.V. & Vajda, V., 2019: Baltica cradle of early land plants? Oldest record of trilete spores and diverse cryptospore assemblages; evidence from Ordovician successions of Sweden. *GFF 141:3*, 181–190.

Scotese, C.R., van der Voo, R. & Barett, S.F.,1985: Silurian and Devonian base maps. *Philosophical Transactions of the Royal Society of Lond*on 309, 57–77.

Gee, D.G., 2020: Swedish Caledonides: key components of an early−middle Paleozoic Himalaya-type collisional orogen. In: Stephens, M.B. & Bergman Weihed, A. (eds) *Sweden: Lithotectonic Framework, Tectonic Evolution and Mineral Resources*. Geological Society London Memoirs 50, 577–599.

Wellman, C.H., 2010: The invasion of the land by plants: when and where? *New Phytologist 188*, 306–309.

0.9–0.6 Ga break-up of Rodinia and Pannotia resulting in the birth of the ancient Iapetus Ocean and continent Baltica

Linda M. Wickström

Geological Survey of Sweden, Box 670 75128 Uppsala, Sweden, linda.wickstrom@sgu.se

Summary. The Neoproterozoic was a period in Earth history with amalgamation and break-up of landmasses, and major climate changes. Break-up of Rodinia and Pannotia created the Iapetus Ocean separating Laurentia and Baltica as well as the separation of Laurentia and Gondwana. Neoproterozoic rocks in Sweden are not widespread, but can be found in the lower and middle thrust sheets of the Caledonide orogen, along Lake Vättern in southern Sweden and near Sundsvall in central Sweden. They represent marine environments in a rift-related setting, glacial deposits and, in the latter case, an alkaline and carbonatite intrusive complex with some explosive volcanic vent material.

Rodinia is one of several supercontinents that have existed throughout Earth history. It was formed through orogenic processes at 1.1 to 0.9 Ga and lasted for almost 300 million years. Nance & Murphy (2019) suggested that the final break-up of this supercontinent took place at approximately 680 Ma.

After Rodinia, another large Neoproterozoic landmass, Pannotia, was formed, although its existence has been debated (e.g. Murphy et al. 2021, Kroner et al. 2021, contra Evans 2021). It included Gondwana, Baltica, Laurentia and Siberia, and is believed to have existed for a relatively short time period during the Ediacaran. The opening of the Iapetus Ocean between Baltica and Laurentia, and establishment of Baltica as a separate continent took place during the Ediacaran at c. 610–600 Ma (Gee et al. 2020 and references therein). The palaeogeographic configuration of Baltica and Laurentia appears to have stayed the same during both Rodinian and Pannotian times, hence the existence or non-existence of Pannotia does not affect the interpretation of the geological development in the Baltica–Laurentia context.

Neoproterozoic metasandstones and carbonate rocks, deposited along the rifted continental margin of Baltica, are a prominent component of the lower and middle thrust sheets in the Caledonide orogen (Gee & Stephens 2020, Gee et al. 2020). Early attempts at break-up of Rodinia can be observed in the failed rift which created the Vättern half-graben in southern Sweden. This sedimentary basin was filled with Tonian–Cryogenian sediments of the Visingsö Group (e.g. Moczydłowska et al. 2018, Wickström & Stephens 2020) during and after rifting. Sedimentary rocks of the Visingsö Group are today mainly present along Lake Vättern and at a few additional locations north of the lake, showing the existence of an originally larger cover of Neoproterozoic sediments on top of the older crystalline basement.

The lowermost Visingsö Group is a mature white to reddish sandstone deposited in a marine near-shore delta environment during rifting of Rodinia. The middle part represents an ongoing transgression with a change from near-shore deposits to pro-delta sedimentation that continues, in the upper part, into a supratidal to intertidal environment represented by alternating shale, siltstone and dolomitic sandstones, and limestone with stromatolites (Vidal 1976, 1982, 1985).

The Neoproterozoic was also a time of major climate changes with several glaciations, e.g. the Sturtian, the Marinoan and the Gaskier glaciations. Neoproterozoic glacial remains are not widespread in Baltica, but diamictites have been described from the Långmarkberg Formation in the lower thrust sheets of the Caledonide orogen in northern Jämtland and southern Västerbotten, Sweden (Gee & Stephens 2020 and references therein) and from autochthonous cover rocks resting on top of the crystalline basement in Finnmark, northern Norway.

During the Ediacaran, Baltica comprised a geologically stable paleoenvironment with erosion of the crystalline basement and final formation of the subcambrian peneplain (Fig. 1). However, there is also evidence of Ediacaran magmatic activity in central Sweden, at Alnön near Sundsvall, at c. 584 Ma (Meert et al. 2007). The Alnö complex is an alkaline and carbonatite intrusive complex with some ex-

Figure 1. The sub-Cambrian peneplain at Nordkroken, west of Vänersborg, forming the shore of Lake Vänern, with overlying Palaeozoic strata including a Permian dolerite cap at Mt Hunneberg in the background. Photo: Linda Wickström.

plosive volcanic vent material preserved, all related to extensional tectonic activities possibly steered by the tectonic evolution of Pannotia.

References

Evans, D.A., 2021: Pannotia under prosecution. *Geological Society, London, Special Publications 503*, 63−81.

Gee, D. G. & Stephens, M.B., 2020: Lower thrust sheets in the Caledonide orogen, Sweden: Cryogenian–Silurian sedimentary successions and underlying, imbricated, crystalline basement. In: Stephens, M.B. & Bergman Weihed, J. (eds) *Sweden: Lithotectonic Framework, Tectonic Evolution and Mineral Resources.* Geological Society, London, Memoirs 50, 495–515.

Gee, D. G., Klonowska, I., Andréasson, P.-G. & Stephens, M.B., 2020: Middle thrust sheets in the Caledonide orogen, Sweden: the outer margin of Baltica, the continent-ocean transition zone and late Cambrian–Ordovician subduction–accretion. In: Stephens, M.B. & Bergman Weihed, J. (eds) *Sweden: Lithotectonic Framework, Tectonic Evolution and Mineral Resources.* Geological Society, London, Memoirs 50, 517–548.

Kroner, U., Stephan, T., Romer, R.L. & Roscher, M., 2021: Paleozoic plate kinematics during the Pannotia–Pangaea supercontinent cycle. *Geological Society, London, Special Publications 503*, 83–104.

Meert, J.G., Walderhaug, H.J., Torsvik, T.H. & Hendriks, B.W.H., 2007: Age and palaeomagnetic signature of the Alnö carbonatite complex (NE Sweden): Additional controversy for the Neoproterozoic palaeoposition of Baltica. *Precambrian Research 154*, 159–174

Moczydłowska, M., Pease, V., Willman, S., Wickström, L. & Agić, H., 2018: A Tonian age for the Visingsö Group in Sweden constrained by detrital zircon dating and biochronology: implications for evolutionary events. *Geological Magazine 155*, 1175–1189.

Murphy, J. B., Nance, R. D., Cawood, P. A., Collins, W. J., Dan, W., Doucet, L. S., Heron, P.J., Li, Z-X., Mitchell, R., Pisarevsky, S., Quesada, C., Spencer, C.J., Strachan, R.A. & Wu, L., 2021: Pannotia: in defence of its existence and geodynamic significance. *Geological Society, London, Special Publications 503*, 13–39.

Nance, R. D. & Murphy, J. B., 2019: Supercontinents and the case for Pannotia. *Geological Society, London, Special Publications 470*, 65–86.

Vidal, G., 1976: Late Precambrian microfossils from the Visingsö beds in southern Sweden*. Fossils and Strata 9*, 1–57.

Vidal, G., 1982: Den prepalaeozoiska sedimentära berggrunden. In: Wikman, H., Bruun, Å., Dahlman, B. &Vidal, G. (eds) *Beskrivning till berggrundskartan Hjo NO.* Sveriges geologiska undersökning Af *120*, 52–76.

Vidal, G., 1985: Prepalaeozoisk sedimentberggrund. In: Persson, L., Bruun, Å.& Vidal, G. (eds) *Beskrivning till berggrundskartan Hjo SO.* Sveriges geologiska undersökning Af 134, 77–91.

Wickström, L.M. & Stephens, M.B., 2020: Tonian−Cryogenian rifting and Cambrian−Early Devonian platformal to foreland basin development outside the Caledonide orogen. In: Stephens, M.B. & Bergman Weihed, J., (eds) *Sweden: Lithotectonic Framework, Tectonic Evolution and Mineral Resources*, Geological Society, London, Memoirs 50, 451–477.

General Session 2
Geology and society

Session Chairs:
Katarina Persson Nilsson (katarina.nilsson@svemin.se)
Erika Ingvald (erika.ingvald@sgu.se)
Pär Weihed (par.weihed@ltu.se)

Storm surges in the Swedish Holocene geological record – a key to better risk assessments for coastal flooding

Helena Alexanderson[a], Caroline Hallin[b], Lykke Lundgren Sassner[a], Magnus Larson[b], Timothy Ley[b]

[a]Department of Geology, Lund University, Lund, Sweden, e-mail helena.alexanderson@geol.lu.se, lykkesassner@gmail.com; [b]Department of Building and Environmental Technology, Lund University, Lund, Sweden, e-mail caroline.hallin@tvrl.lth.se, magnus.larson@tvrl.lth.se, timoothy.ley@gmail.com

Summary. The risk of coastal flooding is increasing globally, also in Sweden. Knowledge of past events is needed to assess the risks and to determine which countermeasures should be taken. By investigating coastal sediments and landforms the storm surge record (frequency, extent) can be extended back in time, but so far there are very few such studies in Sweden. We present a review of geological methods that can be used in combination with hydrodynamical modelling and extreme-value analysis to improve predictability of extreme floods, a map with potential study sites and exemplify with a case study.

Rising sea levels and increased population density in coastal areas lead to an increased risk of flooding, and flood risk assessment, risk reduction measures, and risk awareness are crucial for a sustainable societal development and safety in coastal areas. The post-glacial land uplift has kept coastal flood risk in Sweden relatively low, but accelerating sea-level rise increases flood risk in southern Sweden already today. Furthermore, a study on historical storm events by Fredriksson et al. (2017) showed that the probability of flooding is higher than expected, because conventional frequency analysis underestimates low-probability events.

Here we present the results of a multidisciplinary review and synthesis of how historical documentation and geological deposits can be used to extend data series, how flood risk is affected by climate variability and climate change, and how hydrodynamical modelling and statistical methods can be used to improve predictability of extreme floods (Hallin et al. in press/2022).

Estimation of probabilities of extreme events is a key factor in risk analysis and design of coastal protection but analysis of extreme sea-water levels is typically based on relatively short time series in comparison with the required frequency of the events to be analysed. To improve predictability of extreme water levels and their duration in combination with waves, data from longer time periods are needed and the geological record could provide this.

Coastal sediments and landforms constitute geological archives that may record storm events over several thousand years. Geomorphological mapping, geophysical methods and sedimentological investigations combined with macro- and micropalaeontological and geochemical analyses can be used to identify and map the extent of storm deposits. These can then be used to estimate runup elevations, water levels, and storm impact. Geological dating methods such as radiocarbon or luminescence dating, or, for young events, also lead and cesium dating, are required to provide an age for the event.

The choice of methods must be adapted to the conditions and settings of individual areas and no general recommendation for Swedish coasts can be given. For example, on the Swedish west coast, with highly saline sea water, methods based on the identification of microfossils that live in saltwater but during storm floods have been washed onshore (i.e. into freshwater environments) can be useful. Along the coast of the Baltic Sea this can be more difficult since the salinity difference, and thus the difference in microfauna, is smaller. Instead, it may be more beneficial to use sedimentological or geochemical proxies, such as mapping sandy washover deposits in coastal wetlands.

So far, very few geo-focussed studies of coastal flooding in Sweden have been published and there are even fewer studies of their traces in the geological record (Hallin et al. in press/2022). This is in contrast to neighbouring countries such as Denmark and Poland where several studies have been carried out (e.g. Clemmensen et al. 2014; Moskalewicz et al. 2020). There is thus much that can be done and large potential to retrieve more information about past storm surges from the Swedish geological record.

In a pilot study, a number of areas and sites that potentially could contain records of past storm surges have been identified in western and southern Sweden, based on a combination of risk factors for storm surges and geological aspects of sediment accumulation and preservation (Lundgren Sassner 2021). One of these sites, outside Trelleborg, was investigated and a probable storm surge in the 1950s was identified (Lundgren Sassner 2021).

The reconstructions based on the geological data can be used in hydrodynamical modelling and in extreme-value analysis. There is no international standard that recommends specific analytical methods for extreme-value analysis, and the role of historical and geological observations in such analyses varies between countries. International and interdisciplinary collaboration between statisticians and oceanographers has potential to advance this field of research and reduce the uncertainty of the analyses. Here, hydrodynamical modelling plays a key role, partly through the possibilities to produce large volumes of synthetic data that make statistical analyses more robust, but also by examining the boundary conditions of oceanographic systems and assess the feasibility of results from statistical analysis.

References

Clemmensen, L. B., Bendixen, M., Hede, M. U., Kroon, A., Nielsen, L. & Murray, A. S. 2014: Morphological records of storm floods exemplified by the impact of the 1872 Baltic storm on a sandy spit system in south-eastern Denmark. *Earth Surface Processes and Landforms 39*, 499-508.

Fredriksson, C., Feldmann Eellend, B., Larson, M. & Martinez, G. 2017: The role of historical storm events in risk analysis - A study of the coastal flood events in 1872 and 1904 along the south and east coast of Scania, Sweden. *VATTEN – J. Water Manag. Res. 73*, 93-108.

Hallin, C., Alexanderson, H., Larson, M. & Ley, T. in press/2022: Stormfloder – en kunskapsöversikt av metoder för att identifiera och kvantifiera extrema havsvattenstånd. *LUNDQUA Report.* Department of Geology, Lund University, Lund.

Lundgren Sassner, L. 2021: *A method for evaluating and mapping terrestrial deposition and preservation potential for storm surge traces. Remote mapping of the coast of Scania, Blekinge and Halland, in southern Sweden, with a field study at Dalköpinge Ängar, Trelleborg*. Lund University, MSc thesis. 53 pp. http://lup.lub.lu.se/student-papers/record/9052188.

Moskalewicz, D., Szczuciński, W., Mroczek, P. & Vaikutienė, G. 2020: Sedimentary record of historical extreme storm surges on the Gulf of Gdańsk coast, Baltic Sea. *Marine Geology 420*, 106084.

Society stalls without bedrock mapping

Jenny Andersson[a,b], Karin Högdahl[a], Lena Lundqvist[b], Emma Rehnström[c], Kirsten Holme[d]

[a]Department of Earth Sciences, University of Uppsala, Uppsala, Sweden, jenny.andersson@geo.uu.se; karin.hogdahl@geo.uu.se, [b]Geological Survey of Sweden, Uppsala/Göteborg, Sweden, jenny.andersson@sgu.se, lena.lundqvist@sgu.se, [c]Skanska Sverige AB, Malmö, Sweden, emma.rehnstrom@skanska.se, Holme Geoconsulting, Lund Sweden, kirsten.e.holme@gmail.com.

Summary. Long-term systematic basic mapping of the Swedish bedrock is today virtually non-existing. The result is outdated or too generalized bedrock information in many parts of the country. In several densely populated and construction intensive areas the lack of up-to-date bedrock map information have resulted in protracted permit processes, severe delays and even termination of construction projects. Insufficient bedrock map information is also at risk to aggravate future developments of subsurface projects, for example, facilities for extraction and storage of energy.

Background

Mineral exploration has long been a major focus in bedrock geology and an obvious reason why bedrock mapping is important for the society. The societal need for bedrock mapping and bedrock information has, however, a much wider scope. Bedrock maps and information retrieved in conjunction with the mapping provide critical information for assessment of the quantity and quality of ground water reserves, the geological premises for construction and building of houses, infrastructure, and subsurface facilities, such as tunnels, nuclear waste repositories and carbon capture storage, and facilities for extraction and storage of thermal energy. It is also used in the fields of environmental geochemistry, archaeology, forensics, historical industrial development, and forestry. All these applications depend on a long-term build-up of knowledge that can only be achieved by continuous mapping of the bedrock in close interplay with development of analytical techniques, changing societal demands, and research. Long-term and systematic basic mapping of the Swedish bedrock is, however, today virtually non-existing. This development is at serious risk to halt a sustainable societal development and have negative effects on economic growth and technical development, as well as on the climate and the environment. The problem is illustrated by two cases: one topical example from the urban areas of Mälardalen where lack of modern bedrock information result in slowdown of development and high costs for building and construction projects, and one general example concerning the success of future investments in affordable and clean energy.

Example 1: Geogenic contamination of surface and groundwater related to production of crushed rock aggregates

Parts of the Swedish bedrock include low grade mineralizations that contribute to elevated background levels of sulphur (S), arsenic (As), and heavy metals (e.g. Pb, Ni, Cd, Cu, Zn). These are poorly investigated, probably due to their insignificant economic value and that they are difficult to detect in the field. Low-grade mineralizations, however, in places cause contamination of surface and groundwater, and problems for aggregate production and handling of construction and tunnelling waste. The bedrock in the northern Mälardalen contain elevated levels of As, illustrated by high-As in the groundwater (e.g. Thunholm et al. 2009). The construction intensive areas at around the Arlanda airport are especially problematic as quarry aggregates and construction and tunnelling waste occur with As content exceeding several 100 ppm (e.g. Länsstyrelsen Stockholm, 2019). High-As in the bedrock has led to costly delay of construction and remediation actions and is a major challenge for construction and building activities (e.g. Bidros 2014; Law & Jakobsson 2014). In the southern Mälardalen, problems with acid rock drainage and metal-rich leachate have caused severe problems for construction projects at Södertörn (e.g. Mattsson, 2018). Bedrock mapping in these areas of Mälardalen was mainly carried out in the 1960's and the early 1970's. Therefore, critical up-to-date geological information is largely missing (e.g. trace element geochemistry) and very few, if any (?), geologists are well experienced with basic and systematic mapping of the local bedrock. It will take decades of mapping to build up the requested knowledge, a perspective too far ahead for the present urgent societal needs. While knowledge is lacking on the composition of the bedrock and its ability to produce leachate hazardous to health and the environment, construction projects are facing huge costs for surveying, remediation efforts and delays. The lack of knowledge also prevents effective incorporation of construction and tunnelling waste in a circular economy, resulting in costly dumping of rock masses, increased production of virgin aggregates and increased transports.

Example 2: The subsurface as a future source and storage of energy

Heat in Earth´s interior is a potential source of affordable, clean, and renewable energy, with little demand for land use, unaffected by weather and climate, and without CO_2-emissions. New technology may make it possible to construct geothermal plants also at the depths of several kilometres that are required for large-scale extraction of heat from the Swedish bedrock. Moreover, the subsurface basement may be used for storage of energy. Such projects are high-cost and high-risk investments, and their success critically depends on the ability to predict the structure, composition, hydrology, and seismic behaviour of the deep bedrock. Ongoing deep drilling projects in Sweden, e.g. the scientific drilling Collisional Orogeny Scandinavian Caledonides (COSC) in west central Jämtland, and the EON commercial drilling project for building an Enhanced Geothermal energy System (EGS) facility in Malmö, both show that the physical conditions and structure of the bedrock is different from previously thought (cf. Lorenz et al. 2022; Rosberg & Erlström 2021). Deep drilling is an expensive investment and must be guided by solid knowledge of the bedrock at the surface. Similar to areas in Mälardalen, however, basic mapping of Precambrian crystalline basement units in the Caledonides of west central Jämtland and the horsts in southwestern Skåne is outdated, and with little focus on the subsurface Precambrian basement. This lack of up-to-date bedrock map data delimits interpretation of data from the deep drilling projects.

Concluding remarks

Bedrock mapping is conceptual, it includes not only observations of the mineralogy, geochemistry, fabric, structure, and possible fossil content of rocks, but to a large extent rely on empiric and analytical evidence. The bedrock map itself is a model that result from a combination of measurements and observations in the field, interpolation of data, and conceptual thinking on the build-up of the bedrock. Therefore, it intimately relies on technology and research and must be conducted as a continuous long-term build-up of knowledge, not achieved through short term occasional and intermittent projects.

Bedrock mapping provides information that is critical for a sustainable societal development and has a central role in delivering the United Nations Sustainable Development Goals. We urge decision makers to acknowledge the importance of long-term continuous bedrock mapping to ensure an economical, ecological, and social sustainable societal development of Sweden.

References

Bidros, S., 2014: Påträffande av naturlig arsenik vid produktion och dess hantering: En fallstudie av Trafikplats Rosersberg. Student project 2013:76. *KTH Royal Institute of Technology, Stockholm, 2014*, pp 52.

Mattsson, E., 2018: Increased leaching of metals as a result of foundation work. Degree project in environmental engineering, 30 credits). *KTH Royal Institute of Technology, Stockholm, 2018*, pp 75.

Länsstyrelsen Stockholm, 2019: 551-12826-2019. Yttrande till Nacka tingsrätt, *Mark- och miljödomstolen (M8264-18)*.

Law, H-.K., & Jakobsson, J., 2014: Påträffande av naturlig arsenik vid produktion och dess påverkan: Nybyggnation av trafikplats Rosersberg. Student project 2013:75. *KTH Royal Institute of Technology, Stockholm, 2014*, pp 55.

Lorenz, H., Rosberg, J. E., Juhlin, C., Klonowska, I., Lescoutre, R., et al., 2022: COSC-2–drilling the basal décollement and underlying margin of palaeocontinent Baltica in the Paleozoic Caledonide Orogen of Scandinavia. *Scientific Drilling, 30*, 43-57.

Rosberg, J. E., & Erlström, M., 2021: Evaluation of deep geothermal exploration drillings in the crystalline basement of the Fennoscandian Shield Border Zone in south Sweden. *Geothermal Energy, 9(1),* 1–25.

Thunholm, B., Johansson, O., & Söderholm, H., 2009: Vattenkvalitet i bergborrade brunnar i Sigtuna kommun. *SGU-rapport 2009:9. Uppsala 2009*, 35 sidor.

EPOS Sweden: A national contribution to the European Plate Observing System-European Research Infrastructure Consortium

Santiago Arellano[a], Gerhard Barmen[b], Mikael Calner[b], Savka Dineva[c], Lars Jacobsson[d], Christopher Juhlin[e], Martin Lidberg[f], Henning Lorenz[e], Björn Lund[e], Paola Manzotti[g], Maxime Mouyen[a], Victoria Pease[g], Michael Roth[e], Björn Schouenborg[d], Maxim Yu. Smirnov[c], Holger Steffen[f]

[a]Chalmers University of Technology, santiago.arellano@chalmers.se, maxime.mouyen@chalmers.se; [b]Lund University, gerhard.barmen@tg.lth.se, mikael.calner@geol.lu.se; [c]Luleå Technical University, savka.dineva@ltu.se, maxim.smirnov@ltu.se; [d]RISE Research Institutes of Sweden, lars.jacobsson@ri.se, bjorn.schouenborg@ri.se; [e]Uppsala University, christopher.juhlin@geo.uu.se, henning.lorenz@geo.uu.se, bjorn.lund@geo.uu.se, michael.roth@geo.uu.se; [f]Lantmäteriet, Martin.Lidberg@lm.se, holger.steffen@lm.se; [g]Stockhom University, paola.manzotti@geo.su.se, vicky.pease@geo.su.se

Summary. The pan-European "European Plate Observing System (EPOS)" is focussed on Europe and adjacent regions and includes geophysical monitoring networks, local observations (including permanent in-situ and volcano observatories), topographic/surface dynamics information, surface and subsurface geological information, experimental and laboratory data and functions, and satellite data. In 2021 the Swedish Research Council (VR) approved an application for Sweden to join EPOS-ERIC, formally establishing existing collaborations between EPOS and Swedish research infrastructures.

EPOS-ERIC

EPOS-ERIC is a distributed research infrastructure for data and facilities related to studies of the solid Earth. It is genuinely pan-European, with 25 countries and six partners participating in the previous

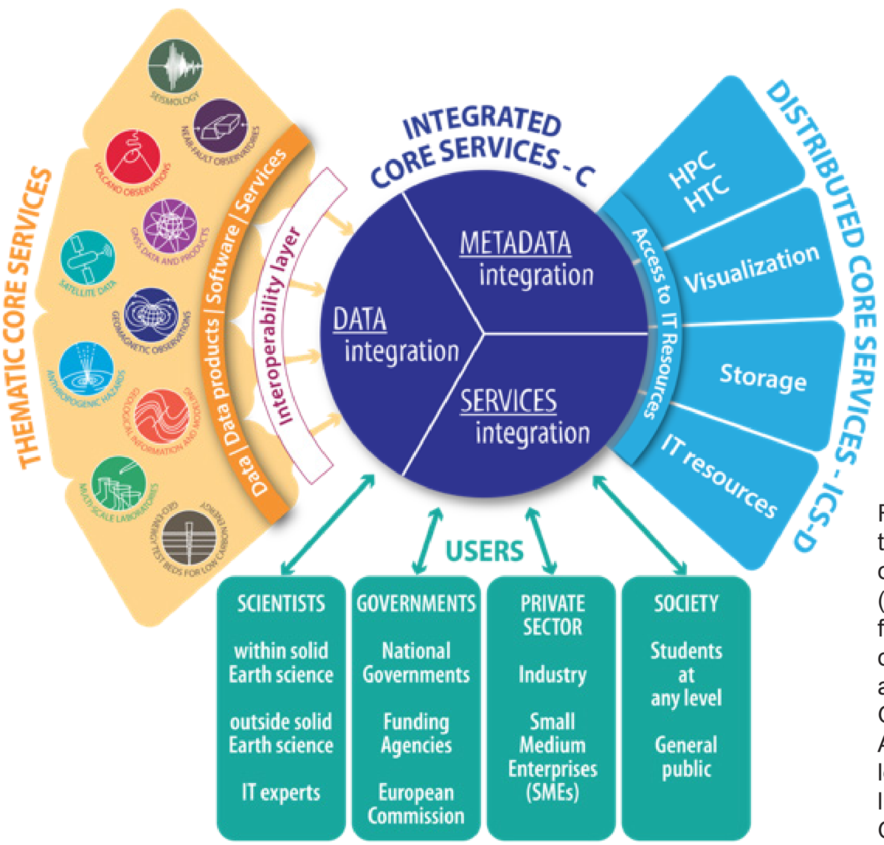

Figure 1. Schematic view of the EPOS design. The names of the Thematic Core Services (left) are; Seismology, Near-fault observatories, Volcano observations, GNSS data and products, Satellite data, Geomagnetic observations, Anthropogenic hazards, Geological information and modelling, Multi-scale laboratories, Geo-Energy test beds.

project phases. The ERIC (European Research Infrastructure Consortium) with its first twelve members was established in November 2018 as the result of two EU projects; "EPOS Preparatory Phase" and "EPOS Implementation Phase". More countries have joined since then and in 2021 the Swedish Research Council (VR) approved an application for Sweden to join the ERIC. Participation comes with commitments, but also with opportunities to cooperate in solid Earth science on an European level that would not be possible otherwise. Currently there are seven research organizations involved in the direct Swedish participation, and the door is open to further cooperation within Sweden.

Swedish contribution

Sweden already delivers services and/or data to the majority of the five Thematic Core Services (TCS) it is involved in (Seismology, GNSS Data and Products, Geoelectromagnetic Observations, Anthropogenic Hazards, and Geological Information and Modelling). Swedish scientists have participated in the EPOS PP (2010-2014) and EPOS IP (2015-2019), and have continued to contribute to the EPOS TCS development also when organisations no longer were an official partner of the EPOS community (EPOS SP, EPOS-ERIC). Sweden will further develop the present commitments to EPOS and find suitable ways of engaging the appropriate communities in additional TCS. The TCS Geoelectromagnetic Observations is at the time of writing coordinated by Sweden (LTU). In the remaining TCS, Sweden participates in the connection to the Integrated Core Services (ICS) via the individual TCS consortia. EPOS Sweden as a consortium will closely follow the development of national priorities and strategies in Earth Sciences and include these in the existing TCS work and new Swedish commitments. The consortium will also relay such information to VR, who will represent Sweden in the EPOS General Assembly. The EPOS Sweden consortium will actively pursue outreach to the Swedish science community and beyond. Once the EPOS portal is public and the Swedish core group is confident in its usage and potential, training will become a part of related university education, of training courses at meetings and of outreach, thus building a user community that can exploit the full opportunities and benefits provided by EPOS. Many Swedish research infrastructures have a strong collaboration with the other Nordic countries, a collaboration which is being stream-lined according to EPOS data sharing strategies, e.g. in the Nordforsk funded Nordic EPOS project, and which may serve as a model for further international collaboration. Swedish research will contribute to or initiate EU projects when opportunities with relevance for EPOS arise.

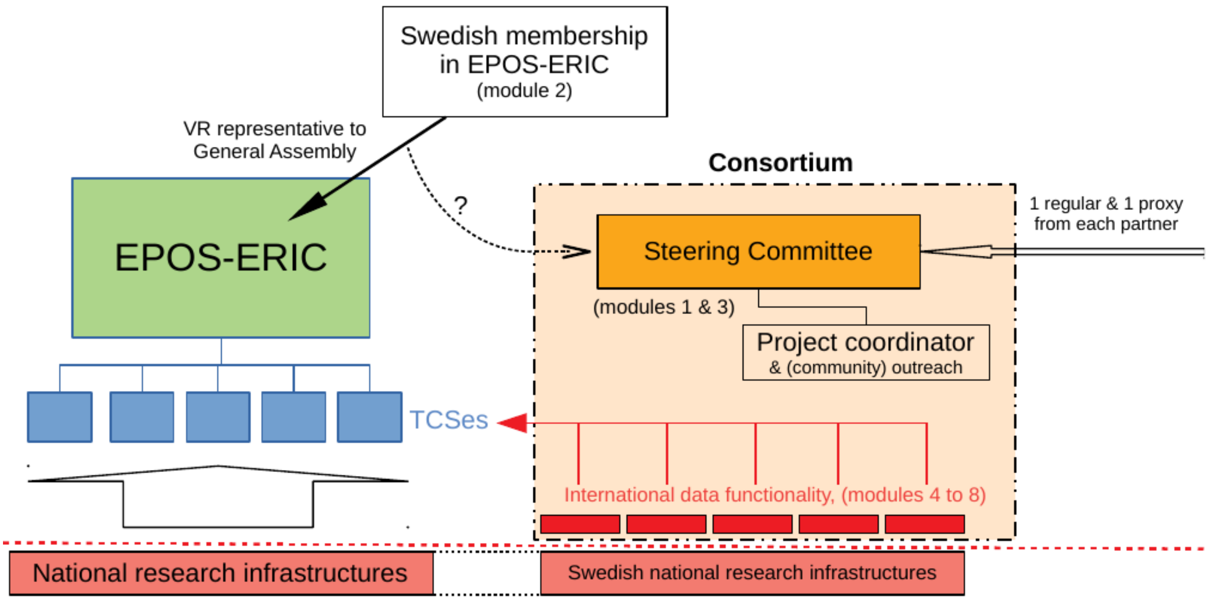

Figure 2. Sketch of the organisation of "Swedish contribution to EPOS-ERIC" in relationship to EPOS and the national research infrastructures.

Postglacial faults, society and mitigation planning

Maria Ask[a], Ilmo Kukkonen[b], Odleiv Olesen[c], Björn Lund[d], Åke Fagereng[e], Jonny Rutqvist[f], Jan-Erik Rosberg[g], Henning Lorenz[h], Bjarne Almqvist[i], Christian Schiffer[j]

[a]Department of Earth Sciences, Uppsala University, Uppsala, Sweden, maria.ask@geo.uu.se; [b]Department of Geosciences and Geography, Helsinki University, Helsinki, Finland, ilmo.kukkonen@helsinki.fi; [c]Geological Survey of Norway, Trondheim, Norway, odleiv.olesen@ngu.no; [d]Department of Earth Sciences, Uppsala University, Uppsala, Sweden, bjorn.lund@geo.uu.se; [e]School of Earth and Environmental Sciences, Cardiff University, Cardiff, UK, fagerenga@cardiff.ac.uk; [f]Earth and Environmental Sciences Area, Lawrence Berkeley National Laboratory, Berkeley, CA, USA, jrutqvist@lbl.gov; [g]Engineering Geology, Lund University, Lund, Sweden, jan-erik.rosberg@tg.lth.se; [h]Department of Earth Sciences, Uppsala University, Uppsala, Sweden, henning.lorenz@geo.uu.se; [i]Department of Earth Sciences, Uppsala University, Uppsala, Sweden, bjarne.almqvist@geo.uu.se; [j]Department of Earth Sciences, Uppsala University, Uppsala, Sweden, christian.schiffer@geo.uu.se.

Summary. Based on recorded earthquakes, Fennoscandia is considered a low-seismicity region. The geological records show that large-great earthquakes were triggered along postglacial fault scarps near the end to just after deglaciation. New results suggests that repeated events have occurred as recent as ~600 years before present day. Geological records are not yet included in probabilistic hazard models. Direct dating of faulting activity and deep investigation of the fault zones with scientific drilling are needed for increased understanding of the phenomena and appropriate mitigation planning.

Postglacial fault scarps and intraplate seismicity

Postglacial fault (PGF) is an all-encompassing designation for the faults and fault scarps of Fennoscandia that also have been referred to as glacially-triggered, glacially-induced, early Holocene, late-glacial or end-glacial faults. These faults represent a particular type of intraplate deformation, with large earthquakes triggered near the end or just after the last deglaciation. Earthquake mechanisms and the nature of faulting along PGFs is poorly understood but may pose high risks to society. A major reason is that intraplate earthquakes occur infrequently and no mitigation planning is in place.

Over a dozen large PGFs have been observed in Sweden, Finland, and Norway. The scarps offset glacial deposits, and have surface offset to scarp length ratio significantly larger for than for contemporary reverse slip earthquakes (e.g. Leonard 2010). In Sweden, north of latitude 66°N, 71% of recorded earthquakes are within 30 km to SE and 10 km to NE of the PGF surface scarps; the focal depths down to ~35 km imply that they are crustal-scale structures (e.g. Lindblom et al. 2015). Four of the Swedish PGFs are located within 30 km from 14 hydropower stations (e.g. Sourva, Vietas, Kvistforsen), and at least 5 mines and tailing dams (e.g. Kirunavaara, Boliden). The Burträsk PGF is located ~35 km from the Rönnskär underground storage of heavy metals, and the Bollnäs PGF lies ~150 km from the planned final repository of high-level radioactive nuclear waste in Forsmark.

Relying on the historical and instrumental earthquake record, Sweden is assessed as a low-seismicity and low-seismic hazard area. The largest earthquake instrumentally observed is the magnitude 5.4 earthquake outside the Koster islands in 1904. The historical record reveals the occurrence of larger earthquakes (e.g. magnitude 5.9 earthquake in Lurøy, Norway in 1819). The geological record in Norway and Finland has documented recurring earthquakes along PGFs, with estimated magnitudes from ~4.9 to 8.0 (e.g. Olesen et al. 2021, Sutinen et al. 2021). These results are game changers, signalling the occurrence of recurring earthquakes from ~11 000 to ~600 years before present. Similar critical data on the timing of large earthquake activity in Sweden is not yet existing.

The DAFNE project: Drilling Active Faults in Northern Europe

The DAFNE project of the Integrated Continental Drilling Program (ICDP) plans to drill the central parts of the postglacial Pärvie fault system (PFS) in Sweden (Ask et al. 2021). The project addresses the gap in knowledge from direct observations and measurements of the fault structures at depth. The central PFS has a complex structure, that must be investigated by multiple boreholes to achieve four-dimensional sampling, testing and long-term monitoring of the fault system. A wide range of fault properties are to be acquired from direct measurements on drill cores, logging and in-situ testing in the borehole, and long-term monitoring (seismicity, fluid properties) within borehole observatories.

The scientific objectives are: (1) Make fundamental in-situ observations of the nature of the fault system, including measurements of fluid pressure, temperature, state of stress, and characterization of fault strength parameters; (2) Measure the accumulation and release of strain along a postglacial intraplate fault zone, including how large intraplate earthquakes are triggered and why seismicity persists for very long time periods in areas of previous large ruptures; (3) Document and understand the thermal and hydrogeological regimes and the deep biosphere within a PGF and the surrounding bedrock, as well as revealing thermal and hydrological consequences of seismic slip and associated stress change; and (4) Use the local data to calibrate and test regional models of glacial isostatic adjustment. There are also objectives of societal relevance: (1) Assess seismic risk for mines, tailing dams and hydropower dams near PGFs; (2) Predict the future behaviour of bedrock, including exposure of more PGFs, during forthcoming glaciations/deglaciations at high latitudes worldwide, in particular for safe disposal of toxic waste in bedrock and stability of tailing dams; and (3) Support the development of enhanced geothermal systems in crystalline basement (by using DAFNE as a test bed).

ICDP has conducted a detailed evaluation with respect to quality of science and societal objectives, qualification of proponents and science team, cost-effectiveness, and the need-to-drill with an appropriate target. ICDP also funds 25% of total costs for establishing the infrastructure. The proponents are now working on attracting co-funding, the strategy is to combine scientific drilling with dating of fault scarps from surface measurements.

Probabilistic seismic hazard analysis

If large earthquakes are triggered on the PGFs, the consequences to society could potentially be severe, and not only in the immediate surroundings. Probabilistic seismic hazard analysis is based on statistical analysis of recorded earthquake catalogues. Hazard models are consulted to perform risk analyses and to define building codes for various infrastructures. Current probabilistic hazard models that encompass Sweden do not include large earthquakes on the PGFs. An underestimation of low-probability, high-magnitude earthquakes, that may not follow existing hazard models could lead to large damage to infrastructure, in particular (a) basic industry for production of raw materials and energy, (b) building and transport infrastructure and (c) spread of pollutants from failure of dams, tailing dams, toxic waste (heavy metals), with potentially major effects on ecosystems, health, forestry and agriculture.

It is essential for a sustainable society and economy to understand these postglacial earthquakes and their recurrence in order to improve hazard and risk analyses for infrastructure, communicate that knowledge to stakeholders (local communities, regional and national government and agencies, mining and energy companies) and to assess updates to building codes, safety norms and regulations. We recommend that the recurrence rate of large earthquakes in Sweden to be assessed by a combination of direct measurements of the timing of earthquakes on the PGFs at the surface and constraining of in-situ conditions at depth through scientific drilling.

References

Ask, M., Kukkonen, I., Olesen, O., et al., 2021: Proposed drilling into postglacial faults: The Pärvie fault system. *In* H. Steffen, et al. (Eds.), *Glacially-Triggered Faulting*, Cambridge university press, 151–174.

Leonard, M., 2010: Earthquake Fault Scaling: Self-Consistent Relating of Rupture Length, Width, Average Displacement, and Moment Release, *Bulletin of the Seismological Society of America 100* (5), 1971–1988.

Lindblom, E., Lund, B., et al., 2015: Microearthquakes illuminate the deep structure of the endglacial Pärvie fault, northern Sweden, *Geophysical Journal International 201*, 1704–1716.

Olesen, O., et al., 2021: Postglacial faulting in Norway: Large magnitude earthquakes of the Late Holocene age. *In* H. Steffen, et al. (Eds.), *Glacially-Triggered Faulting*, Cambridge university press, 198–217.

Sutinen, R., et al., 2021: Glacially induced faults in Finland. *In* H. Steffen, et al. (Eds.), *Glacially-Triggered Faulting*, Cambridge university press, 231–245.

Arctic Sweden's glacial and emerging post-glacial environments: glacial waters, ecosystems and people

Jamie Barnett[a,b], Annika Granebeck[a,c], Martin Jakobsson[a,d], Nina Kirchner[a,b]

[a]Tarfala Research Station (TRS), Stockholm University, Stockholm, Sweden, tarfala@natgeo.su.se; [b]Department of Physical Geography, Stockholm University, Stockhom, Sweden, jamie.barnett@natgeo.su.se, nia.kirchner@natgeo.su.se; [c]Department of Environmental Science and Analytical Chemistry, Stockholm University, Stockholm, Sweden, annika.granebeck@su.se; Department of Geological Sciences, Stockholm University, Stockholm, Sweden, martin.jakobsson@geo.su.se

Summary. Hydrological changes caused by retreating glaciers are a so called Reason For Concern (IPCC, 2022) because they imply changes in downstream hydrology with yet unknown implications for ecosystems, biodiversity, and people. Here, we give examples of how these changes materialize in the wider area around Tarfala Research Station, Arctic Sweden, and how we strive to combine classical academic methods with traditional Sami knowledge to jointly prepare for wise decision-making related to society's adaptation to a warmer world, and to contribute to the fullfillment of SDG 13 and SDG 15.

Tarfala Research Station (TRS) – a time-machine like natural laboratory in the Kebnekaise Mountains

TRS is not only surrounded by Sweden's highest mountains and several glaciers, including Storglaciären – the glacier with the World's longest mass balance record – but also by the grazing areas of the reindeer of the Laevas Sami Village. This makes TRS a unique location to combine classical glaciological mass balance measurements with novel approaches such as 3D numerical modelling of glacier dynamics including glacial meltwater runoff, along side traditional Sami knowledge and observations how changing climatic conditions affect traditional livelihoods, by e.g. threatening the foundations of the Sami people's reindeer herding.

TRS is also located in a time-machine like natural laboratory because climate warming is more pronounced in the Arctic than at lower latitudes and higher than the global average ("Arctic Amplification", Previdi et al., 2021). This renders the 260 Swedish glaciers, all of which are relatively small and vulnerable, an expected short lifespan (Hock et al., 2019). Shrinking glaciers and emerging postglacial environments and the associated changes to hydrological regimes and ecosystems, can therefore be studied at and around TRS before they occur at places not yet exposed to pronounced climate warming.

Determining future glacial meltwater runoff, including both intensity and timing, provides the foundation for studying the impacts of these changes on ecosystems and biodiversity, and contributes to take urgent action to combat climate change and its impacts, and the loss of biodiversity (UN Sustainable Development Goals 13 and 15). Numerical modeling of glacier dynamics and mass loss, translating into glacial meltwater runoff, has therefore been initiated at Storglaciäern, using the open source code Elmer/Ice (Gagliardini et al., 2013). The timing of melt emerges as a new challenge for the modeling because traditional seasonality can be interrupted by extreme meteorological events including shifts between opposing weather conditions such as melt and freeze, with risk for misalignment with other natural systems (Casson et al., 2019). We present first results from the numerical modeling, and related them to the challenges described above and other ongoing work at TRS.

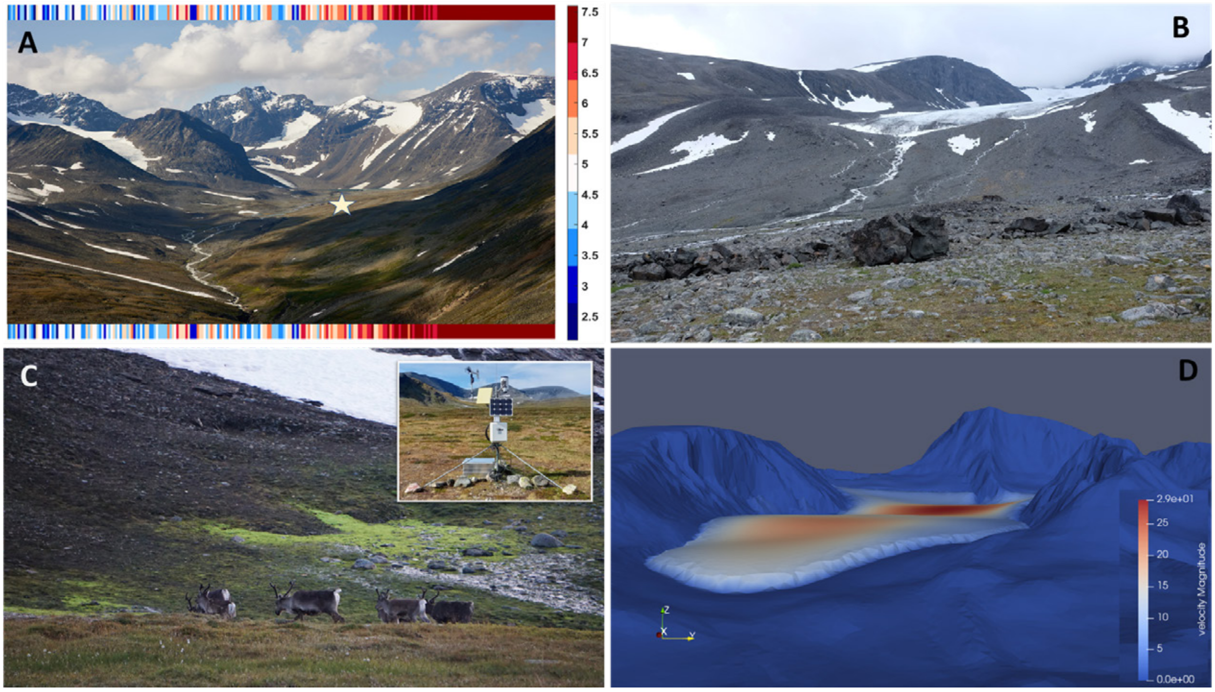

Figure:A. Tarfala valley (Darfálvággi) with Tarfala Research Station (pale yellow star), c. 60 km west of Kiruna/ northern Sweden. The valley is dominated by glaciers, glacial meltwater streams and lakes, permanently frozen soil, and sparse vegetation. Picture-framing: Warming Stripes, displaying color-coded annual air temperature for Sweden 1860–2100 (measurements since 1860, colorscale in degrees Celsius to the right). Temperatures for 2022–2100 are obtained from computer simulations assuming that emissions of greenhouses gases to the atmosphere continue according to a ”Business as Usual” scenario (the RCP8.5 scenario in the IPCC terminology). Photo: J. Strömberg, 2021. Warming Stripes: N. Kirchner. B. Storglaciären, with main glacial meltwater stream. Photo: N. Kirchner. c. Summer-grazing reindeer, northern Sweden, and Automated Weather Station in Laevasvággi, neighboring Tarfala valley. D. Storglaciären, 3D numerical reconstruction in Elmer/Ice. Modelling: Jamie Barnett.

References

Casson, A. et al. 2019. Winter Weather Whiplash: Impacts of Meteorological Events Misaligned With Natural and Human Systems in Seasonally Snow-Covered Regions. Earth's Future. doi.org/10.1029/2019EF001224

Gagliardini O. et al. 2013. Capabilities and performance of Elmer/Ice, a new-generation ice sheet model. Geoscientific Model Development, doi.org/10.5194/gmd-6-1299-2013

Hock, R. et al. 2019. SROCC, IPCC Speccial Report on the Ocean and Cryosphere in a Changing Climate, Cahpter 2: High Mountain Areas. *Cambridge University Press*, www.ipcc.ch/srocc/chapter/chapter-2/

IPCC, Eds. H.-O. Pörtner et al. 2022.Climate Change 2022: Impacts, Adaptation and Vulnerability**.** *Cambridge University Press*, ipcc.ch/report/ar6/wg2/

Previdi, M. et al. 2021 Arctic amplification of climate change: a review of underlying mechanisms. *Environ. Res. Lett*. 16 093003, doi.org/10.1088/1748-9326/ac1c29

Is the Swedish onshore bedrock suitable for carbon dioxide sequestration?

Emelie Crafoord, Glenn Bark, Christina Wanhainen

Department of Civil, Environmental and Natural Resources Engineering, Luleå University of Technology, Luleå, Sweden, emelie.crafoord@ltu.se

In 2020, the paper and pulp industry in Sweden contributed 6% of the total industrial CO_2 emissions (Naturvårdsverket 2022). Given Sweden's climate targets of achieving net-zero emissions until 2045, implementation of Carbon Dioxide Removal (CDR) technologies is needed (IPCC 2022). According to a governmental investigation made in 2020, the CDR technology Bioenergy with Carbon Capture and Storage (BECCS) is mentioned as one of the 'complementary measures' needed to reduce the remaining 15% that will be required beyond national emission reductions until 2045 (SOU 2020). The paper and pulp industry, as well as other CO_2 emitting process and base industries, are now looking for ways to include BECCS in their strategies to limit their emissions.

In an interdisciplinary scientific BECCS project (INSURANCE - Utilization of industrial residues for an efficient geological BECCS), the two research groups biochemical process engineering and ore geology have joined forces together with the packaging company BillerudKorsnäs to cover the entire value chain of BECCS, from capture to storage. The project has two main parts 1) to advance the CO_2 capturing technique using a more environmentally friendly CO_2 capturing agent (enzymes) together with the industry's own waste streams and 2) to investigate the potential for onshore geological storage of CO_2 in the Swedish bedrock. In this contribution, the geological storage potential is in focus.

Onshore geological storage through mineral carbonation

Sites considered 'optimal' for CO_2 storage through mineral carbonation typically include relatively young, porous and unaltered basaltic rocks (McGrail et al. 2017, Oelkers et al. 2008) However, to discover the full potential for mineral carbonation as well as its limitations, there is a need of investigating a broader range of mafic and ultramafic rocks of different ages (Snæbjörnsdóttir et al. 2020, Marieni & Oelkers 2018). Requirements for mineral sequestration to be successful includes suitable mineralogical and chemical conditions, provision of adequate reactive surfaces in terms of porosity and permeability, and the right reservoir pressure and temperature conditions. How reactive the reservoir rock will be, and thereby the suitability for CO_2 sequestration, is an interplay between all these parameters (Oelkers et al. 2008, Snæbjörnsdóttir et al. 2020).

In this early phase of the project, we are investigating favorable sites with regards to minerology, mineral chemistry, textures, primary and secondary porosity. Age, areal extent, and coverage of a varied range of the rock types have also been taken under consideration. The Karlsborg paper and pulp plant in Kalix in northern Sweden, is the project's main target area, but lithologies around six other paper and pulp plants throughout Sweden will also be investigated for potential implementation of BECCS. Sampling and mapping of mafic rock types around the Kalix area took place during August and September 2021. The targeted rock units include two intrusive formations, northeast and northwest of Karlsborg, and the supracrustal volcanoclastic bedrock underneath the Karlsborg plant. The two intrusions are of Svecokarelian age and are dated at c. 1.88 Ga (Bergman et al. 2015). They derive from the Haparanda suite of intrusive rocks (Elming 1985, Bergman et al. 2014). The two rock units studied, have an intermediate to mafic composition between diorite and gabbro. Petrographic analysis shows anorthite, biotite, muscovite, hornblende, augite and accessory apatite and zircon. Opaque minerals consist of ilmenite and magnetite. The metamorphosed supracrustal rocks underneath the Karlsborg plant extending southwest towards Storön and the Baltic archipelago belongs to the Karlsborg formation and is the lowermost formation of the Kalix Group (Åhman et al. 1990). Rocks from the Karlsborg formation consists mainly of banded metabasaltic tuff with locally associated lava flows of similar basic composition, appearing, usually, only a couple of meters thick. Preliminary results from the petrographic studies from the samples from the metabasaltic tuff show lath-shaped hornblende crystals altering with silicate phases of plagioclase and quartz in preferred orientation (Fig. 1). Sericite-altered plagioclase is common.

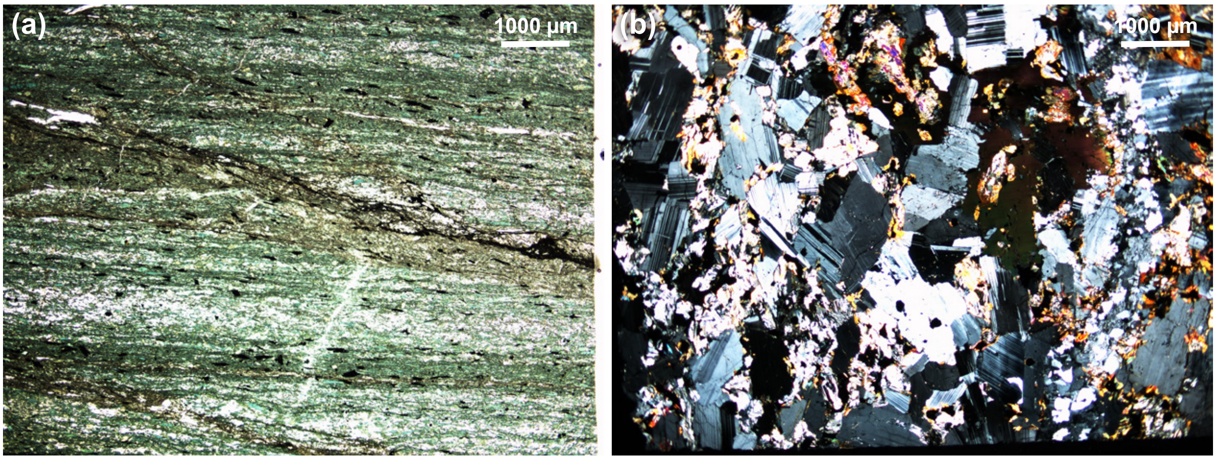

Fig. 1 a) Microphotograph of sample KB2101 (Karlsborg formation) under plain polarized light showing common features of the metabasaltic tuff, with banded layers of (darker green) needle-shaped hornblende crystals alternating with (lighter) layers of microcrystalline quartz and plagioclase. Opaque phases consist primarily of pyrite. b) Microphotograph of sample BG2104 under crossed polarized light from a mafic intrusion northeast of Karlsborg (Haparanda suite) showing the gabbro-diorite with larger grains of primarily anorthite and micas. Surrounding the larger grains amphibole occurs (primarily hornblende) and the lighter grains are sericite alteration.

Further investigations of these intrusions are currently being undertaken, and the second mapping and sampling season will include six additional sites throughout Sweden. Results from this project will enable an evaluation of the CO_2 sequestration potential in the different sampled rock units during aqueous carbonation experiments that later will be carried out in the project. During these experiments, where the capturing and storage sub-projects meet, samples will be tested in a CO_2 buffered solution in a reactor with geologically realistic pressure/temperature conditions. The experiments are conducted to quantify the release rates of divalent metal cations in silicates for different altered and metamorphosed rock types.

References

Bergman, S., Bergström, U., Bastani, M., Jönberger, J., Juhojuntti, N., & Johansson, P. 2014: Regionalkartering i kartområdet 25N Haparanda, tidigare arbeten och resultat från fältarbetet 2013. Sveriges geologiska undersökning rapport, 7.

Bergman, S., Hellström, F., & Bergström, U. 2015: U-Pb zircon age of a metaquartz monzonite in the type area of the Haparanda suite. Sveriges geologiska undersökning SGU-rapport 2015.

Elming, S. Å. 1985: A palaeomagnetic study of Svecokarelian basic rocks from northern Sweden. Geologiska Föreningen i Stockholm Förhandlingar, 107(1), 17–35.

IPCC. 2022: *Climate Change 2022: Mitigation of Climate Change; Working Group III contribution to the Sixth Assessment Report of the Intergovernmental Panel on Climate Change*. Cambridge University Press. Cambridge, New York. https://report.ipcc.ch/ar6wg3/pdf/IPCC_AR6_WGIII_FinalDraft_FullReport.pdf.

Marieni, C., & Oelkers, E. 2018: Carbon sequestration potential of altered mafic reservoirs. Energy Procedia, 146, 68–73.

McGrail, B. P., Schaef, H. T., Spane, F. A., Horner, J. A., Owen, A. T., Cliff, J. B., ... & Sullivan, E. C. 2017: Wallula basalt pilot demonstration project: post-injection results and conclusions. Energy Procedia, 114, 5783–5790.

Naturvårdsverket. 2022: *Naturvårdsverkets underlag till klimatredovisning enligt klimatlagen*. Case number: NV-08742-21

Oelkers, E. H., Gislason, S. R., & Matter, J. 2008: Mineral carbonation of CO2. Elements, 4(5), 333-337.

Snæbjörnsdóttir, S. Ó., Sigfússon, B., Marieni, C., Goldberg, D., Gislason, S. R., & Oelkers, E. H. 2020: Carbon dioxide storage through mineral carbonation. Nature Reviews Earth & Environment, 1(2), 90-102.

SOU. 2020: *Vägen till en klimatpositiv framtid* SOU 2020:4.

Åhman, E., Wikström, A., & Henkel, H. 1990: Berggrundskartan 25M Kalix SO. Sveriges geologiska undersökning Ai 45.

Coastal erosion in Skåne: present and future threats

Bradley W. Goodfellow[a], Magnus Larson[b], Sebastian Bokhari-Irminger[c], Johan Nyberg[d], Jonas Ising[e], Lisa Van Well[f], Björn Almström[g], Per Danielsen[h], Anna Adell[i], Caroline Hallin[j]

[a]Geological Survey of Sweden, Lund, Sweden, bradley.goodfellow@sgu.se; [b]Division of Water Resources Engineering, Lund University, Lund, Sweden, magnus.larson@tvrl.lth.se; [c]Swedish Geotechnical Institute, Malmö, Sweden, sebastian.bokhari-irminger@sgi.se; [d]Geological Survey of Sweden, Uppsala, Sweden, johan.nyberg@sgu.se; [e]Geological Survey of Sweden, Lund, Sweden, jonas.ising@sgu.se; [f]Swedish Geotechnical Institute, Gothenburg, Sweden, lisa.vanwell@sgi.se; [g]Division of Water Resources Engineering, Lund University, Lund, Sweden, bjorn.almstrom@tvrl.lth.se; [h]Swedish Geotechnical Institute, Gothenburg, Sweden, per.danielson@sgi.se; [i]Division of Water Resources Engineering, Lund University, Lund, Sweden; anna.adell@tvrl.lth.se; [j]Division of Water Resources Engineering, Lund University, Lund, Sweden caroline.hallin@tvrl.lth.se

Summary. Erosion is a problem along parts of the Skåne coastline and is expected to worsen through sea level rise (SLR). The Skåne coastline is uniquely sensitive in Sweden to SLR-driven erosion because of topographic, geologic, and social characteristics. Although there is considerable background information (historical erosion, wave fields, geology), we lack measurements of processes and applicable theoretical models to make predictions of future SLR-driven erosion. This information is essential to calculate future erosion risks and developing mitigation strategies. Ongoing research is addressing these knowledge gaps through data analysis, predictive modeling, and co-creation processes involving stakeholders.

The problem of coastal erosion and research aims

Erosion has been a problem over recent decades along several segments of the Skåne coastline and is expected to increase in magnitude and become more widespread because of sea level rise (SLR). The Skåne coastline is uniquely sensitive in Sweden to SLR-driven erosion because it is mostly formed of sediments. SLR now outpaces glacial isostatic rebound, and low-lying topography is overprinted by extensive urban and infrastructure development. Although there is considerable information on historical wave fields and erosion, coastal topography, nearshore bathymetry, and seabed substrates, we lack measurements of processes that drive coastal erosion and, critically, lack quantitative models to predict future SLR-driven erosion. This information is essential both to calculate future erosion risks to society and to develop appropriate adaptation and mitigation strategies. There has been an increasing focus on coastal erosion in Sweden over recent years and research is now under way to address knowledge gaps in coastal erosion processes and to provide predictions of future SLR-driven erosion.

Recent knowledge development and public resources

Knowledge of the Skåne coastline has expanded over recents years and includes academic literature, reports and databases provided by government agencies, and site-specific consultancy reports. Maps of areas inundated under varying future sea level scenarios (but without considering the effects of erosion), a wave model, bathymetry, sediment distributions both on land and on the sea floor, a database of existing coastal structures, historical patterns of erosion and accumulation, and modelling of longshore sediment transport from historical weather records are publically available. These data can be accessed through SGIs mapviewer "SMHI medvattenstand" at https://gis.swedgeo.se/smhi_havsniva/# and SGUs mapviewer "Stranderosion och geologi, kust" at https://apps.sgu.se/kartvisare/kartvisare-skanestrand.html and SGIs mapviewer "Vågmodell" at https://gis.swedgeo.se/vagmodell/#.

Regional Kustsamverkan Skåne/Halland (RKS)

RKS (Regional Kustsamverkan Skåne / Halland; swedgeo.se) is a collaboration between the Swedish Geotechnical Institute (SGI), the County Administrative Boards in Skåne and Halland, the Swedish

Geological Survey (SGU), coastal municipalities, and other authorities, higher education institutions, and stakeholders interested in coastal issues affecting Skåne and Halland.

RKS was established to deal with challenges posed by coastal flooding and erosion, particularly in relation to SLR. These challenges are both scientific and societal, and adressing them requires coordination between the various involved state and private actors, an appropriate legal framework, and suitable levels of funding. RKS is actively working to create sustainable adaptation and mitigation measures to deal with SLR-driven erosion and flooding. This is being done, for example, through research and through engaging national decision-makers in providing the required organisational, legal, and funding conditions.

Why research is needed and what is being done

Through RKS, it has become clear that the scientific basis for coastal adaptation to SLR presently provides an inadequate guide by which to develop policies for planning the built environment, which characterises much of the Skåne coastline. A key issue is that there is currently little research describing the effects of SLR on erosion along Swedish coasts. It is therefore difficult for coastal municipalities to fully comply with their legal requirements to include climate- and erosion-related risks in their spatial planning and it is difficult for the County Administation Board to evaluate whether SLR-induced erosion has been sufficiently considered in municipal spatial planning. New research is motivated by this feedback and is designed to inform adaptation of the built environment of Skåne to SLR, through co-creation of understanding and needs assessments with projected end-users.

Examples of current research include projects funded by Trafikverket and Formas hosted at Lund University. Key goals include developing methods to predict SLR-driven erosion that are applicable to the Skåne coastline, which displays variations in key hydrodynamic, sediment, and geologic conditions. For example, much of the Skåne coastline is hosted on glacial tills, which are characterized by mixed grain-sizes, rather than just sand, and therefore pose a challenge to predict SLR-driven erosion. Modelling of SLR-driven erosion along the Skåne coastline also includes exploring the sensitivity of the model and resulting erosion predictions to future regional climate scenarios, including storminess. Knowledge co-creation with projected end users, through combining the erosion predictions developed for each coastal compartment with existing inundation mapping to show positions of the coastline under different predicted future sea levels is a crucial on-going step in the research. Predictions should be presented in such a way that they they are understood by end users and can be applied to planning decisions. It is anticipated that future coastline predictions are illustrated probabalistically to account for scientific uncertainties.

Need of increased geochemical knowledge on sulphide bearing rock in civil engineering

Cajsa J. Hägglund

Department of civil, environmental and natural resourses engineering, University of Luleå university of technology, Luleå, Sweden, cajsa.hagglund@ltu.se

Within the field of civil engineering, some projects require large amounts of rock to be excavated, crushed and reused as aggregates in e.g. concrete or as unconsolidated materials in e.g. road beds. Bedrock excavated during e.g. tunnel construction sometimes contain higher amounts of sulphides that, when exposed to atmospheric conditions, produce acidity and/or discharge metals in elevated concentrations into surrounding water pathways. Such drainage is often called acid rock drainage (ARD) or neutral metalliferous drainage (NMD) and is generated through oxidation of sulphide minerals exposed to oxygen and water (e.g. Nordstrom 2009, Heikkinen et al. 2009). Depending on which sulphide is weathered and if the rock contain sufficient amounts of buffering minerals, e.g. carbonates, the drainage may be acidic, in addition to increased metal concentrations if compared to background concentrations.

Placement of e.g. highways is governed by many factors, originating in fields varying from biology and geotechnology to archeology and medicine (Trafikverket, 2020). Thus it is rarely possible to adjust the placement of a new e.g. highway tunnel due to elevated sulphide concentrations within the bedrock. Subgoals 9.4 and 12.2 within the 9th and 12th goals of the UN Sustainable Development Goals (SDG) both address the need for increased efficiency regarding the usage of natural resources (UN, 2015). Rock material is a non-renewable natural resource and to reach a circular economy with sustainable management of non-renewable resources, it is necessary to ensure reusage of as much as possible of rock raw materials generated as biproducts through excavation during construction projects (SGU, 2015). Quarrying new rock materials requires usage of previously undeveloped land areas and thus works against the fulfillment of the 15th UN SDG, particularly subgoal 15.5.

Awareness of the risk of formation of ARD in infrastructure construction projects has risen in Sweden in recent years, especially in areas where ballast resources and spaces for temporary rock storage are limited. There is an increased demand on knowledge of rock characteristics and its potential environmental impact before excavation, storage or reuse may be allowed by local authorities. This knowledge is today sought mainly through static or kinetic prediction tests for potential acid generation, e.g. acid base accounting (ABA) or humidity cell tests (HCT), developed within the mining industry. Even as most prediction tests are well-established in the mining industry, they have inherent limitations (Karlsson 2022, Parbhakar-Fox & Lottermoser 2015) and can not take all parameters affecting the potential of negative environmental impact from excavation of sulphide bearing rock into consideration. For one, the risk of NMD is not evaluated through the common prediction tests for potential acid generation. Additionally, the conditions of management of excavated rock and environmental monitoring around the materials' final placement vary greatly between the infrastructure construction and mining industries. Rock material produced through excavations in e.g. highway tunnel constructions can be reused at several different sites, either within the same project or sold to other projects in need of suitable ballast, with mostly geotechnical needs governing how and where the material is placed. Comparatively, waste rock from mining is typically stored in piles engineered to minimize ARD or NRD production and the leachate quality is monitored.

The proportion of reused ballast generated as a secondary product in construction projects is decreasing due to the risk of ARD formation often feared as too large, partly due to insufficient understanding of how to efficiently study the material and interpret test results from case to case. In order to increase the reusage proportion, it is necessary to clarify which geochemical parameters are most influential on if an excavated sulphide bearing rock material may have negative environmental impact. It is important to build this clarification on knowledge and experience from previous scientific findings on mine waste rock, its management and other related geoscientific fields.

To reach a circular economy it is vital to reuse as much rock material as possible without risking negative impact on the local environment. There is a need to better understand which parameters mainly influence if usage of sulphide bearing rock materials produced during construction-related excavations risks negatively impact its surroundings. An increased understanding of the environmental geochemistry of sulphide bearing rock produced outside mining facilities can aid in raising the proportion of reusage of such secondarily produced geomaterials.

References

Heikkinen, P., Räisänen, M., Johnson, R., 2009: Geochemical characterisation of seepage and drainage water quality from two sulphide mine tailings impoundments: Acid mine drainage versus neutral mine drainage. *Mine Water and the Environment 28(1),* 30-49.

Karlsson, T., 2022: Geochemical and Mineralogical Characterization of Waste Rocks for Preliminary Mine Drainage Quality Prediction. *PhD dissertation, Luleå University of Technology.*

Nordstrom, D., 2009: Acid rock drainage and climate change. *Journal of Geochemical Exploration 100 (2-3),* 97-104.

Parbhakar-Fox, A. & Lottermoser, B., 2015: A critical review of acid rock drainage prediction methods and practices. *Minerals engineering 82*, 107-124.

Sveriges Geologiska Undersökning, 2015: Resurseffektivisering och minskade transporter – Förslag till hur insamling av produktionsuppgifter från entreprenadberg kan utformas. *SGU-rapport 2015: 39*.

Trafikverket, 2020: Transportsystemet i samhällsplaneringen – Trafikverkets underlag för tillämpning av 3-5 kap. miljöbalken och av plan- och bygglagen. *Rapport 2020:078*.

United Nations, 2015: Transforming our world – the 2030 agenda for sustainable development. *A/RES/70/1*.

The crucial role of groundwater for Swedish watersupply

Björn Holgersson

Geological Survey of Sweden, Uppsala, Sweden, bjorn.holgersson@sgu.se

Summary. This session focuses on groundwater, playing an important role for our water supply system. Sweden was early in developing groundwater resources for municipal water supply. Taking off from this legacy, a brief explanation of hydrogeological conditions and is given and how this controls and supports the use of groundwater. Swedish groundwater resources management is explained and how the water framework directive has been implemented. Examples on current environmental issues will be given. Emerging drought conditions and water shortages are taking place in parts of Sweden. In spite of this, groundwater will continue to be an important resource also in the future.

Historical background

During the last century groundwater resources were exploited in many areas in Sweden – forming an essential part of municipal water supply. Many, both larger and smaller communities, expanded their water supply systems, introducing municipal groundwater plants for extraction, treatment, and distribution.

In the later decades of the last century enhanced groundwater recharge was implemented through artificial infiltration of surface water into groundwater ponds. Another common solution has been to place the well close to a surface water body so that the groundwater extraction would be enhanced by induced infiltration.

Administrative framework – the EU Water Framework Directive

The Water Framework Directive was decided on October year 2000. The Directive has been implemented into Swedish legislation. Sweden has divided its waters into 5 administrative bodies, headed by one representative county administrative board in each district. These offices have been appointed by the government to act as water district authorities.

In article 7 of the directive a lower limit is assigned, stating that if more than 10 m^3 groundwater per day is extracted, or if groundwater is distributed to more than 50 persons, than the groundwater in that aquifer is to be treated as a groundwater body for drinking water. Water administration calls for monitoring, classification, setting of environmental standards and action plans to identify problems and implement measures for restoration.

Hydrogeological setting in Sweden

The groundwater resources in Sweden are to a large extent dominated by quaternary deposits, often noticed in the landscape as eskers, or ridges, of sand and gravel. In some regions sedimentary rock can also form important groundwater resources which then are considered within Swedish water administration.

Emerging drought conditions and water shortages

Sweden is known as a country of vast water resources. There are almost 100 000 lakes larger than 2 acres. Sand and gravel deposits with good groundwater potential are rather common compared to other countries. Average precipitation generally exceeds potential evaporation, leaving a surplus of water for groundwater- and surface water runoff.

However, due to climate change with increasing temperatures, some regions show trends with increasing periods of very little groundwater recharge. Most obvious are these climate related effects in the south-eastern parts of Sweden. Some streams that previously were perennial tend to run dry during summer months. Groundwater levels (or relative fill rate) in some aquifers go down. Problems with water supply and water shortages become more common.

Groundwater will still be an important resource in the future

Even with the emerging problems related to climate change, groundwater resources will continue to play an important role for future water supply. It is important to notice the differences between various types of aquifers. Some of the shallow aquifers will face severe problems – a meter of drawdown during summer months might be devastating for dug wells leaving no other options than to drill for deeper wells or connect to municipal supply systems. On the other hand, many of Sweden's larger aquifers will continue to be robust even during periods of summer drought. A meter of drawdown in an esker is no big problem if only the levels will be regenerated during winter.

Future monitoring and management will however be crucial, both in small-scale and larger-scale aquifers. It is mor important than ever before to get to know and to protect our groundwater resources.

References

Eklund, F, Vattenmyndigheten i Södra Östersjön & Holgersson, B, SGU, 2022; Vattenmyndigheterna i Sveriges fem vattendistrikt, Rapport 2022:1, Diarienummer 537-3829-20222022: Torka och vattenbrist - Förslag till fortsatt arbete.

Riksriggen: the Swedish research infrastructure for scientific drilling, in-situ testing, project support, and data handling

Jan-Erik Rosberg[a], Henning Lorenz[b], Maria Ask[c,d], Mark Dopson[e], Gerhard Barmen[f]

[a]Division of Engineering Geology, Lund University, Lund, Sweden, jan-erik.rosberg@tg.lth.se; [b]Department of Earth Sciences, University University, Uppsala, Sweden, henning.lorenz@geo.uu.se; [c]Department of Civil and Natural Resources Engineering, Luleå University of Technology, Luleå, Sweden, maria.ask@ltu.se; [d]Department of Earth Sciences, Uppsala University, Uppsala, Sweden, maria.ask@geo.uu.se; [e]Centre for Ecology and Evolution in Microbial Model Systems (EEMiS), Linnaeus University, Kalmar, Sweden, mark.dopson@lnu.se; [f]Division of Engineering Geology, Lund University, Lund, Sweden, gerhard.barmen@tg.lth.se

Summary. Technology development is critical to earth sciences. The Swedish research infrastructure for scientific drilling "Riksriggen" is a versatile platform for core drilling and testing capacity to 2.5 km depth. Riksriggen is managed by Lund University and has been in operation since 2012. In 2018 Riksriggen became an infrastructure of national importance, with Uppsala and Linneus Universities contributing with project support plus data management and expertize in microbiology, respectively. In 2023, the Riksriggen infrastructure will also include the Stress trailer, built and designed at Luleå University of Technology in collaboration with experts from France and Sweden.

Scope of Riksriggen projects

The Swedish national research infrastructure for scientific drilling "Riksriggen" and the "Stress trailer" are versatile instruments for multidisciplinary subsurface research. Drilling and in situ testing in boreholes are the ony direct methods for in situ access to the subsurface apart from larger-scale underground constructions (e.g. tunnels).

Riksriggen is a versatile scientific concept because it is mainly the researchers' ideas that set the limit that range from large concepts to carefully delimited point studies, for example:

- Study the evolution of major mountain chains and how these processes affect mankind (Lorenz et al. 2015; 2022)
- Characterize active deformation zones in the Earth's crust (Ask et al. 2021)
- Reconstruct the ground surface temperature history and its variations for up to 100 000 years; gather new knowledge about the Weichselian glaciation and climate evolution in northern Europe during the Holocene, including industrial age trends
- Study deep microbial communities: composition, energy sources, predation, evolution, and origin of life
- Study the little-known deep hydrosphere (>1 km depth) in general and deep groundwater circulation in mountain belts in particular
- Establish a detailed understanding of the paleoenvironmental conditions for the reconstruction of paleoclimate, global biologic crises and faunal turnover, and major glacial events
- Establish and improve geological time scales based on high-resolution drill core profiles
- Study the physical and mechanical properties of the subsurface in situ and on drill cores
- Constrain the state of stress and its variation with depth to increase the understanding of its interaction with bedrock stability, the onset of earthquake formation (natural and induced), and of crustal fluid flow and -pressure.

General description

The Riksriggen research infrastructure is unique as it i) combines high technical and scientific expertise that is consistently available to the project; ii) is adopted for scientific work with all necessary components/equipment integrated; and iii) lacks commercial interests (affordable and works on the premises of the scientific project). It is also a platform for technological research and development and a bridge between academia and industry. Riksriggen as a national research infrastructure is financed by the Swedish Research Council, with an open data policy that is in line with data policy and work flows of the the Integrated Continental Scientific Drilling Program (ICDP). The policy makes data and samples accessible, research transparent, and allows continued research on the sample material and data. The Riksriggen's consortium has members from Lund University, Uppsala University, Luleå Technical University, and Linnaeus University. A steering committee is the decision body for Riksriggen.

Riksriggen is a modern wire-line core-drilling rig that complies with the latest safety and environmental regulations. The Atlas Copco Christensen CT20C drill rig can handle three common hole/core sizes P, H, and N (123/85 mm, 96/63 mm and 76/48 mm hole/core diameter, respectively) and has a depth capacity of around 1050 m, 1600 m, and 2500 m, respectively (assuming a vertical water-filled hole). The rig is equipped with a data acquisition system for monitoring and recording operational parameters, which is specially designed by Lund University. The in-hole equipment includes complete core retrieval systems for all three core sizes including drill rods in sufficient length to cover the maximum drilling depth for each size. Both dual and triple tube core assemblies are accessible for each size. Other equipment belonging to the infrastructure include a mud cleaning and mixing system, cementing equipment, fishing tools, well heads, and a blow-out preventer (BOP). The infrastructure is complemented with a fully-equipped workshop container with an integrated diesel tank and a terrain-going truck with a crane and hook-system for equipment transport. The infrastructure includes an advanced hydraulic testing system with single/straddle wireline packers in all three dimensions, pressure sensors, and submersible pumps. The geophysical borehole measurement system consists of probes for electrical, caliper, formation density, full waveform compensated sonic, fluid conductivity and temperature measurements, and of an acoustic and an optical televiewer. The logging system has a cable capacity of 3 km, but the majority of the probes have a pressure rating of 20 MPa. A gas and fluid sampler is also available.

The Stress trailer is a unique state-of-the-art slim-hole wireline activated hydraulic stress measurement system for measuring the complete stress field, which has been designed to conduct tests in boreholes drilled by Riksriggen. It uses a wire-line activated straddle-packer equipped with an electrical imager. Imaging data are used to produce a pre-log to select test sections and to identify potential de-coupling zones, and to produce a post-log after completed pressure testing to analyze the orientation of tested fractures. The equipment is mounted in a 40-foot container on a mega-trailer and includes three winches, low- and high-pressure water hydraulics, manifold, water tanks, borehole equipment (straddle-packers, electric imager for three borehole dimensions) and heater for measurements in cold climate. At surface, approximately 45 data streams (electrodes, pressure sensors, orientation sensors, temperatures) from the borehole are integrated with those from surface sensors (pressure sensor, flow-meter, length, speed, cable tension). It was funded by the Swedish Research Council as part of the Swedish Deep Drilling Program, designed and built at Luleå University of Technology and University of Strasbourg with an industry partner (Geosigma AB), and is in operation since 2018. As of 2023, the Stress trailer will reside within the Riksriggen consortium with an own expert infrastructure manager.

References

Ask, M., I. Kukkonen, O. Olesen, et al., 2021: Proposed drilling into postglacial faults: The Pärvie fault System. In H. Steffen, et al. (Eds.), Glacially-Triggered Faulting, Cambridge university press, 151-174.

Lorenz, H., J.-E. Rosberg, C. Juhlin, et al. 2015: COSC-1 – drilling of a subduction-related allochthon in the Palaeozoic Caledonide orogen of Scandinavia. *Scientific Drilling*, 19, 1–11.

Lorenz, H., Rosberg, J-E., Juhlin, et al. 2022: COSC-2 - drilling the basal decollement and underlying margin of palaeocontinent Baltica in the Paleozoic Caledonide Orogen of Scandinavia. *Scientific Drilling*, 30: 43-57

The importance of palaeoecology in nature conservation: A study of the establishment of beech forest in Söderåsen National Park

Mats Rundgren[a], Maja Damber[a,b], Dan Hammarlund[a], Johannes Edvardsson[a], Karl Ljung[a]

[a]Department of Geology, Quaternary Sciences, Lund University, Lund, Sweden, mats.rundgren@geol.lu.se
[b]Department of Environmental Sciences, University of Basel, Basel, Switzerland

Summary. Palaeoecological studies are important for nature conservation, because they provide the long-term perspective on ecosystem devlopment necessary to define reference states for ecosystem management and restoration. A case study was carried out in Söderåsen National park based on pollen and plant macrofossil records from a lake sediment sequence and dendrochronological data. The results reflect establishment of the present beech forest after 1860 CE, following a period of open conditions beginning in the mid-16th century and culminating after the mid-18th century attributed to intense land use.

The contribution of palaeoecological studies to nature conservation

Sweden's (and Europe's) first national parks were established in 1909. At that time, national parks were formed to protect areas with pristine landscapes and valuable ecosystems from threats posed by human activities, e.g. hydropower plant construction and forestry, but also to make these areas accesible for outdoor life. As reflected by the term nature conservation, management of these early national parks aimed at maintaing landscapes and ecosystems in their existing state. Little attention was, however, paid to their history. For remote areas with historically limited land use, this was usually not a problem, but for other areas there would be unwanted surprises. The qualities motivating conservation were sometimes found to deteriorate as the floral splendour of a meadow faded or as majestic old trees died from shadowing by new trees. Often prompted by an interested public or scientists, this urged responsible authorities to understand how to halt the development. From studies of historic documentation it became clear that many protected ecosystems had been used as hay meadows or wood pastures, or subject to small-scale felling, within the last centuries or decades. Ironically, it was often found that the management designed to preserve the qualities of the protected ecosystems did not allow the land-use activities responsible for their composition.

Today, it is clear that almost no areas in Sweden can be considered truly natural. What we call nature is, with few exceptions, a cultural landscape, and this understanding is reflected in the motivation and management of new national parks and nature reserves. Recently, it has also become possible to protect areas as cultural reserves that are managed in ways that resemble traditional practices. However, knowledge of past land use is usually only derived from historical documentation and therefore typically limited to the last few centuries. Because most ecosystems can be expected to partly be shaped by processes acting on multi-centennial and millennial timescales (Willis & Birks 2006), it is important for conservation to also have access to information about ecosystem dynamics on these longer timescales, and this is provided by palaeoecological studies of plant and animal remains preserved in lake sediments and peat.

Although palaeoecological records are still not regularly considered within conservation in Sweden, there is an increasing interest in long-term landscape and ecosystem development among the authorities involved. There are even cases where authorities fund scientists to perform palaeoecological studies in areas that already are, or are in the process of becoming, protected. Moreover, a growing international scientific interest in biodiversity conservation and ecosystem management and restoration has resulted in an increasing number of palaeoecolocal studies within protected areas, and the authorities responsible for their management can benefit greatly from the results from these studies.

Palaeoecological studies provide important information about long-term ecosystem stability, as well as the nature, scale and rate of past ecosystem changes, but they also give insight into the processes responsible for these changes, e.g. climate change, fire and land use (Willis & Birks 2006). Consequently, palaeoecological records are necessary to define adequate reference states or baselines for ecosystem management and restoration. However, palaeoecological studies also highlight important questions that must be addressed before designing methods of ecosystem management and restoration: Which ecosystem do we want to have, the present one or one that existed earlier in the area? If we want to restore an ecosystem, which previous ecosystem state is our target, and how do we motivate this choice? What methods are required to preserve the existing ecosystem or restore the previous ecosystem, and is it possible to maintain this ecosystem in the future? These are all difficult questions, but they must be answered if we want to continue to move away from the rather romantic and naïve concept of nature conservation characterising the early 20th century towards a more science-based type of conservation. Future conservation cannot only aim at providing areas with pristine, or close to pristine, nature but must also help to secure a level of landscape, habitat and species diversity that can supply the other ecosystem services (e.g. food, building materials, fuels, water, air quality, medicine, and carbon storage) that our society is dependent on.

The establishment of beech forest in Söderåsen National Park

Söderåsen National Park, located on the eastern flank of the Söderåsen horst ridge in Sweden's southernmost province Scania, was established in 2001 and features deep fissure valleys with streams, spectacular views and deciduous forests dominated by beech (*Fagus sylvatica*). According to the management plan, the area was protected because of its unique terrain and vegetation, its geological and biological qualities, and its value for outdoor life and science (Naturvårdsverket 2001). Natural vegetation is to be left largely unmanaged, while areas of cultural importance are to be preserved through active management. Areas with alien vegetation or previously used for forestry are to be restored, primarily as broad-leaved forest.

At the time of establishment, there was no information available about long-term landscape and ecosystem devlopment within the park beyond historical documentation. To provide this perspective, we approached the park administration and were permitted to perform a palaeoecological study primarily based on the sediments of Lake Odensjön, known to be partly varved and therefore providing an exceptionally precise chronology. Moreover, an already available freeze core diplayed large amounts of beech leaves above 26 cm, corresponding to c. 1930 CE, suggesting a major vegetation change around this time. The upper 86 cm were analysed for pollen and plant macrofossils with the aim to reconstruct changes in forest composition and openness in the lake surroundings from c. 1500 CE and to identify the causes for any such changes. A dendrochronological study was also carried out to further determine the establishment of the local beech population. Historical maps and photographs were used to support interpreation of the palaeoecological records.

Together, the data suggest an initial decline of a beech-dominated forest in the mid-16th century, due to a combination of factors such as over-exploitation, over-grazing, and implementation of land reforms. The area is believed to have reached its most open stage during the mid-18th to mid-19th century, as indicated by sparse macrofossil and pollen records of tree taxa along with high pollen percentages of juniper (*Juniperus communis*), herbs and graminids. During the second half of the 19th century, the forest is inferred to have grown denser, as reflected by increasing pollen frequencies and macrofossil concentrations of deciduous tree taxa, in particularly beech, and decreasing values for shrubs, herbs and graminids. The shift towards a denser forest is attributed to a change in land use, in particular less intense grazing. The dendrochronological data indicate that the present beech population around Lake Odensjön was established after 1860 CE. The pollen and plant macrofossil records suggest that the main shift from an open landscape to a closed forest did not take place precisely at 1930 CE, as hypothesised based on the abrupt increase in leaves visible in the core, but rather occurred in the beginning of the 20th century, whereafter the beech forest continued to expand until the mid-20th century.

References

Willis, K.J. & Birks, H.J.B., 2006: What is natural? The need for a long-term perspective in biodiversity conservation. *Science 314*, 1261-1265.

Naturvårdsverket, 2001: Skötselplan för Söderåsens nationalpark. Naturvårdsverket, Stockholm, 55 s.

Cancer risk assessment related to terrestrial gamma radiation – an example and future predictions using register data in Sweden

Martin O. Tondel[a], Mats R. Isaksson[b], Peter SO. Molnar[c]

[a]Department of Medical Sciences, Uppsala University, Uppsala, Sweden, martin.tondel@medsci.uu.se;
[b]Department of Radiation Physics, University of Gothenburg, Gothenburg, Sweden, mats.isaksson@radfys.gu.se;
[c]Department of Occupational and Environmental Medicine, University of Gothenburg, Gothenburg, Sweden, peter.molnar@amm.gu.se.

Summary. Exposure to ionizing radiation to the population from natural occuring radionuclides in the ground can be assessed by linking digital maps on the sum of gamma radiation from ^{238}U, ^{232}Th and ^{40}K in nanoGray/hour (nGy/h) to the population using the dwelling coordinates. In Västra Götaland county there is a high contrast of exposure with a population average of 37 nGy/h in the municipality of Borås and 101 nGy/h in Strömstad, respectively. By combining digital databases it is possible to estimate the collective dose (manSievert) from terrestrial gamma radiation for cancer risk assessment.

Background

In many populations, the terrestrial gamma radiation (TGR) accounts for a significant part of the total radiation dose from natural sources. Some areas in the world have significantly elevated naturally occurring terrestrial radiation due to special geological features. One of the highest dose rates have been recorded in ^{232}Th rich monazite sands in Kerala, India showing an average of 1,500 nGy/h. In Ramsar, Iran high content of ^{226}Ra in the soil gives an average of 765 nGy/h. Other areas with high natural background radiation have been seen in Orvieto, Italy with vulcanic ground rich in ^{238}U, ^{232}Th and ^{40}K with an average of 560 nGy/h compared to the world average of 59 nGy/h (UNSCEAR 2010). In Sweden the terrestrial radiation is mainly derived from ^{238}U, ^{232}Th and ^{40}K in bedrock and soil. Aerial measurements carried out by the Geological Survey of Sweden (SGU) have shown that the average radiation dose rate from TGR in Sweden is 90 nGy/h with a range from 15 to 8,500 nGy/h (Åkerblom et al. 2005). TGR is shielded mainly in brick buildings and concrete houses (which also in themselves emit gamma radiation). The population is also exposed to radon gas emitted from ground or building material, in Sweden predominantly lightweight alum shale concrete. The aim of this study is to evaluate a technique of matching the population on their dwelling coordinates with a map of TGR in Västra Götaland county and to discuss possibilites for cancer risk assessment.

Methods

SGU conducts regular aerial measurements of gamma radiation ^{238}U, ^{232}Th and ^{40}K. Because these radionuclides give rise to unique gamma spectra, they can be measured separately in the flight measurements. These aerial measurements take place 60 meters above the ground and with flight lines at a distance of 200 meters (Aaro et al. 2000). ^{238}U and ^{232}Th are expressed in ppm (parts per million) and ^{40}K in percent. These geophysical measurements are collected in a database with coordinates from the Swedish RT90 in a grid map of 200x200 meters. With conversion factors from SGU, the total sum of TGR can be calculated in nanoGray/hour (nGy/h). One percent ^{40}K corresponds to 13.296 nGy/h and one ppm ^{238}U to 6.625 nGy/h and one ppm ^{232}Th to 2.309 nGy/h, respectively.

Each dwelling in Sweden has been appointed a coordinate by the National Land Survey of Sweden and made available from the Statistics Sweden. The accuracy of the coordinate has been calculated to 100 meters. With the help of GIS (Geographical Information System) the database on TGR can be linked to the dwelling coordinates. Thus, each resident in Västra Götaland County can be assigned a an approximate value of TGR in nGy/h.

Results

The average and median value on TGR was 56 and 60 nGy/h, respectively in Västra Götaland County (n=1,557,997). For the largest municipality Gothenburg (n=500,242) the average was 60 and the median 63 nGy/h, respectively. There is a large differences comparing the distribution of TGR between different muncipalities (n=49 in Västra Götaland), here examplified by Borås and Strömstad municipalities with averages of 37 nGy/h and 101 nGy/h, respectively.

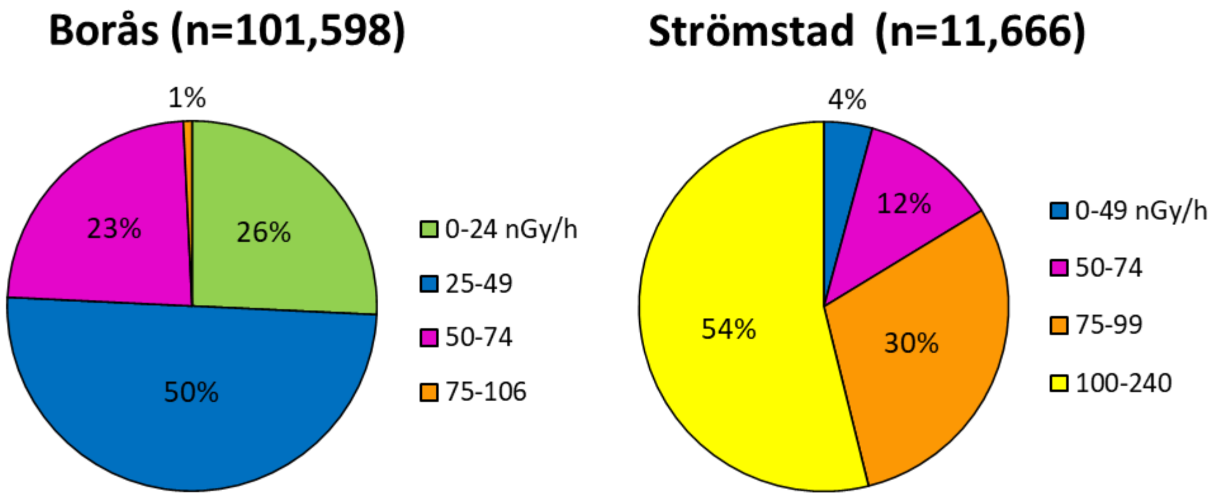

Discussion

The TGR levels in Västra Götaland County is lower than the Swedish national average, but with great geographical variability which make it suitable for epidemiological studies. The method creating individual exposure assessment by linking dwelling coordinates with a map on TGR is rewarding and makes it possible to scale up into the national level including all 290 municipalities in Sweden. The population census 1980 (FoB) at Statistics Sweden is a comprensive data base on building materials classified in to wood or stone (concrete, bricks) buildings. Building material can be used for classifying gamma-radiation, but also applying shielding factors when calculating external effective doses to the population. Between 1979 and 1981 an extensive measurment campaign was performed by SGU with cars equipped with scintillometers measuring the gamma-radiation from the house facades as detectable from more than 25 meters. In total 700 000 addresses were measured in 143 municipalities in 20 out of 24 counties in Sweden (Hesselbom & Berglund 1982). These results has not yet been be digitized, but will be a valuable source for assessing gamma-exposure from the building materials. Moreover, using a compilation on survey data on radon measurements will make it possible to assess the dose contribution from radon to the population dose (Barregård & Andersson 2012). By combining all these databases it will be possible to estimate the collective dose in manSievert (manSv) from natural background radiation to the Swedish population for cancer risk assessment, also make it possible to compare to collective dose in Sweden from the radionuclide fallout from the Chernobyl nuclear power plant accident in 1986.

References

Aaro, S. & Byström, S., 2000: Flyggeofysiken och de nationella miljökvalitetsmålen. *Geologiskt forum 28,* 12–16.

Hesselbom, Å. & Berglund, P., 1982: Bilmätningar i syfte att spåra hus byggda av alunskifferbaserad gasbetong. Slutrapport. FM-rapport 8233. Sveriges Geologiska Undersökning.

Barregård, L., & Andersson, E.M., 2012. Hur många lungcancerfall kan undvikas om radonhalterna i svenska bostäder sänks? Sahlgrenska akademin, Göteborgs Universitet, Göteborg.

United Nations Scientific Committee on the Effects of Atomic Radiation., 2010: UNSCEAR 2008 Report to the General Assembly with Scientific Annexes. Sources and effects of ionising radiation. Volume I. New York: UNSCEAR.

Åkerblom, G., Falk, R., Lindgren, J., Mjönes, L., Östergren, I., Söderman, A.L., Nyblom, L., Möre, H., Hagberg, N., Andersson, P., Ek, B-M., 2005. Natural radioactivity in Sweden, exposure to external radiation. *SSI rapport 15,* 207–210.

Society and geology, what is the future?

Pär Weihed[a], Erika Ingvald[b], Katarina P. Nilsson[c]

[a]Luleå University of Technology, Luleå, Sweden, par.weihed@ltu.se;
[b]Geological Survey of Sweden, Uppsala, Sweden, erika.ingvald@sgu.se;
[c]Svemin, Stockholm, Sweden, katarina.nilsson@svemin.se

Summary. The society needs to invest more in geoscience research and education. Focus on raw materials supply, ground water supply, geohazards, the built environment and energy is required. Actions include increased support for these areas within the geological survey, an introduction of geosciences in the high school curriculum, mission driven action within innovation related to the topics, and enhanced support to both fundamental and need driven research from research councils and other agencies.

Is there a role for geosciences in the green transition to a society built on sustainable solutions for energy, raw materials supply and a minimised anthropogenic impact on the climate? The answer is probably yes. But what is this role and who will define it? Geosciences have for the last two centuries been instrumental in building the modern society as we know it today. We live longer and have a higher standard of living than ever before even though the global population in the near future will reach 10 billion. However, at the same time as we build a fully digitised society we also see a decline in the interest to engage in scientific societies, fake news are spreading in social media and there is a trend in society to base decisions on feelings rather than on scientific facts.

In Sweden, the number of members of the geological society has halved over a period of 30 years. In the 1970ies the geological survey employed close to 800 people, today it is around 300. The geological departments have increased staff over the years, but the number of researchers engaged in research directly related to regional Swedish geological conditions has dramatically gone down. The latter has had the effect that the understanding of Swedish regional geology is undercritial to a degree that there are now geological time spans and geolocical domains of which knowledge is lacking and we must rely on historical records.

In a potentially resource constrained future this is a dangerous development. In the coming decades, besides combatting climate change and the consequences thereof, the following fundamentally important areas need to be considered by society with a direct link to the role of geosciences:

1. Raw materials supply
2. Ground water supply
3. Geohazards
4. The built environment
5. Energy solutions

There has never been a higher demand for metallic and mineral raw materials than today (European Commission, 2018). The driving mechanisms are several, but population growth in combination with urbanisation and the green transition drives the use of almost all commodities. While infrastructure metals such as iron and base metals are in high demand for green solutions and new technologies related to the electrification of the society, also a number of minor metals are in high demand for new energy solutions (see below). The number of critical raw materials is growing in the EU at the same time as the degree of self sufficiency is decreasing. This is a key area for geoscientific knowledge that needs to be upgraded at regional, national and European level.

When population is growing and climate change causes fundamental changes also in global water supply, the demand for knowledge about ground water has never been higher than today (United Nations, 2022). Shortage of water supply is no longer something that affects people in other parts of the world.

It will also be a big issue for Sweden. Therefore we will need to invest much more in hydrogeological research in the future.

With changing climate, changing weather patterns and sea level rise, geohazards is an area that needs much more attention in Sweden. The recent landslide in Gjerdum outside Oslo is a sign of what we can expect to occur more frequently in the future. Therefore a much better understanding of geological risks is important and both regional and national authorities will need to invest heavily in knowledge in this area (cf. European Science Foundation, 2015).

The threat that the environmental permit would not be granted to Cementa for the supply of lime for concrete production was a clear sign of how sensitive the supply chain is for building material. Besides cement and concrete the built environment largely depends on the supply of wood and steel, if we don't include fossil products (for asphalt etc.). Geological knowledge of occurrences and qualities of these products will be in high demand in the future. Today this knowledge is undercritical and investment in both education and research will need to be improved in both industry, academia and responsible authorities in order to safeguard sustainability in the built environment.

There is hardly anything as important for the fate of mankind as identifying and implementing a sustainable energy production based on fossil-free soultions. While decisions on which energy solutions should be chosen is political, it is important to realise that for all fossil-free solutions raw materials are a critical factor, be it for production, distribution or storage. For battery production, solar cells or wind parks metals such as REEs, Li, Co, In, Ga, Ge, Sc and others are fundamental and the European union is basically fully import dependent (European Commission, 2020). So, in order for the green transition to happen, a radical improvement in the knowledge of where these raw materials occur and how they can be sustainably extracted and produced is a fundamental requirement.

So, besides being an integral part in the science and research needed to mitigate climate change, there are a number of critical areas for the future society where geosciences are needed. The question is if the society at large is aware of this, and if there is a political will to make the necessary investments in research and education to meet these needs?

More resources must be invested in geosciences at large. This includes:

- An increased focus on the five topics discussed above from the Geological Survey of Sweden. This will need a substantially increased budget.
- A curriculum in high school that includes geology as a subject.
- Mission driven topics identified and supported by the Swedish Innovation Agency within these areas.
- A substantial increase in targeted funding for both fundamental geoscientific reasearch and the more need-driven and applied research needed within these areas. This in turn will require a larger budget in the research council for geosciences, and a larger external research grant for the Geological Survey of Sweden.

References

European Commission, 2018: Report on Critical Raw Materials in the Circular Economy, 76 pp.

European Commission, 2020: Critical materials for strategic technologies and sectors in the EU - a foresight study, 97 pp.

European Science Foundation, 2015: Extreme Geohazards: Reducing the Disaster Risk and Increasing Resilience. A Community Science Position Paper, 67 pp.

United Nations, 2022: The United Nations World Water Development Report 2022: Groundwater: Making the invisible visible. UNESCO, Paris, 246 pp.

General Session 3
Geoeducation

Session Chairs:
Anders Scherstén (anders.schersten@geol.lu.se)
Magnus Hellqvist (gyttjelera@gmail.com)
Emma Rehnström (emma.f.rehnstrom@gmail.com)

Geoscience education and the use of digital (field) tools, testbeds, drones, and modern pedagogics at Luleå University of Technology

Joel B.H. Andersson[a], Christina Wanhainen[a], Glenn Bark[a], Nils F. Jansson[a], Tobias E. Bauer[a], Hesham Ahmed[b]

[a]Division of Geosciences and Environmental Engineering, [b]Division of Minerals and Metallurgical Engineering, Luleå University of Technology, SE-971 87 Luleå, Sweden.

Summary. Education in Geosciences in Sweden has never been more important. Meanwhile, low student numbers at Geoscience programs have lead to decreasing educational budgets. Within this reality, Geoscience educators must work hard to maintain an education which is both attractive for a younger digitized generation, and still relevant for preparing students for the various challenges of their professional careers. This contribution summarizes how LTU approaches the situation by utilizing digital tools in combination with project-oriented-learning (POL) and problem-based-learning (PBL).

Geoscience in society

Higher education in Sweden plays a key role in supplying expertise to a wide spectrum of different strategic areas in the Swedish society, including the Geosciences. The exploration of metals and minerals is a prerequisite for Europe and Sweden to full-fill the Paris Agreement, underground infrastructure is increasing as our towns grow bigger, and nuclear waste will be stored in our bedrock. These challenges, and many more, position Geosciences as one of the most critical subjects for modern society, but despite its importance, its relevance appears to be problematic to communicate to non-geoscientists. The number of geology students at universities worldwide has been dwindling for a long time (Editorial 2021), which has had a negative effect on the educational area. To solve this, strategic and long-term investments such as increasing the weight of Geosciences in the curriculum of the elementary school and other political priorities are required. Meanwhile, innovative pedagogic approaches and relevant digital tools can be utilized in an extremely cost-effective manner to shape young and self-thinking Geoscientists while being constrained by lower budgets. This contribution is a summary of how Luleå University of Technology is tackling the situation and how we try to push the frontlines of pedagogy within the framework we are acting within.

Fieldwork, virtual mapping, and the testbed Arctic Tests

Fieldwork plays an essential role in any geoscientific curriculum. However, the relatively high costs involved together with short snow-free periods during the semesters in the northern hemisphere are hinders to be tackled. Online adaption using state-of-the-art technology combining virtual excursions with 360° views (Fig. 1A), virtual mapping utilizing photogrammetric models and quasi in-situ structural measurements (Fig. 1B), geochemical software packages, and virtual core logging of tomography-scanned drill cores, has allowed for hands-on and virtual “field based” geological exploration-focused education even during the Covid-19 pandemic (e.g. Jansson et al. 2020). The course development for such a digitized format is work-intensive but the budget is eased already the second year when the course is ready to be delivered fully on-line or combined with field mapping in a format that takes the full advantage of the pedagogical benefits of working with same field localities both in the field and virtually. Being able to do virtual fieldwork is an excellent addition to hands-on field experiences that the students do in for instance the Arctic Tests testbed. This is a testbed situated at the Kaunisvaara mine site north of the Arctic Circle in Pajala municipality where the university students work closely together with the mining company and external small and medium-size companies (consultants, entrepreneurs etc.), through entire project courses and/or separate course modules. Being embedded in an active mining operation, working side-by-side with the mining company, makes this a unique opportunity for the students to interact directly with the industry and potential future employers. Furtermore, the currently large industrial investments in northern Sweden that aim at producing batteries and fossil-free steel serve the area of geo-education a platform for the up-skilling of geoscientists and other life-long learning activities in close collaboration with relevant industry partners.

Drone technologies

Unmanned aerial systems (UAS: Fig. 1C) has torpedoed geoscientific research during the last decade. Today, UASs competent enough to produce terrain models with sub-centimetre precision can be bought off-the-shelf within budget of any geology-department and is a tool that helps bringing the field-situation into the classroom. This is beneficial from many aspects as it allows the field exercise to be performed in field and later processed further in the classroom in the virtual reality which increases the inclusiveness of geological education by providing "field-experience" for people with disabilities and/or other special needs available in a way that is beneficial for all, also during winter, at low cost. This approach is best integrated with a virtual reality studio (Fig. 1B), such as the one installed at Luleå University of Technology or with a hololens, but mapping together in a virtual terrain model displayed on a normal computer screen also full-fills the pedagogical aim. It is emphasized that whereas we see large potential in utilizing digital tools for augmenting or supporting field work, or facilitating mapping excercises during lock downs, we are still far from a point where these could actually replace classical field work.

Figure 1. Examples of innovative geo-education at Luleå University of Technology. A) Screenshot from a virtual fieldtrip with 360° views and embedded lectures at key localities, Skellefte district. B) A photogrammetric 3D-model acquired by UAS of a field locality along the Parvie fault displayed in the Virtual Reality Studio. C) PhD student about to fly a drone in relatively dense forest during the course development of a virtual field course in exploration.

Educational programs at Luleå University of Technology

Complementary to the existing geo-programs at Luleå University of Technology, Natural Resources Engineering (5y) and MSc Exploration and Environmental Geoscience (2y), a new international bachelor program in Mineral Resource Engineering covering the full value-chain of mineral and metal extraction will soon start. The program structure is based on project-oriented-learning (POL) principles, and problem-based-learning (PBL) will permeate the pedagogics applied in the orientation courses. In parallel with courses like Geoscience, Structures and deformation, Mineralogy and crystallography, Sustainable mining methods, Linear algebra and calculus, Mathematical statistics etc., a project course is running where the knowledge and skill sets acquired are applied. After three years the students specialize within their area of interest within the mineral extraction value chain. By this approach, we aim to motivate students to reach the higher and more complex levels of the Bloom´s pedagogical taxonomy as early as possible in the education and to prepare them for the challenges they will meet when Mineral Resource Engineers are going to solve future challenges of the resourceintensive green transition of the society.

References

[Editorial] 2021: Geoscience on the chopping block. *Nature Reviews Earth & Environment 2(9)*, 587–587. https://doi.org/10.1038/s43017-021-00216-1

Jansson, N., Ranta, J-P., Berthet, T., & Suopajärvi, K., 2020: From oil digger to energy transition enabler: the critical role of exploration geosciences education in Europe. *European Geologist 50*, htttp://doi.org/10.5281/zenodo.4311695

What do students learn about stratigraphy through fieldwork?

Abigail K. Barker[a], Sebastian Willman[a], Rie H. Malm[b], Mattias Arrhenius[c]

[a]Department of Earth Sciences, Uppsala university, Uppsala, Sweden, abigail.barker@geo.uu.se
[b]Department of Science Education, University of Copenhagen, Copenhagen, Denmark,
[c]Department of Education, Uppsala university, Uppsala, Sweden

Summary. Stratigraphy is a key concept within geology education and we set out to investigate what students understand about stratigraphy from studying the topic during fieldwork in an introductory course on Earth Science at Uppsala University. We surveyed the students before and after being in the field. The students show a wide range of conceptual understanding of stratigraphy associated ten themes. The basic understanding features rock types, fossils and layering. More nuanced understanding shows interconnection of ideas associated with depositional environments, time and climate.

Sedimentary rocks vary in shape and composition depending on the environments of deposition. In addition to lithological changes, the rocks may contain additional data in the form of fossils. Earth Science focuses on temporal and spatial relationships, for example rocks in the field can be investigated for differences and similarities from one place to another showing past processes, in a particular snapshot of time. Additionally sequences of rock in the same place reveal temporal relationships. This is the foundation of stratigraphy, the description and interpretation of layers of rock in a vertical section that was built up over time. Comparison of several such sections provide the spatial dimension. In this study our aim was to investigate what students learn and understand about stratigraphy.

We studied students learning before and after a one day field excursion in an introductory course in Earth Science at Uppsala University in the autumn 2020. The students were in the first year of their BSc and had just entered university with a school science background, there were 23 students enrolled in the course. We gave them a questionnaire to fill out before they went on the field excursion and a second one for after the excursion, to examine the influence of the fieldwork. Seven people responded to the short answer questions before the excursion and 11 afterwards. We used content analysis to inductively identify critical factors in the responses of both before and after questionnaires. Resource graphs are used to analyse the responses from individuals both before and after fieldwork and look for connections between ideas.

Content analysis revealed ten themes within the answers, the content provides a wide range of conceptual understanding from very basic to well developed. There were very few alternative conceptions found within the responses. Resource graphs show a wide range of patterns from a few connected ideas to highly complex interconnected patterns between themes.

We found three levels of complexity within the responses. Students who showed little insight, have simple resource graphs with a few connected ideas, they notice minerals, fossils, lithology and layering. They consider the rock record as an archive of time very generally. Moderate insight considers stratigraphy to show order of events, time and depositional environments. Good insight is associated with resources graphs that are complex and feature time, depositional environment and spatial scale. These students make connections between fossils and depositional environment, as well as demonstrating conceptal understanding of sedimentation rate and climate. The analysis thereby show a diversity in the complexity of students conceptual understanding and provide us with insights into the challenges of teaching and learning stratigraphy.

Engaging future generations in the challenges of the raw materials sector

Magnus Johansson[a], Anna Apler[a], Jonathan Hamisi[a], Armida Torreggiani[b], Renata Lapinska-Viola[b]

[a]Department of Mineral Resources, Geological Survey of Sweden (SGU), Uppsala, Sweden, magnus.johansson@sgu.se, anna.apler@sgu.se, jonathan.hamisi@sgu.se;
[b]Institute of Organic Synthesis and Photoreactivity (ISOF), National Research Council of Italy (CNR), Bologna, Italy, armida.torreggiani@isof.cnr.it, renata.lapinska-viola@isof.cnr.it

Summary. Raw materials demand and supply, as well as relevant sustainability concerns are often little or poorly known by the public, despite their important role in sustaining our modern way of life. EIT RM@Schools is a European project targeting primary and secondary schools pupils, informing them about sustainable raw materials supply and use. The project aims to promote better understanding of the importance and complexity of the extractive industry and encourage science education and career in STEM by promoting active learning at school thanks to hands-on lab activities and communication work.

The RM@Schools project

Metals and minerals are essential to our everyday life as well as to support the transition to a sustainable economy. The raw material value chain has been identified by Europe as a sector requiring education of highly skilled professionals because the supply of a certain group of raw materials (RMs) is a major concern for the growth of the European industry (EC, 2020). Thus, it is important to create a strategic plan to face this challenge by integrating better exploitation of resources, substitution of critical or toxic elements in products and for optimized performance, and design of products and services to help the transition from linear to circular economy.

Education and social awareness are mandatory elements in the actuation of such strategy. For this reason, the European Commission, through the European Institute of Innovation and Technology (EIT) in the sector of Raw Materials (EIT RawMaterials), the largest consortium in the raw materials sector worldwide, has funded Raw Matters Ambassadors at Schools (RM@Schools) since 2016. In the project name, "Raw MatTERS", the key message resonates: raw materials are the key focus, whatever their origin and "Tackling European Resources Sustainably (TERS)" underlines that it is necessary to actively tackle the challenge ahead of us.

RM@Schools proposes active learning pathways linked to sustainable challenges, solutions explored by research to schools, and improvement of students' technical and non-technical skills. The paths have a modular structure, including lessons, experiments and visits to industries, museums and research centers, and a final step focused on the communication work (Torreggiani et al., 2020; Torreggiani et al., 2021). The latter is the core element of the RM@Schools approach: to empower students to communicate with peers and wider society about critical concepts related to RMs and their use. Thus, students are asked to become Young RM Ambassadors themselves (science communicators) and to create a "product" to be communicated outside of the class (i.e. videos, cards, etc).

In addition, teachers are trained to become RM Ambassadors themselves in the future at school, and selected groups of students are trained on activities suitable to be proposed during Public Events in order to work together with RM Ambassadors (Figure1a).

The RM@Schools activities merge industry-relevant scientific contents with teamwork and creativity-training tasks, which will be useful for students to develop flexibility and ability to handle changes in their future work (Kind and Kind, 2007).

The active learning approach is encouraged by involving students in experiments using raw material-related hands-on educational toolkits. These are distributed within learning pathways such as Exploration & Mining, Recycling, Circular economy and Substitution. The toolkits are promoted within schools and other education organisations, and project partners are then invited by interested schools to present a lecture in classes using the toolkit. Teachers and project partner discuss the content of the toolkit and adapt a suitable presentation module according to the pupils needs and the current curriculum. Interactive exercises including discussions are used to emulate the debate and raise awareness about how raw materials are used in our day-to-day life.

The EIT-funded project is now in the 6th year of activity and 30 partners of 20 European countries have developed and translated more than 50 different stand-alone experiment toolkits with detailed explanations for use at school. Many thousands of people have taken part in events organised by the project partners.

By participating, students develop relevant skills such as creativity, critical thinking awareness of responsibility and teamwork, which are key elements for a successful career (Davidson, 2016). In all, the project has been perennially successful in outreach activities, informing and engaging participants in schools as well as in the wider society.

a) b)

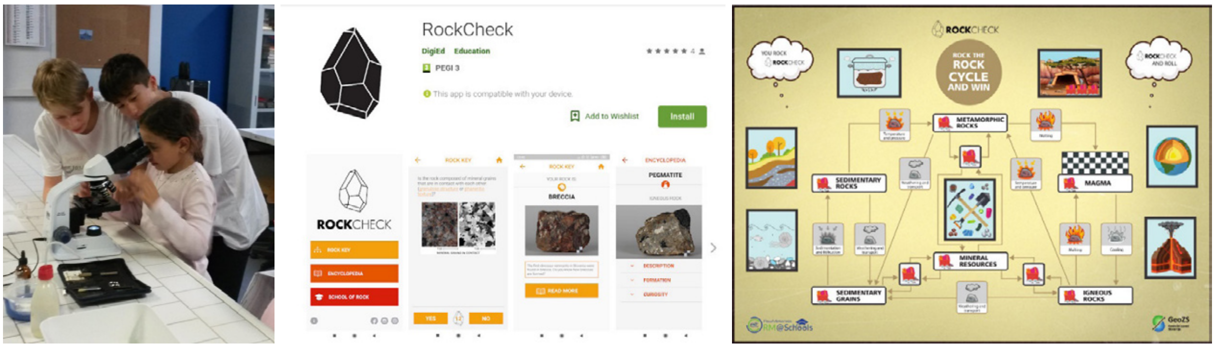

Figure 1. a) Young RM Ambassadors in action during European Researchers' Night; b) two toolkits focused on geology.

References

Davidson, K. (2016). Employers Find Soft Skills Like Critical Thinking in Short Supply. https://www.wsj.com/articles/employers-find-soft-skills-like-critical-thinking-in-short-supply-1472549400 [Accessed: March 10, 2021]

European Commission. (2020). European Commission, Critical materials for strategic technologies and sectors in the EU - a foresight study, 2020. https://op.europa.eu/en/publication-detail/-/publication/8e167f11-077c-11eb-a511-01aa75ed71a1 [Accessed: March 10, 2021]

Kind, P. M., and Kind, V. (2007). Creativity in Science Education: Perspectives and Challenges for Developing School Science. Studies in Science Education 43, 1-37.

Torreggiani, A., Zanelli, A., Canino, M., Sotgiu, G., Benvenuti, E., Forini, L., Aluigi, A., Polo, E., Lapinska-Viola, R. and Degli Esposti, A. (2020). RM@Schools: Fostering Students' Interest in Raw Materials and a Sustainable Society. In: 10th International conference the future of education, virtual edition, Firenze (Italy) virtual conference pp 446-452.

Torreggiani, A., Zanelli, A., Degli Esposti, A., Polo, E., Dambruoso, P., Lapinska-Viola, R, Forsberg, K. and Benvenuti, E. (2021). How to Prepare Future Generations for the Challenges in the Raw Materials. In Rare Metal Technology 2021, G. Azimi et al. (eds.), The Minerals, Metals & Materials Series, pp 277-287.

http://rmschools.eu/

SGU Geological Survey of Sweden

RawMaterials RM@Schools

Co-funded by the European Union

Geoscience education for the future, a Norwegian perspective

Anders Mattias Lundmark

Department of Geosciences, University of Oslo, Oslo, Norway, mattias@geo.uio.no,
and Centre for Integrated Earth Science Education (iEarth), Norway

Summary. This contribution introduces initiatives to strengthen Norwegian geoscience higher education led by iEarth, a Centre for Excellence in Education. An integral part of efforts within iEarth is to work in partnership with students. I will describe some of the benefits and challenges of this approach, with recent examples from iEarth. Our experiences have strengthened our belief that this approach can promote enthusiasm, creativity and motivation for both staff and students, and can ultimately contribute to a transformation of geoscience in higher education.

Challenges and opportunities – current developments in geoscience education in Norway

Geoscience has a privileged position in Norway. The oil and gas industry is responsible for much of the country's wealth. The mountainous and partly arctic terrain facing the North Atlantic weather systems means that geohazards are a constant, and due to climate change, increasing concern. A growing awareness of global environmental degradation and climate change is highlighting the interdependence between human society and our planet, expressed in the UN's Sustainable Development Goals and embodied in the Earth system science perspective. The importance attributed to geoscience is exemplified by the launch in 2006 of geoscience as an elective subject in its own right in Norwegian high schools, though availability depends on the school.

In higher education, the Centre for Integrated Earth Science Education, iEarth, was founded in 2018 by the Geoscience departments at the University of Bergen, University of Oslo, the Arctic University of Norway at Tromsø and the University Centre on Svalbard. The goal of iEarth is to develop higher education geosciences in Norway to answer to future societal needs. This includes e.g. research on and strengthening of fieldwork teaching, integrating an Earth system science perspective in geoscience educations, enhance work life relevance, and increase the coherence in study programmes (www.iEarth.no).

In 2020, iEarth was awarded status as a Centre for excellence in education, a prestigious Norwegian program to promote development of higher education. The award included 36 million Norwegian kronor over 5 years in funding, with a further 40 million kronor from the constituent geoscience departments.

iEarth promotes a change from teaching as an individual undertaking, where teachers work alone with little support and input from colleagues, to a collegial effort, and from teaching practices grounded in tradition to evidence-based teaching practices. We also recognize that the students bring unique and valuable experiences, perspectives and aspirations to their education. We therefore aim to bring students' expertise into courses and study programs through continuous, collaborative educational development, where students and staff co-create a dynamic and inclusive education.

This presentation will discuss some of the ongoing work in iEarth, challenges and opportunities we face, and lessons we are learning. Here, the focus will be on our two greatest resources, students and staff at our geoscience departments. Our approach draws heavily on Student and Staff Partnership work (e.g. Barrineau et al. 2019; Bovill 2020), and iEarth is now starting research into how such partnerships can be a force for transformation of higher geoscience education in a Scandinavian setting. iEarth may not have the roadmap to the geoscience education of the future, but we strongly believe that student-staff partnership is the process that can take us there.

References

Barrineau, S., Engström, A. & Schnaas, U., 2019: An active student participation companion. Avdelningen för kvalitetsutveckling-Enheten för universitetspedagogik.

Bovill, C., 2020: Co-creating learning and teaching: Towards relational pedagogy in higher education. Critical publishing.

Geokids – an outdoor learning activity on geology, cultural heritage and sustainability

Emma F Rehnström, Ola Göransson

Geoforum Skåne, c/o Rehnström, Rosengatan 1, 235 31 Vellinge,
emma.f.rehnstrom@gmail.com, ola.goransson@cellma.se

Summary. Geokids is a concept that have been developed within the framework of the Geopark Skåne project. It is a concept with an interactive outdoor learning experience, that has been adapted both for school classes and as a family acitivity. The activity is typically 2–3 hours, but can be extended. It centres around a geological timeline, with emphasis on the geological development in Skåne. At relevant points along the timeline stops are made and practicals performed with full involvement of the participants. The activity is finalized with a diploma and a badge marking the “membership” in maskot Geo’s club, namely Geo’s heroes.

A pyramid of knowledge

Geokids was developed based on the “Mini ambassador” concept used in several Biosphere areas in Sweden. It is constructed as a pyramid, with a common base of knowledge used at all locations, including several of the practicals. The base consist of general geological facts and processes, as well as an introduction to geological resources. The middle part is where local knowledge is presented, local geology, local cultural heritage, industrial heritage and local geological resources. The top of the pyramid marks the knowledge testing that is done mainly during the practicals that is rewarded with a diploma and a badge with the Geokids logotype as a proof of being a member of Geo’s heroes (Geohjälte).

Practicals

The number of practicals during the Geokids activity is not fixed and should to some degree be adapted to local conditions.

The first practical is located around 800 Ma on the geological timeline and is an erosion-sedimentation practical marking the weathering down of the Sveconorwegian orogen and the deposition of Early Cambrian sandstone.

The second practical is located around 250 Ma, because at this point all the three major rock types: magmatic, sedimentary and metamorphic, have been aquinted with and the rock cycle is presented, together with minerals and rock types. Locally avaliable rocks are practised on and sorted into the different categories.

The third and later practicals are usually more local and could consist of geological bingo that consist of photos of geological phenomena to be found in the area or fossil hunting, if permitting. There can also be a practical connected to the cultural heritage. The last practical is at the end of the geological time line and concerns the difference between finite and infinite resources, whereof geological are almost ubiqutously finite. Common household things, such as glass bottles, plastic, wood etc. are sorted into the finite and infinite materials.

The logo

The Geokids logotype is a dark grey hexagon representing columnar jointing commonly found in Jurassic and Createaceous basaltic rocks outcropping in central Skåne (e.g. Bergelin 2009). In the centre of the hexagon is theropod dinosaur foot print. This partical foot print has been drawn after the description of the Vallåkra occurencies in western Skåne by Gierliński & Ahlberg (1994).

Quality assurance

Geokids can be performed only by trained crew and it is mandatory to attend at least one Geokids as assistant before conducting them yourself. This is to maintain the quality of the concept that has three levels of quality control: quality controlled locations, quality controlled content and qualified performers. The diploma is also a way to increase the perception of quality of the experience.

Several guides have been produced to support the performer and in the case of school children activities there is a teachers guide in order to make the most out of the Geokids experience. Care has been taken to connect the Geokids content to the Swedish elementary school curriculum.

References

Bergelin, I., 2009: Jurassic volcanism in Skåne, southern Sweden, and its relation to coeval regional and global events. *GFF 131*, 165-175.

Gierliński, G. & Ahlberg, A., 1994: Late Triassic and Early Jurassic dinosaur footprints in the Höganäs formation of southern Sweden. *Ichnos 3*, 99-105.

Metals4U+: Mineral raw materials for a green and digital future

Lotta Sartz, Stefan Sädbom, Mattias Bäckström

Bergskraft Bergslagen AB, Kumla, Sweden,
lotta.sartz@bergskraft.se; stefan.sadbom@bergskraft.se; mattias.backstrom@bergskraft.se

Summary. Awareness of where metals and minerals come from and how they are mined and produced is low among the general public and not least among children and young people, whose future strongly depend on how we can solve energy and material supply in the future, while meeting climate goals. To increase knowledge and dialogue about mining, permits, land use and how we can use our natural resources in a sustainable way, Metals4U+ work to describe mining and the mineral industry, the scope of the industry and the connection to our everyday lives.

Metals, minerals, and geoscience in schools

To prepare and educate the next generation of professionals, scientists, engineers, and technicians we need to find ways of engaging them in our huge sustainability challenge. With geology/geoscience and natural resources education as natural components in Swedish schools, young people would be equipped with knowledge and tools to solve future sustainable supply of materials for green energy.

In a survey conducted by a pre-study to Metals4U+, 150 school children, age 11 and 14, in Sweden, were asked what they know and feel about the mining industry. The five most common associations to mining were metals, machine, industry, environmental disruption, and natural resource, closely followed by dangerous, pickaxe and waste. The survey shows the urge and importance of working with these questions, implement in schools and find ways to engage the children.

One way to do this is to demonstrate the features of modern autonomous mines: high-technology, safe work, and gender equal environments. But still, the most important thing is the why, what is close to me, my everyday life. The project therefore mainly focuses on increasing the understanding on a personal level of how we are connected to metals and minerals that we use and depend on. This is achieved by creating works of art that have a local connection to mining, complemented with digital educational tools made available for schools via a web-based learning platform (Figure 1).

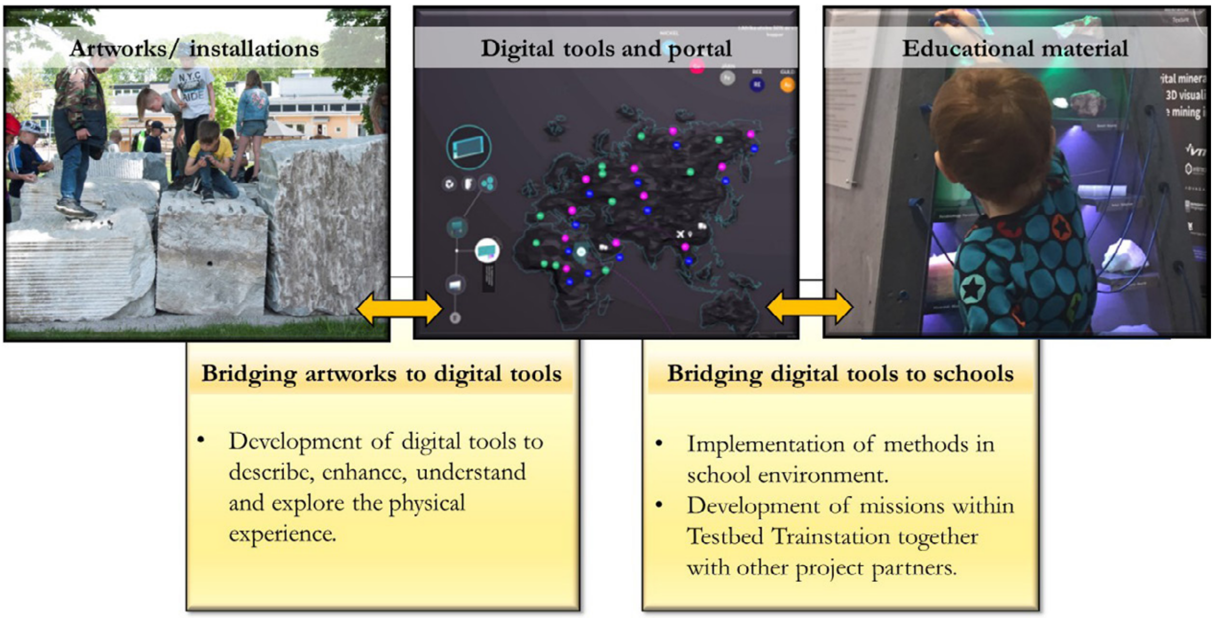

Figure 1. Summative figure of different blocks in the project Metals4U+, and how they are connected.

The project develops physical installations (interactive exhibitions, works of art, and geologically interesting sites) amended with digital tools that explain, further explore or in other ways contribute to a deeper understanding of metals and minerals in our modern society. Questions like how a rock feels like – is it light or heavy? hard or soft? does it smell? can be combined with a digital experience, for instance a measurement saying what the density of this rock is, making it possible also to compare with other rocks.

Studies of the human brain and its way of storing information have shown that when the brain can connect information to a feeling or experience, as when we use multiple senses, e.g. being able to touch, smell, and listen, we get an increased capacity for memorization and understanding (Boström & Svantesson 1998; Dunn et al. 1992). When we use both sides of the brain, we get a complete picture and understand the context. The success of more self-exploring and close to reality assignments were also shown in a study by Sartz & Bäckström (2014), when pupils in ages 13–15 had their own real research projects running at the school. This also showed the importance of open questions, that there were real questions, and someone was truly interested in their results.

Starting point of the work is around four physical installations: Skellefteå in the north, Askersund and "Blue Marble" *Örebro* in mid Sweden and "Geonodes Skåne" in the south. Installation in Skellefteå focus on an interactive mining exhibition at science center Exploratoriet, whereas the installation in Skåne consists of geologically interesting sites with remnants from past mining, industrial heritage, and even dinosaurs. By works of art people are reached at another level, and questions arise that come from ourselves.

Digital tools, educational portal, and mining map

Digital tools are incorporated in a portal, together with previously produced information and educational tools, such as MineFacts, Geologisk, and Minecraft BetterGeo. From there the project moves into developing educational modules and missions, together with science centers and industry partners, suitable for school environment and connected to the school curriculum.

An interactive mining map with information on national and global production of metals and minerals: import, export, and recycling, is further developed from its current form to fit the purposes and needs for the starting page of the educational portal.

Educational material is developed at makerspace/learning lab and testbed Trainstation Vivalla, using the methodology of "missions and skills". Each educational area contains several missions, and to complete the mission, you need to master the skills it is comprised of. Missions are related to school curriculum and the skills pupils get can be found in the curriculum´s central content. The way children can learn, with a more self-exploring and lust-filled methodology, creates a drive and a will to want to learn more. Trainstation methodology offers new ways of learning and thereby gives the children essential survival tools for the future.

References

Boström, L. & Svantesson, I. (1998) *Inlärningsstilar i praktiken*.

Dunn, R., Dunn, K. & Treffinger, D.J. (1992) Alla barn är begåvade – på sitt sätt. *John Wiley & Sons, Inc*.

Sartz, L. & Bäckström, M. 2014: Chemistry and environmental science research as a part of education – an example from Sweden. In: Oral, A.Y. and Bahsi, Z.B. (eds.) 1st International Congress and Exhibition on Current Trends on Science and Technology Education. Pp. 27-32; SCITEED 2014, ISBN 978-1-63266-650-5.

Rocks, Facades, and Pavements of Uppsala – Interactive Geochase to Enhance the Learning Outcome

Thorben Schöfisch[a], Teun Vogel[b]

[a] Department of Earth Sciences, Uppsala University, Uppsala, Sweden, thorben.schofisch@geo.uu.se;
[b] Department of Environmental Sciences, Wageningen University, Wageningen, Netherlands;

Summary. The city centre of Uppsala provides a great opportunity for teaching basics in Geosciences and the rock cycle. With the help of the Peek app, an interactive chase trough the city is developed and engages students to enhance fundamental knowledge and skills in Geosciences. The usage of an app unburdens the lecturer with administrational and technical problems. The Geochase as additional teaching activity has a great potential to improve the learning outcome of the students. Feedback from students suggests integration of interactive geochase into curriculum among field trips.

Interactive Geochase through Uppsala as teaching activity to enhance the learning outcome

At the beginning of the Covid19-pandemic, field trips in the subject Geology were postponed or cancelled. Lectures in Geology around the globe adapted to the current circumstances and developed several ideas to provide alternatives to the students and to compensate the missing learning experiences form field work (Toy et al., 2021). Learning experiences from field work are an increase in knowledge and the gain of skills that are related to the studied subject (e.g. soft skills as teamwork, social interactivity, learn how to make observation and noting them down etc). However, the organisation and logistics of a field work take a lot of time for lecturers and lot of knowledge does not reach every student during the field work. To compensate a field trip for undergraduate students, in which basic geology and rock analyses are taught, an alternative is created by an geologic tour/chase through the city centre of Uppsala. Small groups of students were asked to walk around the city centre and to answer certain geoscientific questions at different locations that show rocks or other geological features (Fig. 1). The questionary was designed to cover different aspects of the rock cycle, identifying rocks, and fundamental concepts in Geosciences.

The city centre of Uppsala provides a great opportunity to study different types of rock and to refer to fundamental concepts of Geosciences. Many facades, pavements or sculptures in Uppsala are made out of different magmatic, metamorphic or sedimentary rocks. Especially, the cathedral provides a great overview from hidden fossils in the pavement up to pillars made out of marble. Moreover, the rock gardens of SGU, Geocentrum, and the Botanical Garden of Uppsala contain a large variety of rocks. The castle of Uppsala is located on top of an esker and from a view point next to the castle, basic concepts of isotacy and geomorphology can be taught. Additionally, typical Swedish red houses, oxidsed copper roofs, iron bridges or bridges made out of concrete with little stalactites have a potential to illustrate geochemistry and to give insights in mining. The river Fyrisån with fish stairs and the old pump house provide information about geo-ecology and hydrology. Several interdisciplinary relations and links can be made during the chase and challenges in Geosciences can be highlighted (not forgetting about the Sustainable Development Goals).

The geochase was initiated by pen and paper, which has the advantage to make sketches and to formulate detailed observations from the location. However, evaluating the answers of the questionary with lots of free text and sketches takes a lot of time. To save time, the geochase was transferred to an app, called *Peek* (peek.app), which was developed by Wageningen University. The app makes the chase interactive and provides a better overview of the participants and answers for the lecturer during and after the chase. Also, it provides additonal fun, enhances decision-making, and stimulates the active engagement of the students. The app is userfriendly and saves time as it unburdens the lecturer in administrational and technical problems during developing a field trip. Feedback of the students is collected for improving the geochase and to discuss the usage of pen and paper or the Peek app. The stu-

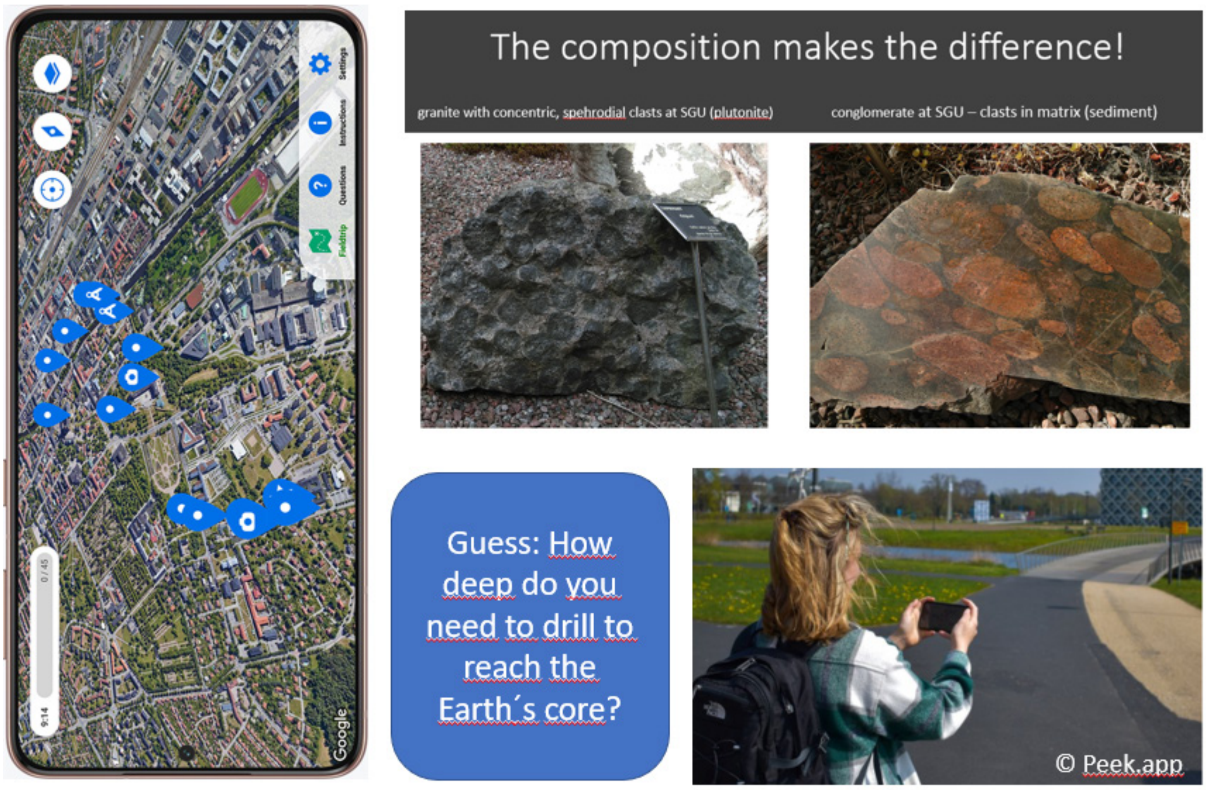

Figure 1: Schematic overview of the app with map showing the geochase locations of Uppsala (left), potential information about rocks and questions (top right and middle), and student how received a question on the app while walking through the chase (bottom right).

dents loved this alternative "field work" and stated that they walk now differently through the city and seeing "geology" everywhere. Such gamification of transfering knowledge to students with the interactive geochase, claims to has an sustainable impression to the students and basic concepts of geology are manifested. The students enjoyed the interactive geochase and suggest to include the geochase into the curriculum although the original field trips take place again after the pandemic.

In conclusion, a combination of the geochase and the *Peek app* has a great potential to support lecturers, to improve the teaching method, and to enhance the learning outcomes of the students. The interactive geochase provides an additional learning activity for basic geology courses and enriches teaching in Geosciences.

References

Toy, V.; Villeneuve, M.; Buckley, S.; Whitmeyer, S. & Buiter, S. (Eds), 2021: Virtual geoscience education resources. *Special Issue of Solid Earth and Geoscience Communication*

GNIST – creating opportunities using the geological heritage in Sweden and Norway.

Linda M. Wickström[a], Rolv Dahl[b], Nelly Aroka[a]

[a]Geological Survey of Sweden, Box 670 75128 Uppsala, Sweden, linda.wickstrom@sgu.se, nelly.aroka@sgu.se ,[b]Geological Survey of Norway,Box 6315 Torgarden NO-7491 Trondheim, Norway, rolv.dahl@ngu.no

Summary. Including geology in the development of the local economy through geotourism is not something new. Geoparks have been doing this for more than 20 years, but not all areas fulfill the requirements of a geopark. The GNIST project aims to target local buisnesses and the usual visitor to the increase the interest of geology and the knowledge of geological sites suitable for tourism developement. Through new geological exhibitons at Naturum Dalarna and Naturum Fulufjället, visitors and local entrepeneurs can get access to the latest geological knowledge.

A common method for assessing the geological conditions has been implemented to sites in Norway and Sweden and data is stored in databases at SGU and NGU. Information about the sites in both countries is displayed together in webmap services.

Tourism is one of the basic industries in Scandinavia and before the Covid-19 pandemic tourism in Sweden had a revenue of 2,4–2,7% of the GDP. Geotourism is part of the nature and culture tourism and today there are several examples where buisnesses, organisations and destinations incorporate geology in their portfolio. The development of geoparks is one such example where areas with interesting geology turn into destinations. These areas can also serve as role models and inspiration for others on how to include geology in the local sustainable economy.

As geologist we know that geology in itself has the ability to create oceans of opportunities within tourism and therefore geology will continue to be an innovation within the sector. Sustainable geotourism is the future and necessary in the promotion and use of geoloigcal sites within the development of destination areas where geology is a natural part. i.e. geoparks, world heritage sites with geological values, protected areas with geological values (e.g. national parks and nature and cultural reserves) or mines with visitor opportunities. A prerequisite for sustainable geotourism is good practice of geoconservation and land use planning. These are areas of expertise that require good knowledge about geodiversity and geoheritage in order to facilitate maintainence and availability of the geoloigcal sites.

GNIST (2020–2022) (Geologisk arv i Naturbasert Innovasjon for Skandinavisk Turisme; Geologiskt arv i Naturbaserad innovation för Skandinavisk Turism) is a project within Interreg Sweden-Norway, aiming to develop the nature and culture tourism in the west of Dalarna, Sweden and Innlandet, Norway through the target audience which includes nature and culture guides, local museums, Geopark Siljan and bodies managing protected areas and other geological sites used in tourism. GNIST is a follow up project of GEARS (2016–2019), where the method to describe and assess geological sites was developed. GNIST partners are SGU (Geological Survey of Sweden), NGU (Geological Survey of Norway), County Administrative Board of Dalarna, Visit Dalarna, the council of Rättvik, Norske Parker and NINA (Norweigan institute for nature research).

GNIST offer platforms to create increased geological knowledge within the tourism industry in the project area. It involves a new approach of landscape characterisation including geological features, the development of a transnational webmap service including sites of geological interest in both Sweden and Norway, new geological exhibitions at Naturum Dalarna and Naturum Fulufjället and a marketing platform within Geopark Siljan. Local organisations and small buisnesses have been involved to create user stories and provide feedback on the different outcomes. The new exhibitions will also serve as knowledge banks in the area and the marketing kit will provide a common approach for communication within Geopark Siljan.

Interviews with the nature, culture and experience tourism show that there is a demand of geological knowledge, but these businesses can rarely participate in traditional education offers, since it means days with lack of income. Their need is to be able to explain and describe the local and regional geological and geomorphologial conditions. Therefore, GNIST offered a web-based lecture series on interpretation and regional geology for those with a non-geological background with focus on the conditions in the Siljan area and along the Swedish-Norwegian border in western Dalarna and Trysil. It was very popular and attracted more than 100 participants, mainly from the project area of Innlandet (Norway) and Dalarna (Sweden), but also from Finland and Faeroe islands. Geological information about sites of interest have been collected from the literature, using LIDAR and during field work in Sweden and Norway. We have implemented the method developed in GEARS (Lundqvist and Dalh eds) in the process of describing and assessing the geological importance of sites.

Information about the sites have been registered in the new databases for sites of geological interest at SGU and NGU using ESRI-based mobile apps for field data collection and webapps for desktop registration. Throughout the project different needs have developed in the two countries and it has been taken into consideration during database development. Data is stored in open-access databases according to FAIR principles (Findable, Accessible, Interoperable and Reusable). In Sweden data will be available through the webmap service and open data of the entire database available through the SGU website.

References

Lundqvist, S. & Dahl, R., (eds) 2020: Slutrapport för projekt inom Interreg Sverige-NorgeSlutrapport GEARS. *SGU-rapport 2020-25*. 311 pp.

General Session 4
150 years anniversary – the evolution of geoscience through time

Session Chair:
Jörgen Langhof (Jorgen.langhof@nrm.se)

Speaking of anniversaries: Who was the first modern mineralogist?

Dan Holtstam

Department of Geosciences, Swedish Museum of Natural History, Stockholm, Sweden, dan.holtstam@nrm.se

Summary. Mineralogy is an old science that has evolved since prehistoric times. An outstanding figure in the early modern period was Axel Fredrik Cronstedt (1722–1765), who dicovered new minerals and metals, and made effective use of the blowpipe in qualitative analysis. He created a revolutionary system for classification of minerals, based on chemical characteristics, that gave significant impetus to the development of modern mineralogical taxonomy.

Introduction

Mineralogy is among the oldest sciences and a core discpline of geology. Already in the Neolithic period, the recognition and use of various minerals was important knowledge for humans. Writers of the Antiquity on the subject, Theophrastus and Pliny the Elder, treated rocks and minerals from a natural-philosophical point of view. Polymaths like Avicenna (Persia) and Shen Kuo (China) in the 11th century AD also documented the minerals known to exist then. European authors of the Renaissance, with Georgius Agricola as the foremost, used the intrinsic physical properties of minerals to describe and classify them in systematic way, an approach that essentially established mineralogy as a science. In Sweden, there was little development in the field before the 18th century (a notable exception is the contributions of Urban Hjärne). During the Age of Liberty, works relating to various aspects of minerals, by natural scientists like Johan Gottschalk Wallerius, Henrik Teofil Scheffer, Carl Linnaeus and Torbern Bergman, came to have a wide influence, far beyond Sweden's borders. Among the mineralogists active in this dynamic period, Axel Fredrik Cronstedt stands out as an exeptionally innovative and forsighted character.

Cronstedt's contributions to mineralogy

Cronstedt was born 300 years ago, on December 23, 1722 (for biographical data, see e.g. Zenzén 1931). He attended lectures at Uppsala University at the age of 16, and three years later joined the Board of Mines (*Bergskollegium*), where he remained until his premature death in 1765. Among his mentors, tutors and friends were the premier mining experts and chemists of the time: Daniel Tilas, Sven Rinman, Wallerius and Georg Brandt. In addition to multifarious administrative duties as a mining official, Cronstedt conducted investigations of minerals and ores, using the blowpipe, calcination and other state-of-the-art methods (he set up his own chemical laboratory). He discovered nickel during investigations of ore samples from the Los cobalt mine, presumably containing gersdorffite. The name was derived from *kupfernickel* (old designation for nickeline), shown by him to contain the new metal as well. Some of Cronstedt's observations also paved the way for future discoveries of new minerals and metals. In a short article (seven pages) published in 1751, he carefully reported properties of three minerals that later came to be named cerite-(Ce), scheelite and hisingerite.

In 1756, Cronstedt described a new kind of mineral, a zeolite. He introduced the name, meaning "boiling stone" in Greek, because of the loosely bound water molecules that produce visible steam on heating. Members of the zeolite mineral family of framework-structured aluminum-silicates have proved very useful in numerous technical applications. The zeolite facies defines the lowest degree of metamorphism in petrology. A search for "zeolite" in Google Scholar gives more than one million hits, 266 years after Cronstedt's original publication.

Cronstedt's greatest achievement, at least as it was perceived by his contemporaries and in the decades following his death, was the system for classification and identification of earth materials he designed. A leave of absence from his official duties allowed him to produce a comprehensive manuscript and it was published anonymously in 1758, with many editions printed thereafter, in several languages including one in English (Cronstedt 1770). Four main classes (*flockar*) were recognized: earths, inflammables, salts and metals, based on reactions upon heat, solubility in water or oil, and ductility. The earths (*jordar*) encompasses most of the present classes of modern nomenclature (oxides, carbonates, sulphates, silicates) and was in turn divided into nine orders (*avdelningar*). In the introduction the author states: "The Mineral Kingdom contains all those bodies which have been formed under the surface of our Earth, whether at the first creation, or any other time since that period… ". From the general definition, it is implicit that minerals are naturally formed and of inorganic nature, and that the mineral world is not static.

In the novel system, Cronstedt emphasised chemical constituents as a basis for classification. These were determined qualitatively by observation of melting reactions, treatment with acids etc. A practical prerequisite for the new approach was that chemical analyses could be carried out in a simple way; the refinement of the blowpipe technique by Swedish chemists in this period was crucial (cf. Abney Salomon 2019). Previous authors on the subject, like Linnaeus, who organized all known species including those of the mineral kingdom in *Systema Naturae*, entirely used external physical properties like shape (morphology), colour, density, hardness etc. as a basis for classification. Some contemporaneous, less well-known systems, by e.g. Magnus von Bromell and Wallerius, were mixed in the sense that chemical properties to a certain extent were considered as well. With Cronstedt, a transparent crystal of calcite and a piece of compact grey marble logically belongs to the same category (pure calcareous earths, *rena kalkarter* = calcium carbonate). He also made clear for the first time that there is a fundamental difference between minerals and compound rocks (*hällearter*; treated in a separate appendix), and he eschewed things that do not belong to the mineral kingdom, like fossils and calculi.

Discussion

Johann Gottlob Werner, in his widely spread mineral classification of 1789, used the same four classes as Cronstedt, and several other elements borrowed from his system; there was, however, still a strong emphasis on the traditional physical properties for determinations. It was not until the work of Jacob Berzelius, more than half a century after Cronstedt's publication, that a system entirely relying on chemistry could be adopted (ultimately based on the type of anions or anion complexes). In the late 18th century, analysis of the crystal forms of minerals and measurement of interfacial angles laid the foundation for a parallel, crystallographic classification system, with René Just Haüy as the main proponent. In mineral taxonomy, there are thus three main lines historically, with focus on physical character, crystallography or chemistry, respectively. Only the last one reflects the temporal character of Earth's mineralogy, i.e. mineral evolution due to chemical differentiation, and in this sense it has triumphed over the other two (Heaney 2016).

There are a few personalities in the history of science that can be considered for the epithet "the first modern mineralogist", but Cronstedt is certainly one of the strongest candidates. "Modernity" is often linked to the Enlightenment, and Cronstedt is associated with that movement. It might also be noticed that Cronstedt was "modern" in the sense that he was very critical towards alchemy, which still was held in esteem by some of his contemporary fellow scientists (Fors 2008). He did not create the science of mineralogy, but gave it a solid scientific foundation.

References

Abney Salomon, C.A., 2019: The pocket laboratory: The blowpipe in eighteenth-century Swedish Chemistry. *Ambix, 66*, 1–22.
Cronstedt, A.F., 1770: *An Essay towards a System of Mineralogy*. 1st edition. E. & C. Dilly, London. 329 pp.
Fors, H., 2008: Speaking about the other ones: Swedish chemists on Alchemy, c. 1730-70. *Neighbours and territories: The evolving identity of chemistry. Proceedings, 6th International conference on the history of Chemistry*, 283–290.
Heaney, P.J., 2016: Time's arrow in the trees of life and minerals. *American Mineralogist 10*, 1027–1035.
Zenzén, N., 1931: Axel Fredrik Cronstedt – bergmästare, kemist, mineralog. *Svensk Biografiskt Lexikon 9*, 279–284.

GENERAL SESSION 4 • GEOSCIENCE THROUGH TIME

Ice Ages in Scandinavia – from initial discovery to authorized fact, 1823–1858

Geir Hestmark

Center for Ecological and Evolutionary Synthesis, Department of Biosciences, CEES, University of Oslo, Oslo, Norway, geir.hestmark@ibv.uio.no

Summary. The discovery of Ice Ages was first announced in Scandinavia, when in April 1824 Danish-Norwegian geoscientist Jens Esmark published a paper stating that there was indisputable evidence that Norway and other parts of Northern Europe had previously been covered by enormous glaciers carving out valleys and fjords, depositing moraines and boulders. After doubts and debate extending over decades, the reality of ice ages in Scandinavia was only officially recognized after the first field mappings of soils performed by the newly established Swedish and Norwegian state geological surveys in 1856-58, directed by Axel Erdmann and Theodor Kjerulf.

Putting the pieces together

The discovery of Ice Ages is one of the most revolutionary advances made in the Earth sciences (Frängsmyr 1976, Imbrie & Imbrie 1986, Rudwick 2008, Krüger 2013). In Scandinavia this discovery was made in the late summer of 1823 by Danish-Norwegian geoscientist Jens Esmark and published in April 1824 (Esmark 1824, 1826, Hestmark 2017a, 2018). Esmark's friend, the famous chemist Jacob Berzelius, initially supported Esmark's claim in a review of his paper (Berzelius 1825), but later had doubts.

Although Esmark's Ice age paper has often been seen as coming right out of the blue, recent studies document that his discovery happened on a prepared background: 1) he had a deep and life-long interest in meteorological phenomena, and in effect was the first Norwegian state meteorologist (Hestmark & Nordli 2016); 2) inspired by the 'physiographic' alpine researches of de Saussure, de Luc, Ramond and von Humboldt, Esmark from 1798 and onward made altitude measurements of treelines, snowlines and several of the highest peaks in Norway (Hestmark 2009); 3) to numerous exploreres of Scandinavian glaciers before 1823 he supplied instruments, notably barometres for altitude measurements, and encouragement (Hestmark 2017a).

Esmark's main achievement was one of *synthesis*: Some of the geomorphological phenomena he realized to be caused by a single agent – former enormous glaciers – were well recognized and studied separately before 1823–24. Foremost among these were the abundant *erratic boulders* of various rock types that lie scattered over the North European and North American landscapes.

After the promotion of ice age theories by several Swiss naturalists in the 1830s, the debate raged for several decades in Scandinavia and other parts of Europe, with a continued study of the phenomena, for instance the furrowed and striated rock surfaces (Sefström 1838, Keilhau 1842), and a number of foreign savants making field trips to Scandinavia to assess the pros and cons, e.g. Robert Chambers (Hestmark 2017b).

The official, authorized national recognition of Scandinavian ice ages only came in the second half of the 1850s with establishment of the state geological surveys of Norway and Sweden and their initial mapping and categorizations of the 'unconsolidated terrain', i.e. the loose deposits of gravel, sand and clay forming the meager soils of Scandinavian agriculture (Erdmann 1857, 1868, von Post 1857, Kjerulf 1858, Sars & Kjerulf 1860). One major effect of the Scandinavian glaciations, the *land rise*, was only understood as an ice age effect later (Nordlund 2001).

In commemoration of professor Tore Frängsmyr, Uppsala historian of science and ideas, friend and mentor.

References

Berzelius, J. 1825: Allmänna idéer öfver jordens bildning. Årsberättelse om Framstegen i *Physik och Chemie* [in 1824]. Pp. 282-285 in Årsberättelser om Veten*skapernas Framsteg, afgifne af Kongl. Vetenskaps-Academiens Embetsmän d. 31 Mars 1825*. Stockholm: P. A. Norstedt & Söner.

Erdmann, A. 1857: *Några ord till belysning af den geologiska kartan öfver Fyris-åns dalbäcken.* Stockholm: P.A. Norstedt & Söner.

Erdmann, A. 1868: *Bidrag til Kännedomen om Sveriges Qvartära Bildningar.* Sveriges Geologiska Undersökning, på Offentlig Bekostnad Utförd under Ledning af A. Erdmann. Sammanfattad Redogörelse för dervid vunna Resultater. I. Qvartära Bildningar (Glacial- och Postglacial-Perioderna). Stockholm: P.A. Norstedt & Söner.

Esmark, J. 1824: Bidrag til vor Jordklodes Historie. *Magazin for Naturvidenskaberne*. (Anden Aargangs förste Bind, Förste Hefte) [3], 28-49.

Esmark, J. 1826: Remarks tending to explain the Geological History of the Earth. *The Edinburgh New Philosophical Journal 2* [First part October-December 1826], 107-121.

Frängsmyr, T. 1976: *Upptäckten av istiden. Studier i den moderna geologins framväxt.* Lychnos Bibliotek 2. Uppsala: Almqvist & Wiksell.

Hestmark, G. 2009: «Her ligger sneen evig» – da Dovre falt for Esmarks barometer. *Historisk Tidsskrift 88*, 231-249.

Hestmark, G. 2017a: *Istidens Oppdager. Jens Esmark, pioneren i Norges fjellverden*. Oslo: Kagge Forlag.

Hestmark, G. 2017b: Tracings of the north of Europe: Robert Chambers in search of the Ice Age. *Annals of Science 74*, 262-281.

Hestmark, G. 2018: Jens Esmark's mountain glacier traverse 1823 – the key to his discovery of Ice Ages. *Boreas 47,* 1-10. Open access.

Hestmark, G. & Nordli, Ø. 2016: Jens Esmark's Christiania (Oslo) meteorological observations 1816-1838: The first long term continuous temperature record from the Norwegian capital homogenized and analysed. *Climate of the Past 12*, 2087- 2106. Open access.

Imbrie, J. & Imbrie, K.1986: *Ice Ages. Solving the Mystery.* 2ed. Cambridge. Mass.: Harvard University Press.

Keilhau, B. M. 1842: Om Merkerne efter en almindelig Afskuring, som vort Nordens Klippegrund har været underkastet. *Nyt Magazin for Naturvidenskaberne* 3: 115-168.

Kjerulf, T. 1858: Om Jordbundens Beskaffenhed i en Del af Romeriget og Aker. *Polyteknisk Tidsskrift* Vol. 5 (No. 21, 15 November): 321-332 & No. 22 (30 November): 337-344. Kristiania.

Krüger, T. 2013: *Discovering the Ice Ages: International Reception and Consequences for a Historical Understanding of Climate*. Leiden, Brill.

Nordlund, C. 2001: *Det upphöjda landet: Vetenskapen, landhöjningsfrågan och kartläggningen av Sveriges förflutna 1860-1930*. Acta Regiæ Societatis Skytteanæ nr. 53. Landskapet som arena 3. Umeå.

Post, H. von 1857: Om kross-stensbäddar i Skedvi socken. *Öfversigt af Kongl. Vetenskaps-Akademiens Förhandlingar, 13*. 1856 (No. 9 & 10), 235-241.

Rudwick, M. J. S. 2008: *Worlds Before Adam. The Reconstruction of Geohistory in the Age of Revolution.* Chicago, The University of Chicago Press.

Sars, M. & Kjerulf, T. 1860: *Iagttagelser over den postpliocene eller glaciale Formation i en Del af det sydlige Norge*. Christiania. Universitets-Program for 1ste Halvaaar 1860.

Sefström, N. G. 1838: Undersökning af de räfflor, hvaraf Skandinaviens berg äro med bestämd riktning fårade, samt om deras sannolika uppkomst. *Kongl. Vetenskaps-Academiens Handlingar, för År 1836*, 141-227. Stockholm.

GENERAL SESSION 4 • GEOSCIENCE THROUGH TIME

Geological nomenclature in Sweden

Nils F. Jansson[a], Linda M. Wickström[b], Stefan Bergman[b], Mikael Calner[c], Mark D. Johnson[d], Risto A. Kumpulainen[e], Stephen McLoughlin[f], Peter Bengtson[g], Annika Wasström[h]

[a]Division of Geosciences and Environmental Engineering, Luleå University of Technology, Luleå, Sweden, niljan@ltu.se; [b]Geological Survey of Sweden, Uppsala, Sweden, linda.wickstrom@sgu.se, stefan.bergman@sgu.se; [c]Department of Geology, Lund University, Lund, Sweden, mikael.calner@geol.lu.se, ORCID: 0000-0003-1096-3153; [d]Department of Earth Sciences, University of Gothenburg, Gothenburg, Sweden, markj@gvc.gu.se; [e]Department of Geological Sciences, Stockholm University, Stockholm, Sweden, risto.kumpulainen@geo.su.se, ORCID: 0000-0001-6065-3343; [f]Department of Palaeobiology, Swedish Museum of Natural History, Stockholm, Sweden, steve.mcloughlin@nrm.se;[g]Institute of Earth Sciences, Heidelberg University, Heidelberg, Germany, Peter.Bengtson@geow.uni-heidelberg.de, ORCID: 0000-0002-1186-6382; [h]Exploration, Boliden Mines, Boliden, Sweden, annika.wasstrom@boliden.com

Summary. The geoscience community has long needed national coordination of geological names in Sweden. Issues of formalization, priority, definition, and distribution of stratigraphic units and other geological features have long been matters of contention among Swedish geoscientists. Several years of discussions have led to the publication of a Swedish guide for naming geological units and structures (Kumpulainen 2016) and, in 2019, to the establishment of the Swedish Committee for Geological Nomenclature (SCGN).

The need for a systematic geological nomenclature

Carl von Linné (1707–1778) taught the world to systematize science. He systematized “everything”: the plant kingdom, the animal kingdom and even the ‘stone kingdom’. However, his attempts to systematize the ‘stone kingdom’ turned out to be difficult and complex, and his system is not used today. Nevertheless, his attempts inspired subsequent scientific efforts to increase our knowledge of rocks and minerals, and their systematic classification—work that continues to the present day.

Efforts to rationalize and simplify communication among geologists — and between geologists and the broader community — requires naming and describing rock units of various kinds in a clear and uniform manner. This concerns both the proper *terminology* for classification, which refers to rock and mineral names, geological structures, and processes, all of which should be based on rigorously defined criteria. Clear communication also requires a proper *nomenclature* applied to geological units and structures, which refers to the unique, geographically named 3D bodies and structures. Examples are the File Haidar Formation (which includes the Cambrian sandstone on Kinnekulle) and the Vistas Granite. Over time the meaning of old names may have changed as geological knowledge has advanced; also, different names may have been used for a certain unit by various investigators. If such changes are left undocumented and uncorrected, misunderstandings ensue, with potentially major consequences, such as impeding scientific advances or provoking uninformed decisions during mineral exploration.

The Swedish Committee for Geological Nomenclature (SCGN)

The members of the SCGN are appointed by the Royal Swedish Academy of Sciences, Class V, on proposal of the Swedish National Committee for Geological Sciences.

The main task of the SCGN is to review and to approve or reject proposals for new and revised, currently informal, names of geological units and other geological features in Sweden. This work is restricted to nomenclature; the SCGN does not take a stance on terminological questions. The SCGN makes decisions on proposed names for geological features (formations, lithodemes, complexes, structural features, etc.), but not geographical features. Geographical and geopolitical names are managed by other authorities. The SCGN addresses name proposals for new geological units and proposals for the formalization of existing ones. All existing names are treated as informal until a proposal for formalization that meets the criteria in the "Guide for geological nomenclature in Sweden" (Kumpulainen 2016) has been approved. The SCGN shall also assist the Swedish National Committee for Geological Sciences in communications regarding nomenclatural issues with international sister organizations, including the International Commission on Stratigraphy (www.stratigraphy.org).

More than just stratigraphy

It is important to emphasize that formal nomenclature refers not only to lithified stratigraphic units (such as the Alum Shale Formation). Unlithified Quaternary units can also be defined formally as lithostratigraphic units. The focus so far in Swedish geology has been on litho-, bio-, and chronostratigraphy. However, in a land dominated by crystalline rock, lithodemic units (e.g. intrusions, complexes, and suites), and geological structures (e.g. deformation zones and folds) should also be formally defined. Even large-scale landforms (e.g. peneplains and mountain chains) can be formally named as a geological feature according to the guide. The guide for geological nomenclature (Kumpulainen 2016) and current work of the SCGN emphasize the efforts to formalize units within the extensive Archean and Proterozoic rocks of Sweden. For example, we recognize the need for a more systematic usage of terms, such as 'suite' and 'complex', when referring to plutonic rocks, for which local usage remains problematic.

How to contribute

Anyone can submit a proposal to the SCGN. The committee expects that submissions of proposals for new units or for the formalization of existing names will come from geologists who have in-depth knowledge of the unit or structure in question. The website (https://www.sgu.se/om-geologi/geologiska-namn-i-sverige) provides information about the committee and how to submit a proposal for a new name or to formalize an existing name. Guidelines for approval were published in the journal *GFF* (Kumpulainen 2016). This publication is the official Swedish guide for naming geological units and structures, along with additional information by Kumpulainen et al. (2016) and a recent emendation on the nomenclature of lithodemic units by the SCGN (submitted).

References

Kumpulainen, R.A. (Ed.), 2016: Guide for geological nomenclature in Sweden. *GFF 139* [for 2017], 3–20, DOI: https://dx.doi.org/10.1080/11035897.2016.1178666

Kumpulainen, R.A., Bergman, S. & Claesson, S., 2016: Sweden to review its geological nomenclature. *GFF 139* [for 2017], 1–2, DOI: https://dx.doi.org/10.1080/11035897.2016.1227366

SCGN: Amendment to the term complex in "Guide for geological nomenclature in Sweden" (Kumpulainen 2016). *Submitted to GFF*.

Thematic Session 1
Applied geosciences

Session Chair:
Paul Evins (paul.evins@wsp.com)

Preliminary analysis of the regional distribution of sulfide-bearing rock in the Stockholm area

Immanuel Åhrberg[a], Paul M. Evins[b]

[a]Institution of geoscience, Uppsala university, Uppsala, Sweden. Immanuel.ahrberg@gmail.com
[b]Department of geology and rock engineering, WSP, Stockholm, Sweden. paul.evins@wsp.com

Summary. Results from statistical and spatial analysis of sulfur content in a large dataset of rock samples from Stockholm are presented. Sedimentary gneiss and amphibolite are confirmed as the main lithologies containing elevated sulfur concentrations. Furthermore, trends in the spatial distribution of sulfur concentrations reveal a risk for higher sulfur content in sedimentary gneiss in the southern half of Stockholm.

The last few years have seen a dramatic increase in attention towards acid rock drainage from excavated rock caused by elevated sulfur concentrations in the Stockholm bedrock (e.g. Albyberg, Haninge). Focus has therefore been on sampling procedures and setting classification limits for infrastructure projects that generate large amounts of excavated rock.

To date there has been no statistical or spatial analysis on which lithologies are prone to higher sulfide contents and how they are spatially distributed. This project was hence initiated to gain a better understanding of which lithologies may contain elevated sulfur levels, and their spatial distribution across the city of Stockholm. The total sulfur content of 336 samples included in WSP's internal database taken during various rock engineering projects, as well as from publicly available reports, were digitised and subject to closer examination. Samples were categorized into 7 simplified lithologies based on their field descriptions and compared to Stålhös' (1968) geological map of Stockholm's bedrock. Amphibolite, metatexitic sedimentary gneiss, and sedimentary gneiss have been identified as having the highest risk of elevated sulfur content in the Stockholm bedrock (Figure 1). The spatial distribution of results show that the southern half of Stockholm has an elevated risk to contain high sulfur levels

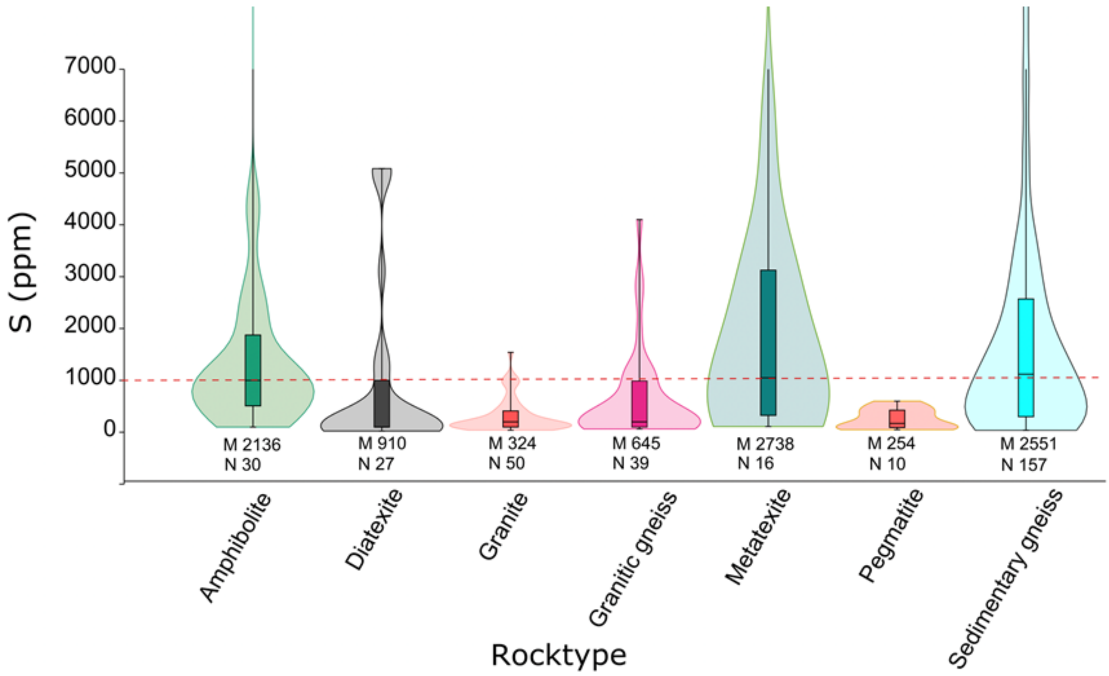

Figure 1. Boxplot and whisker diagrams with symetrical histograms (violin plots) of total sulfur concentrations from the different lithologies of Stockholm. M is the mean value and N is the number of measurements. The red dashed line is the limit upper limit for sulfur concentration for classifying a rock as potentially acid producing according to Fältmarsch (2021).

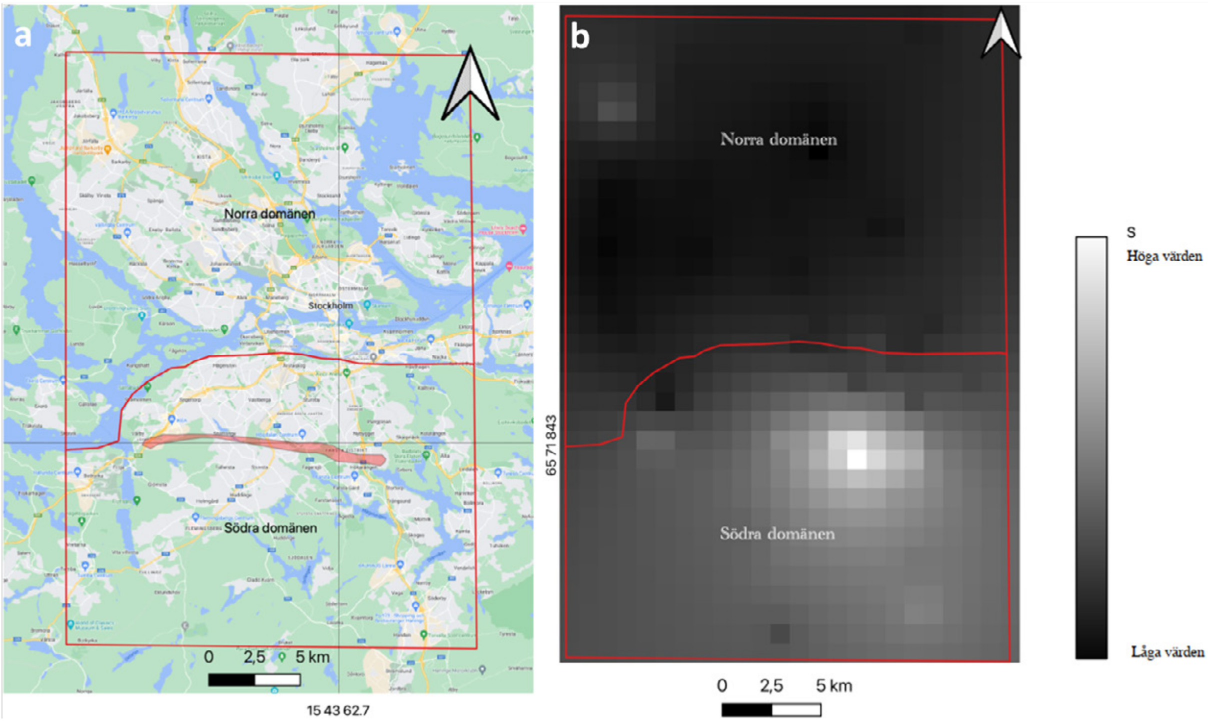

Figure 2. a) Analysed area over Stockholm City framed in red with rough geological subdivsion of Stockholm into northern and southern halves. The red field in the southern half is a lens in the sedimentary gneiss with higher risk for elevated sulfur concentrations in the bedrock. Coordinates are Sweref 99 18 00. b) Inverse distance weighting interpolation of all sulfur concentrations in the study. Lighter shades indicate higher sulfur concentrations.

(Figure 2a). A lens within the sedimentary gneiss in the southern half of Stockholm with particularly high sulfur concentrations has been identified (Figure 2b).

References

Fältmarsch, R., 2021. Vägledning – provtagning och klassificering av sulfidförande berg. *Exploateringskontoret, Stockholms stad.* Dokument E2020-04235. 33 s.

Stålhös, G., 1969: Stockholmstraktens berggrund. *SGU ser. Ba 24*.

Rock strengths of lithologies in Kiirunavaara from point load tests and correlations with other methods

Ulf B. Andersson[a], Georgios Doulamis[b,c]

[a]Luossavaara-Kiirunavaara AB, Research & Development, TG, FK9, SE-981 86 Kiruna, Sweden (ulf.b.andersson@lkab.com), [b]Institute of Earth Sciences, Uppsala University, Villavägen 16, 752 36 Uppsala, [c]Avannaa Exploration Services AB. Blockvägen 27, 981 42 Kiruna, Sweden (geodoulamis@gmail.com).

Summary. About 6350 point load tests have been performed on rocks from the Kiirunavaara area and evaluated with respect to lithology and alteration, as well as correlated to Leeb hardness and uniaxial compressive strength. Country rocks to the iron ore have high rock strengths, particularly the trachyandesites of the foot wall, while the ore has significantly lower strength. Correlations to the Leeb hardness scale are poor because different rock properties are tested in each respective method. Correlation factors between point load and uniaxial compressive strengths are rock specific and higher for harder than for softer rocks.

Background

Point load testing (PLT) was developed by Broch & Franklin (1972) as a method of testing the strength of rocks in a quick and practical way, without any additional specimen preparation. The method can be used on drill cores (axial or diametral) or hand samples and the technique has been formalised by ISRM (1985) and ASTM (2008). The device consists of two steel cones in between which the samples are mounted and compressed until failure when a maximum load is read on a manometer. The results are then normalized to $I_s(50)$ following the formalized procedure to the equivalent of a diametral test on a 50 mm core.

In this project, 5236 previously PLT tested samples in the LKAB database and 1113 new tests were evaluated with respect to lithology and type of alteration. In addition, 569 measurements of the Leeb hardness test (LHT) method (Leeb 1979) were performed and correlated with the PLT results. The Leeb method is based on the rebound velocity relative to the incident velocity (L_D) on the rock surface by a 3 mm hardened steel ball. In addition, based on previous data sets of uniaxial compressive strength tests (UCS) (Andersson 2021), correlation factors of PLT to UCS were calculated for a number of lithologies and compared with previous data.

Results and discussion

The PLT data show large variations within, but also overlaps between lithologies (Fig. 1). The least altered country rocks to the iron ore show the highest strengths with $I_s(50)$ 11–19 MPa for the foot wall trachyandesites and 10–14 MPa for the hanging wall rhyodacites, while ore types generally are lower, 6–11 MPa. Among the altered varieties, clay, mica, and sulphate alterations tend to give the lowest values, while alterations by silicate minerals give the highest values, but with some aberrant results.

The LHT results are completely overlapping for all country rock lithologies in the range 800–900 L_D, while the ore types fall in the range 600–700, and anhydrite at c. 500 L_D. The correlation between PLT and LHT is rather poor (Fig. 2). The LHT tests the mineral hardness/elasticity of the rock surface, while the PLT tests the tensional strength of the whole rock piece, and the methods are thus not equivalent.

The correlation factors for converting PLT to UCS have been calculated using an extensive UCS compilation for Kiirunavaara (Andersson 2021). These range from 13 to 30, depending on lithology (Fig. 3). For strong lithologies they are mostly in the range 25–30 while for less strong types they vary from 13 to 20, similarly to previous estimates (Lindgren & Andersson 2014; Vatcher et al. 2016). Such variations between softer and harder lithologies have typically been reported also by other workers and various conversion formulas suggested (e.g. Kahraman 2001; Fener et al. 2005; Singh et al. 2012).

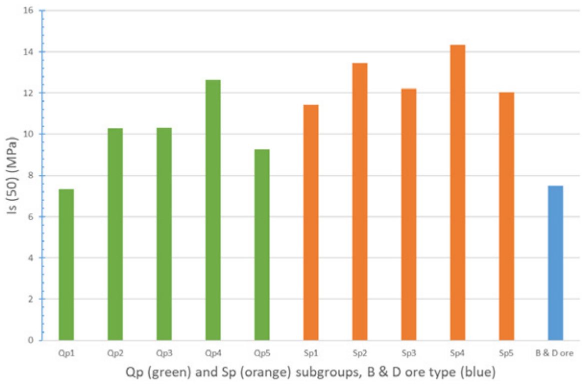

Figure 1. Average PLT results for mineralogical varieties in the country rock. Qp is rhyodacites of the hanging wall and Sp is trachyandesites of the foot wall. B ore is pure, high-Fe, and D ore is apatite-containing.

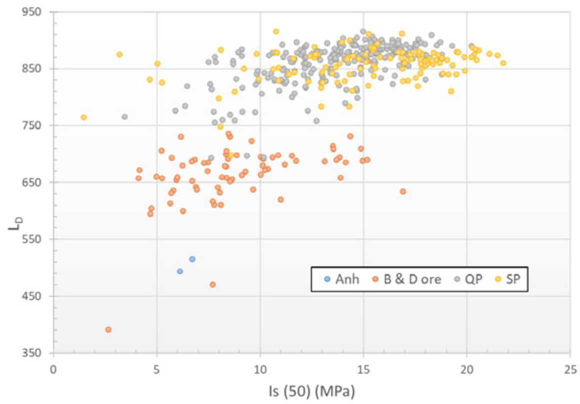

Figure 2. 569 PLT and LHT results for the same rock samples, indicating the poor correlation.

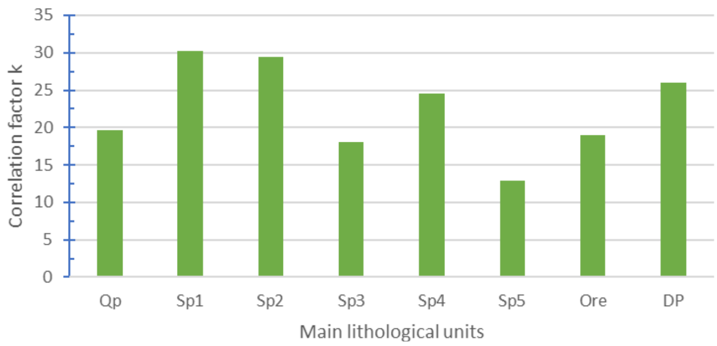

Figure 3. PLT to UCS correlation factors for various lithologies showing the lithology specific nature of the correlation factor. DP is dyke porphyry.

Conclusions

The unaltered country rocks to the Kiirunavaara ore body generally show high rock strengths, particularly the trachyandesites of the foot wall, while ore and altered lithologies generally show lower strengths, as expected. The present extensive PLT data set in conjunction with the compilations of UCS data of the same lithologies clearly indicate that the correlation factors are lithology specific and lower for softer rocks compared with harder ones. The LHT cannot substitute for the PLT, as the correlation between the two is poor and they test different properties of the rock.

References

Andersson, U.B., 2021: Compilation and evaluation of uniaxial compressive strength tests of rocks from Kiirunavaara. *LKAB Investigation 2021-20061,* 20 pp. + App. 5 pp.

ASTM D5731-08., 2008: Standard Test Method for Determination of the Point Load Strength Index of Rock and Application to Rock Strength Classifications. 11 pp. doi:10.1520/D5731-08

Broch, E., & Franklin, J. A., 1972: The point-load strength test. *International Journal of Rock Mechanics and Mining Sciences And*, *9*(6), 669–676.

Fener M., Kahraman S., Bilgil A. & Gunaydin O., 2005: A comparativa evaluation of indirect methods to estimate the compressive strength of rocks. Technical note. *Roch Mech. Rock Engng. 38* (4), 329-343.

ISRM, 1985: Suggested Method for determining point load strength. ISRM Commission on Testing Methods. *Int. J. Rock Mech. Min. Sci. & Geomech, Abstr. 22*(2), 51-60.

Kahraman, S., 2001: Evaluation of simple methods for assessing the uniaxial compressive strength of rock. *Int. J. Reock Mech. Mining Sci. 38,* 981-994.

Leeb, D., 1979: Dynamic hardness testing of metallic materials. *Non Destructive Testing International, 12(6),* 274-278.

Lindgren, K. & Andersson, U.B., 2014: Observations from point load testing of variable rock types in the footwall of the Kiirunavaara iron ore, northernmost Sweden. *31st Nordic Geological Wintermeeting, Lund 2014.* Abstracts vol. p. 48.

Singh, T. N., Kainthola, A., & Venkatesh, A., 2012: Correlation between point load index and uniaxial compressive strength for different rock types. *Rock Mechanics and Rock Engineering*, *45*(2), 259–264.

Mapping by pictures: simplified rock mass classification for better consistency

Paul M. Evins

WSP, Stockholm, Sweden, paul.evins@wsp.com

Summary. A picture-based, simplified rock mass classification based on the Geological Strength Index (GSI) system (Hoek et al. 2013) has been developed and tested. The resulting rock mass classification system reduced subjectivity between observers, streamlined the mapping process and improved consistency.

The most common rock mass classification systems are fraught with well-known weaknesses. The most common criticisms of the Q system (Barton et al. 1974) are the subjectivity in joint roughness (Jr) and scale-dependence of the number of joint sets (Jn). The Rock Mass Rating (RMR) system (Bieniawski 1989) suffers from subjectivity in several of the parameters. The Rock Quality Designation (RQD) parameter (Deere 1968) present in both systems is also inferior to fracture frequency. These uncertainties lead to such inconsistency between geologists' classification to a degree that the same rock mass may fall into 3 different rock support classes depending on each geologist's estimation. Furthermore, Q and RMR mapping can cost precious production time in infrastructure projects. Example sketches or photographs of different classes of blockiness and fracture quality reduces this subjectivity and can be applied to the simpler, two-variable GSI rock mass classification system (Figure 1). Direct comparison of these pictures to the observed rock mass determines the variables and reduces

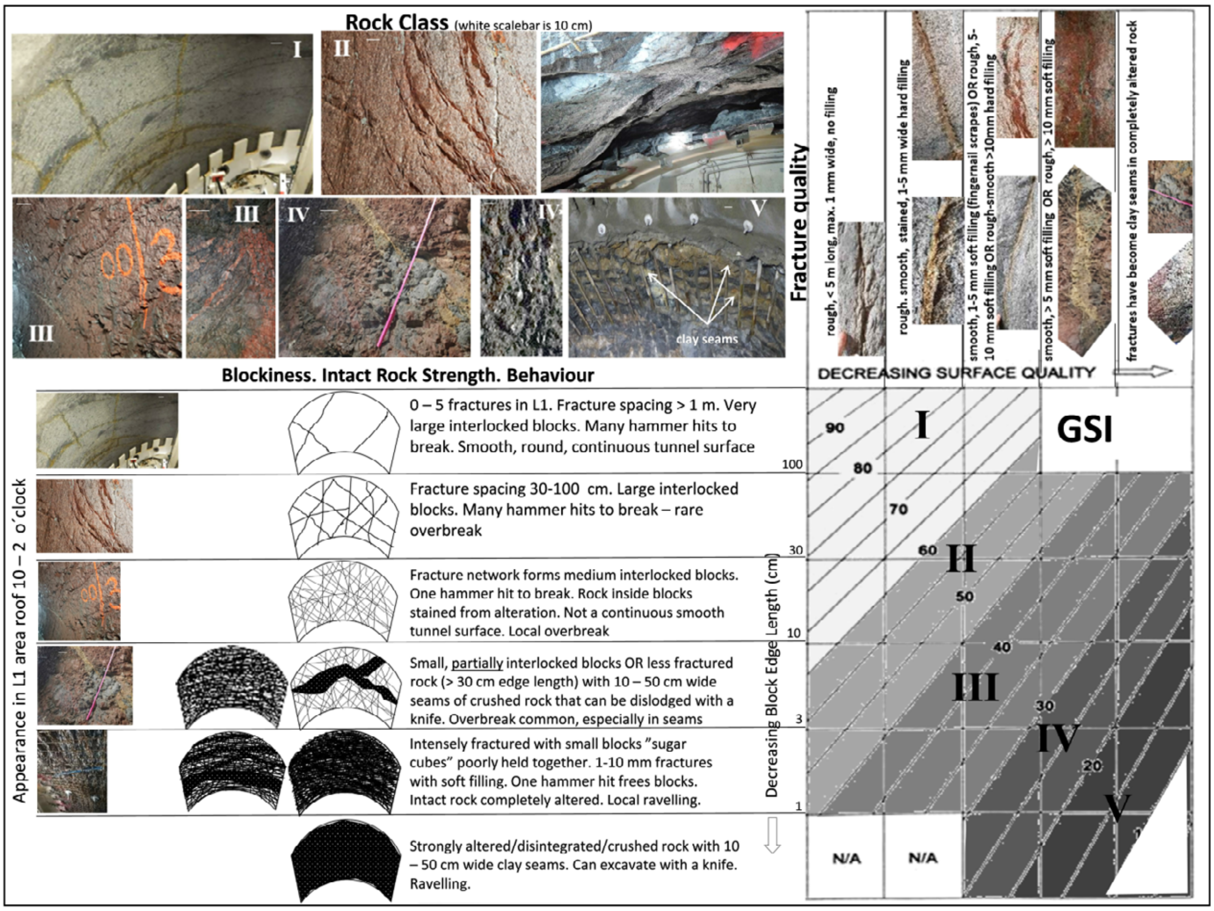

Figure 1. Simplified, picture-based rock mass classification for a TBM tunnel based on GSI.

subjectivity and mapping time. This picture-based, modified GSI classification was tested on geologists, engineers and site managers and implemented in an infrastructure project. The resulting rock mass classification system streamlined the mapping process and provided more consistency between all parties.

References

Barton N.R., Lien R., & Lunde J., 1974. Engineering classification of rock masses for the design of tunnel support. *Rock Mechanics,* 6, 189–236.

Bieniawski, Z., 1989. *Engineering rock mass classification*. New York: Wiley Interscience.

Deere, D.U. 1968. Geological considerations. In *Rock mechanics in engineering practice*, *Chapter 1*. Editors K.G. Stagg and O.C. Zienkiewicz. Wiley, New York. 1–20.

Hoek, E., Carter, T. & Diederichs, M., 2013. Quantification of the Geological Strength Index Chart. *San Francisco, American Rock Mechanics Association,* p. 9.

Seismic risk assessment in the post-closure safety analysis of the planned Swedish repository for spent nuclear fuel

Susanne Grigull, Frederic Wagner, Jenny Gåling

Svensk Kärnbränslehantering AB (SKB), Box 3091, 169 03 Solna, Sweden. susanne.grigull@skb.se

Summary. We present SKB's approach to handle seismic risk in the post-closure safety analysis of the planned geological repository for spent nuclear fuel in Forsmark, Sweden.

The Swedish Nuclear Fuel and Waste Management Organisation (SKB) have obtained a permit to construct a geological repository for spent nuclear fuel at c. 450 m depth in crystalline bedrock at Forsmark, Sweden. The long half-life of the radioactive material requires the post-closure safety assessment for the repository to cover at least 100 000 years (i.e. at least until after the next glaciation) and even up to 1 000 000 years.

As part of the Fennoscandian Shield, Sweden is today considered to be a region with low seismic activity. However, clear evidence of episodic paleoseismicity in Sweden and elsewhere exists in the form of so-called Glacially Triggered Faults (GTFs) (Lagerbäck & Sundh 2008, see also Steffen et al. (eds) 2022). This special kind of intraplate faulting is thought to have been triggered, predominantly, by excess horizontal stresses and elevated fluid pressure after the latest deglaciation and to have resulted in large earthquakes (M>8) especially in northern Scandinavia (e.g. Arvidsson 1996, Lindblom et al. 2015). Therefore, due to the long period of time covered by the safety assessment, the possibility of large future earthquakes needs to be considered and the risk of damage to the future repository needs to be assessed.

Seismic hazard analysis (SHA) in low-seismicity regions is challenging and a probabilistic approach (PSHA) is not necessarily the most conservative way to estimate seismic risk, especially in view of the long time intervals in question. Amongst others, this is because the recurrence intervals for high magnitude earthquakes are on the order of, or longer than, the time period of instrumental observation, and the episodicity of seismic fault activity is afflicted by high uncertainty.

We present the approach adapted by SKB to assess and handle the seismic risk for the spent nuclear fuel repository after closure. The method involves:

- deterministic numerical and probabilistic modelling
- structural geological modelling
- discrete fracture network modelling
- rock mechanical modelling
- and results of paleoseismic investigations of GTFs

The outcomes are ultimately one factor affecting the design of the repository. The method has been under constant development for the past 20 years or more (e.g. Munier & Hökmark 2004, Hökmark et al. 2019).

References

Arvidsson, R., 1996. Fennoscandian earthquakes: whole crustal rupturing related to postglacial rebound, Science, 274, 744–746.

Hökmark H., Fälth B., Lönnqvist M., Munier R., 2019. Earthquake simulations performed to assess the long-term safety of a KBS-3 repository. SKB TR-19-19, Svensk Kärnbränslehantering AB.

Lagerbäck R., Sundh M., 2008. Early Holocene faulting and paleoseismicity in northern Sweden. SGU C 836. Sveriges geologiska undersökning.

Lindblom E., Lund B., Tryggvason A., Uski M., Böðvarsson R., Juhlin C., Roberts R., 2015. Microearthquakes illuminate the deep structure of the endglacial Pärvie fault, northern Sweden. Geophys. J. Int., 201, 1704-1716.
Munier R., Hökmark H., 2004. Respect distances. Rationale and means of computation. SKB R-04-17, Svensk Kärnbränslehantering AB.
Steffen H., Olsesen O., Sutinen R. (eds.), 2022. Glacially-triggered faulting. Cambridge University Press, 438 pp.

Experimental program to study scale effects on mechanical properties of large rock fractures

Lars Jacobsson[a], Diego Mas Ivars[b,d], Hossein A. Kasani[c], Fredrik Johansson[d]

[a]Department of Chemistry and Applied Mechanics, RISE Research Institutes of Sweden, Borås, Sweden, lars.jacobsson@ri.se; [b]SKB, Swedish Nuclear Fuel and Waste Management Company, Stockholm, Sweden, diego.masivars@skb.se; [c]Nuclear Waste Management Organization (NWMO), Toronto, ON, Canada, hkasani@nwmo.ca; [d]Division of Soil and Rock Mechanics, Department of Civil and Architectural Engineering, KTH Royal Institute of Technology, Stockholm, Sweden, fredrik.johansson@byv.kth.se

Summary. The scale effect of natural and artifically induced rock fractures and replicas up to a 500 mm length are experimentally studied by direct shear tests in a testing program including a newly manufactured large shear testing equipment. The fractures are chatacterised pre-, syn-, and post-shear test. Combinations of different measurements provide a high-quality dataset enabling deeper understanding of, and constitutive model development for rock fractures used for safety assessment of deep geological respoitories for nuclear waste disposal.

Background and motivation

Fracture displacement around a geological repository for spent nuclear fuel is one of the factors considered in the safety assessment of the repository. A hypothetical scenario is a secondary fracture undergoing shear displacement in excess of 50 mm during an earthquake following glacial retreat. If such a fracture intersects deposition holes it is considered a threat to the integrity of the copper canister in the KBS-3 repository concept (SKB 2011).

The POST project (Siren et al. 2017), a collaboration between the nuclear waste management organizations of Finland, Sweden and Canada, aimed to develop predictions for the onset and magnitude of shear slip along large fractures at depths of approximately 400 m in a sparsely fractured crystalline rock mass. There are several practical problems associated with studying shear displacement at depth including lack of understanding of the scale (size) effects, limitations of current constitutive models which are generally based on small scale laboratory direct shear test results, and lack of available large scale direct shear equipment with the capacity to apply normal stresses and contant normal stiffness (CNS) values representative of greater depths. Therefore, it was recommended to investigate the scale effect of natural rock fractures under controlled laboratory conditions to increase the accuracy and reduce the cost compared to in-situ experiements and by full scale replicas of rock joints to permit controlled parameteric studies.

Experimental program

This project is a sequel to the POST project and the experimental program is based on the recommendations from the previous phases. This project also supplies data to parallel on-going projects in Sweden and Canada.

The experimental program contains both natural and tensile-induced fractures manufactured from quarried granite blocks at three different fracture sizes of 35×60 mm, 70×100 mm and 300×500 mm. Both natural and tensile-induced fractures are used to study two fracture types: tensile induced fresh, matched fractures and natural slightly weathered fractures. All the fracture and replica samples are also characterized in detail pre-, syn-, and post-shear test, utilizing high resolution optical scanning and contact pressure measurements. This will provide unique opportunities for detailed analysis of the potential factors affecting fracture behavior. Acoutic emission measurements are used to complement other measurements and to add information on the wear processes within the joint during shearing. The workflow and measurements are illustrated in Figure 1.

The development of a large direct shear machine with a high stiffness capable of testing fracture samples of up to 600 mm in length under high normal stress and stiffness conditions, which does not exist elsewhere, was a key objective of this project (Figure 2). With that, accurate experiments can be undertaken on large specimens under normal stresses up to 20 MPa as well as high normal stiffness values. In addition to the traditional measurements of the relative displacement between the two halves of the shear box, direct displacements are measured on the specimens over the joint using digital image correlation (DIC) technology enabling a reduction of measurement errors related to the deformations in the testing system. The effect of high versus low system stiffness is shown in Figure 2. The influence from the system stiffness of the machine is also compensated for during the CNS experiements.

This program provides a novel data set which will help reduce the knowledge gap in understanding of fracture behavior. A more detailed description of the project can be found in Jacobsson et al. (2021).

Workflow and measurements

Before mechanical tests		**During mechanical tests**		**After mechanical tests**
• Specimen preparation • Photo documentation • Surface scanning • Contact pressure distribution	⇨	• Normal stiffness • Shear stress response • Shear induced dilatancy • Acoustic emission	⇨	• Photo documentation • Surface scanning

Contact wear zones & combined measurements = additional understanding

Before mechanical tests		**During mechanical tests**		**After mechanical tests**
Contact pressure distribution • Match with scanning data	⇨	Evolving contact zones • Match AE with shear response	⇨	Wear determination • Match AE and scanning data

Figure 1. Top: Workflow and measurements; and Bottom: Example of integrated measurement and interpretation steps used for studying contact wear zones.

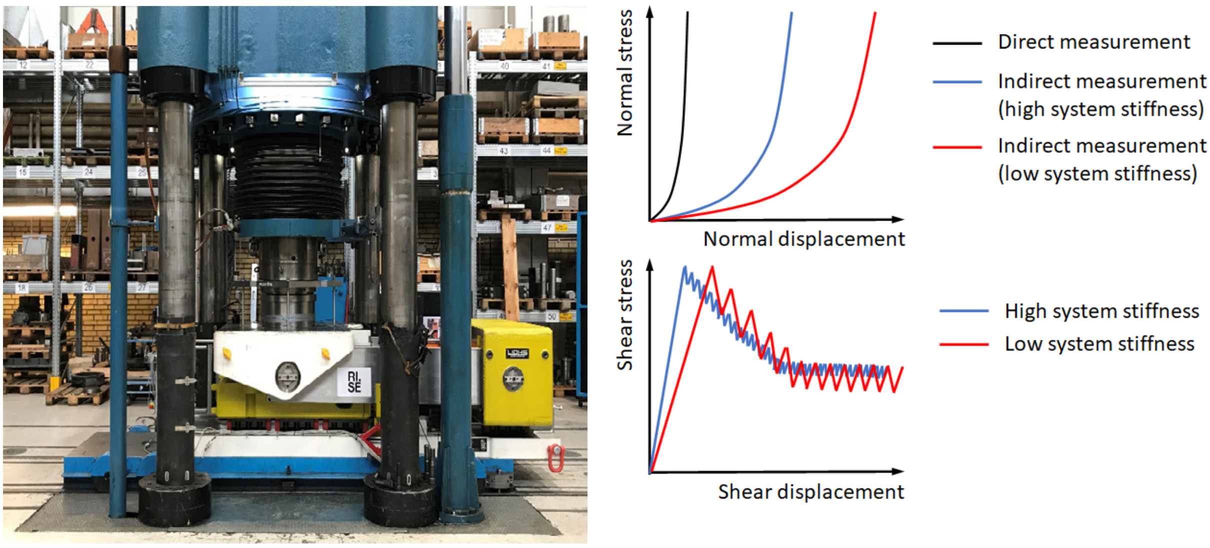

Figure 2. Left: direct shear testing machine; Right: illustration of direct and indirect deformation measurements during normal loading stage and the effect of system stiffness on shear stress-displacement results.

References

SKB, 2011: *Long-term safety for the final repository for spent nuclear fuel at Forsmark main report of the SR-Site project.* SKB TR-11-01, Svensk Kärnbränslehantering AB, Stockholm, Sweden.

Siren, T., Hakala, M., Valli, J., Christiansson, R., Mas Ivars, D., Lam, T., Mattila, J. & Suikkanen, J., 2017: *Parametrisation of Fractures - Final Report*, Posiva Report 2017-1, Posiva OY, Eurajoki, Finland.

Jacobsson, L., Mas Ivars, D., Kasani, H.A., Johansson, F. & Lam, T., 2021: Experimental Program on Mechanical Properties of Large Rock Fractures. In *IOP Conference Series: Earth and Environmental Science*, 833:012015.

Episyenites in Stockholm – observations from ongoing tunnel projects

Felix Makowsky[a], Mathilda Nyzell[b]

[a]Afry, Stockholm, Sweden, felix.makowsky@gmail.com; [b]Afry, Stockholm, Sweden, mathilda.nyzell@gmail.com

Summary. Episyenite is a type of porous, quartz-depleted granitoid that has been encountered more and more frequently in Stockholm. This rock poses a challenge to tunnel production due to its heterogenous porosity and unpredictable nature and the industry currently lacks proven tools to prevent groundwater leakage from episyenite bodies. A thorough investigation of episyenite distribution in Stockholm and establishment of the physical characteristics of this rock is needed to lower costs during planning and production of tunnels.

Multiple infrastructure projects have encountered a rare type of altered rock in Stockholm in recent years. The rock, a quartz-leached granitoid, is called *episyenite* and has caused problems with reinforcement and, to a greater extent, inflow of water. This rock has previously been reported in Bohuslän (Pettersson & Eliasson 1997) and Forsmark (Petterson et al. 2012) but not in Stockholm in academic journals. The name "episyenite" can be somewhat misleading, since the rock is merely a syenite from a strict mineralogical point of view (i.e. low quartz/feldspar ratio) and "quartz-leached leached granitoid" might be more suitable as a descriptive term. The key characteristic of episyenite is the porosity: although the formational history of episyenite alteration can be complex (Suikkanen & Rämö 2019), involving multiple stages of alteration, the initial leaching of quartz by a hydrothermal and silica-undersaturated fluid resulting in the formation of a porous rock, is shared by all episyenite bodies. However, the formation of secondary phases in these quartz-turned-vugs makes cement-based grouting – the most common technique used to prevent leakage of groundwater into tunnels in Sweden – unreliable in episyenite.

At the moment, more than ten observations of episyenite have been verified by the authors in Stockholm. The number of mapped bodies in tunnels and on outcrops is expected to be higher since the term episyenite and the corresponding description is not well established in the industry. Observations range from Barkarby in the northwest (Wallen, A., personal communication, 2022), Lovö in the west, down to Nacka in the southeast (Iskender, C., personal communication, 2022) (see figure). A probable but not verified occurrence in Södermalm has also been noted. Based on the alteration process (Suikkanen & Rämö 2019) it can be concluded that episyenite formation is restricted to a granitoid precursor and is more likely to occur close to major, steeply dipping fault zones with a high hydraulic conductivity at the time of episyenitization. Rare occurrences of episyenite bodies without any visible connection to brittle faults have, however, also been observed. Some of the episyenite-altered bodies have gone through brittle deformation after leaching, resulting in areas with a mix of clay and partially crushed rock, while others are without any visible traces of deformation.

Experiences from tunnel production indicate that cement-based grouting of episyenite bodies generally leads to inadequate volumes of cement penetrating into the rock, resulting in continued leakage from unsealed pores and pathways. A possible explanation for this is that the cement is designed to seal open faults, not a network of pores. Furthermore, most of the cement-based grouting theory assumes a two-dimensional spread of cement, whereas grouting of an episyenite body most likely requires another approach. Now, the authors know of no tests where chemical-based grouting has been used to seal episyenite, but the more fluid-like behaviour of chemical-based grout could prove to be more successful where traditional cement-based grouting has failed.

Although the near-tunnel extent of episyenite bodies can be estimated from drilling data, the critical information – whether the porous mass is connected to an aquifer – remains unknown in most cases. Various geophysical methods that rely on the presence of groundwater could be useful for predicting

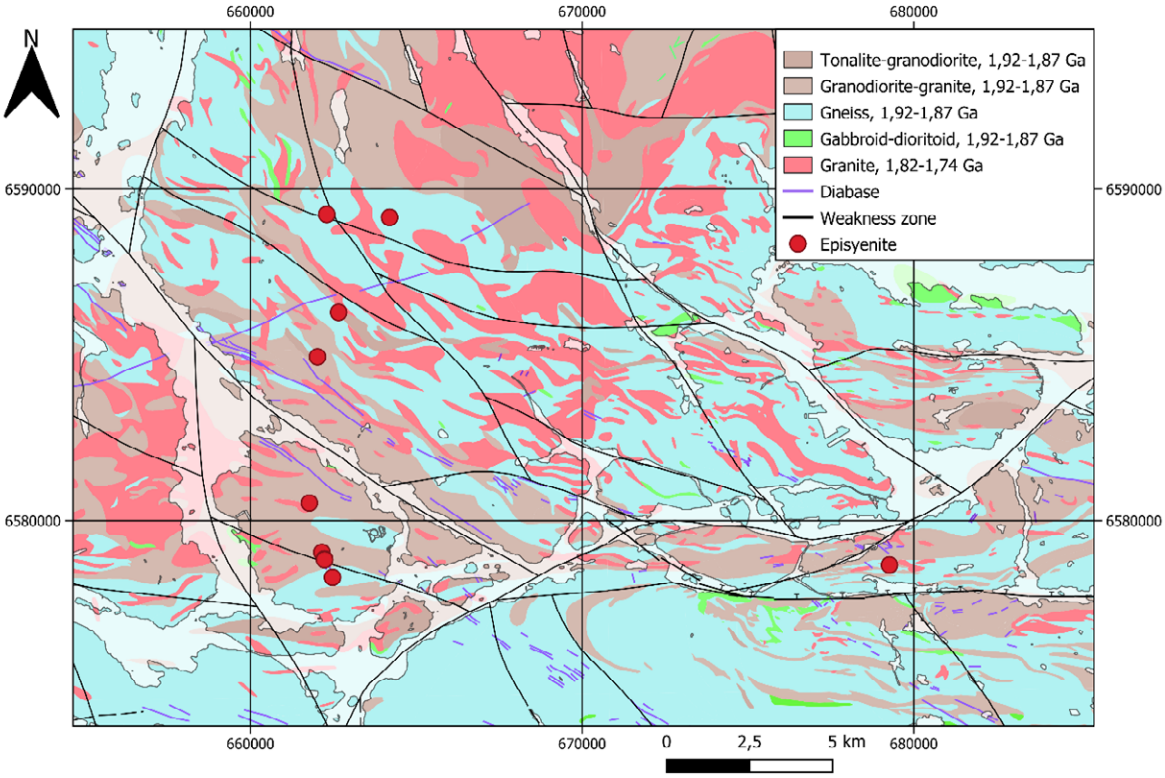

Geological bedrock map of Stockholm from SGU (downloaded in May 2022) with verified episyenite occurrences. Most of the observations reported here are made in the E4 Stockholm Bypass tunnel project, except for the northwesternmost observation (FUT 4, Barkarbystaden) and the southeasternmost observation (FUT 6, Nacka). © Sveriges geologiska undersökning

episyenites, given that observed occurrences seem to act as aquifers on their own, but distinguishing episyenites this way from weakness zones could still be difficult.

More research is needed to establish how to grout episyenite bodies, predict their occurrences, and investigate their hydrogeological behaviors.

References

Petterson, J., Stephens, M., Mattson, H. & Möller, C., 2019: Albitization and quartz dissolution in Paleoproterozoic metagranite, central Sweden, - Implications for the disposal of spent nuclear fuel in a deep geological repository. *Lithos 42*, 123-146.

Petterson, J. & Eliasson, T., 1997: Mineral evolution and element mobility during episyenitization (dequartzification) and albitixation in the postkinematic Bohus granite, southwest Sweden. *Lithos 148*, 10-26

Suikkanen, E. & Rämö, O., 2019: Episyenites – Characteristics, Genetic Constraints, and Mineral Potential. *Mining, Metallurgy & Exploration 36*, 861-878.

Thematic Session 2
Economic geology

Session Chairs:
Erik Jonsson (erik.jonsson@sgu.se)
Iain Pitcairn (iain.pitcairn@geo.su.se)
Christina Wanhainen (christina.wanhainen@ltu.se)

Platinum-group elements exploration in Sweden: new insights by QanTmin

Thomas Aiglsperger[a], Olof Martinsson[a], Joaquín A. Proenza[b]

[a]Department of Civil Engineering and Natural Resources, Luleå University of Technology, Luleå, Sweden, thomas.aiglsperger@ltu.se; [b]Departament de Mineralogia, Petrologia i Geologia Aplicada, Facultat de Ciències de la Terra, Universitat de Barcelona, Barcelona, Spain, japroenza@ub.edu

Summary. In this contribution we present new geochemical and mineralogical data from platinum-group elements (PGE) targets in Sweden. Samples were collected at SGU´s drillcore archive in Malå after literature study and studied using quantitative element screening combined with quantitative target mineralogy (QanTmin). Whole-rock geochemistry revealed PGE anomalies up to 4.2 ppm in samples with hydrothermal overprints. Mineralogical and textural evidence show that these events have mobilized PGE, preferentially palladium.

Background and methods

This contribution is based on a VINNOVA SIP STRIM pre-study that aimed to give an overview for the potential of platinum-group elements (PGE; i.e. Os, Ir, Ru, Rh, Pt, Pd) hosted by Swedish sulfide Ni-Cu deposits. PGE have, due to their specific physical and chemical properties, a wide range of technological applications and are essential raw materials being used, for example, in the production of catalytic converters in the automotive industry. Today, the worldwide supply of PGE is mainly controlled by two countries, South Africa and Russia, that together provide about 80% of the global PGE production (USGS, 2021). Because of their high economic importance for western industries, in combination with existent and emerging supply risks, PGE are defined as critical materials for the EU (EC 2020).

Sweden is considered one of the most mineralized and yet underexplored mining regions worldwide. With respect to PGE, a more complete knowledge is needed for an accurate evaluation of the potential of Sweden as a possible future supplier. Several PGE targets occur throughout the country and some have been investigated on PGE in the past. However, according to available literature data, most targets lack detailed information on PGE geochemistry and on their mineralization. In this contribution we provide new geochemical and mineralogical insights with the aim to support successful PGE exploration in Sweden.

A total of 40 samples from 11 localities were selected after literature research and resampled at SGU’s drillcore archive in Malå. Whole-rock geochemistry by multi-element screening was done at ALS Scandinavia. Samples that showed increased contents of PGE were subsequently investigated in more detail using the quantitative target mineralogy (QanTmin) flowsheet at LTU. QanTmin combines different methods from e.g. (i) initial sample preparation to (ii) hydroseparation (concentration technique for heavy minerals) to (iii) SEM-based automated mineralogy on polished monolayers. Identified PGE-bearing phases were further investigated by electron probe micro-analyzer (EPMA) at the Centres Científics i Tecnològics de la Universitat de Barcelona (CCiTUB), Spain.

PGE geochemistry

Total PGE contents vary from 1 ppb to 4200 ppb with a median value of 31 ppb. Palladium is the most abundant PGE reaching contents of up to 3400 ppb in samples with hydrothermal modification of primary mineralogy. Platinum is the second most abundant PGE reaching contents of up to 770 ppb in massive sulfide ores. Iridium is strongly depleted in all samples and does not exceed contents of 27 ppb. Figure 1 shows primitive mantle normalized patterns for PGE, Ni, Cu, Ag and Au of the investigated samples.

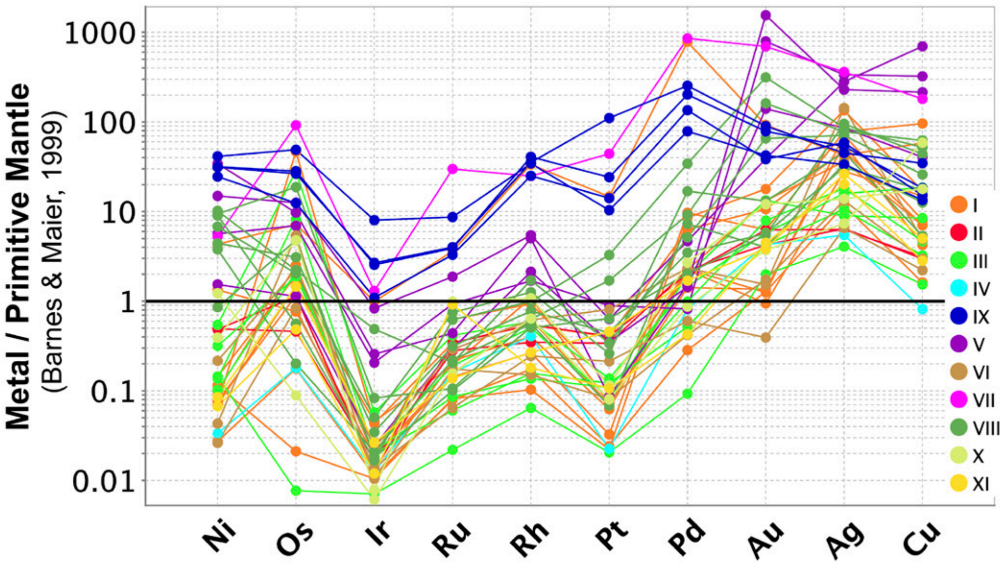

Figure 1. Overview of geochemical patterns from investigated samples (40 samples from 11 localities).

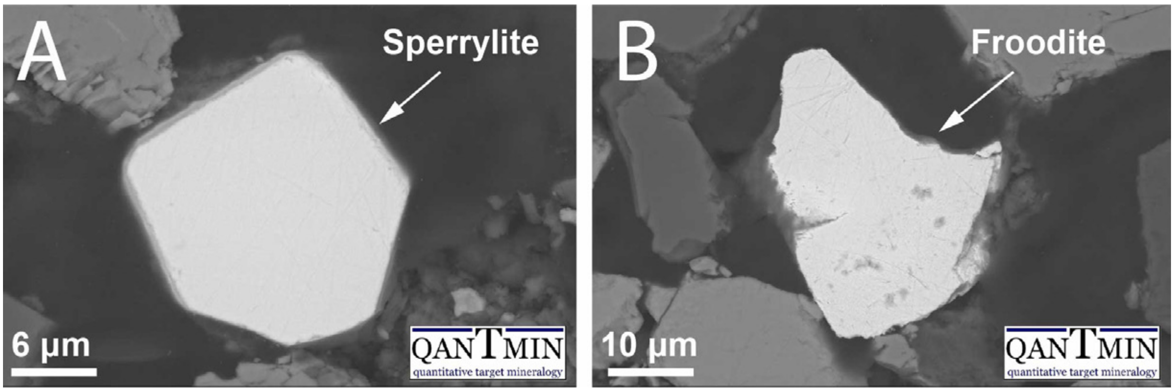

Figure 2. Back-scattered electron (BSE) images of sperrylite (A) and froodite (B) found in heavy mineral concentrates applying the QanTmin flowsheet at LTU.

PGE mineralogy

Preliminary results show that five different types of PGE mineralization occur: (i) platinum-group minerals (PGM), (ii) PGE-bearing sulphides, (iii) PGE-bearing arsenides, (iv) PGE-bearing tellurides and PGE-bearing bismuthides. Overall, sperrylite ($PtAs_2$) is the most abundant PGM in heavy mineral concentrates, followed by froodite ($PdBi_2$) (Fig. 2). Mineralogical and textural evidence, such as the observation of PGM occurring along Cl-rich and serpentine-hosted cracks, as well as Pt-bearing parkerite ($Ni_3(Bi,Pb)_2S_2$) (up to 1.2 wt% Pt) suggests PGE redistribution and accumulation distal to magmatic intrusions due to hydrothermal activity. This should be considered more in future PGE exploration campaigns in Sweden.

References

Barnes, S.-J. & Maier, W.D., 1999: The fractionation of Ni, Cu and the noble metals in silicate and sulphide liquids. In: Keays, R.R., Lesher, C.M., Lightfoot, P.C. & Farrow, C.E.G. (eds.), Dynamic processes in magmatic ore deposits and their application to mineral exploration. *Geological Association of Canada, Short Course Notes* 13, 69–106.

EC (European Commission), 2020: Communication from the commission to the European parliament, the council, the European economic and social committee and the committee of the regions on the 2020 list of critical raw materials for the EU. Brussels, Belgium (2020). Available at https://eur-lex.europa.eu/legal-content/EN/TXT/?uri=CELEX-:52020DC0474. Accessed 10 May 2021).

USGS, 2021: Mineral commodity summaries 2021. Available at: https://pubs.usgs.gov/periodicals/mcs2021/mcs2021-platinum.pdf. Accessed 10.05.2021.

A synthesis of polymetallic (Cu-Co-Mo-Au) sulphide, Fe oxide and REE-U mineralisation types in the Västervik region, SE Sweden

Stefan S. Andersson

Geological Survey of Sweden, Department of Mineral Resources, Uppsala, Sweden, stefan.andersson@sgu.se

Summary. The Västervik region in SE Sweden hosts different known mineralisation types with Fe, Cu, Co, Au, REE and U. The metallogenesis of the region is, however, poorly studied and understood. This contribution synthesises the metal mineralisations in the region and briefly discusses their characteristics.

Introduction

The Fennoscandian Shield is highly prospective regarding a diverse suite of metals, ranging from base-, precious to critical metals, such as the rare earth elements (REE). Many of the well-known ore regions in Sweden (e.g. Norrbotten, Skellefte and Bergslagen) have been studied quite extensively. One of the least studied regions utilising modern geoanalytical methods is the Västervik region in SE Sweden. It is known to host various mineralisation types, including different polymetallic (Cu, Co, Mo, Au) sulphide, Fe oxide, REE and U types (cf. Andersson et al. 2018; Fig. 1). This contribution synthesises the known metal mineralisations in the region from available literature and databases.

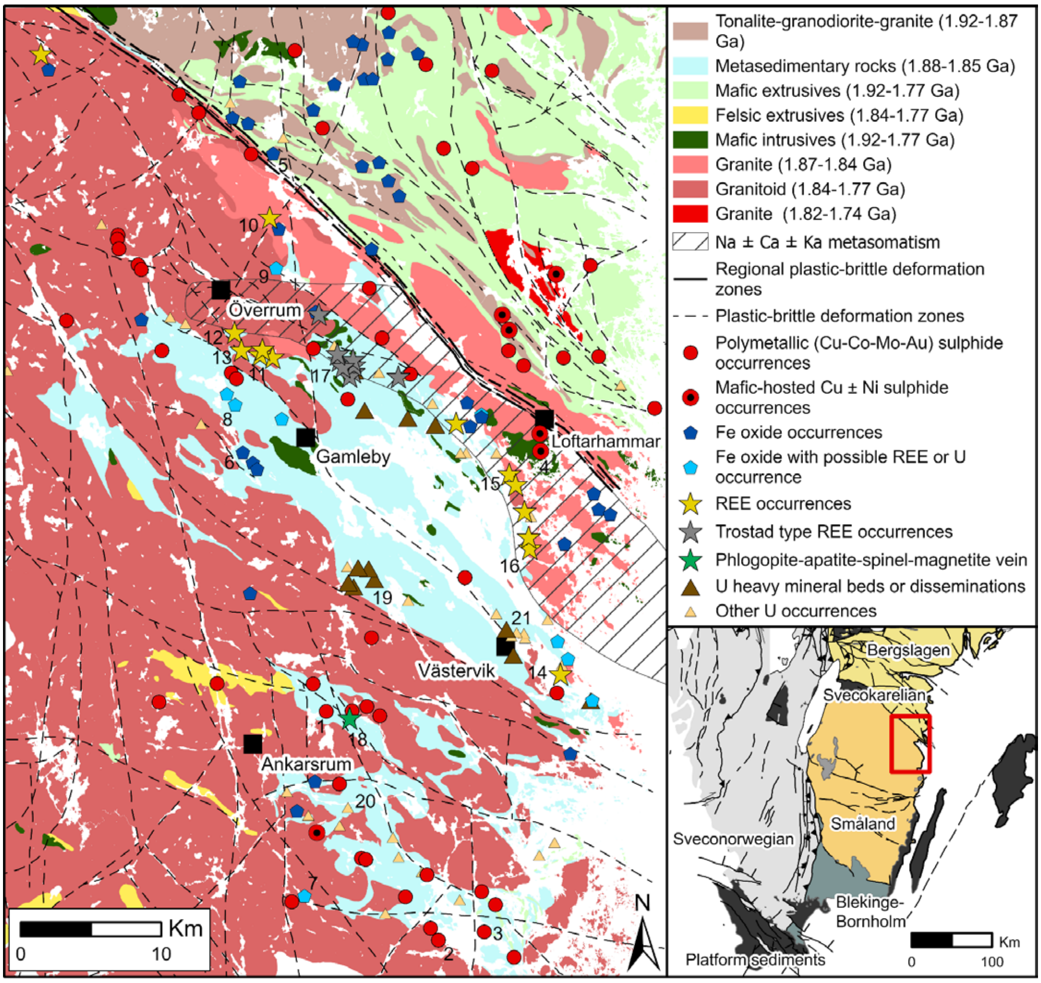

Figure 1. Bedrock map of the Västervik region showing locations of known mineralisations; compiled from the mineral resource database of SGU with supplementary data from Uytenboogardt (1960), Hoeve (1974), Löfvendahl & Åkerblom (1976), Hallgren et al. (1986) and Gustafsson (1992). The inset map shows the lithotectonic units and major deformation zones in southern Sweden. The bedrock maps are based on the database of SGU.

Synthesis of mineralisation types in the region

Polymetallic (Cu-Co-Mo-Au) occurrences in the region are the main sulphide type, with known examples such as the Gladhammar (1), Solstad (2) and Skälö (3) mines. Many of these occurrences have been interpreted as epigenetic and host different Cu-Fe ± Co sulphides with variable amounts of Fe oxides. Mafic-hosted Cu ± Ni sulphide occurrences (e.g. Stora Grundemar, 4) is a subordinate type.

Fe oxides represent the main mineralisation type in the region, comprising magnetite (e.g. Stenebo, 5) or hematite (e.g. Svensbo, 6) ores hosted in diverse host rocks. Many of them are associated with known U anomalies (e.g. Öbälen, 7) and others share features with REE occurrences in the region (e.g. Ramstad, 8, and Borsjö, 9) but have not been studied in recent time. A similar Fe oxide occurrence at Hylleled (10) was recently shown to be REE-bearing (Jonsson et al. 2019).

The most studied REE-rich type is the Olserum-Djupedal REE-phosphate mineralisation at Olserum (11), Djupedal (12) and Bersummen (13; Andersson et al. 2018). Other REE occurrences sharing similar features include the Gränsö (14) and potentially other magnetite-dominated oxide occurrences. A lesser-known REE type occurs in the Västervik archipelago (e.g. Björkö, 15 and Norra Malmö, 16). Here, REE are hosted by davidite and minor allanite occurring with Ti-Fe-bearing oxides in fissures associated with Na ± Ca metasomatism (Hoeve, 1974). Around Trostad (17), a similar REE mineralisation with davidite is exposed associated with K metasomatism in mafic intrusives. A rare phlogopite-apatite-spinel vein has been reported near Gladhammar (18; Kresten 1976). Uranium ± REE in heavy mineral palaeoplacers are known from different locations in the Västervik metasedimentary formation (e.g. Klockartorpet, 19). Other types include U mineralisation associated with cordierite-rich horizons in gneisses and quartzites (e.g. Häggebytorp, 20) and in the contact zone of mafic dykes (e.g. Norrlandet, 21). Secondary U mineralisation in fractures is also common.

Discussion and conclusion

The metal mineralisations in the region host a diverse suite of elements, e.g. Fe, Cu, Co, Au, REE and U in different styles of mineralisation. They are mostly located at known lithological or tectonic boundaries or along deformation zones (Fig. 1). Mineralisation pre- or post-dates regional deformation and metamorphism in the region. Morever, they can be temporally associated with chemically diverse intrusive rocks. Yet, specific magmatic suites acting as a source of fluids or/and metals are not known. The significance and extent of the large-scale alkali metasomatism (Na, K and Ca) that has affected the region, and its relation to mineralisation is not well known. In summary, the region shares many metallogenetic features with the iron oxide copper gold (IOCG) class of deposits (Groves et al. 2010) and should be studied more extensively with modern geoanalytical techniques.

References

Andersson, S.S., Wagner, T., Jonsson, E., Fusswinkel, T., Leijd, M. & Berg, J.T., 2018: Origin of the high-temperature Olserum-Djupedal REE-phosphate mineralisation, SE Sweden: A unique contact metamorphic-hydrothermal system. *Ore Geology Reviews 101*, 740–764.

Groves, D.I., Bierlein, F.P., Meinert, L.D. & Hitzman, M.W., 2010: Iron oxide copper-gold (IOCG) deposits through Earth history: Implications for origin, lithospheric setting, and distinction from other epigenetic iron oxide deposits. Economic Geology 105, 641–654.

Gustafsson, B., 1992: Sällsynta jordartsmetaller – Regional fältkontrol 1991 av arkivuppslag. *PRAP 91047*, 1–22.

Hallgren, U., Nilsson, B. & Luppichini, L.E., 1986: Norra Kalmar Län 1985-1986. *PRAP 86520*. 1–53.

Hoeve, J., 1974: Soda metasomatism and radio-active mineralisation in the Västervik area, southeastern Sweden. *PhD thesis, Vrije University, Amsterdam,* 191 pp.

Jonsson, E., Nysten, P., Bergman, T., Sadeghi, M., Söderhielm, J. & Claeson, D.T., 2019: REE mineralisations in Sweden. *Geological Survey of Sweden reports and communications 146*, 20–111.

Kresten, P., 1976: A spinel-apatite-phlogopite dyke near Västervik, south-eastern Sweden. *GFF 98*, 175–179.

Löfvendahl, R. & Åkerblom, G., 1976: Uranprospektering i Västervikområdet: Rapport över av SGU utförda prospekteringsarbeten åren 1970–1974. *BRAP 87003*, 1–85.

Uytenbogaardt, W., 1960: Uranium mineralization in the Västervik area. *The 21st International geological congress, part 15,* 114–122.

Contrasting Na–Ca ± Fe ± K brines explain differences in REE mineral alteration in the Olserum–Djupedal mineralisation, Sweden

Stefan A. Andersson[a], Erik Jonsson[a,b], Tobias Fusswinkel[c], Thomas Wagner[c]

[a]Geological Survey of Sweden, Department of Mineral Resources, Uppsala, Sweden, stefan.andersson@sgu.se; [b]Department of Earth Sciences, Uppsala University, Uppsala, Sweden; [c]Institute of Applied Mineralogy and Economic Geology, RWTH Aachen University, Aachen, Germany

Summary. Fluid inclusions from the Olserum-Djupedal REE-phosphate mineralisation in the Västervik region, SE Sweden, comprise different brine types with contrasting major cation compositions. Highly saline, Ca-rich brines occur in the Djupedal area and explain why different Ca-bearing REE minerals only formed in this area during alteration. This contrasts with the Olserum area, where the fluids were Na-dominated. The alteration fluids likely evolved from an initial Na-K-Fe-Ca-rich REE-mineralising fluid through alkali exchange and mixing with metamorphic fluids during regionally extensive Na ± Ca alteration.

Introduction

Fluid inclusion petrography, microthermometry and laser-ablation inductively coupled mass spectrometry (LA-ICP-MS) analysis were carried out on quartz-hosted inclusions from the high-temperature (c. 600°C), hydrothermal Olserum–Djupedal REE-phosphate mineralisation in the Västervik region, SE Sweden. Mineralisation here primarily occurs as veins comprising fluorapatite, xenotime-(Y) and monazite-(Ce), with subordinate fergusonite-(Y) and samarskite-(Y), all hosted by metasedimentary rocks within the contact aureole of a c. 1.8 Ga granite and within the granite itself. The primary REE minerals were variably altered during cooling of the system, leading to contrasting alteration features between the mineralised areas. This is mostly manifested as extensive replacement of primary monazite-(Ce) to fluorapatite ± allanite-(Ce)–ferriallanite-(Ce) in the Djupedal area. Nearby host rocks in Djupedal were also altered to distinct quartz-plagioclase rocks. Late-stage REE-fluorocarbonates formed by the alteration of allanite-(Ce)–ferriallanite-(Ce) (Andersson et al. 2018a, 2018b).

Fluid inclusion types and chemistry

The oldest fluid inclusions identified are different aqueous brine inclusions (Fig. 1A). The petrography of the fluid inclusions is complex, and all brine types locally co-exist with CO_2-rich inclusions. Combined microthermometry and LA-ICP-MS analysis show that the major cation compositions of the brine inclusions are different between Olserum and Djupedal. In Djupedal, they are extremely saline (45–55 wt% $CaCl_2$ + NaCl) and Ca-rich (Ca-Na brines). In Olserum, they occur as two types, an early Na-Fe-K-Ca brine with c. 40–45 wt% NaCl eq., and a Na-Ca brine with c. 31 wt% NaCl + $CaCl_2$ (Fig. 1B). The latter has a similar appearance and molar volume as the Ca-Na brine in Djupedal.

Discussion and conclusions

The fluid inclusions are hosted in quartz related to later stages of the hydrothermal system. Yet, the Na-Fe-K-Ca brine was trapped at a temperature of c. 400°C and is the closest candidate to an original REE-mineralising fluid. This early fluid has halogen ratios (Br/Cl and I/Cl) and Cl-normalised Zn-Pb ratios indicating a magmatic origin (Fig. 1C–D). The Ca-Na brine in Djupedal and Na-Ca brine in Olserum were trapped at lower temperatures (250–300°C) and show contrasting compositions, particularly in the Na/Ca ratio. The later brines probably evolved from the earlier Na-Fe-K-Ca brine through a combination of cooling, alkali exchange and mixing with metamorphic fluids. These contrasting fluid compositions had a strong control on alteration and explains why secondary Ca-bearing REE minerals such as allanite-(Ce)–ferriallanite-(Ce) and REE-fluorocarbonates only formed in the Djupedal area. The fluid was most likely responsible for the formation of the quartz-plagioclase rocks in the area, and the regional Na ± Ca alteration that has affected the Västervik region (Hoeve 1974, Andersson et al.

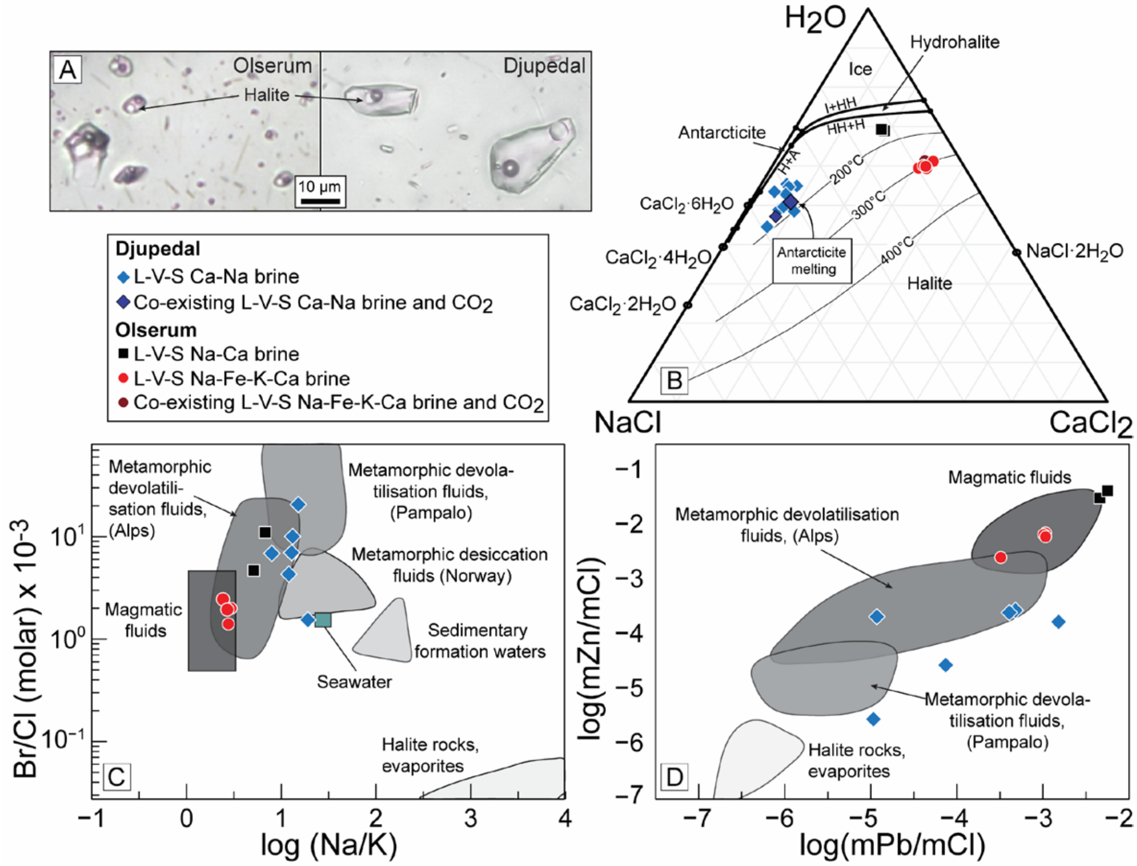

Figure 1. Composite figure illustrating the appearances and compositions of the brine inclusions. A) Photomicrograph of halite-bearing inclusions at Olserum and Djupedal. B) Fluid inclusion compositions based on LA-ICP-MS analysis and microthermometry. The H_2O–NaCl–$CaCl_2$ ternary diagram is from Steele-MacInnis et al. (2011). C and D) Variation diagrams showing the origin and evolution of the brine inclusions. Data from Svensen et al. (2001), Li et al. (2015), Rauchenstein-Martinek et al. (2016), Fusswinkel et al. (2017), Audétat & Zhang (2019).

2018b). Differences in lithology of nearby rocks can explain the different fluid compositions and thus have a strong control on the type and intensity of alteration occurring in the REE-mineralising system.

References

Andersson, S.S. Wagner, T., Jonsson, E. & Michallik, R.M., 2018a: Mineralogy, paragenesis and mineral chemistry of REEs in the Olserum-Djupedal REE-phosphate mineralization, SE Sweden. *American Mineralogist 103*, 125–142.

Andersson, S.S., Wagner, T., Jonsson, E., Fusswinkel, T., Leijd, M. & Berg, J.T., 2018b: Origin of the high-temperature Olserum-Djupedal REE-phosphate mineralisation, SE Sweden: A unique contact metamorphic-hydrothermal system. *Ore Geology Reviews 101*, 740–764.

Audétat, A. & Zhang, D., 2019: Abundances of S, Ga, Ge, Cd, In, Tl and 32 other major to trace elements in high-temperature (350–700 °C) magmatic-hydrothermal fluids. *Ore Geology Reviews 109*, 630–642.

Fusswinkel, T., Wagner, T. & Sakellaris, G., 2017: Fluid evolution of the Neoarchean Pampalo orogenic gold deposit (E Finland): Constraints from LA-ICPMS fluid inclusion microanalysis. *Chemical Geology 450*, 96–121.

Hoeve, J., 1974: Soda metasomatism and radio-active mineralisation in the Västervik area, southeastern Sweden. *PhD thesis, Vrije University, Amsterdam,* 191 pp.

Li, W., Audétat, A. & Zhang, J., 2015: The role of evaporites in the formation of magnetite-apatite deposits along the Middle and Lower Yangtze River, China: Evidence from LA-ICP-MS analysis of fluid inclusions. *Ore Geology Reviews 67*, 264–278.

Rauchenstein-Martinek, K., Wagner, T., Wälle, M., Heinrich, C.A. & Arlt, T., 2016: Chemical evolution of metamorphic fluids in the Central Alps, Switzerland: insight from LA-ICPMS analysis of fluid inclusions. *Geofluids 16*, 877–908.

Svensen, H., Jamtveit, B., Banks, D.A. & Austrheim, H., 2001: Halogen contents of eclogite facies fluid inclusions and minerals: Caledonides, Western Norway. *Journal of Metamorphic Geology 19*, 165–178.

Steele-MacInnis, M., Bodnar, R.J. & Naden, J., 2011: Numerical model to determine the composition of H_2O-NaCl-$CaCl_2$ fluid inclusions based on microthermometric and microanalytical data. *Geochimica et Cosmochimica Acta 75*, 21–40.

A time-constrained structural framework of the Kiruna mining district in northern Sweden

Joel B.H. Andersson[a], Leslie Logan[a], Olof Martinsson[a], David Chew[b], Ellen Kooijman[c], Melanie Kielman-Schmitt[c], Tobias C. Kampmann[a], Tobias E. Bauer[a]

[a]Division of Geosciences and Environmental Engineering, Luleå University of Technology, SE-971 87 Luleå, Sweden, joel.bh.andersson@ltu.se; [b]Department of Geology, School of Natural Sciences, Trinity College Dublin, Ireland, chewd@tcd.ie; [c] Department of Geosciences, Swedish Museum of Natural History, SE-104 05, Stockholm, Sweden, ellen.kooijman@nrm.se.

Summary. To provide a time-constrained structural framework of the type locality for iron oxide-apatite deposits, stratigraphic-structural investigations and U-Pb geochronology on zircon, titanite, and apatite in the Kiruna mining district was undertaken. Results indicate the iron ores were emplaced in a syn-extensional basin and that syn-volcanic faults likely controlled magmatic-hydrothermal transport in the ore-system. Reverse reactivation of syn-volcanic faults during the regional D_2 event led to crustal exhumation and juxtaposition of rocks from different crustal levels.

Introduction

The Kiruna mining district is the type locality for iron oxide-apatite (IOA) deposits and is responsible for a significant portion of total European iron ore production. The area is relatively well studied but its tectonothermal history remains unresolved. In this contribution, we summarize key results reported in Andersson et al. (2021, 2022). These studies focused on the structural geology and stratigraphy as well as U-Pb dating of deformation events to better understand the geological setting generating the IOA deposits, to resolve the subsequent crustal shortening and its effect on the crustal architecture, and to provide a U-Pb age-record that constrains the deformation and the medium-temperate evolution of the area.

Method

Geological mapping and sampling focusing on stratigraphy and structural geology were performed during the field seasons 2016–2020 (848 outcrop observations, 1127 structural measurements, 68 oriented samples) in the Orosirian portion of the Kiruna mining district stratigraphy. The mapping data combined with microstructural analysis, 2D-forward modelling (MOVE by Petroleum), and U-Pb geochronology provided the framework for time-constrained conceptual modelling. Detailed method descriptions are reported in Andersson et al. (2021, 2022, and references therein).

Result and discussion

The Orosirian stratigraphic column of the Kiruna mining district indicates the development of a basin dominated by basal alluvial conglomerates and greywakes followed by bi-modal volcanic and volcanosedimentary rocks hosting two IOA horizons in the lower and middle portions of the basin. Towards the upper levels, the sedimentary rocks have no volcanic component and thus mark the end of the Orosirian volcanism. The IOA deposits were emplaced during the basin development phase, prior to crustal shortening. A U-Pb SIMS zircon concordia age of a volcanic intercalation within the conglomerates of the basal unit indicates the onset of the basin development and the earliest Orosirian volcanism took place at 1887 ± 3 Ma.

Titanite analysed in-situ on hydrothermally altered fracture planes in the damage zone of a fault developed in the footwall rocks to the Luossavaara IOA deposit are cataclastic and yield complex U-Pb data due to a variable uptake of common Pb combined with additional scatter. The most concordant data yield a weighted mean $^{207}Pb/^{206}Pb$ age of 1889 ± 26 Ma which represents the minimum age of the fracture planes and brittle deformation in Kiruna. The obtained minimum age of the fault structure is identical to published protolith ages of the faulted rock and the IOA emplacement (e.g. Westhues et al. 2016) which indicates that the fault structure is syn-volcanic and of a similar age as the ore forming system.

Regional D_1-fabrics are typically developed in northern Norrbotten. However, D_1-fabrics appear to be lacking in the Orosirian rocks of the Kiruna mining district. We hypothesize that the absence of D_1-fabrics reflects a higher crustal level during the 1.87–1.86 Ga time-interval. In contrast, regional D_2-fabrics are abundant in Kiruna. An apatite Tera-Wasserburg lower intercept age of 1805 ± 26 Ma combined with the occurrence of greenschist-facies mineral assemblages and the absence of metamorphic hornblende indicate that the basin was subsequently buried and experienced upper greenschist facies metamorphism. Under these conditions, the basin was inverted as a response to c. E–W crustal shortening, a shortening direction normally associated with the regional D_2 event (e.g. Bergman et al. 2001). Much of the finite non-coaxial strain was taken up by pre-existing syn-volcanic normal faults and bedding was transposed into parallelism due to reverse reactivation of these structures. Strain was also taken up by lithological contacts and relatively incompetent rocks producing layer-parallel shearing, forming moderately to steeply east-dipping brittle-ductile shear zones with mylonite fabrics recording consistent reverse oblique- to dip-slip sense-of-shear. In low strain blocks of competent volcanic rocks, deformation was solely brittle and the movement was taken up by fracture planes with slickensides sub-parallel to the stretching lineation. Folding associated with this inversion event is relatively rare in the Kiruna mining district but where folding developed, fold axes plunge either north or south with predominantly south-plunging fold axes. The competent iron ore bodies were boudinaged along strike and parallel with the stretching lineation but only rarely developed a tectonic foliation. The basin inversion resulted in a thrust-stack with geometries that are partly reconstructable by 2D-forward modelling using pre-existing listric faults as a control on the inversion and supports the transposition of bedding into the direction of pre-existing faults.

Syn-tectonic shear zone-hosted titanite records a protracted deformation event responsible for the basin inversion. Titanite grains show well-developed zonation and limited common Pb yields a concordia age of 1812 ± 3 Ma, which constitutes the first direct age constraint on deformation in Norrbotten and confirms the basin inversion in Kiruna as part of the regional D_2 event. Titanite grains that show a less developed zonation yield a concordia age of 1802 ± 8 Ma indicate that the tectonothermal D_2 event may have lasted up to c. 20 m.y. Sodic-calcic alteration is typically associated with the early geological evolution in Norrbotten and is related to IOA-IOCG formation, but the reported model ages show that sodic-calcic alteration also developed during the late-orogenic stages.

The inverted basin was subsequently gently refolded as a response to c. N–S crustal shortening. The resultant structures are subtle and manifested by a crenulation of rocks and structures dominated by phyllosilicates. Currently, the timing of the refolding event lacks absolute age constraints but is bracketed between the younger age of the inversion obtained in this study (1802 ± 8 Ma) and the last identified hydrothermal/deformation event manifested by late hydraulic quartz-calcite breccias, the timing of which is probably coeval with hydrothermal monazite ages ranging between c. 1.71 Ga and 1.61 Ga (e.g. Blomgren 2015).

References

Andersson, J.B.H., Bauer, T.E., & Martinsson, O., 2021: Structural evolution of the central Kiruna area, northern Norrbotten, Sweden: Implications on the geological setting generating iron oxide-apatite and epigenetic iron and copper sulfides. *Economic Geology, 116*, 1981-2009.

Andersson, J.B.H., Logan, L., Martinsson, O., Chew, D., Kooijman, E., Kielman-Schmitt, M., Kampmann, T.C., & Bauer, T.E., 2022: U-Pb zircon-titanite-apatite age constraints on basin development and basin inversion in the Kiruna mining district, Sweden. *Precambrian Research, 372*, 106613.

Bergman, S., Kübler, L., & Martinsson, O., 2001: Description of regional geological and geophysical maps of northern Norrbotten County (east of the Caledonian orogen). *Geological Survey of Sweden, Ba56*, 110p.

Blomgren, H., 2015: U-Pb dating of monazites from Kiirunavaara and Rektorn ore deposits. *Master thesis, University of Gothenburg, Gothenburg, Sweden,* 39p.

Westhues, A., Hanchar, J.M., Whitehouse, M.J., & Martinsson, O., 2016: New constraints on the timing of host rock emplacement, hydrothermal alteration and iron oxide-apatite mineralization in the Kiruna district, Norrbotten, Sweden. *Economic Geology, 111,* 1595-1618.

Gold mineralization in the Lappberget deposit, Garpenberg mine, Sweden: towards a geometallurgical approach

Leo Barbosa[a], Glacialle Tiu[b], Nils F. Jansson[b], Christina Wanhainen[b], Lena Lilja[c], Yousef Ghorbani[a]

[a]Division of Minerals and Metallurgical Engineering, Luleå University of Technology, 971 87 Luleå, Sweden; [b]Division of Geosciences and Environmental Engineering, Luleå University of Technology, Luleå, glacialle.tiu@ltu.se; [c]Garpenberg Mine, Boliden Mineral AB, SE-77698 Garpenberg, Sweden

Summary. This study investigates the mineralogy and texture of gold-bearing phases in the Lappberget deposit, Garpenberg Mine, and how these characteristics affect gold recovery during mineral processing. Multiple methods such as optical microscopy, SEM-EDS, EPMA, LA-ICP-MS, and bulk chemical analysis were applied on drill core samples, and samples from the processing plant's Knelson gravity concentrator. Electrum-type alloys were recognized as the most common gold hosts.

Gold mineralization in the Lappberget deposit

Located in south-central Sweden (Fig. 1), the Lappberget Zn–Pb–Ag–(Cu–Au) deposit is one of the main ore bodies of the Garpenberg Mine, the oldest Swedish mine in operation (Bindler et al. 2017). The ore mined and processed from the Lappberget deposit yields four different concentrates; Zn, Pb, Cu and a gravimetric concentrate of silver and gold, the latter being a by-product. The geology of the Garpenberg area is well described in the literature (e.g. Allen et al. 2003, 2013, Jansson 2011). There is, however, ongoing detailed research about the mineralogy and distribution of ore minerals in the Lappberget deposit. A recent detailed investigation carried out by Tiu et al. (2021a, 2021b) focused on the mineralogical characterization of sulfides and silver. Nevertheless, there is still a lack of understanding of the occurrence and distribution of gold-bearing minerals in the deposit and its deportment in the mineral processing plant. For that reason, the present study aims to examine the occurrence and distribution of gold-bearing minerals in the Lappberget deposit, to characterize the gold mineralization (mineralogy, composition, grain size range, textures, mineral association, gold carriers and occurrence), and to evaluate its effect on gold recoveries in the beneficiation process, as well as contributing to a better understanding of this deposit. In order to achieve the goals of this work different sets of samples were studied: drill core thin sections from the Lappberget deposit and polished epoxy mounts from the Knelson gravimetric concentrator at Boliden's processing plant. The applied analytical methods for gold characterization were optical microscopy (OM), automated microscopy (AM), and SEM-EDS (Scanning electron microscopy with energy dispersive X-ray Spectroscopy) for studying mineralogy, grain sizes, textures, associations, and mineral compositions. EPMA (electron probe microanalysis) and LA-ICP-MS (laser ablation inductively coupled plasma mass spectrometry) were used to further investigate mineral chemistry and to determine the trace elements in sulfides, respectively. Bulk chemical analysis was done to assess the composition of the samples from the processing plant.

The main findings

The main contribution of the present work was the detailed examination of the gold mineralization at this deposit, conducted within a geometallurgical and gold deportment approach. The main results and conclusions are presented in the table below.

<table>
<tr><th>In ore sample</th><th>In Knelson concentrator streams</th></tr>
<tr><td>

- “Electrum” is the main gold-bearing phase (Fig. 2), with general chemical formulae of $Au_{0.22\text{-}0.85}Ag_{0.15\text{-}0.78}$. Au-dominated compositions prevail.
- The gold mineralization is closely associated with sulfide dissemination, occurring (1) as intergrowths with sulphides, (2) as inclusions in sulfides, (3) as rims on sulfide edges, (4) enclosing sulfides, and (5) as gold minerals filling space in between sulfides and gangue. Gold minerals also occur disseminated among gangue minerals and as inclusions in biotite and muscovite.
- The gold content of electrum appear to increase with depth; however, the current sample set is not enough to determine if it reflects a deposit scale metal zonation.
- Categorization of gold occurrence was made according to its mineralogy, texture, grain size, and association. These characteristics influence gold processing, especially textures and grain size, which implicates its liberation in milling and its recovery.

</td><td>

- The majority of the electrum is completely liberated in the concentrate samples. Some are attached to mainly pyrite and galena. Fine sulfides are found included in the electrum.
- Sulfides seem to be the main carrier and source of Au and Ag. Nevertheless, results show a low potential for invisible gold in the crystal lattice of the sulfides according to the trace element investigation.
- Hydrothermal alteration, metamorphism and polyphase deformation play an important role in the remobilization, redistribution, reconcentration and recrystalisation of gold. The observed features corroborate the abovementioned aspects recognized in previous research.

</td></tr>
<tr><td>

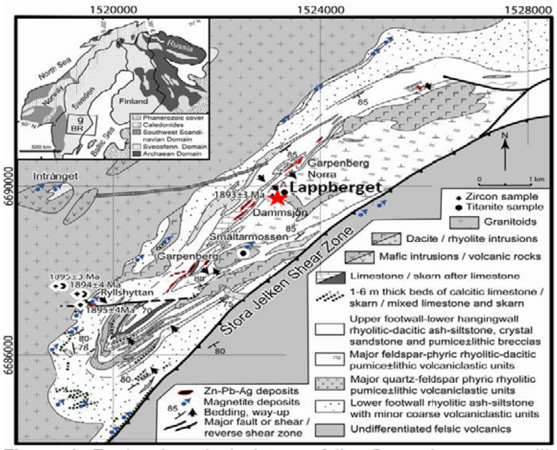

Figure 1. Regional geological map of the Garpenberg area with inset showing the location of the Bergslagen (BR) region where Garpenberg (g) is located (Jansson and Allen 2011b). Ages refer to dated metavolcanic rocks intrusions presented in Jansson and Allen (2011a). Grid is Swedish National Grid RT90.

Figure 1. The location of the Lappberget deposit is shown by the red star. Insert map indicates the location of the Bergslagen (BR) region, where the Garpenberg mine is located; Swedish National Grid RT90 (from Allen et al. 2003, further adapted by Tiu et al. (2019).

</td><td>

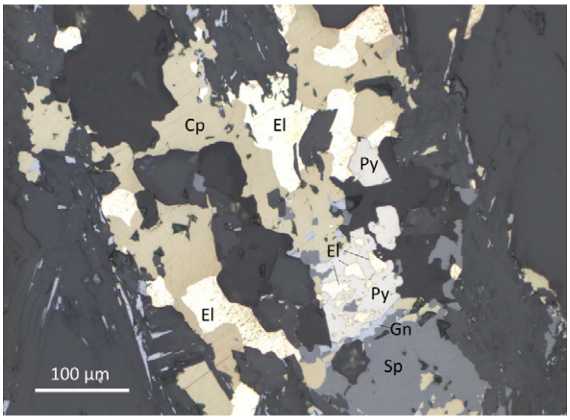

Figure 2. Photomicrograph of electrum (El) grains occuring as intergrowths and inclusions in sulfides: chalcopyrite (Cp), sphalerite (Sp), pyrite (Py) and galena (Gn). (DBH2561e256.05, reflected light).

</td></tr>
</table>

References

Allen, R., Bull, S., Ripa, M. & Jonsson, R., 2003: Regional stratigraphy, basin evolution, and the setting of stratabound Zn–Pb–Cu–Ag–Au deposits in Bergslagen, Sweden. *Sveriges geologiska undersökning, FoU-rapport* 3 (1203), 99 p.

Allen, R., Jansson, N. & Ripa, M., 2013: Bergslagen: Geology of the volcanic-and limestone-hosted base metal and iron oxide deposits. *Excursion Guidebook Swe 4 for the 12th Biennial SGA Meeting,* 102 p.

Bindler, R., Karlsson, J., Rydberg, J., Karlsson, B., Nilsson, L. B., Biester, H. & Segerström, U., 2017: Copper-ore mining in Sweden since the pre-Roman Iron Age: lake-sediment evidence of human activities at the Garpenberg ore field since 375 BCE. *Journal of Archaeological Science: Reports* 12, 99–108.

Jansson, N., 2011: The origin of iron ores in Bergslagen, Sweden, and their relationships with polymetallic sulphide ores *(Doctoral dissertation, Luleå tekniska universitet ISSN 1402-1544),* 73 p.

Tiu, G., Jansson, N., Wanhainen, C., Ghorbani, Y. & Lilja, L., 2021a: Ore mineralogy and trace element (re) distribution at the metamorphosed Lappberget Zn-Pb-Ag-(Cu-Au) deposit, Garpenberg, Sweden. *Ore Geology Reviews* 135, 104223.

Tiu, G., Ghorbani, Y., Jansson, N. & Wanhainen, C., 2021b: Tracking silver in the Lappberget Zn-Pb-Ag-(Cu-Au) deposit, Garpenberg mine, Sweden: towards a geometallurgical approach. *Minerals Engineering* 167, 106889.

A continuum between 1.8 Ga IOCG and orogenic gold deposits in northern Sweden?

Tobias E. Bauer, Joel B.H. Andersson

Division of Geosciences and Environmental Engineering, Luleå University of Technology, Luleå, Sweden, tobias.bauer@ltu.se

Summary. The late stage of the Svecokarelian orogeny in northern Sweden is characterized by c. 1.8 Ga crustal shortening. Syntectonic intrusions caused hydrothermal fluid flow along re-activated shear zones and formation of (Cu-) Au deposits in lower order structures. Differences in mineralogy between individual deposits can be explained by local variations in host rock/fluid compositions and emplacement conditions. Based on these differences the deposits are classified as either iron oxide-copper-gold (IOCG) or orogenic gold style, suggesting there is a continuum between the two deposit types.

Introduction

The northern Fennoscandian Shield is characterized by a long tectonic history with several overprinting tectonothermal events. The most significant metallic mineral deposits in the northern Fennoscandian Shield formed during the Svecokarelian orogeny. An early phase of c. 1.9 Ga subduction-related arc and back-arc extension resulted in the formation of volcanic massive sulfide (VMS) deposits in the arc-region in Västerbotten and iron oxide-apatite (IOA) deposits in the back-arc-region in Norrbotten. A first deformation event at c. 1.87–1.86 Ga resulted in few iron oxide-copper-gold style (IOCG) deposits (e.g. Rakkurijärvi). A late-orogenic phase of c. 1.8 Ga crustal shortening was accompanied by the emplacement of voluminous intrusions and shear zone-reactivation. These reactivated shear zones host several IOCG-style deposits in Norrbotten (Martinsson et al. 2016, Bergman & Weihed 2020, Bauer et al. 2022) and orogenic gold (lode gold) style deposits in Västerbotten (Skyttä et al. 2020).

Tectonic setting and evolution of 1.8 Ga IOCG and orogenic gold deposits

The late-orogenic phase of the Svecokarelian orogeny is caused by E–W-directed crustal shortening at c. 1.81–1.79 Ga (Andersson 2021, Bauer et al. 2022). The structural characteristics of this deformation event gradually change from north to south. In northern Norrbotten, typical structures comprise distinct folding of bedding, ore bodies, as well as folding of an earlier tectonic fabric that developed during the 1.87–1.86 Ga deformation phase. Further south, the late-orogenic folding is less pronounced and grades into a crenulation. In the Skellefte district, the folds and crenulations of the 1.8 Ga phase are generally absent. Hence, the overall deformation intensity decreases slightly from north to south.

A pronounced characteristic of deformation during the late stage orogeny throughout the northern Fennoscandian Shield is strain partitioning. The majority of strain was taken up by pre-existing N-S-trending crustal-scale shear zones that formed during the early-orogenic phase. A prominent example in northern Norrbotten is the Nautanen deformation zone (NDZ) hosting the Nautanen Norra and Kiskamavaara IOCG deposits as well as the Aitik deposit (Andersson 2021, Bauer et al. 2022). The Nautanen deposits comprise a cluster of Cu-Au mineralizations that are hosted by lower-order structures within the NDZ overprinting an earlier magnetite-amphibole-bearing shear fabric. The deposits formed under high temperature-low pressure brittle-ductile conditions with a close spatial relation to syn-tectonic (partly pegmatitic) felsic intrusions. Hydrothermal alteration in the NDZ formed during several phases. A biotite + amphibole + garnet + magnetite + tourmaline + sericite alteration assemblage is typically associated with chalcopyrite + pyrrhotite + pyrite and is locally overprinting earlier scapolite + sericite ± feldspar alteration. Late-stage epidote ± quartz ± feldspar alteration forms selectively pervasive zones and epidote veinlets across the area and is partly related to brittle faulting (Bauer et al. 2022). The southern continuation of these major N-S-trending shear zones into southern Norrbotten and Västerbotten are spatially related to orogenic gold (gold lode) deposits spatially associated to c. 1.80 Ga pegmatitic granites (e.g. Björkdal, Barsele, Svartliden; Andersson 2012, Bauer et al. 2019, Skyttä et al. 2020). The Barsele gold deposit is hosted by 3rd order structures of a crustal-scale N-S-trending shear zone. The distribution of alteration minerals and polymetallic quartz veins suggests multiple phases of fluid flow and remobilisation and a close spatial relation to late-orogenic (pegmatitic) granites. The main phase of enrichment is coupled to low-angle thrusting from ESE and brittle reactivation of earlier structures with emplacement of quartz veins along fault planes and tensile structures in an oblique Riedel system. A series of quartz, quartz-calcite, quartz-tourmaline-bearing veins and polymetallic quartz veins are related to the brittle faulting.

IOCG deposits in Norrbotten as well as orogenic gold deposits in Västerbotten form in lower-order structures of crustal-scale, N–S-trending shear zones. Furthermore, both deposit types show a close spatial relation to late-orogenic (pegmatitic) granites, they are hosted in similar structural settings and likely formed synchronously in a wider perspective during the latest stages of the Svecokarelian orogeny (c. 1.81–1.78 Ga). This event is characterized by high temperature and relatively low pressure conditions throughout the northern Fennoscandian Shield and represents a regional hydrothermal event under a contractional regime. Differences between the deposits can be attributed to variances in regional host rock and/or fluid compositions resulting in different metallogenic signatures. Differences in structural styles are probably an affect of different crustal levels of formation. While the IOCG deposits mainly formed under brittle-ductile conditions (e.g. Bauer et al. 2021), the orogenic gold deposits formed under brittle conditions (e.g. Bauer et al. 2019), indicating a slighly higher crustal level of formation, or higher strain rates. The overall similarities in timing, setting, and character suggest that there might be a continuum between IOCG and orogenic gold deposits in northern Sweden, which would explain the apparent local metallogenic difference in this geological time-window in this part of the Fennoscandian shield. Furthermore, the major 1.8 Ga deformation and (Cu-) Au mineralizing event is also recorded in the Trans-Hudson orogen in Canada and Greenland (cf. Guarnieri & Baker 2022), hence representing a major phase of crustal growth and ore formation with global significance. Applying a zoomed-out mineral-systems perspective on these coeval and structurally controlled hydrothermal deposit types makes a clear distinction between the two less motivated.

References

Andersson, J.B.H., 2012: The Svartliden granite: Petrography, whole rock geochemistry and stable isotope composition. *Msc thesis, Luleå University of Technology, Luleå*, 78 p .

Andersson, J.B.H., 2021: Paleoproterozoic deformation in the Kiruna – Gällivare area in northern Norrbotten, Sweden: Setting, character, age, and control of iron oxide-apatite deposits. *PhD thesis, Luleå University of Technology, Luleå*, 37 p.

Bauer, T.E., Imaña, M., Höglund, K. & Thomas, H., 2019: The structural setting of the Barsele Au deposit, Sweden. *Proceedings of the 15th SGA Biennial Meeting, 27-30 August 2019, University of Glasgow,* 627-630.

Bauer, T.E., Lynch, E.P., Sarlus, Z., Drejing-Carroll, D., Martinsson, O., Metzger, N. & Wanhainen, C., 2022: Structural controls on iron oxide copper-gold mineralization and related alteration in a Paleoproterozoic supracrustal belt: insights from the Nautanen deformation zone and surroundings, northern Sweden. *Economic Geology* 117, 327–359.

Bergman, S. & Weihed, P., 2020: Archean (>2.6 Ga) and Paleoproterozoic (2.5–1.8 Ga), pre- and syn-orogenic magmatism, sedimentation and mineralization in the Norrbotten and Överkalix lithotectonic units, Svecokarelian orogen. In: Stephens, M.B. & Bergman Weihed, J., (eds.), *Sweden: lithotectonic framework, tectonic evolution and mineral resources. Geological Society, London, Memoirs* 50, 27–81.

Guarnieri, P. & Baker, N., 2022: Tectonic inversion of listric normal faults in the foreland of the Rinkian orogen (Maarmorilik, central West Greenland). *Journal of Structural Geology* 159, 104598.

Martinsson, O., Billström, K., Broman, C., Weihed, P. & Wanhainen, C., 2016: Metallogeny of the northern Norrbotten ore province, northern Fennoscandian Shield with emphasis on IOCG and apatite-iron ore deposits. *Ore Geology Reviews* 78, 447–492.

Skyttä, P., Weihed, P., Högdahl, K., Bergman, S. & Stephens, M.B., 2020: Paleoproterozoic (2.0–1.8 Ga) syn-orogenic sedimentation, magmatism and mineralization in the Bothnia–Skellefteå lithotectonic unit, Svecokarelian orogen. In: Stephens, M.B. & Bergman Weihed, J., (eds.), 2020. *Sweden: Lithotectonic Framework, Tectonic Evolution and Mineral Resources. Geological Society, London, Memoirs* 50, 27–81.

Investigation of potential secondary raw materials in tailings at Morkulltjärnen, Yxsjöberg tungsten mine, Bergslagen, Sweden

Patrick Casey, Lena Persson

Geological Survey of Sweden, Uppsala, Sweden, patrick.casey@sgu.se, lena.persson@sgu.se

Summary. In 2020, the Geological Survey of Sweden received a parliamentary directive to identify potential secondary sources of critical raw materials (CRM) in mine waste throughout Sweden. Mine waste sampled within this study includes tailings, the residual product after ore has been crushed and the economic fraction has been removed. During this project several tailings repositories including Morkulltjärnen at the former Yxsjöberg tungsten mine were investigated with geophysical and geochemical methods to estimate the amount of waste material, and quantify concentrations of CRM within the tailings.

Background

In 2011 The European Commission released a list of 14 critical raw materials (CRM) that are vital to our industries such as tungsten, and in several cases also to the transition to green energy, such as the rare earth elements. In 2020 this list grew to include 30 CRM (Regeringskansliet 2020). "Critical" raw materials are classified as such for their economic importance, limited occurrence and high potential for limitations in their supply due to geopolitical factors. By identifying secondary sources of CRM such as mine waste or recycling, these materials can potentially be supplemented with domestic production without the long process of opening new mines. The tailings repositories at Yxsjöberg provide an excellent case study due to the large amount of waste generated, and apparent poor recovery of the economic fraction of the ore.

Figure 1. Sample of tailings collected from Yxsjöberg showing the fluorescence of the tungsten mineral scheelite (blue) under shortwave UV-light, indicating relatively poor tungsten recovery at Yxsjöberg.

The Yxsjöberg mine was the largest source of tungsten in Sweden until its closure in 1989. Mining activity began in the mid-19th century extracting copper, shifting to production of tungsten and fluorite from the skarn ore in 1918. The ore contained an average of 0.27 wt% tungsten and 5.88% fluorite (AB Statsgruvor 1990). Recovery of tungsten from the crushed and processed ore varied from between 50–75%, with the unrecovered fraction disposed in the tailings. Previous sampling at Yxsjöberg has shown tungsten concentrations of up to 0.22 wt% in Morkulltjärnen, as well as high levels of other CRMs such as beryllium, tin, bismuth and indium (Hallberg & Reginiussen 2020). According to the SGU mine production database (MALMdb) 2.80 Mt of tailings were deposited at Morkulltjärnen, pointing to potential economically viable amounts of tungsten and other CRM in the waste. Discussion potential environmental hazards in the Yxsjöberg tailings has been raised by Hällström et al. (2020)

Methods

In preparation for drilling an initial surface sampling campaign was conducted in 2021 at the tailings pond at Morkulltjärnen. A total of 9 samples were collected from between 0.75 and 1.0 m depth using a handheld auger and shovel. These samples were then analysed to determine distribution of CRM throughout the tailing pond and identify which areas were likely to provide ideal drilling targets.
A total of five boreholes were drilled, and samples were taken every meter or at clear differences in

sediment properties. Samples were analyzed by ALS Sweden for major and trace elements, including fluorine. The density of the tailings for every sample was measured, and selected samples were sieved to three fractions (+63µm 63–45µm and –63µm) to determine distribution of grain size through potential sedimentary processes during deposition of the tailings.

A geophysical survey was conducted to better understand the structures within the sand, and to identify the thickness of the tailings. Several different geophysical methods were tested to map the electrical properties within the tailings and the surroundings (fig. 2). Figure 2b shows the resistivity models obtained from electrical resistivity tomography (ERT) measurements along two profiles. The tailings can be clearly identified as a layer with low resistivity underlain by other sediments and bedrock. Using these data, suitable drilling sites were located. The electrical properties of the sand can then be compared to the geochemistry to potentially identify layers rich in CRM. The resistivity models obtained from the measurements can further be used to construct a 3D model and estimate the volume of the tailings.

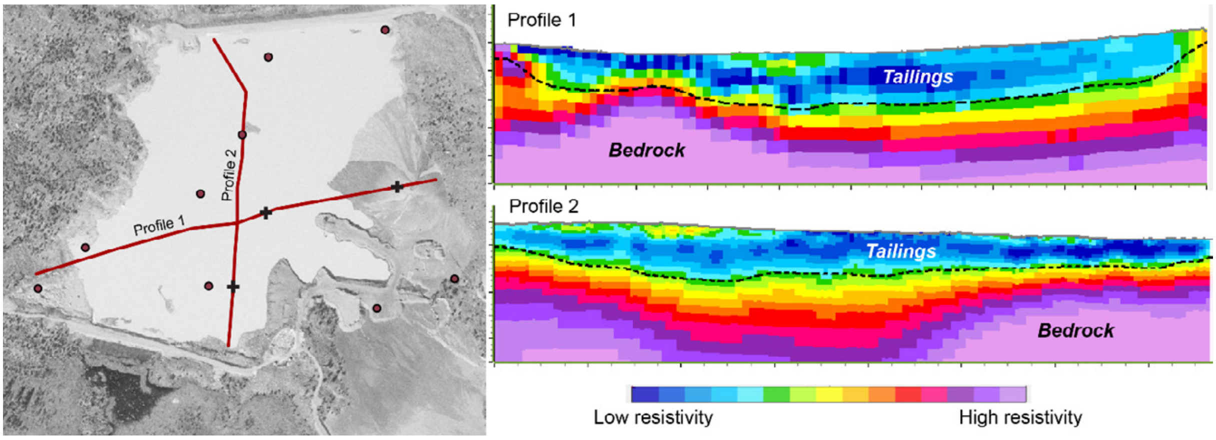

Fig. 2. A: Aerial photo of Morkulltjärnen from 1975, with location of measured ERT profiles, surface sampling (dots) and planned drilling points (crosses). B. Resistivity models from two ERT profiles. Black dotted line indicates bottom of the tailings.

Observations and application of results

Initial observations of material sampled during drilling using UV light demonstrated large quantities of scheelite remaining in the tailings (Fig. 1). An important observation made during drilling is the presence of a strongly oxidized zone above the water table indicating low pH and potentially affecting distribution of CRMs. By combining the data from the 3D models produced from geophysical surveys with density measurements and the results of geochemical analyses from the boreholes, a picture of the potential secondary resources in the tailings at Yxsjöberg will be created and used as a guide for further investigations and potential resource extraction in the future and mitigation of harmful elements entering groundwater. These methods have been applied to other tailings repositories in Bergslagen, and a full report will be released by the Geological Survey of Sweden in 2023, documenting the results.

References

AB Statsgruvor, 1990: Yxsjöbergs gruvkarta 333 och slutrapportering, 3–5.

Hallberg, A. & Reginiussen, H., 2020: Critical raw materials in ores, waste rock and tailings in Bergslagen. Sveriges geologiska undersökning, SGU-rapport 2020:38, 60 p.

Hällström, L.P., Salifu, M., Alakangas, L. & Martinsson, O. 2020: The geochemical behaviour of Be and F in historical mine tailings of Yxsjöberg, Sweden. *Journal of Geochemical Exploration* 218, 106610.

MALMdb, 2022; The SGU database of ore production and mineral processing in Sweden.

Regeringskansliet 2020: Meddelande om kritiska råvaror. *Faktapromemoria* 2020/21:FPM 52, 3–4.

Mobility of REEs during alkali alteration, Bergslagen, Sweden

Robert P. Dunst[a], Iain Pitcairn[a], Nils F. Jansson[b], Alexander Lewerentz[c]

[a]Department of Geological Sciences, Stockholm University, Stockholm, Sweden, robert.dunst@geo.su.se; [b]Devision of Geosciences and Environmental Engineering, Luleå University of Technology, Luleå, Sweden, nils.jansson@ltu.se; [c]Department of Mineral Resources, Geological Survey of Sweden, Uppsala, Sweden, alexander.lewerentz@sgu.se;

Summary. The Bergslagen ore province in central Sweden hosts several rare earth element (REE)-rich deposits, which have recently come back into focus with the increasing demand for REE. In order to understand and potentially predict the occurrence of these deposits, it is crucial to understand the hydrothermal processes that formed them. This study presents new geochemical and mineralogical data on regional alkali alteration zones in the metavolcanic rocks that host the deposits, which show strong depletion of light REE.

Introduction and geological setting

Rare earth elements (REEs) are an essential raw material for our modern technology, and especially for renewable energies, but their supply is heavily dependent on few mines in a small number of countries (Blengini et al. 2020). Therefore, they are classified as so-called critical metals (CM's) by many countries and the EU. To reduce the supply risk, western countries including Sweden are investigating mineral deposits within their borders. The Bergslagen region in central Sweden is the place where many of these, now considered critical, elements were first described in the 18th and 19th century. Mining in this part of Sweden has a long history of over 1000 years and targeted mainly iron-oxide and polymetallic sulfide deposits (Frietsch 1975). The geology of the Bergslagen ore province is defined by a 1.91–1.86 Ga old metavolcanic to metasedimentary succession forming inliers in a series of 1.91–1.87 Ga old intrusions which are dominating the region by area. The metavolcanic succession formed in a shallow marine environment in a continental back-arc setting and is dominantly rhyolitic with some variation over the region. The magmatism is bimodal felsic and mafic with a dominance of the felsic compositions. The rocks were regionaly metamorphosed under low P and variable T conditions. In many areas of Bergslagen the exposed rock has been metamorphosed to amphibolite facies which obliterate the primary features of the rock. In the area of western Bergslagen; however, the metamorphism peaked at significantly lower temperatures. This allows a detailed investigation of the primary volcanic features as well as early hydrothermal alteration (Stephens et al. 2009).

Genetic models for the formation of ore deposits in Bergslagen include mobilisation of metals during hydrothermal alkali-alteration by seawater derived fluids (e.g. Lagerblad & Gorbatschev 1985), and precipitation of ore from metal-bearing magmatic fluids (e.g. Sahlström et al. 2019). The hydrothermal mobilisation model is widely applied to the formation of the base metal sulfide deposits in Bergslagen (e.g. Jansson et al. 2013). The aim of this study is to test whether the alkali alteration could also have mobilised REEs on a regional scale and as such have been the source of metal enrichments in some of the REE-bearing deposits.

Results and discussion

The study area between Hällefors and Hjulsjö in western Bergslagen exposes a 1 km thick stratigraphical section of metavolcanic rocks overlain by pelitic metasedimentary rocks (Allen et al. 1996). 125 samples were collected from the metavolcanic part of the stratigraphy, including proximal volcanic facies formed during a period of intense volcanism. The sampling focused on known areas of hydrothermal Na- and Mg-alteration, which were suggested to have developed in connection with mineralisation (Lagerblad & Gorbatschev 1985). All samples were analysed for major and trace elements by ALS Scandinavia (Piteå) with quantification by ICP-AES for major element oxides and ICP-MS for trace elements following both multi-acid and Li-tetraborate fusion digestions. A representative set was selected for thin-section petrography and semi-quantitative mineral chemical analysis by energy-dispersive scanning

(EDS). For the geochemical study a suite of least altered samples was defined based on geochemical thresholds, and mineralogical- textural characteristics. The median composition of this sample suite was used as baseline to investigate trace element mobility. A set of Na-altered and one of Mg-altered rocks was defined relative to the least altered composition.

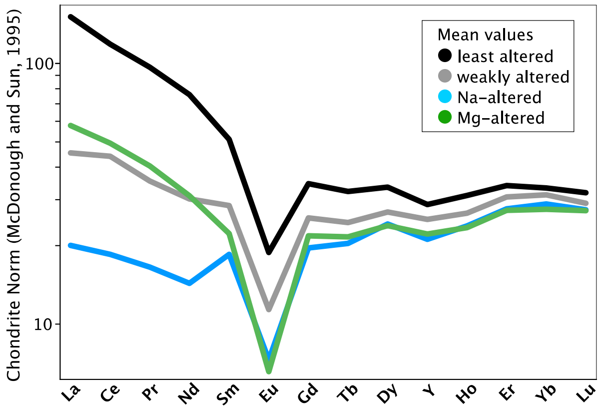

Fig. 2 Chondrite normalized REE spider plot based on the chondrite composition by McDonough and Sun (1995). The lines show the mean of the respective group.

All samples show remnants of a primary porphyritic texture and classify as rhyolite. In least-altered samples, the porphyritic texture is defined by mm-sized microcline, plagioclase and quartz phenocrysts set in a matrix dominated by very fine-grained feldspar and quartz plus variable amounts of biotite and chlorite sensu lato. Allanite group minerals are common accessory- and secondary-minerals. The Na-altered rocks are commonly indistinguishable from the least-altered in the hand sample, but are devoid of K-feldspar phenocrysts and are exclusively dominated by albite which have replaced feldspars with different compositions in the matrix and phenocrysts. Relative to the least altered samples, these samples show a depletion in K_2O, CaO, LOI and Fe_2O_3 and an enrichment in Na_2O and SiO_2. The Mg-altered rock resembles mica schist and is mostly feldspar-free and dominated by quartz (in ground mass and as relict phenocrysts), muscovite, clinochlore and minor tourmaline (dravite). These samples are depleted in most elements except for MgO which is strongly enriched. SiO_2 remains more or less unchanged.

The results of the study show that the light REEs were strongly depleted by regional alkali-alteration (Fig. 2) making REE mobilisation from the metavolcanic rocks of Bergslagen during hydrothermal alkali alteration a fertile source for the REE-rich deposits in the region.

Acknowledgements

This project is funded by the Geological Survey of Sweden (Project number 1929/2019) and the Department of Geological Sciences at Stockholm University.

References

Allen, R.L., Lundström, I., Ripa, M., Simeonov, A., Christofferson, H., 1996: Facies analysis of a 1.9 Ga, continental margin, back-arc, felsic caldera province with diverse Zn-Pb-Ag-(Cu-Au) sulfide and Fe oxide deposits, Bergslagen region, Sweden. *Economic Geology* 91(6), 979–1008.

Blengini, G. A., EL Latunussa, C., Eynard, E., Torres de Matos, C., Wittmer, D., Georgizikis, K., Pavel, P., Carrara, S., Mancini, M., Unguru, M., Blagoeva, D., Mathieux, F., Pennington, D., European commission, 2020: Study on the EU's list of Critical Raw Materials – Final Report (2020), 1-47.

Frietsch, R., 1975: Brief outline of the metallic mineral resources of Sweden. Sveriges Geologiska Undersökning.

Holtstam D., Andersson U.B., Broman C. & Mansfeld J., 2014: Origin of REE mineralization in the Bastnäs-type Fe-REE-(Cu-Mo-Bi-Au) deposits, Bergslagen, Sweden. *Mineralium Deposita* 49(8), 933–966.

Jansson, N.F., Erismann, F., Lundstam, E. & Allen, R.L., 2013: Evolution of the Paleoproterozoic volcanic-limestone-hydrothermal sediment succession and Zn-Pb-Ag and iron oxide deposits at Stollberg, Bergslagen Region, Sweden. *Economic Geology* 108, 309–355.

Lagerblad, B. & Gorbatschev, R., 1985: Hydrothermal alteration as a control of regional geochemistry and ore formation in the central Baltic Shield. *Geologische Rundschau* 74(1), 33–49.

McDonough, W.F. & Sun, S., 1995: Composition of the Earth. *Chemical Geology* 120, 223-253.

Sahlström, F., Jonsson, E., Högdahl, K., Ghaderidosst, J., Luth, S., Lynch, E., ... & Sädbom, S., 2019: Textural evolution of the Lovisa Zn-Pb-(Ag) deposit, Bergslagen, Sweden: Insights from microscopy and 3D X-ray tomography. In Proceedings of the 15th Biennial SGA Biennial Meeting, Glasgow, UK (pp. 27-30).

Stephens, M.B., Ripa, M., Lundström, I., Persson, L., Bergman, T., Ahl, M., Wahlgren, C-H., Persson, P-O. & Wickström L., 2009: Synthesis of the bedrock geology in the Bergslagen region, Fennoscandian Shield, south-central Sweden. Sveriges Geologiska Undersökning.

Critical mineral raw material potential in the Nordic countries – relevance for Europe in the 2020s and further

Pasi Eilu

Geological Survey of Finland, Espoo, Finland, pasi.eilu@gtk.fi

Summary. The Nordic countries form a large resource base of an extensive set of mineral commodities critical for the economy of Europe. The main reason for the Nordic resource richness is the diversified geology covering nearly all major orogenic events from the Palaeoarchaean to the Cenozoic.

Introduction

Since the early 2000s, all major mineral-consuming countries and the EU have been assessing the access to raw materials essential for their industries. Everywhere, we see similar sets of metals and minerals as critical (CRM), being of high importance to the economy and having major risks of supply (e.g. Blengini et al. 2020, Lee & Cha 2021). The latest CRM list for the EU contains 28 mineral/metal commodities, of which three are metal groups (HREEs, LREEs and PGMs). The number of commodities listed as critical just keeps increasing. The reasons having had an effect for the recent decades include: increasing global demand of manufactured products, increasing range and complexity of modern technologies, and the acute need towards a low-carbon society to mitigate climate change (IEA 2021). Also affecting this is the fact that, for all of the CRMs, there are no indications that the demand from almost any industrial sector is significantly decreasing. On top of these factors, we now have another, extremely acute issue: the war in Ukraine which has an immediate effect on global supply of not just fossil energy and foodstuffs, but also on the metals and minerals that Russia, Ukraine and/or Belarus have had a large share in for international trade (BGS 2022). In one of the worst-case scenarios, the World may be heading to a siloed and protectionist state of trade, not unlike what the Cold War era was, but resulting in even more restricted availability of commodities of any kind, into a ‘global fragmentation’ (WEF 2015). There currently are no major indications that any of these issues would go away in short nor medium term. This development means that probably more commodities will be added into the near-future CRM lists, especially for Europe.

Nordic CRM production, resources, and potential

Finland, Norway, Sweden, and the ice-free part of Greenland jointly form perhaps the most significant domain of CRM mine production, resource base, and potential in Europe. This is essentially grounded in that: 1) the bedrock is similar to major mineral-rich terrains globally but uniquely for Europe, 2) the Nordic countries comprising a land area comparable in size to the most mineral-rich parts of Canada, USA, Australia, South Africa, or Brazil, 3) there is a continuous presence of modern mining, and 4) locally developed leading-edge mineral exploration, mining and ore processing technology (e.g. Eilu 2012, Boyd et al. 2016, Kolb et al. 2016, Eilu et al. 2021).

For the EU, EAA, and EU-member candidate countries (excluding Turkey), we see the following for the current CRMs and for metals that may become CRMs soon (end-2020 data): 1) The only mine production of Co and phosphate is from *Finland*, and of Ti from *Norway*. Also, Finnish mines produce 95% of the PGEs and 60% of Cr, Norwegian mines 90% of flake graphite, and Swedish mines 95% of Te in Europe (Zhou & Damm 2020, BGS 2022). 2) *Finnish* known resources would cover 70–150 times the current global annual demand of Sc. For *Greenland*, the figures are 70 times for Ga, 10,000 times for Hf, 80 times for Nb, 170 times for REE, 35 times for Sr, 650 times for Ta, and 25 times for Ti. *Norwegian* known resources would cover 40 times the global annual Ti demand, and the *Swedish* V resources 40 times the global annual demand (Eilu et al. 2021, BGS 2022). 3) In addition, there is the assumed additional mineral potential: indirect information suggests that large further resources in the European context, at least, are present for Cr, Li, Ni, PGE, REE, Ta, Ti, V, and Zr in

Finland, for Cr, Nb, Ni, phosphate, Ta, Ti, and V in *Greenland*, for graphite, high-purity quartz, and Ti in *Norway*, and for graphite, Ta, Te, REE, and V in *Sweden* (Eilu et al. 2021 and references therein).

This large resource base and potential is directly related to the geology of the Nordic bedrock and cover units, combined with the extensive exploration, bedrock geology investigations, and metallogeny and mineral potential assemments done in the region (e.g. Henriksen et al. 2009, Eilu 2012, Boyd et al. 2016, Kolb et al. 2016). Essentially, there are rocks from nearly all major orogenic events since the Palaeoarchaean. In the Archaean, rifting and craton-related processes produced magmatic Ni-Co-PGE, Cr, Ti-V, and phosphate deposits. In the Proterozoic and Phanerozoic, craton and supercontinent rifting and breakup produced mafic–ultrafic intrusion-hosted Ni-Co-PGE±Ga, Cr, Ti-V, and alkaline–peralkaline and carbonatite intrusion-related REE-Nb-Ta-Hf-Zr-phosphate±Sr±Be deposits. Especially, disintegration of Kenorland (2.45–2.06 Ga) and of Columbia (1.30–1.14 Ga) produced very large deposits in Fennoscandia and Greenland, respectively. Assembly of the supercontinents Columbia and Pangaia (Laurasia) produced significant graphite, Li-Ta, Ni, Sc and W deposits. In addition, euxinic passive margin settings post-dating Kenorland and Rodinia were relevant for very large black shale-hosted Ni-Co-Cu-Zn and V-U-Mo deposits in Fennoscandia. Mesozoic to Recent passive margins have created environments for large placer Ti-V±REE±Zr deposits in Greenland.

Acknowledgements

This review is largely based on joint work between GEUS, GTK, NGU, SGU, MMR (Govt. Greenland), Reykjavik University, and the National Energy Authority of Iceland – people crucial in the work are the authors of the report by Eilu et al. (2021), and in a two-decade long work in the FODD Project (www.gtk.fi/en/fennoscandian-mineral-deposits-application-ore-deposits-database-and-maps/). The opinions expressed here are those of this author, however.

References

BGS, 2022: World mineral production 2016−2020. *British Geological Survey*, Nottingham. 88 p. Online: https://www2.bgs.ac.uk/mineralsuk/download/world_statistics/2010s/WMP_2016_2020.pdf

Blengini, G.A., Latunussa, C.E.L., Eynard, U., Torres de Matos, C., Wittmer, D., Georgitzikis, K., Pavel, C., Carrara, S., Mancini, L., Unguru, M., Blagoeva, D., Mathieux, F. & Pennington, D., 2020: Study on the EU's list of Critical Raw Materials, Final Report. 152 p. doi:10.2873/11619

Boyd, R., Bjerkgård, T., Nordahl, B. & Schiellerup, H., (eds.) 2016: Mineral resources in the Arctic. *Geological Survey of Norway, Special Publication*. 483 p.

Eilu, P., (ed.) 2012: Mineral deposits and metallogeny of Fennoscandia. *Geological Survey of Finland, Specical Paper 53*. 401 p. https://tupa.gtk.fi/julkaisu/specialpaper/sp_053.pdf

Eilu, P., Bjerkgård, T., Franzson, H., Gautneb, H., Häkkinen, T., Jonsson, E., Keiding, J.K., Pokki, J., Raaness, A., Reginiussen, H., Róbertsdóttir, B.G., Rosa, D., Sadeghi, M., Sandstad, J.S., Stendal, H., Þórhallsson, E.R. & Törmänen T., 2021: The Nordic supply potential of critical metals and minerals for a Green Energy Transition. *Nordic Innovation Report*. 93 p. Online: https://norden.diva-portal.org/smash/get/diva2:1593571/FULLTEXT02

Henriksen, N., Higgins, A.K., Kalsbeek, F. & Pulvertaft, T.C.R., 2009: Greenland from Archaean to Quaternary. Descriptive text to the 1995 Geological map of Greenland, 1:2 500 000. 2nd edition. *Geological Survey of Denmark and Greenland, Bulletin* 18. 126 p. Online: https://geusbulletin.org/index.php/geusb/article/view/4993

IEA, 2021: The role of critical minerals in clean energy transitions. Special Report of the World Energy Outlook (WEO) team of the IEA. *IEA, Paris*. 283 p. Online: www.iea.org/reports/the-role-of-critical-minerals-in-clean-energy-transitions

Kolb, J., Keiding, J.K., Steenfeldt, A., Secher, K., Keulen, N., Rosa, D. & Stensgaard, B.M., 2016: Metallogeny of Greenland. *Ore Geology Reviews* 78, 493–555. https://doi.org/10.1016/j.oregeorev.2016.03.006

Lee, K. & Cha, J., 2021: Towards improved circular economy and resource security in South Korea. *Sustainability 13*, 17. dx.doi.org/10.3390/su13010017

WEF, 2015: Mining & metals in a sustainable world 2050. Industry Agenda. *World Economic Forum*, Geneva. 43 p. Online: http://www3.weforum.org/docs/WEF_MM_Sustainable_World_2050_report_2015.pdf.

Zhou, Q. & Damm, S., 2020: Supply and demand of natural graphite. *DERA Rohstoffinformationen 43*. 36 p. Online: https://www.deutsche-rohstoffagentur.de/DERA/DE/Downloads/Studie%20Graphite%20eng%202020.pdf?__blob=publicationFile&v=3

Mineralization and alteration paragenesis of Fe-oxide-sulfide-REE mineralization in the Bastnäs area, Bergslagen ore district, Sweden

Jesse Haag[a], Iain Pitcairn[a], Alexander Lewerentz[b], Nils F. Jansson[c], Michael Eigler[d], Hein Raat[d]

[a]Department of Geological Sciences, Stockholm University, Stockholm, Sweden, thehaag@gmail.com; iain.pitcairn@geo.su.se; [b]Department of Mineral Resources, Geological Survey of Sweden, alexander.lewerentz@sgu.se; [c]Division of geoscience and environmental engineering, Luleå University of Technology, Luleå, Sweden, nils.jansson@ltu.se; [d]EMX Royalty Corp., meigler@emxroyalty.com; hraat@emxroyalty.com

Summary. The Bastnäs area hosts complex Fe-oxide-sulfide-REE mineralizations in extensively hydrothermally altered and metamorphosed wall-rocks. This study presents a partial paragenetic sequence of alteration and mineralization in the area using petrographic observations, lithogeochemistry, and thermodynamic modeling of PT conditions. Preliminary results show that the alteration assemblage proximal to the remobilized ball-ore sulfide mineralization developed after the cordierite-bearing peak metamorphic assemblage in the area.

Introduction, sample descriptions, and methods

The Bergslagen ore district contains a wide variety of mineralisation styles dominated by Fe-oxide and polymetallic sulfide mineralisation. Many deposits in the district are enriched in critical metals (CMs), such as Co, In, W and the rare earth elements (REEs). The district is considered to be a potential producer of CMs from both primary ore deposits as well as secondary resources including mine waste and tailings. There is a rich history surrounding the REE-bearing mineral deposits as many of the REEs were discovered here in the 18th century. REE-ore was produced from the Nya Bastnäs deposit in the late 19th and early 20th century (Andersson 2004). The area is a focus for a government-funded initiative to evaluate the possibility of recovering a REE mineral resource from old mine waste.

This study investigates the alteration and ore mineral paragenesis surrounding the Bastnäs type Fe-oxide-sulfide-REE mineral deposits in the Riddarhyttan area. The temporal and genetic relationships between magnetite skarn, Cu sulfide, and REE mineralisation, as well as extensive alkali metasomatism of the metamorphosed host rocks in the area are not fully understood. We report an alteration and mineral paragenesis from drill core RID-19-006 to investigate the genetic relationships between the different mineralization types and variable alteration assemblages. We integrate petrographic observations from optical microscopy and SEM combined with whole rock lithogeochemical data. As part of the project, we will also carry out thermodynamic P-T modeling to constrain the conditions at which the different alteration assemblages developed.

Results and discussion

The RID-19-006 drill core shows a large volume of cordierite-blastic rock of a presumed volcanic ash-siltstone precursor (Fig. 1a). This unit grades into a zone of anthophyllite-rich hydrothermally altered rock (Fig. 1b), which hosts sulfide mineralization (Fig. 1c) and relics of a banded iron formation (BIF). The sulfide mineralisation in this drill core is pyrrhotite-dominated and consists of both disseminated mineralization and massive ball ore. Cordierite, which grew during amphibolite facies metamorphism of a Mg-metasomatized rock (e.g. Trägårdh 1991) occurs distal to the sulfide mineralisation and the BIF which together are surrounded by an envelope of anthophyllite-altered rock. Potential explanations for this are that either 1) the anthophyllite-altered rock represents a different protolith which produced a different mineral assemblage after hydrothermal alteration and metamorphism, or 2) that the anthophyllite has replaced the cordierite-bearing assemblage during a later hydrothermal alteration event. Anthophyllite overprinting hydrated and pinite-altered cordierite could suggest that the development of amphibole occurred via breakdown of the cordierite (Fig. 1d). The implications are that this assemblage developed after the metamorphic event that caused growth of the cordierite and the deformation event that produced the foliation in the rocks. Anthophyllite also appears to replace

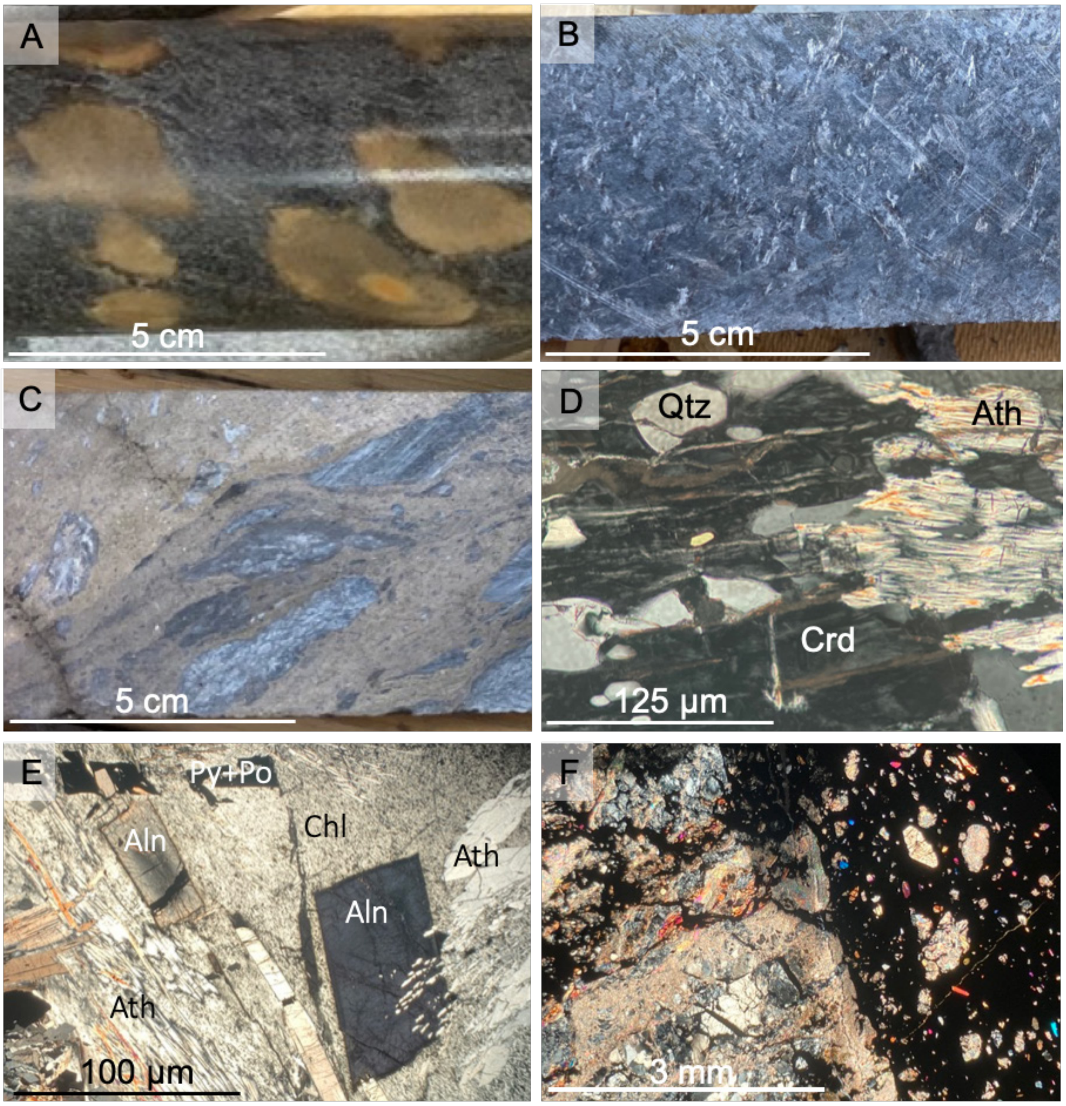

Figure 1. Core photos and thin section photomicrographs of Bastnäs drill core RID-19-006. (A) Cordierite-blasted metavolcanic rock. (B) Anthophyllite-bearing felsic rock. (C) Foliated pyrrhotite-rich massive sulfide ball ore. (D) Anthophyllite (Ath) partially replacing hydrated cordierite (Crd) and quartz (Qtz). (E) Euhedral allanite (Aln) porphyroblasts in a fine-grained chlorite (Chl) matrix partially replaced by anthophyllite (Ath). (F) Anthophyllite showing extensive talc alteration on the margin of a sulfide ball ore zone.

euhedral allanite group minerals which along with bastnäsite group minerals are the main REE-bearing minerals in the drill core (Fig. 1e). The alteration assemblage directly adjacent to the sulfide ball ore is dominated by anthophyllite that has been altered to talc (Fig. 1f). These observations place the remobilization of the sulfide ball ore as being post-peak metamorphic. The disseminated sulfide mineralization and ball ore are of very similar composition, suggesting that the ball ore represents a local remobilization from a pre-existing sulfide mineralization. The P-T conditions during the deformation event that caused the remobilization of the sulfide ball ore are not yet understood. However, preliminary results indicate the cordierite-bearing mineral assemblage was stable above c. 500°C and below c. 4.4 kbar.

References

Andersson, U.B., 2004: The Bastnäs-type REE-mineralisations in north-western Bergslagen, Sweden – a summary with geological background and excursion guide. *SGU Rapporter och meddelanden* 119, 34 pp.

Trägårdh, J., 1991: Metamorphism of magnesium-altered felsic volcanic rocks from Bergslagen, central Sweden. A transition from Mg-chlorite- to cordierite-rich rocks. *Ore Geology Reviews*, 6, 485–497.

Variations in stable C and O isotopes in metacarbonates in Bergslagen; relationships to mineralisation

Kevin Hatton[a], Iain Pitcairn[b]

[a]Institutionen för geologiska vetenskaper, Stockholms universitet, Stockholm, Sweden, Kevinhatton1998@gmail.com; [b]iain.pitcairn@geo.su.se

Summary. Carbonate samples from the Håkansboda Cu-Co deposit were analysed for C and O isotopes to investigate the extent of isotope variation during ore-related alteration. C and O isotopes can be slightly depleted when proximal to ore horizons and a weak trend to lighter $\delta^{18}O$ and $\delta^{13}C$ values can be seen in the samples overlying the main ore horizon. When comparing these isotopes regionally, distinct groupings occur for carbonate from different ore deposits. It is not yet clear if the grouping is related to ore fluid composition or other factors such as interaction with later metamorphic fluids.

Results and discussion

Bergslagen province is an important mining district that has produced metals for many centuries. Many of the deposits in Bergslagen are either hosted by, or spatially associated with carbonate units which increase in abundance in the upper parts of the Bergslagen Lithotectonic Unit. Carbonates in Bergslagen can act as host rocks for sulfide mineralisation (e.g. Sala and Garpenberg) and can be a commodity in their own right in the fom of dolomitic and calcitic marbles which is mined in a number of locations in the province (e.g. Jansson et al. 2022). The province is also well known for skarn alteration where carbonate rocks have reacted during hydrothermal alteration and/or metamorphism to form calc-silicate mineral assemblages. These calcitic and dolomitic carbonates are interbedded with thick felsic volcanosedimentary succesions, likely formed as stromatolitic growths or chemical sediments in a shallow sea between episodes of sedimentary and volcanosedimentary sedimentation. The carbonate layers commonly act as host rocks to sulfide deposits as the carbonate is partially dissolved and recrystallised by the low-pH metal-bearing ore fluids (Jansson et al. 2018).

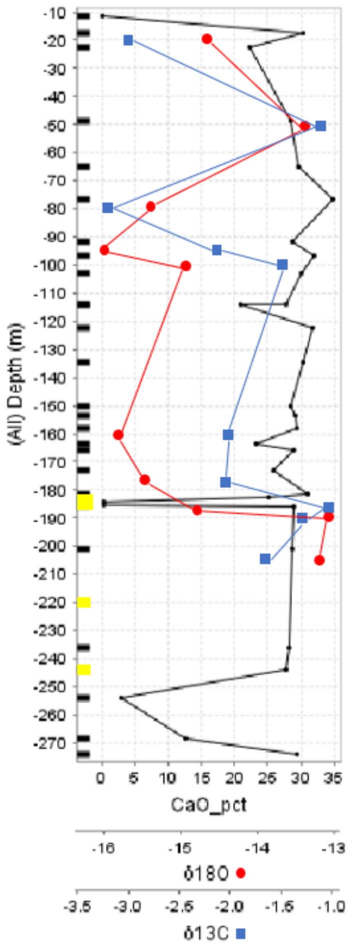

Figure 1: Downhole plot of $\delta^{13}C$ and $\delta^{18}O$ against Ca. The Yellow boxes indicate the sulfide layers.

This project focuses on the Håkansboda limestone, a dolomitic marble unit up to 250 m thick located near Lovisagruvan. The unit hosts the Håkansboda Cu-Co mineralisation horizon which occurs mainly in the upper part of the section as massive sulphide horizons surrounded by a halo of disseminated sulphides. The alteration surrounding the mineralisation is limited indicating that the fluid was most likely neutral to weakly acidic (Jansson et al. 2018). We report a suite of C and O isotopic compositions, expressed in per mil (‰) values relative to the Vienna Pee Dee Belemnite (VPDB), from from drill core DDH 371 in the Håkansboda limestone. Geochemical analyses and petrographic observations from the drill core were reported by Månbro (2021). 12 samples were analyzed using a Finnigan Mat 252 IRMS coupled with a Finnigan Gasbench II device at the Stable Isotope Lab, Department of Geological Sciences, Stockholm University and compositions range from 13.03‰ to 16.03‰ for $\delta^{18}O$ and –1.00‰ to –3.27‰ for $\delta^{13}C$ (Fig. 1). The samples show coupled variation down the drill core and samples from the stratigraphic hangingwall of the massive sulphide horizon trend towards lighter values for both isotopes closer to the ore. Further sampling is required to con-

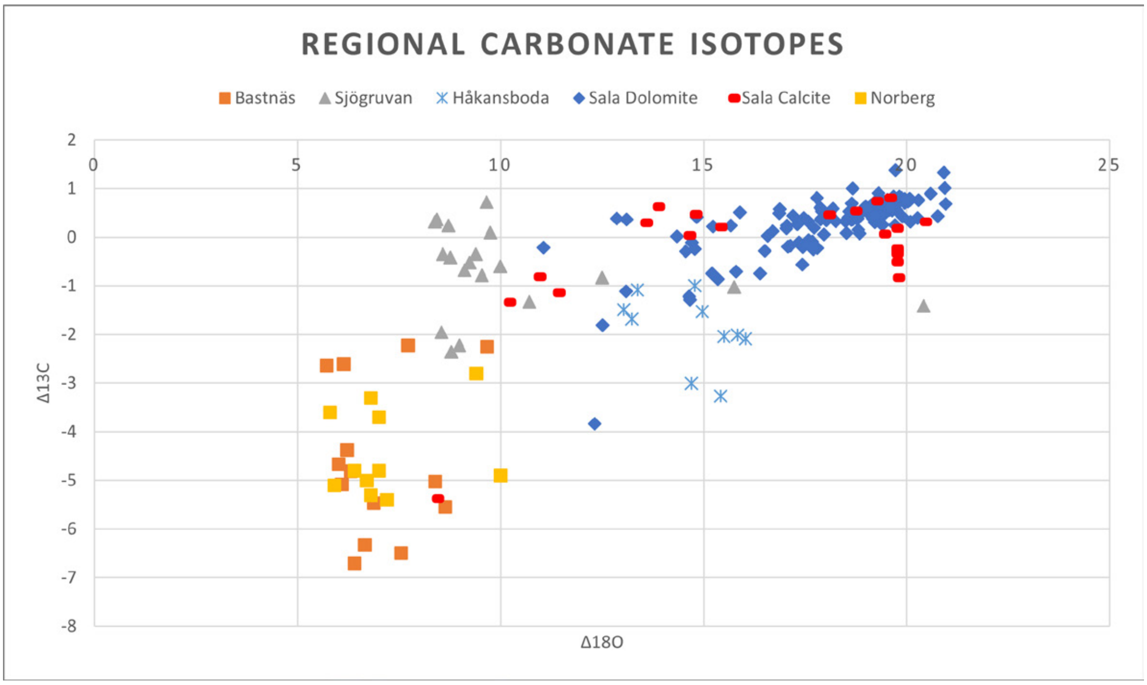

Figure 2: C and O isotopes collected from several studies across Bergslagen. The localities are distinct when displayed in this isotopic space. Sala data from Jansson et al. (2022), Sjögruvan data from Holtstam and Mansfeld (2001), Bastnäs data from Holtstam et al. (2014), Norberg data from Sahlström et al. (2019).

firm this trend. Selected C and O isotopic data from other ore deposits in the Bergslagen province are compared to those from Håkansboda in figure 2. The plot shows clusters of isotopic compositions from specific ore deposits. The heavier isotopic values from the Sala area reported by Jansson et al. (2022) are most likely representative of the primary isotopic composition of carbonate units in accordance with observations from De Groot and Shepperd (1998). The dolomites from Håkansboda plot within the array of dolomitic isotopic composition recently reported from Sala (Jansson et al. 2022). Samples from many of the other deposits show lighter O and C values and the trend to lighter values may be caused by a number of processes including more extensive dolomitisation during diagenesis, interaction with ore fluids of different composition, temperature variation, or interaction with later metamorphic fluids. A wider survey of C and O isotopes needs to be conducted in order to establish a systematic understanding of C and O isotopes in carbonate rocks in Bergslagen and the relative roles of dolomitisation, interaction with ore forming fluids of different composition formation, and metamorphism in controlling the stable isotopic compositions of these rocks.

References

De Groot, P.A and Shepherd, S.M.F. 1998: Carbonate rocks from W. Bergslagen, Central Sweden: isotopic (C, 0, H) evidence for marine deposition and alteration by hydrothermal processes. *Geologie en Mijnbouw* 67, 177-188.

Holtstam, D. and Mansfeld, J. 2001: Origin of a carbonate-hosted Fe-Mn-(Ba-As-Pb-Sb-W) deposit of Långban-type in central Sweden. *Mineralium Deposita* 36**,** 641–65.

Holtstam, D., Andersson, U.B., Broman, C.*, Mansfeld J.* 2014: Origin of REE mineralization in the Bastnäs-type Fe-REE-(Cu-Mo-Bi-Au) deposits, Bergslagen, Sweden. *Mineralium Deposita* 49**,** 933–966.

Jansson, N.F., Allen, R.L., Skogsmo, G. *Turner T.,* 2022: Origin of Palaeoproterozoic, sub-seafloor Zn-Pb-Ag skarn deposits, Sala area, Bergslagen, Sweden. *Mineralium Deposita* 57**,** 455–480.

Jansson N.F., Sädbom S., Allen R.L., Billström K. and Spry P.G., 2018: The Lovisa Stratiform Zn-Pb Deposit, Bergslagen, Sweden: Structure, Stratigraphy, and Ore Genesis. Economic Geology, 113, 699–739.

Månbro, C., 2021: The geology and geochemistry of the Håkansboda Cu-Co deposit, Bergslagen, Sweden. *Unpublished MSc Thesis, Stockholm University* 2021, 87 pp.

Sahlström, F., Jonsson, E., Högdahl, K., Troll, V. R., Harris, C., Jolis, E. M. and Weis, F. 2019: Interaction between high-temperature magmatic fluids and limestone explains 'Bastnäs-type' REE deposits in central Sweden. *Scientific Reports* 9, 1–9.

Magmatic origin of the Malmberget apatite-iron oxide deposit

Jens Henriksson[a,b], Valentin R. Troll[a], Ellen Kooijman[c], Ilya Bindeman[d]

[a]Department of Earth Sciences, Uppsala University, Uppsala, Sweden;[b]Near Mine Exploration, LKAB, Malmberget, Sweden, jens.henriksson@lkab.com; [c]Department of Geosciences, Swedish Museum of Natural History, Stockholm, Sweden; [d]Department of Earth Sciences, University of Oregon, Eugene, USA.

Summary. Fe-O isotope data from six massive magnetite samples indicates a magmatic to magmatic-hydrothermal origin of the Malmberget Apatite-Iron Oxide (AIO) ore deposit. Fe-O isotope variations between ore bodies can be explained by their structural position and proximity to the ore-forming magmatic system.

The Malmberget AIO ore deposit is considered a lower amphibolite facies analogue of the world famous Kiruna deposit (Geijer 1930). Both deposits are situated in the Paleoproterozoic northern Norrbotten ore province, northernmost Sweden. The Malmberget AIO ore deposit comprises 20 ore bodies, hosted within a package of extensively altered and deformed mafic to felsic metavolcanic rocks (Geijer 1930, Martinsson 2016). Bauer et al. (2018) grouped the ore bodies in Malmberget into two separate ore horizons. The stratigraphically lower ore horizon forms a c. 5 km semi-continuous ore zone, from the Western Field, through Printzsköld-Alliansen to ViRi in the east. The upper ore horizon sits in the fold hinge of the Malmberget synform and includes the Fabian, Kapten and Selet ore bodies. Several modes of formation have historically been proposed for AIO ore deposits (e.g. Geijer 1910, Hildebrand 1986, Knipping 2015, Parák 1975). However, recent thermometry studies, based on stable isotopes, suggest a high-temperature origin (>800°C), attributing low-temperature hydrothermal features to a progressively cooling magmatic system (e.g. Bilenker et al. 2016, Jonsson et al. 2013, Troll et al. 2019). In this contribution we aim to: (1) Investigate the Fe-O isotope composition of the Malmberget deposits and compare the signatures to Fe-O isotope signatures of global AIO ore deposits, (2) Evaluate potential differences in Fe-O isotope signatures between the two ore horizons (i.e. Bauer et al. 2018).

Six massive magnetite samples were collected along two drill cores transecting the Fabian (n=5) and ViRi (n=1) ore bodies, at depths of –1550 m and –1220 m, respectively. Here we present the first Fe-O isotope for massive magnetite samples from the Malmberget AIO ore deposit. $\delta^{18}O$-values are reported relative to SMOW and $\delta^{56}Fe$-values are reported relative to IRMM-014. Additionally, available literature Fe-O isotopes from global AIO ore deposits are included together with reference values for volcanic, igneous, Low-T hydrothermal and hydrothermal replacement magnetites (Fig. 1).

The Malmberget magnetite samples plot within the range of common igneous magnetites ($1‰ < \delta^{18}O < 4‰$ and $0.05‰ < \delta^{56}Fe < 0.9‰$), reflecting the original, magmatic origin of the Malmberget deposit, despite observed equilibrated textures (Geijer 1930). Moreover, all the Malmberget samples plot within the field of the Kiruna AIO ore deposit established in Troll et al. (2019) and emphasise the similarities of the two AIO ore deposits. Equilibrium calculations (Table 1) have been conducted to evaluate the potential magnetite source(s). Potential sources include basaltic to dacitic magmas (900°C) and magmatically derived High-T fluids (800°C). For $\delta^{18}O$-values, three samples are in equilibrium with a basaltic source, five samples with an andesitic source, five samples with a dacitic source, and all six samples with a High-T fluid

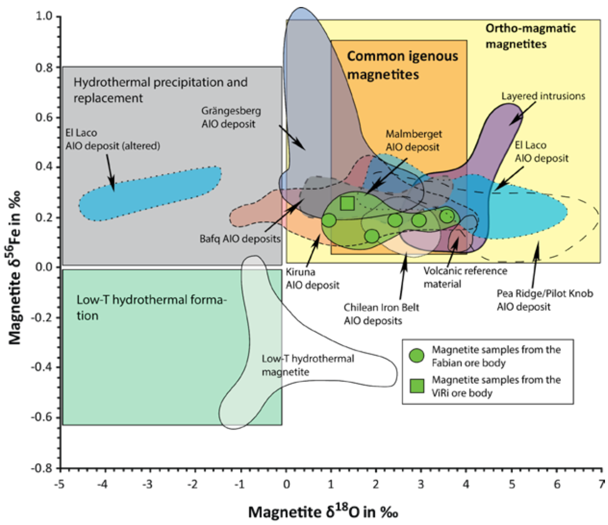

Figure 1. Discriminatory diagram for magnetite based on $\delta^{18}O$-values and $\delta^{56}Fe$-values. The coloured fields correspond to the distribution of values reported in Troll et al. (2019) and Xie et al. (2021).

Table 1. Results for the magnetite-magma (900°C) and magnetite-magmatic fluid (800°C) equilibrium calculation.

Sample	$\delta^{18}O$	2σ	$\delta^{56}Fe$	2σ	$\delta^{18}O$ Basalt	$\delta^{18}O$ Andesite	$\delta^{18}O$ Dacite	$\delta^{18}O$ Fluid	$\delta^{56}Fe$ Magma	$\delta^{56}Fe$ Fluid	Formation Temp.
FA-001	2.0	±0.2	0.16	±0.07	5.4	**6.0**	**6.3**	**7.2**	**0.13**	**–0.08**	≥800°C
FA-003	1.1	±0.2	0.18	±0.07	4.5	5.1	5.4	**6.3**	**0.15**	**–0.06**	≥800°C
FA-004	3.7	±0.2	0.19	±0.07	**7.1**	**7.7**	**8.0**	**8.9**	**0.16**	**–0.05**	≥800°C
FA-005	2.5	±0.2	0.18	±0.07	**5.9**	**6.5**	**6.8**	**7.7**	**0.15**	**–0.06**	≥800°C
FA-006	3.2	±0.2	0.18	±0.08	**6.6**	**7.2**	**7.5**	**8.4**	**0.15**	**–0.06**	≥800°C
ViRi-01	1.7	±0.2	0.25	±0.07	5.1	**5.7**	**6.0**	**6.9**	**0.22**	0.01	>800°C

Bold=in equilibrium. **Oxygen**: 1000lnα mt - (basalt) or (andesite) or (dacite) or (magmatic water 800°C) = (–3.4‰), (–4.0‰), (–4.3‰), (–5.2‰); regular range for basalts, arc andesites/dacites +5.7 to +8‰ (ref[56,57,160] in Troll et al. 2019); regular range for High-T magmatic fluids 5–10‰ (ref[161,162] in Troll et al. 2019). **Iron**: 1000lnα mt - (magma) or (magmatic water 800°C) = (0.03‰), (0.24‰); regular range of arc andesites/dacites +0.00 to +0.12‰ (ref[39] in Troll et al. 2019); regular range for High-T magmatic fluids 0.00 to –0.35‰ (ref[39,70] in Troll et al. 2019).

source. All the samples have δ^{56}Fe-values in equilibrium with a magma source, whereas all samples except ViRi-01 are in equilibrium with a High-T fluid source.

Consequently, uniform equilibrium for the Fabian magnetites is exclusively attained with a High-T fluid source, whereas the ViRi magnetite is in equilibrium with a dacitic to andesitic magma. The observed magnetite-source dissimilarity between the ViRi and Fabian ore bodies is in agreement with the two ore horizons interpreted in Bauer et al. (2018), where ViRi sits in a structurally lower position, more proximal to the magmatic centre of the ore-forming system.

Acknowledgements

We thank Vetenskapsrådet (grant number 2020-03789) for funding this project.

References

Bauer, T., Andersson, J.B.H., Sarlus, Z., Lund, C. & Kearney, T., 2018: Structural Controls on the Setting, Shape, and Hydrothermal Alteration of the Malmberget Iron Oxide-Apatite Deposit, Northern Sweden. *Economic Geology 133*, 377–395.

Bilenker, L.D., Simon, A.C., Reich, M., Lundstrom, C.C., Gajos, N., Bindeman, I., Barra, F. & Munizaga, R., 2016: Fe–O stable isotope pairs elucidate a high-temperature origin of Chilean iron oxide-apatite deposits, *Geochimica et cosmochimica acta 177*, 94–104.

Geijer, P., 1910: Igneous rocks and iron ores of Kiirunavaara, Luossavaara and Tuollavaara. Scientific and Practical Researches in Lapland arranged by the Luossavaara-Kiirunavaara Aktiebolag, *Geology of the Kiruna district 2*, Stockholm, 278 p.

Geijer, P., 1930: Gällivare malmfält: geologisk beskrivning. *Sveriges Geologiska Undersokning C 22*, 115 p.

Hildebrand, R.S., 1986: Kiruna-type deposits; their origin and relationship to intermediate subvolcanic plutons in the Great Bear magmatic zone, Northwest Canada. *Economic Geology 81*, 640–659.

Jonsson, E., Troll, V.R., Högdahl, K., Harris, C., Weis, F., Nilsson, K.P. & Skelton, A., 2013: Magmatic origin of giant 'Kiruna-type' apatite-iron-oxide ores in Central Sweden. *Scientific reports 3*, 1644–1644.

Knipping, J.L., Bilenker, L.D., Simon, A.C., Reich, M., Barra, F., Deditius, A.P., Lundstrom, C., Bindeman, I. & Munizaga, R., 2015: Giant Kiruna-type deposits form by efficient flotation of magmatic magnetite suspensions. *Geology 43*, 591–594.

Martinsson, O., Billström, K., Broman, C., Weihed, P. & Wanhainen, C., 2016: Metallogeny of the Northern Norrbotten Ore Province, northern Fennoscandian Shield with emphasis on IOCG and apatite-iron ore deposits. *Ore geology reviews 78*, 447–492.

Parák, T., 1975: Kiruna iron ores are not "intrusive-magmatic ores of the Kiruna Type. *Economic Geology* 70, 1242–1258.

Troll, V.R., Weis, F.A., Jonsson, E., Andersson, U.B., Majidi, S.A., Högdahl, K., Harris, C., Millet, M., Chinnasamy, S.S., Kooijman, E. & Nilsson, K.P., 2019: Global Fe-O isotope correlation reveals magmatic origin of Kiruna-type apatite-iron-oxide ores. *Nature Communications 10*, 1712–1712.

Xie, Q.H., Zhang, Z.C., Hou, T., Cheng, Z., Campos, E., Wang, Z.C. & Fei, X.H., 2019: New insights for the formation of Kiruna-type iron deposits by immiscible hydrous Fe-P melt and high-temperature hydrothermal processes; evidence from El Laco Deposit. *Economic Geology 114*, 35–46.

A preliminary comparison of the Per Geijer and Kiirunavaara apatite-iron oxide (AIO) deposits

Johan Hilmo, Jo Miles, Iana Bacquet

LKAB, Prospektering Fält, Kiruna, Sweden, exf.prospektering.falt@lkab.com

Summary. Located ~3 km northeast of the world-class Kiruna deposit, the neighbouring Per Geijer (PG) apatite-iron oxide deposit lies stratigraphically higher in the Kiirunavaara Group and contains significantly more hematite and phosphorus. Here, stratigraphy and textures suggest that Fe-rich fluids breached the paleosurface during formation of the mineralisation. We consider PG to have extended into the submarine environment with ore-forming processes similar to that of magmatic-hydrothermal-exhalative systems.

Background

The Per Geijer (PG) area is located ~3 km northeast of the Kiirunavaara deposit and Kiruna town in Norrbotten, Sweden (Fig. 1). The area hosts several apatite-iron oxide (AIO) lenses of magnetite, but also hematite and mixed magnetite-hematite ore bodies. During the early and mid-20th century, four surface occurrences were actively mined, but recent exploration (since 2010) has targeted the 'PG Deep' ore body. With a stratigraphy consistently dipping towards the east, PG Deep lies down-dip in the continuity of the surface ores extending to depths beyond 500 m.

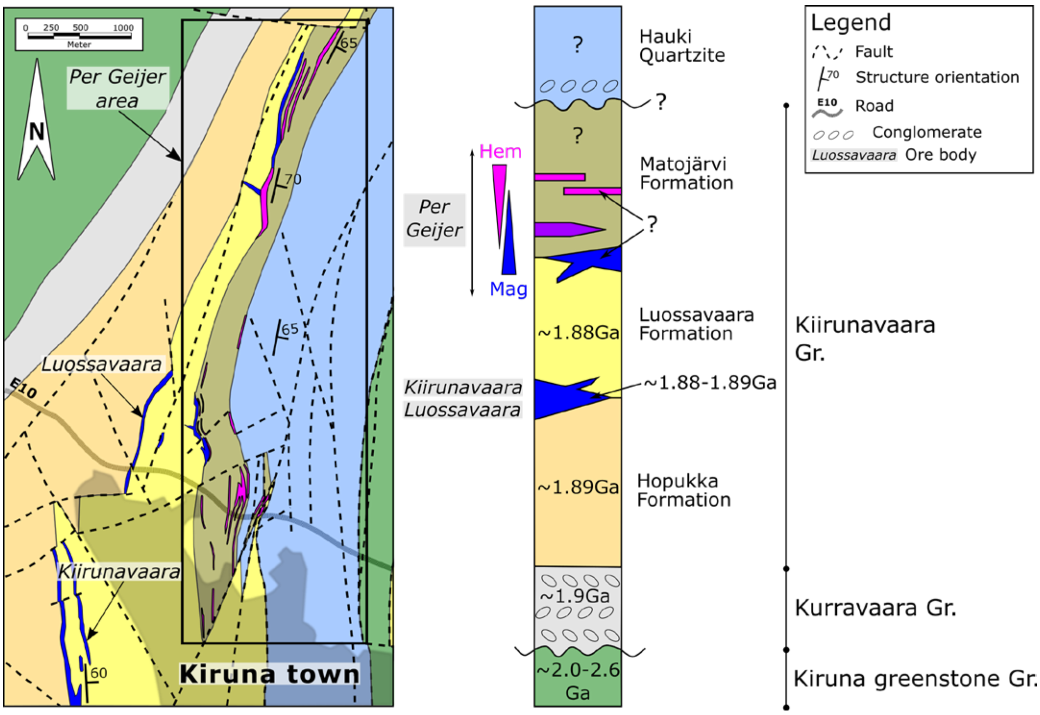

Figure 1: Geological map and stratigraphy of the PG area. Map simplified after Martinsson and Erlandsson (2009).

Geology and mineralisation of Per Geijer: how does it compare to Kiruna?

The stratigraphy of the PG area begins in a subaerial to submarine environment, with the emplacement of a subaerial rhyodacitic flow unit (pyroclastic and lava flows) of the Luossavaara Formation. This unit is commonly the footwall for PG Fe-mineralisation and laterally grades up into the volcanic-sedimentary units of the Matojärvi Formation (siltstones to sandstones, conglomerates, tuffs and flows). The Matojärvi Formation also hosts mineralisation itself, although it is often dominated by hematite. It is overlain by the Hauki Quartzite Formation (quartzite, conglomerates and phyllites) that reflect basin infill. The stratigraphy is later affected by greenschist facies metamorphism. Textures observed in drill core (e.g. graded bedding), suggest a likely submarine deposition of the Matojärvi Formation and its upper hematite ore that is disseminated within basinal sands (Fig. 2A). Preferential replacement of laterally extensive mafic units occurs within the Matojärvi volcanic pile (Fig. 2B), suggesting a hydrothermal component to ore emplacement at PG. However, the lower Fe-ore (PG Deep) occurring at the stratigraphic contact between the Luossavaara and Matojärvi Formations share textural similarities to ores of Kiirunavaara (Fig. 2C). They are often massive and intrusive-like (± flow banding). Alternatively, delicate laminations and graded bedding of layers of apatite and magnetite (Fig. 2D), may also reflect exhalation of P-rich fluids. With increasing host-rock interaction, the matrix of the Luossavaara rhyodacite footwall can also be partially replaced (Fig. 2E).

While Kiruna is the type-locality for AIO deposits, the origin remains controversial (e.g. Troll et al. 2019). Unlike the Kiirunavaara magnetite ores, PG contains significant hematite from the transformation of magnetite to hematite (martitisation). This can result in the formation of mixed ore when the martitisation process is not entirely complete. In general, textures observed at PG Deep can be most likened to Kiirunavaara (Nyström & Henríquez 1994). However, the genetic relationship between Kiirunavaara and PG remains unknown, except for the proximity in stratigraphy. The textures at PG suggest variable processes for ore formation and evolution of the volcanic-sedimentary pile within a dynamic subaerial to submarine environment.

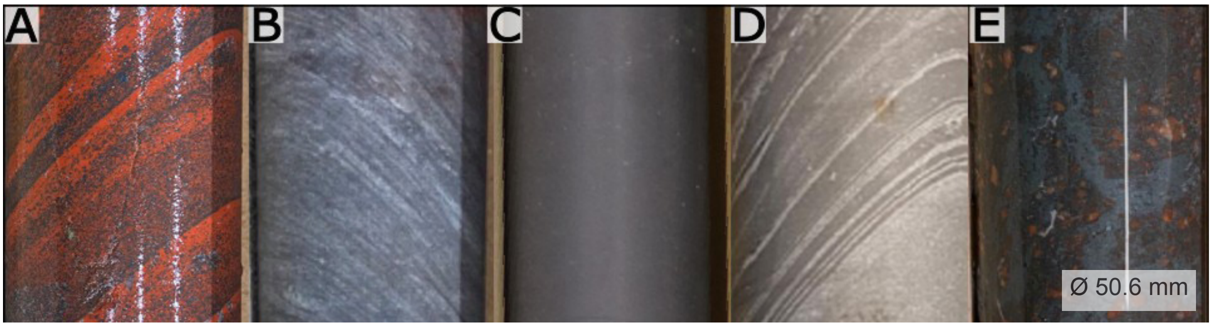

Figure 2: Mineralisation styles found in Per Geijer ores: A) Stratified sandstone/siltstone + hematite dissemination; B) Replacement-style hematite with relict amygdales and sericite-rich feldspar laths within an andesite; C) Massive magnetite, almost texture-less; D) Magnetite-apatite rock with well-preserved lamination; and E) Replacement-style hematite mineralisation with relict quartz-feldspar phenocrysts of a rhyodacitic lava/ignimbrite.

Exploration implications

Textures at PG suggest Fe-rich fluids likely breached the seafloor, resulting in partial oxidation (martitisation), sedimentary-like features within the ore itself, and a dynamic depositional environment for the volcanic-sedimentary pile. Apatite-iron oxide ores are not known to extend into this type of environment and our preliminary observations allows us to draw upon knowledge from known submarine systems and their processes, i.e. exhalites. It appears that PG may be a hybrid magmatic-hydrothermal-exhalative system and consequently, a shallow analogue to that of the Kiirunavaara ores, that extended into the submarine environment. Per Geijer Deep occurs at a stratigraphic break between the Luossavaara and Matojärvi Formations, and the upper 'sedimentary-like' Fe-ores were likely emplaced between pulses of sedimentation in a basin environment. However, basin environments can also be subjected to erosion and transportation, which may impact the preservation potential of submarine AIO-ores.

References

Martinsson, O. & Erlandsson, M., 2009: Fältarbete 2006-2008: objekt Lappmalmen. GeoVista Ab, *Internal Consultant report* GV 09018, 8–9.

Nyström, J.O. & Henríquez, F., 1994: Magmatic features of iron ores of the Kiruna type in Chile and Sweden: ore textures and magnetite geochemistry. *Economic Geology 89*, 820–839.

Troll, V.R., Weis, F.A., Jonsson, E., Andersson, U.B., Majidi, S.A., Högdahl, K., Harris, C., Millet, M.-A., Chinnasamy, S.S., Kooijman, E. & Nilsson, K.P., 2019: Global Fe–O isotope correlation reveals magmatic origin of Kiruna-type apatite-iron-oxide ores. *Nature Communications 10*, 1–12.

Mass-dependent Zn and Cd isotope fractionation in Swedish base metal sulphide deposits

Nils F. Jansson[a], Christina Wanhainen[a], Emma Engström[a,b], Ilia Rodushkin[a,b], Glacialle Tiu[a], Ingeborg Hjorth[a], Jonathan Rincon[a]

[a]Division of Geosciences and Environmental Engineering, Luleå University of Technology, SE-971 87 Luleå, Sweden, nils.jansson@ltu.se, [b]ALS Laboratory Group, ALS Scandinavia AB, Luleå, Sweden, Emma.Engstrom@alsglobal.com

Summary. The ZnTrace project has assembled the first extensive dataset on non-conventional metal isotopes (Zn, Cd, Fe, Cu) from Zn-rich sulphide deposits in Sweden. The dataset amounts to 61 analyses of sphalerite concentrates and Zn-rich pulps from nine major sulphide deposits, including all active Zn mines in Sweden. Elemental analyses and isotope ratio measurements were performed by ICP-SFMS and MC-ICP-MS, respectively, at ALS Scandinavia AB in Luleå. This contribution presents some preliminary findings and implications from the dataset with a focus on the Zinkgruvan deposit.

Zn/Cd–δ^{66}Zn–$\delta^{114/110}$Cd systematics in sphalerite

Cadmium and zinc have broadly similar geochemical and crystallographic characteristics, whereby Cd commonly substitutes for Zn in the sphalerite lattice. Thermodynamic modelling by Wen et al. (2016) suggest that this substitution is favored by high temperatures, yet differ depending on other physicochemical parameters in the hydrothermal fluid, e.g. redox state and salinity. Moreover, rapid precipitation of sphalerite from hydrothermal fluids at T<300°C commonly cause kinetic fractionation effects for isotopes of both elements, leading to the enrichment of the lighter isotopes in sphalerite (e.g. Wen et al. 2016; Kelley et al. 2009). However, at T>300°C, T-dependent fractionation can cause an elevated δ^{66}Zn in hydrothermal precipitates (Toutain et al. 2008). Hence, δ^{66}Zn, Zn/Cd and $\delta^{114/110}$Cd can be useful for better constraining processes of Zn ore formation.

In our sample set of hand-picked sphalerite concentrates from Swedish Zn deposits, we obtain clear correlations between Zn/Cd and δ^{66}Zn at Sala ($R^2 = 0.75$, n = 6), Garpenberg ($R^2 = 0.91$, n = 5), Lovisa ($R^2 = 0.84$, n = 7), Zinkgruvan ($R^2 = 0.90$, n = 4) in Bergslagen, and samples of Skellefte district VMS deposits ($R^2 = 0.52$, n = 12). Stratabound, marble- and skarn-hosted Zn-Pb-Ag±(Cu)±(Au) mineralization from Sala and Garpenberg exhibit anomalously high δ^{66}Zn in relation to stratiform Zn-Pb±Ag mineralization from Zinkgruvan and Lovisa. Massive sulphide mineralization from Falun and from four Skellefte district VMS deposits (Kristineberg, Rävliden N, Långträsk, Renström) plot in-between these groups.

The vertical separation of deposit-grouped δ^{66}Zn data mirror broad formation temperature estimates deduced from various geological critera, which suggest a high-T (>250°C) contact metasomatic skarn origin for Sala, hybrid VMS-skarn and VMS-SEDEX models for Garpenberg and Lovisa respectively, and a relatively low-T (150–250°C), SEDEX model for Zinkgruvan. The results are hence in agreement with existing genetic models, and with more general inferences on δ^{66}Zn, Zn/Cd and $\delta^{114/110}$Cd in natural ore-forming systems. A transition in fractionation mechanism from T-dependent to kinetic with falling T is the most likely reason why sphalerite from vent-proximal Cu mineralization at Zinkgruvan shows a high δ^{66}Zn in relation to stratiform ore from this deposit. Alternatively, the different δ^{66}Zn values point to key differences in the source rocks of the deposits.

To test the applicability of the results above to impure, non-concentrated samples of sphalerite mineralization, we analyzed 20 whole-rock pulps from different parts of the Zinkgruvan deposit, ranging from 1.4 to 70.1 wt% sphalerite (Hjorth 2022). Measured $\delta^{114/110}$Cd values exhibit a clear positive trend against Zn/Cd. Earlier studies have shown that proximal sphalerite at Zinkgruvan is enriched in Fe, Cd and Co (Hjorth 2022). There is a strong negative correlation between measured pulp Zn/Cd values, and Co content in sphalerite from the same pulps, independently determined using LA-ICP-MS

(Hjorth, 2022). Hence, we conclude that Zn/Cd is an excellent proxy for proximal vs. distal position at Zinkgruvan, and that $\delta^{114/110}$Cd increase from proximal to distal at this deposit most likely reflect Rayleigh distillation.

Pulp samples from distal mineralization at Nygruvan plot along the δ^{66}Zn vs. Zn/Cd trendline defined using concentrate data, whereas samples of proximal mineralization from the Knalla mine (Sävsjön, Mellanby, Burkland) generally exhibit higher δ^{66}Zn. The isotopic variations hence mirror a deposit-scale transition from distal stratiform mineralization, to proximal stratiform and stratabound mineralization in marble, tuffite and skarn at Zinkgruvan. Mineralization from the Dalby area north of Knalla mine plot close to the vent-proximal mineralization at Knalla mine, consistent with the inferences of Dalby being a northern continuation of the Zinkgruvan vent zone (Hjorth 2022)

Conclusions

The Zn/Cd–δ^{66}Zn–$\delta^{114/110}$Cd systematics in the sampled deposits are sufficiently distinct to differentiate between the main types of Zn deposits in Sweden, and for providing information on mineralization types and vent-proximity. Thus, metal isotopic data could provide an empirical tool for fingerprinting specific deposits or deposit types, with implications for both classic ore genetic studies and exploration, but also for traceability applications such as e.g. providing analytical fingerprints that can aid sustainability certification of concentrates from Swedish zinc mines.

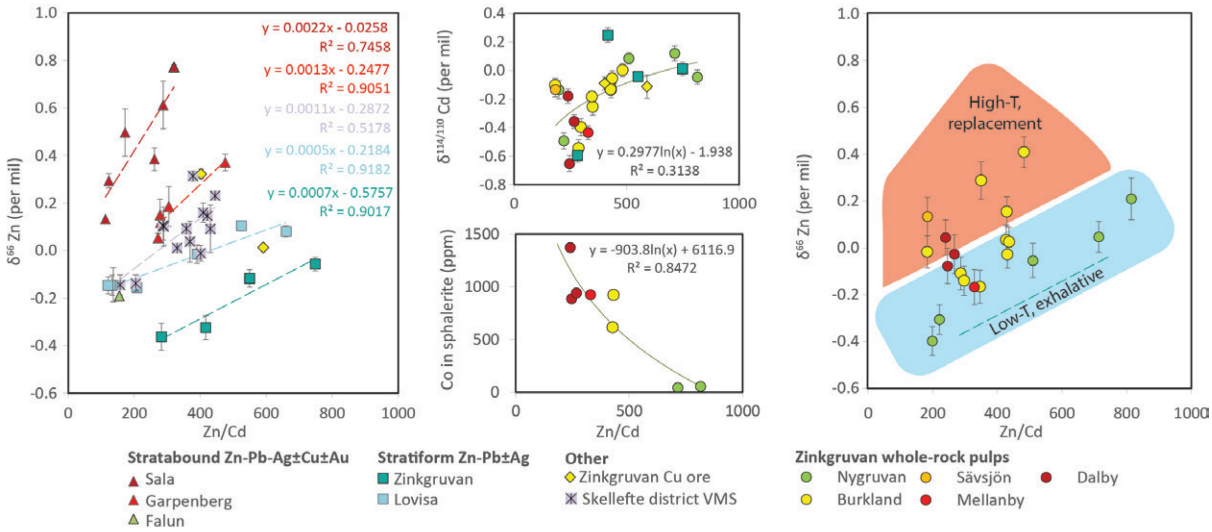

Acknowledgments

This research has been carried out within the strategic innovation program Swedish Mining Innovation, a joint venture by Vinnova, Formas and the Swedish Energy Agency, and within the the Center of Advanced Mining and Metallurgy (CAMM) at Luleå University of Technology. Boliden Mineral AB, Lovisagruvan AB and Zinkgruvan Mining AB are thanked for providing samples for analysis and additional financial support to help cover the analytical costs.

References

Hjorth, I., 2022: Characterization of the cobalt content in zinc ore from Zinkgruvan, Sweden. MSc thesis, Luleå University of Technology, 123 p.

Kelley, K.D., Wilkinson, J.J., Chapman, J.B., Crowther, H.L. & Weiss, D.J., 2009: Zinc isotopes in sphalerite from the base metal deposits in the Red dog district, Northern Alaska. *Economic Geology* 104, 767–773

Toutain, J-P., Sonke, J., Munoz, M., Nonell, A., Polvé, M., Viers, J., Freydier, R., Sortino, F., Joron, J.-L. & Sumarti, S., 2008: Evidence for Zn isotopic fractionation at Merapi volcano. *Chemical Geology* 253, 74–82

Wen, H., Zhu, C., Zhang, Y., Cloquet, C., Fan, H. & Shaogon, F., 2016: Zn/Cd ratios and cadmium isotope evidence for the classification of lead-zinc deposits. *Scientific Reports* 6:25273, DOI:10.1038/srep25273, 8 p.

Evidence for metamorphic ore melts in the Palaeoproterozoic Enåsen gold deposit, central Sweden?

Erik Jonsson[a,b], Simon Pieslinger[b]

[a]Department of Mineral Resources, Geological Survey of Sweden, Uppsala, Sweden; erik.jonsson@sgu.se,
[b]Department of Earth Sciences, Uppsala University, Uppsala, Sweden

Summary. During a current project on the Palaeoproterozoic Enåsen gold deposit in Hälsingland, central Sweden, we have initiated studies of ore mineral assemblages in the sillimanite quartzite host rock. These are dominated by sulphides, sulphosalts, tellurides and native gold. Combining existing P-T-data with our observations of complex symplectitic and related intergrowths of tellurides and sulphides/sulphosalts, including Se-bearing Bi tellurides and the Cu tellurides rickardite ($Cu_{3-x}Te_2$) and vulcanite (CuTe), we interpret the former as relics of quenched syn-regional metamorphic ore melts.

The Enåsen deposit and current project

The Enåsen gold(-copper) deposit, hosted by Palaeoproterozoic, mainly metasupracrustal rocks within the Ljusdal lithotectonic unit in central Sweden (Högdahl & Bergman 2020), was mined between 1984 and 1991 (Wik et al. 2009). Based mainly on geochemical evidence including isotope systematics combined with its mineralogical-petrological character, the Enåsen Au-Cu mineralisation and its immediate host rock, a sillimanite-rich quartzite, was interpreted as a high-grade metamorphosed epithermal system (Hallberg 1994, Hallberg & Fallick 1994). Regional metamorphic conditions were estimated to 600–700°C and 4–6 kb (Nysten & Annersten 1984, Hallberg & Fallick 1994). The ore mineralogy of in particular gold-associated assemblages, including Co-bearing minerals and diverse Bi, Sb and Se-bearing tellurides, was described by Nysten & Annersten (1984). An on-going project at the Geological Survey of Sweden (SGU) is focused on the Enåsen deposit and surroundings (Bergman et al. 2022) and includes the present study of the ore mineralogy and petrology. Considering the present demand for critical metals such as Bi, Co and Sb, as well as non-critical semi-metals such as Te and Se, there may also be by-product potential for these and others in Enåsen-type deposits.

Ore mineral melting in nature and laboratory

While the existence of sulphide melts in orthomagmatic ore-forming systems is well known and accepted as fundamental for many Cu-Fe-Ni sulphide deposits, the concept of metamorphogenic ore mineral melting has not reached a similar degree of consensus. Yet, mounting evidence from natural systems and experimental work suggest that such processes have operated in metamorphic environments over time (e.g. Frost et al. 2002, Mavrogenes et al. 2013, and references therein). Notably, the melting temperatures of sulphide and telluride assemblages may decrease by the addition of so-called low-melting-point chalcophile elements, e.g. As, Au, Bi, Hg, Sb, Se, Sn, Tl, Te, Cu and Pb (e.g. Frost et al. 2002, Sparks & Mavrogenes 2005). This can vitally assist the metamorphic generation and associated remobilisation of metal-rich melts under suitable conditions.

Observations and interpretations

The most abundant ore minerals in the studied samples are chalcopyrite, pyrrhotite, pyrite and bornite, as well as variable amounts of tennantite-subgroup sulphosalts. Native gold mainly occurs as minute anhedral grains or aggregates. Telluride minerals are variably abundant and a predominant one is a Se-substituted Bi-telluride corresponding to a selenian tellurobismuthite [$Bi_2(Te,Se)_3$], which often hosts symplectites, in which Cu sulphides, typically Se and Te-bearing bornite or chalcopyrite, occur as vermicular to droplet-like inclusions (Fig. 1). Complex intergrowths of Cu tellurides, mainly vermiform rickardite, with Cu sulphides and Bi tellurides also occur, locally with possibly epitactic intergrowths between rickardite and vulcanite. Another important host for in part symplectitic intergrowths

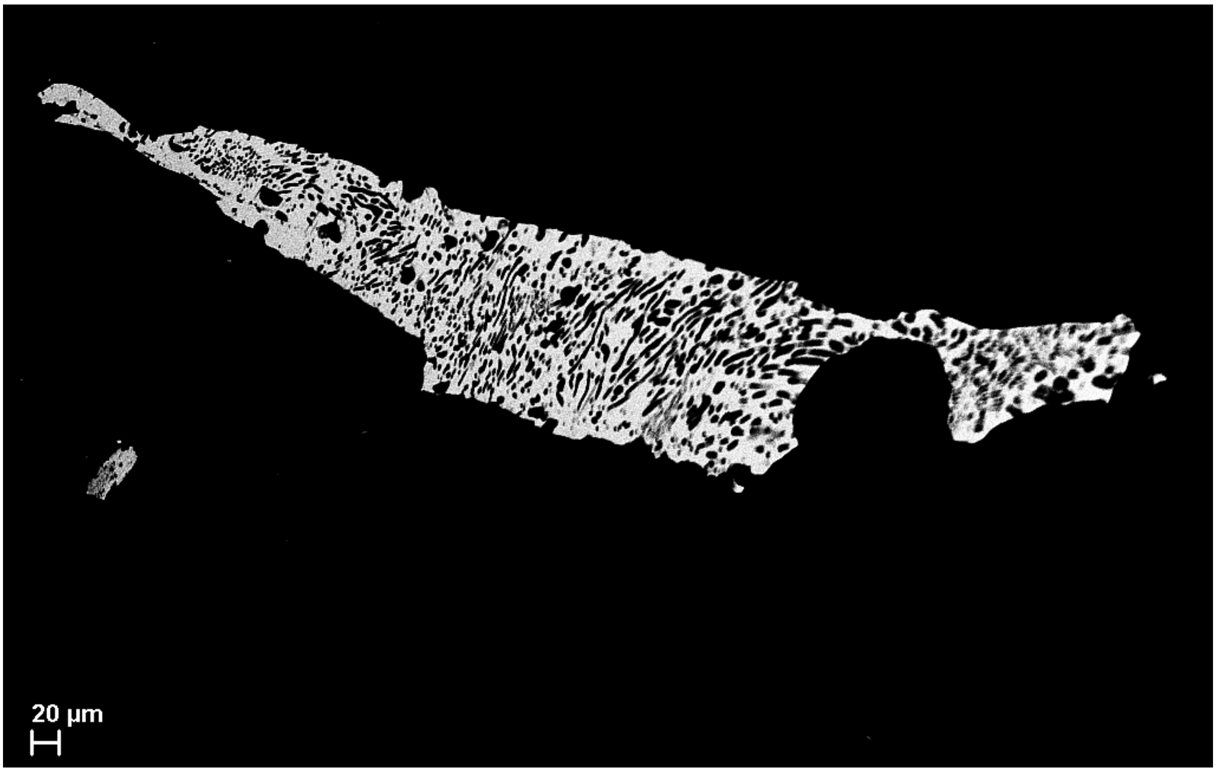

Fig. 1.Scanning electron microscope high-contrast back-scattered electron (BSE) image of a symplectite with vermicular to rounded selenian-tellurian bornite inclusions (BSE-black to dark grey) and host selenian tellurobismuthite (BSE lightest grey-white) from the Enåsen deposit. Black groundmass is host quartzite.

is a tennantite-subgroup mineral which may contain multiple mineral inclusions, mainly Cu sulphides, abundant tellurides and native gold.

Given the known P-T-conditions of regional metamorphism at Enåsen, we interpret these and similar complex symplectitic intergrowths as likely to represent quenched Te-rich polymetallic, syn-metamorphic melts which were generated within the pre-existing deposit. Additionally, the potential effects of crystal fractionation and immiscibility processes during the evolution of such ore melts (cf. Mavrogenes et al. 2013) may help to explain additional features observed in the Enåsen assemblages which we have so far not been able to fully interpret.

References

Bergman, S., Jonsson, E., Jönberger, J. & Luth, S., 2022: Mineraliseringar i området kring Enåsen – sammanfattning av pågående undersökning 2021. Sveriges geologiska undersökning, SGU-rapport 2022:05, 29 p.

Frost, B.R., Mavrogenes, J.A. & Tomkins, A.G. 2002: Partial melting of sulfide ore deposits during medium- and high-grade metamorphism. *Canadian Mineralogist* 40, 1-18.

Hallberg, A., 1994: The Enåsen gold deposit, central Sweden. 1. A Palaeoproterozoic high sulphidation epithermal gold mineralization. *Mineralium Deposita* 29, 150–162.

Hallberg, A. & Fallick, A. E., 1994: The Enåsen gold deposit, central Sweden. 2. Light element stable isotope evidence of pre-metamorphic hydrothermal activity. *Mineralium Deposita* 29, 163–169.

Högdahl, K. & Bergman, S. 2020: Paleoproterozoic (1.9–1.8 Ga), syn-orogenic magmatism and sedimentation in the Ljusdal lithotectonic unit, Svecokarelian orogen. In: Stephens, M.B. & Bergman Weihed, J. (eds.): *Sweden: Lithotectonic Framework, Tectonic Evolution and Mineral Resources*. Geological Society, London, Memoirs 50, 131–153.

Mavrogenes, J., Frost, R. & Sparks, H.A., 2013: Experimental evidence of sulfide melt evolution via immiscibility and fractional crystallisation. *Canadian Mineralogist* 51, 841-850.

Nysten, P. & Annersten, H., 1984: The gold mineralization at Enåsen, central Sweden. *Geologiska Föreningens i Stockholm Förhandlingar* 106, 245–256.

Wik, N.-G., Albrecht, L., Bergman, S., Kübler, L. & Sundberg, A., 2009: Malmer, industriella mineral och bergarter i Gävleborgs län. Sveriges geologiska undersökning, *Rapporter och meddelanden* 130, 310 pp.

Augen apatites and apatite pegmatites: new observations from the Långblå Fe-P-REE deposit, Bergslagen, Sweden

Erik Jonsson[a,b], Karin Högdahl[b], Camilla Perttula[b]

[a]Department of Mineral Resources, Geological Survey of Sweden, Uppsala, Sweden; erik.jonsson@sgu.se,
[b]Department of Earth Sciences, Uppsala University, Uppsala, Sweden

Summary. The Långblå deposit in the Grängesberg apatite-iron oxide ore district in northwestern Bergslagen, Sweden, is a previously mined apatite-iron oxide ore body interpreted as mega-xenolithic. Recent investigations at Långblå led to the discovery of several uncommon features, including augen apatites and lenses or dykes of pegmatitic apatite (both specifically fluorapatite). These exhibit low rare earth element (REE) contents but variable amounts of associated REE minerals formed from later fluid-mediated processes, such as allanite-(Ce), monazite-(Ce) and, unexpectedly, monazite-(La).

The Bergslagen apatite-iron oxide ores

So-called apatite-iron oxide (AIO) ores are the overall biggest sources of iron in Sweden and Europe, and the closed AIO mines in the Grängesberg-Blötberget area in the northwestern part of the Palaeoproterozoic Bergslagen ore province represent the largest known iron deposit concentration in Sweden south of Norrbotten. Besides iron these ores also host large amounts of the critical metals phosphorus and rare earth elements (REE). The Grängesberg and Blötberget AIO ores are widely recognised as metamorphosed and deformed deposits of Kiruna-type (e.g. Jonsson et al. 2013, and references therein). Additional AIO deposits occur in the region, outlining an incoherent and probably faulted "belt" with a roughly NE–SW strike.

The Långblå deposit

The Långblå AIO deposit, located between the Grängesberg and Blötberget mine fields, was mined during the early part of the 20th century and observed to occur as irregular (mega-)xenoliths of apatite, biotite and amphibole-bearing coarse magnetite ores with associated metavolcanic rocks, all hosted by a gneissic granitoid similar to the one forming the hangingwall at Grängesberg; the ore itself carried 64.7% Fe and 1.54% P (Geijer & Magnusson 1944). Samples for the present study were collected from outcrops and the present, overgrown dumps at the Långblå mine, and analysed by optical and electron microscopy as well as bulk geochemical and electron microprobe (EPMA) methods.

Comparisons between Långblå and the much bigger and more well-studied AIO deposits in the region, in particular Grängesberg, show some marked contrasts. Whereas apatite (specifically fluorapatite) in the ore of the Grängesberg Export field is mainly fine and even-grained and, as its associated magnetite, mainly exhibits a recrystallised granoblastic texture, the apatite at Långblå exhibits a diversity of grain sizes and textures, ranging from similarly relatively fine-grained types, to coarse or very coarse-grained anhedral to subhedral in prismatic crystals to several cm, as well as deformed and partly recrystallised c. 0.5 to 1.5 cm augen (Fig. 1A). The coarse-prismatic type of apatite forms near-monomineralic aggregates to several dm in size and essentially represent a "pegmatitic" type of apatite that locally seems to appear as dykes or lenses occasionally cross-cutting earlier-formed ore assemblages. These crystals are pervasively fractured on microscale and show extensive evidence for representing an early or primary feature within the deposit. The augen may represent more isolated, originally pegmatitic apatite crystals.

Most Långblå fluorapatites exhibit very low or not detectable REE contents, in contrast to the variability observed in Grängesberg, ranging from (very) low contents up to totals near 2.5 wt% REE_2O_3 (Jonsson et al. 2016). Yet, as in the latter location, monazite and allanite are quite abundant at Långblå, particularly as scattered, locally epitactically oriented euhedral to anhedral inclusions in fluorapatite, suggesting a dissolution-reprecipitation mode of formation from REE+P originally contained within

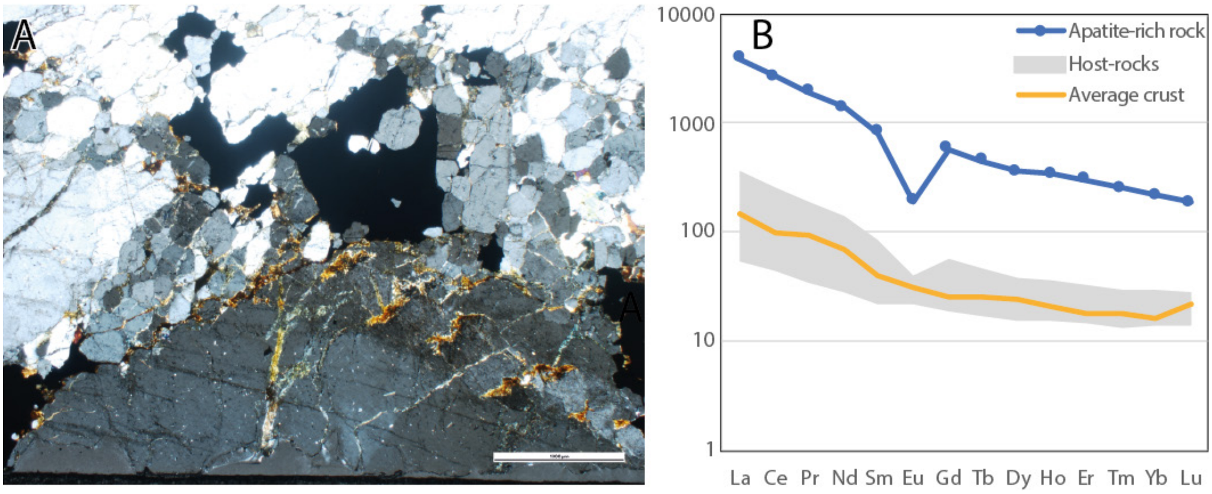

Figure 1. A. Photomicrograph of "augen" fluorapatite; thin section in cross-polarised light. The rounded and porphyroclastic fluorapatite in the lower part of the image is surrounded by finer-grained fluorapatite. The fractures in the augen apatite contain yellowish-brownish aggregates of allanite, while the interior of the fluorapatite hosts abundant small inclusions of subhedral monazite (white). The surrounding fluorapatite grains appear to form small pressure-shadows. B. Bulk geochemical analyses of samples from Långblå with reference average crustal values from Cox (1989), all chondrite-normalised (McDonough & Sun 1995).

the fluorapatite, as observed in other Palaeoproterozoic AIO deposits (e.g. Harlov et al. 2005, Jonsson et al. 2016). While the majority of analysed monazites are Ce-dominated, as are all allanites, some monazite grains had La>Ce, and are thus monazite-(La), which has not been observed previously. Cerium-dominated REE-fluorocarbonates also occur relatively widespread. The total REE concentrations are overall relatively modest in the studied samples (Fig. 1B) but exhibit patterns comparable to other AIO deposits in the region. Based on the present first impressions, we note that several textural-structural features exhibited by the Långblå ore assemblages are unique among the Bergslagen AIO ores, most importantly the occurrence of coarse "pegmatitic" fluorapatite masses that appear (on meso-scale) to cross-cut magnetite ore, but which have also been affected by both fluid-mediated REE-mobilisation as well as deformation and metamorphism. A possible interpretation is that they represent a relatively early, volatile-rich product of unmixing of the AIO magma, which could have acted as localised "intrusives" during the crystallisation of the ore body.

References

Cox, P.A., 1989: The elements. Oxford University press, 207 pp.

Geijer, P. & Magnusson, N.H. 1944: De mellansvenska järnmalmernas geologi. Sveriges Geologiska Undersökning Ca 35, 654 pp.

Harlov, D.E., Wirth, R. & Förster, H.J., 2005: An experimental study of dissolution-reprecipitation in fluorapatite: fluid infiltration and the formation of monazite. *Contributions to Mineralogy and Petrology* 150, 268–286.

Jonsson, E., Nilsson, K.P., Hallberg, A. & Högdahl, K., 2010: The Palaeoproterozoic fluorapatite-iron oxide deposits of the Grängesberg area: Kiruna-type deposits in central Sweden. *NGF abstracts and proceedings* 1, 88–89.

Jonsson, E., Troll, V.R., Högdahl, K., Harris, C., Weis, F., Nilsson, K.P. & Skelton, A., 2013: Magmatic origin of giant central Swedish "Kiruna-type" apatite-iron oxide ores. *Scientific Reports* 3, 1644, 1-8.

Jonsson, E., Harlov, D.E., Majka, J., Högdahl, K. & Persson-Nilsson, K., 2016: Fluorapatite-monazite-allanite relations in the Grängesberg apatite-iron oxide ore district, Bergslagen, Sweden. *American Mineralogist* 101, 1769-1782.

McDonough, W.F. & Sun, S.-S. 1995: The composition of the Earth. *Chemical Geology* 120, 223-253.

Persson Nilsson, K., Högdahl, K., Jonsson, E., Troll, V.R., Weis, F., Persson, L., Majka, J. & Skelton, A. 2013: The Grängesberg apatite-iron oxide deposit. Geological Survey of Sweden, SGU-rapport, 45 pp.

Age of Cu-Co-mineralised skarns, Vena mines, Bergslagen: insights from titanite LA-ICP-MS U-Pb geochronology

Alexander Lewerentz[a], Dino Leopardi[b,c], Tomas Næraa[c], Ulf Söderlund[c], Erik Jonsson[a,d]

[a]Department of Mineral Resources, Geological Survey of Sweden, alexander.lewerentz@sgu.se; erik.jonsson@sgu.se; [b]Mineral Systems Analysis Group, Institut für Mineralogie, TU Bergakademie Freiberg, Germany, dino.leopardi@mineral.tu-freiberg.de; [c]Department of Geology, Lund University, Sweden, ulf.soderlund @geol.lu.se; tomas.naeraa@geol.lu.se; [d]Department of Earth Sciences, Uppsala University, Sweden.

Summary. LA-ICP-MS U-Pb analyses of titanite from a metavolcanic rock from the Vena mines in southern Bergslagen yield a magmatic crystallisation age of 1905±30 Ma. Analyses of titanite from two skarn samples yield an age of 1906±18 Ma, interpreted as the timing of crystallisation of the skarn assemblage. These results show that skarn formation predates regional metamorphism at 1.86–1.80 Ga.

Introduction, sample descriptions and methods

The Vena mines (*Vena gruvfält*) is a historic mine field situated in the southernmost parts of the Bergslagen lithotectonic unit, where Cu and Co were extracted from polymetallic sulphide mineralisations during the years of c. 1770–1870 AD (Tegengren et al. 1924). The geology is dominated by volcanic rocks, with subordinate carbonate, calc-silicate, and sedimentary horizons. Formation of nearby volcanic rocks is constrained to c. 1.90 Ga (Kumpulainen et al. 1996). Granitoid rocks intruded at c. 1.89–1.87 Ga, after which metamorphism affected the area at c. 1.86 and c. 1.80 Ga (Stephens & Jansson 2020). In this study, we use titanite U-Pb geochronology and textural observations to explore the temporal relationship between volcanism, skarn formation, and sulphide mineralisation at the Vena mines.

Sample VNA007A, a pyrrhotite-, pyrite-, and chalcopyrite-bearing metavolcanic rock was sampled from outcrop in the walls of the Långgruvan mine. Titanite crystals reach 0.3 mm in length. Samples ALZ180089A1 and -A2 are pyrite-, pyrrhotite-, chalcopyrite-, sphalerite-, and cobaltite-bearing skarns collected from the waste piles of Nya Galtgruvan, in which up to 0.5 mm, euhedral titanite crystals are found intergrown with mainly zoisite, clinopyroxene, garnet, and calcite.

Similar mineralogy and textures of the two skarn samples strongly suggest they represent a common skarn-forming event. Textural relations in the studied skarn assemblages suggest that titanite formed significantly prior to syn-metamorphic remobilisation of, *inter alia*, sulphides (Fig. 1a). Thus, the titanite data may also represent a bracketing age for the later ore remobilisation process.

U-Pb isotope LA-ICP-MS analysis of titanite was carried out in thin sections at Lund University. Data was calibrated against the MKED1 titanite standard (Spandler et al. 2016). Data reduction was done using the Iolite software (Paton et al. 2011). The method was validated by analysis of the ONT2 titanite (Spencer et al. 2013), which resulted in common lead (Pbc) corrected ratios within 95% concordant with the preferred age. Titanite grains were imaged prior to analysis using SEM-BSE.

Results and discussion

Preliminary processing and interpretation of the titanite U-Pb data show that the U-Pb system in titanite has been disturbed in all samples. Pbc concentrations are generally high and correction of common Pb results in over-corrected ages. Instead, we consider the lower intercept of the uncorrected data as a more appropriate approach. The lower intercept obtained from sample VNA007A yields 1905 ± 30 Ma (Fig. 1b) and is interpreted as a magmatic crystallisation age. The lower intercepts for the two skarn samples yield ages of 1907 ± 31 Ma (Fig. 1c) and 1897 ± 28 Ma (fig. 1d), respectively. Data from the two skarn samples combined give a lower intercept of 1906 ± 18 Ma (n = 51, MSWD = 10), which we interpret as the timing of skarn formation. Thus, all obtained ages are within error identical.

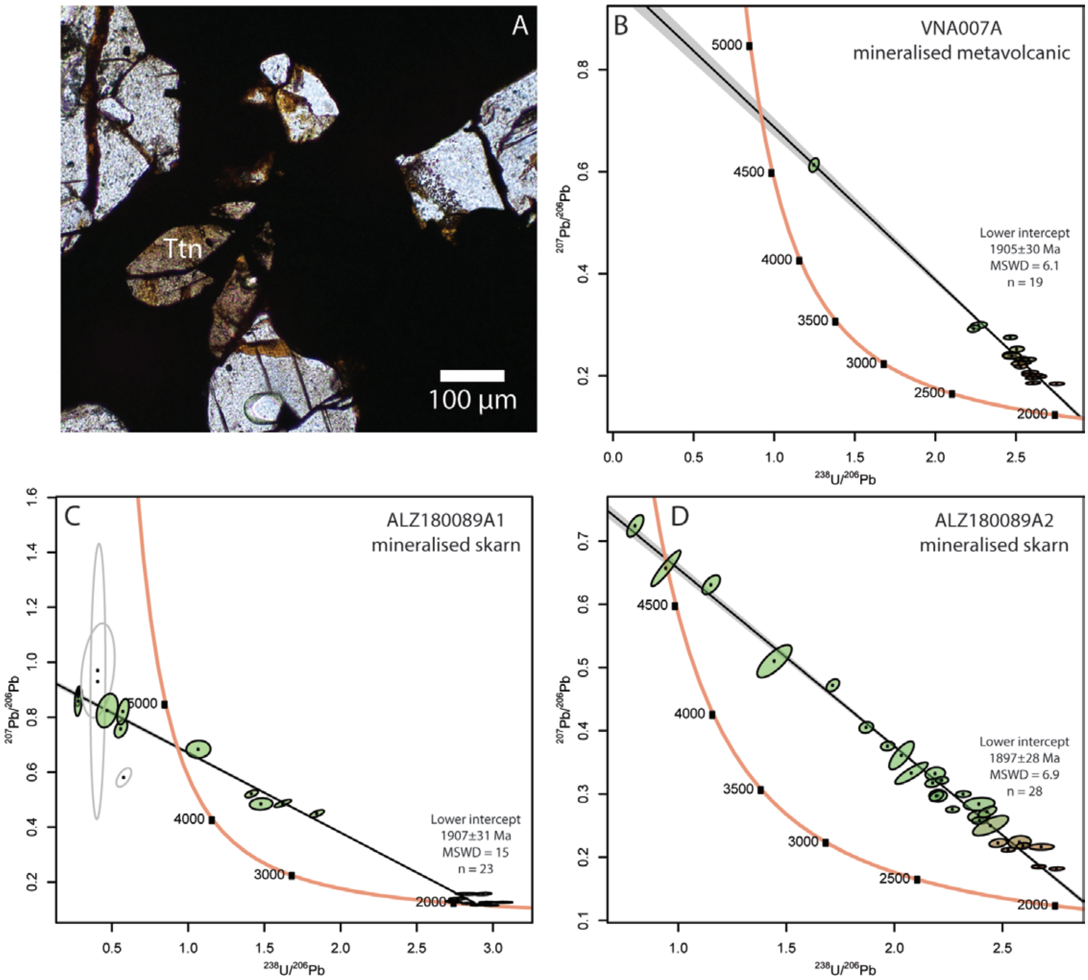

Fig. 1. A. Photomicrograph (ppl) of sample ALZ180089A-2, in which titanite and other skarn silicate crystals are brecciated by pyrrhotite (opaque) due to syn-metamorphic mechanical sulphide remobilisation. B-D. Tera-Wasserburg diagrams with results of U-Pb analyses of titanite from three samples from the Vena mines. Hollow ellipses show data filtered out due to bad spot positioning (partially outside the titanite grain).

Considering the relatively large errors of the almost identical ages, significant time may have passed between volcanism and crystallisation of the skarn assemblage. The age of 1906 ± 18 Ma, however, rules out that skarn formation was related to regional metamorphism at c. 1.86–1.80 Ga, which leaves hydrothermal processes related to either 1.90 Ga volcanism or 1.89–1.87 Ga magmatism as plausible alternatives.

References

Kumpulainen, R.A., Mansfeld, J., Sundblad, K., Neymark, L. & Bergman, T., 1996: Stratigraphy, age, and Sm-Nd isotope systematics of the country rocks to Zn-Pb sulphide deposits, Åmmeberg district, Sweden. *Economic Geology 91*, 1009–1021.

Paton, C., Hellstrom, J., Paul, B.,Woodhead, J. & Hergt, J., 2011: Iolite: Freeware for the visualisation and processing of mass spectrometric data. *Journal of Analytical Atomic Spectrometry*. doi:10.1039/c1ja10172b.

Spandler, C., Hammerli, J., Sha, P., Hilbert-Wolf, H., Hu, Y., Roberts, E. & Schmitz, M., 2016: MKED1: A new titanite standard for in situ analysis of Sm–Nd isotopes and U–Pb geochronology. *Chemical Geology 425*, 110-126.

Spencer, K.J., Hacker, B.R., Kylander-Clark, A.R.C., Andersen, T.B., Cottle, J.M., Stearns, M.A., Poletti & J.E. Seward, G.G.E., 2013: Campaign-style titanite U–Pb dating by laser-ablation ICP: Implications for crustal flow, phase transformations and titanite closure. *Chemical Geology 341*, 84-101.

Stephens, M.B. & Jansson, N.F., 2020: Chapter 6, Paleoproterozoic (1.9–1.8 Ga) syn-orogenic magmatism, sedimentation and mineralization in the Bergslagen lithotectonic unit, Svecokarelian orogen. In M.B. Stephens & J. Bergman Weihed (eds.): Sweden: lithotectonic framework, tectonic evolution and mineral resources. *Geological Society of London Memoirs 50*, 105–206.

Tegengren, F.R. et al., 1924: Sveriges ädlare malmer och bergverk. *Sveriges geologiska undersökning Ca 17*. 406 pp.

Late-orogenic timing of the Pahtohavare Cu±Au deposits constrained by a structural framework model

Leslie Logan, Joel B.H. Andersson, Ervin Veress, Olof Martinsson, Tobias E. Bauer

Division of Geosciences and Environmental Engineering, Luleå University of Technology, Luleå, Sweden, leslie.logan@ltu.se

Summary. The Kiruna mining district, known for the type locality for Kiruna-type iron oxide-apatite (IOA) deposits, also contains several Cu-mineralized ore bodies including the Pahtohavare Cu±Au sulfide deposits. To understand the broader mineral systems related to Cu mineralization, a structural investigation was conducted to assess the structural controls on the ores and place them into a regional tectonic framework. Results show that the Pahtohavare deposits formed syn- to post- F_2 folding during a late phase of the Svecokarelian orogeny.

Introduction

The Pahtohavare Cu±Au sulfide deposits are located in the southern part of the Kiruna mining district, Sweden, hosted in a SE-plunging anticline in the Kiruna greenstone group. Two of the four mineralized bodies were mined during the 1990s and produced 1.7 Mt of Cu and Au ore at 1.9% and 0.9 ppm, respectively (Martinsson et al. 1997). The orebodies are structurally and lithologically controlled with the main ore (dominantly chalcopyrite and pyrite) occurring disseminated and as breccia infill and veins in strongly albitized graphite schist and tuffite horizons. The Cu-bearing deposits in the Kiruna mining district are largely undated, except for the Rakkurijärvi IOCG deposit approximately 5 km SW of Pahtohavare, which was radiometrically constrained to have formed during the early crustal shortening phase of the Svecokarelian orogeny around 1.86 Ga (Smith et al. 2007, 2009, Martinsson et al. 2016). Furthermore, the timing of introduction and possible remobilization of Cu has not been investigated within the constraints of a regional tectonic framework, for which increasing evidence shows that mineralization is associated to two time-separated deformation events during the orogeny (e.g. Bauer et al. 2022). In this study, a structural investigation in the Pahtohavare-Rakkurijärvi areas was conducted as a part of a mineral systems approach to assess the structural controls on the mineralization in order to illuminate the relative timing of mineralization within a regional tectonic framework.

Method

Geologic mapping in the Pahtohavare-Rakkurijärvi areas took place during the 2019–2021 field seasons. Planar and linear structures were measured as dip/dip direction and plunge/azimuth conventions, respectively. Structural measurements were recorded and processed using Petroleum Experts Ltd. Field Move application and Move software. Microstructural analysis was done on thin sections prepared by Precision Petrographics Ltd. Sampling was conducted in the field and from drill core at the Geological Survey of Sweden National Drill Core Archive in Malå.

Results and discussion

The fold in the Pahtohavare-Rakkurijärvi area is bound by two shear zones: one to the south that trends NW-SE and one to the east that trends NE–SW. The geometry of the fold expressed by bedding measurements indicates it is asymmetric, non-cylindrical, with a fold axis that plunges moderately to the southeast (34/149). Parasitic fold axes along the limbs vary and may deviate from the overall orientation of the 1^{st} order fold structure. Microstructural investigations show bedding-parallel S_1 foliation is characterized by schistose or mylonitic textures. Asymmetric sigmoidal clasts with recrystallized pressure shadows suggest the fabric is tectonic and formed from non-coaxial strain. A bedding-parallel fabric is also observed in outcrop especially in biotite-scapolite-altered metavolcanosedimentary rocks. In some samples, a spaced S_2 fabric is observed occurring parallel to axial planes of F_2 folds. In the field, examples of preserved S_1 and S_2 cleavages are also observed in felsic igneous rocks outcropping 3 km southwest of the Pahtohavare area.

The evidence for both S_1 and S_2 fabrics is in contrast to the structural patterns in the Orosirian stratigraphy in the central Kiruna area, where an S_1 fabric is absent or masked. The area is hypothesized to reflect a higher crustal level that did not experience ductile deformation during the early orogenic phase, which is supported by the absence of any overprinted M_1 mineral generation and radiometric data (Andersson et al. 2021, 2022). Interestingly, the results from this study indicate that an S_1 cleavage is preserved in the volcanic and sedimentary rocks of the underlying Rhyacian and early Orosirian sections of the stratigraphy 5 km south of the central Kiruna area. This result indicates that further modeling of the structural and metamorphic evolution in the Kiruna mining district is needed and that it helps delineating areas of different crustal levels during the early orogenic phase.

The cleavage data from the Pahtohavare area mimics the overall folding pattern seen in the bedding data. This implies that the Pahtohavare fold must be an F_2 fold and formed as a result of the late orogenic deformation event in the Kiruna area. This deformation event is seen regionally, and in Kiruna is characterized by brittle-plastic conditions resulting in both shearing and brittle fracturing (Andersson et al. 2021) at 1.81 Ga (Andersson et al. 2022). Importantly, quartz-carbonate veins related to ore formation are observed in the open pit at the Pahtohavare Southern deposit cross cutting foliation. Additionally, the deposits have previously been mapped to be hosted in brittle features cross cutting the fold (Martinsson et al. 1997). Microstructural results further constrain a late generation of Cu-sulfides which are hosted (and possibly remobilized) in S_2 cleavages parallel to the axial planes of F_2 folds. Given the assumption that the quartz-carbonate (-sulfide) veins are associated to the main mineralizing event and that the ore is controlled by brittle structures from F_2 folding, the combined results indicate that the Pahtohavare epigenetic deposits must have formed syn- to post- F_2 folding. The role of remobilization of earlier mineralization (e.g. Pahtohavare Southern deposit) remains to be determined. This marks the first late orogenic relative age determination of epigenetic Cu mineralization in the Kiruna mining district, indicating that a later IOCG-style mineralization event occurred up to 80 m.y. after the formation of IOA deposits. The results from this study supports that a well-characterized tectonic framework is pivotal for gaining a holistic understanding on mineral systems.

References

Andersson, J.B.H., Bauer, T.E. & Martinsson, O., 2021: Structural evolution of the central Kiruna area, northern Norrbotten, Sweden: Implications on the geologic setting generating iron oxide-apatite and epigenetic iron and copper sulfides. *Economic Geology* 116, 1981–2009.

Andersson, J.B.H., Logan, L., Martinsson, O., Chew, D., Kooijman, E., Kielman-Schmitt, M., Kampmann, T.C., & Bauer, T.E., 2022: U-Pb zircon-titanite-apatite age constraints on basin development and basin inversion in the Kiruna mining district, Sweden. *Precambrian Research* 372, 106613.

Bauer, T.E., Lynch, E.P., Sarlus, Z., Drejing-Carroll, D., Martinsson, O., Metzger, N. & Wanhainen, C., 2022: Structural controls on iron oxide copper-gold mineralization and related alteration in a Paleoproterozoic supracrustal belt: insights from the Nautanen deformation zone and surroundings, northern Sweden. *Economic Geology* 117, 327–359.

Martinsson, O., Hallberg, A., Söderholm, K. & Billström, K., 1997: Pahtohavare - an epigenetic Cu-Au deposit in the Paleoproterozoic Kiruna Greenstones (Paper III), in Martinsson, O., Tectonic setting and metallogeny of the Kiruna Greenstones (PhD Thesis). Luleå, Sweden, Luleå University of Technology, 37 p.

Martinsson, O., Billström, K., Broman, C., Weihed, P. & Wanhainen, C., 2016: Metallogeny of the northern Norrbotten ore province, northern Fennoscandian Shield with emphasis on IOCG and apatite-iron ore deposits. *Ore Geology Reviews* 78, 447–492.

Smith, M., Coppard, J., Herrington, R. & Stein, H., 2007: The Geology of the Rakkurijärvi Cu-(Au) prospect, Norrbotten: a new iron oxide-copper-gold deposit in northern Sweden. *Economic Geology* 102, 393–414.

Smith, M.P., Storey, C.D., Jeffries, T. E. & Ryan, C., 2009: In situ U-Pb and trace element analysis of accessory minerals in the Kiruna District, Norrbotten, Sweden: new constraints on the timing and origin of mineralization. *Journal of Petrology* 50, 2063–2094.

Source-to-sink controls on granite-related W-Mo-F mineralization, western Bergslagen

Edward P. Lynch, Stefan Bergman, Robert Berggren

Department of Mineral Resources, Geological Survey of Sweden, Uppsala, Sweden,
edward.lynch@sgu.se, stefan.bergman@sgu.se, robert.berggren@sgu.se

Summary. We present an updated assessment of regional- to deposit-scale (source-to-sink) factors controlling W-Mo-F ± Cu mineralization associated with c. 1.8 Ga granites in western Bergslagen. New petrological, structural, geochemical, and geochronological (U-Pb, Re-Os) data provide insights into the petrogenesis of mineralization-related granites and local factors controlling intragranitic and skarn-hosted W-Mo-F mineralization.

Introduction and geological background

The 'Western Bergslagen W-Mo' metallogenic area includes more than 100 known W-Mo-F ± Cu deposits and prospects that show a spatial and/or genetic association with late orogenic (c. 1.8 Ga) granitic intrusions (Fig. 1A; e.g. Bergman 2012). Mineralization typically comprises intragranitic disseminated molybdenite ± fluorite, and scheelite-bearing skarn zones in supracrustal rocks adjacent to granites. The southeastern margin of the W-Mo metallogenic area coincides in general with the 'Western Bergslagen Boundary Zone' (WBBZ, Beunk & Kuipers 2012), a composite regional-scale structure comprising discontinuous northeast-trending shear zones (Fig. 1A–B). Thus, the WBBZ acts as a major structural-deformational boundary separating mineralization-related granitic intrusions in the NW from equivalent, generally barren granites in the SE.

Late orogenic granites in western Bergslagen are characteristically high-silica, peraluminous and ferroan intrusions enriched in certain lithophile elements (e.g. K, Rb, U, Th). Across the district, their spatial distribution corresponds with elevated U-Th-K signatures in regional radiometric data reflecting their evolved character (Fig. 1B). Structurally, the granites are typically massive (undeformed) bodies that crosscut earlier metamorphic fabrics (Fig. 1C) and locally act as 'stitching plutons' with respect to regional-scale deformation zones. Southeast of the WBBZ, the granites comprise equigranular to megacrystic syenogranite to alkali feldspar granite types and lack mineralization (Fig. 1D). Northwest of the WBBZ, similar biotite granite occurs and may contain country rock xenoliths and/or mafic microgranular enclaves. Closer to skarn W prospects, reddish pink, massive, equigranular alkali feldspar granite associated with sulfide-bearing aplite-pegmatite dykes, veins and segregations are common (Fig. 1E).

Sequential, multi-scale factors controlling Bergslagen W-Mo-F mineralization

From a petrogenetic perspective, the ages and character of the studied granites supports the idea of parental magmas formed at c. 1.81–1.78 Ga by melting of c. 1.9 Ga (Svecofennian) source rocks modified by earlier subduction and/or metamorphic processes. Granite trace element systematics, inherited zircon signatures, and isotopic (Sm-Nd) compositions support an infracrustal origin and mainly metaigneous heritage. Subduction-related magmatism also occurring at c. 1.8 Ga (e.g. TIB 1 magmatic front, Fig. 1B) may have played an indirect role in granite formation via heat advection and/or mafic melt input, initiating anatexis of a metasomatized lithospheric mantle or lower to mid crust pre-enriched in ore and volatile elements (e.g. W, Mo, F). Granite geochemical trends across the WBBZ suggest fractional crystallization during magma ascent and emplacement was a key control on forming 'specialized' melts with increased potential for W-Mo-F mineralization (Fig. 1F).

At the deposit-scale, mineralized and skarn-proximal granites show textural features consistent with high degrees of fractionation and volatile enrichment including aplite-pegmatite variants depleted in mafic minerals, quartz-rich segregations, and alkali metasomatism. A mineralogical overlap between some granitic bodies and W-bearing skarns – such as fluorite, molybdenite, chalcopyrite and/or garnet

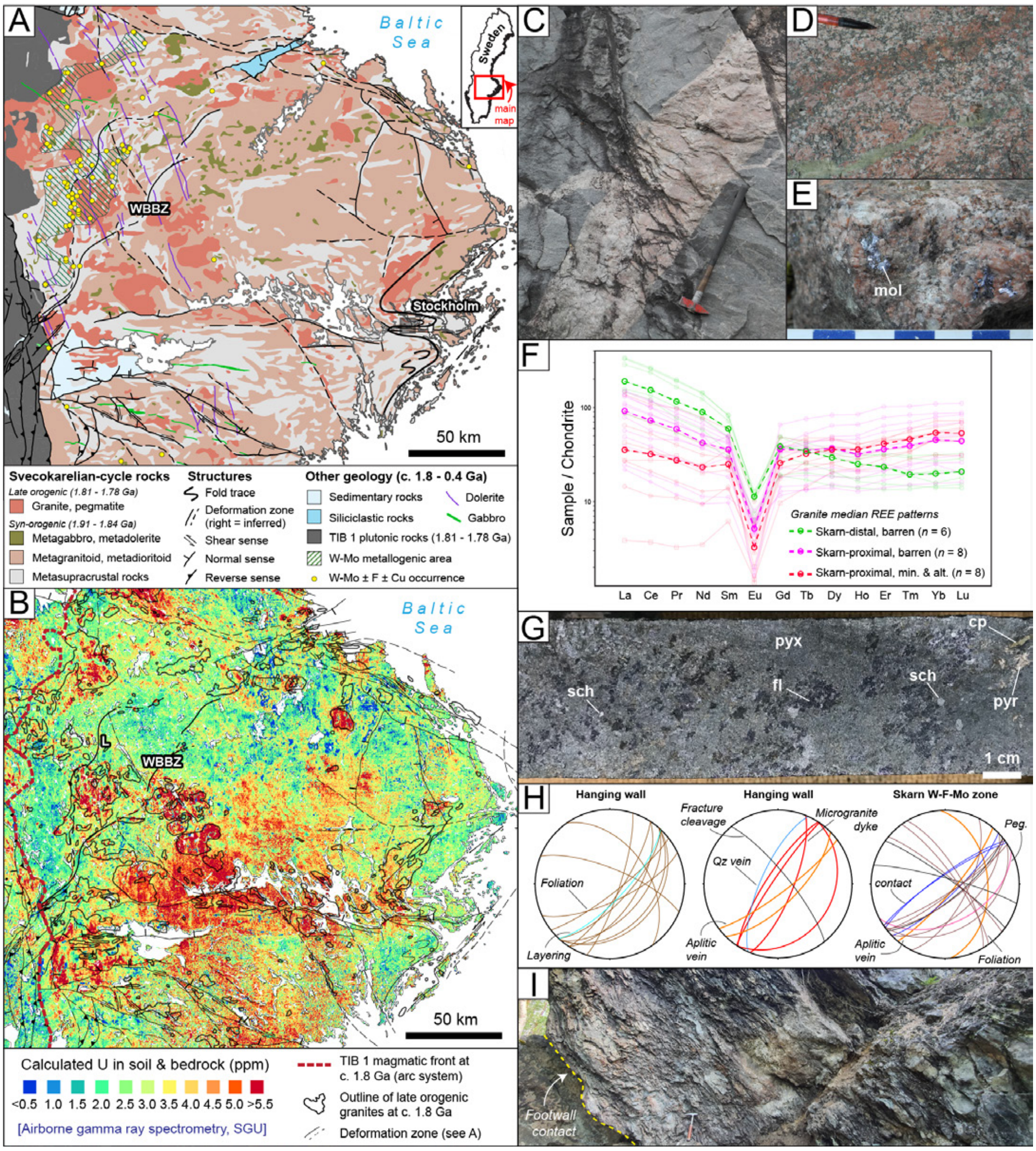

Figure 1. (A) Summary geology of Bergslagen showing W-Mo-F metallogenic area and occurrences. WBBZ = Western Bergslagen Boundary Zone, L = Ludvika, TIB = Transscandinavian Igneous Belt. (B) Regional U distribution map with 1.8 Ga granitic intrusions outlined. (C) Typical 1.8 Ga granite dyke crosscutting foliated metavolcanic rock. (D) Example of megacrystic granite, Fellingsbro area. (E) Biotite granite with molybdenite (mol) at Bispbergs Klack. (F) REE patterns for 1.8 Ga granitic intrusions. (G) Pyroxene (pyx)-rich skarn rock from Yxsjöberg with scheelite (sch), fluorite (fl), pyrrhotite (pyr) and chalcopyrite (cp). (H) Orientations of planar structures and granitic bodies at the Wigström W deposit. (I) Deformed marble-skarn zone, Wigström deposit. View to NE.

occurring in both settings (Fig. 1G) – supports granite-skarn consanguinity and common genetic controls at the site of mineralization. Granitic bodies with orientations similar to earlier planar fabrics suggest preexisting structures provided controlling pathways for melt migration and exsolved mineralizing fluids (Fig. 1H). Critically for skarn systems, the availability of intrusion-proximal trap rocks (e.g. marble; Fig. 1I) to facilitate fluid-rock interaction and mineral deposition represents a key local controlling factor.

References

Bergman, T., 2012: Western Bergslagen W-Mo. *In* P. Eilu (Ed.): Mineral deposits and metallogeny of Fennoscandia. *Geological Survey of Finland Special Paper 53*, 162 pp.

Beunk, F.F. & Kuipers, G., 2012: The Bergslagen ore province, Sweden: Review and update of an accreted orocline, 1.9–1.8 Ga BP. *Precambrian Research 216–219*, 95–119.

Potential REE-resources in northern Sweden

Olof Martinsson, Thomas Aiglsperger

Division of Geosciences and Environmental Engineering, Luleå University of Technology, Luleå, Sweden, olof.martinsson@ltu.se, thomas.aiglsperger@ltu.se

Summary. Rare earth elements (REE) are metals important in many high-tech applications, and are classified as critical raw materials by the EU. There may be potential for several types of REE deposits in northern Sweden. These include apatite iron ores, stratiform/stratabound base metal deposits, epigenetic Cu deposits, IOCG deposits, skarn deposits, carbonate vein deposits, phosphorite deposits, hydrothermally altered rocks, pegmatites, and granites. Most common REE minerals are allanite and monazite but in the apatite iron ores a significant part of REE is related to apatite.

Introduction

The demand for Rare Earth Elements (REE) has increased significantly during the last 20 years and they have many different applications of which many are classified as high-tech and important in the energy sector for production of renewable electricity and for the EV sector. Most of the supply of REE is from China and exploration for REE deposits in the rest of the world is important, to add other producers and reduce this dependence. Although these metals are classified as critical in the EU, only limited exploration focused on REE has been done in Sweden. However, based on existing knowledge there could be a significant potential for a number of different REE deposits in Sweden (Jonsson et al. 2019, Sadeghi et al. 2013), but most previous studies have mainly been focused on occurrences in southern and central Sweden. The known occurrences in northern Sweden are mainly related to apatite iron ores with REE enriched in apatite.

Method

The object of this contribution is to focus on REE occurrences in northernmost Sweden and their character and possible economic potential. The identification and characterization of these REE occurrences is based on published papers, exploration reports and unpublished research data.

Results and discussion

Northern Norrbotten is an important mining district containing world-class deposits of iron and copper. These are apatite iron ores and of porphyry-Cu type, but several other types of deposits are also known from the area including stratiform/stratabound base metal deposits, epigenetic Cu±Au deposits, IOCG deposits, and iron formations. Several of these deposits have elevated contents of REE as a characteristic minor component or as local enrichments.

The apatite iron ores were recognized already in the 1960s for their elevated contents of REE, with several studies of REE content in apatite (e.g. Parak 1973). The possibility to recover REE using hydrometallurgical processes has been investigated recently (Peelman et al. 2018) and LKAB has demonstrated the economic potential of REE as a by-product from iron mining in the ReeMAP project. Production is planned for the near future and may cover a significant part of EU demand of REE (LKAB 2021). However, previous studies have shown that only parts of the total REE content in the Kiirunavaara deposit is hosted by apatite and that the remaining content is mainly occurring in monazite, allanite and titanite (Martinsson et al. 2012, Wanhainen et al. 2017). This suggests possible additional REE production from the apatite iron ores in Norrbotten.

Other types of REE occurrences in Norrbotten are mainly indicated by elevated contents in whole rock analyses of drill cores and outcrop samples done within exploration and research projects. These includes complete REE analyses or only selected REEs (mostly La, Ce, Y). This means that total REE-content is only sometimes available and here analyses with a total REE content >0.1% or a con-

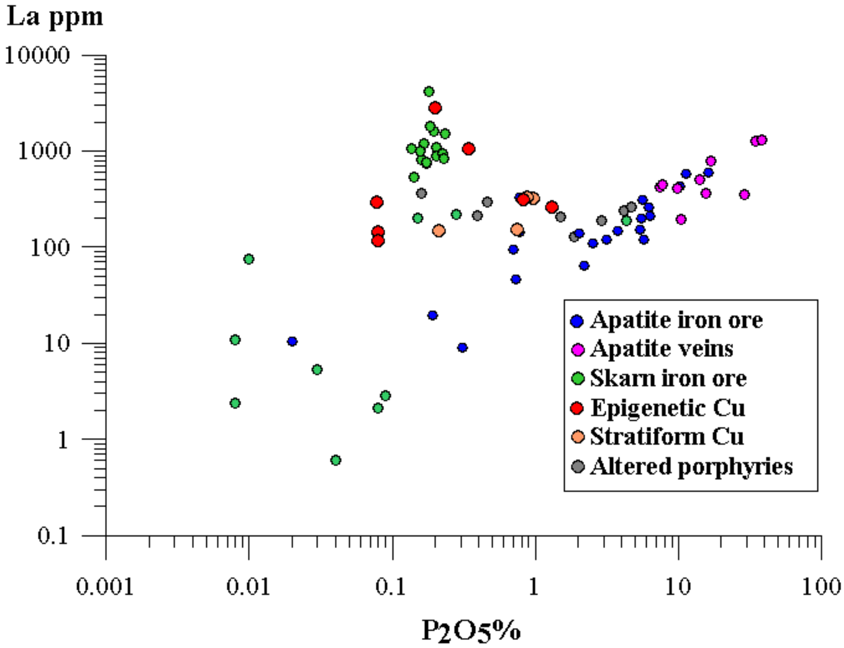

Figure 1. Content of La and P in different types of mineral deposits and altered rocks.

tent >0.05% for individual REEs have been considered. These include samples with up to 4.5% REE from hydrothermally altered rocks, skarn deposits, apatite iron deposits, stratiform sulphide deposits, epigenetic sulphide deposits, and carbonate veins. In some cases, a strong correlation with phosphorous indicate apatite to be an important REE-carrier while others do not, and instead suggests the occurrence of specific REE-minerals (Fig. 1).

Preliminary mineralogical data supports this with monazite and allanite as the most common REE-minerals with xenotime and synchysite type minerals occurring more rarely. Deposits where REE are hosted by specific REE-minerals have the potential to have higher grades, or at least have the possibility to produce concentrates with higher REE content compared to when apatite is the main carrier. Important aspects are also the occurrence of deleterious elements like U and Th that could negatively affect the value of the concentrate. On the other hand, there might also be components that could add value as by-products. Many REE occurrences in northern Sweden have low contents of U and Th and often contain Fe or Cu in elevated concentrations making them attractive as potential REE-resources. However, so far, their economic potential is unclear and more detailed studies are needed.

References

LKAB, 2021: LKAB's exploration results confirm potential for production of phosphorus mineral fertiliser and rare earth elements. https://ree-map.com/exploration-confirms-potential/

Martinsson, O., Öberg, E. & Fredriksson, A., 2012: Apatite for extraction - mineralogy of apatite and REE in the Kiirunavaara Fe-deposit. Abstract. XXVI International Mineral Processing Congress - IMPC 2012, New Delhi, India, September 24–28, 2012.

Parak, T., 1973: Rare earths in the apatite iron ores of Lappland together with some data about the Sr, Th and U content of these ores. *Economic Geology* 68, 210–221.

Peelman, S., Kooijman, D., Sietsma, J. & Yang, Y., 2018: Hydrometallurgical recovery of rare elements from mine tailings and WEEE. *Journal of Sustainable Metallurgy* 4, 367–377.

Jonsson, E., Nysten, P., Bergman, T., Sadeghi, M., Söderhielm, J. & Claeson, D. 2019: REE mineralisations in Sweden. In: Sadeghi, M. (ed.), Rare earth elements distribution, mineralisation and exploration potential in Sweden. *Rapporter & Meddelanden 146, Sveriges geologiska undersökning*, 20–111.

Sadeghi, M., Morris, G.A, Carranza, E.J.M., Ladenberger, A. & Andersson, M., 2013: Rare earth element distribution and mineralisation in Sweden: An application of principal component analysis to FOREGS soil geochemistry. *Journal of geochemical exploration* 133, 160–175

Wanhainen, C, Pålsson, B.I. & Martinsson, O., 2017: Rare earth mineralogy in tailings from Kiirunavaara iron ore, northern Sweden: Implications for mineral processing. *Minerals & Metallurgical Processing* 34, 189–200.

Character and origin of the graphite deposits in Norrbotten, northern Sweden

Olof Martinsson, Thomas Aiglsperger

Division of Geosciences and Environmental Engineering, Luleå University of Technology, Luleå, Sweden, olof.martinsson@ltu.se; thomas.aiglsperger@ltu.se

Summary. Several graphite deposits are known from northern Sweden but so far only limited exploitation has occured. However, significant graphite production is planned from large and high grade deposits in northern Norrbotten. They are part of extensive graphite bearing units in the c. 2.1 Ga Karelian greenstones and may constitute world-class deposits. The carbon isotope composition and their chemical characteristics indicate accumulation of biogenic carbon in marine to non-marine basins. In total these graphite bearing units could contain at least 0.1 to 0.5 billion tons of graphite.

Introduction

Graphite is an important industrial mineral with many different uses due to its unique properties. Graphite deposits are mostly of metamorphic origin, formed from sedimentary rocks containing organic carbon, but historically vein-style graphite of hydrothermal origin has also been an important source. The growing EV-market has increased the demand of graphite for electrodes and with a rapid expansion of battery production in EU the dependence of import is addressed as a problem as China is strongly dominating the market. In Europe, Norway has a minor production of graphite and several graphite projects are under development in Sweden and Finland. The Kringeltjärn deposit in Hälsingland (indicated+measured resources 2.5 Mt @ 9.3% graphite) and Nunasvaara area in Norrbotten (probable ore reserve 1.94 Mt @ 23.5% graphite and inferred + indicated resource 19.5 Mt @ 24.0% graphite) are the most promising deposits in Sweden (Martinsson & Wanhainen 2022; Talga Group 2022). The Nunasvaara deposit is regarded to be a world-class graphite deposit (Pearce et al. 2015; Martinsson & Wanhainen 2022).

The Norrbotten graphite deposits

Graphite has historically been mined in small scale in the coastal area of Norrbotten. These deposits are small and low grade occurrences of flaky graphite in metasedimentary rocks. Trial mining was made in the mid to late 20th century in larger and more high-grade graphite deposits at Nunasvaara and Nybrännan in northern Norrbotten. These two, and several other more important graphite deposits in northern Norrbotten have recently been claimed. Some of them contain flaky graphite, as Raitajärvi in the Övertorneå area with an inferred and indicated resource of 4.3 Mt @ 7.1% graphite (Talga Group 2021). However, the largest and most important deposits are mainly classified as "amorphous" graphite and are known from the Nunasvaara area from investigations in early 1900s (Geijer 1918). These include the Nunasvaara and Niska deposits, which have been recently investigated by extensive drilling and subjected to metallurgical studies and are both planned for production of graphite electrodes to EV batteries (Talga Group 2021).

The most extensive and graphite rich units in northern Norrbotten are found within the c. 2.1 Ga Karelian greenstones and is part of a lithostratigraphic sequence of (meta-)volcaniclastic rocks extending from Kiruna in west to Pajala in the east (Martinsson 2004). They occur at two main stratigraphic levels and have different lithological associations, chemical characteristics, and carbon isotopic compositions. The stratigraphically lower unit constitutes a distinct marker horizon 10–20 m thick and with 10–30% graphite, that is easily identified using geophysical methods as it produces a strong anomaly on electromagnetic maps. It is situated within the upper part of volcaniclastic rocks of intermediate composition that are located between a dolomitic carbonate unit below and mafic volcaniclastic rocks above. It has a carbon isotope composition of –19.6 to –23.8‰ and with a graphite content that increases from west (5–15% C) to east (15–35% C). It is mostly poor in sulphides (0.1–1% S) with only minor pyrite-pyrrhotite mainly occurring in veinlets and locally some sphalerite in calcite fracture fillings.

The upper graphite unit is more varying in character with graphite-bearing intercalations within a mafic volcaniclastic unit below an extensive unit of dolomite constituting the top of the Karelian greenstones. The thickness of graphite schist intercalations vary from a few meters up to several tens of meters and they are mostly rich in pyrite/pyrrhotite occurring disseminated and as veinlets. The graphite content is mostly low (mainly < 10% C but could be up to 15% C) while the content of sulphur is rather high (3–10% S) and can locally reach 25% S. The carbon isotopic compositions vary mostly from –29.2 to –31.4‰ but values around –25‰ are also found. In contrast to the lower graphite unit these upper graphitic units are commonly enriched in V, Ni, Mo and U typical for rocks formed in a marine environment (Huyck 1990). The strongly negative carbon isotope composition in both the lower and upper graphitic units supports a biogenic origin for carbon and the huge amount of carbon deposited in these units demonstrates extensive biogenic activity at that time. Total amount of carbon in the preserved parts of the lower unit could be in the range of 0.1 to 0.5 billion tons and in the upper graphite unit at least 0.1 billion tons.

The economically most important graphite unit is the lower one hosting the Nunasvaara and Niska deposits in the Vittangi area but also Nybrännan and Suinavaara further east in the Masugnsbyn area. In the Vittangi area the graphite unit occurs at the flanks of dome structure and can be followed for c. 16 km in outcrops, prospect pits and geophysical maps. In the Masugnsbyn area the combined length of this lower graphite unit could be as much as 30 km according to geophysical data. Further east in the Pajala area graphite-bearing units of unclear stratigraphic position within the Karelina greenstones have been intersected by drilling at several places. Some of them are rich in graphite (25–40% C) and have mostly a low content of sulphides (<2% S). Graphite has also been found in sedimentary rocks suggested to be of Svecofennian age. In 1990–1992 several occurrences of graphite schists in the Pajala–Tärendö area (the Jalkunen, Tiankijokki, and Lehtosölke deposits) were investigated for possible production of flaky graphite. These deposits have graphite contents varying from 12 to 40%. For Lehtosölke the estimated tonnage to a depth of 40 meters is 1.72 Mt with 12.3% C (Bergman et al. 2001). For the Jalkunen deposit an inferred resource of 31.5 Mt @ 14.9% C has been estimated (Talga Group 2021).

The crystallinity of graphite is a function of metamorphic grade and has also importance for the quality of graphite products. Several studies have shown a systematic relation between peak metamorphic temperature and graphite crystallinity, based on Raman spectroscopy (Beyssac et al. 2002, Couzi et al. 2016). Preliminary Raman results from graphite occurrences in Norrbotten give temperatures in accordance with metamorphic grades estimated from metamorphic mineral assemblages and geothermometers given by Bergman et al. (2001). The Raman data are also useful for indicating the quality of a graphite deposit as it gives information about graphite crystallinity.

References

Bergman, S., Kübler, L. & Martinsson, O., 2001: Description of regional geological and geophysical maps of northern Norrbotten County (east of the Caledonian orogen). *Sveriges geologiska undersökning Ba* 56, 110 pp.

Gautneb, H., Knezevic, J., Gloaguen, E., Melleton J., Gourcerol, B. & Törmänen, T., 2019: Occurrence of energy critical elements; litium-cobalt and graphite in Europe, a preliminary overview. *15th SGA Biennial Meeting 2019* 4, 1784-1787.

Geijer, P., 1918: Det grafit- och järnmalmsförande området vid Vittangi. *Sveriges geologiska undersökning C* 284, 106 pp.

Huyck, H., 1990: When is a metalliferous black shale not a black shale? In: Grauch, R.I. & Huyck, H.L.H. (eds.), Metalliferous black shales and related ore deposits - Proceedings, 1989 United States Working Group Meeting, International Geological Correlation Program Project 254, *U.S. Geological Survey Circular* 1058, 42-56.

Martinsson O., 2004: Carbon isotopes as a tool for stratigraphic correlation within the Palaeoproterozoic Kiruna Greenstones, northern Sweden. In: Mansfeld, J. (ed.), *The 26th Nordic Geological Winter Meeting, Uppsala, Abstract volume, GFF* 126, 30.

Martinsson. O. & Wanhainen, C., 2022: Economic potential of battery metals and minerals in Sweden. *16th SGA Biennial Meeting 28-31 March 2022 Rotorua, New Zealand, Proceedings 1,* 27-30.

Pearce, M.A., Godel, B.M. & Thompson, M., 2015: Microstructures and mineralogy of a world-class graphite deposit. *Society of Economic Geologists, Annual Conference 2015 Hobart, Australia. Program and abstracts*.

Talga Group, 2021: Annual report 2021, , https://talgagroup.eu-central-1.linodeobjects.com/app/uploads/sites/2/2022/03/24033633/AnnualReporttoshareholders.pdf

Metal mobilization during the evolution of the Central Lapland Greenstone Belt, Finland: implications for orogenic Au deposits

Clifford G.C. Patten[a], Ferenc Molnár[b,c], Iain K. Pitcairn[d], Jochen Kolb[a], Satu Mertanen[b], Simon Hector[a]

[a]Institute of Applied Geosciences, Chair of Geochemistry and Economic Geology, Karlsruhe Institute of Technology, 76131 Karlsruhe, Germany, clifford.patten@kit.edu; [b]Geological Survey of Finland, P.O. Box 96, Espoo FI-02151, Finland; [c]Institute of Geography and Earth Sciences, Budapest University, 1117 Budapest, Hungary; [d]Department of Geological Sciences, Stockholm University, SE-106 91 Stockholm, Sweden

Summary. The sources of Au, base metals, metalloids and ligands enriched in orogenic Au deposits are still not fully constrained. Investigation of element mobilization during prograde metamorphism of the Central Lapland Greenstone Belt (CLGB), Finland, shows that metavolcanic rocks can release significant Au, As, Sn, Te and S while metasedimentary rocks can release significant S, C, Cu, As, Se, Mo, Sn, Sb, Te and U, but limited Au. Mass balance calculations show that prograde metamorphic devolatilization of various lithologies can account for the metal endowment of the CLGB orogenic Au deposits.

Introduction

Precambrian greenstone belts are prospective terrains for orogenic Au deposits worldwide but the sources of Au, base metals and metalloids (e.g. Cu, Co, As, Se, Mo, Sn, Sb, Te, U) and ligands trapped within the deposits are still debated. Three main geological processes produce Au-rich hydrothermal fluids which ultimately can lead to orogenic Au deposit formation: metamorphic devolatilization of supracrustal rocks, subcontinental lithospheric mantle fluid release and magmatic-hydrothermal fluid generation. The role of metamorphic devolatilization in generating Au-rich hydrothermal fluids in Precambrian greenstone belts remains controversial and the respective role of the metavolcanic and metasedimentary rocks present within these belts in releasing Au, ligands, metals and metalloids remain poorly understood (Goldfarb & Groves 2015).

The Central Lapland Greeenstone Belt (CLGB), Finland, is one of the largest known Paleoproterozoic greenstone belts and hosts numerous orogenic Au deposits with typical (Au-only) and atypical (Au-Cu-Co-Ni) metal associations (Eilu 2015; Fig. 1). The orogenic Au deposits are preferentially located along the Kiistala shear zone (KiSZ) and the Sirkka shear zone (SiSZ). Within the CLGB, the Kittilä suite and the Savukoski groups, which host most of the orogenic Au deposits, are characterized by various metavolcanic (protoliths defined MORB, WPB and komatiite) and metasedimentary rocks (protoliths defined as volcanoclastic rock, shale, wacke and black shale) which are variably metamorphosed from greenschist facies to upper amphibolite facies (Fig. 1).

Results and discussion

In this study, we investigate the extent to which each lithological unit present in a greenstone belt contributes to the generation of metal-rich metamorphic fluids during metamorphic devolatilization. Characterization of the distribution and behavior of S, C, Co, Ni, Cu, As, Se, Mo, Sn, Sb, Te, Au and U during prograde metamorphism of rocks from the Kittilä and Savukoski groups highlights that 1) metavolcanic rocks (MORB and WPB) release significant Au, As, Sn, Te and S, 2) metasedimentary rocks release significant S, C, Cu, As, Se, Mo, Sn, Sb, Te and U, but limited Au, and 3) metakomatiites release C and possibly Au.

Based on mass balance calculations and careful review of the tectonic, metamorphic and magmatic evolutions of the CLGB during the Svecofennian orogeny, a multi-source and multi-stage model is proposed for the formation of orogenic Au deposits: 1) metamorphic devolatilization during the early accretionary stages (1.92–1.86 Ga) of the CLGB led to preferential release of Au, As and S from the metavolcanic rocks and the minor metasedimentary rocks of the Kittilä suite accounting for the forma-

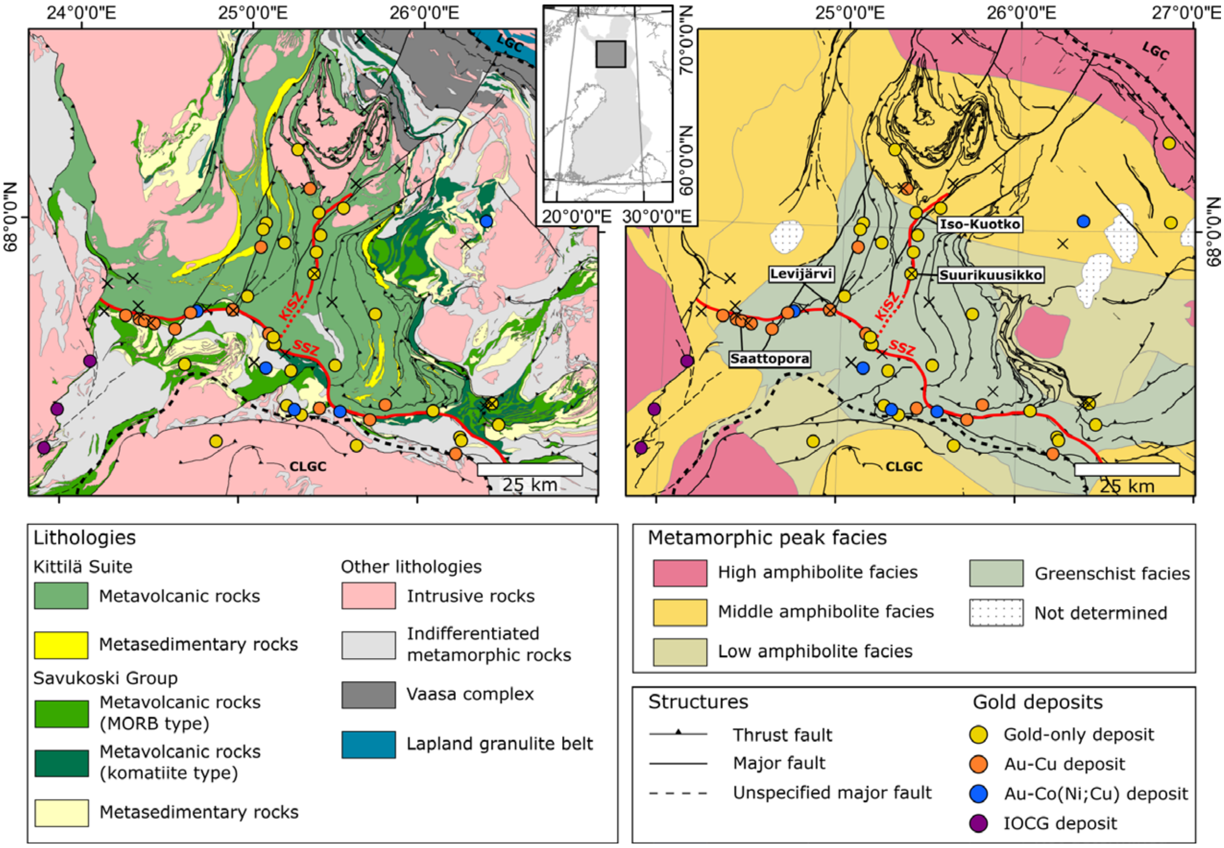

Figure 1. Regional geological (A) and metamorphic map of the CLGB (B) showing major lithological units, orogenic Au deposits and showing major fault zones (KiSZ=Kiistala Shear Zone, SiSZ=Sirkka Shear Zone), complexes (CLGC=Central Lapland Granitoid Complex, LGC=Lapland Granulite Complex), and sampled drillcore locations (black crosses)

tion of typical orogenic Au deposits such as the Suurikuusikko deposit; 2) late-stage (1.83–1.76 Ga) metamorphism and magmatism associated with a regional-scale thermal event led to metamorphic devolatilization dominantly from the metasedimentary-rich Savukoski group, promoting S, C, Cu, As, Se, Mo, Sn, Sb, Te and U-rich metamorphic fluids and accounting for the formation of atypical orogenic Au deposits. Deep crustal or sublithospheric fluids could also be involved during this stage.

The complex lithologic diversity, tectonic evolution and metamorphic history of the CLGB highlights that metal mobilization can occur at different stages of an orogenic cycle and from different sources stressing the necessity to consider the complete dynamic and long-lasting evolution of orogenic belts when investigating the source of Au, ligands, metals and metalloids in orogenic Au deposits.

References

Goldfarb, R.J. & Groves, D.I., 2015: Orogenic gold: Common or evolving fluid and metal sources through time. *Lithos 233*, 3–17

Eilu. P., 2015: Overview on gold deposits in Finland. *In: Mineral Deposits of Finland. Elsevier*, 377–410

Niobium-tantalum mineralisation in Sweden: an overview

Helge Reginiussen[a], Erik Jonsson[a,b]

[a]Department of Mineral Resources, Geological Survey of Sweden, Uppsala, Sweden; helge.reginiussen@sgu.se, erik.jonsson@sgu.se, [b]Department of Earth Sciences, Uppsala University, Uppsala, Sweden.

Summary. Based on present knowledge, niobium-tantalum mineralisations in Sweden are essentially restricted to three major genetic types: 1) rare metal-type granitic pegmatite-aplite systems, 2) alkaline-peralkaline igneous rocks, and 3) carbonatite complexes. These deposits occur in both the Palaeoproterozoic bedrock as well as in younger intrusive complexes and in Caledonian nappe sequences. Here we outline the main types of Swedish Nb-Ta mineralisations and briefly assess their exploration and future sourcing potential.

Background

The chemically closely related metals niobium (Nb) and tantalum (Ta) are critical metals according to present EU classification. Both elements have unique properties and are essential in a range of applications and products including electronics, steel alloys and superalloys. Tantalum is particularly problematic as it is extensively sourced from conflict mineral production in the central African region, although the EU and USA have recently imposed regulations to prevent the use of conflict minerals/metals in industrial products. In the case of Nb, the EU relies entirely on imports (mainly from Brazil) to meet its industrial demand. Among several relevant regions in Europe, the Proterozoic bedrock of the Fennoscandian shield and its cover units host diverse Nb-Ta mineralisation; specifically in Sweden, deposits are known carrying these and other potential commodities.

Nb-Ta deposit types in Sweden

Three main types of Nb-Ta mineralisation occur in Sweden; 1) rare metal-type granitic pegmatite-aplite systems, 2) alkaline-peralkaline igneous rocks, and 3) carbonatite complexes. The most abundant are variably evolved granitic pegmatites, of which many have been exploited for one or several commodities over time. They are locally associated with aplites or aplitic units, occurring both singularly or in zoned fields (e.g. Sundius 1951, Brotzen 1959, Smeds 1990). Yet, only some are rare element pegmatite systems corresponding to the LCT-type classification of Černý (1991), which are known to host Ta-enriched oxide minerals of "columbite" type. These may have exploitation potential for in particular Ta, not least in combination with potential hard rock lithium (Li) resources, based on their contents of spodumene ± petalite. Others which belong to the rare element class, in particular those classified as of NYF type, may carry Nb-(Ta) mineralisation; yet, we judge that the economic potential of such Nb-enriched pegmatite systems is small today.

The most important regions with LCT-type granitic pegmatite-(aplite) systems in Sweden are the eastern part of the Skellefte district in northern Sweden; the Sollefteå area and the Räggen and Mårdsjön areas in north central Sweden (Västernorrland and Jämtland counties), and eastern Bergslagen with the Stockholm archipelago, specifically the "Utö-Mysingen field", in southeast central Sweden (cf. Smeds 1990). A more recent discovery of a Li-Ta-Nb-(Cs)-mineralised granitic pegmatite-aplite system near Bergby in east central Sweden, in the Hamrånge metasupracrustal rocks, led to recognition of a new prospective area (Jonsson 2007, Jonsson 2018).

Among few known Swedish Nb-(Ta) mineralisations in alkaline-peralkaline rocks, the Prästrun complex stands out. It occurs along the contact between the Caledonian Seve and Särv thrust nappes in Jämtland, west central Sweden, and contains metamorphosed and deformed syenitic, variably nepheline-bearing, mostly relatively fine-grained, but locally also pegmatitic rock units (e.g. Holmqvist 1989). The pyrochlore mineral "betafite" is the main Nb-(Ta) host here (e.g. Hålenius 1990).

The carbonatite complex at Åkersjön is located in a similar tectonostratigraphic position as Prästrun; the actual ages of formation of either of these rock units are presently not known, but based on field evidence, they are likely to predate Caledonian orogenic deformation and thrusting (Jonsson & Stephens 2004, 2006). The Åkersjön complex comprises silicic to carbonatitic metamorphosed rocks featuring mineral assemblages in which pyrochlore-group minerals are the likely main hosts of Nb-(Ta). Alnö island outside of Sundsvall in east central Sweden hosts an early Phanerozoic carbonatite complex with associated silicic rocks and fenitised host rocks; several additional dykes and potential buried (and submerged) intrusions are known as well as inferred in the area (e.g. Kresten 1990, Andersson et al. 2013, and references therein). Perovskites and pyrochlore-group minerals (+ unknown distribution of Nb-enriched zirconolites) together with titanite are the main hosts of Nb (± Ta), and while they predominantly occur in the carbonatites and locally in the contact fenites, their overall distribution and compositions are less well known (cf. von Eckermann 1974, Kresten 1990). Due to its location, and from a land-use point of view, most of the main intrusion is probably not accessible for exploration or mining, but the wide and in part unknown extent of carbonatitic rocks with multi-metal/mineral contents in the area makes it relevant for further study.

Conclusions

Based on present knowledge we judge that a handful of deposits or districts in Sweden have potential to host relevant mineralisations of Ta and/or Nb, but more detailed exploration and research is needed to identify their full economic potential. Viable sources are most probably deposits where Ta and/or Nb can be extracted as by-products. The on-going green energy transition has increased the demand for certain metals (e.g. Li for e-vehicle batteries), which has resulted in a renewed focus on European LCT-pegmatite systems. When, or if, Li ore production starts from the latter type of deposits, they could become future sources of Ta in addition to Li.

References

Andersson, M., Malehmir, A., Troll, V.R., Dehghannejad, M., Juhlin, C. & Ask, M., 2013: Carbonatite ring-complexes explained by caldera-style volcanism. *Scientific Reports* 3, 1677, 1-9.

Brotzen, O., 1959: Mineral association in granitic pegmatites. A statistical study. *Geologiska Föreningens i Stockholm Förhandlingar* 81, 231–296.

Černý, P., 1991: Rare-element granitic pegmatites, part 1. Anatomy and internal evolution of pegmatite deposits. Part 2. Regional to global environments and petrogenesis. *Geoscience Canada* 18, 49-81.

Hålenius, U., 1990: Holmslättmyren mineralogi. SGAB report PRAP 90 010. 8 pp.

Holmqvist, A., 1989: Prästrun. Ett nytt alkalint bergartsområde. SGAB PRAP 89 019. 8 pp.

Jonsson, E., 2007: Fältbesöksprotokoll, spodumen Stor-Igeltjärnen. SGU/Mineraljakten 2007. Kbl 14H SV. ID:07359.

Jonsson, E., 2018: Pegmatite-hosted lithium mineralisation in Sweden: an overview. In: J. Mansfeld (ed.), *Mineralogical Society of Sweden, Lithium 200 years,* Meeting Proceedings and field-trip guide book, 9-11.

Jonsson, E. & Stephens, M.B., 2004: Investigation of alkaline rocks in the Prästrun and Åkersjön areas, Jämtland. *SGU report* 08/1129/2004

Jonsson, E. & Stephens, M.B., 2006: Metamorphosed U-Nb-Ta-REE-bearing alkaline rocks from the Swedish Caledonides in Jämtland. *Bulletin of the Geological Society of Finland*, Special issue 1, 63.

Kresten, P., 1990: Alnöområdet. In T. Lundqvist (ed.), Beskrivning till berggrundskartan över Västernorrlands län. SGU Ba 31, 238-278.

Smeds, S.-A., 1990: Regional trends in mineral assemblages of Swedish Proterozoic granitic pegmatites and their geological significance. *Geologiska Föreningens i Stockholm Förhandlingar* 112, 227-242.

Sundius, N., 1951: Kvarts, fältspat och glimmer samt förekomster därav i Sverige. SGU C 520, 231 pp.

von Eckermann, H., 1974: The chemistry and optical properties of some minerals of the Alnö alkaline rocks. *Arkiv för Mineralogi och Geologi* 5 (8), 93-210.

Pyrite and sphalerite trace element redistribution during metamorphism of the Rävliden North VMS deposit, northern Sweden

Jonathan Rincon[a], Nils F. Jansson[a], Helen Thomas[b], Majka C. Kaiser[b], Mac F. Persson[b], Filip Simán[a], Christina Wanhainen[a]

[a]Department of Civil and Environmental Engineering, Luleå University of Technology, Luleå, Sweden, jonathan.rincon@ltu.se, nils.jansson@ltu.se, filip.siman@ltu.se, christina.wanhainen@ltu.se, [b]Exploration department, Boliden Mineral AB, Boliden, Sweden,helen.thomas@boliden.com, christiane.kaiser@boliden.com, mac.persson@boliden.com.

Summary. The Rävliden North volcanogenic massive sulphide (VMS) deposit and its host rocks exhibit a shared history of metamorphism during the 1.88–1.86 Ga deformation phases of the Svecokarelian orogeny. Predominantly internal sulphide remobilisation produced minor modifications to the overall pre-metamorphic trace element distribution including remobilisation. Post-Svecokarelian sulphide-bearing zeolite- and calcite veinlets cross-cut the stratigraphic hanging wall suggesting mobilisation of sulphides in a fluid phase during an overprinting later event unrelated to the VMS mineralisation.

Introduction

Pyrite and sphalerite trace element compositions have previously been used to contextualise the genesis and deformation of mineral deposits (Cook et al. 2009, Large et al. 2009). In the Skellefte district, such a study coupled to detailed textural characterization remains underutilised, with the greenschist to low amphibolite facies metamorphosed Rävliden North Zn-Pb-Cu-Ag VMS deposit providing an excellent opportunity. The deposit is hosted at the transition from the dominantly rhyolitic metavolcanic rocks of the Skellefte group (SG) to the predominantly metasiliciclastic rocks of the Vargfors group (VG). Locally, cryptodomes occur close to the SG-VG contact spatially related to synvolcanic normal faults that acted as mineralisation conduits. Flattening and transposition of the ore lenses into faults during tectonic inversion as well as stretching parallel to F2 fold hinges occurred during the 1.88–1.86 Ga D1 and D2 events in the Skellefte district. Massive to semi-massive sphalerite, pyrrhotite, galena, pyrite (Sp+Pyh+Gn±Py), and chalcopyrite, pyrrhotite, pyrite (Ccp+Pyh+Py) mineralisations comprise the main ore lenses. Sub-economic mineralisation includes pyrite, pyrrhotite and minor arsenopyrite (Pyh+Py±Apy), and sparse occurrences of late veinlets and breccias composed of sphalerite, galena and minor Ag-Sb-sulphosalts (Sp+Gn±SS) in association with calcite and zeolites. Sulphosalts are typically hosted in the stratigraphic hanging wall as well as in the periphery of the main ore lenses.

Results and discussion

Internal remobilisation of sulphides during metamorphism of the Rävliden North mineralisation retained a bulk metal zonation characteristic of VMS deposits (e.g. Hannington 2013), with Zn- and Pb-rich ore lenses (Sp+Pyh+Gn±Py) located structurally and stratigraphically above Cu-rich lenses (Ccp+Pyh+Py). However, remobilisation is apparent as sulphides are aligned sub-parallel to a penetrative S1 foliation in addition to the spaced S2, and S2L described by Skyttä et al. (2013), as well as hosted in brittle-ductile and brittle structures. Micro-scale analysis reveals that ductile deformation of sulphides, likely through dislocation flow, was the main responsible mechanism of deformation.

We compared trace element maps of pyrite porphyroblasts performed with Laser Ablation Inductively-Coupled Mass Spectrometry (LA-ICP-MS) from two proximal samples, one from the Sp+Pyh+Gn±Py, and the other from the Pyh+Py±Apy mineralisation. Both samples hosted in the vicinity of a deposit-scale shear zone. Pyrite from the Sp+Pyh+Gn±Py sample is characterized by cores rich in galena and sulphosalt inclusions, surrounded by euhedral inclusion-free overgrowths. The cores show elevated Co, As and Ni content, whereas pyrite haloes are commonly depleted in trace elements. Pyrite porphyroblasts from the Pyh+Py±Apy sample were formed syn-to-post S2 foliation. They are characterized by an inclusion-rich zone surrounded by an inclusion-poor zone in contact with strain shadows.

LA-ICPMS trace element maps reveal that the inclusion-rich zone is usually composed of an anhedral core enriched in As and Co, surrounded by overgrowths defined by alternating zones of As and Co. The inclusion-rich zone also presents variable concentrations of Sb, Pb, and Ag, attributed to release of metals during D2 remobilization of galena and Ag-sulphosalts hosted in the Sp+Pyh+Gn±Py mineralisation. The inclusion-poor zone records a later stage of pyrite growth, defined by concentrations of Ni and a general depletion in trace elements.

LA-ICP-MS spot analysis of sphalerite grains hosted in brittle ductile structures in the Ccp+Pyh+Py mineralisation contain higher concentrations of Fe, In, Co, and Cu relative to the Sp+Pyh+Gn±Py mineralisation. This high concentration is common in sphalerite that crystallized at higher temperatures during pre-metamorphic ore formation (Cook et al. 2009). In addition, sphalerite recrystallisation and trace element redistribution during metamorphism can lead to a relative enrichment of these elements (Frenzel et al. 2016). Germanium is notably absent in the sphalerite from the Sp+Pyh+Gn±Py and Ccp+Pyh+Py mineralisation compared to sphalerite hosted in late veinlets of the Sp+Gn±SS mineralisation. Germanium, Ga and Sb form oscillatory zoning in growth twins in the late veinlets as shown by trace element maps (Fig. 1), indicating a low crystallisation temperature (<250°C) (Cook et al. 2009, Frenzel et al. 2016). The temperature, mineralogy and style of mineralisation of the late veinlets are similar to Mississippi Valley Type (MVT) Lycksele-Storuman deposits located just west of the Kristineberg area (Billström et al. 2012). We suggest that the origin of the late veinlets is a low-temperature overprinting, unrelated mineralization event. However, this post-Svecokarelian event may have remobilised Ag and Sb from the Rävliden North deposit.

Conclusions

The metamorphism of the Rävliden North deposit produced internal remobilisation of sulphides and trace element redistribution in pyrite and sphalerite in the deposit. These two minerals show chemical changes consistent with the relative timing and temperature attained by the mineralisations during the 1.88–1.86 Ga D1-D2 deformation phases of the Svecokarelian orogen in the Skellefte district. The presence of Zn-Pb-Ag-S minerals in the stratigraphic hanging wall is due to a late post-Svecokarelian, likely Phanerozoic event.

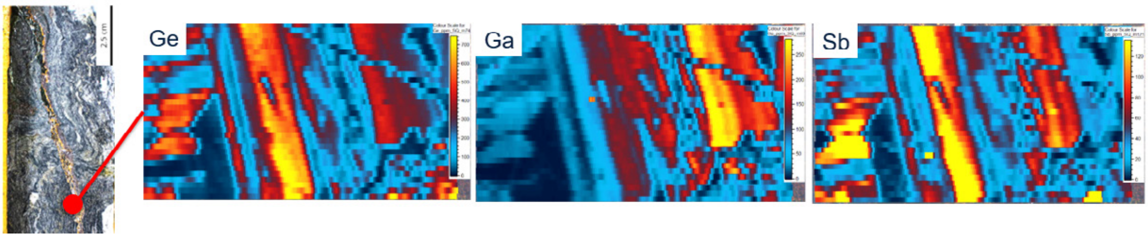

Figure 1. Germanium, Ga and Sb trace element maps of sphalerite from a late zeolite-sphalerite veinlet crosscutting folded graphitic phyllite in the hanging wall of Rävliden North.

References

Billström, K., Broman, C., Schneider, J., Pratt, W. & Skogsmo, G., 2012: Zn-Pb ores of Mississippi valley type in the Lycksele-Storuman district, Northern Sweden: A possible rift-related cambrian mineralisation event. *Minerals* 2, 169–207.

Cook, N.J., Ciobanu, C.L., Pring, A., Skinner, W., Shimizu, M., Danyushevsky, L., Saini-Eidukat, B. & Melcher, F., 2009: Trace and minor elements in sphalerite: A LA-ICPMS study. *Geochimica et Cosmochimica Acta* 73, 4761–4791.

Frenzel, M., Hirsch, T. & Gutzmer, J., 2016: Gallium, germanium, indium, and other trace and minor elements in sphalerite as a function of deposit type - a meta-analysis. *Ore Geology Reviews* 76, 52–78.

Hannington, M.D., 2014: Volcanogenic massive sulfide deposits. *in: Holland, H.D., Turekian, K.K. (Eds.), Treatise on Geochemistry. Elsevier*, p. 463–488.

Large, R.R., Danyushevsky, L., Hollit, C., Maslennikov, V., Meffre, S., Gilbert, S., Bull, S., Scott, R., Emsbo, P., Thomas, H., Singh, B. & Foster, J., 2009: Gold and trace element zonation in pyrite using a laser imaging technique: implications for the timing of gold in orogenic and Carlin-style sediment-hosted deposits. *Economic Geology* 104, 635–668.

Skyttä, P., Bauer, T., Hermansson, T., Dehghannejad, M., Juhlin, C., García Juanatey, M., Hübert, J. & Weihed, P., 2013: Crustal 3-D geometry of the Kristineberg area (Sweden) with implications on VMS deposits. *Solid Earth 4*, 387–404.

Fitting Rävliden North Zn-Pb-Ag-Cu deposit host stratigraphy into regional Skellefte district nomenclature

Filip Simán[a], Nils F. Jansson[a], Sean Johnson[b], Foteini Liwicki[c], Jonathan Rincon[a], Erik Nordfeldt[b], Mac F. Persson[b], Paul McDonnell[b], Tobias Hermansson[b]

[a]Department of Civil and Environmental Engineering, Luleå University of Technology, Luleå, Sweden, filip.siman@ltu.se; nils.jansson@ltu.se; jonathan.rincon@ltu.se; [b] Exploration Department, Boliden Mineral AB, Boliden, Sweden, sean.johnson@boliden.com; erik.nordfeldt@boliden.com; mac.persson@boliden.com; paul.mcdonnell@boliden.com; tobias.hermansson@boliden.com; [c] Department of Computer Science, Electrical and Space Engineering, Luleå University of Technology, Luleå, Sweden, foteini.liwicki@ltu.se;

Summary. Lithofacies logging from Rävliden North in the Skellefte district is presented, and the use of lithostratigraphic names in deposit scale mapping is discussed. The authors conclude that while Skellefte district nomenclature can be applied, it cannot preserve the level of detail relevant to exploration.

Results and discussion

Nomenclature is a system of naming objects and should be stable, understandable, consistent, self-evident, and easy to apply (Kumpulainen 2017) allowing geologists to communicate efficiently whilst preserving information. This study is an attempt to correlate observations at Rävliden North with established Swedish nomenclature. Rävliden North, c. 5 km west of the Kristineberg mine in the western Skellefte district, is a volcanic-hosted massive sulphide (VHMS) Zn-Pb-Ag-Cu deposit formed in a Palaeoproterozoic volcanic arc environment. The ore lenses are composed of semi-massive to massive sphalerite-pyrrhotite-galena-pyrite mineralisation structurally above vein-hosted chalcopyrite-pyrrhotite-pyrite mineralisation. Two principal lithostratigraphic units are recognised in the Rävliden area and broader Skellefte district: 1) the c. 1.90–1.88 Ga Skellefte group (SG) consisting of predominantly felsic–intermediate volcanic rocks, and 2) the overlying c. 1.88–1.87 Ga Vargfors group (VG) comprised of siliciclastic sedimentary rocks and lesser volcanic rocks. The SG-VG contact is important to exploration since most VHMS deposits in the Skellefte district are located at or adjacent to it. Additionally, it is important to target syn-volcanic faults and cryptodome-tuff volcanoes in the succession (Allen et al. 1996). Thus, mapping lateral variations along the regionally expansive contact is critical.

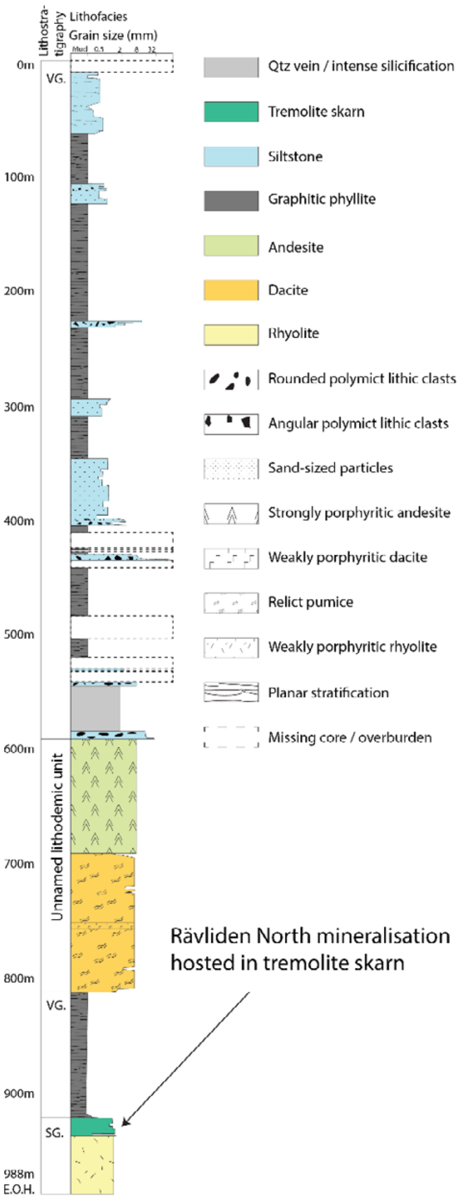

Figure 1. Graphical log and lithostratigraphy of Rävliden North.

Systematic lithofacies observations (Figure 1) and review of available maps and profiles reveal that the Rävliden stratigraphy defines a transition from a weakly porphyritic rhyolite with sphalerite-galena-rich sulphide mineralization in tremolite skarn to a volcano-sedimentary succession. The overlying succession comprises interbedded graphitic phyllite, silt- and sandstones, and breccia conglomerates with clast populations possibly originating from stratigraphically deeper coherent and volcaniclastic andesitic-dacitic rocks. Some rocks have seen intense

Table 1. Logged lithologies and facies, type and suggested name in Skellefte district nomenclature.

Logged lithologies and facies	Type	Name in Skellefte district nomenclature	
		Formation / Suite	**Group**
Mafic sills and dykes	Lithofacies	Gallejaur volcanics?	VG?
Strongly porphyritic andesite	Lithofacies	Jörn GI?	VG?
Weakly porphyritic dacite	Lithofacies	Jörn GI?	VG?
Pumiceous dacite	Lithofacies	Unnamed	VG
Graphitic phyllite	Lithology	Elvaberg formation?	VG
Polymict clasts (breccia-conglomerate)	Facies	Unnamed (similar to Abborrtjärn conglomerate)	VG
Silt- and sandstone	Lithology	Elvaberg formation?	VG
Weakly porphyritic rhyolite	Lithofacies	Unnamed	SG

hydrothermal alteration overprinting many primary textures. All rocks are metamorphosed to greenschist-lower amphibolite facies (Barrett et al. 2005).

Lateral discontinuities and local occurrences of polymict breccia-conglomerate units indicate syn-volcanic faulting at the time of deposition. Altogether, this reflects a palaeoenvironment typical of waning volcanism and basin subsidence that is characteristic of host stratigraphies for VHMS deposits (Allen et al. 1996). Stratigraphic discontinuity, deformation, difficulty correlating rocks over short distances, and difficulty in interpreting relict textures, makes the systematic application of lithostratigraphic names to lithofacies observations challenging during logging. Correlating current observations with existing schemes results in the division into SG and VG with suggestions for possible lower ranked units within (Table 1). The andesitic-dacitic rocks could arguably belong to Jörn GI suite due to similarities with the Viterliden intrusion (a Jörn GI intrusion) described at the nearby Kristineberg mine (Jansson & Persson 2014). Alternatively, the co-genetic pumiceous volcaniclastic dacitic rocks could also be grouped with the coherent rocks as a complex. The breccia-conglomerates are comparable to the Abborrtjärn conglomerates (Allen et al. 1996; Kautsky 1957) with a key similarity being clasts from Jörn GI suite rocks, however, observations do not fully match original descriptions. The weakly porphyritic rhyolites have few primary textures preserved after intense quartz-sericite alteration and sub-division is done almost purely by lithogeochemistry (Barrett et al. 2005), rendering detailed lithostratigraphic subdivision virtually impossible. As such, we find that the conditions for applying a lithostratigraphic scheme differ in different parts of the stratigraphy.

With the uncertainties of applying finer ranking than "group" and "suite" at Rävliden, the only certain lithostratigraphic division is that of the SG and VG which does not show important information regarding lateral facies variation. Clearly, the usefulness of applying established nomenclature is scale-dependent, and at the deposit-scale a different approach that is understandable, consistent, self-evident, and easy to apply, is needed. A first-principles, observation-based approach is thus recommended since it forces us to first consider how rocks are recognised, before attempting at putting them into broad genetic groups. This will be of crucial importance for rigorous classification schemes needed to progress mineral exploration into the age of data-driven rock classification.

References

Allen, R. L., Weihed, P., & Svenson, S.-A. 1996: Setting of Zn-Cu-Au-Ag massive sulfide deposits in the evolution and facies architecture of a 1.9 Ga marine volcanic arc, Skellefte District, Sweden. *Economic Geology* 91(6), 1022-1053.

Barrett, T. J., MacLean, W. H., & Areback, H. 2005: The Palaeoproterozoic Kristineberg VMS deposit, Skellefte district, northern Sweden; Part II, Chemostratigraphy and alteration. *Mineralium Deposita 40*(4), 368-395.

Jansson, N., & Persson, M. F. 2014: Results from exploration drilling in the area between the abandoned Rävliden and Rävlidmyran mines, Skellefte district, Sweden. *Boliden AB Internal Report* 2013-17, 76 p.

Kautsky, G. 1957: Ein Beitrag zur Stratigraphie und dem bau des Skelleftefeldes, Nordschweden (English Summary). *Sveriges Geologiska Undersökning 49*(3), 57-66.

Kumpulainen, R. A. 2017: Guide for geological nomenclature in Sweden. *GFF 139*(1), 3-20.

Norra Kärr alkaline complex, from mantle melt to mineral deposit

Axel S.L. Sjöqvist[a], Filip Manneberg Kozlowski[b]

[a]Department of Earth Sciences, University of Gothenburg, Göteborg, Sweden, axel.sjoqvist@gu.se;
[b]Leading Edge Materials Corp., Vancouver, Canada, filipkozlowski@leadingedgematerials.com

Summary. Rare-earth elements (REE) are essential in many technologies, some of which are crucial for the transition to sustainable energy and transportation. Nepheline syenites in the Norra Kärr alkaline complex in Sweden host the largest defined REE deposit in Europe: one of few in the world with a high abundance of heavy REE. The rocks formed by extreme fractional crystallisation of mantle-derived magma at c. 1.5 Ga. Sveconorwegian metamorphism caused remobilisation of REE. Eudialyte is the main REE ore mineral. Potential by-products include Zr, Nb, and a nepheline syenite industrial mineral product.

Geology and petrology

The Norra Kärr alkaline complex in southern Sweden (58°06'N, 14°34'E; c. 1.5 by 0.45 km) is made up of varieties of agpaitic nepheline syenite with rare silicate minerals from the eudialyte, catapleiite, and rinkite groups. These exotic rocks were the topic of pioneering studies (e.g. Törnebohm 1906, Adamson 1944), and have been reevaluated since exploration drilling for REE began in 2009.

The main rock type is generally known by its local name grennaite (Sw. *grännait*), which accounts for c. 80% of the known volume. It is a fine-grained (nearly aphanitic) green peralkaline nepheline syenite that consists of nepheline, albite, microcline, aegirine(-jadeite), eudialyte, and catapleiite. The remaining volume consists of phanerocrystalline enclaves of varieties of less evolved nepheline syenite, primarily pulaskite and the locally-named lakarpite and kaxtorpite.

The grennaite magma intruded rocks of the 1.8-billion-year-old Transscandinavian Igneous Belt at 1.49 ± 0.01 Ga (2σ), determined by U–Pb dating of metasomatic zircon in the fenitised granitic wall-rock. The highly radiogenic $^{176}Hf/^{177}Hf$ ratio ($\varepsilon_{Hf} \approx 6$) in the metasomatic zircon differs from the typical Svecofennian crustal signature, but overlaps the isotopic ratio measured in Lu-poor eudialyte and suggests a mantle origin for the parental magma of the agpaitic rocks (Sjöqvist et al. 2017).

The grennaitic magma formed by extensive fractional crystallisation of an inferred alkali basaltic parental magma. Concentrations of incompatible elements, such as Zr, Nb, Sn and REE, are frequently enriched to more than 1000 times chondrite/primitive mantle values, corresponding to c. 98% fractional crystallisation. Early depletion of i.a. Cu, Ni, Co, Cr, Ti, V, Sc, P, Sr, and Eu as well as a tenfold enrichment of incompatible elements in the most primitive syenite (pulaskite) correspond to an initial removal of a gabbroic cumulate. Late depletion of i.a. Li, K, Ba, Ti, V, Th, and U as well as a further increase in incompatible elements suggests grennaite may have formed by fractional crystallisation of an alkali syenitic cumulate from an intermediate magma (Sjöqvist 2021).

All rock units in Norra Kärr contain evidence of pervasive metamorphism and deformation. Marginal facies of grennaite are intensely sheared, while the central units are tightly folded. The metamorphic fabric of the grennaite is frequently cross-cut by eudialyte-rich pegmatoids (nepheline syenite pegmatites). Detailed characterisation of one eudialyte crystal from a cross-cutting vein by LA-ICP-MS and ID-TIMS revealed that the vein crystallised at 1.144 ± 0.053 Ga (2σ). Sjöqvist et al. (2020) suggested the veins to be the result of partial melting of the grennaite during Sveconorwegian metamorphic overprinting, leading to local remobilisation of REE into eudialyte-rich pegmatoids.

Economic geology and permitting

Norra Kärr was investigated during the 1940s by Boliden AB as a potential resource of zirconium and nepheline. Two sites were test mined in 1949, but the company did not succeed in beneficiating the minerals sufficiently for commercial use. Two test trenches were dug and sampled in 1974, returning high grades of zirconium and REE. Boliden AB sold the land in 2001.

In 1994 the Geological Survey of Sweden (*Sveriges geologiska undersökning*) designated Norra Kärr as an area of national interest (*riksintresse*) for particularly valuable mineral substances. Detailed demarcation of the deposit was decided in May 2011.

Renewed mineral exploration began in 2009 by Tasman Metals Ltd. (now Leading Edge Materials Corp.), which led to the discovery of a large REE deposit. The Mining Inspectorate (*Bergsstaten*) granted a mining lease in May 2013. The mining lease was appealed to the Government, which in January 2014 affirmed the mining lease. Following an appeal against the Government's decision, the Supreme Administrative Court (SAC, *Högsta förvaltningsdomstolen*) cancelled the Government's decision, which in turn reverted the mining lease back to application status in February 2016. Central to the SAC's ruling was a new interpretation of the interplay between the Minerals and Environmental Act, thus now requiring an Environmental Impact Assessment not only within the concession area but extending to auxilliary facilites outside the concession area and possible indirect impacts on the surrounding environment. The Mining Inspectorate decided not to grant a new mining lease in May 2021 based on this new legal precedent, specifically due to the absence of a Natura 2000 permit for potential indirect impact on such areas in the vicinity of the project. The rejection has been appealed to the Government. In May 2022, the Government announced an investigation to evaluate legislative change that negates the need for a Natura 2000 permit for the granting of a mining lease, with results to be announced in February 2023.

The latest NI 43-101-compliant inferred mineral resource comprises 110 Mt containing 0.5% total rare earth oxides, featuring 52% heavy rare earth oxide, 1.7% ZrO_2, 0.05% Nb_2O_5, and 65% nepheline syenite (Bowell et al. 2021). Eudialyte contains more than 95% of the REE in Norra Kärr, and only minor amounts are hosted in other minerals such as fluorbritholite-(Ce) and mosandrite-(Ce) (Saxon et al. 2015). Based on the re-evaluation of Bowell et al. (2021), the deposit could be exploited by open pit mining with a 260-metre-wide exclusion zone from the E4 highway. The mine design assumes an annual mining rate of 1.15 Mt over 26 years to a pit depth of 150 m, resulting in 29.7 Mt of RoM and 9.2 Mt of waste rock, exploiting only 27% of the inferred mineral resource.

Beneficiation of the REE ore can be achieved by dry magnetic separation due to the paramagnetic nature of eudialyte (Saxon et al. 2015), leaving a non-magnetic nepheline syenite product to be sold as industrial mineral. A second stage of magnetic separation of the primary concentrate will separate gangue aegirine from eudialyte. Wet chemical processing using a low-temperature dry digestion method to extract and recover Zr, Nb, and REE from eudialyte is planned at an off-site industrial facility (Bowell et al. 2021). Production of REE from Norra Kärr could offer a reduced environmental footprint compared with current REE production in and outside of China (Zapp et al. 2022).

References

Adamson, O.J., 1944: The petrology of the Norra Kärr district: An occurrence of alkaline rocks in southern Sweden. *Geologiska Föreningens i Stockholm Förhandlingar 66*, 113–255.

Bowell, R.J., Chapman, C., McDougall, C., Martindale, R. & Pittuck, M., 2021: Preliminary Economic Assessment of the Norra Kärr Rare Earth Deposit and Potential By-Products, Sweden. SRK Consulting Internal Report, 275 pp.

Saxon, M., Leijd, M., Forrester, K. & Berg, J., 2015: Geology, mineralogy, and metallurgical processing of the Norra Kärr heavy REE deposit, Sweden. *Symposium on Strategic and Critical Materials Proceedings. British Columbia Ministry of Energy and Mines, British Columbia Geological Survey Paper 2015-3*, 97–107.

Sjöqvist, A.S.L., 2021: *Ample Rare Elements: A Geochemical Anomaly in the Earth's Crust at Norra Kärr*. PhD thesis, University of Gothenburg. 86 pp.

Sjöqvist, A.S.L., Cornell, D.H., Andersen, T., Christensson, U.I. & Berg, J.T., 2017: Magmatic age of rare-earth element and zirconium mineralisation at the Norra Kärr alkaline complex, southern Sweden, determined by U–Pb and Lu–Hf isotope analyses of metasomatic zircon and eudialyte. *Lithos 294–295*, 73–86.

Sjöqvist, A.S.L., Zack, T., Honn, D.K. & Baxter, E.F., 2020: Modification of a rare-earth element deposit by low-temperature partial melting during metamorphic overprinting: Norra Kärr alkaline complex, southern Sweden. *Chemical Geology 545*, 119640.

Törnebohm, A.E., 1906: Katapleiit-syenit, en nyupptäckt varietet af nefelinsyenit i Sverige. *SGU Serie C 199*, 1–54.

Zapp, P., Schreiber, A., Marx, J. & Kuckshinrichs, W., 2022: Environmental impacts of rare earth production. *MRS Bulletin 47*, 1–9.

3D geologic modeling of the Kiruna mining district

Ervin C. Veress, Tobias E. Bauer

Division of geosciences and environmental engineering, Luleå University of Technology, Luleå, Sweden, ervin.veress@ltu.se, tobias.bauer@ltu.se

Summary. Three-dimensional geologic modeling of iron oxide-apatite (IOA) deposits from the Kiruna Mining District aims at providing a wider spatial context of the mineral system. Leveraging all available data and existing conceptual models, the 3D architecture of the area is built by combining densely and sparsely drilled areas.

Introduction

The Kiruna mining district is situated in the northern Norrbotten ore province of Sweden and belongs to the northwestern part of the Fennoscandian Shield (Bergman 2001). The study area stretches over a distance of 15 km (NE–SW) by 7,5 km (NW–SE) by 2 km (depth). Due to its high economical potential, numerous geological, geochemical, and geophysical studies have been carried out resulting in extensive mapping, prospecting, and drilling campaigns. This ongoing work is currently producing a geological 3D model of deposits and host rocks in the Kiruna mining district in close collaboration with LKAB.

Geological background

In Norrbotten, gneissic granitoid Archean rocks form the basement which are unconformably overlain by Paleoproterozoic metasupracrustal rocks. The Rhyacian-Orosirian pile in Central Kiruna is the best-preserved sequence within Norrbotten and consists of greenstones, trachyandesitic to rhyodacitic volcanic rocks, and clastic sedimentary rocks which are younging and dipping towards the east (Andersson et al. 2021).

The Kiirunavaara and Luossavaara iron oxide-apatite (IOA) deposits are hosted in porphyritic rocks between a trachyandesitic footwall (Hopukka formation) and a rhyodacitic hangingwall (Luossavaara formation). At a stratigraphically higher level, between the Luossavaara formation and the Matojärvi formation, the Per Geijer ores are situated (Geijer & Ödman 1974). The genesis of the deposits is debated and different ore forming processes have been suggested, ranging from magmatic to hydrothermal and mixed models. The structural evolution of the area is interpreted to result from intracontinental back-arc extension and related emplacement of IOA bodies, followed by crustal shortening and basin inversion. Strain was partitioned into rheologically weak rocks and a series of faults were reactivated during basin inversion, generating moderate to steeply east-dipping structures (Andersson et al. 2021).

Modeling methodology

The economic mineral potential of the region leads to the collection of abundant datasets, which must be compiled, analyzed, and interpreted to maximize their value. In the Kiruna area, the basin architecture was studied by several authors (e.g Vollmer et al. 1984, Wright 1988, Andersson et al. 2021), resulting in conceptual geological profiles and models. However, these models do not offer a 3D view of the subsurface structural setting and due to the lack of constraints they cannot be tested and reconciled. The 3D geospatial environment strenghtens interpretation and visualization of the data, which in turn can be used for key economic decisions, such as exploration targeting (De Kemp et al. 2016). However, 3D camp-scale models must integrate regions with sparse data availability with regions having abundant data available from local clusters of measurements such as drillholes (cf. De Kemp et al. 2016, Schetselaar et al. 2016). To connect these highly heterogeneous spatial datasets, interpretive support is needed, and therefore the elements of the models are variably constrained ranging from areas constrained by a few measurements to areas where thousands of measurements are available. In the present study, a similar approach is used for the Kiruna mining district, which aims at producing a wider spatial perspective of the structural and stratigraphic geology of the subsurface focusing on the IOA ore bodies and their relationship with the hosting horizons.

To achieve a robust 3D model, standardized processing and parameter selection steps must be defined (i.e. a workflow). These steps can be used by different people given the same dataset and processing parameters to ultimately produce the same or similar results (De Kemp et al. 2016). The workflow applied in this study (Fig. 1), contains six iterative user-driven steps which mutually contribute to the final model and which were implemented and executed in Leapfrog Geo 2021.2 software (developed by Seequent). The input data contains surface measurements, including 832 structural measurements from a previous study by Andersson et al. (2021), local geologic maps, elevation data, geophysical data, and existing 2D/3D models. Subsurface measurements include structural, lithological, and geotechnical data from 5987 drillcores and 106,372 structural and rock-mass strength measurements from underground face mapping. Quality check and data import include steps to organize the spatial data (standardizing, georeferencing, visual inspection in 3D), compilation, and extraction of drillhole data from the database using SQL (Structures Query Language) queries. During the interpretation and conceptualization steps, the data is organized into characteristic domains (spatial regions) based on the structural analysis, lithological and geophysical information, and existing conceptual models. Validation is done to verify the geologic reasonability of the outcome, by estimating the errors of the input data and the uncertainty based on secondary constraints, such as previously existing models. It can be noted that each step contributes to the central modeling method and steps are iterative, making it possible to import new data at later stages.

The study complements previous studies on the geological architecture of the Kiruna Mining District (e.g. Andersson et al. 2021) and provides new insights on geometries and relationships of the structures that are not evident on 2D maps and cross-sections.

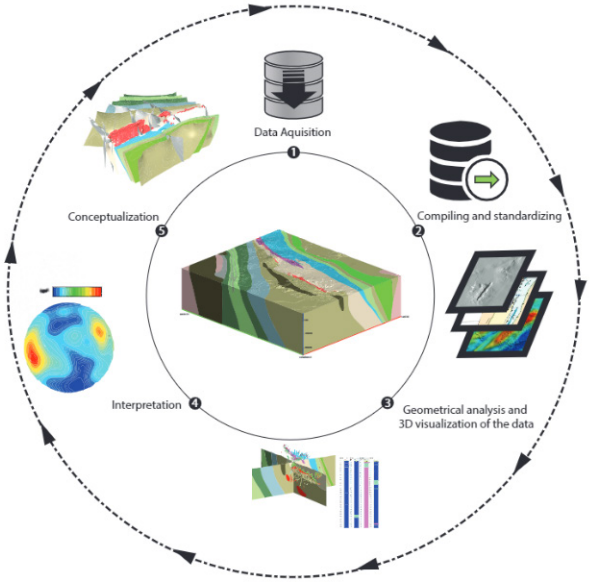

Figure 1. Workflow diagram illustrating the 3D modelling steps.

References

Andersson, J.B.H., Bauer, E.T. & Martinsson, O., 2021: Structural evolution of the central Kiruna area, Northern Norrbotten Sweden: Implications on the geological setting generating iron oxide-apatite and epigenetic iron and copper sulfides. *Economic Geology* 116, 1981-2009.

Bergman, S., Kübler, L. & Martinsson, O., 2001: Description of regional geological and geophysical maps of northern Norrbotten County (east of the Caledonian orogen). *Geological Survey of Sweden Ba* 56, 110p.

Dekemp, E., Schetselaar, E., Hillier, M., Lydon, J. & Ransom, P., 2016: Assessing the workflow for regional-scale 3D geologic modeling: An example from the Sullivan time horizon, Purcell Anticlinorium East Kootenay region, southeastern British Columbia. *Interpretation 2016; 4:3, SM33-SM50.*

Geijer, P. & Ödman, O.H., 1974: The emplacement of the Kiruna iron ores and related deposits. *Geological Survey of Sweden C* 700, 48p.

Schetselaar, E., Pehrsson, S., Devine, C., Lafrance, B., White, D. & Malinowski, M., 2016: 3-D Geologic modeling in the Flin Flon mining district, Trans-Hudson Orogen, Canada: Evidence for polyphase imbrication of the Flin Flon-777-Callinan volcanogenic massive sulfide ore system. *Economic Geology* 111, 887-901.

Vollmer, F.W., Wright, S.F. & Hudleston, J.P., 1984: Early deformation in the Svecokarelian greenstone belt in the Kiruna iron district, northern Sweden. *Geologiska F*öreningens *i Stockholm F*örhandlingar 106, 109-118.

Wright, S.F., 1988: Early Proterozoic deformational history of the Kiruna district, northern Sweden. *Ph.D. thesis (8823582), University of Minnesota, 170p.*

Thematic Session 3
Environmental geosciences

Session Chairs:
Lena Alakangas (lena.alakangas@ltu.se)
Karin Eliaeson (Karin.Eliaeson@sgu.se)
Geoffrey Lemdahl (Geoffrey.lemdahl@lnu.se)

Geochemistry in the Arctic – The legacy of GEOTRACES

Per S. Andersson

Swedish Museum of Natural History, Stockholm, Sweden, per.andersson@nrm.se

Summary. This presentation gives an overview of the GEOTRACES programme with focus on specific scientific issues in the Arctic that might impact marine biogeochemical cycles on a broader scale. Data from Arctic cruises is used to illustrate the important influence of the Arctic region on marine biogeochemistry. During its first decade of operation scientists from about 35 nations have been involved in the programme, which has produced a range of extraordinary results that will serve as a benchmark for future marine biogeochemistry.

The GEOTRACES programme is an international scientific collaboration to map and study the Marine Biogeochemical Cycles of Trace Elements and Isotopes (TEI). Several trace elements are critical micronutrients (e.g. Fe, Zn, Cd, Cu) for marine life and therefore influence the functioning of ocean ecosystems and the global carbon cycle. Some trace elements are also of concern as contaminants (e.g. Pb, Hg), while others, together with a diverse array of isotopes, are used to assess modern-ocean processes and the role of the ocean in past climate change (e.g. ^{231}Pa, ^{230}Th, Nd-isotopes). Despite the recognised importance of TEI in the ocean, our ability to exploit knowledge of their significance is limited by uncertainty about their sources, sinks, internal cycling and chemical speciation. GEOTRACES fills this critical gap with knowledge of the marine biogeochemical cycles of TEI at an unprecedented scale.

The GEOTRACES planning began in 2003 and the programme had a pre-start with the International Polar Year, 2007–2008, marine expeditions to the Arctic Ocean and the Southern Ocean. Since the start of the programme 19 nations have completed more than 132 cruises throughout the world oceans. A key component of GEOTRACES is open data sharing (IDP 2021). When generating a high quality global data product sampling and anlytical methods needs to be tested and verified. This has been carried out through an ambitious and rigourous intercalibration program with the establishment of a best practice "cookbook" for sampling and sample-handling protocols.

GEOTRACES cruises in the Arctic generated data of dissolved trace elements that among other features showed high concentrations of trace elements in surface waters around the North Pole (Charette et al. 2020). The Transpolar Drift (TPD), a surface current that carries ice and continental river-shelf-derived materials from Siberia across the North Pole to the North Atlantic Ocean, is the major conveyor of trace elements originated from land and into the Arctic Ocean and further onward to the Atlantic. The trace element inputs are expected to increase as a result of permafrost thawing and increased river runoff in the Arctic, which is warming at a rate much faster than anywhere else on Earth. Recent studies (Krisch et al. 2022) predicts that trace elements from the Arctic region may stimulate primary production and atmospheric CO_2 drawdown in regions downstream to the Arctic-Atlantic gateways.

The Nd-isotopic composition, ε_{Nd}, have been videly used as a water mass tracer for studies of large-scale oceanographic and paleoceanographic circulation. The restricted Arctic Ocean basin is surrounded by large continental shelves, covering more than 50% of its total area. Distinct from other oceans, with surface water Nd depletion, there is throughout the Arctic a pattern of higher Nd concentrations at the surface that gradually diminish with depth. A range of isotopic variations across the Arctic and within individual depth profiles reflects the different sources of waters. Radiogenic ε_{Nd} signatures can also be traced in Pacific water flowing into the Chukchi Sea. Improving our knowledge of how sea water aquire its ε_{Nd} signature and how it is modified across shelf areas and ocean boundaries is not fully understood. The Arctic Ocean with vast shelfs and large river water input with contrasting e_{Nd} constitute an excellent area both to delinate and understand key geochemical process and also how these process might impact the Oceans on a larger scale.

References

Charette, M. A., Kipp, L. E., Jensen, L.T., Dabrowski, J. S., Whitmore, L. M.,Fitzsimmons, J. N., et al. (2020). The Transpolar Drift as a source of riverine and shelf-derived trace elements to the central Arctic Ocean. *Journal of Geophysical Research: Oceans*, 125, e2019JC015920. https://doi.org/10.1029/2019JC015920

IDP (2021). The GEOTRACES Intermediate Data Product 2021. NERC EDS British Oceanographic Data Centre NOC. DOI: 10.5285/cf2d9ba9-d51d-3b7c-e053-8486abc0f5fd .

Krisch, S., Hopwood, M. J., Roig, S., Gerringa, L. J. A., Middag, R., Rutgers van der Loeff, M. M., et al. (2022). Arctic – Atlantic exchange of the dissolved micronutrients iron, manganese, cobalt, nickel, copper and zinc with a focus on Fram Strait. *Global Biogeochemical Cycles*, 36, e2021GB007191. https://doi.org/10.1029/

The Ce anomaly in hemiboreal headwater streams

Sarah Conrad[a], Johan Ingri[a], Stefan Löfgren[b]

[a]Department of Civil, Environmental and Natural resources Engineering, Luleå University of Technology, Sweden, firstname.lastname@ltu.se; [b]Department of Aquatic Sciences and Assessment, Swedish University of Agricultural Sciences, Uppsala, Sweden, stefan.lofgren@slu.se

Summary. Rare-earth element (REE) concentrations were measured on over 100 hemiboreal headwater stream samples during summer (drought period), late autumn, and spring. Element concentrations and calculated anomalies (δCe) are used to discover and verify different flow pathways from the groundwater into the headwater streams. The geochemistry of headwater streams is very responsive to natural and anthropogenic changes and spatial and seasonal discharge studies are necessary to understand the transport mechanisms and pathways of nutrients and elements. Especially changes in the redox conditions affect element mobility.

The Ce anomaly is defined as δCe calculating the deviation between the expected and measured Ce concentrations (Lidman et al., 2019, Eq. 1). During transport in the soil profile, redox reactions cause Ce to separate from the other REE, leading to a distinct negative δCe in the soil solution, which eventually discharges into surface waters. This process is also known as oxidative scavenging (Bau, 1999; Davranche et al., 2005)Rare Earths and Yttrium (ΣREY: ~61 µg/L. Within organic-rich soil layers, Ce and other REE are complexed by organic matter, which prevents oxidation (Davranche et al., 2008, 2005)whereas steady state is not reached before 10 d when REE occur as REE-humate complexes. The distribution coefficients (KdREE and inhibits the development of a negative δCe in solution. Therefore, the δCe signal of stream water offers the possibility to determine the groundwater origin and the redox state along the dominant groundwater flow paths. The Ce anomaly is an excellent addition to the Environmental Geoforensic approach, determining sources of and pathways between different water bodies.

$$\delta Ce = \frac{(Ce/Ce_N)}{\frac{2}{3}(La/La_N) + \frac{1}{3}(Nd/LNda_N)} - 1 \qquad \text{Eq.1}$$

This study was performed on data from 104 randomly chosen hemiboreal headwater streams in southeast Sweden (Conrad et al., 2019; Löfgren et al., 2014). The unfiltered headwater stream waters were sampled in summer, late autumn, and spring. Analyses of total organic carbon (TOC), pH, SO_4^{2-}, alkalinity/acidity, and other ions (Ca^{2+}, Mg^{2+}, K^+, Na^+, Cl^- and NO_3^-) needed for estimating ANC were performed at SLU (Löfgren et al., 2014). Multi-elemental analysis of bulk water samples was carried out in a clean laboratory (Class 10,000) on a ICP-SFMS (Rodushkin et al., 2005).

The REE concentrations between summer, late autumn, and spring in the single streams varied, but no significant changes in the normalized REE patterns between the sampling events occurred. Compared to the late autumn and spring surveys, some streams showed different element concentrations in summer due to drought and low flow conditions. In another study based on data from these three surveys, sulfate and nitrate concentrations and Fe isotope compositions were used to show that the soils were reduced along the main groundwater flow paths being the source for stream water runoff (Conrad et al., 2019). Similar reduced conditions were observed in northern Sweden linked to a drought period in the Summer 2018 (Gómez-Gener et al., 2020). High TOC concentrations in headstream water during the summer drought (12.5 mg L^{-1}) indicate a strong influence by runoff from organic-rich and reduced riparian soils and wetlands, increasing the normalized REE_N concentrations and keeping the negative Ce anomaly close to zero (–0.15 in summer). During the following late autumn and spring surveys, decreasing TOC concentrations (3.7 and 2.7 mg L^{-1}, respectively) and a slight decrease in Ce anomaly (–0.19 and –0.17, Table S3) indicate less influence by organic-rich soils and very restricted changes in redox. Contradictory, headwater streams with low TOC concentrations (0.9 to 2.8 mg L^{-1}) showed low variations in TOC and REE_N between the different surveys. These streams also exhibited tangible negative Ce anomalies (–0.65, –0.73, –0.72) at all three surveys, indicating strong influence by groundwater discharge from oxidized and Fe-rich mineral soils during summer baseflow and seasons with high runoff. This information was paired with the catchment composition (SGU database) and the catchment slope, allowing us to define two source endmembers; the *reduced groundwater* has a Ce anomaly between –0.3 and zero. In contrast, the *oxidized groundwater* has a δCe between –0.8 and –0.4 in the hemiboreal headwater streams of this study. In the interval –0.3 to –0.4, the variation in stream water chemistry indicates a relatively even influence by oxidized and reduced groundwater, causing uncertainties in the end-member classification.

Acidic headwater streams with reduced groundwater generally showed a wide variation of element concentrations (Figure). We observed up to five times higher concentrations in headwater streams fed by reduced groundwater than oxidized groundwater. Redox-sensitive elements, e.g. Mn, Fe, and Pb, showed trends with up to three-, four-, and five-times higher concentrations in streams fed reduced groundwaters. The elements Al, As, and Cd showed low concentrations in streams fed by oxidized groundwaters and about twice as high in streams fed by reduced groundwater. On the contrary, Ca and Mg were depleted in streams fed by reduced groundwater than oxidized groundwater. Streams with high Ca and Mg concentrations are fed by oxidized groundwater and most likely lateral transport through the less influenced by OC and offering a longer travel time through the soil. The Ce anomaly offers great potential to identify the source of headwater streams during seasonal variations. While the concentrations were affected by seasonal drought events, the extent of the Ce anomaly stayed constant throughout the seasons.

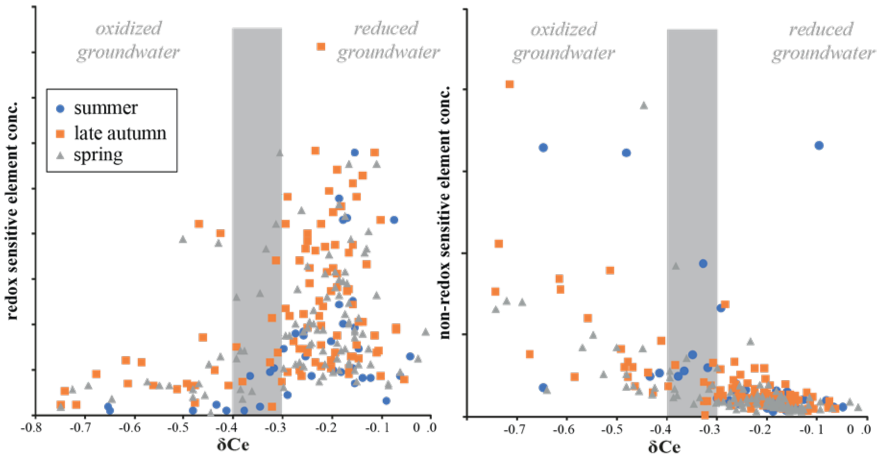

The Ce anomaly versus element concentration of two different behaving elements, showing the behavior of redox-sensitive and non-redox sensitive elements The general behavior of redox-sensitive elements, such as Mn, Fe, Pb, as well as Al, As, and Cd is shown on the left side, while the general behavior for elements such as Ca and Mg, which are not influenced by redox conditions is shown on the right side.

References

Bau, M., 1999. Scavenging of dissolved yttrium and rare earths by precipitating iron oxyhydroxide: Experimental evidence for Ce oxidation, Y-Ho fractionation, and lanthanide tetrad effect. Geochim. Cosmochim. Acta 63, 67–77.

Conrad, S., Löfgren, S., Bauer, S., Ingri, J., 2019. Seasonal Variations of Redox State in Hemiboreal Soils Indicated by Changes of δ 56 Fe, Sulfate, and Nitrate in Headwater Streams. ACS Earth Sp. Chem.

Davranche, M., Pourret, O., Gruau, G., Dia, A., Jin, D., Gaertner, D., 2008. Competitive binding of REE to humic acid and manganese oxide: Impact of reaction kinetics on development of cerium anomaly and REE adsorption. Chem. Geol. 247, 154–170.

Davranche, M., Pourret, O., Gruau, G., Dia, A., Le Coz-Bouhnik, M., 2005. Adsorption of REE(III)-humate complexes onto MnO2: Experimental evidence for cerium anomaly and lanthanide tetrad effect suppression. Geochim. Cosmochim. Acta 69, 4825–4835.

Gómez-Gener, L., Lupon, A., Laudon, H., Sponseller, R.A., 2020. Drought alters the biogeochemistry of boreal stream networks. Nat. Commun. 11.

Lidman, F., Laudon, H., Taberman, I., Köhler, S., 2019. Eu anomalies in soils and soil water from a boreal hillslope transect – A tracer for Holocene lanthanide transport? Geochim. Cosmochim. Acta 267, 147–163.

Löfgren, S., Fröberg, M., Yu, J., Nisell, J., Ranneby, B., 2014. Water chemistry in 179 randomly selected Swedish headwater streams related to forest production, clear-felling and climate. Environ. Monit. Assess. 186, 8907–8928.

Rodushkin, I., Nordlund, P., Engström, E., Baxter, D.C., 2005. Improved multi-elemental analyses by inductively coupled plasma-sector field mass spectrometry through methane addition to the plasma. J. Anal. At. Spectrom. 20, 1250–1255.

Secondary minerals affecting the mobility of critical metals (Be and W) – determined by sequential extraction combined with DXRD and SEM-EDS

Lina P.B. Hällström, Emma Flodin

Applied Geochemistry, Luleå University of Technology, Luleå, Sweden; lina.hallstrom@ltu.se

Summary. Be and W are critical elements with the potential to be mined in Sweden. The knowledge regarding their geochemical behavior is limited and needs to be understood to ensure sustainable mine waste and water management. White crystals formed secondarily at the shore of W-skarn tailings were analyzed with sequential extraction, DXRD and SEM. The results showed that secondary gypsum temporarily scavenged Be, but dissolution by rainfall released high concentrations of Be to downstream surface water. W adsorbed to hydrous ferric oxides (HFO), and the particles settled close to the tailings. This needs to be considered when evaluating remediation techniques for Be and/or W mine waste.

Introduction

Beryllium and W are identified as EU-critical raw materials based on supply risk and economic importance. The EU aims for a higher domestic production to secure that the European Green Deal is reached by 2050. Both Be and W have the potential to be mined in Sweden (Eilu et al., 2021). Still, to maintain sustainable mining, research is needed regarding the geochemical behavior of both elements. Without this knowledge, mine waste and water management containing Be and W might be insufficient, and reclamation to "pre-mining conditions" after mine closure will be hard to achieve. The poor knowledge of their geochemical behavior can adversely impact groundwater due to element leaching. Both Be and W have previously been considered as immobile elements (Koutsospyros et al., 2006; Taylor et al., 2003), but Hällström et al. 2021 found that both elements were released from their primary minerals in W-skarn tailings in Yxsjöberg and transported to the groundwater in high concentrations. Beryllium is identified as the most toxic element in the periodic table if inhaled (Taylor et al., 2003). Tungsten is classified as an emerging contaminant of concern in the USA (US EPA 2014). The risk of having groundwater polluted with Be and /or W highly depends on the stability of the hosting minerals and the geochemical environment in which they are located. The mobility of Be and W and co-precipitation with secondary minerals were studied at the shore of Smaltjärnen Repository in Yxsjöberg, Sweden.

Method

A white precipitate from the tailings shore was collected and analyzed with SEM-EDS. The first four steps of the sequential extraction described by Dold (2003) were carried out on the sample. The sample was analyzed by XRD and SEM between each step of the sequential extraction. The eluates were sent to ALS Scandinavia for screening analyses of 71 elements using inductively-coupled plasma sector field mass spectrometry (ICP-SFMS).

Results and discussion

The tailings shore at Smaltjärnens repository acts as a chemical barrier, scavenging Be temporarily and W more permanently by adsorption/co-precipitation with gypsum and HFO, respectively, Fig 1. The groundwater of the tailings contains high concentrations of Ca, Fe, and S (615, 50, 590 mg/L, respectively), primarily released from pyrrhotite oxidation (Fe, S) and calcite neutralization (Ca) in the upper parts of the tailings. The tailings have been oxidized during >50 years of storage, and no dams are controlling the tailings (Hällström et al., 2021). The groundwater in the tailings flows out to the shore and makes the tailings saturated. White crystals, defined by SEM and XRD as gypsum ($CaSO_4*2H_2O$), formed on the tailings and vegetation, probably due to evaporation. HFO has formed due to the oxidation of Fe^{2+} when the groundwater comes in contact with the atmosphere.

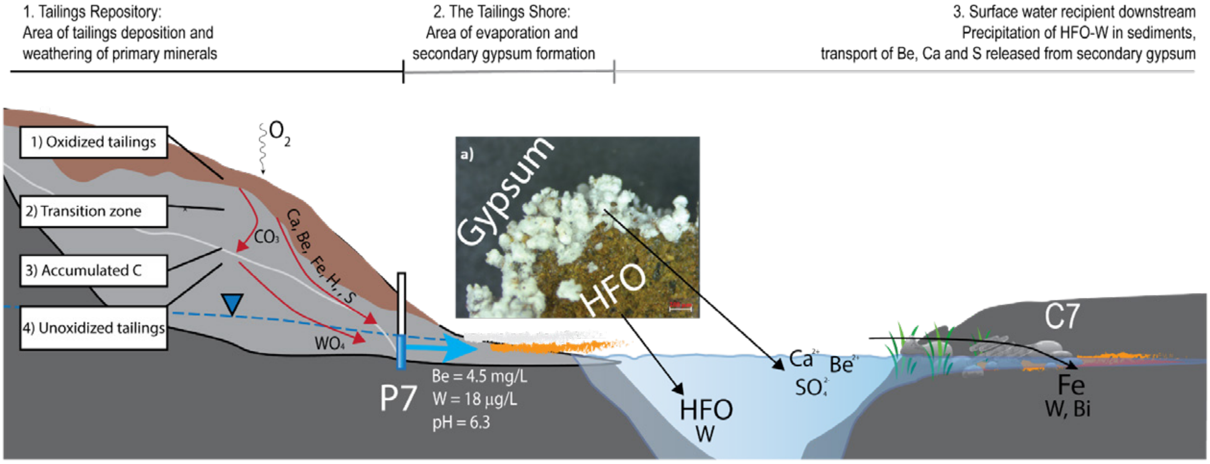

Figure 1. A schematic figure illustrating 1. Beryllium and W mobility from different zones in the tailings to groundwater, 2. Uptake by secondary gypsum and HFO at the shore of the tailings, and 3. Beryllium is released to surface water downstream.

Sequential extraction combined with XRD and SEM showed that Be preferentially adsorbed/co-precipitated with secondary gypsum. Thus, high concentrations of Be, Ca and S released during the first step in sequential extraction were correlated with removing gypsum peaks in the XRD spectra and decreasing appearance of Ca and S during SEM-EDS mapping. This is interesting since Be previously has been considered to have a high affinity for HFO (Taylor et al. 2003), but studies regarding Be uptake in gypsum are limited. Correlated concentrations of Be, Ca and S in the surface water downstream the tailings suggest that secondary gypsum has been dissolved due to rainfall and released Be in high concentrations. According to the sequential extraction, tungsten released from weathering of scheelite in the tailings was mainly associated with HFO. Both Fe and W were found as suspended matter in the surface water, and erosion from the shore has probably transported the particles there. Tungsten settled into the sediment close to the tailings repository, whereas Be was transported in concentrations above guideline values from aquatic organisms more than 5 km from the Yxsjöberg mine site. This shows that the stability of the secondary minerals formed at the shore plays an important role regarding the impact on the surface water quality.

Conclusions

This study shows that Be preferentially adsorbes/co-precipitates with secondary gypsum, while W has a high affinity for HFO. Beryllium is released in high concentrations to downstream surface water due to gypsum dissolution by rainfall. Tungsten settled to the sediments a few 100 m from the repository together with HFO and did not pose a threat to ecosystems. This needs to be considered when evaluating methods for remediation of mine waste containing Be and W.

References

Eilu P, Bjerkgård T, Franzson H, Gautneb H, Häkkinen T, Jonsson E et al. 2021. *The Nordic Supply potential of critical metals and minerals for a Green Energy Transition.* Nordic Innovation Report. ISBN 978-82-8277-115-3

Dold, B., 2003. *Speciation of the most soluble phases in a sequential extraction procedure adapted for geochemical studies of copper sulfide mine waste*. J. Geochem. Explor. 80, 55-68.

Koutsospyros A, Braida W, Christodoulatos C, Dermatas D, Strigul N. 2006. *A review of tungsten: from environmental obscurity to scrutiny.* J. Hazard. Mater. 136, 1-19.

Hällström L. 2021. *Source, mobility and fate of critical Be, Bi, F and W from historical sulfidic-oxidic skarn tailings: Re-mining as remediation method?* Doctoral thesis, Luleå University of Technology.

Taylor T.P, Ding M, Ehler D.S, Foreman T.M, Kaszuba J.P, Sauer N.N. 2003. *Beryllium in the environment: A review.* J. Environ. Sci. Health A Tox. Hazard. Subst. Environ. 38, 439-469.

U.S Environmental Protection Agency. 2014. *Technical Fact Sheet – Tungsten,* EPA 505-F-14-004.

Using ion-exchange resin and Itrax XRF Core Scanning to pinpoint heavy metal pollution sources

Ludvig Löwemark

Department of Geosciences, National Taiwan University, Taipei, Taiwan, ludvig@ntu.edu.tw

Summary. Locating sources of intermittent heavy metal pollution in natural and man-made waterways can be challenging, labour intensive, and expensive using conventional analytical methods. Ion-exchange resin deployed in the waterways and analysed using XRF scanners can be a cost-efficient, fast and easy way to locate point sources in complex waterways. Here two case studies and a newly developed sample carrier are described.

Environmental application of Itrax XRF core scanning

To find heavy metal pollution sources in natural and man-made waterways is often difficult, time-consuming and expensive. Continuous monitoring by autonomous devices requires the installation of analytical instruments that may break down, be stolen, or be tampered with, while manual monitoring requires frequent visits and the risk of missing pollution events in case these fall between the sampling dates. A recent approach utilizing ion-exchange resins can overcome many of these issues. In short, ion-exchange resins are placed into a large number of small sachets, which are then deployed all over the area to be investigated. After a certain time period, the sachets are collected, brought back to the lab where they are dried and then analysed using XRF core scanning techniques (Fig. 1). Because the ion-exchange resin takes up metal ions in relation to the concentrations in the waters where the sachets were deployed, XRF counts from the scanned ion-exchange resin will be directly proportional to the pollution level in the water. This method was first tested in a polluted former farmland in central Taiwan (Huang et al., 2019), and a second test is being performed in a creek passing through a now abandoned copper smelter (MSc-project, Jian, in progress).

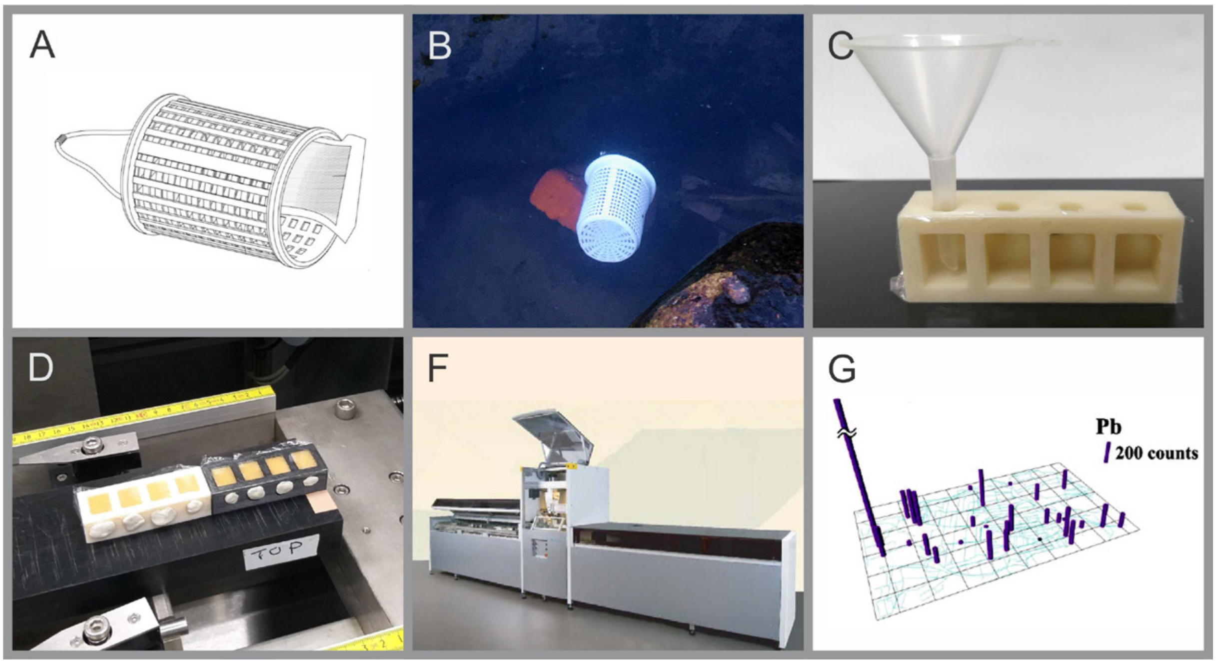

Figure 1. Schematic outline of the ion-exchange resin approach. A) Ion-exchange resin is filled into sachets that are attached to a protective cage. B) Resin sachets are deployed in the water and left for several days. C) Resin is retrieved, dried, and filled into the sample carrier using a funnel. D) The sample carrier is sealed, flipped 90 degrees, and placed onto the Itrax sample holder. F) The sample carrier is scanned in the Itrax XRF core scanner. G) Data can be plotted using GIS applications to pinpoint pollution sources (Huang et al. 2019).

In order to streamline the analysis of large numbers of ion-exchange resin samples, a dedicated sample carrier was designed (Löwemark et al., 2021). The sample carrier consists of a bar with a number of rectangular compartments for the ion-exchange resin and was designed with holes on the side for rapid loading. To load the carrier, a XRF transparent foil is attached over the compartment openings, the carrier is flipped 90 degrees, and a funnel is attached to the filling hole. When the compartment is filled, the filling hole is sealed with putty, and the carrier can then be placed on the Itrax XRF Core scanner for analysis. After analysis, the compartment can be easily emptied by removing the XRF film covering the compartments. Not only does this speed up the loading and cleaning of the sample carrier, but it also minimizes the risk of cross-contamination between different samples and reduces the risk of sample loss during handling in the laboratory.

The outlined method is particularly suited for citizen science projects designed to monitor metal pollution of waterways. Sachets with ion-exchange resin can be sent out to participants from schools or environmental organizations, deployed over large areas and then mailed back to the lab where the resin is dried and analysed, with results being made available to participants almost in real-time using geographical information systems (GIS).

References

Huang, J.-J.S., Lin, S.-C., Löwemark, L., Liou, S.Y.H., Chang, Q., Chang, T.-K., Wei, K.-Y., Croudace, I., 2019. Rapid assessment of heavy metal pollution monitoring using ion-exchange resin sachets and micro-XRF-core scanning. Scientific Reports 9, 10.1038/s41598-41019-43015-x.

Jian, Y.-C., In progress. Using ion-exchange resins and XRF-core scanning to monitor heavy metal contamination and pinpoint pollution sources, Department of Geosciences. Natioanl Taiwan University.

Löwemark, L., Liao, A.C.-Y., Liou, Y.-H., Godad, S., Chang, T.-Y., Kunz, A., 2021. Potential and pitfalls of XRF-CS analysis of ion-exchange resins in environmental studies. Scientific Reports 11.

GIS-modelled estimation of peat volumes and peat carbon stock in Sweden

Caroline Morin[a], Gustav Sohlenius[b], Elin Norström[c]

[a] The Geological Survey of Sweden, Uppsala, Sweden, and the Department of Physical Geography, Stockholm University, Stockholm, Sweden. Email: caroline.morin@sgu.se. [b] The Geological Survey of Sweden, Uppsala, Sweden, Email: gustav.sohlenius@sgu.se. [c] The Geological Survey of Sweden, Uppsala, Sweden, Email: elin.norstrom@sgu.se (corresponding author)

Summary. Digital information on the spatial and stratigraphical distribution of peat available at The Geological Survey of Sweden is included in a GIS-modelled estimation of the total volume of peat present in Sweden. From the modelled volumes of peat, an aproximate estimation of the the total carbon stock contained in the Swedish peatlands can be calculated. The project runs through 2022 and the model outcome will be presented at the conference.

Peatlands represent unique ecosystems providing numerous ecosystem services. They act as efficient nutrient traps, effective carbon sinks and they have capacity to regulate and store water (e.g. Gao et al. 2016, Walton et al. 2020). Around 15% of the land area in Sweden is covered with peatlands (The Geological Survey of Sweden). Drainage of peatlands for forestry and agricultural purposes have however exposed the peat for oxidation over centuries, turning them into a major carbon source (Loisel et al. 2021). Today drained peatlands in Sweden are emitting greenhouse gases in the range of 11.6 million ton CO_2-equivalents per year, which is equal to 25% of the country's yearly territorial emissions (The Swedish Environmental Protection Agency).

This project aims to compile digital data on peat available at The Geological Survey of Sweden (SGU), in order to estimate the total peat volume and carbon stock in Sweden. SGU hosts spatial as well as stratigraphic data on peat in Sweden (SGU, 2022a-c). Detailed stratigraphic data from peatlands are available for specific parts of Sweden, providing information about peat thickness and peat properties such as the degree of humification (see figure). The spatial data of the areal extension of peatlands in Sweden, is divided into bogs and fens, with level of details varying geographically (SGU, 2022a). Peatlands affected by human activities are considered by identifying areas affected by drainage and agriculture.

First part of this project involved an estimation of the total peat volume in Swedish soils. The estimation was performed through a GIS modelling approach. Data from areas where detailed information is available i.e. from observations and mapping, was extrapolated to areas where data is less abundant or less detailed. Moreover, the extent of peat affected by drainage was estimated by using spatial mapping of diked soils (The Swedish Environmental Protection Agency). Secondly, the carbon stock was calculated by applying the expected carbon content per volume unit, for different types of peat. This estimation was based on a division of the total peat into e.g. the degree of humification, compaction from drainage, land use etc. (e.g. von Post and Granlund 1926; Päivänen 1969; Mäkilä & Goslar 2008; Schoning 2014; Schoning 2015).

The study highlights peat as an important carbon sink in Sweden. However, it also highlights its role as a huge carbon source through the extensive areas affected by drainage - a process that can only be reversed by restoration and re-wetting of the drained wetlands.

The project is running through 2022, and the first outcome from the model will be available later this year. It should be stressed that the modelling apporoach involves several uncertainties, including limitations in both spatial and stratigraphical resolution of source data. It is, for example, possible that the model underestimate peat volumes due to the occurrence of small peat areas not shown on SGU:s soil maps (SGU, 2022a). The outcome of the model should thus be considered an approximate estimation of peat volumes and carbon stocks. One aim for the future is to improve the model by using the large amount of analogue peat information that is available in SGU:s archive.

The project was initiated by SGU and is funded by The Swedish Environmental Protection Agency.

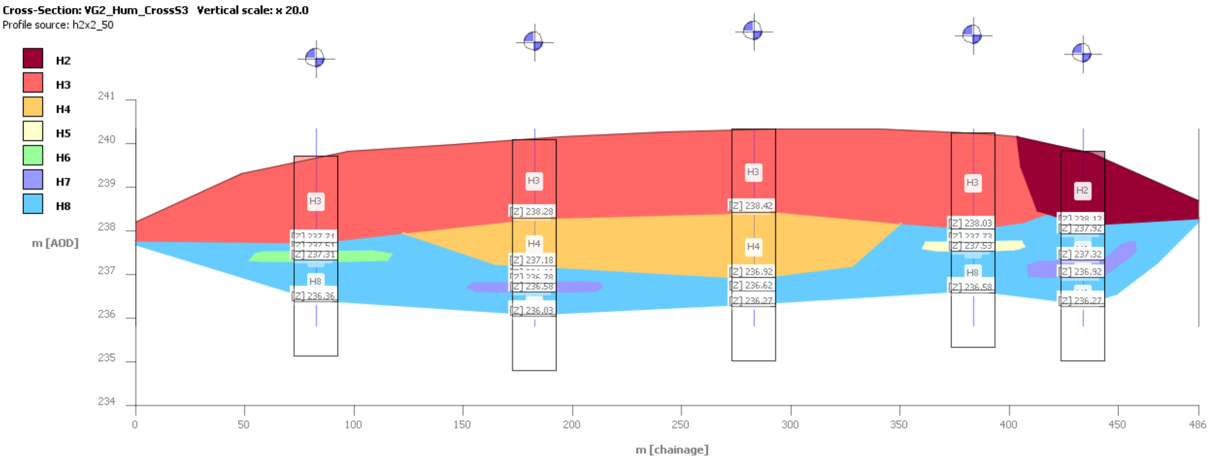

Figure. A digitalized cross section through a typical peat bog located in Västergötland, Sweden. The humification levels are based on boreholes drilled in the peat. Humification is categorized from H1 (lowest humification) to H10 (highest humification). The cross section indicates the typical stratification expected from this type of peat, with lower humification at the top and higher humification further down. Stratigraphic data is based on digitalised data from SGU (SGU, 2022b). The cross section was digitalized in *Groundhog* software (British Geological Survey, BGS). Based on crossections like this, 3D modelling of peat volumes are conducted using the same software.

References

Gao, J., Holden, J., Kirkby, M., 2016. The impact of land-cover change on flood peaks in peatland basins. Water Resource Research 52, 3477–3492.

Loisel et al., 2021. Expert assessment of future vulnerability of the global peatland carbon sink. Nature Climate Change volume 11, pages70–77

Mäkilä, M, & Goslar T. 2008: The carbon dynamics of surface peat layers in southern and central boreal mires of Finland and Russian Karelia. Suo 59(3): 49–69, Finnish Peatland Society.

Päivänen, M., 1969: The bulk density of peat and its determination. Silva Fennica 3, 1–19.

von Post, L., & Granlund, E., 1926: Södra Sveriges torvtillgångar. Sveriges geologiska undersökning, Serie C 355. Sveriges geologiska undersökning.

SGU, 2022a: Jordarter 1:25 000–1:100 000 (Databas) www.sgu.se/produkter/geologiska-data/

SGU, 2022b: Torvlagerföljder (Databas) www.sgu.se/produkter/geologiska-data/

SGU, 2022c: Jordlagerföljder (Databas) www.sgu.se/produkter/geologiska-data/

Schoning, K. 2014: Torvtillväxt och kolackumulation hos unga torvmarker i Uppland. SGU-rapport 2014:35. Sveriges geologiska undersökning.

Schoning, K. 2015: Förändringar i torvegenskaper, markanvändning och vegetation hos södra och mellersta Sveriges torvmarker. SGU-rapport 2015:09. Sveriges geologiska undersökning.

Walton, CR, et al. 2020. Wetland buffer zones for nitrogen and phosphorus retention: Impacts of soil type, hydrology and vegetation. Science of The Total Environment 727, 138709.

Investigations on fibre sediments in Sweden

Johan Norrlin[a], Lijana Gottby[a], Johan Nyberg[b], Anna Apler[a], Olof Larsson[a], Sarah E. Josefsson[a], Lovisa Zillén Snowball[a]

[a]Geological Survey of Sweden (SGU), Box 670, 751 28 Uppsala, johan.norrlin@sgu.se;
[b]Ramboll, Sidenvävargatan 11, 753 19 Uppsala, johan.nyberg@ramboll.com

Summary. Paper, pulp, and fibre board production until late 20th century led to discharge of fibres in marine and limnic waters. The fibres accumulated into fibre sediments that often contain chemical pollutants. SGU has so far investigated 46 sites in Sweden, using an in-house combination of methods including hydroacoustics, sediment sampling and environmental chemistry. An area of c. 31 km^2 of fibre sediments have been described. Regional authorities have identified 300 additional sites where fibres have been produced. Further investigations, risk assessments, and remediation priorities are needed.

Background

In many regions in Sweden the forest industry was, and partly still is, very important. Unfortunately, the manufacturing of different types of wooden products, such as paper pulp and particle board, caused large amounts of fibrous material to be discharged with the wastewater in the late 19th and most of the 20th century. The existence of fibre banks has been noted at least since the 1970s. Site-specific studies have been conducted with varying methods and levels of ambition by e.g. environmental authorities, the industry and as research projects (Apler 2021 with references). The fibres accumulated in calm aquatic environments in the near vicinity of the factories or further downstream in the catchment area. In addition, various chemicals were used or produced in the processes, and therefore, in many locations, the fibrous sediments contain large amounts of contaminants and are considered as environmental risks. Several natural and anthropogenic processes may cause a dispersal of hazardous contaminants from these sediments to the aquatic environment.

Aim

To get a uniform and comparable overview of the spatial extent and other properties of fibrous sediments at different sites in Sweden, the Swedish Environmental Protection Agency and the Swedish Agency for Marine and Water Management have financed inventory surveys. This overview is a necessary basis for further assessment, monitoring and remediation of these contaminated sites.

In collaboration with the county of Västernorrland, which is situated at the northern part of the Bothnian Sea, the Geological Survey of Sweden (SGU) has developed a method for inventory of fibrous sediments. It is based on a combination of hydro acoustic (geophysical) measurements and sediment sampling resulting in stratigraphic descriptions, radiometric dating and sub-samples for environmental chemical analyses and characterization . The method has now been applied in several parts of Sweden to investigate expected fibrous sediment areas, mostly in coastal areas but also in lakes and rivers. These marine-geological tools, normally used in conventional bottom floor mapping, can be used to facilitate the mapping of contaminated fibrous sediments.

Conclusions

In total, 46 sites with potential fibrous sediments have so far been investigated by SGU, covering a total area of c. 259 km^2. At these sites 49 fibrebanks, consisting almost entirely of cellulose fibres, have been identified and estimated to cover a total area of almost 3.0 km^2. In addition, fibre-rich sediments, i.e. natural sediments displaying a pronounced content of fibres and/or wood and bark chips, have also been mapped and estimated to cover a total area of c. 28 km^2. Further work on these deposits, in terms of e.g. risk classification and priorities for remediation, will need to be carried out by regional authorities in order to deal with the risk posed by this contaminated type of sediment.

An estimate from Swedish county boards shows that there are more than 300 sites in Sweden where soil contaminated from paper, pulp or fibreboard industries is or may be present. Since these industrial processes are very water-consuming, it is likely that they have discharged wastewater and potentially caused formation off fibrebanks or fibre-rich sediments. During 2019–2022 SGU, in cooperation with other authorities, has a government assignment to enhance the knowledge of polluted sediments in Sweden. Several sites, in addition to those mentioned above, with potential fibrous sediments are investigated as a part of the assignment.

The reported inventory method can be used for all types of fibrous sediments and can thus be applied to such deposits worldwide.

References

Apler A., 2021: Contaminated organic sediments of anthropogenic origin: impact on coastal environmenst. *Acta Universitatis Upsaliensis*. Uppsala.

Acid sulfate soil in Sweden – distribution, machine learning maps, and environmental impact in a changing climate

Christian Öhrling[a], Gustav Sohlenius[b], Marina Becher[b]

[a]Geological Survey of Sweden, Gothenburg, Sweden, christian.ohrling@sgu;
[b]Geological Survey of Sweden, Uppsala, Sweden

Summary. In many coastal areas in Sweden, especially along the Bothnian Bay coast, acid sulfate soil occurs, which can have a negative impact on nearby surface waters. This has sometimes caused the environmental quality standards for water could not be achieved. The Geological Survey of Sweden aims to map the national distribution of the occurrence of this soil. For help and efficiency, we use machine learning to predict the occurrence. Based on water-balance forecasts, we evaluate the environmental risks posed by acid sulfate soil in a changing climate.

Acid sulfate soil (AS-soil) can cause significant economic and environmental issues due to its ability to lower pH and mobilize elements to surface waters (see Becher et al. 2019 and references therein). The problems arise when the soils are oxidized, which commonly occurs due to land use, ditching and excavations. Furthermore, periods with low groundwater levels can cause soil oxidation and following periods with high runoff can affect surface waters negatively. It is assumed that such periods will be more common in the future. We used analyses from climate scenarios, water balance, and AS-soil maps to assess future environmental impact.

The work by the Geological Survey of Sweden has been done within several EU projects, in collaboration with The Geological Survey of Finland (primarily) and Norway, the County Administrative Board in Sweden, and several other institutions in Sweden and Finland.

With machine learning techniques, we have produced probability maps of AS-soil along the Bothnian coast of Sweden, where these soils are common. The maps are compared with results from the hydrological runoff model HYPE regarding different IPCC scenarios in a catchment area of Hertsångerälven, Västerbotten. However, AS-soil has been sampled along almost the entire coast of Sweden, in southern Sweden, often within university-student projects.

The map predicts the distribution of three classes: 1) No AS-soil, 2) Active AS- soil on top of potential, and 3) Potential AS-soil. The model was produced by using data from field observations and several environmental covariates such as maps of Quaternary deposits, and most importantly, a high-resolution elevation model from which several derivatives were extracted (Figure 1). The modelled map shows that active AS-soils are common in flat areas with fine-grained sediments close to the sea level where the groundwater level has been lowered by ditches. Potential AS-soils are common in peat-covered wetlands and are found in larger geographical areas than active acid soils. Models from all climate scenarios show an increase in runoff during autumn and winter, where the increase in winter is the largest. Spring runoff is clearly estimated to be smaller. The summer results are more uncertain but indicate less runoff – more drought.

The described future conditions could lead to increased oxidation and the formation of active AS-soil during the summer drought. If these dry periods are followed by high water flow, a significant acid shock might occur. Consequently, there is a risk that AS-soils in the future may periodically, to an increased extent, adversely affect surface waters. The map data from SGU can highlight areas where the geohazard from AS-soils, in a changing climate, are the greatest. Further, to take actions to mitigate the negative influence from AS-soils or for recognising sites suitable for restoration of wetlands to prevent further negative impact.

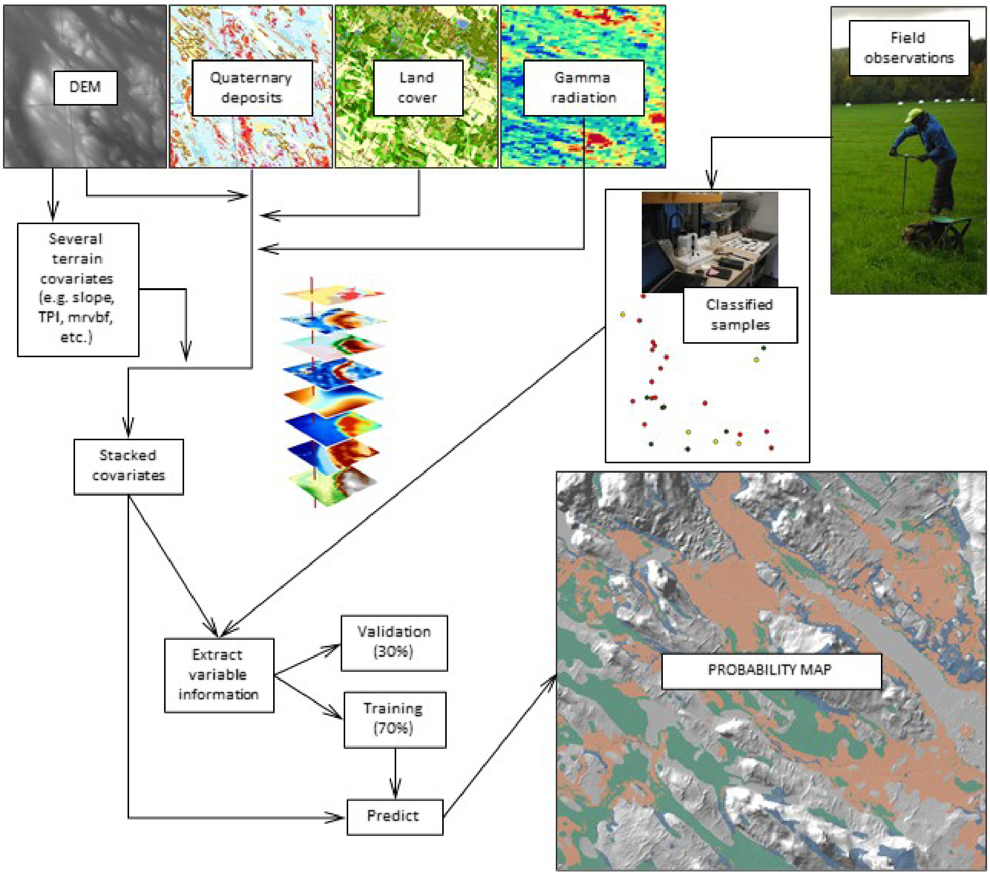

Figure 1: The machine learning workflow. The model is trained with landscape covariates and point observations. The model is then used to predict AS soil occurrence and plot a map (active=red, potential=green, not ASS=blue).

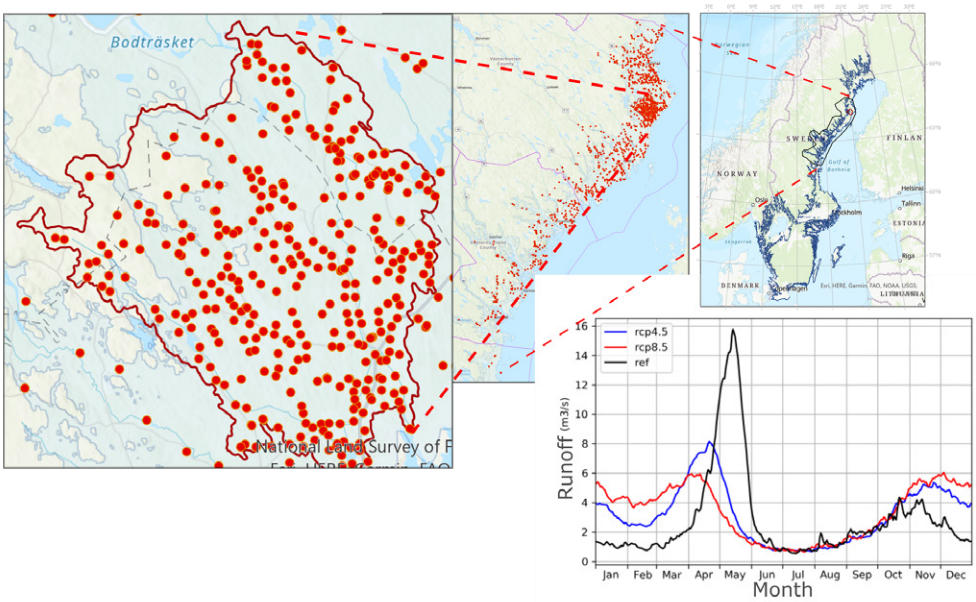

Figure 2: Right to left, the location of the project area and the detailed studied catchment. The blue line on the map represents the marine limit; red dots are sampling locations. The graph shows the modelled runoff over a year; black is historical data, and red and blue are changes in a future climate predicted from two main scenarios from IPCC.

References

Becher, M., Sohlenius, G., & Öhrling, C., 2019: Sur sulfatjord – egenskaper och utbredning. *Sveriges Geologiska Undersökning SGU-rapport* 2019:13.

Distribution and sources of natural and anthropogenic rare earth elements in Trondheimsfjord, Norway

Anna-Lena Zocher[a], Michael Bau[b], Tomasz Ciesielski[c], Stefania Piarulli[d], Julia Farkas[e]

[a]Department of Physics and Earth Sciences, Jacobs University Bremen, Bremen, Germany, a.zocher@jacobs-university.de; [b]Department of Physics and Earth Sciences, Jacobs University Bremen, Bremen, Germany, m.bau@jacobs-university.de; [c]Department of Biology, Norwegian University of Science and Technology, Trondheim, Norway, tomasz.m.ciesielski@ntnu.no; [d]Department of Climate and Environment, SINTEF Ocean, Trondheim, Norway, stefania.piarulli@sintef.no; [e]Department of Climate and Environment, SINTEF Ocean, Trondheim, Norway, julia.farkas@sintef.no

Summary. Rare Earths and Yttrium (REY) are increasingly used in high-tech applications and hence are also increasingly released into the environment. Compared to other water systems, rather little is known about the distribution and sources of REY in Norwegian coastal waters. We present REY data for several sites and depths in Trondheimsfjord, for rivers discharging into the fjord and for waste water treatment plant samples from Trondheim as (potential) source of anthropogenic gadolinium (Gd). We also discuss the role of nanoparticles and colloids for REY behaviour in the fjord.

The REY have become crucial constituents for many high-technology products and processes, such as renewable energies, fertilisers, catalysts, and medical contrast agents. The REY are included in the lists of critical raw materials as defined by the European Union and the United States Geological Survey, which highlights their great economic relevance. The large and ever-growing number of applications of REY causes increasing emissions of anthropogenic REY into the environment. Concomitantly, concerns regarding their (bio-)geochemical behaviour are rising.

Today, many waterbodies worldwide show large positive anthropogenic Gd anomalies in shale-normalised ($_{SN}$) REY patterns (e.g. Bau & Dulski, 1996; Kulaksız & Bau, 2013). These anomalies result from the application of Gd-based contrast agents (Gd-CAs) in Magnetic Resonance Imaging (MRI). Such contrast agents are manufactured as very stable, non-reactive chemical complexes since free Gd is highly toxic to humans. Unfortunately, the Gd from these water-soluble Gd-CA complexes passes waste-water treatment plants (WWTPS) nearly completely and eventually reaches natural waters such as rivers, lakes and groundwater. In contrast to the particle-reactive geogenic REY, anthropogenic Gd is truly dissolved, behaves conservatively during estuarine mixing processes and is not removed from the water column by aggregation of nanoparticles and colloids (NPCs).

Although REY have been widely studied in many types of natural waters and their behaviour during estuarine processes is rather well-known (e.g. Kulaksız & Bau, 2007; Lawrence & Kamber, 2006; Sholkovitz, 1995), they have received little attention yet in waters of the Norwegian west coast.and knowledge on REY in Norwegian coastal waters is still scarce. Therefore, we here present REY data for the dissolved fraction (0.2 µm-filtered) in water samples from different depths at several sites in Trondheimsfjord, located in Trøndelag county in central Norway, and for four of the main rivers entering the fjord (Orkla, Gaula, Nidelva, Stjørdalselva). Additionally, data of influent and effluent samples from two WWTPs in Trondheim are presented. A previous study has shown that their effluents contain notable amounts of Gd (Farkas et al., 2020).

At most stations in Trondheimsfjord, the REY show similar concentration ranges despite considerable depth differences, but the deepest sample at each of these sites always has the lowest total REY concentration. The REY_{SN} patterns of the different depths resemble each other and reveal the typical features of a seawater-like REY_{SN} pattern: an increase from light REY (LREY) to heavy REY (HREY), small positive geogenic La_{SN} and Gd_{SN} anomalies, large positive Y_{SN} anomalies and relatively large negative Ce_{SN} anomalies. However, compared to “true” seawater the increase over the LREY series is flatter. Only the stations located in the vicinity of the Nidelva mouth clearly show different REY_{SN}

patterns for different depths. While the deeper samples also show the seawater-like REY_{SN} patterns, the samples from shallower waters are characterised by notably higher total REY concentrations and a flat REY_{SN} pattern with only a small negative Ce_{SN} anomaly. These are typical features of the REY_{SN} patterns of boreal rivers in Sweden, which are usually very rich in NPCs (e.g. Ingri et al., 2000). Accordingly, the Nidelva REY_{SN} pattern reflects the same features as these shallow fjord water samples, but the river's total REY concentrations are even higher. The positive Gd_{SN} anomalies in the REY_{SN} patterns of the effluents from the WWTPs confirm that they release notable amounts of anthropogenic Gd into the fjord due to incomplete removal of Gd-CAs from sewage during waste water treatment. However, this anthropogenic Gd has no major imprint on the REY inventory of the fjord waters, probably due to the immediate strong dilution with fjord waters.

References

Bau, M. & Dulski, P., 1996: Anthropogenic origin of positive gadolinium anomalies in river waters. *Earth and Planetary Science Letters 143*, 245–255.

Farkas, J., Polesel, F., Kjos, M., Carvalho, P.A., Ciesielski, T., Flores-Alsina, X., Hansen, S.F. & Booth, A.M., 2020: Monitoring and modelling of influent patterns, phase distribution and removal of 20 elements in two primary wastewater treatment plants in Norway. *Science of the Total Environment 725*, 138420.

Ingri, J., Widerlund, A., Land, M., Gustafsson, Ö., Andersson, P. & Öhlander, B., 2000: Temporal variations in the fractionation of the rare earth elements in a Boreal river; the role of colloidal particles. *Chemical Geology 166*, 23–45.

Kulaksız, S. & Bau, M., 2007. Contrasting behaviour of anthropogenic gadolinium and natural rare earth elements in estuaries and the gadolinium input into the North Sea. *Earth and Planetary Science Letters 260*, 361–371.

Kulaksız, S. & Bau, M., 2013. Anthropogenic dissolved and colloid/nanoparticle-bound samarium, lanthanum and gadolinium in the Rhine River and the impending destruction of the natural rare earth element distribution in rivers. *Earth and Planetary Science Letters 362*, 43–50.

Lawrence, M.G. & Kamber, B.S., 2006: The behaviour of the rare earth elements during estuarine mixing – revisited. *Marine Chemistry 100*, 147–161.

Sholkovitz, E.R., 1995: The aquatic chemistry of rare earth elements in rivers and estuaries. *Aquatic Geochemistry 1*, 1–34.

Thematic Session 4
Hydrogeology

Session Chairs:
Roger Herbert (Roger.Herbert@geo.uu.se)
Bo Olofsson (boolof@kth.se)

Establishing a baseline understanding of the hydrogeology in Forsmark

Robert Earon, Magnus Odén, Sven Follin

The Swedish Nuclear Fuel and Waste Management Co, Solna, Sweden, robert.earon@skb.se

Summary. Comprehensive site investigations were carried out by SKB in two campaigns, 2002–2007 and 2008–2010. Following these investigations, new hydrological and hydrogeological data in the form of monitoring time-series, single- and cross-hole hydraulic tests have been collected. Integration of this data into the current understanding of the Forsmark Site and site-descriptive modelling will reduce uncertainties identified in the site descriptive modelling process and allow for the establishment of a baseline understanding of the pre-construction conditions as reference for future construction.

Comprehensive site-descriptive modelling (Follin & Selroos 2013) of the Fosrmark area was conducted in preparation for the site selection of and application for a deep geological repository for spent nuclear fuel (SFK) during the period of 2002–2007 (SKB 2008). During this period several methods of single hole hydraulic testing were conducted in more than 21 core-drilled and 32 percussion drilled boreholes as well as several hydraulic interference tests and the creation of a multi-disciplinary integrated Site-Descriptive Model (SDM). A site investigation for the extension of the short-lived low- and intermediate-level radioactive waste (SFR) was subsequently carried out (SKB 2011) some two kilometers north of the planned location for the SFK, which involved hydraulic tests in additional boreholes. Since both of these investigation campaigns, the number of existing boreholes with single-hole hydraulic test data numbers 50 core-drilled and 56 percussion-drilled, and several hydraulic interference tests have been conducted. Additionally, several more years of hydrological and hydrogeological modelling data exist, all of which aid in the refinment and verification of the existing SDM.

In preparation for the construction phase of the SFK, it is necessary to establish a baseline understanding of the current hydrogeological conditions of the Forsmark area. This entails a detailed categorization and integration of data collected during and after the two site investigation phases within the current hydrogeological site understanding. Integrated hydrological and hydrogeological modelling campaigns will be carried out to test and implement the modelling methodology derived from experiences from the two site-descriptive modelling campaigns, SDM-Site and SDM-PSU. The establishment of a hydrogeological and hydrological baseline in the Forsmark area will be an important reference for forthcoming underground SDM-campaigns, which will be conducted to detail the existing understanding of the Forsmark Site from a safety assessment point of view prior to the start of deposition.

References

SKB, 2008: *Site description of Forsmark at completion of the site investigation phase SDM-Site Forsmark*. SKB TR-08-05, Svensk Kärnbränslehantering AB.

SKB, 2011: *Site description of the SFR area at Forsmark at completion of the site investigation phase: SDM-PSU Forsmark*. SKB TR-11-04, Svensk Kärnbränslehantering AB.

Follin, S. & Selroos J.O., 2013: Overview of hydrogeological site-descriptive modeling conducted for the proposed high-level nuclear waste repository site at Forsmark, Sweden. *Hydrogeology Journal,* DOI 10.1007/s10040-013-1077-x.

In-situ injection of colloidal activated carbon to reduce PFAS spreading in groundwater from a contaminated site

Fritjof Fagerlund[a], Georgios Niarchos[a], Lutz Ahrens[b], Dan Berggren Kleja[c], Jonny Bergman[d], Anna Larsson[d], Gareth Leonard[e], Jim Forde[e], Matilda Schütz[f], Henning Persson[g]

[a]Department of Earth Sciences, Uppsala University, Uppsala, Sweden, fritjof.fagerlund@geo.uu.se; [b]Department of Aquatic Sciences and Assessment, Swedish Univ. of Agricultural Sciences (SLU), Uppsala, Sweden, lutz.ahrens@slu.se; [c]Department of Soil and Environment, SLU, Uppsala, Sweden, Dan.Berggren@slu.se; [d]RGS Nordic, Sweden; [e]Regenesis, UK; [f]NIRAS, Sweden; [g]Swedish Geological Survey, Uppsala, Sweden

Summary. Per- and polyfluoroalkyl substances (PFAS) are contaminants of increasing concern due to their extreme persistence in the evironment and their adverese health effects already at part-per-billion concentrations in drinking water. Here, a method to reduce further spreading to the environment from a PFAS contaminated hotspot was tested using a pilot-scale field trial of *in-situ* injection of colloidal activated carbon (CAC). CAC was able to adsorb and reduce PFAS concentrations in the groundwater, but due to the hydrogeological complexity of the site, complete interception of contaminant transport pathways was not achieved and the final reduction in concentration of a sum of 11 PFASs was approx. 44%.

Introduction

Due to their extreme persistence, often combined with high aqueous mobility, per- and polyfluoroalkyl substances (PFAS) are challenging to remediate and remove from the environment. Stabilisation by activated carbon (AC) is a method that can potentially stop or at least reduce the migration of PFAS and limit further spreading to the environment from contaminated hot spots. Reduced mobility of the contaminants is achieved by adding fixation agents (sorbents) to the subsurface, which immobilize contaminants by sorbing them from the groundwater to the solid phase. AC in various forms, such as granular (GAC) or powdered (PAC) have been identified as promising sorbents for many PFASs, although short chain PFASs are more difficult to adsorb than their long-chain counterparts and remain challenging to completely remove from the water phase (Sörengård et al. 2020). Colloidal activated carbon (CAC) is a novel sorbent for PFAS stabilisation that consists of AC particles up to 1 or 2 µm in diameter. CAC particles are small enough to be injected into the pores of an aquifer and their mobility can be further enhanced by adding polymers to the injection fluid. In this study a pilot-scale field trial was performed by injecting CAC at a PFAS contaminated site in Arboga, Sweden. The main objective was to take the method from the controlled environment in the lab to the real complexity of a field site and evaluate the feasibility of CAC for PFAS stabilisation *in situ* as well as investigate the potential challenges and pitfalls for the given hydrogeological setting.

Method

The study site is a small firefighting training area connected to a facility for airplane manufacturing and repair south of the town Arboga, Sweden. The site was in use from the 1950s to 1990s and the PFAS contamination originates from aqueous film forming foams (AFFF) used in the firefighting training with burning airplane fuel. The exact composition of the firefighting foams is not known and may have changed over time. In the early times, firefighting was done directly in pits in the ground. The site was investigated 2016 and 2018 as part of the normal procedures to characterize the state of contaminated sites in Sweden. From February 2019 additional characterization was performed within the StopPFAS research project including regular sampling and analyses of PFAS concentrations in selected wells and the small stream going though the site, continuous measurements of groundwater levels, analyses of groundwater chemistry, some characterisation of the soil – bedrock interface and groundwater flow direction using iFLUX measurements.

In November 2019 CAC was injected as a small V-shaped (permeable) barrier, aimed to intercept the PFAS plume in the groundwater arriving from upstream sources to the well B2. Additional wells were also installed to add monitoring points for the evaluation of the effect of CAC on PFAS concentrations in the groundwater.

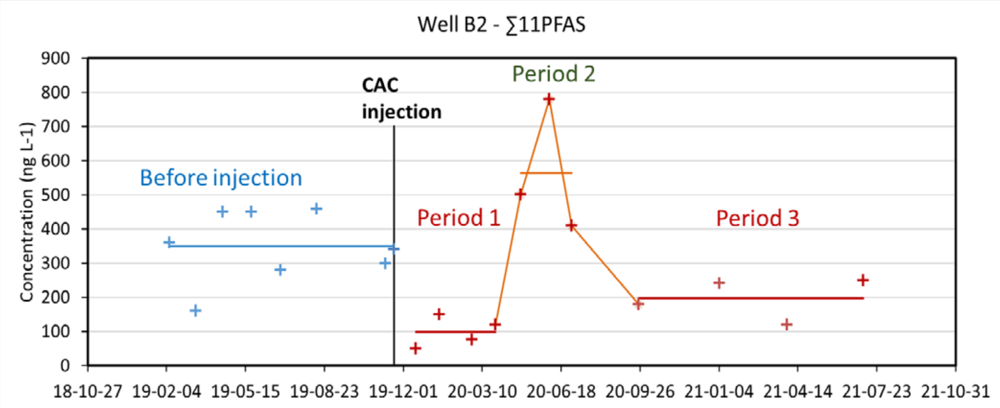

Figure 1. Sum of 11 PFASs in well B2 before and after injection of CAC (Plumestop®) (Niarchos et al., manuscript in preparation).

Results and discussion

After CAC injection, there was an initial reduction in PFAS concentrations in well B2 by approximately 72% for a sum of 11 PFAS, referred as period 1 in Figure 1. Later however, the PFAS concentrations rebounded to levels equal or higher than before CAC injection (period 2), but after this rebound concentrations again declined to lower than before CAC injection (period 3).

The reduction in PFAS concentrations by sorption is related to the amount of CAC that the PFAS come in contact with. An *in-situ* CAC barrier acts as a filter that is emplaced in the subsurface and a critical aspect of the effectiveness of this filter is to intercept as much of the PFAS-transporting flow as possible. Bypass of the barrier in flow paths that were not reached by the CAC injection or by flow from the side or around the barrier may allow PFAS transport to go past it.

The site had a complex geology with a clayey till soil of approximately 3–5 m depth on top of a potentially fractured crystalline bedrock. The groundwater table was very flat in the area of CAC injection and likely prone to changes in local groundwater flow direction with small changes in groundwater levels. An iFLUX measurement of groundwater flow direction in well B2 just before CAC injection indicated that the planned injection would intercept the PFAS plume towards B2. However, CAC injection proved challenging because there were preferential flow zones and the barrier became shorter than planned to avoid a fast transport of CAC into a stream through such zones. The monitoring of groundwater levels and PFAS composition in different wells also indicated seasonal variations in groundwater flow directions.

The initial reduction in PFAS concentrations was significant, but not complete, indicating that there were still flow paths where the PFAS transport was not intercepted by CAC also in period 1 (Figure 1). The most reasonable explanation to the post-CAC-injection changes in downstream PFAS concentrations was deemed to be changes in the groundwater flow direction causing bypass or partial bypass of the injected CAC in periods 2 and 3. It was concluded that the soil characteristics including texture, heterogeneity and existence of preferential flow channels are important factors for the resulting CAC distribution. In a treatment with CAC to limit PFAS migration the goal is to catch as much as possible of the contaminant transport with the injected CAC. Our results show that complex hydrogeological conditions pose a challenge to this goal. For optimal design and placement of a sorptive CAC barrier, it is essential to have a detailed characterization and understanding of soil conditions, groundwater flow directions, including seasonal variations, and flux-zone locations on the local scale of flow through and around the CAC barrier.

References

Niarchos, G., Ahrens, L., Berggren Kleja, D., Leonard, G., Bergman, J., Forde, J., Schütz, M., & Fagerlund, F., *In-situ* application of colloidal activated carbon for PFAS-contaminated soil and groundwater at a hydrologically complex site. *Manuscript in preparation*.

Sörengård, M., Östblom, E., Köhler, S. & Ahrens, L., 2020: Adsorption behavior of per- and polyfluoroalkyl substances (PFASs) to 44 inorganic and organic sorbents and use of dyes as proxies for PFAS sorption. *J. Env. Chem. Engineer. 8.*

Laboratory low-transmissivity tests on natural rock fracture under varying normal load

Michele Godio[a], Lars Jacobsson[b]

[a] Department of Chemistry and Applied Mechanics, RISE Research Institutes of Sweden, Borås, Sweden, michele.godio@ri.se, [b] Department of Chemistry and Applied Mechanics, RISE Research Institutes of Sweden, Borås, Sweden, lars.jacobsson@ri.se

Summary. There is limited available data on natural rock fractures with low hydraulic transmissivity. In this study, we measured the transmissivity of a granite specimen with a 200×200 mm naturally-induced closed fracture under varying normal load. We repeated the measurements after opening the fracture to investigate how this affects its transmissivity. At each stage, we ensured laminar flows by setting Reynolds numbers << 1. Finally, we resorted to the parallel-plate theory to obtain the equivalent hydraulic aperture, that we compared to the mechanical aperture derived from the observed deformation.

Introduction

Knowing the in-situ flow in rock fractures is relevant for hydrogeological problems. Determining the hydraulic transmissivity of a fractured rock mass is of particular importance in, e.g. deep underground nuclear waste repositories, where the groundwater flow and the transport of solutes must be assessed to evaluate their safety. Long-term thermo-hydro-chemo-mechanical processes are usually simulated in the rock mass in the vicinity of the repositories. Nonetheless, modelling these processes exactly is difficult and necessitates the use of established laboratory methodologies to build reliable models. Here, we describe the laboratory work undertaken to characterize the hydro-mechanical behaviour of a natural rock fracture under varying normal loading.

Specimen

We extracted the specimen from a large block of medium-grained granite from the Flivik quarry in the southeast part of Sweden. The block had a natural fracture across the block oriented along the grain plane and was originally subdivided into smaller blocks within the POST2 project (Jacobsson et al., 2021)there is a knowledge gap in terms of the impact of high normal stresses on the mechanical properties of large-scale fractures under Constant Normal Stiffness (CNS. The rock type belongs to the 1.8–1.7 Ga Transscandinavian Igneous Belt (TIB) and has a low matrix permeability. One of the blocks was processed in several steps in order to obtain the final specimen, of size of 200 × 200 × 250 mm (length × width × height). In said specimen, the fracture was pseudo-planar, approximately aligned with the horizontal plane, and with only few minor branches (Figure 1).

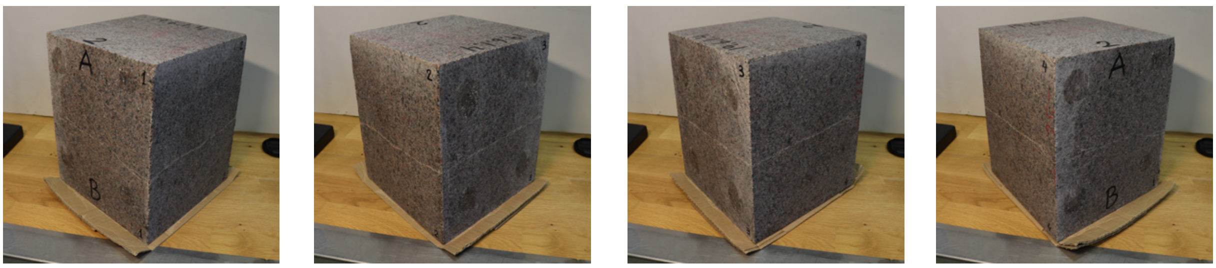

Figure 1 Pictures of the rock specimen and the natural fracture.

Laboratory tests

We measured the fracture transmissivity at the rock mechanics laboratory of RISE Research Institutes of Sweden (Borås, Sweden). We designed the setup in order to provide a uniform laminar flow in one direction of the fracture at a time, while subjecting the specimen to a constant normal compression force (Figure 2). During the tests, we recorded the following quantities: the water pressure, measured on three different points, namely, p_{in}, p_{out} and $p_{in,top}$; the water volume flow rate, Q_w, derived from the measure of the weight of the vessel V3, M_w taking water evaporation into account; the temperature of the water, T_w, measured in the vessel V2, and of the rock material, T_r, measured on the specimen surface; the force exerted by the actuator, F, applied on the top of the specimen; the mechanical deformation of the fracture, by displacement transducers positioned at the four corners of the specimen. The applied force determined the normal stress σ, which was derived as $\sigma = F/A$, with A the nominal cross-sectional area of the specimen.

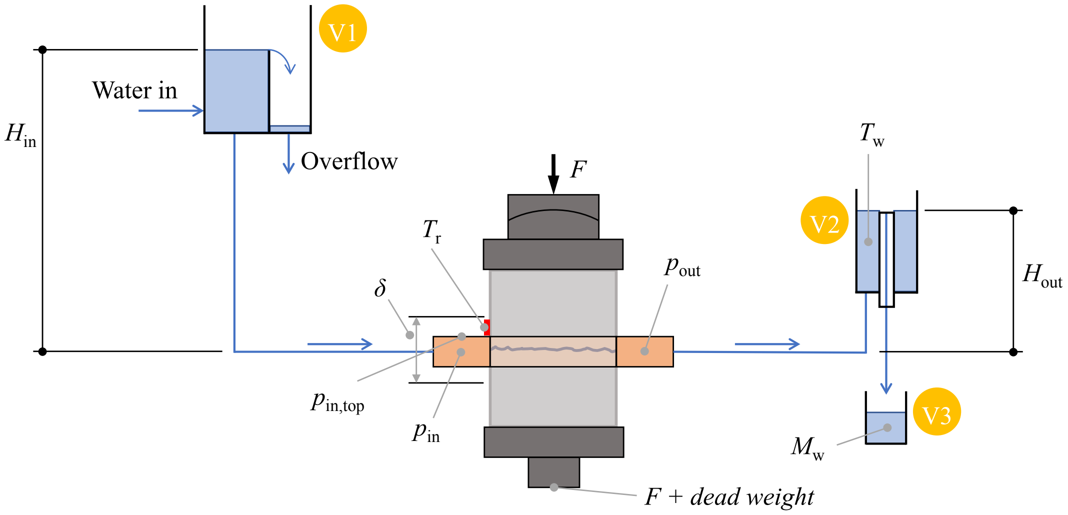

Figure 2 Test setup used to measure the transmissivity of rock fractures under normal loading.

Results

We experimentally derived the value of the transmissivity by setting the pressure different ($p_{out} - p_{in}$) and measuring the corresponding flow rate Q_w. The equivalent hydraulic fracture aperture a could be determined by resorting to the parallel-plate hydrogeological model (Singhal and Gupta, 2010). The results achieved in this campaign shed light on the transmissivity of natural rock fractures under sealed and opened conditions, and its dependency to the applied normal load at low to very-low flow rates. By way of example, Figure 3 shows a cross-section of the results obtained by the tests, highlighting the dependency of the fracture transmissivity to the applied normal stress.

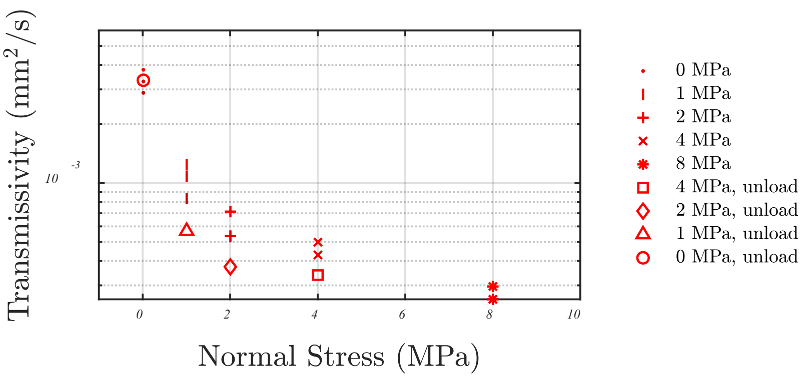

Figure 3 Transmissivity-stress diagram resulting from the tests performed in the direction 1-3 of the fracture, in its closed unperturbed state.

References

Jacobsson, L., Ivars, D.M., Kasani, H.A., Johansson, F., Lam, T., 2021: Experimental program on mechanical properties of large rock fractures, *IOP Conference Series: Earth and Environmental Science*. p. 012015. https://doi.org/10.1088/1755-1315/833/1/012015

Singhal, B.B.S., Gupta, R.P., 2010: Hydraulic Properties of Rocks, *Applied Hydrogeology of Fractured Rocks*. https://doi.org/10.1007/978-90-481-8799-7_8

Dominating hydrochemical processes in a coastal bedrock aquifer along the Baltic Sea

Roger B. Herbert

Department of Earth Sciences, Uppsala University, Uppsala, Sweden, roger.herbert@geo.uu.se

Summary. Saltwater intrusion is a risk in coastal regions in Sweden where groundwater extraction is intensive. In groundwater, increasing chloride concentrations and electric conductivity are common indicators that saltwater intrusion is occurring, while sodium concentrations may not increase at the same rate due to ion exchange processes. In this study, mixing, ion exchange, and calcium carbonate equilibrium are investigated as the primary hydrochemical processes controlling the chemical composition of groundwater in a bedrock aquifer used for drinking water by a coastal community on Väddö.

Background

The study site is a small coastal community on the island of Väddö on the Swedish east coast, approximately 90 km northeast from Stockholm. The community consists of 180 houses which are primarily used as summer residences, although a small fraction of the residents live permanently in the community. Drinking water is produced from groundwater and provided to the community from either private wells or from three community-operated well fields.

The bedrock geology of the area consists of metamorphic intrusive rock types of either dacite-rhyolite or granodiorite-granite composition; marble (containing calcium carbonate) occurs locally. The bedrock is generally covered with a thin layer (0–4 meters) of recent or calcium carbonate – rich glacial sediments. Recent sediments include peat deposits, while the glacial sediments consist of clay-rich glacial till and gravelly outwash sediments. All wells in the area obtain water from the bedrock aquifer.

For this investigation, groundwater data from private wells were voluntarily provided by residents in the community. Groundwater data from the community well fields were provided by the community water board. In all cases, chemical analyses were performed by accredited laboratories; water samples used in this study were sampled and analyzed within the past five years.

Methods

Hydrochemical facies and groundwater mixing were investigated by plotting groundwater and Baltic sea water chemistry data in a Piper diagram. The potential impact of ion exchange on groundwater composition was studies using a one-dimensional transport simulations with PHREEQC (Parkhurst & Appelo, 1999).

Results

Initial results indicate that groundwater composition in the coastal community lies along a mixing line between Ca-HCO_3 type water and Na-HCO_3 type water (see Figure 1). These facies are attributed to groundwater of more recent, surficial origin and deeper groundwater that is impacted by ion exchange processes, respectively. One-dimensional transport simulations with PHREEQC (Parkhurst & Appelo, 1999) suggest that the Na-HCO_3 groundwater is created by the freshing of the bedrock aquifer, where Ca^{2+} in recent groundwater replaces Na^{+} on cation exchange sites in deeper bedrock fractures. Groundwater extracted from depths of c. 90 m exhibit the presence of organic carbon (i.e. color), which supports the interpretation that groundwater from shallower depths is drawn into wells during extraction.

References

Parkhurst, D.L. & Appelo, C.A.J. 1999: User's guide to PHREEQC (version 2): a computer program for speciation, batch reaction, one-dimensional transport, and inverse geochemical calculations. Denver (CO): USGS; 1999. (Water-Resources Investigations; no. 99–4259).

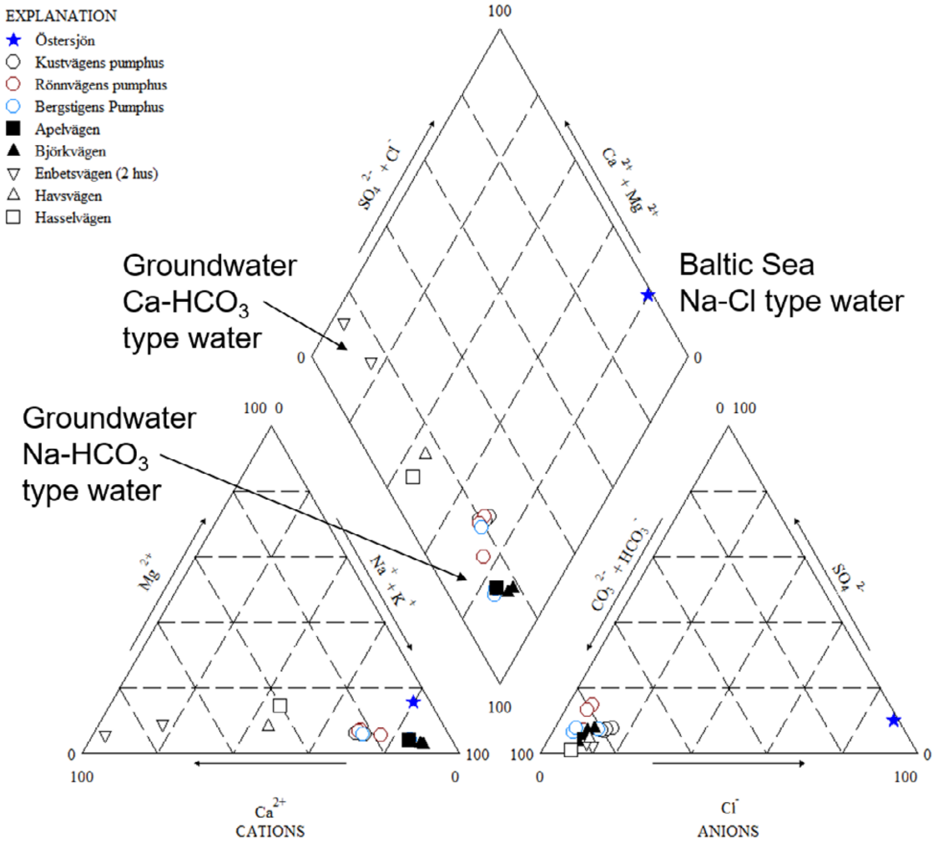

Figure 1. Piper diagram of hydrochemical facies in coastal aquifer

Understanding the flow path of reagents in groundwater remediation actions, by cross-borehole electrical monitoring

Léa Lévy[a], Aristeidis Nivorlis[a], Thue S. Bording[b], Rasmus Thalund-Hansen[c], Poul L. Bjerg[c], Torleif Dahlin[a], Anders Vest Christiansen[b]

[a]Engineering Geology Division, Lund University, Sweden, lea.levy@tg.lth.se; [b]Department of Geoscience, Aarhus University, Denmark, anders.vest@geo.au.dk; [c]Department of Environmental Engineering, Technical University of Denmark, rath@env.dtu.dk

Summary. In-situ remediation of contaminated groundwater relies on full contact between contaminant and reagent, to enable degradation of contamination plumes and hot spots. Adequate delivery of reagents in the whole target volume is a challenge. Monitoring the spatial distribution of injected reagents is important for decision-makers, to determine the need of more careful injection in some areas. We present here the lessons learnt from monitoring by electrical resistivity tomography (ERT) the injection of chemical reagents at three sites in Denmark and Sweden.

Introduction

Soil and groundwater contamination is a world-wide challenge related to different waste types: chlorinated solvents from dry cleaning, hydrocarbons spills, and pharmaceutical and plastic factories. In 2017, a total of 1.3 million and 2.8 million contaminated sites were estimated in the US and Europe, respectively (Pérez and Rodríguez, 2018). While excavation is an effective remediation technique, it generates waste in air and water and requires a large amount of resources (Søndergaard et al., 2018). In situ remediation technologies, involving strong chemical oxidants (Tsitonaki et al., 2010), enhanced bioremediation and bioaugmentation or micro-scale zero-valent-iron (ZVI) (Xin et al., 2015), to “treat” contamination hot spots or plumes have been under development for years.

Regardless of the injected reagent, adequate delivery in the target volume is a major challenge for *in-situ* remediation (Stroo and Ward, 2010). Electrical resistivity tomography (ERT) is well suited for providing spatial and temporal views of the chemical changes in groundwater.

Two strategies can be adopted for laying-out electrodes in an ERT survey: “surface ERT” where electrodes are located at the surface and cross-borehole ”XB-ERT”, where electrodes are inserted at deeper levels within dedicated boreholes. While surface ERT is less expensive and invasive, it has major limitations in terms of resolution and data quality, especially in urban areas. Data quality and spatial resolution can be significantly improved with XB-ERT (Daily and Ramirez, 1995, Madsen et al., 2021), but the operative costs remain high for private businesses.

Three study sites in Denmark and Sweden

Kærgård Plantation is one of the largest polluted sites in Denmark, with over 300,000 tons of pharmaceutical waste dumped in sand dunes in the 1960s. The geology consists of sand and gravel layers of high permeability and the remediation targets the contamination hot spots themselves. Chemical remediation is carried out by injection of peroxide activated persulfate.

The Farum site hosts a pilot scale experiment in a suburb of Copenhagen, where waste and spills from a packaging factory led to several groundwater contamination hotspots. The in-situ remediation there aims at creating a treatment zone intersecting the contaminant plume coming from the different hot spots. Injection of zero-valent-iron takes place in a fine-grained sandy aquifer of intermediate permeability. At these two Danish sites, monitoring was carried out by XB-ERT.

Alingsåstvätteriet is a former industrial-scale dry-cleaning facility located in Alingsås, Sweden. Leakage of minimum 200 litres of perchloroethylene into the ground was documented, while further spills are suspected. The geology mainly contains fine-grain materials in the most contaminated volume.

In-situ remediation was carried-out with direct push injections downstream of the source zone. Two different products were injected, to install two adjacent treatment zones. An autonomous ERT monitoring system was deployed, providing daily ERT data measuring 4 surface ERT and 2 XB-ERT layouts.

Visualization of the remediation cloud

Resistivity imaging by XB-ERT at the two Danish sites provides a dynamic image of the remediation cloud. At the Kærgård site, the cloud is composed of sulphate ions, and as a complex mixture of solid iron and aqueous species at the Farum site. Results allow assessing whether spreading takes place as expected or if limited spreading need to be addressed.

Despite some areas of limited spreading, overall successful spreading is observed in Kærgård. The treatment zone installation is more problematic in Farum: two injection rounds were attempted with different strategies and both led to heterogeneous spreading, as well as significant upstream leakage and surface spills. Based on time-lapse resistivity results, chemical monitoring, as well as solid iron analyses in core sediments, we suspect the creation of preferential pathways during injection at Farum, due to the viscosity of the product and the high pressure used for the injection.

The two reagents injected in Alingsås are composed of (i) a mixture of bacteria with a carbon source and iron particles (Provectus) and (ii) mostly iron particles (CAT100). Preliminary results from surface ERT monitoring during injection indicate a clear signal from CAT100 spreading, in the injection zone, as well as downstream a couple of months later. However, no clear sign of Provectus spreading is observed. Further analysis to assess reagent spreading with XB-ERT and chemical monitoring is on-going.

References

Daily, W. & Ramirez, A., 1995. Electrical resistance tomography during in-situ trichloroethylene remediation at the Savannah River Site, *Journal of Applied Geophysics,* 33**,** 239-249.

Madsen, L.M., Kühl, A.K., Levy, L. & Christiansen, A.V., 2021. Cross-Borehole ERT: Sensitivity, Model Resolution, and Field Data Quality, pp. 1-5European Association of Geoscientists & Engineers.

Pérez, A.P. & Rodríguez, E.N., 2018. Status of local soil contamination in Europe: Revision of the indicator “Progress in the management contaminated sites in Europe” Technical Report.

Søndergaard, G.L., Binning, P.J., Bondgaard, M. & Bjerg, P.L., 2018. Multi-criteria assessment tool for sustainability appraisal of remediation alternatives for a contaminated site, *Journal of Soils and Sediments,* 18**,** 3334-3348.

Stroo, H.F. & Ward, C.H., 2010. Future directions and research needs for chlorinated solvent plumes. *in In Situ Remediation of Chlorinated Solvent Plumes*, pp. 699-725Springer.

Tsitonaki, A., Petri, B., Crimi, M., Mosbæk, H., Siegrist, R.L. & Bjerg, P.L., 2010. In situ chemical oxidation of contaminated soil and groundwater using persulfate: a review, *Critical Reviews in Environmental Science and Technology,* 40**,** 55-91.

Xin, J., Zheng, X., Han, J., Shao, H. & Kolditz, O., 2015. Remediation of trichloroethylene by xanthan gum-coated microscale zero valent iron (XG-mZVI) in groundwater: effects of geochemical constituents, *Chemical Engineering Journal,* 271**,** 164-172.

Geophysical mapping of aquifer properties in infrastructure projects using DCIP and MRS

T. Martin[a], M. A. Kass[b], G. Fiandaca[c], D. Grombacher[b], C. Butron[d], J. Bjergsted Pedersen[b], M. Griffiths[b], M. Østbjerg Vang[b], S. Rejkjær[a], A. Mendoza[a], T. Dahlin[a]

[a]Engineering Geology, Lund University, Lund, Sweden, tina.martin@tg.lth.se; [b]Geoscience Department, Aarhus University, Aarhus; [c]Department of Earth Sciences, University of Milano, Milano, Italy; [d]Trafikverket – Swedish Transport Administration, Sweden

Summary. There is a need for improved methods for evaluating groundwater conditions in infrastructure projects. This includes advanced approaches to map hydraulic properties in both 2D and 3D. This work presents the use of two geophysical methods for both permeability and water content determination at three test sites. These methods are Direct Current resistivity and Induced Polarization, DCIP (permeability) and Magnetic Resonance Sounding, MRS (water content). The results indicate improvements in these applications.

Introduction

Mapping aquifer properties is needed to protect groundwater resources and avoid structural and environmental problems in infrastructure projects. Determining the hydrogeological properties in an aquifer usually involves drilling and hydraulic tests which are reliable but expensive and, in many cases give point-scale information. The use of geophysical methods can help to reduce drillings and costs while providing continuous information. The Induced Polarization (hereafter Direct Current resistivity and time-domain Induced Polarization, DCIP) can give information about the permeability and thus about the hydraulic conductivity (Revil et al. 2012, Weller et al. 2015). In addition, Magnetic Resonance Sounding (MRS) can provide water content information and pore size characteristics and therewith be related to the intrinsic permeability and the hydraulic conductivity (Schirov et al. 1991). By combining both methods in a two- or three-dimensional approach, an elaborated interpretation of the subsurface is possible. We have applied these methods in three different sites in Sweden, which were chosen based on their different geological settings and electromagnetic noise levels.

Test sites and measurements

Site 1 and 2 are located close to Svedala and Mariestad, respectively. At these sites several DCIP profiles were measured using an ABEM Terrameter LS2 and later a number of MRS soundings were conducted with the Apsu system (Larsen et al. 2020). The electromagnetic noise level was higher at site 2 compared to site 1. A third site selected for having low noise level was surveyed subsequently.

The data processing and inversion is done in different subsequent steps. For the DCIP data, a processing according to Olsson et al. (2016) was done before it was manually controlled. The inversion was then conducted based on the inversion routine by Fiandaca et al. (2021). The MRS data were acquired using a steady-state acquisition scheme (Grombacher et al. 2021). Data were subsequently inverted for water content and relaxation parameters related to grain size distribution.

Results and discussion

The DCIP data quality is good with varying resistivity in the different layers. The chargeability values are usually quite small in all profiles. In Figure 1, an example of a DCIP profile in Mariestad, the conductivities on top are characterized by high values whereas at depth the conductivity decreases. That can be related to clay lying above a sandy till. The known hydraulic conductivity value from that profile (in the middle of the profile) is 2×10^{-5} m/s, in agreement with the inverted K-value (10^{-4}–10^{-5} m/s).

The MRS data reveals mostly low water content at test site 1. At test site 2 elevated noise was present which affected the MRS data quality considerably. At test site 3, high-quality data were acquired coincident with the DCIP data with high lateral resolution along 4 lines.

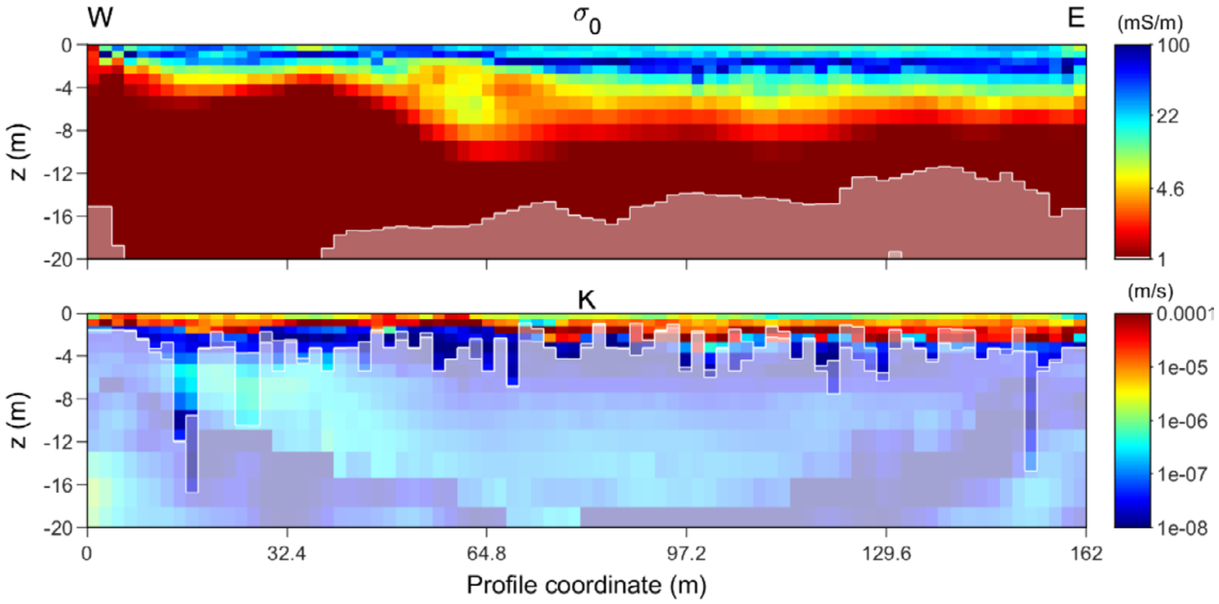

Figure 1. DCIP Inversion results for one profile at site 2, Mariestad. The data is inverted for the electrical conductivity (σ_0) with a known fluid conductivity (σ_w) of 140 mS/cm.

Conclusions and outlook

The DCIP measurement at all test sites shows some layered subsurface with varying resistivities. The IP signal response is quite small but for some profiles significant. The MRS data quality varies throughout the test sites. While the Mariestad site had too high noise level for accurate interpretation, at the third site it provided excellent data quality and laterally varying water content levels as high as >40% in some locations.

The first correlation of the DCIP measurements with known hydraulic conductivity values are promising but further analysis and interpretation is needed. The next steps in the project include finalising the processing and inversion and interpreting the results from both methods. Subsequently, the data will be compared with available hydrogeological information. Additionally, hydraulic tests and laboratory measurements on collected samples will be made.

Acknowledgment

This research project is funded by Trafikverket, the Swedish transport authority (grant number: 2020/122405).

References

Fiandaca G., Meldgaard Madsen L., Olmo M., Römhild L., Maurya P.K., 2021: Inversion of hydraulic conductivity from Induced Polarisation, Part A: methodology and verification. Near Surface Geoscience 2021-27th European Meeting of Environmental and Engineering Geophysics, 1-4.

Grombacher, D., Liu, L., Griffiths, M.P., Vang, M.Ø., & Larsen, J.J. 2021: Steady-state surface NMR for mapping of groundwater, Geophysical Research Letters, 48(23), 9p.

Larsen, J.J., Liu, L., Grombacher, D., Osterman, G., & Auken, E., 2020: Apsu—A new compact surface nuclear magnetic resonance system for groundwater investigation, Geophysics, 85(2), JM1-JM11.

Olsson P.-I., Fiandaca G., Larsen J.J., Dahlin T. & Auken E., 2016: Doubling the spectrum of time-domain induced polarization by harmonic de-noising, drift correction, spike removal, tapered gating and data uncertainty estimation, Geophys. J. Int., 207 (2), 774-784. 10.1093/gji/ggw260

Revil, A., Koch, K., & Holliger, K., 2012: Is it the grain size or the characteristic pore size that controls the induced polarization relaxation time of clean sands and sandstones? Water Resources Research, 48(5).

Schirov M., Legchenko, A., & Creer, G., 1991: A new direct non-invasive groundwater detection technology for Australia. Exploration Geophysics, 22(2), 333-338.

Weller, A., Slater, L., Binley, A., Nordsiek, S., & Xu, S., 2015: Permeability prediction based on induced polarization: Insights from measurements on sandstone and unconsolidated samples spanning a wide permeability range. Geophysics, 80(2), D161–D173.

Contaminants as Tracers of Complex Groundwater Flow Systems: Insights from Field Research

Beth L. Parker

Groundwater Research Institute, University of Guelph, Canada, bparker@uoguelph.ca
and Tage Erlander Visiting Professor, Lund University, Sweden

Summary. Groundwater is a key yet poorly understood component of the hydrologic cycle, and our understanding of this resource is dependent on our ability to resolve spatial and temporal variability in hydrogeological systems. By improving our knowledge of groundwater flow systems through advanced monitoring and characterization methods, we are better equipped to predict groundwater availability, flow paths, residence times and the transport of nutrients and contaminants.

Groundwater – making the invisible visible

Because groundwater is out of sight, it is poorly understood and often mismanaged. Overpumping of groundwater and depletion of aquifers causes several direct and indirect consequences such as land subsidence, sea level rise, reduced river baseflow, changing groundwater quality and soil salinization. Furthermore, we have indiscriminately spilled and dumped wastes and chemicals on and in the ground expecting the groundwater system to degrade or purify these contaminants over time, without concern for limits.

The United Nations has declared 2022 the year of groundwater: making the invisible visible. In keeping with this mission, I aim to show how our understanding of groundwater as a valuable resource depends on higher vertical resolution characterization and monitoring methods, using multiple tools and methods from across the geoscience disciplines. This is warranted because hydrogeological systems are complex, both spatially and temporally; enhanced knowledge of groundwater flow systems can improve prediction of groundwater availability, flow paths, residence times and transport of nutrients and contaminants toward surface water or water well receptors.

The time is now for developing a deeper understanding of our groundwater resources using modern technologies with a commitment to do so sooner rather than later. Groundwater, as a key component of the hydrologic cycle, is a vital resource for sustaining life and providing resilience to changes in climate. Addressing current and future challenges will require a more robust approach to groundwater flow system monitoring tailored to the local geologic conditions.

Hydrogeological applications within SKB's programme for a spent nuclear fuel repository

Jan-Olof Selroos[a,b], Sven Follin[a,c]

[a]SKB, Box 3091, 169 03 Solna, Sweden, jan-olof.selroos@skb.se; [b]Department of Sustainable Development, Environmental Science and Engineering, KTH, Stockholm, Swedenl; [c]SF GeoLogic, Danderyd, Sweden, sf@geologic.nu;

Summary. In this presentation, we highlight the site-descriptive and safety assessment modelling in the field of hydrogeology performed within the programme of the Swedish Nuclear Fuel and Waste Management Company (SKB). We describe what the hydrogeological site-descriptive modelling entails, and how it relates to other scientific disciplines within the integrated site-descriptive modelling. Also, we provide a number of exemples of hydrogeological applications related to performance and safety assessments.

Hydrogeology is a key discipline both in the site investigations and site-descriptive modelling of a potential repository site, as well as in a number of modelling applications such as in the safety assessment of the planned repository. The Swedish Nuclear Fuel and Waste Management Company (SKB) has performed site investigations at both the Forsmark site in the municipality of Östhammar, and at the Laxemar site in the municipality of Oskarshamn (SKB, 2008; 2009). In this talk, we will provide an overview of the site-descriptive modelling performed, and provide examples of a number of performed and planned hydrogeological modelling applications.

While the scientific discipline bedrock geology, and most notably structural geology, provides the structural backbone to the hydrogeological discipline, hydrogeology itself is a central discipline in the integrated site-descriptive modelling due to the control of groundwater flow on both hydro-geochemistry and on transport of solutes. The aim of the the hydrogeological site-descriptive model is thus twofold: first, it is a means to, in a comprehensive and internally consistent manner, explain the hydrogeological data measured; second, it is a means to, in an integrative and consistent manner, simultaneoulsy explain data from several scientific disciplines. The various disciplines and their interactions are shown in the figure below.

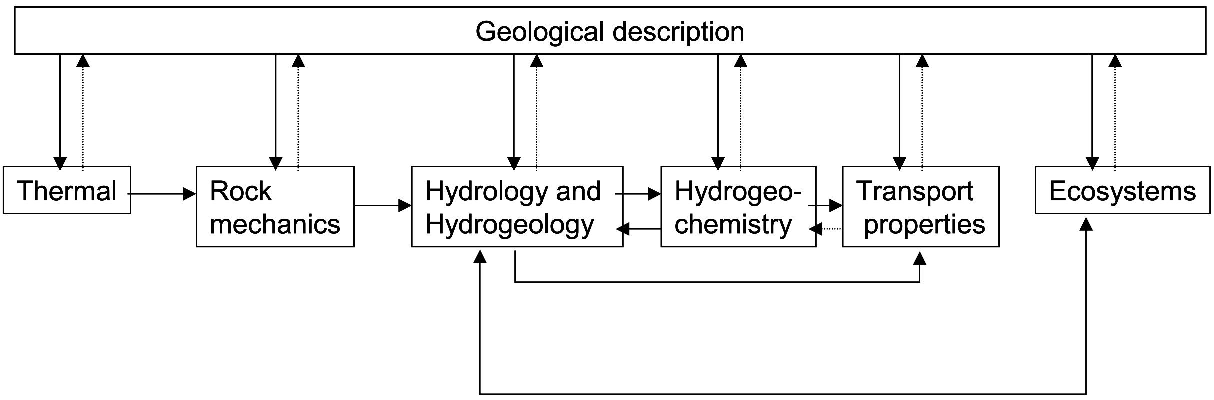

Figure. The scientific disciplines in the site-descriptive model and their interdependencies.

The integrated site-descriptive model and the individual discipline-specific models, such as the hydrogeological site-descriptive model, serve the purpose of "explaining" the site, and as such also provide improved confidence in the subsequent applications. The main hydrogeological modelling applications are: i) environmental impact assessment of primarily the surface system during construction and operation of the repository, ii) water management assessment in the tunnel system during construction and operation, iii) post-closure assessment of the hydrogeological (and hydrogeochemical) evolution in the 1 Myear regulatory time frame, and iv) calculation of transport both to and from the repository.

The former includes substances detrimental to the longevity of the engineered barriers, while the latter concerns transport of radionuclides from a potentially breached waste container.

In the talk, we will provide examples of some modelling studies from the most recently approved license application of a spent fuel repository in Forsmark (Selroos & Follin 2009; SKB 2011). Also, we will provide examples of currently on-going modelling methodology development to be used in future studies.

References

Selroos, J-O & Follin, S., 2010: SR-Site groundwater flow modelling methodology, setup and results. *SKB R-09-22*, Svensk Kärnbränslehantering AB, Stockholm.

SKB, 2008: Site description of Forsmark at completion of the site investigation phase: SDM-Site Forsmark. *SKB TR-08-05*, Svensk Kärnbränslehantering AB, Stockholm.

SKB, 2009: Site description of Laxemar at completion of the site investigation phase. SDM-Site Laxemar. *SKB TR-09-01*, Svensk Kärnbränslehantering AB, Stockholm.

SKB, 2011: Long-term safety for the final repository for spent nuclear fuel at Forsmark. Main report of the SR-Site project. *SKB TR-11-01*, Svensk Kärnbränslehantering AB, Stockholm.

Thematic Session 5
Geochemistry

Session Chairs:
Anna Ladenberger (anna.ladenberger@sgu.se)
Anna Neubeck (anna.neubeck@geo.uu.se)

Geochemical signature and environmental implications of waste from burning black shale in Västergötland, Sweden

Lisa Blomskog[a], Anna Ladenberger[b], Iain Pitcairn[a], George A. Morris[b], Merita Murtola[b]

[a]Department of Geological sciences, Stockholm University, Stockholm, Sweden, lisa.blomskog@gmail.com;
[b]Department of Mineral Resources, Geological Survey of Sweden, Uppsala, Sweden, anna.ladenberger@sgu.se

Summary. The historical waste after burning of alum shale in Västergötland originates from black shale processing to produce lime, crude oil and uranium. It occurs in many locations in Västergötland, including urban, recreational, agricultural and forested areas. The waste shows variable degrees of high temperature processing and lime contamination, which result in modification of its original composition. Due to high metal contents in the original black shale, the waste presents a potential environmental risk via leaching and weathering processes, especially for the quality of soil and groundwater.

Historical waste in Västergötland

Burnt alum shale waste (*rödfyr* in Swedish) is the residual waste product after alum (black) shale has been burned. The black shale source rock belongs to the Alum Shale Formation that was deposited in a marine environment in the Late Cambrian to Early Ordovician and occurs from Finnmark in Northern Norway to Skåne in southern Sweden (Andersson et al. 1985). The Alum Shale Formation has been of economic interest for hundreds of years, and black shale has been mined for alum salt, oil, and uranium, as well as used as fuel source in lime production. Alum was produced in, for example, Latorp (Närke) from 1773–1878. When it was found in the 1800's that alum shale would burn on its own, shale gradually replaced the wood in the quicklime kilns in lime production. Interest in extracting oil from the alum shale started as early as 1873, with the most productive period between 1940–1969. The three areas that were subject to oil extraction (with at least 4% oil content) are Kinnekulle, Kvarn-

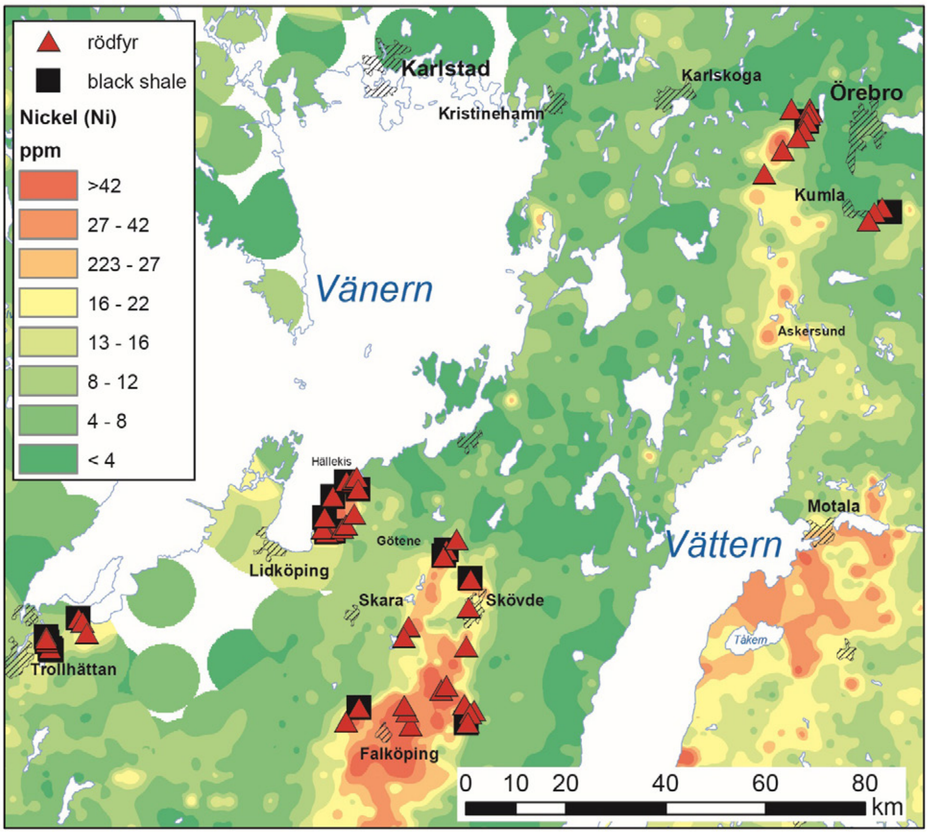

Fig.1. Map with the sites of collected burnt shale and black shale. The background: Ni geochemical map for till (SGU digital database, method: 7M HNO_3 leach by ICP MS).

torp and few localities west of Örebro. High uranium concentrations were found in the kolm lenses in the alum shales as early as 1893 by Nordenskiöd, but it was after World War II when exploration and mining was successful. Uranium was processed through the mill at Ranstad from 1965–1969. Waste from each of these industries can be found in large volumes throughout Västra Götaland. The largest of these heaps is c. 100 m high and covers an area of 450,000 m^2. In 2014 the County Administrative Board of Västra Götaland reported sixty-five burnt shale waste heaps in the county which are now registered in the national database of contaminated sites. In September 2021, 59 samples have been taken in Västra Götalands Län and Örebro Län (Fig. 1). The focus of this study is on the characterisation of the chemistry of burnt alum shale waste and its potential impact on the local environment.

Geochemical signature of burnt shale and environmental implications

Industrial processing of the black shale results in modifications of the primary chemical composition in the waste product. The first consequence of burning alum shale is the loss of volatile elements (e.g. Hg, Se) and removal of organic matter and sulphur. Secondary iron oxidation tends to result in slight enrichment in Fe in the waste products. Calcium (magnesium and strontium) higher content in the waste can be explained by contamination from the lime production (Fig. 2). As a result of iron oxidation the original black colour of the shale changes into orange-red in the waste. High temperatures remobilise the silica and the waste contains up to 30% higher SiO_2 content than original rock, which results in new physical properties of the material which is more 'baked', hard and consolidated. Most of the trace elements, including rare earth elements (REE) and other critical elements are relatively enriched (concentrated) in the waste products, while arsenic, bismuth and tellurium have higher concentrations in unburnt black shale. The environmental risks related to aerial exposure of the waste are mainly related to the degree of enrichment of individual waste piles and the degree of thermal processing, i.e. the higher burning temperature results in more resistant waste to weathering and decomposition. The evaulation of risks related to leaching of potentially toxic elements into soil and groundwater can be furthered compared to the natural geochemical baseline constrained from the till regional mapping carried out by SGU (Fig. 1).

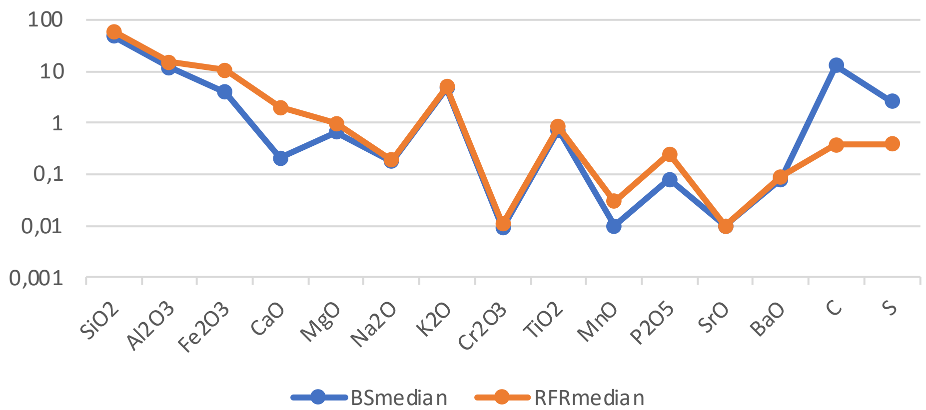

Fig.2. Diagram comparing median concentrations of major elements, C and S (total concentrations) in the source black shale (n=19) and corresponding burnt shale. BS: black shale, RFR: burnt shale (sw. rödfyr). Unit: %.

References

Andersson, A., Dahlman, B., Gee, D. G. & Snäll, S. (1985). The Scandinavian Alum Shale. In *Sveriges Geologiska Undersökning* Vol. 56, pp. 1–50.

Nickel isotope fractionation during iron oxide formation

Madeleine S. Bohlin[a], Christoffer Hemmingsson[a,b], Dilan Ratnayake[c], Ryoji Tanaka[c], Eizo Nakamura[c], Anna Neubeck[a]

[a]Department of Earth Sciences, Uppsala University, Uppsala, Sweden, madeleine.bohlin@geo.uu.se, chris.hemmingsson@gmail.com, anna.neubeck@geo.uu.se; [b]Department of Earth Sciences, Stockholm University, Stockholm, Sweden; [c]Institute for Planetary Materials, Okayama University, Misasa, Japan, dilanrath@s.okayama-u.ac.jp, ryoji@okayama-u.ac.jp, eizonak@misasa.okayama-u.ac.jp

Summary. Nickel (Ni), being a transition metal involved in the major marine redox cycles, as well as being a vital micronutrient has enormous potential as a biogeochemical tracer. This work aims to constrain fundamental Ni isotopic fractionation mechanisms and pathways during the formation of ferrihydrite, one of the most ubiquitous iron oxides on Earth.

Introduction

The isotopic composition of nickel (Ni) in natural samples has great potential as a biogeochemical tracer. Ni is a transition metal involved in the major marine redox cycles and is also a vital micronutrient used by both marine and terrestrial organisms. Biological uptake of Ni is associated with a large isotopic fractionation as organisms preferentially retain the lighter Ni isotopes. Laboratory-grown methanogenic archaea are <1.5‰ (average of 0.7‰) lighter in their Ni isotopic composition relative to their growth medium (Cameron et al. 2009). This is considerably lighter than most terrestrial rocks which have an average composition of ~+0.15‰ (Cameron et al. 2009). This offset has sparked an interest in developing the Ni isotopic system as a biomarker to trace the evolution of the earliest life on Earth as well as in the search for extra-terrestrial life. The biogeochemical cycling of Ni is however strongly dependant on abiotic chemical reactions involving metal-oxides, primarily those of iron (Fe) and manganese (Mn) which are ubiquitous in both the terrestrial and marine environment. Previous experimental work has shown limited isotopic fractionation of Ni during iron oxide formation with solids being ~0.3‰ lighter than the experimental fluids (e.g. Wasylenki et al. 2015, Wang & Wasylenki, 2017). However, these experiments were conducted in simple, low-ionic strength solutions containing only Fe and Ni. In order to reliably use Ni isotopes a biomarker, the uniqueness of the isotopically light biogenic compositions need to be tested.

Ferrihydrite experiments

This work focuses on the Ni isotope fractionation associated with the formation of ferrihydrite, a poorly crystalline Fe-oxide precursor to the more evolved hematite and magnetite. The ferrihydrite was synthesised in high-ionic strength solutions with seawater salinity through a combination of adsorption and co-precipitation experiments yielding 125 unique experimental conditions. Focus was put on Ni incorporation mechanism (adsorption and/or incorporation into the crystal structure), varying Ni concentrations, pH, equilibration time and varying silicon (Si) concentrations. The effects of Si on the chemical behaviour of Ni is of great interest as the Earth's early oceans may have had dissolved Si concentrations reaching 2.2 mM (Konhauser et al. 2009), more than 30 times that of the present-day average of ~70 µM (Tréguer et al. 1995). Further, much of the work on the earliest life on Earth has involved microbial structures found in Si-rich hydrothermal vent deposits (e.g. Djokic et al. 2017), and the search for extra-terrestrial life has found compelling Earth-analogues in similarly Si-rich hydrothermal sinter deposits on Mars (Ruff & Farmer, 2016). If Ni isotopes are to be used as a biomarker in the absence of organic structures, the effects of Si on the isotopic fractionation behaviour of Ni needs to be systematically tested and constrained.

Results and implications

The addition of Si in our experiments systematically decreases the amount of Ni that is sorbed to the ferrihydrite, supporting the hypothesis that Si either outcompetes Ni to sorption sites and/or changes the overall charge balance of the nanocrystals (Konhauser et al. 2009). Co-precipitation leads to higher incorporation of Ni for any given Ni and Si concentration, compared to pure adsorption which is also more sensitive to the addition of Si. The difference between the sorption mechanisms is also seen in the isotopic compositions. Co-precipitated ferrihydrites in high-Si solutions have indistinguishable isotopic compositions to those where Si is not present, similarly to what was found in a recent study by Neubeck et al. (2021). During adsorption however, the isotopic fractionation is greatly increased with solids being <0.8‰ lighter than the experimental solution (Figure 1). These results show that abiotic fractionation of Ni isotopes may start to overlap with the suggested biological fingerprint when Ni is adsorbed to ferrihydrite in solutions containing dissolved silicon (Si). This has implications for reconstructing past seawater compositions on Earth when Si concentrations fluctuated and were much higher than in the modern ocean.

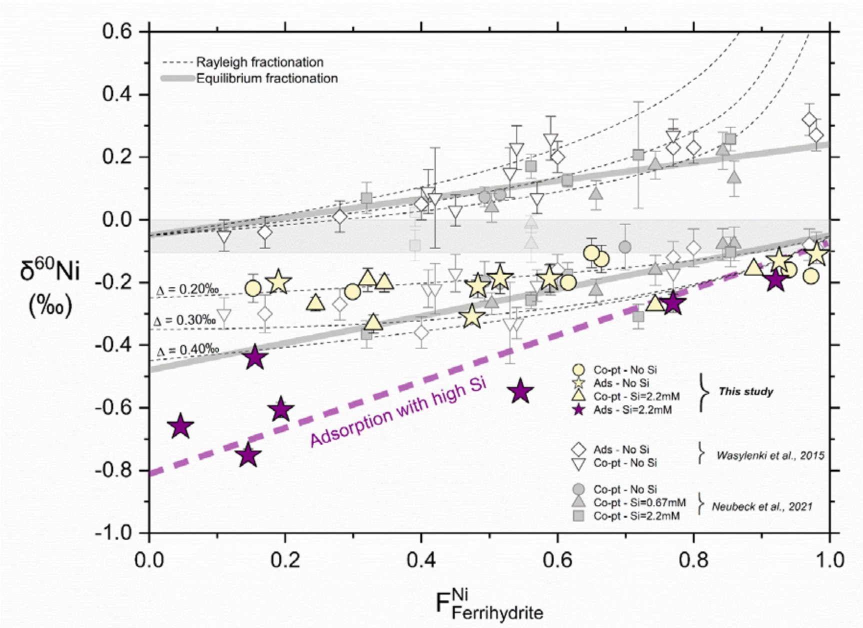

Figure 1. Ni isotopic composition ($\delta^{60}Ni$) against fraction of Ni sorbed to Ferrihydrite ($F^{Ni}_{Ferrihydrite}$). While the presence of Si in the experimental solution does not appear to affect Ni in co-precipitated ferrihydrite solids (yellow triangles), it has a large effect on the surface adsorbed Ni (purple stars). Reference data in grey from Wasylenki et al. (2015) and Neubeck et al. (2021). Ni isotopes analysed following Ratnayake et al. 2022.

References

Cameron, V., Vance, D., Archer, C. & House, C. H., 2009: A biomarker based on the stable isotopes of nickel. *Proceedings of the National Academy of Sciences 106*, 10944-10948.

Djokic, T., Van Kranendonk, M. J., Campbell, K. A., Walter, M. R., & Ward, C. R., 2017. Earliest signs of life on land preserved in ca. 3.5 Ga hot spring deposits. *Nature Communications 8*, 15263

Konhauser, K. O., Pecoits, E., Lalonde, S. V., Papineau, D., Nisbet, E. G., Barley, M. E., Arndt, N. T., Zahnle, K. & Kamber, B., 2009. Oceanic nickel depletion and a methanogen famine before the Great Oxidation Event, *Nature 458*, 750-754

Neubeck, A., Hemmingsson, C., Boosman, A., Rouxel, O. & Bohlin, M., 2021. Ni isotope fractionation during coprecipitation of Fe(III)(oxyhydr)oxides in Si solutions. *Geochemistry 81*, 125714

Ratnayake, D.M., Tanaka, R. & Nakamura, E., 2022. Novel nickel isolation procedure for a wide range of sample matrices without using dimethylglyoxime for isotope measurements using MC-ICP-MS. *Analytica Chimica Acta 1181,* 338934

Ruff, S. W., & Farmer, J. D., 2016. Silica deposits on Mars with features resembling hot spring biosignatures at El Tatio in Chile, *Nature Communications 7*, 13554

Tréguer, P., Nelson, D.M., Van Bennekom, A.J., DeMaster, D.J., Leynaert, A. & Quéguiner, B., 1995. The silica balance in the world ocean: a reestimate. *Science 268*, 375-379

Wasylenki, L. E., Howe, H., D., Spivak-Birndorf, L. J. & Bish, D. L., 2015. Ni isotope fractionation during sorption to ferrihydrite: Implications for Ni in banded iron formations, *Chemical Geology 400,* 56-64

Wang, S-J. & Wasylenki, L. E., 2017. Experimental constraints on reconstruction of Archean seawater Ni isotopic composition from banded iron formations, *Geochimica et Cosmochimica Acta 206*, 137-150

Differences in the mineralogy and geochemical composition of oxidized and waterlogged acid sulphate soils in northern Sweden

Federico Alvarellos, Sarah Conrad, Lena Alakangas

Department of Civil, Environmental and Natural Resources Engineering, Luleå University of Technology, Luleå, Sweden, federico.alvarellos@ltu.se.

Summary. The mineralogical distribution and the geochemical composition of acid sulphate soils (ASS) in northern Sweden varies widely. The aim of this study is to describe and interpret the mineralogy and distribution of chemical elements in ASS. Therefore, sampling was performed on oxidized and waterlogged soil profiles for their subsequent geochemical analysis. The results show dependence between pyrite varieties and its oxidation products as indicator of the environmental conditions that generate different types of ASS.

Introduction and methodology

Acid sulphate soils (ASS) are a common feature along Swedish coastlines with the potential to cause significant negative environmental and economic impacts. When sulphide-rich sediments get exposed to oxygen, their pH value drops below 4, sulphuric acid is generated, causing leaching of harmful elements and precipitation of new minerals (Cook et al.,2000). One of the most abundant sulphide minerals in these soils is pyrite. Activities that exaggerate the oxidation include deforestation, drying of wetlands, agricultural practices such as ditching, and construction of buildings, roads, and railways, which lower the groundwater level and expose the soils to the atmospheric oxygen (D.L. Dent, L.J. Pons, 1995).

We present the mineralogy and the distribution of the chemical elements (Raman spectroscopy, SEM-EDS, ICP-SFMS and XRD) of one oxidized and one waterlogged soil profile at four different sampling sites near Luleå in northern Sweden (Gunnarsson, 2018). The profiles are divided into three different zones depending on the degree of oxidation (oxidation, transition, and reduction zone).

Results and discussion

The results suggest that fluctuations in the groundwater table generate variations in the zone's thicknesses. A permanently lowered groundwater table results in a thicker oxidation zone compared to the transition zone. The waterlogged profiles with varying groundwater levels show opposite results with thinner oxidation zones compared to the transition zone. Iron and sulphur concentrations in all profiles range between 2.5 to 5% (±4.1%) and 0.1 to 2.3% (±1%), respectively, with the highest concentrations in the transition and reduction zones. The chemical distribution of iron and sulphur over the profiles is consistent with the scanning electron microscope (SEM) images which show framboidal (and cubic) pyrite as the most abundant sulphide mineral in the different zones (Figure 1).

The pH varies in the profiles (from 2.87 to 8.49), presenting its highest values in the waterlogged profiles, and increases with depth keeping the framboidal pyrite intact.

The SEM images of the waterlogged and oxidized soil profiles showed a variety of other minerals in the different zones. Oxidation zones contain mainly sulphates and iron oxides. Jarosite, formed as a product of the pyrite oxidation, is found only in the oxidation zone of one of the oxidized profiles. Barite appears frequently in different zones and its precipitation could be due variations in redox conditions combined with the introduction of saline groundwater resulting from fluctuating groundwater levels. (Stoops and Zavaleta, 1978; Carson et al. 1982). Silicates are inferred to be the main source of Ba. In the reduction and transition zones, iron sulphides (pyrite and monosulphides) dominate, although various sulphates and iron oxides were recognized. The identified silicates (mainly quartz and albite) reflect a parent material composition associated with the granitic bedrock.

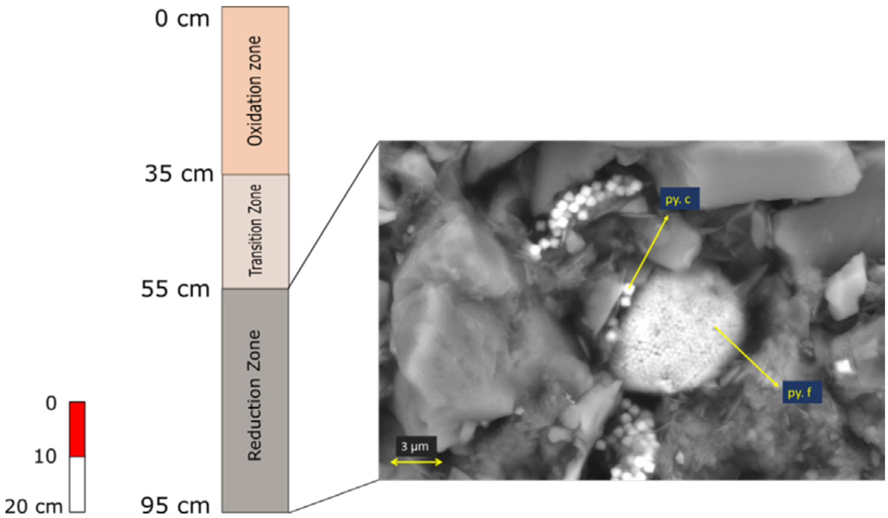

Figure 1. SEM image of framboidal and cubic pyrites (py.f and py.c) found in the reduction zone of a waterlogged profile, Luleå, northern Sweden.

Further, the SEM images suggest variations in appearance of organic matter (OM) in the different profiles. Profiles with higher signs of oxidation showed comparably less OM, in form of decomposition of leaves and roots, whereas the less oxidized profiles, showed more OM mixed into the soil matrix. This feature may help to explain how the organic matter content influences the oxidation processes.

In the future, comparing the chemical elements distribution and the mineralogy of ASS in other areas in northern Sweden (e.g. Skellefteå) would be recommended to increase the understanding of soil geochemistry and thus create a model that allows us to recognize and reduce potential risks to the environment generated by ASS. The variety in size distribution of identified framboidal forms of pyrite requires a detailed mineralogical and geochemical analysis to gain insight into their formation processes and how they are related to the oxidation processes that occur in ASS.

References

Carson, C.D., Fanning, D.S., and Dixon, C.J., 1982, Alfisols and Ultisols with acid sulfate weathering features in Texas, in Kittrick, J.A., ed., Acid Sulfate Weathering: Madison, WI, *Soil Science Society of America*, p. 127-146.

Cook, F.J., Hicks, W., Gardner, E.A., Carlin, G.D., Froggatt, D.W., 2000. Export of acidity in drainage water from acid sulphate soils. *Mar. Pollut. Bull*. 41, 319–326.

Dent, D.L., Pons. L.J. 1995. A world perspective on acid sulphate soils. UK, Netherland: *ELSEVIER*.

Gunnarsson, N. 2018. Mineralogical speciation of sulfur in acid sulfate soils from Luleå, Sweden. Natural Resources Engineering. Luleå University of Technology.

Stoops, G., and Zavaleta, A., 1978, Micromorphological evidence of barite neoformation in soils: *Geoderma*, v. 20, no. 1, p. 63-70.

Determination of phosphorus speciation in soil by XANES spectroscopy – strengths, weaknesses and comparison with other methods

Jon Petter Gustafsson[a], J.R. Marius Tuyishime[a], Gbotemi A. Adediran[b], Stephen Hillier[c]

[a]Department of Soil and Environment, Swedish University of Agricultural Sciences, Uppsala, Sweden, jon-petter.gustafsson@slu.se; [b]UK Centre for Ecology and Hydrology, Wallingford, UK, GboAde@ceh.ac.uk; [c]James Hutton Institute, Craigiebuckler, Aberdeen, UK, Stephen.Hillier@hutton.ac.uk

Summary. Here we summarize results from a number of research projects at SLU dealing with soil phosphorus speciation using XANES spectroscopy. The results show that P of the upper 50 cm of the mineral soil is dominated by Fe- and Al-bound P, where Al-bound P is the most common form. In the subsoil apatite dominates. Organic P is found in the surface layer. XANES-derived Ca-bound P is related to the Ca-bound P obtained by Hedley extraction, while the sum of Fe- and Al-bound P is well represented by oxalate-extractable P. The results help us to understand how P has transformed during soil formation.

Phosphorus is an important nutrient in soils. In agricultural soils, fertilizer P has to be applied to compensate for the removal P that occurs during harvest. This is not usually done in forest soils, which experience a slow P loss due to harvest removal. In addition, if any P is leached, this contributes to eutrophication of surface waters. For these reasons it is important to obtain more understanding of P transformations and speciation in soils. Synchrotron-based P K-edge XANES spectroscopy is one of the few direct methods to study P speciation. The XANES spectra obtained are then interpreted using linear combination fitting with known standards, revealing the combination of species present in the sample. Here we show results for eleven Swedish soil profiles and compare them with other more traditional methods based on various extractions and on X-ray powder diffraction. Most of the XANES data have previously been shown elsewhere (Eriksson et al., 2016; Schmieder et al., 2018; Schmieder et al., 2020; Tuyishime et al., 2022), although they were critically examined and in some cases updated for this work.

The P K-edge XANES results show a consistent picture of the P transformations that have taken place during postglacial soil formation, in which apatite, which often still dominates in the subsoil, is weathered. The released P has been adsorbed to ferrihydrite and imogolite, and transformed to organic P in the surface layer. In the upper 20–30 cm of the soil, apatite is generally completely dissolved or at least nearly so. The exact distribution of P species vary from soil to soil. As an example of the results obtained, Fig. 1 shows the XANES distribution of P species at Skogaby, SW Sweden (from Tuyishime et al. 2022).

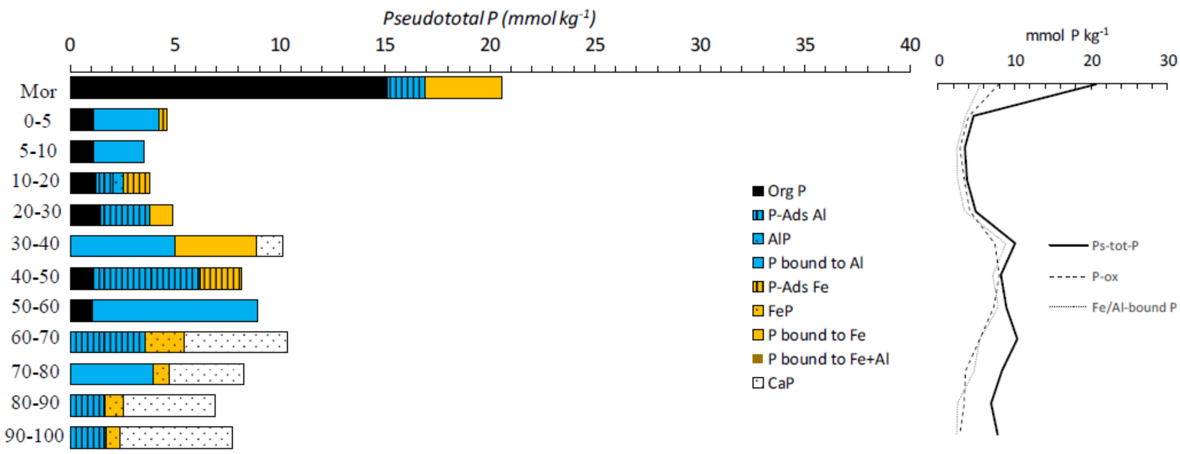

Fig. 1. Distribution of P species as found by XANES spectroscopy (left), and Fe+Al-bound P compared to oxalate-extractable P and total P (right) at Skogaby, SW Sweden.

A strength of the XANES method is that the speciation can be determined directly on undisturbed samples and that a distinction can be made between Fe- and Al-bound P, while a weakness is that it is usually not possible to determine individual species within a compound group, e.g. the method allows for identification and quantification of Ca-bound P in a soil sample, but not for more specific Ca-P species such as hydroxy- or fluorapatite. Best practices for XANES data interpretation with the linear combination fitting method have been summarized by Gustafsson et al. (2020).

As it is not possible to use synchrotron-based XANES spectroscopy for routine analysis, it is of interest to compare commonly used extraction methods to see if they provide the same, or similar, results. Our data show that: (i) oxalate-extractable P usually gives a very good description of the sum of Fe- and Al-bound P (see e.g. Fig. 1), (ii) Ca-bound P according to the Hedley extraction scheme agrees rather well with Ca-bound P from XANES ($r^2 = 0.69$ for a subset of 20 samples), and (iii) apatite as determined by X-ray powder diffraction is less precise as an estimate of Ca-bound P ($r^2 = 0.26$ when compared to XANES results, but can still be considered indicative. The latter observation is related to the low apatite content of the soil, which ranges from 0 to 0.4% – consequently, most of the data are very close, or below, the detection limit of the method.

In summary, the P K-edge XANES data collected from eleven soil profiles constitute a unique data set for Swedish conditions that can act as a baseline for future research in P transformations in soils.

We acknowledge the financial support given by the Swedish Research Council Formas and the Geological Survey of Sweden.

References

Eriksson, A.K., Hillier, S., Hesterberg, D., Klysubun, W., Ulén, B., Gustafsson, J.P., 2016. Evolution of phosphorus with depth in an agricultural soil profile. *Geoderma 180,* 29-37.

Gustafsson, J.P., Braun, S., Tuyishime, J.R.M., Adediran, G.A., Warrinnier, R., Hesterberg, D., 2020. A probabilistic approach to phosphorus speciation using P K-edge XANES spectroscopy with linear combination fitting. *Soil Systems 4,* 26.

Schmieder, F., Bergström, L., Riddle, M., Gustafsson, J.P., Klysubun, W., Zehetner, F., Condron, L., Kirchmann, H., 2018. Phosphorus speciation in a long-term manure-amended soil profile – evidence from wet chemical extraction, ^{31}P-NMR and P K-edge XANES spectroscopy. *Geoderma 322,* 19-27.

Schmider, F., Gustafsson, J.P., Klysubun, W., Zehetner, F., Riddle, M., Kirchmann, H., Bergström, L., 2020. Phosphorus speciation in cultivated organic soils revealed by P K-edge XANES spectroscopy. *Journal of Plant Nutrition and Soil Science 183,* 367-381.

Tuyishime, M., Adediran, G.A., Olsson, B., Spohn, M., Hillier, S., Klysubun, W., Gustafsson, J.P., 2022. Phosphorus abundance and speciation in acid forest Podzols – effect of postglacial weathering. *Geoderma 406,* 115500.

To what degree can the spatial distribution of secondary minerals in porous media be determined?

Helge Hellevang[a], Mohammad Masoudi[a], Mohammad Nooraiepour[a], Hossein Fazeli[b]

[a]Department of Geosciences, University of Oslo, Pb. 1047, Blindern, Oslo 0316, Norway, e-mail helghe@geo.uio.no, [b]Institute of GeoEnergy Engineering, Heriot-Watt University, Edinburgh EH14 4AS, UK

Summary. Mineral nucleation and growth affects the hydrodynamic properties of a porous media, and is important in a range of natural and engineered systems. The spatial distribution of mineral growth and the corresponding changes in por-perm relations is statistical at low temperatures, low supersaturations and (relatively) short time spans, while approaching deterministic at elevated temperatures and supersaturations and at (relatively) long time spans. We here propose a new statistical model and a method of upscaling mineral nucleation and growth from pore- to continuum scale.

Probabilistic or deterministic?

Mineral nucleation and growth is a prime example where (geo)chemical reactions give rise to geometry evolution in porous media. Crystal accumulations can dramatically reduce porosity. Alteration in pore volume, in turn, changes the connectivity of the pore space. Alterations in porosity and connectivity lead to pore space morphology changes, affecting properties such as tortuosity and permeability, and therefore, changes in fluid flow and solute transport. Mineral precipitation may partially or entirely clog pores and throats in the porous medium and change pore size distribution. Even small amounts of solid accumulation may render the pore structure impermeable. Additionally, precipitation reshapes the available surface area for growth, leading to changes in the system's reactivity, reaction progress, and reaction rates.

The process of mineral precipitation and crystal growth begins with nucleation, which is not fully understood and which is usually overlooked in reactive transport simulators. Nucleation controls the location and timing of solid mineral formation in porous media (see Fazeli et al. 2020). For an accurate prediction of the hydrodynamics of the porous medium after mineral precipitation, it is crucial to know the spatial distribution of stable secondary nuclei. Especially when the nucleation events are limited in number.

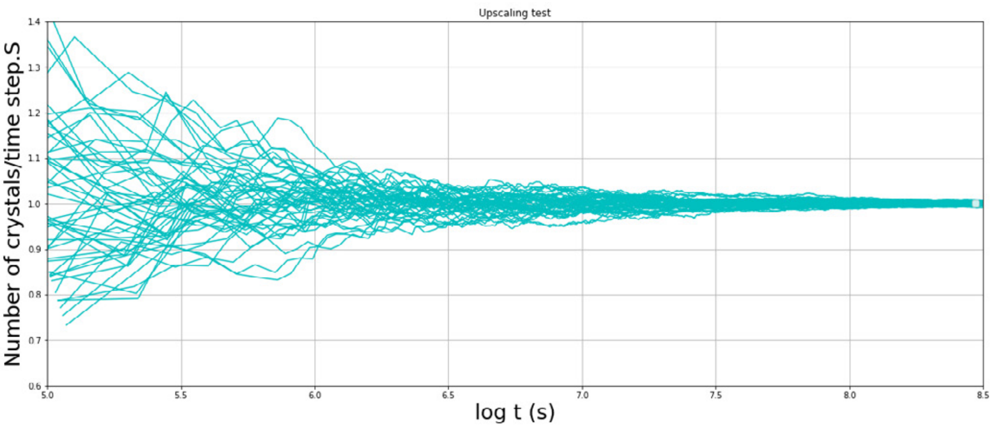

Fig. 1. Average number of stable nuclei/time step as a function of time. See Nooraiepour et al. (2021) for details on the statistical mineral nucleation model.

Nucleation is a statistical phenomenon, but can, as every statistical phenomena, to some degree be upscaled. If the total time of interest is much longer than the average nucleation time for a given substrate, the number and volume of secondary crystals can, to a reasonable degree, be determined. This is illustrated in Fig. 1, showing the normalized average number of crystals forming as a function of time (nucleation events), approaching the mean and determistic number of crystals (in this case 1.0 crystals/

time step). This statistical to deterministic transition is not only valid for small (pore-scale) systems, but also for large engineered systems, such as CO_2 storage reservoirs. It is the total time relative to nucleation time/surface area that determines if a system is probabilistic or not. If a reaction (mineral nucleation) is very slow, such as can be the case for magnesian carbonates at low temperature, the timeframe and system size can be very large before we can determine the spatial distribution of the crystals. This concept is illustrated in fig. 2. In this figure, large-scale engineered systems are generally in the deterministic field, while laboratory experiments, for many minerals, will be in the probabilistic field. The transition from deterministic to probabilistic will, however vary from mineral to mineral.

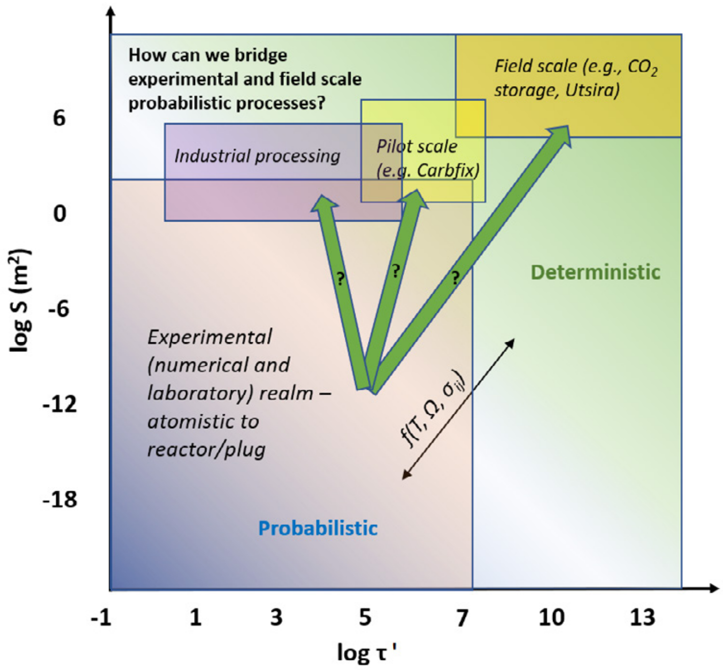

Fig. 2. The transition from probabilistic (non-determinable) to deterministic systems based on the total time of interest compared to nucleation time (τ', non-dimensional) and size of system (m^2).

A major challenge is the numerical modeling of mineral nucleation and growth at large continuum-scale systems and their consequences for hydrodynamic properties. We propose to use an entropy-function to quantify the spatial variability of nucleation at surface scale, and to use the resulting entropy values in upscaling schemes. For example, if very few crystals form in large systems, then hydrodynamic properties, such as the por-perm relation, will be little affected, no matter where in the pore space the crystals form. On the other hand, if crystals form everywhere in the pore space, and in large numbers, then a Kozeny-Carman-type (Kozeny, 1927; Carman,1937) of averaged por-perm relation can be found. We propose to replace the empirical coefficient in the Kozeny-Carman relation with an entropy-function, directly relating the statistical process of nucleation to the por-perm relation. Furthermore, we envisage that other empirical hydrodynamic parameters affected by mineral precipitation can also be formulated in terms of the spatial variability of nucleation, i.e. entropy.

References

Carman, P., 1937: Fluid flow through a granular bed. *Trans. Inst. Chem. Eng.*,15, 150–167.

Claramunt, C., 2005: A spatial form of diversity. (eds. A.G. Cohn & David M. Mark) Spatial information theory. Proceedings COSIT 2005, pp. 218-221.

Nooraiepour, M., Masoudi, M., & Hellevang, H., 2021: Probabilistic nucleation governs time, amount, and location of mineral precipitation and geometry evolution in the porous medium. *Scientific Reports*, 11, 16397.

Kozeny, J., 1927: Uber kapillare Leitung der Wasser in Boden. *Sitzungs-ber. Akad. Wiss. Wien*,136, 271–306.

Chemical gardens mimic electron paramagnetic resonance (EPR) spectra and morphology of biogenic Mn oxides

Sigrid Huld[a], Sean McMahon[b], Susanne Sjöberg[c], Ping Huang[d], Anna Neubeck[a]

[a]Department of Earth Sciences, Uppsala University, Uppsala, Sweden, sigrid.huld@geo.uu.se; [b]UK Centre for Astrobiology, School of Physics and Astronomy, University of Edinburgh, Edinburgh, UK, sean.mcmahon@ed.ac.uk; [c]Department of Geological Sciences, Stockholm University, Stockholm, Sweden, susanne.sjoberg@geo.su.se; [d]Department of Chemistry, Ångström Laboratory, Uppsala University, Uppsala, Sweden, ping.huang@kemi.uu.se.

Summary. Mn oxides in nature occur as both biological and abiotic minerals but distinguishing them is a difficult task. It was reported that biogenic Mn oxides display a characteristic narrow linewidth in electron paramagnetic resonance (EPR) spectroscopy, in contrast to their abiotic counterparts. Here we report two synthetic chemical garden Mn oxide biomorphs in silica and carbonate, of which the former exhibits both morphologically life-like structures and narrow EPR linewidths. Thus, a narrow EPR line may not be reliable evidence for the assessment of biogenicity.

Materials and methods

The chemical gardens were grown in a similar manner to previous work on the subject (McMahon, 2019). Grains of Mn sulphate were manually dispersed into silicate and carbonate solutions and left for approximately 10 minutes before decanting and rinsing four times with distilled water. The resulting filamentous structures were imaged using a normal light microscope and a scanning electron microscope from the department of Earth Sciences at Uppsala University. The chemical composition of these structures was also investigated with various geochemical techniques such as Raman spectroscopy, XRD, Leucoberbelin blue dye and, most importantly, electron paramagnetic resonance (EPR) spectroscopy.

Results and discussion

The reaction between seed salt and alkaline solution produces a pocket of acidic fluid, delimited by a semi-permeable membrane. As the pressure inside the vesicle increases it eventually ruptures, and jets of fluid are released that are immediately surrounded once more by a membrane, thus forming filamentous structures. The formation of successive filaments may occur on the original grain or along an already formed filament, creating branching structures. The morphology and size-range of these filamentous structures often imitate many biological criteria used to identify microfossils in the rock record such as branching, constant diameter, circular cross-sections, hollowness, anastomosis and nestedness (Dodd et al., 2017; McMahon, 2019) (Fig. 1). Hydroxide ions in solution may cross the semi-permeable membrane surrounding the filaments and react with the metal ions resulting in the precipitation of a metal oxide or (oxy)hydroxide coating on the inside of the filaments.

Raman spectroscopy, XRD and leucoberbelin blue all indicated that the Mn oxides precipitated on the chemical garden filaments were oxidized primarily to Mn^{4+} in the silicate solutions whereas in the carbonate solution no oxidation had occurred. In the latter it was evident that Mn^{2+} from the dissolving grains had reacted directly with the carbonate in solution to form Mn carbonate, or rhodochrosite.

Manganese oxides are commonly found in nature as lacustrine and marine ferromanganese nodules, in soils, and in desert varnish, and have also been found on Mars. They occur as both biological and abiotic minerals but empirically distinguishing between the two remains a problem. Many attempts at identifying structural and compositional differences have been made. Recently, electron paramagnetic resonance (EPR) spectroscopy has been used for this purpose (Kim et al., 2011; Ivarsson et al., 2015). EPR is a method used to analyze transition metals with unpaired electrons in their outer shells, and Mn is one such metal with up to five unpaired electrons in the Mn^{4+} ion. As such, a group of researchers led by Soon Sam Kim in 2011 used EPR on a series of biological and abiotic Mn oxide samples to try to find differences in the EPR spectral linewidth (Kim et al., 2011). The results of this paper indicated

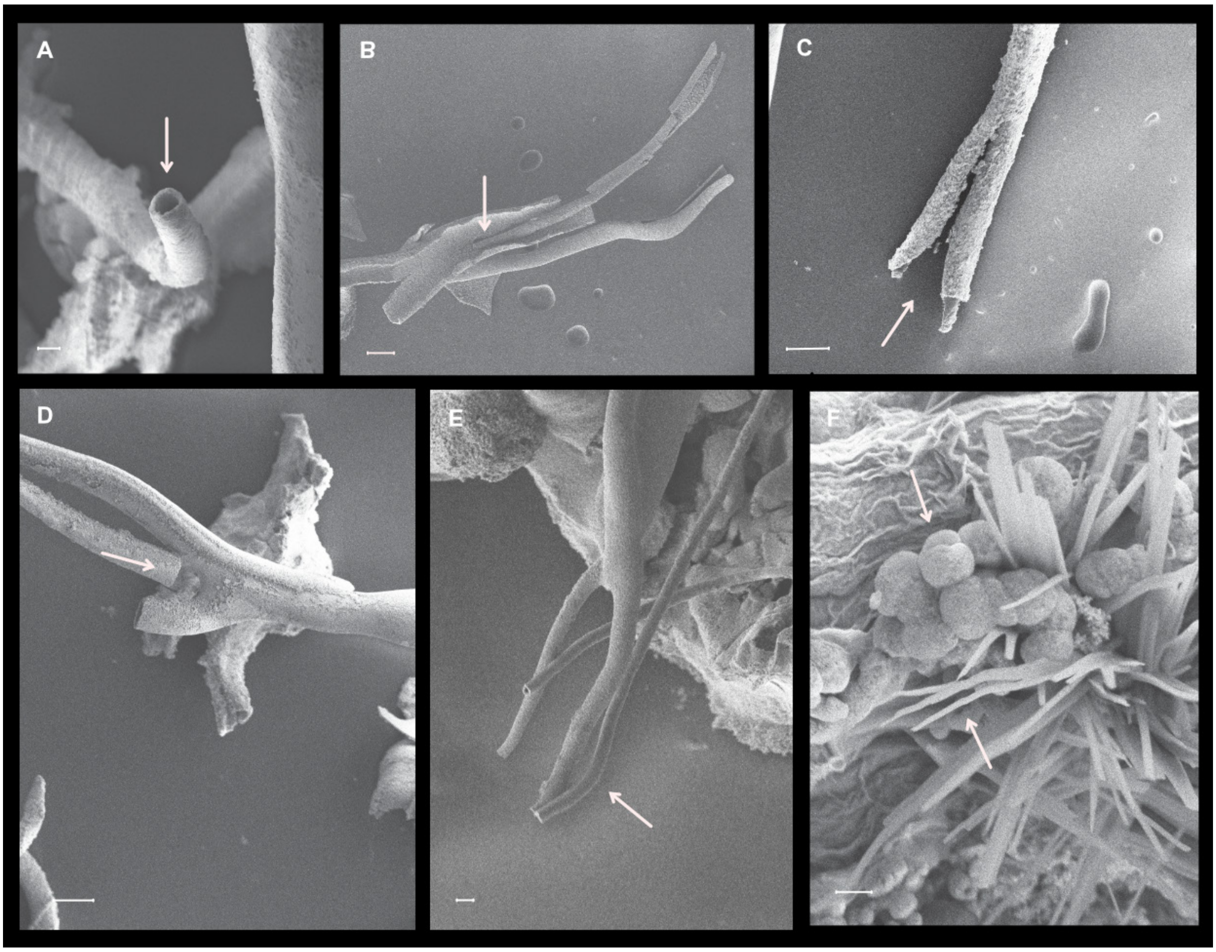

Figure 1. SEM pictures of silicate (A–E) and carbonate (F) chemical garden biomorphs. Arrows indicate hollow and circular cross-section in (A), nestedness in (B), branching structures in (C, D) and long straight filaments with constant diameter of <10μm in (E). (F) shows globular growths in carbonate solutions and small groups of spines. Scale bar: (A) 30μm; (B, C, E) 100μm; (D) 10μm; (F) 3μm.

that EPR can be used to identify biologically produced Mn oxides in nature. In particular, the narrow width of the EPR spectrum with values $\Delta H_{pp} < 580G$ was proposed as an indicator of a biogenic origin for Mn oxides. However, the EPR spectra obtained in the present work from synthetic chemical gardens grown in silica solution also had linewidths well below 580G. In poorly crystalline or amorphous solids several factors may affect the breadth of EPR spectral linewidths, including exchange narrowing phenomena and dipole-dipole broadening. This is often a result of high concentrations of Mn ions in the samples. Therefore, we argue that the EPR linewidth alone may not be reliable for identifying with accuracy a biogenetic origin for natural Mn oxides.

References

Dodd, M.S., Papineau, D., Grenne, T., Slack, J.F., Rittner, M., Pirajno, F., O'Neil, J., and Little, C.T.S., 2017: Evidence for early life in Earth's oldest hydrothermal vent precipitates. *Nature 543*, 60-64.

Ivarsson, M., Broman, C., Gustafsson, H., and Holm, N.G., 2015: Biogenic Mn-Oxides in Subseafloor Basalts. *PLoS ONE 10*, e0128863.

Kim, S.S., Bargar, J.R., Nealson, K.H., Flood, B. E., Kirschvink, J.L., Raub, T.D., Tebo, B.M., and Villalobos, M., 2011: Searching for Biosignatures Using Electron Paramagnetic Resonance (EPR) Analysis of Manganese Oxides. *Astrobiology 11*, 8.

McMahon, S., 2019: Earth's earliest and deepest pur- ported fossils may be iron-mineralized chemical gardens. *Proc R Soc Lond B Biol Sci 286*, 20192410.

Ah soil horizon geochemistry as a tool to detect buried VMS mineralizations in the Skellefte ore field – the Rävliden pilot survey

Majka C. Kaiser[a], David R. Heberlein[b] , Joachim Albrecht[c], Mac F. Persson[d]

[a]Boliden Mineral AB, Boliden, Sweden, christiane.kaiser@boliden.com; [b]Heberlein Geoconsulting, Vancouver, Canada, dave@hebgeoconsulting.com; [c]Boliden Mineral AB, Boliden, Sweden, joachim.albrecht@boliden.com, [d]Boliden Mineral AB, Boliden, Sweden, mac.persson@boliden.com

Summary. To evaluate low level Ah soil horizon geochemistry as tool for the detection of blind massive sulphide mineralization in the Skellefte ore field, Northern Sweden, a pilot survey was carried out over the deep-seated and till-covered Rävliden North ore bodies in the Kristineberg VMS camp. 132 soil samples were taken and subjected to partial extraction before analysis. Except for Hg, which has a true geochemical surface expression over the mineralization, Bi, Cu, Hg, In, Mo, Pb, S, Sb, Tl, W and Zn show convincing high-contrast anomalies after normalization against Al, Fe and Mn.

Introduction

The Skellefte ore field in Northern Sweden contains over 87 pyritic Zn-Cu-Au-Ag massive sulphide deposits of which 27 have produced over 100,000 tons of ore (Allen et al. 1996). The Kristineberg VMS camp with the operating Kristineberg and the closed Rävlidmyran and Rävliden mines is one of the most important mining districts in the area. Intensely mineralized but in large parts still underexplored, the till-covered area is considered as to be very endowed in terms of buried, yet undetected ore bodies. As Ah soil horizon sampling has been proven to be effective at identifying sulphide mineralization through Quaternary glacial sediment (Heberlein, 2010), a pilot survey was carried out to test the method as exploration tool in the Skellefte ore field to discover buried mineralization.

Ah soil horizon geochemistry

Ah soil horizon geochemistry is based on analyses of metal ions that have been leached from a buried ore body, migrated upwards (for different mechanisms see Geffen, 2011 and references therein) and adsorbed to soil matrix. When subjected to partial extraction techniques, the adsorbed ions – the exogenic signal of the soil matrix – yield subtle anomalies over the buried mineralization. The lowermost humic layer of podsols (Fig. 1), which develop in boreal climates in 5–15 cm depth, favours the adsorption of metal ions and was therefore chosen as sampling medium.

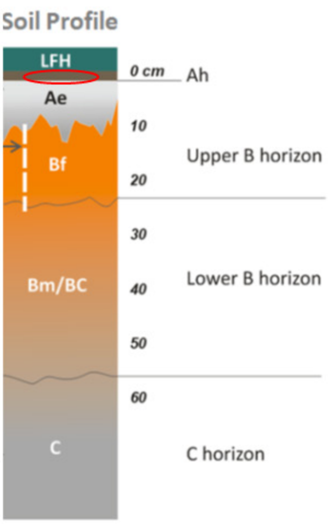

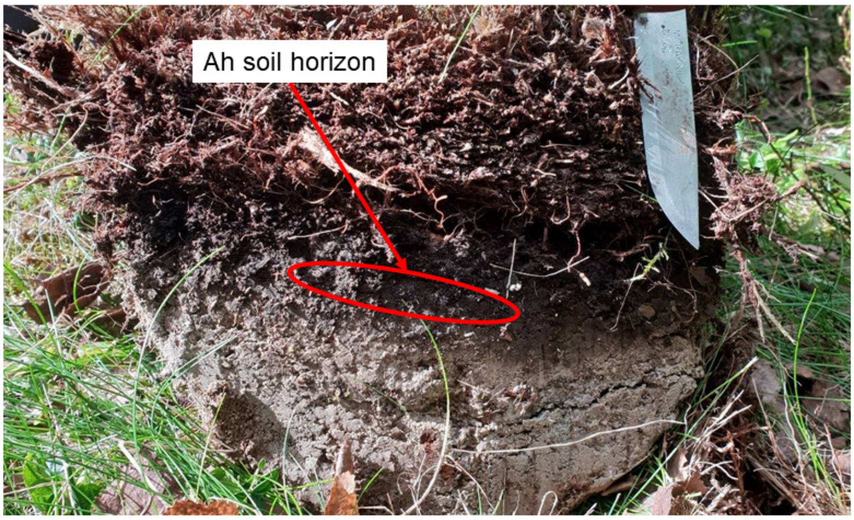

Fig. 1: Left: Ah soil horizon in podsol according to the Canadian soil classification (Heberlein, 2010); right: Ah soil horizon sample

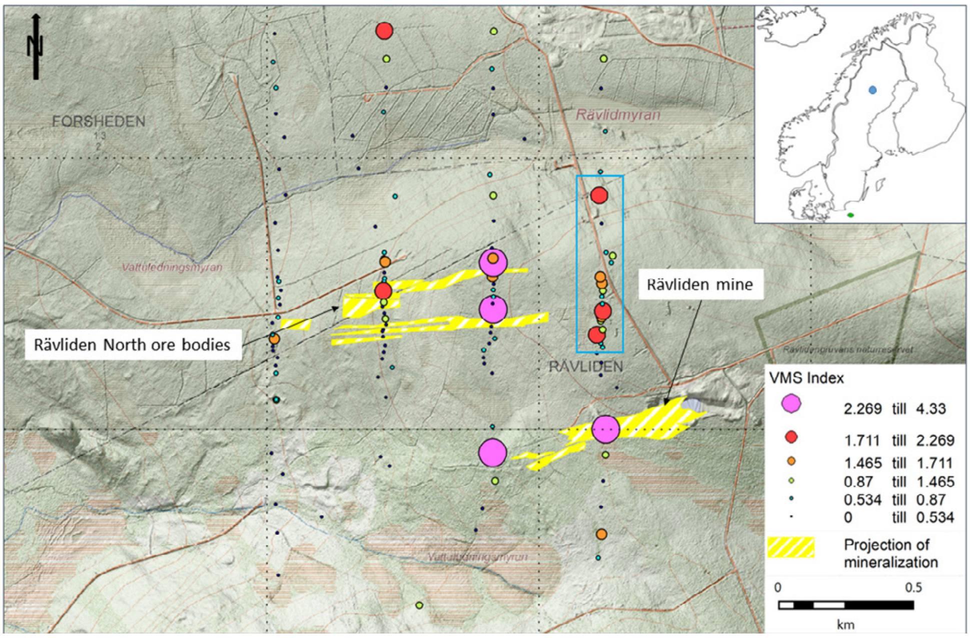

Fig. 2: Results of the Ah soil horizon sampling pilot study at Rävliden, Kristineberg VMS camp, as summative VMS index (Bi, Cu, Hg, In, Mo, Pb, S, Sb, Tl, W and Zn; Heberlein, 2019 b); blue square: Samples possibly affected by road contamination; blue dot in inlay: Sampling area.

Sampling and analysis

For sampling, about 50 × 50 cm pits have been dug (Fig. 1). If the Ah soil horizon was sufficiently developed, about a handfull Ah soil was sampled below the grass sod (c. 0.5 kg). In total, 132 samples along four north-south trending lines have been collected (Fig. 2) avoiding fresh roadcuts, swamps and poorly drained areas. For quality control, duplicates at 20 sample intervals were taken. The samples were leached in aqua regia and analyzed for 53 elements by ICP-ES and ICP-MS at ALS.

Results

Quality control using the duplicates yielded inacceptable high total measurement errors of over 50% (average percent standard deviation) for Au, Ag, Pd (nugget effect) and Se. Hence, these elements were not considered for interpretation. Except for Hg, which has a good response over the mineralization, the other elements show random patterns that appear unrelated to the mineralization. They had to be normalized against Al, Fe and Mn, as these elements (i.e. clays and hydroxides) tending to be hydromorphically concentrated in poorly drained areas, favour metal adsorption. After normalization, true responses are revealed over the blind sulphide mineralization, which define high-contrast anomalies for Bi, Cu, Hg, In, Mo, Pb, S, Sb, Tl, W and Zn (plotted as summative VMS index in Fig. 2, Heberlein, 2019 b). The samples in the central part of the easternmost line either reflect dust contamination from the road nearby or a western continuation of the Rävliden North ore bodies.

References

Allen, R. L., Weihed, P. and Svenson, S.-Å., 1997: Setting of Zn-Cu-Au-Ag massive sulphide deposits in the evolution and facies architecture of a 1.9 Ga marine volcanic arc, Skellefte district, Sweden. *Economic Geology 91*, 1022-1053.

Geffen, P.W., 2011: Geochemical Indicators of buried sulphide mineralization under sedimentary cover near Talbot lake, Manitoba. *PhD thesis, Queen´s University, Ontario, Canad*a.

Heberlein, D.R., 2010: An assessment of soil geochemical methods for detecting copper-gold porphyry mineralization through quaternary glaciofluvial sediments at the WBX-MBX and 66 Zones, Mt. Milligan, North-Central British Columbia. *Geoscience BC Report 2010-08*.

Heberlein, D.R., 2019 a: Interpretation of the 2018 Ah soil horizon geochemistry results, Rävliden project, Sweden. *Unpublished report, Heberlein Geoconsulting*.

Heberlein, D.R., 2019 b: Interpretation of the 2019 Ah soil horizon geochemistry results, Rävliden project, Sweden. *Unpublished report, Heberlein Geoconsulting*.

Stuck in the muck: Reconstructing paleostorms using geochemical tools in peatlands

Malin E. Kylander[a,b], Antonio Martínez Cortizas[c], Jenny K. Sjöström[a,b], Richard Bindler[d]

[a]Department of Geologial Sciences, Stockholm University, Stockholm, Sweden, malin.kylander@geo.su.se; [b]Bolin Centre for Climate Research, Stockholm, Sweden; [c]CRETUS, EcoPast (GI-1553), Universidad de Santiago de Compostela, Santiago de Compostela, Spain; [d]Department of Ecology and Environmental Science, Umeå University, Umeå, Sweden.

Summary. Past variability in storminess can be reconstructed using the mineralogical information archived in peatlands. A challallenge is however, the highly organic matrix. We present a new approach to this problem using a sequence from Store Mosse, Sweden which pairs XRF and FTIR-ATR analyses of the inorganic fraction. Quartz dominates the signal which, being coarser grained, is used as a storm proxy. The variations observed over the last 5 ka generally agree with regional records, although comparisons are complicated by different types of proxy data and the transient nature of storms.

Over the past decades severe winter windstorms have broken new records in Europe (e.g. >190 km h^{-1} winds in Denmark 2013). The most recent predictions suggest a heterogenous future in terms of storm frequency in Europe, although there is poor agreement across climate models (IPCC, 2021). At present we lack a fundamental understanding of the mechanisms driving natural storminess in the Euro-Atlantic sector on pre-instrumental timescales. Only paleoarchives, which incorporate signals of environmental change over time, can give us a window into the undistributed climate system.

It has become increasingly common to use peat archives to reconstruct past storm activity. Ombrotrophic (atmospherically fed) bogs trap minerals transported via aeolian pathways in their organic rich matrices (sometimes even up to 99%). Given that storms are at their strongest as they make landfall on the western coasts of Europe, peat paleostorm records to date have been from coastal areas located downwind from sand dune and beach systems. The basic premise is that stronger winds during stormier conditions transport larger grains such as quartz to these peat bogs. Storm proxies in peat records have thus been focussed on the amount of mineral material coming to the bog as well as its grain size. Storms do not however, stop at coastal areas and can have a devastating impact on the landscape as they move inland. In comparison to peat paleostorm reconstructions from coastal sites, inland sites are faced with two main methodological challenges: (i) there are usually no large sand sources in the landscape and (ii) wind speeds inland are often lower than at the coast, muting the proxy signal. As such, we need more refined methods for identifying temporal changes in the quantity of atmospherically transported particles and their grain size.

The highly organic matrix of peat makes the measurement and identification of the archived minerals and their grain sizes complex. Removal of the organic fraction in peat using combustion methods can impact mineral composition/identification and destroy aggregates. On the other hand, acid-based methods have found to be ineffective in removing such large amounts of organic matter. Once the organic fraction is removed, direct identification of minerals in peat can been made by XRD (Sjöström et al., 2018). Alternatively, multi-element analyses have been used to infer mineralogy, and thereby, grain size (Kylander et al., 2016). More recently, Fourier transform infrared spectroscopy attenuated total reflectance (FTIR-ATR), a quick and non-destructive analysis, has been used on the inorganic fraction in peats to establish the mineral composition (Martinez Cortizas et al., 2021).

We make a first attempt at a paleostorm reconstuction from an inland site using a peat sequence from Store Mosse (N57°13´37´´, E13°55´17´´), a large peatland (77 km^2) located in Småland, south-central Sweden. Peat accumulation started at Store Mosse ~9 ka in the southern portion of the bog complex and a string of sand dunes were emplaced 6–8 ka. These sand dunes are present still today and indeed, the entire peatland is ringed by aeolian deposits (both sand sheets and dunes) and glaciofluvial sediments. There are thus a number of local sources (<5 km) of coarse-grained mineral material and these were sampled in parallel to the peat bog.

We acquired basic peat properties (bulk density, peat accumlation rates, LOI) on the Store Mosse Dune South (SMDS) sequence. In addition, elemental data from XRF and spectral data from FTIR-ATR analyses were made on the inorganic fraction. Both of these datasets were analysed separately by Principal Component Analyses (PCA). Following the approach of Martinez Cortizas et al. (2021), the PCA established six components explaining 99% of the variance in the dataset. The reference minerals showed large loadings in the ash samples, accounting for the spectral signal of four of the components: Cp2: quartz, Cp4: K-feldspar, Cp5: mica and Cp6: Ca-feldspar. Components Cp1 and Cp3 did not correspond to any of the reference minerals and are interpreted to be minerals formed during ashing. The composition of the local aeolian samples was shown to be similar with quartz accounting for the majority of the samples (~70%). Importantly, the bulk and coarse fraction (>63 µm) have nearly the same composition meaning quartz in the landscape has larger grain sizes.

The SMDS paleostorm record was built using the partial communalities of FTIR-inferred quartz and K-feldspar, representing coarse and medium sized fraction, respectively. In addition, we include Cp2 from the PCA on the XRF data which represents the behaviour of Zr, Si, Ti and Al. Changepoint modelling was then applied to identify common periods of increased storminess across these three proxies at 4500–4000 (Event I, EI), 3330–3140 (EII), 2330–1910 (EIII), 1490–1230 (EIV), 1045–780 (EV) and 740–650 (EVI) cal yr BP. Nearly all of these storm periods, with the exception of EII, were also detected in K and Al mass accumulation rates from SMS_{2008}, a core collected from Store Mosse some 5 km to the south. Smaller differences between the records may be linked to their proximity to mineral sources where SMDS is much closer to a aeolian sources than SMS_{2008}.

Comparisons with palestorm records further afield shows some agreement but is complicated by differences in the proxies being examined where we look at FTIR inferred mineralogy, elementally inferred mineralogy and minerogenic input as well as the physical counting of grains. Elementally-based approaches “smear” the mineralogical signal as it necessarily combines the presence of all minerals hosting, in the case of SMDS, Zr, Ti, Si and Al. It must also be kept in mind that each record has errors associated with age modelling of the proxy data. Finally, storms are very short term events lasting hours to days, which may not always be captured in paleostorm records depending on wind directions, the landscape and vegetation cover.

References

Intergovernmental Panel on Climate Change, 2021: Climate Change 2021: The Physical Science Basis. Contribution of Working Group I to the 6th Assessment Report of the Intergovernmental Panel on Climate Change. Cambridge University Press.

Kylander, M.E., Martinez Cortizas, A., Bindler, R., Greenwood, S.L., Mörth, C.-M., Rauch, S., 2016: Potentials and problems of building detailed dust records using peat archives: an example from Store Mosse (the “Great Bog”), Sweden. *Geochimica et Cosmochimica Acta* 190, 156-174.

Martinez Cortizas, A., López-Merino, L., Silva-Sánchez, N., Sjöström, J.K., Kylander, M.E., 2021: Investigating the Mineral Composition of Peat by Combining FTIR-ATR and Multivariate Analysis. *Minerals* 11, 1084.

Sjöström, J.K., Bindler, R., Granberg, T., Kylander, M.E., 2019: Procedure for Organic Matter Removal from Peat Samples for XRD Mineral Analysis. *Wetlands* 39, 473–481.

Geochemical mapping of the historical mining field at Vena, central Sweden

Anna Ladenberger, Jo Snöälv, George A. Morris, Alexander Lewerentz, Merita Murtola

Department of Mineral Resources, Geological Survey of Sweden, Uppsala, Sweden, anna.ladenberger@sgu.se

Summary. The historical Vena mining field is well known for its iron, copper and cobalt mining. The geochemical survey was carried out in 2019 and corresponding samples of C-horizon till and A-horizon topsoil (forest soil) were collected. As expected, the geochemistry of soil and till reflects well the nature of the ore deposit with high content of Fe, V, Co, Zn, As, Mo, Ag, Cd, Sn, Sb, Pb and Bi.

Historical mining at Vena and geology overview

The Vena mining field is located east of the town of Åmmeberg in the southern part of the Örebro County. The area hosts hundreds of small historical mines (Fig. 1) where iron-oxide and polymetallic sulphide ores were mined from at least the 16th century. The Vena copper and cobalt mines were in operation between 1770 and 1880, with an average concentration of 0.1–0.5% Co in cobalt ore (Tegengren et al. 1924). Bedrock in the Vena area is composed of Svecokarelian metavolcanic rocks belonging to the Mariedamm unit, and include lithologies such as rhyolite and dacite occurring as subvolcanic intrusions or volcaniclastic deposits (Lewerentz et al. 2020). Amphibolites and granites occur as elongated bodies and lenses within the metavolcanic rocks. Local presence of carbonates indicates deposition in a marine environment. Deformation and metamorphic overprint varies from low (primary textures present) to high (migmatitisation). The mineralisation at Vena was formed in several stages and the most common ore minerals are chalcopyrite, pyrrhotite, sphalerite, pyrite and subordinate galena. Cobalt minerals are represented by cobaltite, Co-arsenopyrite, willyamite and other rare phases (Lewerentz et al. 2020). Iron-oxide skarn mineralisation just southeast of the Vena field is dominated by magnetite with minor pyrrhotite, pyrite and chalcopyrite.

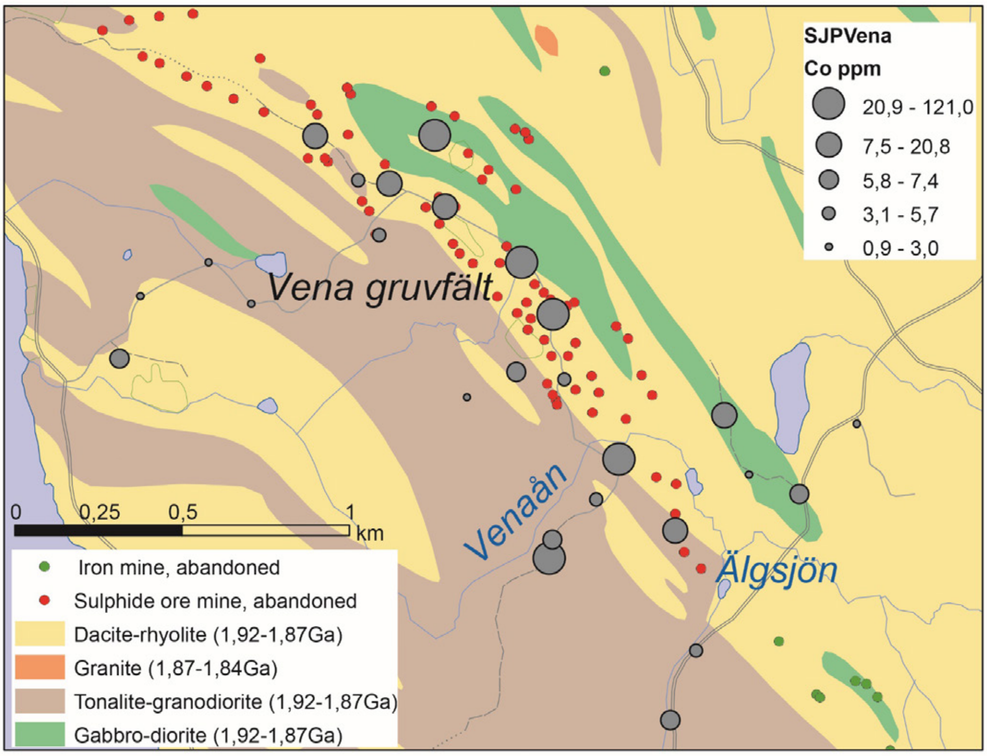

Fig.1. Geological map of the Vena mining field with sites of historical iron-oxide and sulphide mining (SGU digital database) and cobalt concentrations in forest topsoil (method: 7M HNO_3 leach by ICP-MS).

Geochemical signature in till and forest soil

Twenty-six samples of till from the C-horizon (KJP) and 26 samples of corresponding forest topsoil (SJP) were collected in 2019. Till and soil samples were vacuum-dried and sieved to the fraction <0.063 mm. An acid leach method using 7M HNO_3 was applied and chemical composition of the leachate was measured by quadrupole ICP-MS at the SGU laboratory.

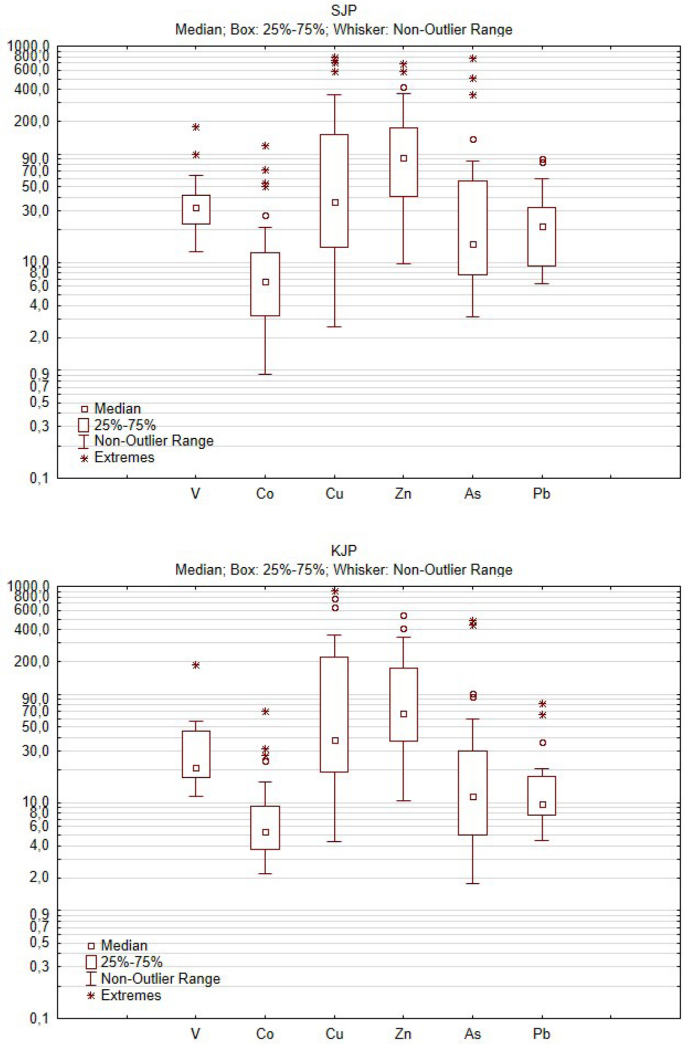

Fig.2. Multivariate boxplots for forest topsoil (SJP) and till (KJP) at Vena mining field (all values in ppm).

The chemical composition of till and soil is to large degree similar but secondary enrichment in topsoil can be observed for many metals and trace elements. Elements which are usually hosted by silicates and carbonates (e.g. K, Y, Zr, Ca, Sr REEs, Sc, Th and U) have slightly higher concentrations in till while metals with high affinity for oxides and sulphides are enriched in surface topsoil, e.g. Fe, V, Co, Zn, As, Mo, Ag, Cd, Sn, Sb, Pb and Bi. Most of the median concentrations do not exceed threshold values for contaminated soil (Naturvårdsverket 2009) with the exeption of As (median in SJP=14.7 ppm, 16 samples exceed threshold value). Extreme As values up to 778 ppm are observed in topsoil (Fig. 2). Several metals closely related to Vena mineralisation types show high concentrations in both till and topsoil, e.g. V, Co, Cu, Zn and Pb (Fig. 2). Spatial distribution of high metal concentrations in both sampling types is closely related to the historical mining sites at Vena where the bedrock is dominated by felsic metavolcanic rocks and mafic lithologies. Most anomalies, such as for cobalt occur in the southeastern part fo the ore field and they correlate well with the rock chemical composition (Lewerentz et al 2020, Fig. 1).

References

Lewerentz, A., Bakker, E., Hedin, P. & Leopardi, D., 2020: Ore-proximal surveys in southern Bergslagen: Vena gruvfält and Tunaberg. *SGU-rapport* 2020:16, 100 pp.

Naturvårdsverket, 2009: Riktvärden för förorenad mark. Modellbeskrivning och vägledning. *Naturvårdsverket, Rapport 5976,* 270 s.

Tegengren, F.R. et al., 1924: Sveriges ädlare malmer och bergverk. *Sveriges geologiska undersökning Ca 17*. 406 pp.

Geochemical mapping of black shales, with applications for environmental risk assessment and exploration

Kirsti Loukola-Ruskeeniemi[a], Eija Hyvönen[b], Jouni Lerssi[c], Hilkka Arkimaa, Meri-Liisa Airo

[a]Geological Survey of Finland, Espoo, kirsti.loukola-ruskeeniemi@gtk.fi; [b]Geological Survey of Finland, Rovaniemi, eija.hyvonen@gtk.fi; [c]Geological Survey of Finland, Kuopio, jouni.lerssi@gtk.fi

Summary. We present the final results of the country-wide black shale mapping of Finland. Black shales host, e.g. sulphide and graphite deposits. They occur in the vicinity of other types of sulphide deposits as well and their chemical composition may be used as a pathfinder in exploration. The black shale database is important for regional and environmental authorities. Black shales may cause acid rock drainage, weaken the quality of well water and contribute to the trace element status of local residents. Black shales occur world-wide in densely populated areas where risk management may be needed.

Black shale deposits

In Finland and in Sweden, Proterozoic black shales represent seafloor mud deposited for 2.50–1.85 Ga ago. They host sulphide deposits such as the Talvivaara Ni-Zn-Co-Cu (e.g. Loukola-Ruskeeniemi & Lahtinen 2013). Moreover, they occur in the vicinity of other types of deposits and their chemical characteristics can be used as a pathfinder in exploration (e.g. Loukola-Ruskeeniemi 1992, 1999). For example, black shales in a komatiite-hosted Ni-Cu-PGE occurrence in Central Lapland show increased Na and Si values compared with black shales studied in other parts of Finland due to alteration processes. The Proterozoic black shales of Finland and Sweden contain graphite because of medium to high-grade metamorphism. Over 30 small graphite mines have operated in Finland in the past. In Sweden, the Palaeozoic 'alum shales' have been mined in the southern part of the country (Figure 1).

Country-wide mapping procedure

Proterozoic black shales of Finland and Sweden are at present schists or gneisses as a result of metamorphic and tectonic deformation. We traced them with geophysical measurements since they are rarely outcropped in glaciated terrains. Airborne geophysical surveys revealed stratigraphy-related, coupled magnetic and electrically conductive patterns. Electrical conductivity was related to the content of graphite and sulphides and produced continuous and bending electromagnetic anomaly patterns. The magnetic anomalies, if present, resulted from ferrimagnetic monoclinic pyrrhotite. We correlated the airborne magnetic and electromagnetic survey with petrophysical and chemical data from drill core samples, geological outcrop observations and geophysical field measurement data. We also interviewed other geologists and geophysicists specialized in different regions of Finland. The first version of the country-wide map and database was published in 2000 (Arkimaa et al. 2000). It has been updated with new drillings and will be completed and published in 2023. The mapping procedure should be tailored for each country according to the mineral composition and petrophysical properties of black shales. However, in the Proterozoic of Sweden, the Finnish procedure will work well.

Geochemistry of black shales

Finnish black shales contain abundant iron sulphides: pyrite and/or pyrrhotite. Quartz, micas, graphite and sulphides are the main minerals. The concentrations of Ca, Si and K vary, largely reflecting the content of carbonate, detritus and clay fractions in the primary organic-rich mud. Considerable differences in geochemistry were observed from site to site and within individual lithostratigraphic units (Loukola-Ruskeeniemi et al. unpublished data). – Swedish 'alum shales' contain more U and Mo, for example, than the Proterozoic black shales of Finland.

Environmental risk assessment and risk management

Sulphide-rich black shales may cause acid rock drainage even under natural conditions in different parts of the world (Parviainen & Loukola-Ruskeeniemi 2019). The distribution of Ni-Mn-rich black shales is reflected in elevated Ni-Mn concentrations of the hair samples of local residents in eastern Finland (Kousa et al. 2021) pointing out the need for risk assessment and subsequently, risk management actions in highly-populated extensive black shale areas like those occuring in China.

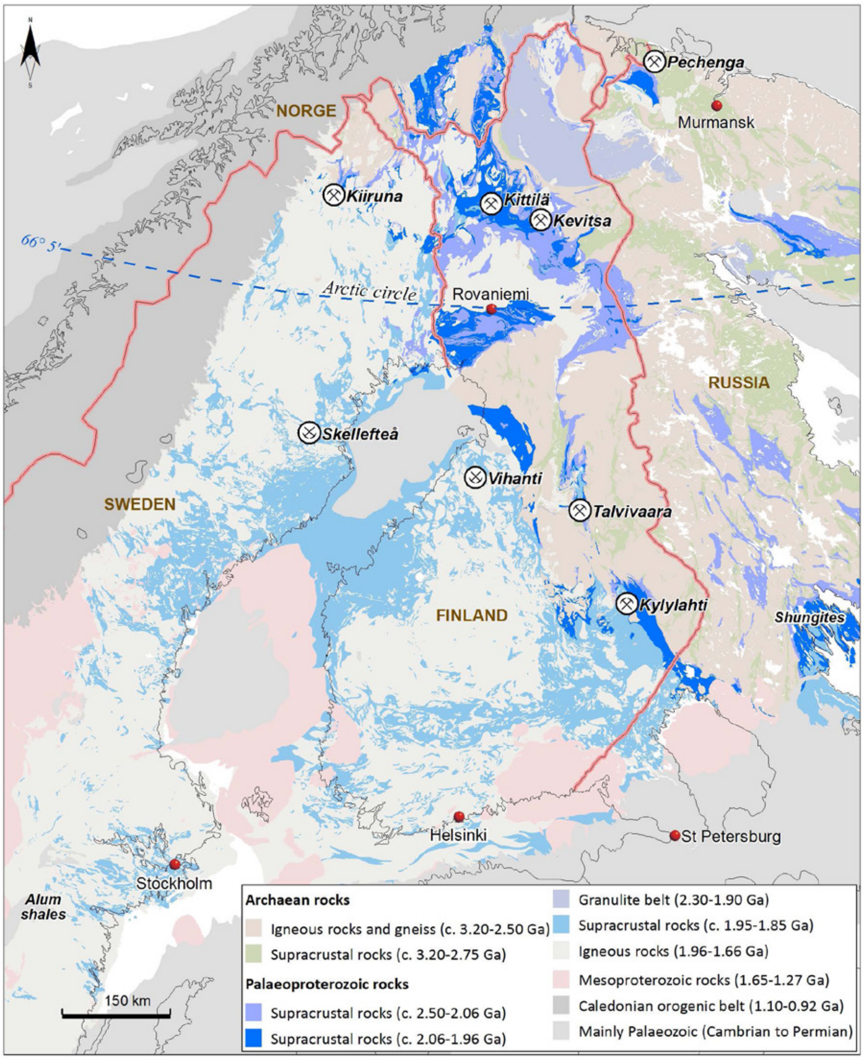

Figure 1. Generalized geological map of the Fennoscandian Shield. In Finland, we have mapped the geochemistry of Proterozoic black shale units all over the country. The 1.95–1.85 Ga units continue in Sweden. Selected sulphide mines are shown with crossed hammers. The hammers are downwards if the mine is closed.

References

Arkimaa, H., Hyvönen, E., Lerssi, J., Loukola-Ruskeeniemi, K., Vanne, J. 2000: Proterozoic black shale formations and aeromagnetic anomalies in Finland. Database and map 1:1 000 000. *Geological Survey of Finland, Special Maps 45*. ISBN: 951-690-762-8

Kousa, A., Loukola-Ruskeeniemi, K., Hatakka, T., Kantola, M. 2021: High manganese and nickel concentrations in human hair and well water and low calcium concentration in blood serum in a pristine area with sulphide-rich bedrock. *Environmental Geochemistry and Health*. https://doi.org/10.1007/s10653-021-01131-6

LoukolaRuskeeniemi, K. 1992: Geochemistry of Proterozoic metamorphosed black shales in eastern Finland, with implications for exploration and environmental studies. *Geological Survey of Finland, Special Publication 9*. 97 p. ej_009.pdf (gtk.fi)

Loukola-Ruskeeniemi, K. 1999: Origin of black shales and the serpentinite-associated Cu-Zn-Co ores at Outokumpu in Finland. *Economic Geology 94,* 1007–1028. http://dx.doi.org/10.2113/gsecongeo.94.7.1007

Loukola-Ruskeeniemi, K., Lahtinen, H. 2013: Multiphase evolution in the Talvivaara Ni-Cu-Zn-Co deposit, Finland. *Ore Geology Reviews 52*, 85–99. https://doi.org/10.1016/j.oregeorev.2012.10.006

Parviainen, A. & Loukola-Ruskeeniemi, K., 2019: Environmental impact of mineralised black shales. *Earth-Science Reviews 192,* 65–90. https://doi.org/10.1016/j.earscirev.2019.01.017

Mineralogy and geochemistry of komatiites associated with Cu-Au deposits: an example from the Mundonguara mine in Manica Greenstone Belt, Mozambique

Laura Mendes[a,b], Olof Martinsson[b], Christina Wanhainen[b], Daud Jamal[a]

[a]Department of Geology, Eduardo Mondlane University, Maputo, Mozambique; [b]Department of Civil, Environmental and Natural Resources Engineering,Luleå University of Technology, Luleå, Sweden

Summary. Komatiites from the Mundonguara mine have been affected by hydration and carbonatization due to hydrothermal alteration and greenschist facies metamorphism. The mineralogical assemblage in these rocks is serpentine + chlorite + talc + tremolite + magnetite + carbonates. The chemical characteristics indicate a mantle origin with a source transitional between OIB and N-MORB. The LREE-depleted character of the komatiites is also a signature that could be related to a depleted mantle source similar to N-MORB.

The Archean rock units in Mozambique includes the Manica Group, the Munhinga Group, the Mavonde Complex, and the Mudzi Complex that are part of the Zimbabwe Craton. The Manica and Munhinga groups are typical of supracrustal greenstone belts, whereas the Mavonde and Mudzi complexes represent granitic basements (Grantham et al. 2011). This greenstone-granite terrain hosts several mineral deposits including komatiite-related Ni-Cu deposits, various epigenetic gold deposits, and secondary enriched banded iron formations (Hofmann et al. 2002, Zeh et al. 2009). The Mundonguara Cu-Au mine, located in the Manica Group, is a rare example of a Cu-Au deposit in this area. The Mundonguara Cu-Au mine is located in a steeply north-dipping succession of ultramafic-mafic volcanic (komatiites and komatiitic basalts) and minor felsic volcanic rocks, at the southern limb of a regional E–W synclinal fold (GTK 2006). The komatiites are intruded by gabbroic dykes in the mine area. These rocks have been investigated by optical microscopy and chemical analyses, including main and trace elements, for characterization and interpretation of tectonic setting.

The komatiites from the Mundonguara mine are highly altered but contain locally relict spinifex textures indicating an extrusive origin for some of these rocks while others have a relict cumulate texture. They all underwent hydrothermal alteration, followed by a low-grade metamorphism. The mineralogical assemblage found in these rocks includes serpentine + chlorite + talc + tremolite + magnetite + carbonates and they are divided into serpentinites, komatiites, and pyroxenitic komatiites.

In an AFM diagram (Fig. 1) the ultramafic rocks occupy the komatiite field and the mafic ones have the character of tholeiitic high-Mg basalts. Serpentinites and komatiites are low in REE, usually with a LREE depletion for komatiites, while the serpentinites have a slight LREE enrichment similar to the pyroxenitic komatiites. Gabbroic rocks have a higher content of REE and are slightly enriched in LREE. Two of the samples show a more fractionated pattern and one of them with a distinct negative Eu-anomaly indicating magma development by plagioclase fractionation.

The tectonic discrimination diagram TiO_2/Yb vs Nb/Yb (Pearce 2008) in figure 2, shows that the komatiites and gabbroic rocks mainly occupies the MORB array field suggesting a mantle origin for the magma. The slightly diagonal trend may indicate a source transitional between OIB and N-MORB. The LREE-depleted character of the komatiites is also a signature that could be related to a depleted mantle source similar to N-MORB. These rocks were probably generated in an extensional continental setting with crustal contamination during the magma ascend indicated by a high Th/Yb ratio.

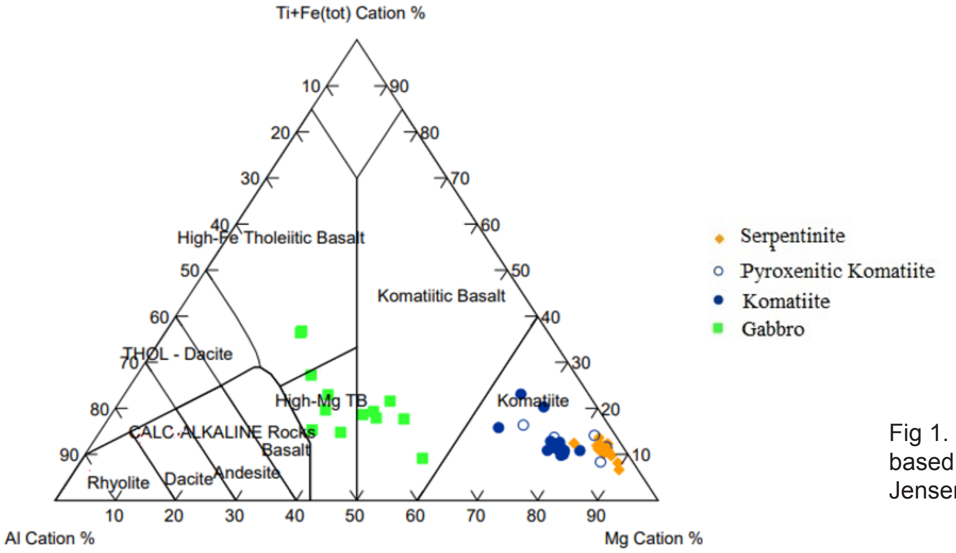

Fig 1. Rock classification based on the AFM diagram of Jensen (1976).

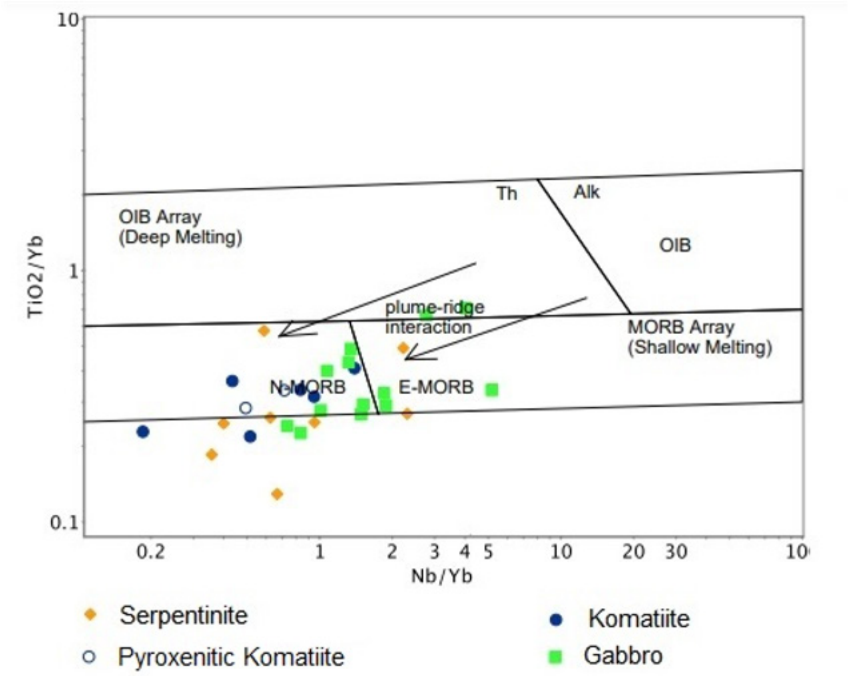

Fig 2. TiO_2/Yb vs Nb/Yb diagram for the ultramafic and mafic rocks at the Mundonguara mine.

References

Grantham, G.H., Marques, J.M., Wilson, M.G.C., Manhiça, V., Hartzer, F.J., 2011: Explanation of the Geological Map of Mozambique, scale 1:1 000 000, 1–383.

GTK Consortium, 2006: Map Explanation Volume 2. *National Directorate of Geology, Maputo, Mozambique*, 411 p.

Hofmann, A., Dirks, P. H. G. M., Jelsma, H. A., 2002: Late Archaean clastic sedimentary rocks (Shamvaian Group) of the Zimbabwe craton: First observations from the Bindura-Shamva greenstone belt. *Canadian Journal of Earth Sciences 39*, 1689–1708.

Jensen, L. S., 1976: A New Cation Plot for Classifying Sub-alkaline Volcanic Rocks. *Ontario division Mines Miscellaneous Paper 66,* 1-22.

Pearce, J. A., 2008: Geochemical fingerprinting of oceanic basalts with applications to ophiolite classification and the search for Archean oceanic crust. *Lithos, 100*, 14–48.

Zeh, A., Gerdes, A., Barton, J. M., 2009: Archean accretion and crustal evolution of the kalahari craton - The zircon age and Hf isotope record of granitic rocks from barberton/ swaziland to the francistown arc. *Journal of Petrology 50*, 933-966.

The National Till Geochemical Mapping program at SGU: producing a uniform regional scale public data set

George A. Morris[a], Anna Ladenberger[a], Merita Murtola[a], Jo Snöälv[a,b], Patrick Casey[a]

[a]Geological Survey of Sweden, Uppsala, Sweden, e-mail: george.morris@sgu.se; [b]now at Southwest Water, UK

Summary. Since 1995, the Geological Survey of Sweden has been working towards producing a uniform till (and other surficial sediments) database covering the whole of Sweden. Initially 34 elements were analysed by ICP-MS and for pH, rising to 60 elements and pH today. Considerable effort is put into ensuring that the database is level over the extended timescale of the project, including the development of an in-house standard as well as routine external quality controls on the data. All data is publicly available and recent innovations include direct provision of analyses online via SGUs Mapviewer.

Collection, analysis and data coverage

Till samples are collected from hand-dug pits from the C-horizon. Approximately 1 sample is collected per 7 km^2. In addition, samples from previous SGU surveys, held in our sample archive at Eggebyholm, and from both internal and external projects are analysed and incorporated as long as the sample collection criteria match that of the regional program. The analytical routine is developed from Swedish Standard method SS 02 83 11 (Swedish Standards Institute, 1997), adapted to suit large numbers of samples and to use modern equipment. Significant emphasis is placed on quality control, including the development of in-house standards, to ensure a level dataset, lab-blind analysis (sample randomisation) to remove systematic bias, and field repeats to monitor analytical precision and sample handling (Morris & Ladenberger, 2017).

Two separate partial leach extractions are used. Most elements are analysed from a 7M HNO_3 extraction while an Aqua Regia partial leach is used to access less soluble elements, with special focus on gold and antimony. Initially 34 elements were analysed from the HNO_3 extraction (Lax & Solenius, 2005), rising to 54 elements from HNO_3 extraction (Li, Be, B, Na, Mg, Al, P, K, Ca, Sc, Ti, V, Cr, Mn, Fe, Co, Ni, Cu, Zn, Ge, As, Se, Rb, Sr, Y, Zr, Nb, Mo, Ag, Cd, Sn, Sb, Cs, Ba, La, Ce, Pr, Nd, Sm, Eu, Gd, Tb, Dy, Ho, Er, Tm, Yb, Lu, W, Tl, Pb, Bi, Th & U) and 11 elements from Aqua Regia extraction (Cu, As, Mo, Rh, Cd, Sb, Te, Ta, Au, Bi, U). There is some overlap in analysed elements in both methods to provide a degree of internal monitoring for quality control (Morris & Ladenberger, 2017; Morris et al., in prep).

Applications

In Sweden, till covers the vast majority of bedrock to depths sometimes in excess of 50 m. Several studies have shown that till provides a good proxy for the bedrock composition with glacial transport generally only displacing the sediment 4–6 km from source. This data is therefore often used by prospecting companies to identify anomalies of interest in the sub-surface. Further, as till is the predominant surface and near-surface material in Sweden, this is the material that most people will come in contact with. As such, knowledge of the chemical composition of the till is important for agriculture, groundwater safety and sand/gravel extraction, where the till is often used as fill or surfacing material in building projects.

Till geochemistry on SGU's Kartvisare

Selected elemental and pH data is public domain and available via SGUs Mapviewer (https://apps.sgu.se/kartvisare/kartvisare-markgeokemi-regional-provtagning.html). In addition to the modern ICP-MS data, a large range of legacy data can be accessed (Fig. 1 & 2). This includes total concentration data by XRF (15 elements) as well as Aqua Regia partial leach data by ICP-AES (7 elements) and ICP-AAS (Au), and a considerable amount of data inherited from the old state prospecting company, NSG-

SGAB. Further, the entire dataset from the Geochemical Atlas of Sweden (Andersson et al., 2014) is available on line.

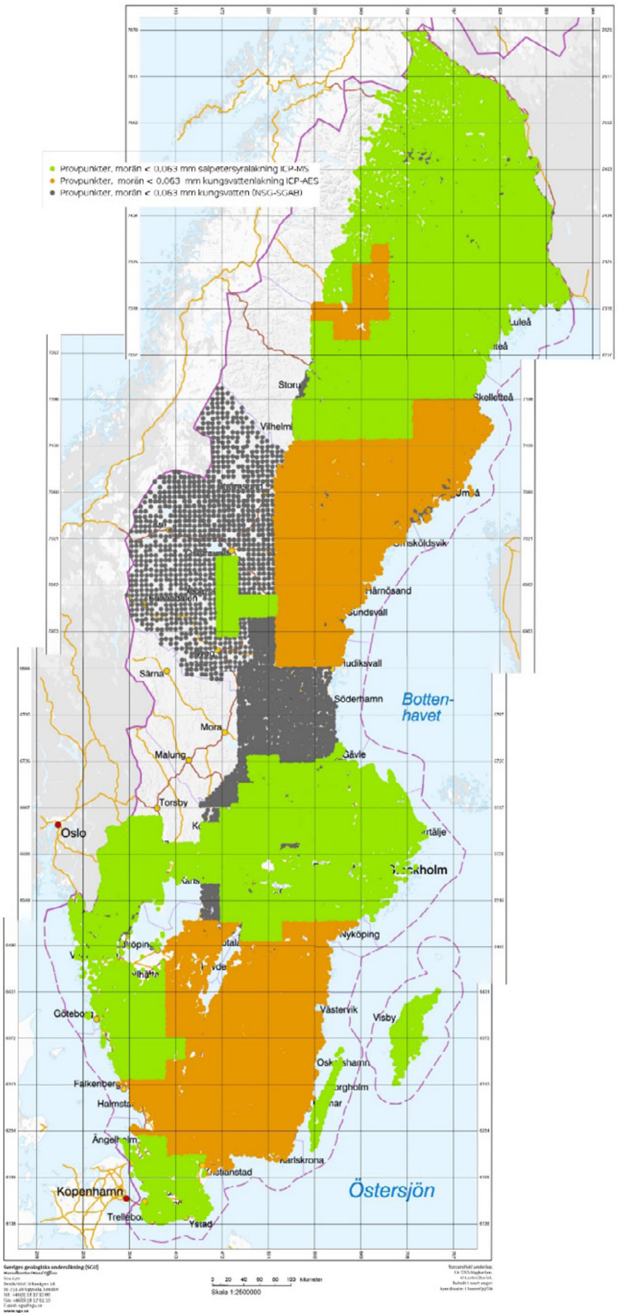

Figure 1. Current extent of data coverage by modern ICP-MS (HNO3 and Aqua Regia partial leach) in green, ICP-AES (Aqua Regia partial leach) in orange, and inherited NGS-SGAS data in grey. Image created using individual sample points with SGUs Kartvisare : https://apps.sgu.se/kartvisare/kartvisare-markgeokemi-regional-provtagning.html

Figure 2. Please scan the qr code and visit our interactive geochemistry maps on SGUs Mapviewer.

References

Andersson, M., Carlsson, M., Ladenberger, A., Morris, G.A., Sadeghi, M., Ulbäck, J., 2014: Geokemisk Altas över Sverige. SGU, 212 pp.

Lax K. & Selinus O., 2005: Geochemical mapping at the Geological Survey of Sweden. *Geochemistry: Exploration, Environment, Analysis 5*, 337–346.

Morris, G.A. & Ladenberger, A., 2017: Till Geochemistry by Nitric Acid (HNO_3) partial leaching at the Geological Survey of Sweden. *SGU-rapport: 2017:14.*

Morris, G.A. et al., in prep: Till Geochemistry by Aqua Regia partial leaching at the Geological Survey of Sweden. *SGU-rapport.*

Swedish Standards Institute, 1997: Soil Analysis – Determination of trace elements in soils – Extraction with Nitric Acid. *Svensk Standard SS 02 83 11.*

Urease aided precipitation of manganese oxides and carbonates

Anna Neubeck[a], Susanne Sjöberg[b], Sigrid Huld[a], Christophe Dupraz[b]

[a]Department of Earth Sciences, Uppsala University, Uppsala, Sweden, anna.neubeck@geo.uu.se; [b]Department of Earth Sciences, Stockholm University, Stockholm, Sweden, susanne.sjoberg@geo.su.se, sigrid.huld@geo.uu.se and christophe.dupraz@geo.su.se

Summary. Urease is a nickel-bearing extracellular and intracellular enzyme widespread in all domains of life. Its major function is the catalytic hydrolysis of urea, an important function for nitrogen assimilation. The hydrolysis of urea results in production of carbonate ions and an increase in pH, which, in the presence of Ca2+ cations, lead to precipitation of calcium carbonates. This process is not only important in nature but also a potential, eco-friendly method for industrial remediation of soils, strengthening of cement and CO2 sequestration (Onal Okyay et al. 2015).

Methods and experiment set up

Manganese oxides, play a critical role in controlling global geochemical cycling of metals and organics due to their exceptionally strong sorption and oxidative degradation properties (Jung et al. 2020). Our study investigates 1) if urease aided hydrolysis of urea may be an important pathway for producing Mn carbonates and Mn oxides in nature, 2) what mineral phases that are produced and how this is governed by parameters such as pH, kinetics etc, and 3) evaluate whether the produced precipitates could be used for industrial applications such as sequestering of CO_2 and remediation of contaminated soils (Hayes et al. 2012). In a series of experiments, the potential of urease aided precipitation of Mn-oxides and Mn-carbonates were investigated. Urease (jack bean) was dissolved in a $MnSO_4$ stock solution and mixed with urea (exp. #4, #5). Control experiments with i) pure water (exp. #1), ii) pure water + $MnSO_4$ (exp. #2), iii) pure water + $MnSO_4$ + urea (exp. #3), were also prepared. All experiments were made in triplicate. Samples were collected after 1h, 24h, 1 week and were filtered and analyzed for precipitates. All filters were treated using Leucoberbelline blue (LBB), a dye indicative of the presence of Mn-oxides.

Preliminary results and discussion

No precipitates were formed in experiment #1–2, with no added urea or urease. In experiment #3–5, precipitates were produced and the blue color from LBB spot tests indicates manganese oxidation. The change in pH from ~6 at the beginning and to ~8–9 at the end of the experiments is consistent with urease activity and concomitant pH rise. At pH>7 manganese precipitates as manganese carbonates in the precence of HCO_3^- (the dominating carbon dioxide and related species at pH between 6.4 and 10.3) and will oxidize at pH>8 (Hem 1963). Our experiments showed putative manganese oxidation already at relatively low pH (faint blue color at #3) and precipitation of various crystal morphologies (Fig.1).

In comparison with previous studies on manganese oxide/carbonate precipitation, our precipitates in #3 are consistent with the morphology of manganese carbonates (Zhu et al. 2021). Qualitative compositional analyses indicate that carbon is present, incorporated as organic carbon in the crystal structure and/or as carbonates.

The morphologies observed in experiment #4 and #5 are similar but not exactly corresponding to previous reports of manganese oxides/carbonates (Zhu et al. 2021). The major rounded cubic features are similar to what has been reported previously but with the difference of showing terassic or hillock crystal structures (Fig.1). It has been reported that nitrate precursors for manganese oxide precipitation results in more angular crystallinity than other organic precursors, such as acetate (Alwera et al. 2020), which is consistent with our results from #4 and #5 experiments.

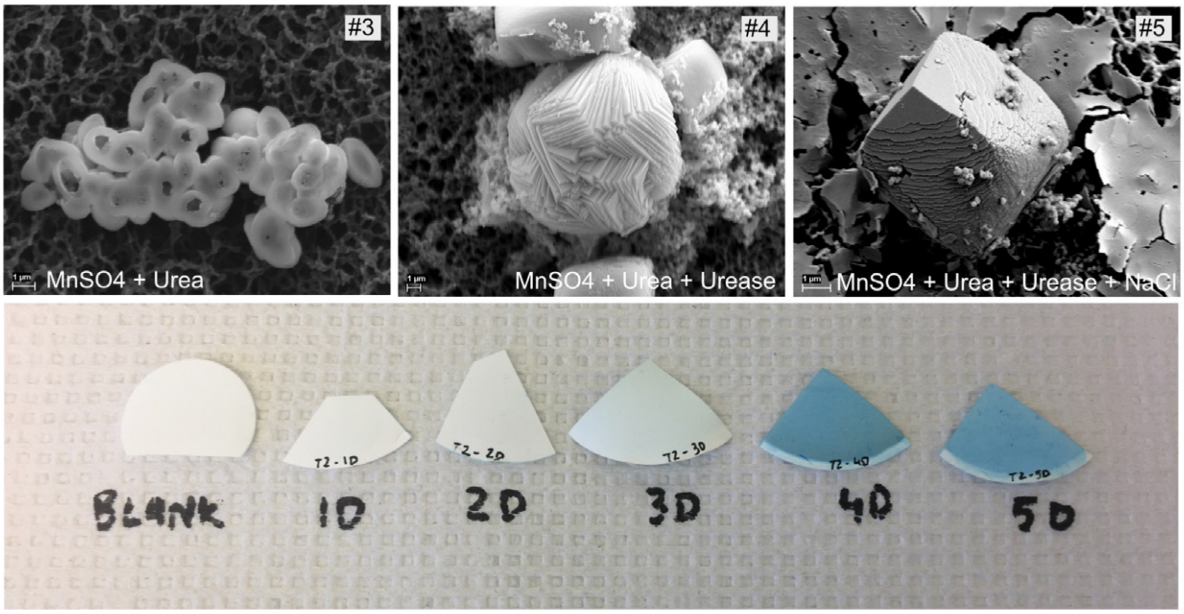

Fig.1. Images showing morphologies (upper panel) and dyed experiments (lower panel) where experiments without urease (#3) forms morphologies similar to calcite-rhodochrosite solid solutions (Zhu et al. 2021) and experiments with added urease (#4, #5) forms precipitates with terrasse or hillock structures. Blanks and experiments with only water (#1) or water + $MnSO_4$ (#2) did not show any coloration from the LBB.

The experiments show that manganese precipitates as carbonates and/or oxides, putatively with incorporated organic matter in the presence of urea and urease even at relatively low pH values (#3). Our results indicates that urea and/or urease are putatively efficient catalysts for precipitation of Mn-carbonates and/or Mn-oxides, which implies that ureloytic bacteria may be used as mild, eco-friendly binders of metal cations in soil and waste rock. Some ureolytic bacteria are also beneficial because they precipitate carbonates without ammonia emissions, which otherwise is a strong greenhouse gas and a problem in agriculture when urea is used as a fertilizer.

References

Hayes R. C., Conyers M. K., Li G. D., Poile G. J., Price A., McVittie B. J., Gardner M. J., Sandral G. A., McCormick J. I., 2012: Spatial and temporal variation in soil Mn2+ concentrations and the impact of manganese toxicity on lucerne and subterranean clover seedlings. *Crop and Pasture Science 63*, 875-885.

Jung J., Taillefert M., Sun J., Wang Q., Borkiewicz O. J., Liu P., Yang L., Chen S., Chen H., and Tang Y., 2020: Redox Cycling Driven Transformation of Layered Manganese Oxides to Tunnel Structures. *Journal of the American Chemical Society 142* (5), 2506-2513

Onal Okyay T., F. Rodrigues D., Biotic and abiotic effects on CO_2 sequestration during microbially-induced calcium carbonate precipitation, *FEMS Microbiology Ecology 91(3)*

John D. HEM (1963) Chemical equilibria affecting the behavior of manganese in natural water, *Hydrological Sciences Journal, 8:3*, 30-37

Zhu Y., Nong P., Mo N., Zhu Z., Deng H., Tang S., Yang H., Zhang L., Wang X. 2021: Dissolution and solubility of calcite-rhodochrosite solid solutions [(Ca1-xMnx)CO3] at 25 °C. *Geochemical Transactions 22:1*

Zhu T., Paulo C., Merroun M.L., Dittrich M. Potential application of biomineralization by *Synechococcus* PCC8806 for concrete restoration. *Ecol. Eng.* 2015;82:459–468

Modelled impact of climate change scenarios on hydrodynamics and water quality of the Rävlidmyran pit lake, northern Sweden

Oscar Paulsson, Anders Widerlund

Dept. of Civil, Environmental and Natural Resources Engineering, Luleå University of Technology, Luleå, Sweden
oscar.paulsson@ltu.se

Modified from: https://doi.org/10.1016/j.apgeochem.2022.105235

Summary. Predictive modelling for three climate scenarios, based on three greenhouse gas emission scenarios, was conducted for the Rävlidmyran pit lake The results indicate that the water outflow from the lake will increase, as well as the temperature in the mixolimnion. A small increase in Zn outflow (4.4%) could be observed for the highest emission scenario. The results indicate that the stratification is relatively stable, and it is predicted to remain meromictic. A sensitivity analysis indicates that a reduction of groundwater inflow element concentrations may result in a weakened stratification.

Despite that there is a large number of existing and future pit lakes, there are relatively few studies that have been published regarding numerical predictions on the evolution of pit lake water quality (Salmon et al., 2017). Climate change can be expected to impact pit lakes through changed temperature and precipitation patterns, which can influence other factors such as water balance, hydrology, limnology, and biogeochemical predictions (Copetti et al., 2013). Similar to most subarctic–arctic regions, the climate in northern Sweden is predicted to change significantly. The temperature is predicted to increase by as much as 6°C and precipitation by 20–40% until the year 2100, depending on the emission of greenhouse gases (GHG) (SMHI, 2020).

The Rävlidmyran pit lake is located in Västerbotten County, northern Sweden, where there are approximately 25–30 existing pit lakes. It has a maximum depth of 28.9 m and volume of approximately 527,000 m^3. It is meromictic with a well-mixed surface layer and a thermocline /chemocline located at a depth of 5–8 m. The lake is a flow through lake without visible surface water inlets or outlets in its normal state and the water level has reached a steady state. (Lu, 2004)

The aim of this study was to perform a long-term prediction of changes in water outflow, water column stratification and water quality of the Rävlidmyran pit lake for three climate scenarios until 2100. The climate scenarios (SMHI, 2020), which have been developed by the Swedish Meteorological and Hydrological Institute (SMHI) are based on three representative concentration pathway (RCP) GHG emission scenarios, RCP 2.6, RCP 4.5 and RCP 8.5, with predictions of temperature and precipitation (IPCC, 2014). As there were limitations on the available data used to model the pit lake the focus of the paper was to look at the overall picture and model general, potential effects of a changing climate on small to medium-sized pit lakes in a subarctic region.

The software PITLAKQ (Müller, 2020) was used to model the pit lake and the results were evaluated based on, pH, temperature, dissolved oxygen (DO), Cl, Fe^{3+}, and Zn, as well as stratification (chemocline, thermocline) and amount of water outflow. Sensitivity analyses were carried out for varying amounts of shallow groundwater inflow and element concentrations to evaluate the stability of the stratification. The modelling input is to a large extent based on actual field measurements in the Rävlidmyran pit lake during 2001–2003 (Lu, 2004). Some of the less well-known model conditions and parameters are, however, based on reasonable, best estimates of conditions in the lake.

The inflows to the pit lake used in the model were divided into shallow groundwater, deep groundwater and direct precipitation whereas the outflows were groundwater, precipitation and a surface outflow that was activated once the lake water level was rising above a certain threshold. Up until 2016, the lake was assumed to be in a steady state condition (inflow equals outflow). After that, adjustments were made to account for the predicted change in precipitation. The deep groundwater inflow was however assumed to be constant for each of the three climate scenarios.

The starting concentrations of the modelled elements were filtered samples (<0.22 μm), averaged for five depth ranges based on sampling on April 23, 2001. The inflow concentrations were average values from six sampling occasions between April 23, 2001 and March 18, 2002 (Lu, 2004). The deep groundwater outflow was used to calibrate the hydrodynamics and was adjusted to achieve a steady state assumption during 1996–2015 (initial water volume matching final water volume). The shallow and deep groundwater inflow temperatures and concentrations were adjusted to achieve a good match between measured and modelled temperature from April 23, 2001 to March 18, 2002.

The modelling results suggests that the geochemical conditions in the lake are relatively stable, and that the lake will continue to be meromictic throughout the modelled 100-year period for the three modelled climate scenarios (RCP 2.6, RCP 4.5, and RCP 8.5). No large differences in redox or oxygen levels could be observed in any of the scenarios. The sensitivity analysis suggests that lake stratification is insensitive to variations in groundwater inflow under all emission scenarios. However, it also indicates that a reduction of groundwater inflow element concentrations by 25–50% may result in a weakened stratification of the lake and episodic oxygenation of the monimolimnion. The number of days with temperatures above 12°C in the mixolimnion is predicted to increase for the higher greenhouse gas emission scenarios (RCP 4.5 and RCP 8.5). The water outflow from the pit lake is also predicted to increase, as is also the outflow of metals occurring in the lake water. For Zn the total outflow is predicted to be 4.4% higher in the RCP 8.5 scenario than in the RCP 2.6 scenario. Dilution could be observed in the higher emission scenarios, where the modelled concentration of the conservative element Cl was reduced by approximately 0.3 mg/L in the monimolimnion and was lower in the RCP 8.5 emission scenario than in the RCP 2.6 and RCP 4.5 emission scenario, both in the mixolimnion and the monimolimnion. Only minor changes in pH (~0.01 pH units) were indicated. Consequently, no significant change in pH is suggested by the model.

Although the exact values of the modelled parameters can be discussed this study suggests that predictive modelling can be used as a simulation tool to investigate possible effects on pit lake water quality under varying climatic conditions.

References

Copetti, D., Carniato, L., Crise, A., Guyennon, N., Palmeri, L., Pisacane, G., Struglia, M.V., & Tartari, G. (2013). Impacts of climate change on water quality. In *Regional assessment of climate change in the Mediterranean* (pp. 307-332). Springer, Dordrecht.

IPCC, (2014). *Climate Change 2014: Synthesis Report.* Contribution of Working Groups I, II and III to the Fifth Assessment Report of the Intergovernmental Panel on Climate Change [Core Writing Team, R.K. Pachauri and L.A. Meyer (eds.)]. IPCC, Geneva, Switzerland, 151 pp.

Lu, M. (2004). *Pit lakes from sulphide ore mining, geochemical and limnological characterization before treatment, after liming and sewage sludge treatments: cases studies at Rävlidmyran and Udden, Sweden* (Doctoral dissertation, Luleå tekniska universitet).

Müller, M. (2020). The PITLAKQ website. http://www.pitlakq.com Accessed 10th Sep 2020

Salmon, S. U., Hipsey, M. R., Wake, G. W., Ivey, G. N., & Oldham, C. E. (2017). Quantifying lake water quality evolution: Coupled geochemistry, hydrodynamics, and aquatic ecology in an acidic pit lake. *Environmental science & technology*, *51*(17), 9864-9875.

SMHI., (2020). Sveriges Meteorologiska och Hydrologiska Institut [SMHI]. *Klimatscenarier* https://www.smhi.se/klimat/framtidens-klimat/klimatscenarier/ [2020-09-16]

Mineral exploration in the glaciated terrain using upper soil and snow geochemistry

Pertti Sarala

Oulu Mining School, University of Oulu, Finland, pertti.sarala@oulu.fi

Summary. Surface geochemical sampling and analysis techniques has opened new way to do environmentally friendly and cost-effective mineral exploration in variable environments. Techniques which are based on the migration of mobile metal ions from mineralization in the bedrock through the sediment cover to the upper part of the soil can be use in exploration for all type of elements and their associations. Huge benefit is that practically all type of materials, i.e. mineral and organic sediments, plants and even snow are suitable sample media. Experiences have been good in the areas of transported cover such as in the glaciated terrains, where secondary transport distances of surface sediments can be long and complex making conventional tracing of mineralized rock sources difficult.

Introduction

Advanced, environmentally friendly sampling and budget leaching and analytical techniques provide cost-effective surface geochemical exploration method for different environments. In the glaciated terrains, conventional till geochemistry based on glacigenic secondary dispersion has been largely used, but due to variable glacial history, multiple glacial advances and complex stratigraphy, tracing the source(s) can be difficult. Instead, the surface geochemical techniques which are based on mobile metal ion migration through the upper part of bedrock and sediment cover give direct signal from underlying suboutcroping or blind mineralizations.

Mobile Metal Ions in different sample media

Different sample materials and geochemical analysis methods have been studied recently for mineral exploration in vulnerable northern areas. In addition, research is going on in new EU-funded project Sustainable exploration for orthomagmatic (critical) raw materials in the EU: Charting the road to the green energy transition (SEMACRET). The mobile metal ion based geochemical signal is seen in upper soil horizons (mineralized and organic), in different parts of plants, and in snow. Migrated metal ions accumulate first to the upper soil onto the surface of mineral grains and organic materials forming exogenic geochemical signal (Fig. 1). So called trap sites can be variable, such as surface of mineral grains, clay minerals, different hydroxides and organic material. Weakly bounded ions are possible to dissolute with weak or selective leaches. There are plenty of commercial leaching methods available for extracting metal ions from certain mineral traps. In addition, easy sampling and sample processing procedure with relative low analytical costs make the use of upper soil geochemistry effective technique in mineral exploration (Fig. 2a).

The same layer, i.e. upper soil is also a main source for nutrients which plants are collecting using roots. Plants use major and trace elements as construction materials for trunk, branches and leaves/needles. The elements which seem to be harmful or surplus are moved and stored in outer shell or extreme parts from where the plant can get rid of them most easily. These parts (e.g. bark, twigs and leaves/needles) are most promising as a sample material for mineral exploration (Fig. 2b) and used in the surface geochemistry known as a biogeochemistry.

One of the latest advances in sample media is snow. During winter time same mobile ions continue moving upward from the upper soil with water vapour and hydrocarbons to accumulate and trap into snow. Metal ions which are travelling with gases trap into snow crystals. The bottom part of the snow cover gives the most stable sampling media (Fig. 2c) because of the longest deposition history and the coverage of the upper snow layers which act as a shelter from atmospheric contamination. In addition, the lowest layer is in contact with the ground and is influenced by the gases and heat coming from the underlying soil and bedrock.

Snow covers the landscape several months each year in large areas in the Northern Hemisphere. For example, in southern Fennoscandia the snow cover exists one to three months, but in the northern parts up to seven months. Snowing periods and the snow properties are constant in a regional scale, which gives a good foundation for large and comparable geochemical exploration. Therefore, snow is a suitable sampling material in mineral exploration, and with low environmental impact, the interest and usability of snow as a sampling media increases with years (Taivalkoski et al. 2019).

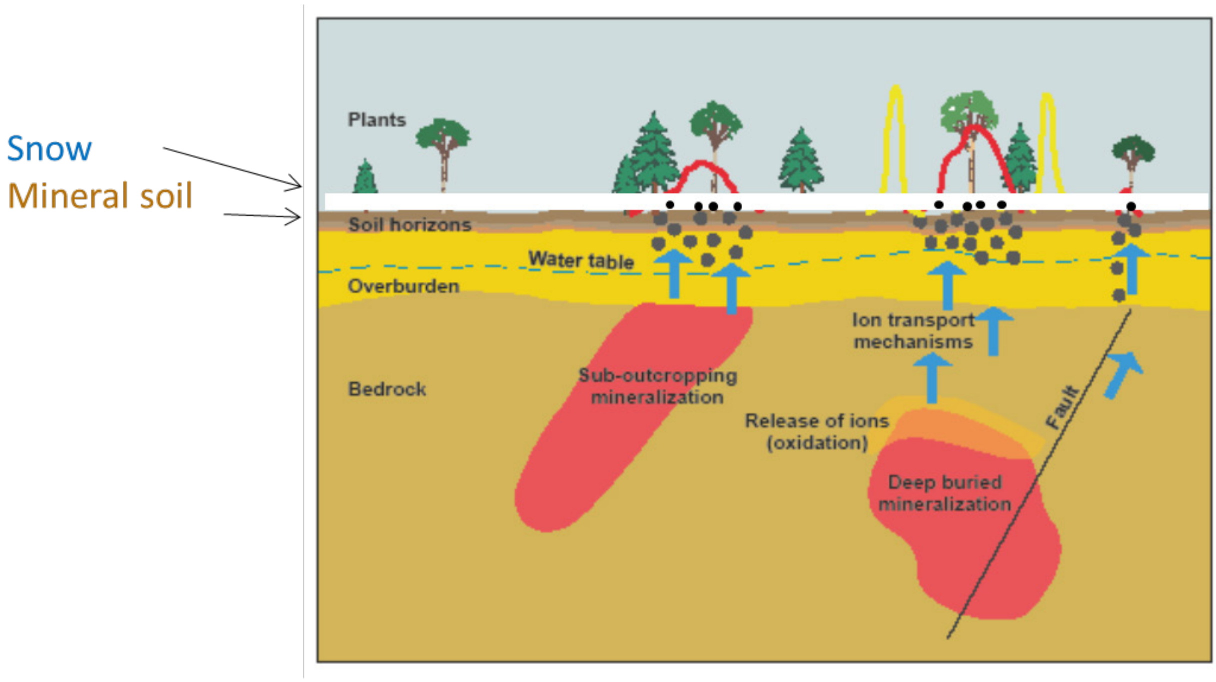

Fig. 1. Theory of Mobile Metal Ions and how they migrate through the sediment cover to upper soils, plants and snow. Modified after Heberlein et al. (2013).

Fig. 2. a) Upper soil sampling form small hand-made test pit, b) bark sampling as a part of biogeochemical sampling, and c) snow sampling using suitable acryl plastic tube. Photos by P. Sarala

References

Heberlein, D.R., Dunn, C. & MacFarlane, B., 2013: Use of organic media in the geochemical detection of blind porphyry copper-gold Mineralization in the Woodjam Property Area, South-Central British Columbia (NTS 093A/03, 06); Geoscience BC, Report 2013-20, 97 p.

Taivalkoski, A., Sarala, P., Lahaye, Y., Lukkari, S. & Sutherland, D., 2019: Snow in mineral exploration - examples and practices in glaciated terrain. Journal of Geochemical Exploration 200, 1-12.

The FOREGS Geochemical Baselines Project – 25 years of European-wide geochemical mapping

Timo Tarvainen[a], Reijo Salminen[a], Alecos Demetriades[b], Tarja Hatakka[a] , Anna Ladenberger[c] and the FOREGS Project Team

[a]Geological Survey of Finland, Espoo, Finland, timo.tarvainen@gtk.fi; [b]Institute of Geology and Mineral Exploration, Athens, Hellas; [c]Geological Survey of Sweden, Uppsala, Sweden, anna.ladenberger@sgu.se

Summary. The EuroGeoSurveys-FOREGS geochemical baseline project started in 1997 and was completed in 2006 with the publication of a two-volume atlas. For 25 years, the FOREGS dataset has provided European scientists and decision-makers with data about the chemical composition of the near-surface environment in Europe. All the data have been freely available as an electronic atlas book since 2006 and used in various projects throughout Europe.

The Geochemical Atlas of Europe 1997–2006

The FOREGS Geochemical Baseline Mapping Programme's main aim was to provide high quality, multi-purpose environmental geochemical baseline data for Europe (Salminen et al. 2005a). The FOREGS Programme was the European contribution to the IUGS/IAGC Global Geochemical Baselines Programme. It was carried out by government insitutions from 25 European countries and 3 Italian universities. The participating organisations applied standardised methods of sampling, chemical analysis and data management throughout the project.

Samples of stream water, stream sediment and three types of soil layers (humus, topsoil and subsoil) were collected from 900 small ctachments (<100 km^2). The sampling density was c. 1 sample/4700 km^2. In addition, the uppermost 25 cm of floodplain sediment was sampled from 790 sites (Salminen et al. 2005b). The floodplain sediments represented large catchments (c. 1000–6000 km^2).

The FOREGS geochemistry group had two meetings in 1997 to prepare the project: one in Aveiro, Portugal, and one in Spisska Nova Ves, Slovakia. Preliminary sampling instructions were tested on the first sampling site by Rekolanoja stream, Vantaa, Finland in July 1997. Stream water, stream sediment and all three layers of soil samples were taken from the small catchment basin. The floodplain sample was later taken from the outlet of River Vantaa in Helsinki. The final sampling manual was published in the beginning of 1998 (Salminen et al. 1998), and the sampling in most of the other participating European countries started in summer 1998.

Fig.1. The front covers of the FOREGS atlas.

Geochemical baseline maps of Europe were published as the first part of the Atlas in 2005 (Salminen et al. 2005b, Figure 1). Figure 2 shows the distribution of Co in European topsoils as an example. These maps show distinct geograhical differences in the levels of potentially harmful elements from geogenic sources and from natural processes. Interpretation of the geochemical maps were published in 2006 as the 2nd volume of the Atlas (De Vos, Tarvainen et al. 2006). One of the conclusions that it was imporant for decision-makers is that the natural variation of the element concentrations across Europe is so variable that it is difficult to define a single background or guideline value for water, soil or sediment to be applied in all countries. Both Atlas volumes as well as all the published data are freely available from a dedicated website hosted by the Geological Survey of Finland: www.gtk.fi/publ/foregsatlas. Today the data are used all over the world and by scientist from various branches of science.

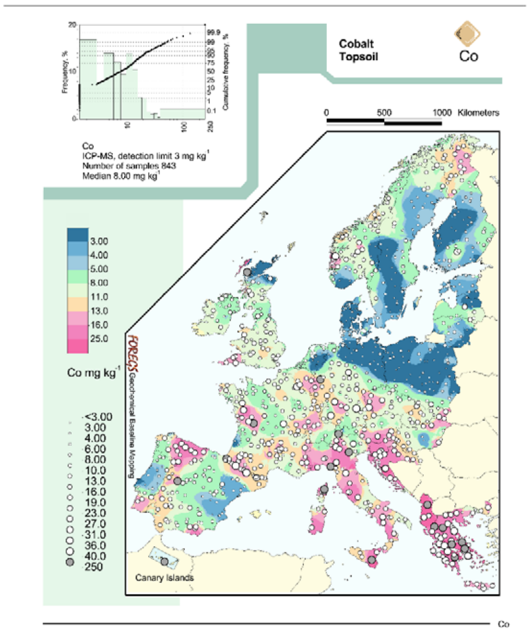

Fig. 2. Distribution of Co in topsoil in Europe. Source: The FOREGS Geochemical Baseline Mapping Programme (Salminen et al. 2005b).

References

De Vos, W.; Tarvainen, T. (Chief-editors); Salminen, R.; Reeder, S.; De Vivo, B., Demetriades, A., Pirc, S., Batista, M. J., Marsina, K., Ottesen, R.T., O'Connor, P.J., Bidovec, M., Lima, A., Siewers, U., Smith, B., Taylor, H., Shaw, R., Salpeteur, I., Gregorauskiene, V., Halamic, J., Slaninka, I., Lax, K., Gravesen, P., Birke, M., Breward, N., Ander E.L., Jordan, G., Duris, M., Klein, P., Locutura, J., Bel-lan, A., Pasieczna, A., Lis, J., Mazreku, A., Gilucis, A., Heitzmann, P., Klaver, G., Petersell, V. 2006. *Geochemical Atlas of Europe*. Part 2: Interpretation of Geochemical Maps, Additional Tables, Figures, Maps, and Related Publications. 692 p. Geological Survey of Finland. Espoo.

Salminen, R., Tarvainen, T., Demetriades, A., Duris, M., Fordyce, F. M., Gregorauskiene, V., Kahelin, H., Kivisilla, J., Klaver, G., Klein, H., Larson, J. O., Lis, J., Locutura, J., Marsina, K., Mjartanova, H., Mouvet, C., O'Connor, P., Odor, L., Ottonello, G., Paukola, T., Plant, J. A., Reimann, C., Schermann, O., Siewers, U., Steenfelt, A., Van der Sluys, J., de Vivo, B., Williams, L. 1998. FOREGS Geochemical Mapping. Field Manual. Geological Survey of Finland. Guide 47. 36 p.

Salminen, R., Demetriades, A. & Reeder, S. 2005a. Introduction. Pages 15 – 21 in Salminen, R. (chief-editor*) Geochemical Atlas of Europe.* Part 1 – Background Information, Methodology, and Maps. 526 p. Geological Survey of Finland. Espoo.

Salminen, R. (chief-editor), Batista, M. J., Bidovec, M., Demetriades, A., De Vivo, B., De Vos, W., Duris, M., Gilucis, A., Gregorauskiene, V., Halamic, J., Heitzmann, P., Lima, A., Jordan, G., Klaver, G., Klein, P., Lis, J., Locutura, J., Marsina, K., Mazreku, A., O'Connor, P. J., Olsson, S. Å., Ottesen, R.-T., Petersell, V., Plant, J. A., Reeder, S., Salpeteur, I., Sandström, H., Siewers, U., Steenfelt, A., Tarvainen, T. 2005b. *Geochemical Atlas of Europe.* Part 1: Background Information, Methodology, and Maps. 526 p. Geological Survey of Finland. Espoo.

Chemical changes and neutralization of acid-generating dredged material

Timo Tarvainen[a], Stefan Mattbäck[b], Anton Boman[b], Jan-Erik Eriksson[c], Thomas Kronberg[c], Jaakko Auri[a]

[a]Geological Survey of Finland, Espoo, Finland, timo.tarvainen@gtk.fi, [b] Geological Survey of Finland, Kokkola, Finland, anton.boman@gtk.fi, [c] Åbo Akademi University, Turku, Finland thomas.kronberg@abo.fi

Summary. Acid sulfate (AS) soils can cause severe environmental harm due to a low pH and mobilization of harmful elements (Peltola & Åström 2002). Acid sulfate soil are formed when oxidation of sulfide minerals causes a drop in pH to <4.0 (actual AS soil) or when the soil contains enough sulfide to potentially do so (potential AS soil). The various remediation methods were applied to neutralise soil excavated and deposited on land in Naantali, SW Finland.

The case study: metodology

In winter 2019–2020, during the development of a new marina in Naantali (southwestern Finland); sulfide-rich subaqueous sediments were excavated and deposited on land, forming a potential AS soil (Jarva et al. 2021). The dredged materials were draped with a thin layer of humus-rich topsoil, but two test patches were left bare for mass stabilization experiments, and oxidation progression monitoring.

The uppermost 15 cm of the dredged materials oxidized during the first year. In May 2021, samples were collected from the oxidized layer (pH 3.6) and the deeper reduced soil material (pH 5.8). Semi-total metal concentrations were studied using aqua regia extraction, whereas leachability of the same elements was studied by using a two stage batch leaching test. The leachability of Cd, Ni, and Zn had increased in the oxidized layer (Fig. 1). These metals had already dissolved while the semi-total concentration was lower in the uppermost oxidized layer after one year (Fig. 2). The same sampling was repeated in September 2021. The oxidation had progressed down to at least 25 cm and the leachability of the aforementioned metals had increased.

Neutralization tests

During a 19-week oxidation period, the influence of various amounts of neutralizing agents and industrial side stream materials (calcium carbonate, fly ash and lime kiln dust) on the dredge spoils were tested in the laboratory. Untreated dredge materials and materials mixed with smaller amounts of the neutralizing agents, acidified clearly within the oxidation period. However, several industrial side stream materials were found to be applicable for neutralization. The amount used was calculated based on the acid producing capacity of the material.

References

Jarva, J. (Ed.), Eriksson, J.-E. Ed.), Larkela, L., Auri, J., Kronberg, T., Tarvainen, T., Kuva, J., Järvinen, M., Hänninen, H., Lehtonen, M., Ketola, M. & Huhtinen, R. 2021: CircVol projekti. Ruoppausmassojen stabiloinnin kenttäkoe Naantalin Matalahdella. Geologian tutkimuskeskus, Tutkimustyöraportti 19/2021. [In Finnish] https://tupa.gtk.fi/raportti/arkisto/19_2021.pdf

Peltola, P. & Åström, M. 2002: Concentrations and leachability of chemical elements in estuarine sulfur-rich sediments, W. Finland. The Science of the Total Environment, 284 (1-3), 109–122. https://doi.org/10.1016/S0048-9697(01)00872-5

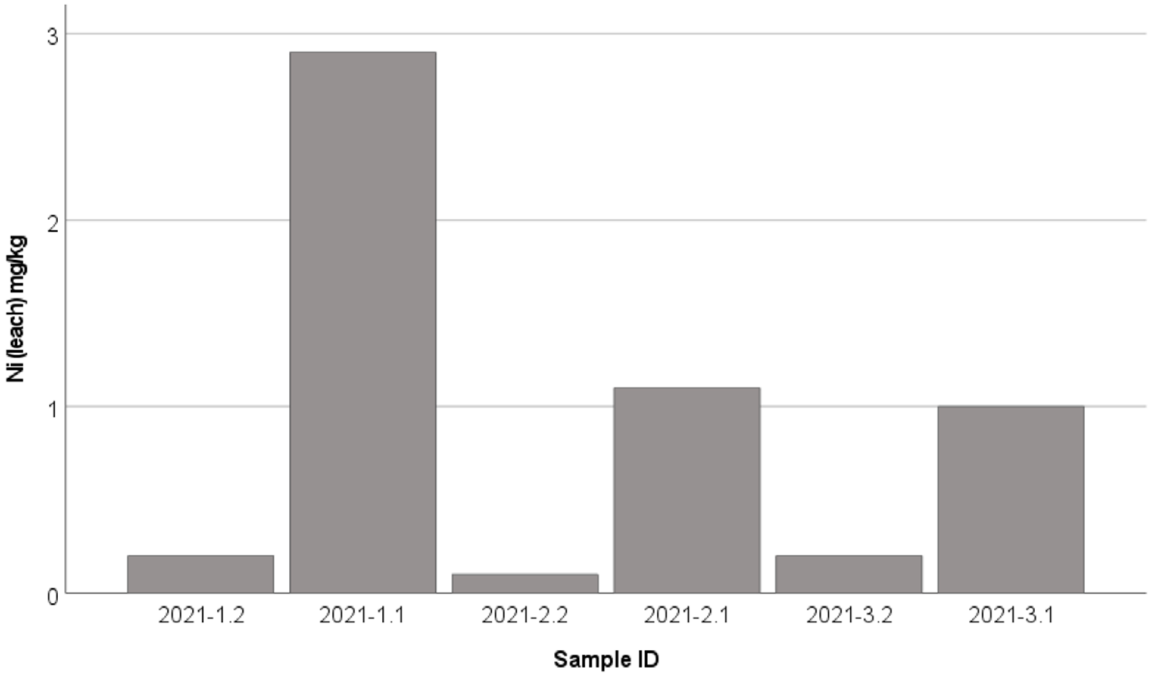

Fig. 1. Leachable Ni concentration in the oxidized layer (samples 2021-1.1, 2021-2.1 and 2021-3.1) and the deeper reduced soil material (samples 2021-1.2, 2021-2.2 and 2021-3.2) in the Naantali test site. The leachability was studied by using a two stage batch leaching test.

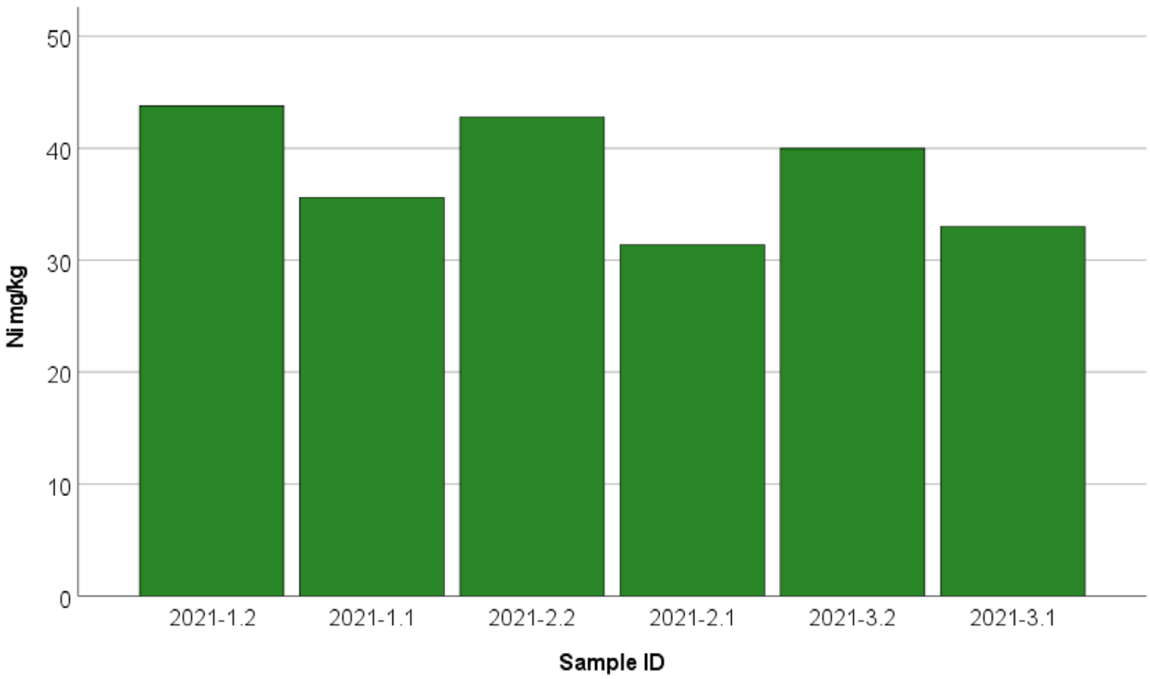

Fig. 2. Aqua regia extractable Ni concentration in the oxidized layer (samples 2021-1.1, 2021-2.1 and 2021-3.1) and the deeper reduced soil material (samples 2021-1.2, 2021-2.2 and 2021-3.2) in the Naantali test site.

Phosphorus speciation in boreal forest soils

J.R. Marius Tuyishime[a], Gbotemi A. Adediran[b], Camille Rivard[c], Jon Petter Gustafsson[a]

[a]Department of Soil and Environment, Swedish University of Agricultural Sciences, 7014, SE-75007 Uppsala, Sweden, marius.tuyishime@slu.se and jon-petter.gustafsson@slu.se; [b]UK Centre for Ecology and Hydrology, Wallingford OX10 8BB, United Kingdom, GboAde@ceh.ac.uk; [c]Synchrotron SOLEIL, L'Orme des Merisiers, Saint Aubin BP 48, 91192 Gif-sur-Yvette Cedex, France, camille.rivard@synchrotron-soleil.fr.

Summary. Phosphorus (P) is a rock-derived nutrient that plants need to build their biomass; however, the occurrence of Al/Fe surface minerals limits P availability to plants, particularly in acidic podzolized soils. These minerals have a strong affinity for dissolved P. By using chemical extractions and X-ray fluorescence/ spectroscopy to study P distribution and speciation in the bulk and micro soil environment, we showed that despite the young age of Swedish forest soils (<15,000 years), reactive apatite in the upper 30 cm has been transformed mainly to Al-bound P, but also to Fe-bound P.

Lithogenic apatite is the primary source of P in natural soils (Walker & Syers 1976). As the forest ecosystem develops the pool of apatite-bound P weathers and gradually declines. Part of this dissolved P is simultaneously retained on the surfaces of secondary Al and Fe minerals (Walker & Syers 1976). To fully understand the processes leading to nutrient limitation in boreal forests, which has often been attributed to nitrogen (N), a detailed knowledge of P chemistry is required. However, it is s difficult to precisely quantify the chemical P composition in the bulk soil when using macroscale analyses such as chemical extractions. Spectroscopic methods such as P *K*-edge XANES spectroscopy on bulk samples may be able to more precisely provide the P speciation, but still there are uncertainties, for example it is difficult to distinguish Al-bound P from Fe-bound P (Gustafsson et al. 2020, Tuyishime et al. 2022).

The objective of this study is to examine how post-glacial soil formation influenced the distribution of P species in forest soils, in particular the formation of secondary Al-, and Fe-bound P phases. Two podzolized soil profiles from Flakaliden and Skogaby sites in northern and southern Sweden, respectively, were used to study the microscale distribution of P, Al, and Fe and the P speciation at the selected micro P-spots. We used micro X-ray fluorescence (µ-XRF) imaging at the P *K*-edge energy, and spotwise µ-XANES. The results were compared to those obtained from bulk P *K*-edge XANES (Tuyishime et al. 2022) and chemical extractions. The latter two were also used to estimate the concentration of reactive apatite from apatite inclusion in weathering-resistant minerals such as quartz.

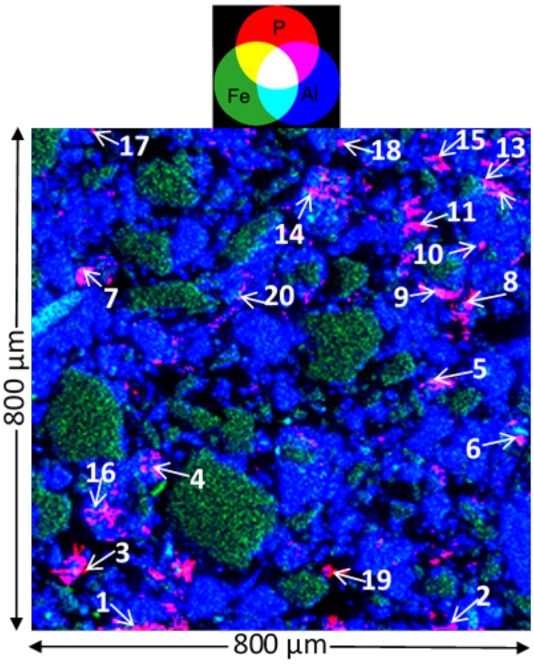

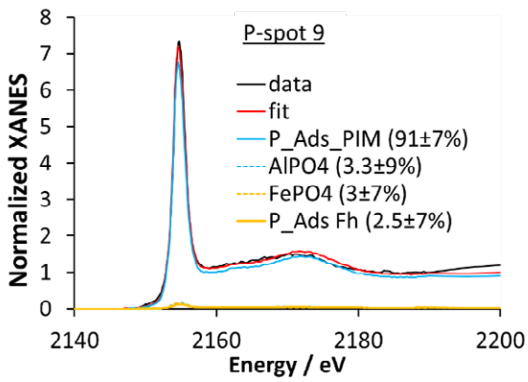

Figure 1: Tricolor µ-XRF map of P (red), Al (blue), and Fe (L-edge) (green) of the thin-section from the B horizon (20–30 cm) of Flakaliden soil profile. Numbers 1 to 20 indicate selected P-points to which µ-P K-edge XANES was applied. P_Ads PIM and P_Ads Fh: P adsorbed protoimogolite and ferrihydrite.

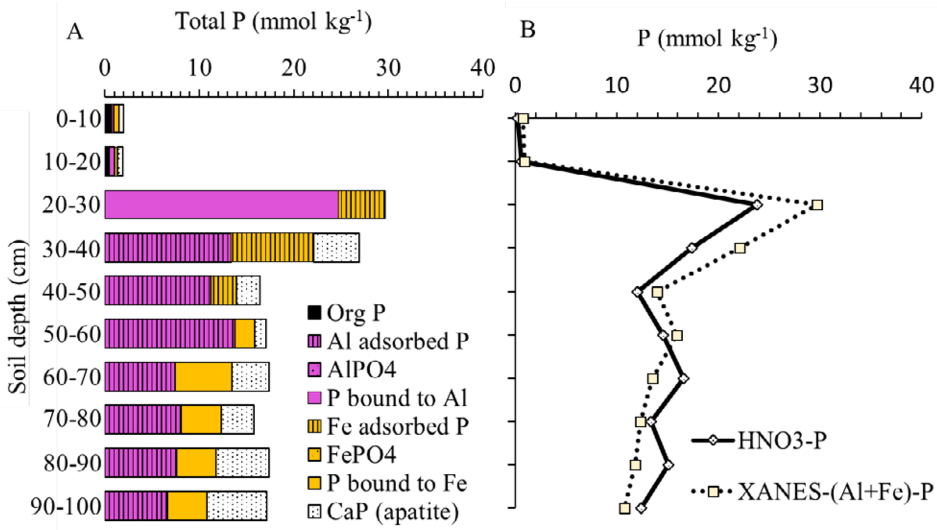

Figure 2A: Relative contributions of different P species to the total P in Flakaliden soil according to bulk P *K*-edge XANES. Org P: organic P, P bound to Al or P bound Fe indicate the sum of all Al-bound P or Fe-bound P when the uncertainty to differentiate the adsorbed and precipitated P forms is large. 2B: XANES-(Al+Fe)-P: the sum of all P bound on Al and Fe according to bulk XANES. The difference between the concentration of HNO_3-extractable P and XANES-(Al+Fe)-P is assigned to reactive apatite.

The µ-XRF map (Figure 1) shows that P mainly co-occurs with Al and, to a lesser extent, with Fe. P seems to occur on their surfaces or somehow mix with them. This is shown by the predominance of the pink-colored P-spots, indicating P and Al colocalization, mainly in the B horizons. Yellow-colored P-spots, although fewer, indicate that P co-occurs with Fe. For some thin sections, especially from the upper 10 cm, some P spots are located in the background space. Those P-spots are mostly red. We found also the red P-spots at a deeper depth, but they do mostly co-occur with Al or Fe. The red color suggests P species other than Al- and Fe-bound P e.g. organic P or apatite, but Ca was not modeled.

The P *K*-edge µ-XANES spectra obtained from the pink-colored P-spots mostly resemble those from Al-bound P reference standards, mainly P adsorbed on protoimogolite (PIM). These spectra are very intense. The P associated with Al contributed between 61 and 72% of the total P weight in the B horizons. At many of the yellow P spots, the spectra show a small pre-edge, indicating that Fe-bound P is detectable. Further, the µ-XANES analysis showed that organic P dominated in many red P-spots in the surface soils. At a deeper depth (C horizon), however, most of the spectra showed a post-edge. These features were also found in some of the P-spots in the upper soil. That is characteristic of apatite.

These results are consistent with those obtained from bulk P *K*-edge XANES (Figure 2) (Tuyishime et al. 2022), although the latter method could not always distinguish the Al- and Fe-bound P with certainty. We also showed that no reactive apatite remains in the top and B horizons. HNO_3-P method allows estimating reactive apatite but can also include some Al-, and Fe-P. This was corrected by combining this method and bulk XANES. Any detectable apatite in the upper mineral soil is probably held as an inclusion in quartz.

In conclusion, despite the young age of Swedish forest soils (<15,000 years), reactive apatite in the upper 30 cm has been transformed mainly to Al-bound P, which is dominated by P adsorbed to protoimogolite, and to a lesser extent to Fe-bound P.

References

Gustafsson, J. P., Braun, S., Tuyishime, J.R.M, Adediran, G. A., Warrinnier, R. & Hesterberg, D, 2020: A probabilistic approach to phosphorus speciation of soils using P K-edge XANES spectroscopy with linear combination fitting. *Soil Systems,* 4**,** 26.

Tuyishime, J.R. M., Adediran, G. A., Olsson, B. A., Spohn, M., Hillier, S., Klysubun, W. & Gustafsson, J. P, 2022: Phosphorus abundance and speciation in acid forest Podzols–Effect of postglacial weathering. *Geoderma,* 406**,** 115500.

Walker, T. & Syers, J. K.,1976: The fate of phosphorus during pedogenesis. *Geoderma,* 15**,** 1-19.

Investigating sources of riverine mercury in the Mackenzie River Basin, Canada, with isotopic (Hg, ^{14}C) and other markers

Christian Zdanowicz[a], Staffan Åkerblom[b], Audrey Campeau[a,c], Karin Eklöf[d], Anne Soerensen[e], Holger Hintelmann[f], Shengliu Yuan[f]

[a]Department of Earth Sciences, Uppsala University, Uppsala, Sweden, christian.zdanowicz@geo.uu.se; [b]Statistiska Centralbyrån, Stockholm, Sweden, Staffan.Akerblom@scb.se; [c]Department of Forest Ecology and Management, Swedish University of Agricultural Sciences, Umeå, Sweden; audrey.campeau@slu.se; [d]Department of Aquatic Sciences and Assessment, Swedish University of Agricultural Sciences, Uppsala, Sweden, Karin.Eklof@slu.se [e]Department of Environmental Research and Monitoring, Swedish Museum of Natural History, Sweden, anne.soerensen@nrm.se; [f]Water Quality Centre, Trent University, Peterborough, Canada, hhintelmann@trentu.ca.

Summary. The Arctic stores vast amounts of mercury (Hg) bound with organic carbon (OC) in soils, some of which could be released in water by climate warming, with risks to ecosystems. We investigated dissolved and particulate riverine mercury (DHg, PHg) and OC (DOC, POC) in the Mackenzie River Basin using Hg isotopes (δ^{202}Hg , Δ^{199}Hg) and radiocarbon (Δ^{14}C-OC). We found that most Hg is transported as PHg with aged OC, suggesting sedimentary rocks and permafrost as the sources. In contrast, DHg is associated with mostly modern OC and carries Hg isotopic signatures of recent atmospheric deposition.

Goals, materials and methods

Over 7000 Mg of Hg may be stored in circumarctic permafrost soils, which, as they warm, could release Hg into waterways and the Arctic Ocean, and lead to higher exposure of aquatic fauna and Arctic people (Dastoor et al. 2022). However predicting Arctic riverine Hg releases is hampered by limited knowledge of its specific sources and mobilization pathways. To address this issue, we investigated sources of Hg in streams of the Mackenzie River Basin (MRB), Canada, a permafrost region that is presently warming at 3–4 times the mean hemispheric rate. In the summers of 2018–2019, we sampled surface waters and suspended sediments from 17 river sites across parts of the MRB (Fig. 1), and we analyzed these waters for dissolved and particulate levels of Hg (DHg, PHg) and its stable isotope ratios (Δ^{199}Hg, δ^{202}Hg), the radiocarbon content of OC, (Δ^{14}C-DOC,-POC) and optical properties of DOC (Campeau et al., 2021, 2022).

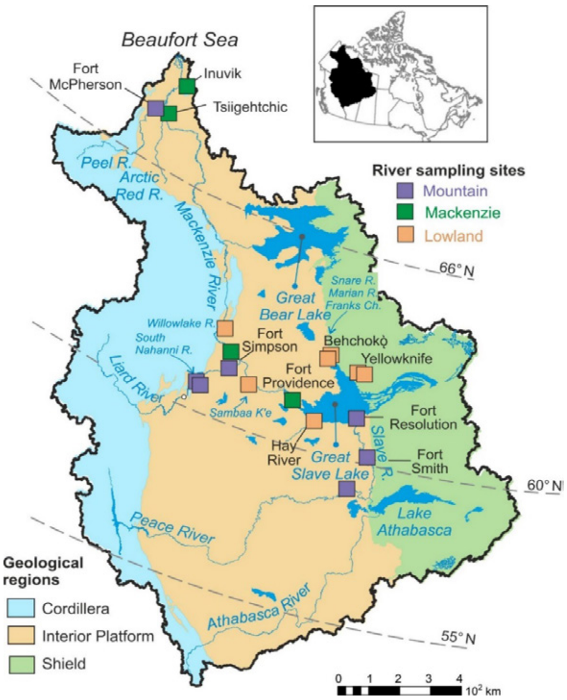

Fig. 1. Location map of the Mackenzie River Basin in northwestern Canada, showing major geological regions (colored shading), lakes and rivers. The Mackenzie River proper begins at the outlet of Great Slave Lake (Fort Providence) and empties in the Beaufort Sea north of Inuvik. Colored squares indicate the sites where river water and suspended sediments were collected during the summers of 2018 and 2109 (Some sites are not distinct at the map scale). The color codes separate the sampled rivers in three categories: Those with their headwaters in the western Cordillera ("Mountain" rivers), those with headwaters in the Interior Platform and/or the eastern Shield ("Lowland" rivers), and the Mackenzie River itself, which receives and blends water and suspended ediment contributions from all three geological regions.

Key findings and implications

We found the largest riverine Hg loads of the MRB are in the Mackenzie River itself near its mouth, and in its large, turbid tributaries fed from waters issued from the western Cordillera (e.g. Peel, Slave and Arctic Red rivers). The Hg in these rivers is primarily PHg (>85%) and correlated with the apparent mean age (^{14}C-depletion; Δ^{14}C) of suspended POC. The PHg isotopic signature also resembles that of borest forest and Arctic tundra soils (Fig. 2). This suggests that this PHg is primarily released by erosion from OC-rich sedimentary rocks (e.g. shales, coal) and the thawing of relatively old permafrost soils in western and northern parts of the MRB. Rivers issued from the Interior Platform and the Canadian Shield lowlands carry much less Hg, with larger shares of DHg, the latter being associated with mostly moderm OC, and bearing Hg stable isotope signatures that resemble those of recent atmospheric deposition (gas phase or precipitation). In the dissolved fraction of rivers, older DOC is associated with higher molecular weight, aromaticity and humic content, and likely has higher DHg-binding potential.

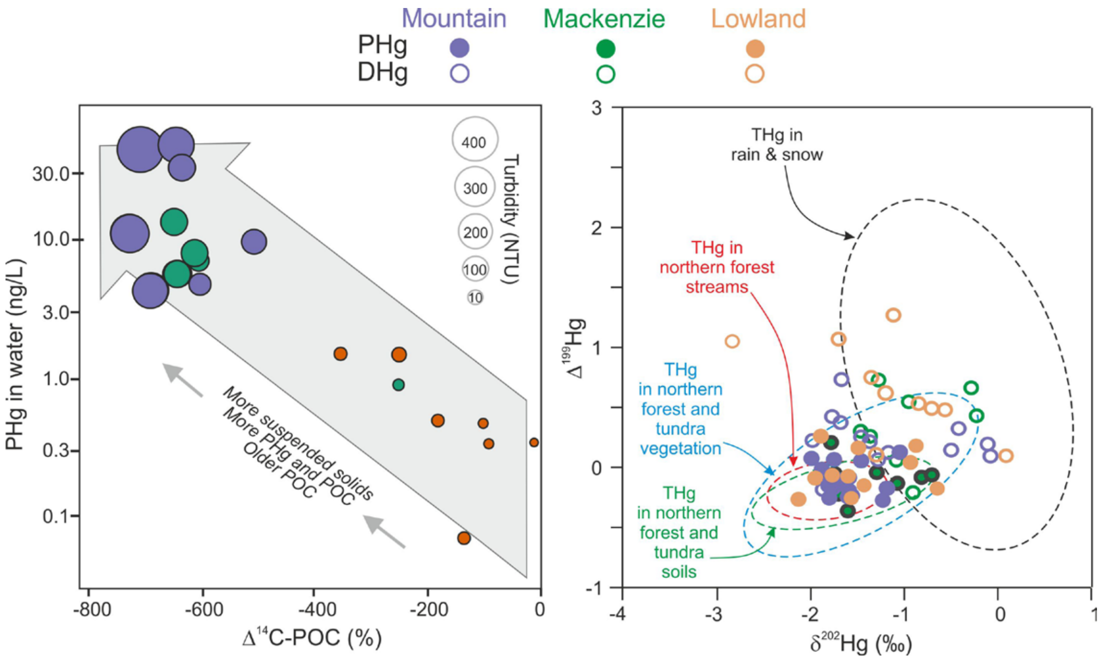

Fig. 2. Left: Plot showing the relationship between PHg levels and the ^{14}C content of POC (Δ^{14}C) in rivers of the Mackenzie Basin. Right: Scatter plot of the stable Hg isotope composition of DHg and PHg (δ^{202}Hg, Δ^{199}Hg) in the same rivers, compared with the range of isotopic signatures in different environmental pools of Hg, as documented in landscapes of North America and northern Europe. Rivers are color-coded as in Fig. 1.

Collectively, our findings imply that Hg entering the Mackenzie River and being discharged to the Beaufort Sea is primarily sourced from the western, more rugged parts of the MRB via riverbank erosion and/or abrupt permafrost thaw (e.g. St. Pierre et al. 2018). Future climate-driven changes in landscape and hydrological conditions across this region (e.g. higher freshet peak discharge, soil thaw subsidence, forest fires) will therefore likely have a disproportionately large impact of riverine Hg loads, and need to be closely monitored.

This project was supported by FORMAS grants 2017-00660 and 2019-01529.

References

Campeau, A. *et al.* 2022: Sources of riverine mecury across the Mackenzie River Basin: Inferences from a combined Hg-C isotopes and optical properties approach. *Science of the Total Environment 806*, 150808.

Campeau, A. *et al.* 2021: Controls on the ^{14}C-content of dissolved and particulate organic carbon mobilized across the Mackenzie River basin, Canada. *Global Biogeochemical Cycles 34*, e2020GB006671.

Dastoor, A. *et al.* 2022: Arctic mercury cycling. *Nature Reviews Earth & Environment 3*, 270–286.

St. Pierre, K. *et al.* 2018: *Environmental Science and Technology 52*, 24, 14099–14109.

Thematic Session 6
Geochronology and isotope geology

Session Chairs:
Renaud Merle (renaud.merle@geo.uu.se)
Martin Whitehouse (martin.whitehouse@nrm.se)

Enriched Archean mantle below northern Sweden; Hf isotopic evidence

Ulf B. Andersson[a], Zmar Sarlus[b,c], Tobias E. Bauer[b], Yann Lahaye[d]

[a]Luossavaara-Kiirunavaara AB, SE-98186 Kiruna, Sweden, ulf.b.andersson@lkab.com; [b]Division of Geosciences & Environmental Engineering, Luleå University of Technology, SE-971 87 Luleå, Sweden, zmar.sarlus@ltu.se; [c]Svensk Kärnbränslehantering AB, Evenemangsgatan 13, Box 3091, 169 03 Solna, Sweden; [d]Geological Survey of Finland, Betonimiehenkuja 4, PL96 02151 ESPOO, Finland; yann.lahaye@gtk.fi

Summary. Hf isotopes of zircon in 1.9–1.8 Ga mafic-intermediate rocks from northernmost Sweden show consistently sub-chondritic ε_{Hf} data with a limited spread, interpreted as indicating extraction from old (Archean), enriched mantle sources, underlying the region. Associated felsic rocks show much larger variations, indicating combined origins in the Archean crustal basement and more juvenile crustal sources.

Background – results

In northernmost Sweden (and neighbouring areas), north of the Luleå-Jokkmokk zone, defined as an Archaean-Proterozoic palaeoboundary (APPB) (Mellqvist et al. 1999), the outcropping Svecofennian successions have been shown to be underlain by an Archaean crustal basement, a basement that is exposed only in a few small areas (Bergman & Weihed 2020). However, little is known about the nature of the underlying mantle in the region, a mantle that has contributed mafic-intermediate magmas to the crust at various times from the Archaean to at least to c. 1.8 Ga.

We have analysed Hf isotopes in zircons from 1.90–1.77 Ga igneous rocks of felsic to mafic compositions from the Gällivare area, north of the APPB. Among these, and other data from the region, the great majority of initial ε_{Hf} data plot below CHUR, being low-radiogenic, irrespective of compostion. Furthermore, the data plot almost completely below the field of the equivalent rocks of the Svecofennian juvenile crust in southern Sweden (Fig. 1). This character is most coherently shown by the mafic-intermediate rocks. Recalculated to 1.80 Ga, few are outside the range $\varepsilon_{Hf} = -6 \pm 3$ (Fig. 2).

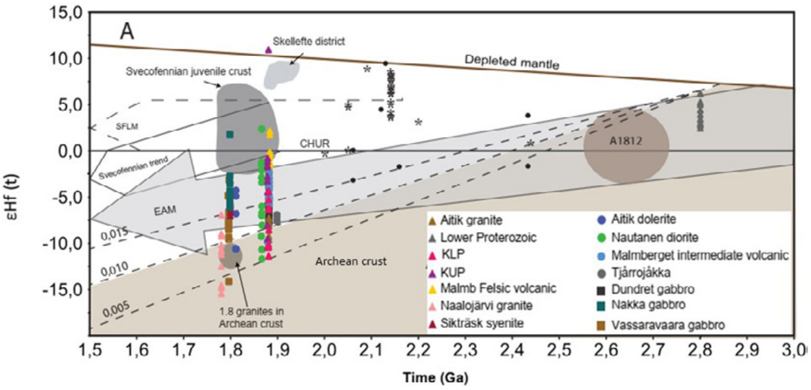

Figure 1. ε_{Hf} vs. time showing various potential sources and evolutionary trends. Additional data and sources as in Sarlus et al. (2018). A1812 is mafic rocks of the Archean Pudasjärvi complex. The upper limit of the Archean crust can be defined by various $^{176}Lu/^{177}Hf$ ratios other than the normal 0.015. Laurent et al. (2019) proposed a value as low as 0.005, based on Archean basement data just north of the study area. KLP and KUP are felsic metavolcanic rocks from the Kiruna area.

In contrast, the felsic rocks show a larger spread, with a large set of data at low values around $\varepsilon_{Hf} = -9$ and another set just below zero.

Discussion and conclusions

Among the *felsic rocks* the spread of values both between and within samples is large (see Figs.). Certain samples, such as the Aitik and Naalojärvi granitods, derive dominantly from the Archean crustal basement, while others (e.g. the Malmberget felsic volcanite) have significantly higher proportion juvenile material. This indicates that, in addition to the Archean basement, some post-Archean crustal source material has to be available at depth, similar to that observed in southern Sweden (Andersen et al. 2009), since the involvment of large fractions of mantle magmas in such silicic rock are unlikely. No such juvenile material is known in the region, except for the 2.45–2.0 Ga greenstone rocks and associated sediments, which may thus be contributing to later crustal magmas.

In contrast, the *mafic-intermediate rocks* show a much more condensed distribution of ε_{Hf} values (Fig. 2), with only few outliers. This does not support an origin by mixing of the Archean crustal basement with the depleted mantle (DM) as this would result in a much wider scatter of values. Instead, we infer that the sources for these rocks are to be found in an enriched Archean mantle (AEM), underlying at least parts of the region. The enrichment thus occurred through subduction fluids rejuvenating a DM already at 2.8–3.0 Ga, or earlier (Fig. 1), where the 2.7–2.6 Ga mafic rocks of the Pudasjärvi complex (Lauri et al. 2011) can be taken as an early example of extraction of such a mantle. Using the latter as a starting point and the 1.9–1.8 Ga rocks analysed in this study, an evolutionary slope of $^{176}Lu/^{177}Hf$ for this proposed AEM can be calculated to c. 0.024 (Fig. 1). This is low, but not unreasonable for strongly enriched mantle sections (e.g. Schmidberger et al. 2002). The limited spread outside the bulk of the data can be accounted for by small local contributions from Archean crustal sources or less enriched mantle material.

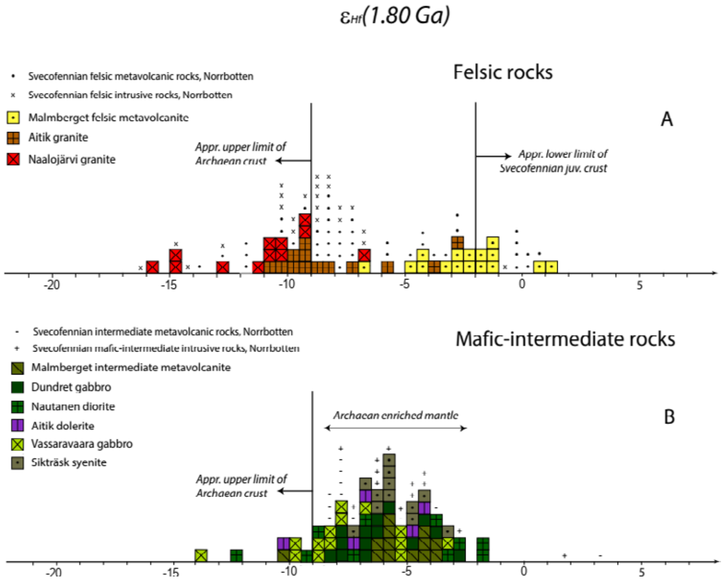

Figure 2. ε_{Hf} data recalculated to 1.80 Ga for all rocks from this study (coloured squares). Additional data for comparison (Westhues et al 2017; Sarlus et al. 2018). Upper limit of Archean crust and lower limit of Svecofennian juvenile crust are from Andersen et al. (2009). The proposed Archean enriched mantle source has approx. $\varepsilon_{Hf}(1.8) = -6\pm3$.

In conclusion, in addition to the established presence of an Archean crustal basement north of the APPB, more juvenile sources can be traced in felsic rocks in the region. We infer, based on the limited spread of initial ε_{Hf} and consistently low values of the mafic-intermediate rocks, that these derive from mantle sections enriched in the Archean and underlying the Archean crustal basement in the region.

References

Andersen, T., Andersson, U.B., Graham, S., Åberg, G. & Simonsen, S.L., 2009, Granitic magmatism by melting of juvenile continental crust: New constraints on the source of Palaeoproterozoic granitoids in Fennoscandia from Hf isotopes in zircon: *Journal of the Geological Society of London, v. 166,* 233–247.

Bergman, S. & Weihed, P., 2020: Archean (>2.6 Ga) and Paleoproterozoic (2.5-1.8 Ga), pre- and syn-orogenic magmatism, sedimentation and mineralization in the Norrbotten and Överkalix Lithotectonic units, Svecokarelian orogen. *Geological Society, Memoir 50,* 27-81.

Laurent, O., Vander Auwera, J., Bingen, B., Bolle, O. & Gerdes, A., 2019: Building up the first continents: Mesoarchean to Paleoproterozoic crustal evolution in West Troms, Norway, inferred from granitoid petrology, geochemistry and zircon U-Pb/Lu-Hf isotopes. *Precambrian Research 321*, 303-327.

Lauri, L.S., Andersen, T., Hölttä, P., Huhma, H., & Graham, S., 2011: Evolution of the Archaean Karelian province in the Fennoscandian Shield in the light of U–Pb zircon ages and Sm–Nd and Lu–Hf isotope systematics. *Journal of the Geological Society London v. 168,* 201–218.

Mellqvist, C., Öhlander, B., Sköld, T. & Wikström, A., 1999: The Archaean–Proterozoic Palaeoboundary in the Luleå area, northern Sweden: field and isotope geochemical evidence for a sharp terrane boundary. *Precambrian Research v. 96*, 225–243.

Sarlus, Z., Billström, K., Martinsson, O., Andersson, U.B., Bauer, T., Lahaye, Y., Belousova, E. & Evins, P., 2018: Variably old components in mafic-felsic magmas; evidence from north of the Archean-proterozoic paleoboundary, northern Norrbotten, Sweden. In, Z. Sarlus: Timing and origin of igneous rocks in the Gällivare area, northern Sweden. *Doctoral thesis, Luleå Univ. of Technology,* 24 pp.

Schmidberger, S. S., Simonetti, A., Francis, D. & Gariépy, C., 2002: Probing Archean lithosphere using the Lu–Hf isotope systematics of peridotite xenoliths from Somerset Island kimberlites, Canada. *Earth and Planetary Science Letters 197,* 245-259.

Westhues, A., Hanchar, J. M., LeMessurier, M. J. & Whitehouse, M. J., 2017: Evidence for hydrothermal alteration and source regions for the Kiruna iron oxide–apatite ore (northern Sweden) from zircon Hf and O isotopes. *Geology v. 45*, 571-574.

LA-ICP-MS U-Pb geochronology of the COSC-1 drillcore, Åre, Sweden

David G. Gee[a], Anna Ladenberger[b] , Yuan Li[c], Iwona Klonowska[d], Pauline Jeanneret[a]

[a]Department of Earth Sciences, Uppsala University, Uppsala, Sweden, David.Gee@geo.uu.se; [b]Department of Mineral Resources, Geological Survey of Sweden, Uppsala, Sweden, anna.ladenberger@sgu.se; [c]State Key Laboratory for Continental Tectonics and Dynamics, Chinese Academy of Geological Sciences, Beijing, China; [d]Faculty of Geology, Geophysics and Environmental Protection, AGH – University of Science and Techonology, Kraków, Poland, klonowska@agh.edu.pl

Summary. The ICDP-COSC-1 drilling project in western Jämtland, penetrated 2500 m of metasediments, amphibolites and gneisses of the Lower Seve Nappe. The psammitic schists and orthogneisses as well as amphibolites have been analysed by LA-ICP-MS. U-Pb geochronology of zircons in these lithologies provides evidence of two main stratigraphic units, one with polymodal age distribution typical of the Middle Seve metasediments and lower units with unimodal Sveconorwegian ages. Orthogneisses record mid Ordovician magmatism and amphibolites point to the Caledonian migmatitic event in the overlying Middle Seve.

Results and discussion

The ICDP - Collisional Orogeny in the Scandinavian Caledonides (COSC-1) drilling project, targeting the lower part of the Seve Nappe Complex (SNC) in western Jämtland, near Åre (Fig.1), penetrated c. 2500 m of mainly psammitic metasediments, amphibolites and a few felsic, pegmatitic/leucogranitic orthogneiss intrusions.

U-Pb dating by LA-ICP-MS of detrital zircons in these Seve metasediments provides evidence of the two main stratigraphic units in the drill cores (Fig. 2). The upper section, down to a depth of c. 1660 m, is dominated by a polymodal age distribution which is common in the Särv (Be'eri-Shlevin et al. 2011) and Middle Seve Nappes (Ladenberger et al. 2014), with dominant Sveconorwegian (early Neoproterozoic to late Mesoproterozoic, c. 900–1100 Ma) and early Mesoproterozoic to late Palaeoproterozoic ages (c. 1400 and 1800 Ma). The lower section has exclusively unimodal distribution with Sveconorwegian detrital ages and only minor representation of both older (Proterozoic and Archean) and younger (Palaeozoic) ages. The latter are similar to those in the Caledonian Middle Ordovician turbidites of the underlying Lower Allochthon that had been derived from the hinterland during early thrusting. These results are in a good agreement with previous investigations of the SNC (Gee et al. 2014) and also the Särv Nappes (Be'eri-Schlevin et al. 2011) in central Jämtland, near the border to Västerbotten (Kirkland et al. 2011) and southern Norrbotten (Gee et al. 2015). The zircon populations are nearly all dominated by Sveconorwegian signatures; many also have a strong late Palaeoproterozoic component and, at the base of the hole, a few significant late Archean zircon ages.

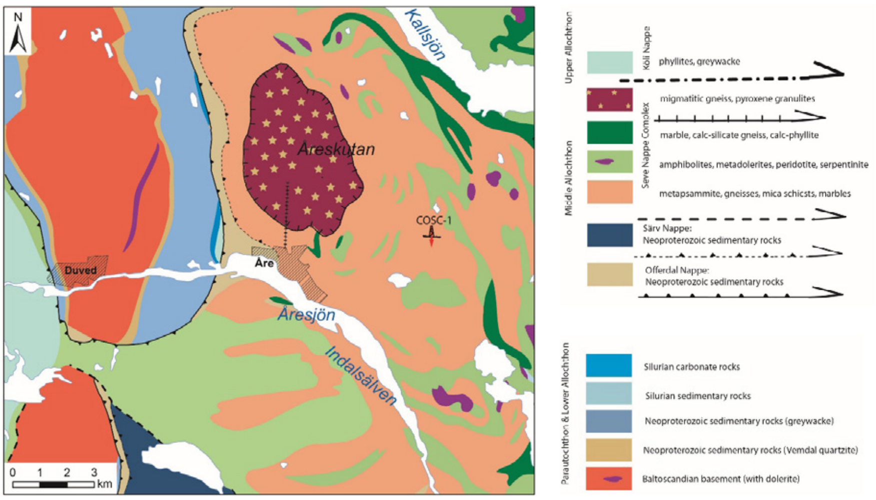

Fig.1. Geological map of the study area (modified digital 50,000–250,000 bedrock map; Geological Survey of Sweden) with the COSC-1 drill site location.

The felsic intrusions (now orthogneiss) of c. 445–460 Ma cut the sediments in several locations and provide evidence of Ordovician magmatism (Li et al., 2021). The age of two amphibolites (gabbro-basalt precursors) is difficult to constrain because they have been subject to a complex metamorphic history; however, they point clearly towards a Caledonian origin.

Along with the data from the Kalak Nappe Complex correlatives of the SNC and Särv Nappes in northernmost Norway (Kirkland et al 2011), the new data emphasize the common character of the provenance of the sediments in all these nappes, derived from the outer margin of Baltica. In this context, it is important to bear in mind that prior to the opening of the Iapetus Ocean in the late Neoproterozoic (c. 600 Ma), Laurentia and Baltica may well have been proximal.

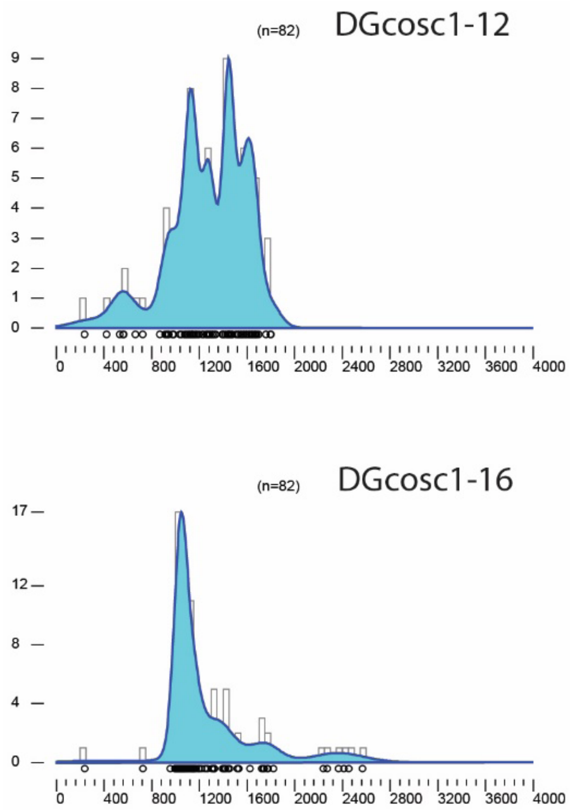

Fig. 2. Examples of detrital ages in the upper (at 1306 m depth) and lower part (at 1847 m depth) of the drill core.

References

Be'eri-Shlevin, Y., Gee, D.G., Claesson, S., Ladenberger, A., Majka, J., Kirkland, C., Robinson, P. & Frei, D., 2011: Provenance of Neoproterozoic sediments in the Särv nappes (Middle Allochthon) of the Scandinavian Caledonides: LA-ICP-MS and SIMS U–Pb dating of detrital zircons. *Precambrian Research* 187, 181–200.

Gee, D.G., Ladenberger, A., Dahlqvist, P., Majka, J., Be'eri-Shlevin, Y., Frei, D. & Thomsen, T., 2014. The Baltoscandian margin detrital zircon signatures of the central Scandes. In F. Corfu, D. Gasser & D.M. Chew (eds.): *New Perspectives on the Caledonides of Scandinavia and Related Areas*. *Geological Society, London, Special Publications* 390, 131-155.

Gee, D.G., Andréasson, P.G., Lorenz, H., Frei, D. & Majka, J., 2015: Detrital zircon signatures of the Baltoscandian margin along the Arctic Circle Caledonides in Sweden: the Sveconorwegian connection. *Precambrian Researc*h 265, 40–56. doi:10.1016/j.precamres.2015.05.012

Kirkland, C.L., Bingen, B., Whitehouse, M.J., Beyer, E. & Griffin, W.L., 2011: Neoproterozoic palaeogeography in the North Atlantic Region: inferences from the Akkajaure and Seve Nappes of the Scandinavian Caledonides. *Precambrian Research* 186, 127–146.

Ladenberger, A., Be'eri-Shevin, Y., Claesson, S., Gee, D.G., Majka, J. & Romanova, I.V., 2014: Tectonometamorphic evolution of the Åreskutan Nappe – Caledonian history revealed by SIMS U–Pb zircon geochronology. In F. Corfu, D. Gasser & D.M. Chew (eds.): New Perspectives on the Caledonides of Scandinavia and Related Areas. *Geological Society, London, Special Publications* 390, 337–368. doi:10.1144/SP390.10

Li, Y., Gee, D.G, Ladenberger, A. & Sjöström, H., 2021: Timing of deformation, metamorphism and leucogranite intrusion in the lower part of the Seve Nappe Complex in central Jämtland, Swedish Caledonides. *GFF* 143, 55-70, https://doi.org/10.1080/11035897.2020.1858341

Cleaning up the record – Revised U-Pb zircon ages and new Hf isotope data from southern Sweden

Åke Johansson

Department of Geosciences, Swedish Museum of Natural History, Stockholm, Sweden. ake.johansson@nrm.se

Summary. Ten granitoid samples from the Eastern Segment of the Sveconorwegian Orogen, previously dated by ID-TIMS on zircon, have been reanalysed using SIMS. A granitoid rock within the Protogine Zone south of Alvesta in Småland yields a revised U-Pb age of c. 1725 Ma, and six samples of orthogneiss from Skåne all yield revised ages between 1680 and 1700 Ma. Two samples of granite and one sample of syenite along the Protogine Zone in northern Skåne yield ages around 1220 Ma. Average initial εHf values for the 1725–1680 Ma rocks fall between +3 and +6, and around +1.5 in the 1220 Ma rocks.

Zircons from ten rock samples from the Eastern Segment of the Sveconorwegian Orogen in southern Sweden, including the southern part of the Protogine Zone, previously analyzed by conventional TIMS technique on multigrain fractions (and in two cases also on single grains) (Johansson 1990, Johansson et al. 1993), have been reanalyzed by SIMS (ion microprobe) spot analysis in individual grains. This has led to a revision of previously published ages, as seen in the table below. In several cases the earlier ages may have been of mixed magmatic-metamorphic origin or otherwise disturbed, leading to blurring of the magmatic record.

Sample	Locality	Rock type	Chemical classification (TAS)	Earlier U-Pb TIMS age	Revised U-Pb SIMS age
Granitoid gneisses					
76314	Flackarp, W Glimåkra	Gneissic granite	Granite	1531 ± 8 Ma	**1698 ± 6 Ma**
86011	South Alvesta	Gneissic granite	Monzonite	1711 ± 3 Ma	**1725 ± 4 Ma**
84093	Mölle, Kullaberg	Gneissic granite	Granite	1497 +47/–34 Ma	**1683 ± 6 Ma**
85015	Stenberget, Romeleåsen	Red gneiss	Granite	1557 +32/–27 Ma	**1696 ± 8 Ma**
85017	Vägasked, NW Höör	Grey gneiss	Syenite	1613 ± 6 Ma	**1693 ± 6 Ma**
85018	Skäralid, Söderåsen	Gneissic granite	Granite	1575 +77/–61 Ma	**1684 ± 11 Ma**
85019	Björnamossa, NW Örkelljunga	Charnockic gneiss	Syenite	1452 +347/–47 Ma	**1698 ± 7 Ma**
Protogine Zone intrusives					
84082	Önnestad	Syenite	Syenite	1224 +140/–14 Ma	**1221 ± 6 Ma**
84083	Åraslöv	Gneissic granite	Granite	1204 +16/–15 Ma	**1218 ± 4 Ma**
86010	Vanås gods	Gneissic granite	Syenite	1232 +80/–46 Ma	**1224 ± 5 Ma**

As can be seen, the revised magmatic crystallization age for most of the granitoid gneisses in the Eastern Segment fall in the interval 1680–1700 Ma, typical for TIB-2-related granitoids in the southern part of the Eastern Segment. There is a possible tendency for the coarser intrusive granitoids at Mölle and Skäralid to yield slightly younger ages (1680–1690 Ma) than the more fine-grained gneiss varieties (1690–1700 Ma). Metamorphic overgrowths with an age around 1460 Ma (Hallandian) was recorded from the charnockitic gneiss northwest of Örkelljunga in northern Skåne. A sample of gneissic granite within the Protogine Zone south of Alvesta in Småland yields a magmatic age of 1725 ± 4 Ma, thereby falling in the gap between TIB-1 granitoids to the east and TIB-2 gneisses to the west. The younger gneissic granitoids (Gumlösa-Glimåkra granite) and syenites along the Protogine Zone in Skåne yield similar ages as before of around 1220 Ma, but with better precision.

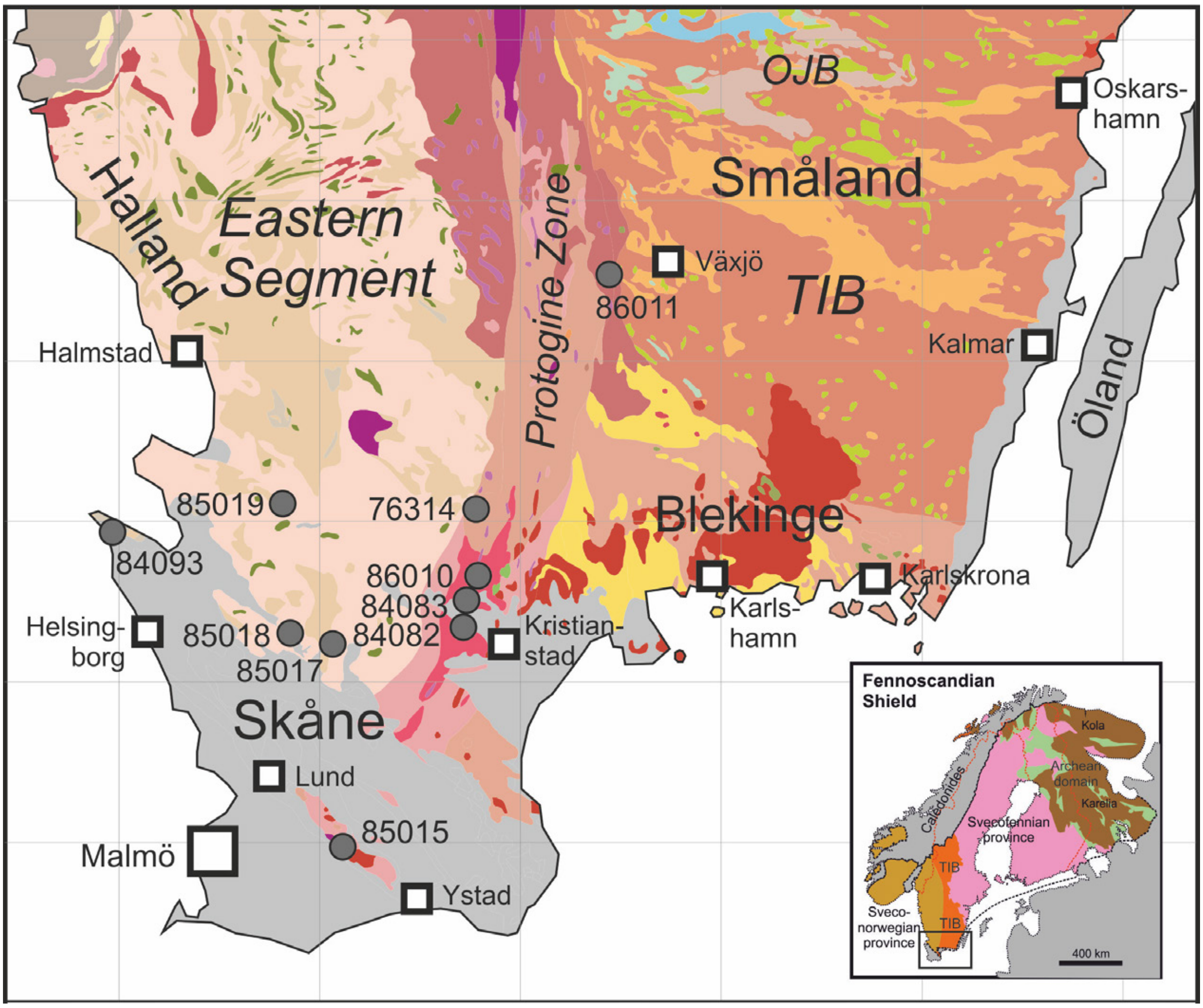

Figure 1. Geological map of southern Sweden, with sample locations indicated. Map source SGU (modified).

The revision of ages has also lead to some revision of previously measured and published whole-rock initial Sr and Nd isotope values for these rocks (Johansson 1990, Johansson et al. 1993). In addition, new Hf isotope values have been measured by LA-ICP-MS on the same zircon grains dated by U-Pb. The initial Sr values are disturbed, but the revised initial ε_{Nd} values fall between +1 and +2 for the older granitoids, and around 0 for the younger PZ intrusives. When it comes to initial ε_{Hf} in magmatic zircon, the average values for the older granitoids fall between +3 and +6 (total range for individual analyses +2 to +8), and for the younger intrusives between +1 and +2 (total range –1 to +4). Both the Nd and Hf isotope values suggest fairly large juvenile contributions (directly from the mantle or from newly formed crust) to the magmas forming all these rocks. The new results have been published by Johansson (2021).

References

Johansson, Å., 1990: Age of the Önnestad syenite and some gneissic granites along the southern part of the Protogine Zone, southern Sweden. In Gower, C.F., Rivers, T. & Ryan, A.B. (eds.): *Mid-Proterozoic Laurentia-Baltica. Geological Association of Canada Special Paper 38*, 131-148.

Johansson, Å., Meier, M., Oberli, F. & Wikman, H., 1993: The early evolution of the Southwest Swedish Gneiss Province: geochronological and isotopic evidence from southernmost Sweden. *Precambrian Research 64*, 361-388.

Johansson, Å., 2021: Cleaning up the record – revised U-Pb zircon ages and new Hf isotope data from southern Sweden. *GFF 143*, 328-359. https://doi.org/10.1080/11035897.2021.1939777

Age and C-O isotopes of the hydrothermal breccias within the Kiruna-Naimakka zone, Norrbotten, Sweden

Laura S. Lauri[a], Jo Miles[b], Xuan Liu[c], Hugh O'Brien[d]

[a]LKAB Exploration, Kiruna, Sweden, laura.lauri@lkab.com; [b]LKAB Exploration, Kiruna, Sweden, jo.miles@lkab.com; [c]Espoo Research Laboratory, Geological Survey of Finland (GTK), Espoo, Finland, xuan.liu@gtk.fi; [d]Espoo Research Laboratory, Geological Survey of Finland (GTK), Espoo, Finland, hugh.obrien@gtk.fi

Summary. Preliminary age and C-O isotope data is presented on hydrothermal carbonate breccias within the Kiruna-Naimakka deformation zone in Norrbotten, Sweden. C-O isotopes of calcite show a texture-related trend from Precambrian limestone and hydrothermal marble values to previously unreported compositions. Zircons were most probably inherited from the Late Archean country rocks whereas monazite crystallization in the mid-Proterozoic is very likely connected to breccia formation, possibly dating the latest activity in the Kiruna-Naimakka zone.

Introduction

The Kiruna-Naimakka zone (KNZ) is one of the crustal-scale shear zones that traverse the Norrbotten craton in northern Sweden (see Bergman et al. 2001). In the Kiruna area the KNZ forms a boundary where the youngest formation in the area, the <1.87 Ga Hauki quartzite, is juxtaposed against the ~2.4–2.0 Ga Kiruna greenstones, with up to 6 km vertical offset in the fault zone (see Bergman et al. 2001 for the age references).

The KNZ was intersected by LKAB drillings in 2021, with several drill holes crossing from the greenstones in the east to the quartzite on the western side of the shear zone. The contact zone is characterized by strong carbonate alteration that extends for tens of meters in the deformed greenstones. In addition, two holes intersected a hydrothermal breccia that is present both as consecutive zones 1–15 m in width and as smaller, irregular pockets within the wall rocks. The breccia is composed of different kinds of clasts cemented by fine-grained, brownish to white carbonate. The clasts are rounded to well-rounded in shape, commonly with a mm-thick reaction rim. They are typically quartz-albitic or mafic metavolcanic in composition (Fig. 1), and have variable (90–10%) volume fractions in different rock types. Cements in the clast-rich breccia are commonly dominated by anhedral calcite, whereas those in the clast-poor breccia are mainly subhedral calcite along with subordinate amounts of muscovite, chlorite and biotite. Vugs in clast-rich breccia commonly contain subhedral calcite crystals with muscovite. Calcite crystal shape shows a relationship with C-O isotopic compositions (see below).

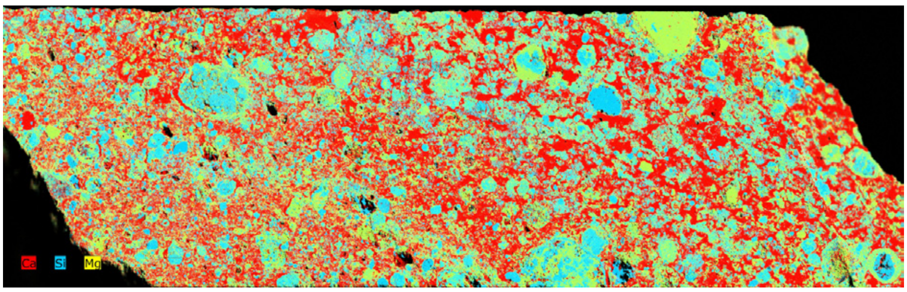

Figure 1. Scanning µ-XRF elemental map of sample No. 2 breccia from drill core PYK 21009. Clasts are mostly rounded to subrounded. Blue dominated are quartz rich, green are mafic clasts (Mg + Si) and red is calcite matrix. The drill core is 3 cm in width.

Geochemistry and isotope geology

Geochemical signatures obtained by the Minalyzer X-ray fluorescence Core Scanner reflect the heterogeneous matrix-to-clast ratio, as well as the varying composition of clasts and matrix that comprise the polymictic breccia. The brecciated zones are commonly depleted in both K and Al, relative to the surrounding greenstones, and locally, Ti and Fe. Ca concentration inversely correlates with the abundance of clasts. In clast-rich breccia, Ca content is commonly between 20–40 wt%, whereas it increases to 50–60 wt% in clast-poor breccia.

Eight breccia samples were selected for microscopic observation and C-O isotope analyses. The samples represent all breccia types. Calcite was separated from crushed materials using heavy liquid technique followed by careful handpicking under a binocular. Calcite separates were crushed to 200-mesh powders and dissolved in phosphoric acid to extract CO_2. Carbon and oxygen isotopes were measured using a MAT-253 EM mass spectrometer. Results are reported in δ-notation relative Vienna Pee Dee Belemnite (V-PDB) for carbon and Vienna Standard Mean Ocean Water (V-SMOW) for oxygen.

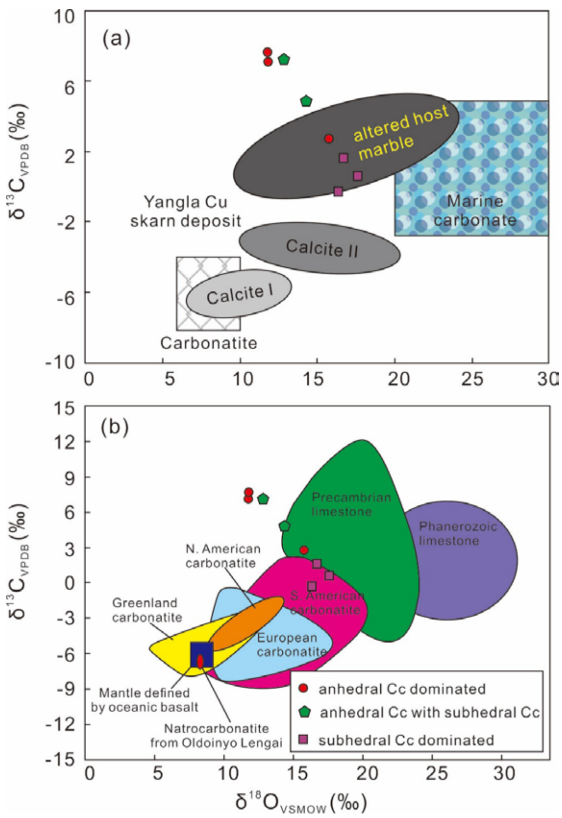

Figure 2. δ18O versus δ13C plots of calcite from the breccia from drill core PYK 21009. Fields in (a) are adapted from Du et al. (2017), and those in (b) are adapted from Bell and Simonetti (2010).

Two samples dominated by anhedral calcite from clast-rich samples display the highest $\delta^{13}C$ values (7.1–7.6‰) yet lowest $\delta^{18}O$ (11.8‰). Another similar sample, however, shows lower $\delta^{13}C$ (2.7‰) and higher $\delta^{18}O$ (15.8‰) values similar to two samples that contain both anhedral and subhedral calcites ($\delta^{13}C$: 4.9–7.3‰; $\delta^{18}O$: 12.8–14.3‰). Three samples mainly consisting of subhedral calcite show consistently lower $\delta^{13}C$ (–0.3–1.6‰) and higher $\delta^{18}O$ (16.4–17.6‰). On $\delta^{18}O$ versus $\delta^{13}C$ plots, the data form a roughly decreasing trend (Fig. 2). The lower end of the trend plots in the fields of the hydrothermal marble of the Yangla Cu deposit (Fig. 2a) and Precambrian limestone (Fig. 2b) as well as the overlapping field of South American carbonatite (Fig. 2b). By contrast, the upper end of the trend plots outside of all other known carbonate or carbonatite fields.

Geochronology

Polished thin sections were made from each of the eight samples and scanned by LV-SEM for U-bearing minerals. Approximately 50 zircon grains and 5 monazite grains large enough for 15 and 12 micron laser spots, respectively, were discovered.

U-Pb analyses were made using a 193 nm Excite laser and Nu Instruments AttoM SC-ICPMS. Preliminary zircon U-Pb data lay on a discordia with a concordia intercept age of approximately 2670 Ma. Despite the fact that the zircons came from 4 different samples, they all appear to lie on or near the same discordia. Grain shapes suggest most of the grains are fragments. These two factors together imply that these zircons represent grains derived from the countryrock clasts in the breccia and provide an age for the countryrock hosting the breccia.

The SEM search revealed sufficiently large monazite grains in 3 samples, and showed that these grains are located within the calcite matrix. Preliminary monazite U-Pb ages are quite distinct from the zircon ages. Two of the samples have an age range from 1780 to 1760 Ma, all plotting along concordia, whereas the single large monazite discovered in sample No. 8 gave an age of 1675 Ma.

References

Bergman, S., Kübler, L. & Martinsson, O., 2001: Description of regional geological and geophysical maps of northern Norrbotten County (east of the Caledonian orogen). *SGU Ba 56*, 114 p.

Du, L.J., Li, B., Huang, Z.L., Zhou, J.X., Zou, G.F. & Yan, Z.F., 2017: Carbon-oxygen isotopic geochemistry of the Yangla Cu skarn deposit, SW China: Implications for the source and evolution of hydrothermal fluids. *Ore Geology Reviews, 88*, pp.809-821.

Bell, K. & Simonetti, A., 2010: Source of parental melts to carbonatites–critical isotopic constraints. *Mineralogy and Petrology, 98(1)*, pp.77-89.

Did the mid-Pleistocene climate transition drive enhanced exhumation in the Karakoram? A detrital provenance perspective

Chris Mark[a], Peter Clift[b], Célia Paolucci[c], Anwar Alizai[d]

[a]Department of Geosciences, Swedish Museum of Natural History, Stockholm, Sweden, chris.mark@nrm.se; [b]Department of Geology and Geophysics, Louisiana State University Baton Rouge, USA; [c]Ecole Supérieure de Physique et Chimie Industrielle, Paris, France; [d]Geological Survey of Pakistan, Quetta, Balochistan, Pakistan.

Around the Nanga Parbat massif in the west and the Namche Barwa massif in the east, the trend of the Himalayan orogen exhibits an abrupt strike change from roughly E–W to N–S, forming two structural syntaxes. Each syntaxis is drained by a major trans-orogenic river system: the Ganges-Brahmaputra in the east, and the Indus in the west. Within each syntaxis, exposed crystalline basement of the underthrust Indian plate exhibits metamorphism up to granulite-facies grade, and records some of the fastest exhumation rates on Earth (up to c. 10 mm/a), together with Plio-Pleistocene mineral (re)crystallisation and cooling ages (Bracciali et al., 2016; Crowley et al., 2009). The Namche Barwa syntaxial massif, although modest in size (c. 3,300 km^2), supplies a remarkable 65% of Brahmaputra sediment load (Enkelmann et al., 2011. However, recent research indicates that its western twin, the Nanga Parbat massif, does not dominate the modern Indus sediment budget in the same way: instead, present-day sediment production (and thus exhumation) are focussed in the east Karakoram (Clift et al., in review).

Here we present data from material sampled during IODP expedition 355 (Arabian Sea Monsoon), which cored the offshore Indus fan and recovered a high-resolution archive of onshore erosion since the mid-Miocene. Preliminary analysis of this data indicates an abrupt increase in sediment sourced from the Nanga Parbat massif at c. 2.2 Ma, in good agreement with onshore bedrock analyses. The Nanga Parbat massif then dominates the sedimentary record until at least c. 1.4 Ma, when the youngest clastic material recovered from the fan was deposited. Analysis of legacy material from Ocean Drilling Program site 117-720 to bridge this temporal gap is in progress.

These observations indicate that at some point in the past c. 1.4 Ma, the dominant sediment source for the Indus system switched from the Nanga Parbat massif to the eastern Karakoram, north-east of Nanga Parbat. The east Karakoram zone includes some of Earth's highest peaks, and the largest extra-polar glaciers on Earth. Therefore, a provocative possibility is that the jump in erosion focus was driven by the well-documented switch from c. 41 ka, obliquity-dominated, to 100 kyr, eccentricity-dominated orbital forcing (the so-called Mid-Pleistocene Transition). This transition occurred at c. 1 Ma, and could have driven enhanced glacially-mediated erosion in the east Karakoram, outpacing Nanga Parbat sediment production.

References

Bracciali, L., et al., 2016: Plio-Pleistocene exhumation of the eastern Himalayan syntaxis and its domal 'pop-up' *Earth-Science Reviews*, 160, 350–385.

Clark, P., et al., 2006: The middle Pleistocene transition: characteristics, mechanisms, and implications for long-term changes in atmospheric pCO2, *Quaternary Science Reviews*, 25, 3150-3184.

Clift, P., et al., Detrital U-Pb Rutile and Zircon Data Show Indus River Sediment Dominantly Eroded from East Karakoram, not Nanga Parbat, *Earth and Planetary Science Letters*, In Review.

Crowley, J., et al., 2009: Pleistocene melting and rapid exhumation of the Nanga Parbat massif, Pakistan: Age and P–T conditions of accessory mineral growth in migmatite and leucogranite, *Earth and Planetary Science Letters*, 288, 408–420.

Enkelmann, E., et al., 2011: Denudation of the Namche Barwa antiform, eastern Himalaya, *Earth and Planetary Science Letters*, 307, 323-333.

Deciphering the timing and mantle sources of lunar magmatism using Pb-Pb dating and Sr-Nd-Pb isotope systematics

Renaud E. Merle[a], Alexander A. Nemchin[b], Martin J. Whitehouse[c], Gavin G. Kenny[c]

[a]Department of Earth Sciences, University of Uppsala, Uppsala, Sweden, renaud.merle@geo.uu.se; [b]School of Earth and Planetary Sciences, Curtin University, Perth, Australia, a.nemchin@curtin.edu.au; [c]Department of Geosciences, Swedish Museum of Natural History, Stockholm, Sweden, martin.whitehouse@nrm.se

Summary. Here we document new SIMS Pb-Pb ages and Pb isotope initial ratios of 7 low-Ti and 2 very rare basaltic meteorites with low-μ ratios ($\mu = {}^{238}U/{}^{204}Pb$). These new data were combined with those from literature and initial $^{87}Sr/^{86}Sr$ and $^{143}Nd/^{144}Nd$ were recalculated using the most recent high-precision Pb-Pb ages. From this dataset, we identify two main periods of activity at 3100–3350 Ma and 3550–4000 Ma. The Sr-Nd-Pb isotope ratios of basalts can be explained by a mixing from 4350 Ma until 3000 Ma between low-μ and KREEP mantle components.

Introduction

The chemical evolution of the lunar mantle through time then the characteristics of mantle sources of the lunar basaltic rocks, remains poorly constrained. This is related to two interconnected issues: (1) the timing of the magmatic activity is still poorly constrained owing the lack of very precise and accurate dates for many lunar basalts and (2) as a consequence of this, very precise radiogenic initial isotope ratios cannot be calculated. In this contribution, we aimed to decipher the chemical characteristics of the mantle sources of the lunar volcanism.

Samples and methods

To achieve this goal, we investigated lunar gabbro and basalt samples from meteorites. We used the in-situ Pb–Pb SIMS approach which proved efficient to date lunar basalts (Snape et al., 2016, 2018, 2019; Merle et al., 2020). Analyses of K-rich feldspars, phosphates and sulphides present in the samples allow us to use the $^{204}Pb/^{206}Pb$ vs $^{207}Pb/^{206}Pb$ isochron method, which has the advantage of yielding precise ages and initial Pb ratios as a by-product but also the assessment of terrestrial Pb contamination. In this study we have analysed lunar meteorites from the Northwest Africa (NWA) 773 clan (NWA 2727, NWA 3333, NWA 2977, NWA 773 and NWA 3170), NWA 4734, Dhofar 287A, Asuka (A) 881757 and Miller Range (MIL) 05035. These latter two samples belong to a very rare chemical group of lunar basalts which are suspected to have low-μ ($^{238}U/^{204}Pb$) ratios. These samples have been selected because they all belong to the dominant chemical group of low-titanium mare basalts but for which there has, to date, been no clear agreement on their age.

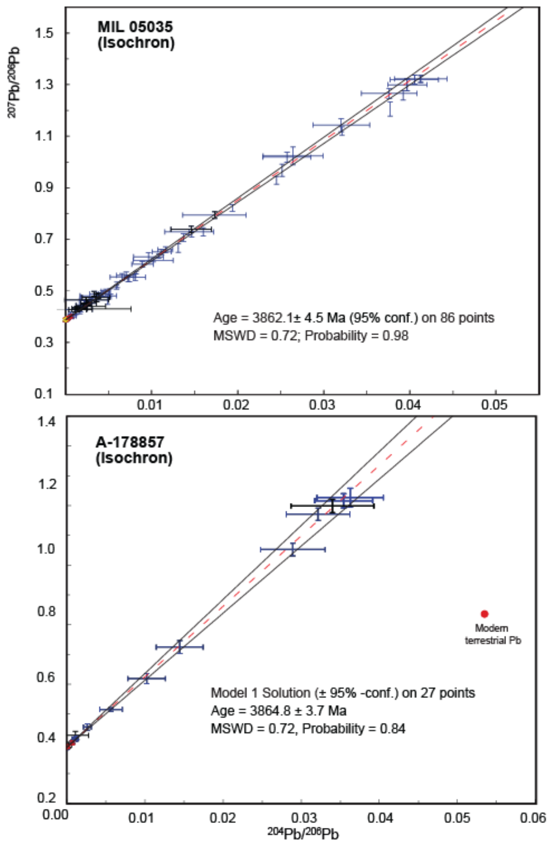

Figure 1: $^{204}Pb/^{206}Pb$ vs $^{207}Pb/^{206}Pb$ isochron for A-881757 and MIL05035 meteorites.

Results

We have obtained ages of 2981±12 Ma for NWA 4734, 3209±21 Ma for Dhofar 287. Four samples of the NWA 773 clan (NWA 2727, NWA 773, NWA 2977, NWA 3170) yielded isochron ages that are identical within uncertainty with an average age of 3087±5 Ma. The gabbro NWA 3333 yielded an age of 3039±20 Ma suggesting that two distinct magmatic events are recorded in the meteorites of the NWA 773 clan. Finally, we obtained reliable ages of 3865±4 Ma for A-881757 and 3862±4 Ma for MIL 05035 (Figure 1). Initial Pb ratios range from 0.842 to 1.344 for $^{207}Pb/^{206}Pb$ and 0.00203 to 0.0404 for $^{204}Pb/^{206}Pb$. The lowest ratios were obtained from NWA4734 while the highest ratios, for A-881757 and MIL 05035. These two samples plot away from any other samples in the $^{204}Pb/^{206}Pb$ vs $^{207}Pb/^{206}Pb$ diagram (Figure 2). The age dataset of mafic lunar meteorites and Apollo samples was filtered to remove data displaying large uncertainties, analytical issues and contamination by terrestrial Pb (Merle et al., 2020). Using this age dataset and literature data, initial Sr and Nd isotope ratios were recalculated.

Interpretations and conclusions

The new and refined dataset combines the ages of mafic lunar meteorites and Apollo samples and suggests pulses in magmatic activity, with two main phases between 4000 and 3550 Ma and between 3350 and 3100 Ma followed by a minor phase at ~3000 Ma.

The evolution of the Pb initial ratios of the lunar basalts between 4300 Ma and 2000 Ma can be interpreted as a progressive mixing between a component representing the source of the 3860 Ma low-µ basalts with a KREEP-like component (Figure 2). The evolution through time of the initial Sr-Nd isotope ratios is compatible with such hypothesis.

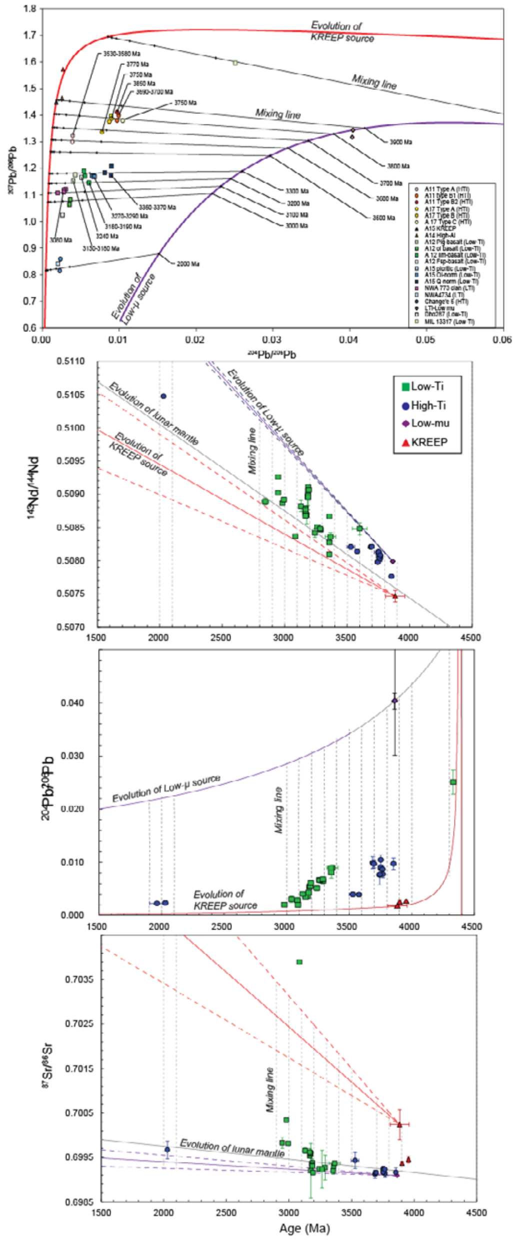

Figure 2: Initial Pb-Sr- isotope ratios of mafic lunar rocks (meteorites and Apollo samples). dataset for Apollo and meteorite samples after Snape et al., 2016, 2018; 2019; Merle et al., 2020 and this work.

References

Merle, R.E., Nemchin, A.A., Whitehouse, M.J., Snape, J.F., Kenny, G.G., Bellucci, J.J., Connelly, J.N. & Bizzarro, M., 2020. Pb-Pb ages and initial Pb isotopic composition of lunar meteorites: NWA 773 clan, NWA 4734, and Dhofar 287. *Meteoritics and Planetary Science* 55, 1808-1832.

Snape J.F., Nemchin A.A., Bellucci J.J., Whitehouse M.J., Tartèse R., Barnes J.J., Anand M., Crawford I.A. & Joy K.H., 2016. Lunar basalt chronology, mantle differentiation and implications for determining the age of the Moon. *Earth and Planetary Sciences Letters* 451, 149-158.

Snape J.F., Curran N.M., Whitehouse M.J., Nemchin A.A., Joy K.H., Hopkinson T., Anand M., Bellucci J.J. & Kenny G. G., 2018. Ancient volcanism on the Moon: Insights from Pb isotopes in the MIL 13317 and Kalahari 009 lunar meteorites. *Earth and Planetary Science Letters* 502, 84-95.

Snape J.F., Nemchin A.A., Whitehouse M.J., Merle R.E., Hopkinson T. & Anand M. 2019. The timing of basaltic volcanism at the Apollo landing sites. *Geochimica et Cosmochimica Acta* 266, 29-53.

Formation of early Archean Granite-Greenstone Terranes from a globally chondritic mantle

Andreas Petersson[a,b], Anthony I.S. Kemp[c], Martin J. Whitehouse[b]

[a] Department of Geography and Geology, University of Copenhagen, Øster Voldgade 10, DK-1350 Copenhagen K, Denmark, ape@ign.ku.dk; [b] Swedish Museum of Natural History, Box 50 007, SE-104 05 Stockholm, Sweden, Martin.Whitehouse@nrm.se; [c] School of Earth Sciences, The University of Western Australia, Crawley, Australia, tony.kemp@uwa.edu.au.

Summary. The zircon Hf and O isotope signatures of ~3.59–3.4 Ga Pilbara do not support remelting of an ancient basement, and reinforce the overwhelmingly near-chondritic zircon Hf isotope composition of Eoarchean meta-igneous rocks from several different Archean cratons. A corollary of this remarkable global consistency is that a significant volume of the mantle maintained a chondritic composition for the Lu-Hf system from the formation of the Earth into the Paleoarchean, as would be the case if stabilised volumes of felsic continental crust prior to 3.5 Ga were relatively small.

Insights from igneous rocks of the Pilbara Craton, Western Australia

The continental crust grows via juvenile additions from the mantle. However, the timing of initial continent stabilisation and the rate of subsequent continental growth during the first billion years of Earth history is widely debated, in part due to uncertainty over the composition of the mantle source of new crust (e.g. Kemp et al. 2015, Fisher & Vervoort 2018, Petersson et al. 2019a). Well-preserved Archean granite-greenstone terranes, as present within the Pilbara Craton (Western Australia), provide insights into the sources of felsic magmas and the processes of continental growth and evolution in the distant geological past at the regional scale.

Zircon U-Pb, oxygen, and hafnium isotope data reported here for nine gneissic samples of the Pilbara Craton provide new insights into the earliest magmatic and growth history of this exceptionally well-preserved section of Earth's Archean crust. Zircon age determinations of a newly identified tonalite gneiss enclave (12TKPB06), and additional zircon U-Pb data from the gneiss enclave GSWA142870, confirm the existence of 3.58 Ga igneous protoliths within the Warrawagine Granitic Complex. This is 160 km northeast of the first documented occurrence of rocks of this age in the Shaw Granitic Complex, and thus markedly expands the geographical extent of the ~3.59–3.58 Ga Mount Webber magmatic event across the Pilbara Craton.

Igneous protolith ages of 3.53–3.49 Ga have been established for gneisses of the Carlindi and Muccan Granitic Complexes. We propose the name Mulgundoona Supersuite for these rocks, which comprise the hitherto "missing" plutonic complement to the felsic extrusive Coucal Formation of the Coonterunah Subgroup. Combined zircon U-Pb, O and Lu-Hf isotopes indicate that magmatic events from ~3.58 Ga to 3.4 Ga in the Pilbara Craton were associated with the emplacement of juvenile continental crust extracted from chondritic mantle.

The overwhelmingly chondritic zircon Hf isotope signatures of meta-igneous rocks in the Pilbara Craton do not support the reworking of even older (>3.8 Ga) crust within the region. Generally, mantle-like zircon $\delta^{18}O$ indicates a limited role for ^{18}O-enriched sources in the production of these rocks, although slightly elevated values (6–6.5‰) in the oldest zircons suggest minor incorporation of a juvenile supracrustal component. Building on the recent findings of Petersson et al. (2019b), we propose a refined model for the earliest evolution of the Pilbara Craton. This involves the assembly of a basaltic plateau that was 'seeded' by a 3.76–3.65 Ga continental nucleus to localise melting above a mantle upwelling zone, and to allow thickened mafic crust to form. The subsequent rifting and collapse of this thickened protocrust attending further mantle melting led to the emplacement of the 3.59–3.58 Ga igneous rocks of the Mt. Webber event, marking the first stabilisation of felsic crust associated with growth of the Pilbara Craton. Such rocks provided a substrate to facilitate the accumulation and stabilisation of voluminous eruptive products of the Warrawoona Group, commencing with pronounced mantle upwelling from 3.53 Ga, which was also associated with the emplacement of felsic magmas of the Mulgundoona Supersuite into the deeper part of the crustal pile. Overturn of the resulting unstable configuration of dense basaltic crust overlying felsic middle crust, and accompanying infracrustal reworking of the foundering basaltic piles, generated the felsic intrusive and extrusive rocks of the granitic complexes and flanking greenstone belts. This process was the critical step in stabilising the Pilbara Craton and led to the distinctive dome and keel architecture.

In assessing the broader relevance of these results, we emphasise that the chondritic zircon Hf isotope compositions reported here for the Pilbara Craton are in line with zircon Hf isotope data from meta-igneous rocks of Eo- to Paleoarchean cratons on a number of other continents (e.g. Kemp et al. 2015, Hiess & Bennett, 2016, Fisher & Vervoort 2018, Petersson et al. 2019a, Petersson et al. 2020). The striking uniformity of these near chondritic Hf isotope signatures on a global scale suggest either that new continental crust separated from a primitive, undifferentiated mantle source from 3.9 to 3.3 Ga, leaving depleted mantle residues that were not re-sampled until later in the Archean, or that the depleted signatures induced by limited continent sequestration were largely erased by crustal recycling and vigorous mantle convection, maintaining a near-chondritic mantle composition. Both scenarios are compatible with the prevalent primitive mantle trace element composition of Archean basaltic rocks (Bédard 2018), although the latter situation would suggest that stabilisation of continental crust prior to 3.5 Ga was not voluminous enough to cause long-term depletion of the mantle source of new crust in incompatible trace elements. If the mantle of the newly assembled Earth was chondritic for involatile elements, it is reasonable to propose that the history of the convecting chondritic mantle extends through the Hadean to the earliest stages of the Earth and is a fundamental aspect of the planet. The gradual slowing of convective activity into the Paleoarchean associated with mantle cooling may have contributed to the initiation of a different tectonic regime that gave rise to the more voluminous continental crust preserved from that time.

Newly identified similarities between the initial growth phases of the Pilbara and Kaapvaal cratons, arguably the best-preserved Archean terranes on Earth, suggest that granite-greenstone terranes may initially form via assembly and differentiation of juvenile crustal contributions sourced from chondritic mantle, and that reworking ancient 'proto'-crust was not an essential process in the growth of Archean cratons.

References

Bédard, J.H., 2018. Stagnant lids and mantle overturns: Implications for Archaean tectonics, magmagenesis, crustal growth, mantle evolution, and the start of plate tectonics. *Geoscience Frontiers 9*, 19–49.

Fisher, C.M. & Vervoort, J.D., 2018. Using the magmatic record to constrain the growth of continental crust—the Eoarchean zircon Hf record of Greenland. *Earth and Planetary Science Letters 488*, 79–91.

Hiess, J. & Bennett, V.C., 2016. Chondritic Lu/Hf in the early crust–mantle system as recorded by zircon populations from the oldest Eoarchean rocks of Yilgarn Craton, West Australia and Enderby Land, Antarctica. *Chemical Geology 427*, 125–143.

Kemp, A.I., Hickman, A.H., Kirkland, C.L. & Vervoort, J.D., 2015. Hf isotopes in detrital and inherited zircons of the Pilbara Craton provide no evidence for Hadean continents. *Precambrian Research 261*, 112–126.

Petersson, A., Kemp, A.I., Hickman, A.H., Whitehouse, M.J., Martin, L. & Gray, C.M., 2019a. A new 3.59 Ga magmatic suite and a chondritic source to the east Pilbara Craton. *Chemical Geology 511*, 51–70.

Petersson, A., Kemp, A.I. & Whitehouse, M.J., 2019b. A Yilgarn seed to the Pilbara Craton? Evidence from inherited zircons. *Geology 47*, 1098–1102.

Petersson, A., Kemp, A.I., Chris, M. Grey. & Whitehouse, M.J., 2020. Formation of early Archean Granite-Greenstone Terranes from a globally chondritic mantle: Insights from igneous rocks of the Pilbara Craton, Western Australia. *Chemical Geology 551*, p. 119757.

Observation and inference in the interpretation of zircon ages obtained from “>3.9 Ga” gneiss in the Saglek Block, Labrador

Martin J. Whitehouse[a], Daniel J. Dunkley[b], Monika A. Kusiak[b], Simon A. Wilde[c], Tanmay Keluskar[b]

[a]Department of Geociences, Swedish Museum of Natural History, Stockholm, Sweden, e-mail; martin.whitehouse@nrm.se; [b]Institute of Geophysics, Polish Academy of Sciences, Warsaw, Poland; [c]School of Earth & Planetary Sciences, Curtin University, Perth, WA, Australia

With due care, most techniques in geochronology can provide precise ages for multiple generations of magmatism and metamorphism in a single complex outcrop. Equally, the same methods can produce spurious interpretations, either through a neglect of statistical reproducibility in age estimates, or through a misunderstanding of the relationships between dated phases (e.g. zircon) and their host rocks. In the Saglek Block of Labrador, NE Canada, evidence for what could be some of Earth’s earliest signs of life in purported >3.95 Ga supracrustal rocks (Tashiro et al. 2017) relies on zircon dating and field relationships that are ambiguous. The age of the supracrustal rocks in which evidence of life is reported was not established directly, but by extrapolating cross-cutting relationships from directly-dated zircon-bearing magmatic rocks. Conclusions were drawn by Tashiro et al. (2017) that contradict evidence from earlier studies (as discussed by Whitehouse et al. 2019). This includes ‘cherry-picking’ a handful of >3.9 Ga analyses from an imprecise dataset from tonalitic gneiss presented in an earlier study by Shimojo et al. (2016). In fact, closer inspection reveals that this dataset contains a subset of statistically equivalent data yielding a more inclusive and robust ‘maximum’ age of c. 3.87 Ga. A similar age of c. 3.86 Ga was obtained from a metagranite that Shimojo et al. (2016) considered syn-metamorphic; consequently, this age was assigned to both the intrusion of the granite and the metamorphism that produced gneissosity in the host tonalite. This interpretation, however, ignores the well-established presence of c. 2.7 Ga granulite-facies metamorphism that has been recognized across the entire Saglek Block (Dunkley et al, 2020).

We present a re-evaluation of critical field relationships together with new ion microprobe U-Pb analyses of the tonalitic gneiss and the metagranite that is clearly transposed into the dominant gneissosity, obtaining ages for their emplacement of c. 3.87 Ga and c. 2.71 Ga, respectively. In the metagranite, c. 3.87 Ga zircon is most likely xenocrystic, being derived from the tonalitic host, whereas ca, 2.71 Ga zircon of a distinct high-U generation represents the actual magmatic age; the latter is in marked contrast to the interpretation of such grains by Shimojo et al. (2016) as having experienced Pb loss after the gneiss-forming metamorphic event. Our interpretation that Eoarchean ages for granitic magmatism and metamorphism as estimated by Shimojo et al. (2016) derive from xenocrystic zircon incorporated into a Neoarchean melt *a priori* implies that these cannot be used to constrain pre-Neoarchean processes, nor, by extension, provide an Eoarchean minimum age for supracrustal rocks that host potentially biogenic remnants. This case study demonstrates the confusion that can arise when the essential interplay between observation and inference in both field geology and zirconology is overlooked.

This research was funded by NCN grant UMO2019/34/H/ST10/00619 and Knut and Alice Wallenberg Foundation grant 2012.0097.

References

Dunkley, D.J., Kusiak, M.A., Wilde, S.A., Whitehouse, M.J., Sałacińska, A., Kielman, R. & Konečný, P., 2020. Two Neoarchean tectonothermal events on the western edge of the North Atlantic Craton, as revealed by SIMS dating of the Saglek Block, Nain Province, Labrador. *Journal of the Geological Society 177*, 31-49.

Shimojo, M., Yamamoto, S., Sakata, S., Yokoyama, T.D., Maki, K., Sawaki, Y., Ishikawa, A., Aoki, K., Aoki, S., Koshida, K., Tashiro, T., Hirata, T., Collerson, K.D. & Komiya, T. 2016. Occurrence and geochronology of the Eoarchean, ~3.9 Ga, Iqaluk Gneiss in the Saglek Block, northern Labrador, Canada: Evidence for the oldest supracrustal rocks in the world. *Precambrian Research 278*, 218-243.

Tashiro, T., Ishida, A., Hori, M., Igisu, M., Koike, M., Méjean, P., Takahata, N., Sano, Y. & Komiya, T., 2017. Early trace of life from 3.95 Ga sedimentary rocks in Labrador, Canada. *Nature 549*, 516-518.

Whitehouse, M.J., Dunkley, D.J., Kusiak, M.A. & Wilde, S.A., 2019. On the true antiquity of Eoarchean chemofossils – assessing the claim for Earth's oldest biogenic graphite in the Saglek Block of Labrador. *Precambrian Research 323*, 70-81.

Extreme initial 87Sr/86Sr ratios through metamorphic overprinting: an example from Balltorp (western Sweden)

Thomas Zack[a], Andreas Karlsson[b]

[a]Department of Earth Sciences, University of Gothenburg, Göteborg, Sweden, thomas.zack@gu.se
[b]Department of Geosciences, Swedish Museum of Natural History, Stockholm, Sweden, andreas.karlsson@nrm.se

Introduction

Rubidium-strontium dating traditionally uses an isochron approach, where phases with varying Rb/Sr ratio are plotted against their $^{87}Sr/^{86}Sr$ ratio, solving simultaneously for an age (slope) and initial $^{87}Sr/^{86}Sr$ ratio (intercept with y-axis; in the following called initial Sr). In the absence of widely varying Rb/Sr ratios, an age can still be calculated by making simple assumptions on likely initial Sr. Rösel & Zack (in press) delineated expected initial Sr ratios for three cases: (1) for mantle-derived rocks from 0.700–0.706, (2) for evolved magmatic rocks from 0.70–0.73 and (3) for crustal rocks from 0.70–0.76. This works well in most applications around the world; still, it is essential to know under which conditions such assumptions are not valid.

Arfvedsonite-bearing monzonite from Balltorp

An extreme case of initial Sr well outside normal values has been encountered in an ongoing study of an arfvedsonite-bearing monzonite from Balltorp, western Sweden (Karlsson & Zack, this conference). The rock assemblage is a peculiar mix of ordinary, mostly major phases (microcline, albitic plagioclase and minor quartz) and rather exotic phases (abundant arfvedsonite and zircon, aegirine, chevkinite-(Ce), astrophyllite, fluorite, etc). The intrusion age of c. 1.33 Ga (from relictic zircon cores; Karlsson & Zack, this conference) corresponds to incipient rift-related bimodal magmatic rocks in this area (Kungsbacka suite; Hegardt et al., 2007), while substantial resetting in the Balltorp monzonites is recorded by strongly modified zircon and concordant zircon rims and tied to c. 1.03 Ga (Karlsson & Zack, this conference). The exact nature of this resetting is currently unclear, as it can be envisioned through substantial fluid circulation and/or through dynamic recrystallization. What can be said is that it likely was triggered by elevated temperatures in this area, documented by contemporaneous zircon ages in leucosome of nearby migmatites (Hegardt et al., 2007).

Rubidium-Strontium systematics in Balltorp

Microcline is the mineral phase in Balltorp monzonite that contains most of the rocks Rb. Compared to other K-feldspars, a Rb content of 2500 µg/g and a common Sr content c. 0.3 µg/g is quite unusual and has otherwise only been encountered in highly fractionated pegmatites. Other phases are much lower in Rb concentration, but also relatively low in Sr: albite has c. 6–12 µg/g Rb and 4–6 µg/g Sr, while aegirine has c. 0.1–1.0 µg/g Rb and 0.5–2.0 µg/g Sr. Under such conditions, microcline will accumulate radiogenic Sr (^{87}Sr by ^{87}Rb decay) to a degree that it will contain the majority of radiogenic Sr of the rock in a few 10's of Ma. Given the circumstance that the Balltorp monzonite recrystallized 300 Ma after formation, it will lead to the redistribution of highly radiogenic Sr from the microcline by incorporating it to other phases, like albite and aegirine.

This effect can be recorded by in-situ Rb-Sr analysis utilizing the LA-ICP-MS/MS facility at the University of Gothenburg (see Rösel & Zack, in press for current setup) with high spatial resolution (50–70 µm spot size). As can be observed in Figure 1, albite and aegirine record some of the highest and most varied initial Sr ratios ever recorded. Using 900 Ma isochrons as reference lines to project to the y-axis (initial Sr), initial $^{87}Sr/^{86}Sr$ ratios between 1.1 and 3.4 have been encountered. Although it is an extreme example, it clearly demonstrates that (1) high grade metamorphic resetting generally lead to elevated initial Sr and (2) isotopic equilibration is far from being reached.

With such heterogeneous and unusual initial Sr ratios it may appear to be impossible to derive meaningful Rb-Sr ages. However, this is actually only partly correct. In the case of arfvedsonite, a sodic amphibole with substantial Rb contents, up to 80 µg/g Rb at 4–6 µg/g Sr, ages can not be calculated (with initial Sr ratios of 1, unrealistic single spot ages of 2.8 Ga are calculated, while with a ratio of 3.4, apparent negative ages are derived). However, calculations using the highly radiogenic microcline are completely inert against uncertainties in the initial Sr. It can be seen in figure 2A that microcline itself has large enough variation in Rb/Sr that useful Rb-Sr ages can be derived (ca 0.89±0.08 Ga). However, a better approach is pooling single spot ages of individual laser spots (for explanation see figure 2B), so that robust Rb/Sr ages for microcline can be reported for Balltorp to be 0.90±0.01 Ga. This age can be interpreted as a general cooling age in this area, although it must be emphasized that exact closure temperatures for Sr are currently not available. Regardless, this age can be taken as the youngest age where microcline behaved as an (partly) open system that was able to “leak” highly radiogenic Sr into the surrounding, explaining the highly variable and elevated $^{87}Sr/^{86}Sr$ ratios of phases like albite and aegirine.

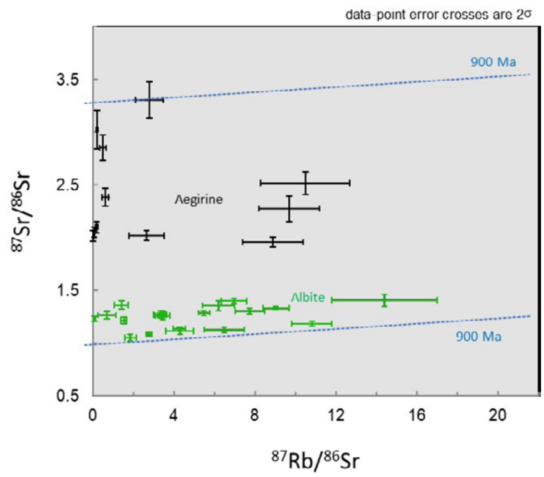

Figure 1. In-situ Rb-Sr data for Albite and Aegirine from Balltorp monzonite. Blue stippled lines show examples of isochrons corresponding to 900 Ma. Please note that initial $^{87}Sr/^{86}Sr$ ratios of above 3 are hardly recorded in the literature.

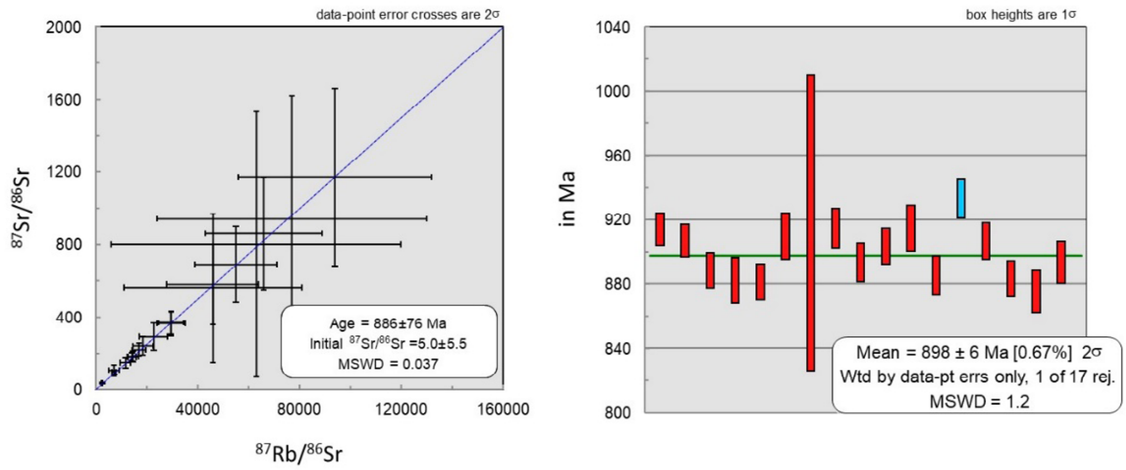

Figure 2. In-situ Rb-Sr data for microcline from Balltorp monzonite. A) On the left is a classical isochron of the data with apparently highly imprecise data. However, this is only an artifact of the plotting method, which disregards the strongly correlated nature of both $^{87}Rb/^{86}Sr$ and $^{87}Sr/^{86}Sr$ data due to the extremely low content of common Sr (^{86}Sr). B) A better method of calculating Rb-Sr ages for low common-Sr phases is the single spot approach by Rösel & Zack (in press). This requires knowledge of a correct initial Sr ratio. In the example shown on the right, an initial Sr value of 1.3 was used. Please note that microclines from Balltorp are so radiogenic that even an initial ratio of 4.0 leads to a reduction of the calculated age by only 10 Ma.

References

Hegardt, E. A., Cornell, D. H., Hellström, F. A., & Lundqvist, I. (2007). Emplacement ages of the mid-Proterozoic Kungsbacka bimodal suite, SW Sweden. *GFF*, *129*(3), 227-234.

Rösel, D., & Zack, T. (in press). LA-ICP-MS/MS single-spot Rb-Sr Dating. *Geostandards and Geoanalytical Research*.

Karlsson, A. & Zack, T. (2022). A mineralogical and geochronological approach to unravel the mysteries of an arfvedsonite-bearing monzonite at Balltorp in western Sweden. *This conference.*

Thematic Session 7
Geophysics

Session Chairs:
Christopher Juhlin (christopher.juhlin@geo.uu.se)
Thorkild Maack Rasmussen (thorkild.maack.rasmussen@ltu.se)
Lena Persson (lena.persson@sgu.se)

Studies of paleomagnetism and rock magnetism in Sweden: history, state-of-the-art and future

Bjarne S.G. Almqvist[a], Ian Snowball[a], Sten-Åke Elming[b], Andreas Nilsson[c], Per Sandgren[c]

[a]Department of Earth Sciences, Uppsala University, Uppsala, Sweden, bjarne.almqvist@geo.uu.se, ian.snowball@geo.uu.se; [b]Exploration Geophysics, Luleå University of Technology, Luleå, Sweden, sten-ake.elming@ltu.se; [c]Quaternary Sciences, Lund University, Lund, Sweden, andreas.nilsson@geol.lu.se, per.sandgren@geol.lu.se.

Summary. Laboratory-based magnetic techniques are broadly used in Earth sciences, from studies of the structure and dynamics of Earth's magnetic field, to plate tectonic reconstruction and paleogeography, paleoenvironment reconstruction and contemporary environmental pollution. Since the 1940's Swedish scientists have played a prominent role in these research fields. Key contributions have been made to Precambrian paleogeography, studies of the paleosecular variation of the magnetic field since the last deglaciation, Quaternary magnetostratigraphy and fundamental aspects of mineral magnetism.

In this contribution we review the history and notable contributions in the fields of paleomagnetism, environmental magnetism and anisotropy of magnetic susceptibility (AMS), as they were advanced in Sweden. Sweden has a long history in the use of magnetic techniques for geological and environmental application and the geological setting of Sweden. This presentation concerns mainly the use of laboratory-based magnetic techniques applied to different geological settings. The Swedish physicist Gustav Ising can arguably be considered as the founder of fields of environmental magnetism and the use of anisotropy of magnetic susceptibility, with key contributions in the early 1940's (Ising, 1942). Ising studied the magnetic properties of varved clays to determine how ferromagnetic minerals in the clay recorded the Earth's magnetic field direction during deposition. His work was later continued by Lars Granar (1958).

Magnetic laboratory methods generally target measurements of magnetic remanence and magnetic susceptibility and, regardless of research aims, high-sensitivity instrumentation is necessary to characterize potentially weakly magnetic geological samples. Gustav Ising can likely be considered one of the premier instrument makers in Sweden during the first half of the 20th century, building (among many other instruments) a torsion magnetometer and a pendulum magnetometer for his geophysical laboratory in Djursholm. The first laboratory principally dedicated to paleomagnetic studies in Sweden was initiated by Göran Bylund in the 1970's, followed by the establishment of a paleomagnetic laboratory in Luleå in the early 1980's. These early laboratories used sensitive astatic and spinner magnetometers and the earliest laboratories were typically established in houses built from non-magnetic materials and in areas with magnetically quiet environments. In the early 1990's, a new generation of cryogenically cooled superconducting (SQUID) magnetometers became widely available and the laboratories in Lund and Luleå were both upgraded with such magnetometers.

Gustav Ising, and later Lars Granar, realized that varved sediments could be ideal for studying secular variation of Earth's magnetic field, potentially providing a (near) continuous recording of the field based on clay varve chronologies. Göran Bylund and Sten-Åke Elming shifted the focus of research to hard-rock paleomagnetism. Among the earliest studies by Bylund, is paleomagnetism of the Dellen impact structure (Bylund, 1974). However, most hard-rock paleomagnetic studies focused on Precambrian rocks in Sweden and other countries (e.g. Elming et al., 2010). Of significant importance in Sweden and in the Nordic countries was the establishment of the Nordic working group in paleomagnetism. This group formed in Helsinki, with its first workshop in 1986 with a theme of establishing a paleomagnetic database. In connection with the workshops, it was realized that establishing quality criteria of paleomagnetic data was crucial in evaluating high-quality data, which led to development of a set of paleomagnetic quality criteria indicators (van der Voo, 1990). The Nordic cooperation resulted most recently in the publication of a state-of-the-art book on ancient supercontinents and the paleogeography of Earth (Pesonen et al., 2021).

In the late 1980's and during the 1990's, paleomagnetic and mineral magnetic studies at Lund University shifted direction towards Quaternary applications. A sabbatical spent in Lund by Roy Thompson from Edinburgh University in 1987 catalysed a transition to environmental magnetic studies (e.g. Sandgren and Thompson 1990). Subsequent magnetic studies of lake sediments provided important insight into the presence and role of fossil magnetosomes as paleomagnetic field recorders. In addition, the fundamental magnetic properties of authigenic greigite (Fe_3S_4) and recognition of its widespread occurrence in reduced sediments were pioneered in Sweden (Snowball, 1991). Inspired by Finnish studies of annually laminated (varved) lake sediments, Ian Snowball and Per Sandgren initiated similar studies in Sweden, which led to a paleosecular variation master curve for Fennoscandia (Snowball et al. 2007). Recently, the research focus at Lund University has shifted towards the development of Holocene geomagnetic field models based on global compilations of sedimentary palaeomagnetic data (Nilsson and Suttie, 2021).

Figure 1. (a) Participants at the Nordic Paleomagnetic workshop, arranged in 2009 by Sten-Åke Elming, and taking place at the Rosfors mansion, west of Luleå. Among the Participants are in rear row (from left to right): Harald Walderhaug (1), Trond Torsvik (2), Joseph Meert (3), Sten-Åke Elming (4), Lauri Pesonen (5), Zheng-Xiang Li (6), Phil McCausland (7), Sergei Pisarevsky (8), David Evans (10), Fabio Donadini (11), Mads Faurschou Knudsen (12), Andreas Nilsson (13), Satu Mertanen (14), Ian Snowball (15); front row (left to right): Ulla Predeen (1), Elisa Piispa (3), Eric Tohver (5), Manuel D'Agrella (8). (b) Per Sandgren (left) and Ian Snowball (right) relax on the ice during coring for paleomagnetic samples on lake Furskogstjärnet in 2000.

References

Bylund, G. (1974). Palaeomagnetism of a probable meteorite impact, the Dellen structure. GFF, 96. 275-278.

Elming, S.-Å., Shumlyanskyy, L., Kravchenko, S., Layer, P., Söderlund, U. (2010). Proterozoic basic dykes in the Ukrainian shield: A paleomagnetic, geochronoloic and geochemical study – The accretion of the Ukrainian shield to Fennoscandia. Precamb. Res., 178, 119-135.

Granar, L. (1958). Magnetic measurements on Swedish varved sediments. Arkiv för Geofysik, 3, 1-40.

Ising, G. (1942). On the magnetic properties of varved clay. Arkiv för Matematik, Astronomi och Fysik, 29a, 1-37.

Nilsson, A., Suttie, N., 2021. Probabilistic approach to geomagnetic field modelling of data with age uncertainties and post-depositional magnetisations. Phys. Earth Planet. Int., 106737.

Pesonen, L.J., Salminen, J., Elming, S.-Å., Evans, D.A.D., Veikkolainen, T. (2021). Ancient Supercontinents and the Paleogeography of Earth. Elsevier Inc.

Sandgren, P., Thompson, R. (1990). Mineral magnetic characteristics of podzolic soils developed on sand dunes in the Lake Gosciaz catchment, central Poland. Phys. Earth Planet. Int., 60, 297-313.

Snowball, I.F. (1991). Magnetic hysteresis properties of greigite (Fe_3S_4) and a new occurrence in Holocene sediments from Swedish Lappland. Earth Planet. Sci. Lett., 68, 32-40.

Snowball, I., Zillén, L., Ojala, A., Saarinen, T. & Sandgren, P. (2007). FENNOSTACK and FENNORPIS: varve dated Holocene palaeomagnetic secular variation and relative palaeointensity stacks for Fennoscandia. Earth Planet. Sci. Lett., 255, 106-115.

Van der Voo, R. (1990). The reliability of paleomagnetic data. Tectonophysics, 184, 1-9.

A review of developments of electromagnetic methods at SGU

Mehrdad Bastani[a,b], Lena Persson[a], Mats Wedmark[a], Henrik Johansson[a]

[a]Department of Mineral Resources, Geological Survey of Sweden, Villavägen 18, 75128, Uppsala, Sweden, mehrdad.bastani@sgu.se; lena.persson@sgu.se; mats.wedmark@sgu.se; henrik.johansson@sgu.se;
[b]Department of Earth Sciences, Uppsala University, Villavägen 16, 75236, Uppsala, Sweden

Summary. The geological survey of Sweden (SGU) has been actively utilizing and developing electromagnetic (EM) methods to map and model the electrical resistivity of the ground. The main purpose of the measurements was initially ore prospecting and later technical developments led to the use in other applications such as bedrock and groundwater mapping and near surface studies (0–50 m depth). In this study a review of electromagnetic methods used and developed at SGU for mapping, modelling, and interpretation of various geological structures is presented. Three examples are selected to demonstrate the results of airborne and ground measurements using various EM methods at SGU.

Introduction

Use of electromagnetic methods at SGU dates back to the 1920's when Sundberg et al. (1923) published the results of studies made with various geophysical methods in Skellefte district. Later in 1936, Sture Werner and Alfred Holm developed the Slingram method (Påsse et al., 2008) to carry out ground measurement over conductive structures in Adak and Kristineberg areas in Skellefte district. Later in 60's Werner developed the method further for airborne applications at SGU. In the 60's Paál discovered the existing signal from distant Very Low Frequency (VLF) transmitters, primarily used to communicate with submarines, which resulted in the tests for investigating the use of VLF-signals for ore prospecting by SGU (Paál, 1968). VLF profiles were measured over known sulphide ores in southern Lapland and showed the usefulness of the method in locating orebodies and other conductive structures. The measuring equipment consisted of a rather simple tunable loop and antenna with earphones. Since early 70's SGU has been extensively utilizing various airborne and ground EM measurements methods in its mapping program. In the following we provide a summary of these methods and example applications.

Airborne-VLF method

The VLF method uses the EM signal from distant radio transmitters in the frequency range 15–30 kHz. A sensor composed of three perpendicular induction coils measures the magnetic field components of the signal. By calculating the ratio between the vertical and horizontal components, the magnetic transfer function, the so-called tipper is estimated. SGU has conducted airborne-VLF measurements since early 70's using a fixed-wing system developed at SGU (Fig. 1a). Maps of tipper and its horizontal derivatives are utilized to locate elongated conductive structures. The tipper maps using just one transmitter contain an intrinsic directional bias and in the 80's SGU started measuring the signal from two transmitters. In the early 90's and in a close collaboration between SGU and Prof. Laust Pedersen at Uppsala University (UU) a new concept called the Tensor-VLF was developed to eliminate the bias. Later Becken and Pedersen (2003) developed a technique to transform tipper to apparent resistivity and phase. Since then, SGU has intensively used the technique for mapping deformation zones, conductive mineralization, and water-bearing fracture zones. Pedersen et al. (2009) presented examples of using airborne Tensor-VLF data collected by SGU in mapping and modeling conductive geological structures. The airborne tipper data along a flight line over the known Viscaria Cu-deposit were inverted in 2D and the resulting resistivity models revealed strong correlations with the existing geological and borehole data.

LF and VLF measurements onboard an Unmanned Aerial Vehicle (UAV)

The use of UAVs in mapping and modeling geology has increased considerably over the past decade. This includes geophysical measurements onboard UAVs. In the frame of the EU-funded Smart Exploration (https://smartexploration.eu/) project a new UAV-EM data acquisition system was developed by

SGU (2017 to 2020). The system is mounted below a dedicated electric UAV with a payload of 8 kg (Fig. 1b) and measures the EM signal in the VLF and extended LF frequency band of 10–350 kHz. The data acquisition system and 3-component induction coil sensor is hanging 10 m below the UAV. By increasing the frequency bandwidth, the resulting resistivity models deliver higher vertical resolution and maps of apparent resistivity can be generated at several frequencies. SGU has conducted UAV-borne EM measurements over three areas during 2020 and 2021. One area is located close to the abandoned Enåsen gold mine in central Sweden. The UAV survey was conducted along 26 lines (each 1.1 km long) with a separation of 100 m. The resistivity maps at six frequencies show a NW–SE running conductive structure and correlates well with the known greywacke unit that hosts copper sulfide mineralization.

Radio Magnetotellurics (RMT)

Like the VLF method, the RMT method also uses EM signal from distant radio transmitters though in a broader band of 10–1000 kHz (Bastani 2001, Tezkan et al. 2008). The RMT method also measures two horizontal components of the electric field and the complex impedance tensor is estimated (Bastani 2001). The RMT data are then inverted in 2D and 3D to model the electrical resistivity. SGU in collaboration with Uppsala University (UU) have been actively involved in development of instruments. In a research project funded by SGU, Bastani et al. (2015) carried out RMT measurements over the Lake Mälaren where they used UU's EnviroMT instrument (Bastani 2001) and developed a new setup, the so-called "Boat-towed RMT". During a three-day field campaign 17 km of RMT data were collected along parallel profiles over the water passages where three tunnels will be excavated within the frame of Stockholm bypass. The resistivity models from 2D inversion of RMT data revealed low resistivity zones within the crystalline bedrock that could be caused by fracture zones filled with clay and/or water.

Figure 1: a) SGU's fixed wing system for airborne-VLF. b) SGU's UAV system for extended VLF-LF.

References

Bastani M., 2001, EnviroMT – A New Controlled Source /Radio Magnetotelluric System. PhD thesis: *Acta Universitatis Upsaliensis, Uppsala Dissertations from the Faculty of Science and Technology* 32

Bastani, M., Persson, L., Mehta, S., and Malehmir, A., 2015. Boat-towed radiomagnetotellurics (RMT)— a new technique and case study from the city of Stockholm. *Geophysics*, 80, B193–B202. doi:10.1190/GEO2014- 0527.1

Becken, M. and Pedersen, L. B., 2003. Transformation of VLF anomaly maps into apparent resistivity and phase. *Geophysics 68*, 497–505.

Paal, G. 1968, Very low frequency measurements in northern Sweden. *Geoexploration* 6, 141-149

Pedersen, L.B., Persson L., Bastani, M., and Byström, S., 2009. Airborne VLF measurements and mapping of ground conductivity in Sweden. *Journal of Applied Geophysics* 140, 250–258.

Påsse Tore, Kim-Andersson Anna, red (2008). Sveriges geologiska undersökning: 150 år i samhällets tjänst : undersökningen, uppdragen, människorna. Uppsala: *Sveriges geologiska undersökning*. sid. 44.

Sundberg, K., Lundberg, H. and Eklund, J., 1923. Electrical Prospecting in Sweden. Årsbok 17, *Sveriges Geologiska Undersökning*, Stockholm.

Tezkan, B., & Saraev, A. 2008, A new broad band radiomagnetotelluric instrument: Applications to near surface investigations, *Near Surface Geophysics*, Vol. 6, 4, 245-252, https://doi.org/10.3997/1873-0604.2008019

A Geophysical Survey of Utö

Nicole C. Flanders

Department of Geological Sciences, Stockholm University, Stockholm, Sweden, nifl0456@student.su.se

Summary. A multidisciplinary geophysical survey on the northeast part of Utö was performed using a variety of analog instruments in order to identify ferromagnetic sources and investigate the extent of Fe bearing sulfides, BIFs, and their probable origins. Through the addition of historical maps, published matter, and previous surveys was this study able to affirm those observations, and with small discoveries during the project adding new information allowed the ability for qualitative reassessment of Utö's structural geology, ore depth and exents, and petrology.

A Multidisciplinary Geophysical Ground Survey

A geophysical investigation on the northeastern part of Utö was carried out between 2020 and 2021 to asses the extent of the iron ore (BIFs) and the Fe bearing sulfides that have been surveyed and mined in the past (Skelton et al. 2018, Talbot 2008, Stålhös 1982, and many more). The survey combined magnetometry, gravimetery, susceptibility, leveling, density, and thin-section microscopy. Analog survey equipment such as the SCINTREX MP-2 magnetometer, Sodin Gravimeter, Malå JH8 susceptibility meter, and Leica Wild NA-20 were used for measurements. Magnetic measurement reduction method was done through SGU's communicated advice (private communication, May 26, 2021) and software used in data analysis were Golden Software's Surfer® 21, Gordon Cooper's Mag2DC and Grav2DC, and QGIS. Additionally, an in depth literature analysis was performed to understand the historical context of mine operations to aid interpretation.

The results of the multidisciplinary analysis show a number of observations: figure 1 below is the interpolated local magnetic anomaly which fit well with current SGU magnetic map. Also the measured gravity data are consistent with the SGU Bouguer anomaly maps. The susceptibilty is observed to follow past reports of localities where Fe bearing sulfides were found. The 2D gravity profile suggests that more BIF ore certainly does exist in the synclinal structure of the seam, very likely corroborating estimated ore depths up to 1000 meters (Halen 1979). Virgin sulfide ore discovered during field work provides evidence to early ore formation and fluid mobilization and pictures taken from divers in Nyköpings and Långgruvan shine a fresh and new light of the structural geology and the reactivation of fractures in later stages of Utö's geological history. Overall, there is evidence to suggest far more BIF ore exists on the island and this result of course requires more inquiry into the geophysical context of its exploration.

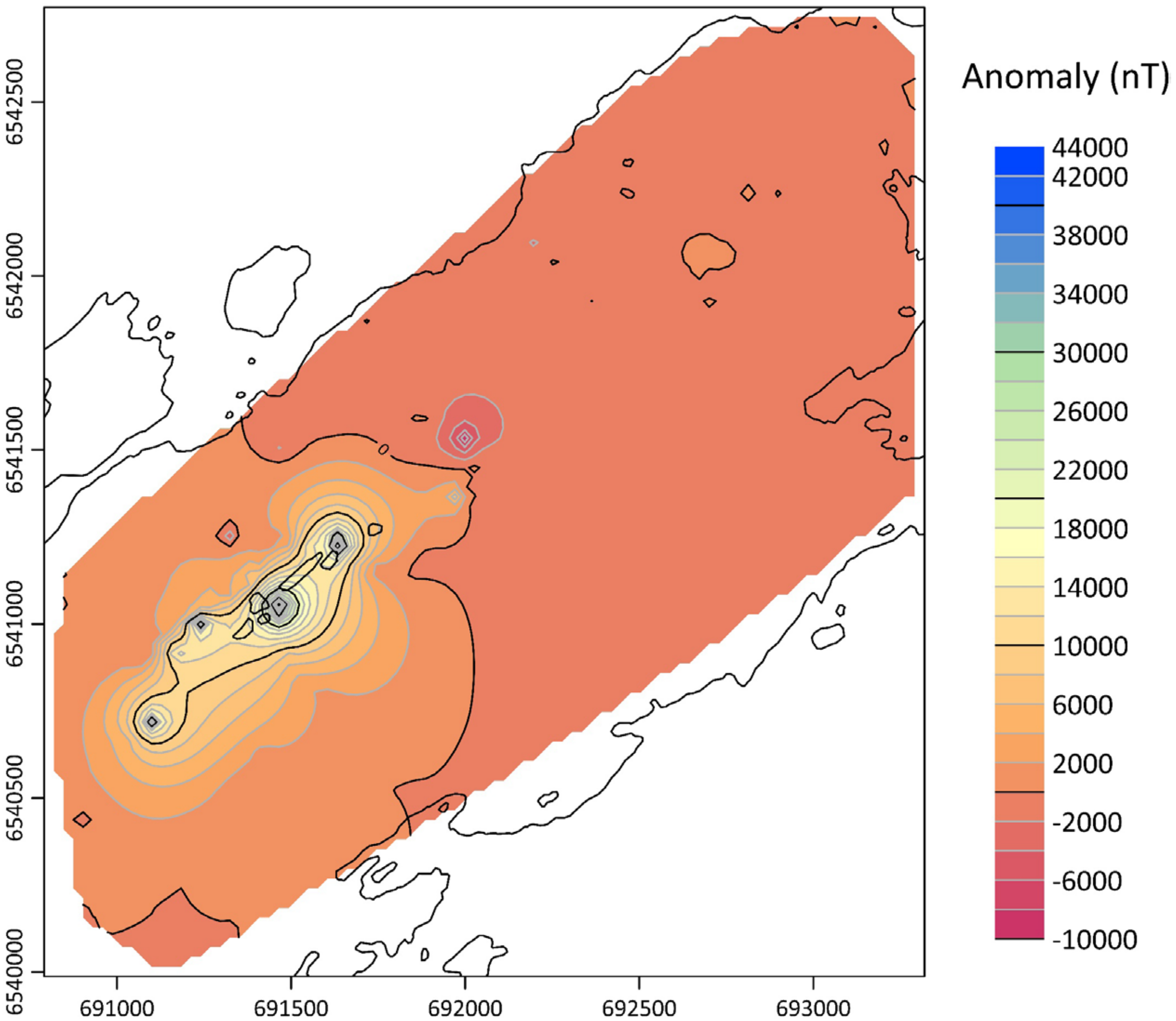

Figure 1: Interpolated local magnetic anomaly grid using Surfer 21® on Utö. Blank areas represent no data.

References

Halen, P. A., 1979: Utö gruvor, Gruvkarta 1, Beskrivning. Sveriges Geologiska Undersökning.

Skelton, A. & Mansfeld, J. & Ahlin, S. & Lundqvist, T. & Linde, J. & Nilsson J., 2018: A compilation of metamorphic pressure–temperature estimates from the Svecofennian province of eastern and central Sweden, *GFF* 140:1, 1-10, DOI:10.1080/11035897.2017.1414074.

Talbot, C. J., 2008: Palaeoproterozoic crustal building in NE Utö, southern Svecofennides, Sweden, *GFF* 130:2, 49-70, DOI: 10.1080/11035890801302049.

Stålhös, G. 1982: Beskrivning till berggrundskartan Nynäshamn NO/SO. Utö med omgivande skärgård. Sveriges Geologiska Undersökning, Af 138.

QGIS Development Team, 2022: QGIS Geographic Information System. Open Source Geospatial Foundation Project. http://qgis.osgeo.org.

Collisional Orogeny in the Scandinavian Caledonides (COSC): Overview of geophysical results from COSC-1 and COSC-2

Christopher Juhlin[a], Bjarne Almqvist[b], Henning Lorenz[a], Simon Rejkjær[b], Jan-Erik Rosberg[b]

[a]Department of Earth Sciences, Uppsala University, Uppsala, Sweden, christopher.juhlin@geo.uu.se;
[b]Engineering Geology, Lund University, Lund, Sweden

Summary. COSC aims to characterise the structure and orogenic processes involved in a major collisional mountain belt by multidisciplinary geoscientific research. Located in western central Sweden, the project has drilled two fully cored deep boreholes into the bedrock of the deeply eroded Early Paleozoic Caledonide Orogen. COSC-1 (2014) drilled a subduction-related allochthon and the associated thrust zone. COSC-2 (2020) extends this section deeper through the underlying nappes, the main Caledonian décollement, and the upper kilometre of basement rocks. A geophysical overview will be presented.

COSC-1

COSC-1 was drilled into the high grade Seve nappe to 2496 m, with almost 100% core recovery, during the summer of 2014 (see Figure for location). The top c. 1700 m consists mostly of sub-horizontal and shallowly dipping intermittent layers of felsic calc-silicates/gneisses and amphibolite. First signs of increasing strain appear shortly below 1700 m in the form of narrow deformation bands and thin mylonites. Below c. 2100 m, mylonites dominate and garnets become common. A transition from gneiss into lower-grade metasedimentary rocks occurs between 2345 and 2360 m. The lower part of the drill core to 2496 m is dominated by quartzites and metasandstones of unclear tectonostratigraphic position that are mylonitized to a varying degree. The lowermost 800 m can be interpreted as a thick shear zone.

Geophysical logging has been performed along the entire borehole with a wide variety of logs run, including P-wave sonic, density and televiewer logs. Geophysical measurements on core include P-wave velocity, density and magnetic susceptibility. Seismic data show the Seve nappe to be represented by a highly reflective package with short dipping reflections in the upper part. Deeper down the reflections become long and more sub-horizontal. The reflectivity is interpreted to be generated at the boundaries between the mafic and felsic rocks. Other important geophysical observations include the detection of discrete zones of fresh water inflow into the borehole along its entire length and that a relatively high temperature gradient of about 20 °C/km.

COSC-2

COSC-2 was drilled from mid-April to early August in 2020 to 2276 m depth (see figure for location), also with excellent core recovery. Drilling targets for COSC-2 included (1) the highly conductive Alum shale, (2) the Caledonian décollement, the major detachment that separates the Caledonian allochthons from the autochthonous basement of the Fennoscandian Shield, and (3) the strong seismic reflectors in the Precambrian basement.

Combined seismic, magnetotelluric (MT) and magnetic data were used to site the COSC-2 borehole about 20 km east-southeast of COSC-1. Based on these data it was predicted that the uppermost, tectonic occurrence of Cambrian Alum shale would be penetrated at about 800 m, the main décollement in Alum shale at its stratigraphic level at about 1200 m and the uppermost high amplitude basement reflector at about 1600 m. Paleozoic turbidites and greywackes were expected to be drilled down to 800 m depth. Below this depth, Ordovician limestone and shale with imbricates of Alum shale were interpreted to be present. Directly below the main décollement, magnetite rich Precambrian basement was expected to be encountered with a composition similar to that of magnetic granitic rocks found east of the Caledonian Front. The actual depths of the main contacts turned out to agree very well with the predictions based on the geophysical data. However, the geology below the uppermost occurrence of Alum shale is quite different from the expected model. Alum shale was only clearly encountered as a highly deformed, about 30 m thick unit, starting at about 790 m. Between about 820 and 1200 m, interpretations are that the rocks mainly consist of Neo-Proterozoic to Early Cambrian tuffs. Further below, Precambrian porphyries are present.

The Alum shale is responsible for the strong high conductivity anomaly observed on the MT data with a predicted top to the shale close to that observed in the borehole. The high amplitude reflections within the Precambrian sequence appear to be generated by dolerite sheets with the uppermost top penetrated at about 1600 m. Several deformed sheets of dolerite may be present down to about 1930 m. Below this depth the rocks are again porphyries. A temperature gradient of about 20 °C/km is also observed at the COSC-2 location.

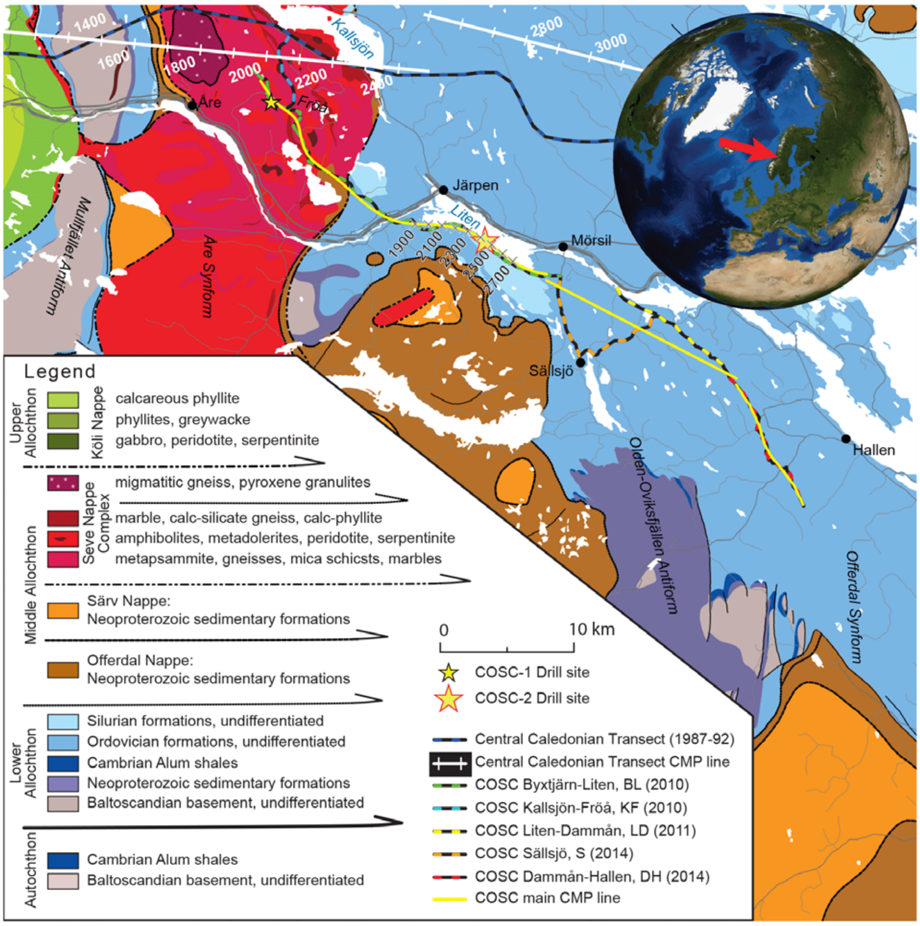

Figure. Tectonostratigraphic map of the Åre–Järpen area (based on the 1 : 200 000 scale geological map by the Geological Survey of Sweden, I2014/00601; Strömberg et al., 1984). The map shows the COSC drill sites, the location of the regional seismic profiles of the Central Caledonian Transect (Palm et al., 1991; Juhojuntti et al., 2001), and the seismic lines of the COSC site investigations. The magnetotelluric survey (Yan et al., 2016) followed the track of the COSC seismics. Figure from from Lorenz et al. (2022).

References

Strömberg, A.G., 1961: On the tectonics of the Caledonides in the southwestern part of the County of Jämtland, Sweden, Almqvist & Wicksell, Uppsala, 1961.

Palm, H., Gee, D.G., Dyrelius, D. & Björklund, L., 1991: A reflection seismic image of Caledonian structure in central Sweden, Sveriges geologiska undersökning, Uppsala.

Juhojuntti, N., Juhlin, C. & Dyrelius, D., 2001: Crustal reflectivity underneath the Central Scandinavian Caledonides, *Tectonophysics 334*, 191–210.

Lorenz et al., 2022: COSC-2 – drilling the basal décollement and underlying margin of palaeocontinent Baltica in the Paleozoic Caledonide Orogen of Scandinavia. *Scientific Drilling 30*, 43-57.

Yan et al., 2016: A magnetotelluric investigation of the Scandinavian Caledonides in western Jämtland, Sweden, using the COSC borehole logs as prior information, *Geophys. J. Int. 208*, 1465–1489,

Geophysical exploration in the Per Geijer area, close to Kiruna

Niklas Juhojuntti, Agnieszka Stoch, Birka Ewig, Joseph McLeod

LKAB Exploration, Kiruna, Sweden, niklas.juhojuntti@lkab.com, agnieszka.stoch@lkab.com, birka.ewig@lkab.com, joseph.mcleod@lkab.com

Summary. The Fe mineralization at Per Geijer responds well to many geophysical surveys, although the higher-grade parts are at the limit for traditional gravity and magnetic surveys from the surface. Recent exploration in the area has therefore included deep-sounding electromagnetic measurements and reflection seismics. The many drill holes in the area have also been used to image the target with higher resolution, to measure the physical properties via wireline logging, and for injecting electric current to illuminate the mineralization for certain geophysical surveys.

Geophysical exploration in the Per Geijer area

The Per Geijer ore field is located just north of the town Kiruna, in northern Sweden, and contains four previously mined iron ore bodies. These are located stratigraphically up-section of the Luossavaara and Kiirunavaara ore deposits, the latter of which is currently being mined.

Already in the 1960s a long-wavelength magnetic anomaly was recognised in the area, indicating the possible presence of a deep Fe mineralization (Fig. 1). This interpretation was confirmed by drilling in 1965, leading to the discovery of the Per Geijer Deep mineralization (at this time called Lappmalmen). Exploration continued in the area until the early 1980s, but was then paused for many years. Around the year 2006 there was a renewed interest in the PG Deep target, and since then various geophysical surveys have been carried out in the area.

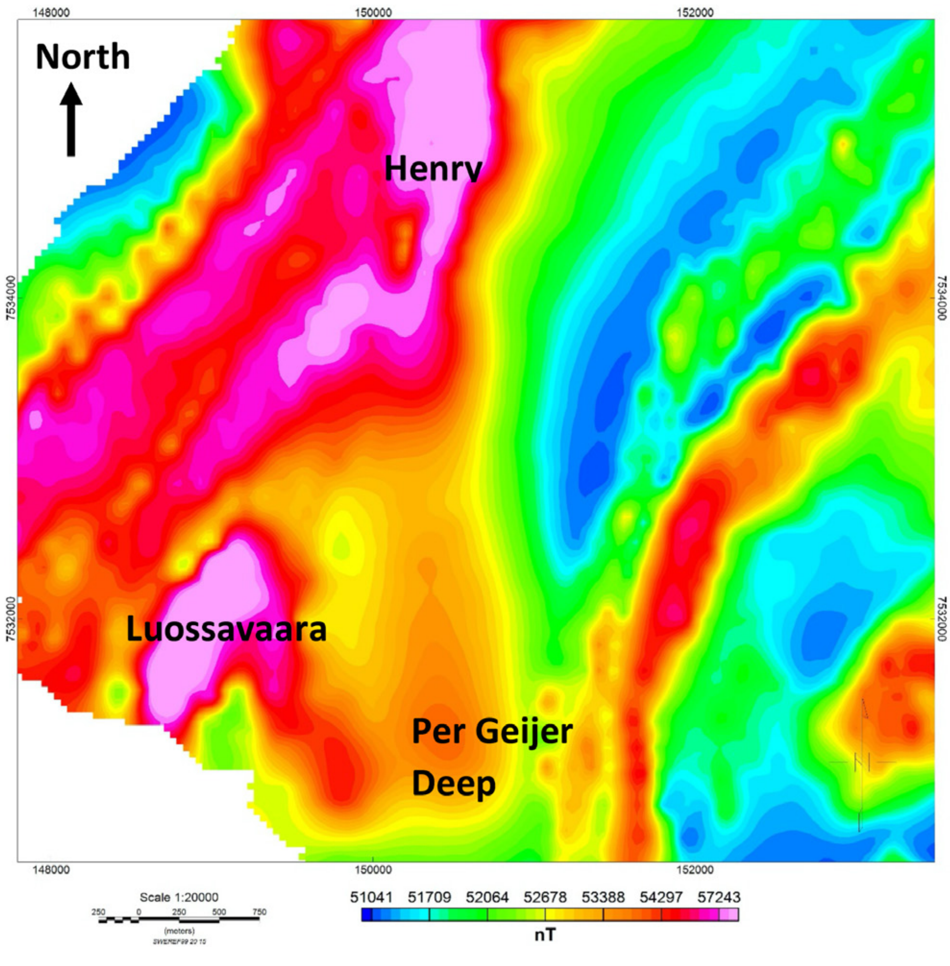

Figure 1. Airborne magnetic map for the Per Geijer area. The airborne measurements were carried out in 2008.

The large volumes of dense, generally highly magnetic, and electrically conductive Fe mineralization at Per Geijer are suitable targets for many geophysical surveys. Magnetic and gravity measurements have of course remained important, although the large depth (>500 m) to the richest part of the mineralization (PG Deep) poses a challenge for potential field surveys at the surface, and the observed anomalies have long wavelengths and moderate amplitude (Fig. 1). Therefore, the recent geophysical exploration in the area has included deep-sounding electromagnetic and seismic reflection measurements, both of which show distinct responses from the Fe mineralization at Per Geijer (Fig. 2).

Given the intense drilling carried out on this target, LKAB also has an active borehole geophysics program, including logging of parameters such as resistivity and magnetic susceptibility, and also downhole TEM and magnetics to detect off-hole mineralization. During 2021, borehole gravity was used in three deep holes, showing pronounced anomalies (>5 mGal), and inversion modelling has been carried out based on data from these measurements.

The boreholes have also been used for injecting electric current into the target, and carrying out mise-à-la-masse and magnetometric resistivity (MMR) measurements to outline the geometry of the mineralization. The first mise-à-la-masse survey in 2012 indicated a connection of the PG Deep mineralization with the shallower ore bodies around the Henry open pit, an interpretation which was verified by subsequent drilling.

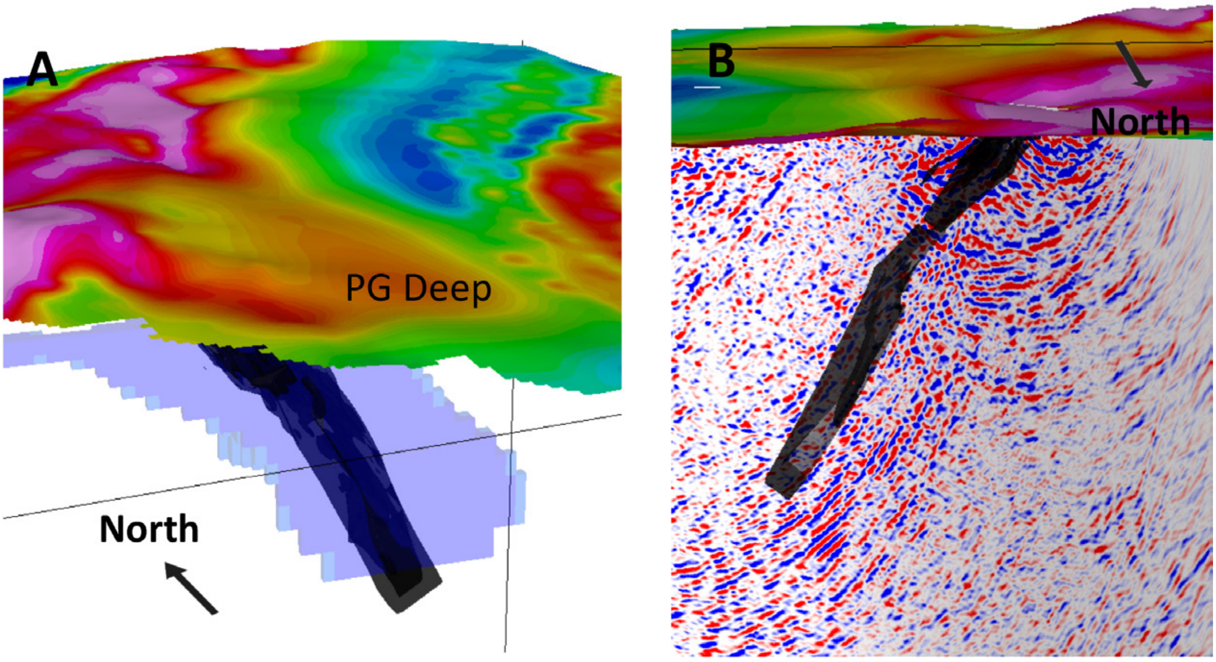

Figure 2. Geophysical data from the Per Geijer area. A) View approximately from southwest, showing the magnetic map draped on the surface, the electrical conductivity model from the 2018 helicopter survey in bluish colour (Smirnova et al., 2020), and the simplified PG Deep ore model in black. B) View from the north, showing a reflection seismic image and the simplified ore model, with the magnetic map draped on the surface. The seismic image is shown to a depth of about 2.2 km.

References

Smirnova, M., Juhojuntti, N., Becken, M., Smirnov, M. & the DESMEX WG, 2020. Exploring Kiruna Iron Ore fields with large-scale, semi-airborne, controlled-source electromagnetics. First Break 38.

Magnetotelluric and geomagnetic activities in Sweden – from space to core

Thorkild M. Rasmussen[a], Maxim Yu. Smirnov[a], Toivo Korja[a] , Roshanak Vadoodi[a], Gerhard Schwarz[b], Niklas Juhojuntti[c]

[a]Luleå University of Technology, Luleå, Sweden, thorkild.maack.rasmussen@ltu.se, Maxim.Smirnov@ltu.se, Toivo.Korja@ltu.se, Roshanak.Vadoodi@ltu.se; [b]Sveriges Geologiska Undersökning, Uppsala, Sweden, Gerhard.Schwarz@sgu.se , [c]LKAB, Kiruna, Sweden, niklas.juhojuntti@lkab.com

Summary. Time variations of the naturally occurring Earth's magnetic and electric fields provide valuable information about the interior of the Earth. Data are measured at geomagnetic observatories and at temporary sites by portable units utilizing, e.g. the magnetotelluric (MT) method. Geomagnetic data are primarily used for space-weather diagnosis and main field modelling and mapping. MT surveys can provide information about the electrical conductivity structure of the entire lithosphere.

Historical perspective and data acquisition

The geomagnetic observatories in Sweden are part of an international network of observatories (INTERMAGNET, e.g. Love & Chulliat 2013). Their data are applied as part of global modelling and mapping of the main field and provide information about the dynamics of the Earth's core. Three geomagnetic observatories are today operated by the Swedish Geological Survey (SGU): The oldest one, Abisko (ABK) is running since 1921. The main observatory of Sweden, Lovö (LOV) was in operation from 1928 to 2004. It was replaced by the Fiby observatory (UPS) close to Uppsala in 1997. Lycksele observatory was set-up in the 1950'ties and run by SGU, in corporation with the Institute of Space Physics (IRF), since 2006.

Geomagnetic data are utilized in the diagnosis of space weather and enhancing its prediction. It describes the variations in the space environment, e.g. particle flux between the sun and Earth. Space weather can impact systems and modern technologies in orbit and on Earth and, therefore, studying this phenomenon is of utmost importance. In the last years, SGU has narrowed the existing gaps in ground magnetometer coverage in Sweden by establishing 6 geomagnetic stations within the MAG-SWE-DAN project, funded by ESA. All stations will provide near-real time data to monitor the geomagnetic conditions, thereby expanding the existing space weather monitoring system. Swedish expertise in the MT method was established when Laust B. Pedersen became chaired professor in Solid Earth Physics at Uppsala University (UU). First systematic MT measurements were performed in 1983 by UU along the FENNOLORA (Fennoscandian Long Range) seismic refraction profile which runs from Karlskrona in southern Sweden to Nordkap in northern Norway. The measurements were made possible after purchase of a five component MT system developed at Aarhus University complemented by a digital recording system, developed at UU. Earlier magnetometer array studies included a few electrical recordings, were performed during the International Magnetospheric Study (IMS) project (Kuipers et al. 1979, Jones, 1980, 1982). These initial measurements were truly experimental since no knowledge was available at that time about the deep electrical conductivity structure of the Fennoscandian Shield. Truly large MT array surveys were supported by EU funding and resulted in acquiring large BEAR array data (Korja 2003). Significant parts of the research have involved Nordic cooperation on instrument development, data processing and interpretations. Development of a broad-band (Audio MT + Long periodic MT = MTU2000) instrument was initiated at UU in 2000 when Knut and Alice Wallenbergs Stiftelsen provided financial support in 1999 (Smirnov et al. 2008). This set of new instruments allowed several projects, starting from investigating deep structures along Trans-European Suture Zone TESZ (Brasse 2005), and further extending to the Sorgenfrei-Tornquist Zone (STZ) in Denmark (Smirnov 2009). Later, extensive deep MT studies were investigating the Caledonian orogen (Korja 2008) along the Jämtland profile and in Norrbotten. There, the Nordic pool of MT instruments was used, together with contribution from other partners around Europe (Cherevatova 2015).

LTU has recently upgraded the MT pool of instruments (0.001–250 kHz range) with ten new Metronix ADU08 systems. These were used in large simultaneous MT array measurements for mineral exploration within D-REX project (see presentation of Smirnov).

Results

The first results from geomagnetic array studies showed the presence of highly conductive structures within the crust, such as the Storavan anomaly (Jones, 1980). It was studied further with MT measurements along the FENNOLORA profile. Modelling of these data (Rasmussen et al. 1988) showed the presence of a highly conductive upper crust south of the Skellefte ore district and a NE dipping conductive slab below. The electrical conductivity structure with a dip of 30 degrees was interpreted as the remnants of a Precambrian subduction zone. The presence of graphite is most likely the cause of the observed high conductivities (Korja 2008). Studies of the Archaen and Precambrian crust and upper mantle in Norrbottten (Cheratova et al., 2015, Vadoodi et al. 2021) indicate several highly conductive structures within the crust. A possible generic relationship between these conductive structures was discussed by Vadoodi et al. (2021) and being a key research topic in the on-going D-REX project (Smirnov et al. 2021).

Correlation between models derived from MT data and reflection seismic images were studied along the Jämtland profile crossing the Caledonides (Korja 2008). Graphite was inferred as the cause of observed high conductivity layers, marking the sole thrust deduced from reflection seismics.

Azimutal electrical anisotropy of the lower crust was interpreted from MT measurements performed in Värmland (Rasmussen, 1988). There, data also indicate an electrical asthenosphere at depth larger than 300 km. This result differs from depth estimates of the asthenosphere of roughly 150 km, observed in the Archaean part of northern Sweden.

References

Brasse, H., Kreutzmann, A., Cerv, V., Ernst, T., Jankowski, J., Jozwiak, W., Neska, A., Pedersen, L. B. rsting, Smirnov, M., Schwarz, G., Sokolova, E., Varentsov, I. M., Hoffmann, N., Palshin, N., & Korja, T. (2006). Probing electrical conductivity of the Trans-European Suture Zone. *Eos Transactions American Geophysical Union*, *87*(29), 281.

Cherevatova, M., Smirnov, M. Yu., Jones, A. G., & Pedersen, L. B. (2015). Magnetotelluric array data analysis from northwest Fennoscandia. *Tectonophysics*. https://doi.org/http://dx.doi.org/10.1016/j.tecto.2014.12.023

Jones, A. (1980). Geomagnetic induction studies in Scandinavia — I. Determination of the inductive response function from the magnetometer array data. Journal of Geophysics, 48(1), 181-194.

Jones, A.G., 1982. Observations of the electrical asthenosphere beneath Scandinavia. In: E.S. Husebye (Editor), The Structure of the Lithosphere-Asthenosphere in Europe and the North Atlantic. Tectonophysics, 90: 37-55.

Kiippers, F., Untiedt, J., Baumjohann, W., Lange, K., Jones, A.G.: A two-dimensional magnetometer array for ground-based observations of auroral zone electric currents during the International Magnetospheric Study. J. Geophys. 46, 429-450, 1979

Korja, T., Smirnov, M., Pedersen, L.B., Gharibi, M., Korja, T., Smirnov, M., Pedersen, L. B., & Gharibi, M. (2008). Structure of the Central Scandinavian Caledonides and the underlying Precambrian basement, new constraints from magnetotellurics. *Geophysical Journal International*, *175*(1), 55–69. https://doi.org/10.1111/j.1365-246X.2008.03913.x

Korja, T., Engels, M., Zhamaletdinov, A. A., Kovtun, A. A., Palshin, N. A., Smirnov, M. Y., Tokarev, A. D., Asming, V. E., Vanyan, L. L., Vardaniants, I. L., & the BEAR working group. (2002). Crustal conductivity in Fennoscandia - a compilation of a database on crustal conductance in the Fennoscandian Shield. *Earth Planets Space*, *54*(5), 535–558. https://doi.org/10.1186/BF03353044

Love, J.J. & Chulliat, A. (2013). An International Network of Magnetic Observatories. EOS, 94, 373-374.

Smirnov, M. Yu., & Pedersen, L. B. (2009). Magnetotelluric measurements across the Sorgenfrei-Tornquist Zone in southern Sweden and Denmark. *Geophysical Journal International*, *176*(2), 443–456. https://doi.org/10.1111/j.1365-246X.2008.03987.x

Smirnov, M., Korja, T., Dynesius, L., Pedersen, L. B., & Laukkanen, E. (2008). Broadband magnetotelluric instruments for near-surface and lithospheric studies of electrical conductivity: A Fennoscandian pool of magnetotelluric instruments. *Geophysica*, *44*(1–2), 31–44.

Rasmussen, T., Roberts, R., Pedersen, L., 1987. Magnetotellurics along the fennoscandian long range profile. Geophysical Journal International 89, 799–820.

Rasmussen, T. M. (1988). Magnetotellurics in southwestern Sweden: Evidence for electrical anisotropy in the lower crust? *Journal of Geophysical Research: Solid Earth*, *93*(B7), 7897–7907. https://doi.org/10.1029/JB093iB07p07897

Vadoodi,R., Rasmussen T.M, Smirnov M., Bauer T. (2021) Towards an understanding of mineral systems–Contributions from magnetotelluric data from the Fennoscandian Shield in northern Sweden, Tectonophysics, 228816. Volume 808, 5 June 2021, 228816.

The Swedish National Seismic Network

Michael Roth, Björn Lund, Peter Schmidt, Hossein Shomali, Gunnar Eggertsson

Department of Earth Sciences, Uppsala University, Uppsala, Sweden, michael.roth@geo.uu.se, bjorn.lund@geo.uu.se; peter.schmidt@geo.uu.se; hossein.shomali@geo.uu.se; gunnar.eggertsson@geo.uu.se

Summary. The Swedish National Seismic Network (SNSN) currently comprises 68 permanent and 13 medium-term seismic broadband stations. SNSN exchanges waveform data with neighboring countries and the seismological community, and automatically processes all data streams in real-time. Since the start of automatic operations in August 2000 the SNSN has recorded more than 11,800 earthquakes in Sweden and contributed data to a large number of studies on crustal and lithospheric structure.

Network operations

Seismic observations in Sweden started in Uppsala on October 4th 1904 with the installation of a Wiechert horizontal pendulum seismograph (Swedish National Seismic Network (SNSN), 1904). From 1969 until 1998 an additional 6 analogue seismic stations were in operation. In the year 1998, a significant modernisation and expansion of the SNSN started which was completed in 2008, when 55 new stations had been built. Since then only a few permanent stations have been added to the network (for a recent review see Lund et al., 2021).

SNSN currently operates 68 permanent and 13 medium-term (3-year) broadband seismic stations (Fig. 1). The network stretches over a distance of about 1500 km from South to North. All stations are sending continuous real-time data to the the SNSN centre located at Uppsala University. Automatic routines at the SNSN data centre are monitoring the state-of-health and the quality of the incoming data streams. Continuous real-time waveform data from about 30 stations of the SNSN are shared with institutes in neighboring countries (Denmark, Finland, Norway, Germany) and with the general international seismological community. SNSN receives additional real-time data streams from about 400 seismic stations abroad.

SNSN uses four different automatic data processing systems for local and regional events:(1) SIL/multi_SIL (Stefansson et al, 1993), (2) a migration stack (MS) system (Wagner et al., 2017), (3) SeisComP (SeisComP, 2008) and (4) Earthworm (Eartworm, 2019), all completely independent from and in parallel which each other. On one hand there is signification overlap of the automatic bulletins from the individual bulletins, which gives a high level of reliability and redundancy. On the other hand, the systems are complementary in terms of both timeliness and detection thresholds. The analyst review uses information from all four systems, but it is performed with SIL system software designed for interactive analysis such as picking, location and focal mechanisms. Most of the

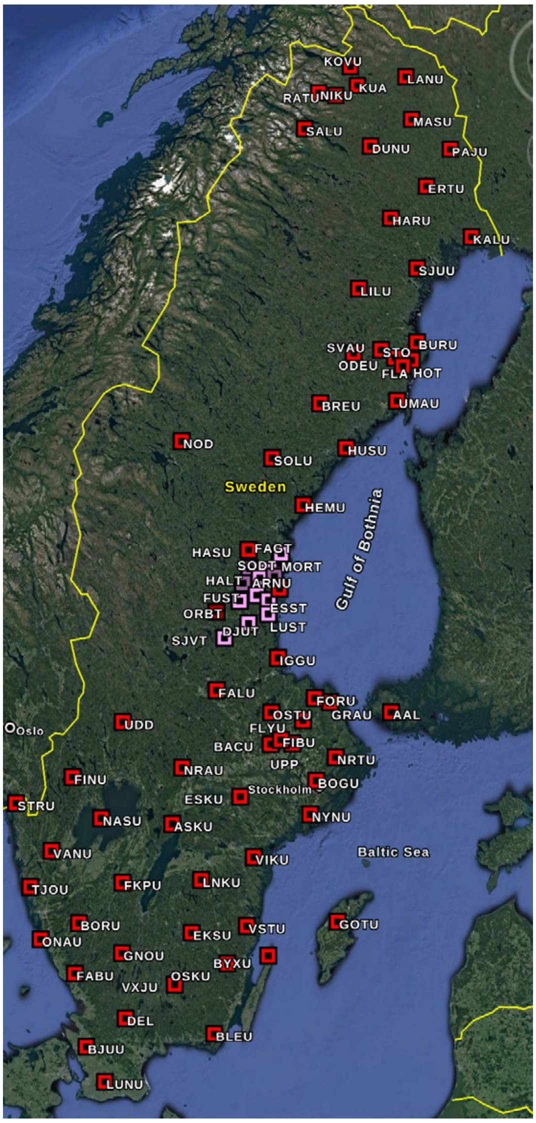

Figure 1: Stations of the Swedish National Seismic Network.

seismic events in Sweden are blasts related to mining (open pit and underground) and to civil works. SNSN is currently developing a neural network classification schema to automatically discriminate between earthquakes and blasts.

Earthquakes and structure

Since the start of automatic operations in August 2000, the SNSN has detected, located and determined the magnitude of approximately 11,800 earthquakes in Sweden. During the last five years approximately 700 earthquakes have been recorded annually, with an average annual rate of 17 magnitude 2+ events. Every year 20–30 earthquakes are reported as felt to the SNSN or to local media. The largest earthquake recorded during these years was the M 4.3 Skåne event on 16 December 2008, an event that shook the cities of Malmö and Copenhagen significantly. The large number of well located earthquakes has significantly increased the detail in the seismically active structures. The new data have confirmed that the area around Lake Vänern is significantly seismically active, as is the northeast coast. The data have also revealed just how seismically active the post-glacial faults in northern Sweden are (Lindblom et al., 2015), that the Burträsk postglacial fault is the most seismically active area in Sweden (Juhlin and Lund, 2011), and that the dip and depth extent of the postglacial faults can be imaged using microearthquakes (Lindblom et al., 2015; Lund et al., 2015). The spatial resolution of the new locations shows that in many areas the seismicity is not generally diffuse, as suggested by the older data, but actually follows geological structures. The continuous data collected in SNSN have also allowed a number of structural studies in Fennoscandia using teleseismic tomography (e.g. Silvennoinen et al., 2016), receiver functions (e.g. Makushkina et al., 2019), surface waves (Köhler et al., 2015), and ambient noise (Sadeghisorkhani et al., 2017).

References

Earthworm, 2019: http://www.earthwormcentral.org/ (last accessed March 2022)

Juhlin, C., Lund, B., 2011: Reflection seismic studies over the end-glacial Burträsk fault, Skellefteå, Sweden, Solid Earth 2, 9–16, doi: 10.5194/se-2-9-2011.

Köhler, A., Maupin, V., Balling, N., 2015: Surface wave tomography across the Sorgenfrei-Tornquist Zone, SW Scandinavia, using ambient noise and earthquake data, Geophys. J. Int. 203, 284–311, doi: 10.1093/gji/ggv297.

Lindblom E., Lund B., Tryggvason A., Uski M., Bödvarsson R., Juhlin C., Roberts R., 2015: Microearthquakes illuminate the deep structure of the endglacial Pärvie fault, northern Sweden, Geophys. J. Int., 201, 1704-1716,.

Lund, B., Lindblom, E., Schmidt, P., Buhcheva, D., 2015: Constraints on endglacial rupture mechanics from estimates of the current stress field, IUGG-5471, 26th General Assembly of the IUGG, Prague, Czech Republic.

Lund B, Schmidt P., Shomali Z. H., Roth M., 2021: The modern Swedish National Seismic Network: Two decades of intraplate microseismic observations, Seismol. Res. Lett. 92: 1747-1758, doi: 10.1785/0220200435

Makushkina, A., Tauzin, B., Tkalcic, H., Thybo, H., 2019: The mantle transition zone in Fennoscandia: Enigmatic high topography without deep mantle thermal anomaly, Geophys. Res. Lett. 46, 3652–3662, doi: 10.1029/2018GL081742.

Sadeghisorkhani, H., Gudmundsson, O., Roberts, R., Tryggvason, A., 2017: Velocity-measurement bias of the ambient noise method due to source directivity, Geophys. J. Int., 209, 1648–1659, doi: 10.1093/gji/ggx115.

SeisComP 2008: Helmholtz Centre Potsdam GFZ German Research Centre for Geosciences and GEMPA GmbH, The SeisComP seismological software package, GFZ Data Services, doi:10.5880/GFZ.2.4.2020.003

Silvennoinen, H., Kozlovskaya, E., Kissling, E., 2016: POLENET/LAPNET teleseismic P wave travel time tomography model of the upper mantle beneath northern Fennoscandia, Solid Earth 7, 425–439, doi: 10.5194/se-7-425-2016.

Stefansson R., Bödvarsson R., Slunga R., Einarsson P., Jakobsdottir S., Bungum H., Gregersen S., Havskov J., Hjelme J., Korhonen H., 1993: Earthquake prediction research in the south Icelandic seismic zone and the SIL project, Bull. Seismol. Soc. Am. 83, no 3, 698-716

Swedish National Seismic Network (SNSN) 1904: Swedish National Seismic Network, Other/seismic network, Uppsala University, Sweden, doi: 10.18159/SNSN.

Wagner F., Tryggvason A., Roberts R., Lund B., Gudmundsson O., 2017: Automatic seismic event detection using migrations and stacking: A performance and parameter study in Hengill, soutwest Iceland, Geophys. J. Int. 209: 1866-1899, doi: 10.1093/gji/ggx127

Comparison of 3D inversions of MT and CSEM-data from Malmberget northern Sweden with a geological model

Oskar Rydman[a], Maxim Yu. Smirnov[a], Tobias E. Bauer[a], Harald Van Den Berg[b], Niklas Juhojuntti[b], Thorkild M. Rasmussen[a]

[a]Luleå University of Technology, Luleå, Sweden, oskar.rydman@ltu.se, maxim.smirnov@ltu.se, tobias.bauerr@ltu.se, thorkild.maack.rasmussen@ltu.se; [b]LKAB, Kiruna, Sweden, niklas.juhojuntti@lkab.com

Summary. During 2020-2022, LTU conducted both MT and CSEM measurements in the Malmberget area, Sweden, in collaboration with LKAB. The surveys consists of two CSEM surveys and one MT survey of the whole area. One CSEM survey measured all five field-components (E_x,E_y,H_x,H_y,H_z) whereas the other only measured magnetic field components (H_x,H_y,H_z). The data have been processed and later inverted using the MR3Dmod code. Consequently, the conductivity models are compared to each other and to the regional geological model.

Survey layout and data processing

During the summers 2020, 2021 and winter/spring 2022 Luleå University of Technology (LTU) in collaboration with Luossavaara-Kiirunavaara Aktiebolag (LKAB) have measured both magnetotelluric (MT) and Controlled source electromagnetics (CSEM) in the Malmberget area, Sweden. The Malmberget iron-oxide apatite deposit is one of Europe's largest underground iron mines operated by LKAB, and is hosted in paleoproterozoic mafic-intermediate metavolcanic rocks. The two CSEM surveys were measured during summer 2021 and winter/spring 2022. The summer survey was conducted using a 4 km grounded dipole source and five field components where measured (E_x,E_y,H_x,H_y,H_z). The area of the survey was 2×3 km^2 and the measurements were spaced with roughly 250 m distance. In the winter/spring survey only magnetic field components (H_x,H_y,H_z) where measured due to the snow-coverage and the survey covered an area of 2×2 km^2 with 250 m receiver spacing using a 1×1 km^2 magnetic loop source. The MT survey consists of measurements done from 2020–2022 which covers an area of 10×15km^2 with roughly 130 measurement points with around 1 km receiver spacing. The CSEM data were then processed to estimate univariate transfer functions between field components and current recording in frequency range 8–3000 Hz. The MT data were processed in the 10^{-3} to 10^3 Hz frequency range. After processing the data were separately inverted using the MR3Dmod code. The resulting electrical resistivity models are compared to each other as well as to geological information. An example of the MT 3D resistivity model can be seen in Figure 1. The surveys are part of two different projects. One focusing on Common Earth modelling (CEM) on deposit scale and the other being (D-Rex) which focuses on connections between regional and deposit scale exploration.

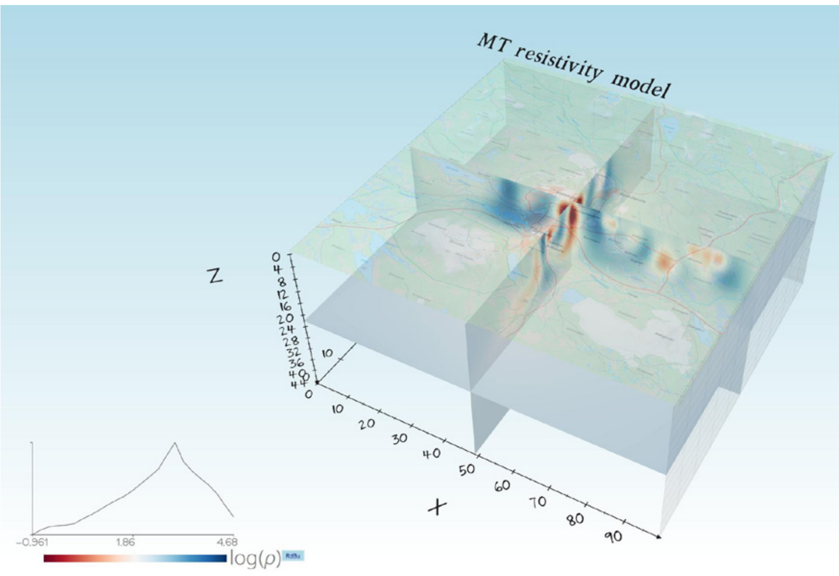

Figure 1: 3D MT electrical resistivity model of Malmberget. Subfigure shows logarithmic resistivity distribution in Ohm-m and spatial axis's shows cell number. The model is $15 \times 15 \times 20$ km^3

Crustal structure and isostasy in Nordland and Troms, Northern Norway – A controversy?

Christian Schiffer[a], Stéphane Rondenay[b], Lars Ottemöller[b], Anne Drottning[b]

[a]Department of Earth Sciences, Uppsala University, Uppsala, Sweden, christian.schiffer@geo.uu.se;
[b]Department of Earth Science, University of Bergen, Bergen, Norway, Rondenay@uib.no, Lars.Ottemoller@uib.no, annedrottning@gmail.com;

Summary. The crustal structure of the Nordland and Troms region, Norway, has received growing scientific attention for two main reasons: (i) The region is one of the most seismically active areas of mainland Norway, the reason of which is poorly understood. (ii) There are different interpretations of the crustal structure of the region and none of the models satisfy gravity and topography via crustal isostasy. Our results detect a coherent low-velocity layer directly below the crust in the uppermost mantle that has not been previously identified, which appears to be relevant to isostasy in the region.

Background

The Nordland and Troms region of Northern Norway comprises the narrow Lofoten-Vesterålen continental rifted margin hosting Permo-Triassic to Cretaceous sedimentary basins, the Lofoten-Vesterålen archipelago and the Scandinavian mainland, and is characterised by Precambrian bedrock overprinted by the northern Scandinavian Caledonides (Mosar et al. 2002). The origin of the high topography in the Caledonian mountain range, and particularly that of the Lofoten and Vesterålen islands, is a matter of debate. Proposed mechanisms include isostatic compensation from within the crust and lithosphere, elastic effects, dynamic topography, as well as uplift caused by glacial erosion (e.g. Nielsen et al. 2009, Gradmann et al. 2017, Maystrenko et al. 2017)

Several complementary geophysical datasets are available in the region, based on gravity, magnetics, active and passive seismic data (Maystrenko et al. 2017, Ben Mansour et al. 2018, Breivik et al, 2020 Shiddiqi et al. 2021). However, interpretations of these datasets show considerable differences leading to controversy concerning the structure, isostatic state and state of stress of the lithosphere – key factors to constrain the cause of intraplate seismicity. The Lofoten-Vesterålen archipelago appears to exhibit considerable crustal thinning from north to south. The prevalent view has been that the crust beneath the southern Lofoten is extremely thin at ~20 km (e.g. Mjelde et al. 1993), but this has been disputed (Breivik et al. 2020). Thus, the structure and isostatic state of the crust and lithosphere is still a matter of vigorous debate.

Study and preliminary results

Here, we present new seismological constraints on the crustal and uppermost mantle structure that help us addressing this debate. Models of velocity structure are computed at 62 broadband seismic stations by joint inversion of teleseismic receiver functions and P-wave polarisation – a method that is complementary to other geophysical approaches previously employed in the region.

Overall, our results are consistent with the regional crustal structure and trends inferred by previous models, including a sharp, N-S directed Moho gradient across the southern Lofoten and an extremely shallow Moho beneath the southern Lofoten Ridge. However, our results also detect a low-velocity layer directly below the interpreted crust in the uppermost mantle that has not been identified in previous work. This layer appears to be highly relevant to isostasy in the region.

In conclusion, the crustal structure in the region may not be as controversial as the recent debate suggests, as of now all geophysical models show very similar results. Yet, the isostatic state of the region, and the concept and applications of isostasy, as well as the depth of lithospheric structures relevant to isostasy seem to be much more urgent to be reviewed in the case of the Nordland and Troms region.

References

Ben Mansour, W., England, R.W., Fishwick, S., and Moorkamp, M., 2018: Crustal properties of the northern Scandinavian mountains and Fennoscandian shield from analysis of teleseismic receiver functions, *Geophys. J. Int., 214*, 386–401.

Breivik, A.J., Faleide, J.I., Mjelde, R., Flueh, E.R., and Murai, Y., 2020: Crustal structure and erosion of the Lofoten/Vesterålen shelf, northern Norwegian margin, Tectonophysics, 776, 228318.

Maystrenko, Y.P., Olesen, O., Gernigon, L., and Gradmann, S., 2017: Deep structure of the Lofoten-Vesterålen segment of the Mid-Norwegian continental margin and adjacent areas derived from 3-D density modeling, *J. Geophys. Res. Solid Earth, 122*, 1402–1433

Mjelde, R., Sellevoll, M.A., Shimamura, H., Iwasaki, T., and Kanazawa, T., 1993: Crustal Structure Beneath Lofoten, N. Norway, From Vertical Incidence and Wide-Angle Seismic Data, *Geophys. J. Int., 114*, 116–126.

Mosar, J., Eide, E.A., Osmundsen, P.T., Sommaruga, A., and Torsvik, T.H., 2002: Greenland–Norway separation: a geodynamic model for the North Atlantic, *Nor. J. Geol.*, *82*, 282.

Nielsen, S.B., Gallagher, K., Leighton, C., Balling, N., Svenningsen, L., Jacobsen, B.H., Thomsen, E., Nielsen, O.B., Heilmann-Clausen, C., Egholm, D.L., Summerfield, M.A., Clausen, O.R., Piotrowski, J.A., Thorsen, M.R., et al., 2009: The evolution of western Scandinavian topography: A review of Neogene uplift versus the ICE (isostasy–climate–erosion) hypothesis, *J. Geodyn.*, *47*, 72–95.

Shiddiqi, H.A., Ottemöller, L., Rondenay, S., Halpaap, F., Gradmann, S., and Michálek, J., 2021: Crustal structure and intraplate seismicity in Nordland, Northern Norway: Insight from Seismic Tomography, in review.

DREX project

Maxim Yu. Smirnov[a], Graham J. Hill[b], Jochen Kamm[c], Jan Vozar[d], Thorkild M. Rasmussen[a], Jirigalatu Jirigalatu[a], Pankaj K. Mishra[c], Kenneth Muhumuza[b], D-REX WG

[a]Luleå University of Technology, Luleå, Sweden, maxim.smirnov@ltu.se, thorkild.maack.rasmussen@ltu.se, jirigalatu.jirigaltu@ltu.se; [b]Institute of Geophysics, Czech Academy of Sciences, Prague, Czech Republic, gjhill@ig.cas.cz, muhumuza@ig.cas.cz; [c]Geological Survey of Finland, Espoo, Finland; jochen.kamm@gtk.fi, pankaj.mishra@gtk.fi, [d]Earth Science Institute, Slovak Academy of Sciences, Bratislava, Slovakia, geofjavo@savba.sk

Summary. The objective of the D-Rex project is to improve the identification of previously unrealized metal endowed regions. Regional electromagnetic (magnetotellurics) surveys are being obtained at three prospective areas in Sweden, Norway and Finland to generate the large scale models needed to identify the deeper footprints of metal concentration. Previous studies of mineralized systems have focused on near surface investigations characterising individual deposits, whilst regional scale geophysical looking at the mineral system as a whole have the ability to identify markers at mid-lower crustal depths indicative of economically viable regions of metal endowment.

Regional to deposit scale exploration based on mineral system concept

Formation and concentration of metals into economic mineral deposits requires a combination of processes operating at different scales. Mineral deposits are themselves a small part of a much larger geological framework, the 'mineral system', which includes an often deeply seated source for fluids, a source region for metals, an energy source for driving hydrothermal circulation, pathways for the migration of enriched fluids, a depositional mechanism responsible for the formation of the deposit and a fluid outflow. Regional scale geophysical modelling of petrophysical properties may have the ability to identify markers at mid-lower crustal depths indicative of economically viable regions of metal endowment (i.e. the near surface mineral deposit). Historically, efforts to understand mineralized systems have focused on the near surface identification and evaluation of individual resource bodies using shallow imaging techniques. Given that surface geologies are often broadly similar in endowed and lesser endowed terrains the difference in endowment level can result either from: (1) a deeper burial depth of endowment beyond the sensitivity of traditional exploration techniques; or (2) differences in the mid to lower crustal evolution of these regions with processes favorable for concentration of metals being localized and potentially identifiable by key structural features at depths greater than typically considered in exploration surveys.

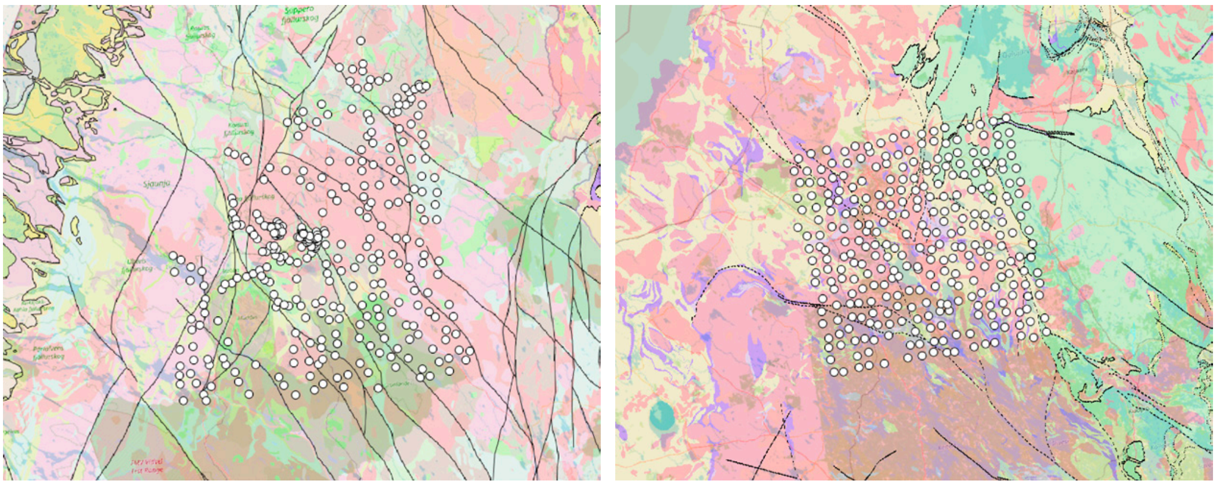

Fig1. MT sites measured during summer 2022 at regional and deposit scales around Gällivare, Sweden (left panel) and Pyhäsalmi, Finland (right panel)

Thus, large-scale deeper looking regional studies are needed to compliment the deposit scale models to clarify the disparate nature of metal endowment in areas characterised by similar surface geology. Construction of a regional model requires collection of a complimentary 3D geophysical datasets sensitive to different physical properties, covering depths from the upper mantle source zone to the near surface mineral deposit.

The manageable logistical requirements and small environmental footprint of magnetotellurics coupled with its broadband depth sensitivity (from 10s of meters to 100+ kilometres) are making it an increasingly important and powerful tool for geophysical studies with multiple depth scales of interest. For these reasons magnetotellurics is the primary new geophysical data set collected in D-Rex.

During summer 2021 regional and local scale magnetotelluric data were collected at two locations in Sweden and Finland. Areas of about 100x100 km^2 were covered with average site spacing of 5 km resulting to about 400 sites at each area. Additional deposit scale measurement around Gällivare and Pyhäsalmi were measured to compliment the regional data set as well as all previously available geophysical data. Extra CSEM data were also measured at both locations.

Original data are currently processed and analysed to derive impedance and tipper transfer functions using conventional robust remote reference processing. We will continue to work with data and apply multivariate techniques which we expect will improve estimates of transfer functions at problematic sites and provide additional information for the inverse modelling. Overall, the data quality is from excellent to good with some few exceptions related to instrumental and measurements problems and in some places human activity. We currently perform the first 3D inversion trials which will be presented.

D-REX Working Group (D-REX WG)

Luleå University of Technology:
Maxim Yu. Smirnov, Jirigalatu Jirigalatu, Thorkild M. Rasmussen, Tobias Bauer, Oskar Rydman

Geological Survey of Finland, Espoo, Finland:
Jochen Kamm, Pankaj K. Mishra, Cedric Patzer, Uula Autio, Jouni Luukas, Jarkko Jokinen

Institute of Geophysics, Czech Academy of Sciences:
Graham J. Hill, Kenneth Muhumuza, Světlana Kováčiková

Earth Science Institute, Slovak Academy of Sciences:
Jan Vozar , Jozef Madzin, Lenka Ondrášová, Vladimír Bezák, Peter Vajda

LKAB:
Niklas Juhojuntti, Harald Van Den Berg

Boliden:
Tobias Hermansson, Kirsi McGimpsey, Katri Vaittinen

NGU:
Sofie Grandmann

BIFROST – A Global Navigation Satellite System project serving Earth sciences since three decades

Holger Steffen[a], Jan Johansson[b], Halfdan Pascal Kierulf[c,d], Martin Lidberg[a], Hans-Georg Scherneck[e]

[a]Geodetic Infrastruture, Lantmäteriet, Gävle, Sweden, holger.steffen@lm.se, martin.lidberg@lm.se; [b]Department of Space, Earth and Environment, Chalmers Tekniska Högskola, Gothenburg, Sweden, jan.johansson@chalmers.se; [c]Geodetic Institute, Norwegian Mapping Authority, Hønefoss, Norway, Halfdan.Kierulf@kartverket.no; [d]Department of Geosciences, University of Oslo, Oslo, Norway; [e]Onsala Space Observatory, Chalmers Tekniska Högskola, Gothenburg, Sweden, hgs@chalmers.se;

Summary. Since three decades, displacements in Fennoscandia are precisely measured using a Global Navigation Satellite System (GNSS) within the Baseline Inferences for Fennoscandian Rebound, Sea-level, and Tectonics (BIFROST) project. The latest velocity field for geophysical applications published in 2021 shows dominating signals of plate motion (c. 2 cm/a from SW to NE) and Glacial Isostatic Adjustment (GIA) (up to c. 1 cm/a uplift near the city of Umeå). In recent years, also climate change effects have notable impact (up to 0.9 mm/a uplift). Work on a new velocity field commenced recently.

The scientific employment of the GNSS technique since the late 1980s has revolutionized many geoscientific fields. In solid Earth sciences and geodynamics precise determination of any plate motion and deformation cannot be imagined without the help of GNSS. The BIFROST project, started in 1993, is one of the very early and still continuing GNSS projects in geodynamics. Its original mission was primarily the measurement of vertical crustal motion, especially the postglacial rebound after last glaciation in northern Europe (Scherneck et al. 1998). It started with a network of more than 40 GNSS stations in mainly Sweden and Finland, which since then has been increased to more than 160 stations covering almost whole northern Europe.

Since the late 1990s there is a steady flow of new velocity field results based on an increasing number of stations with longer observation time, thereby densifying and enlarging the network as well as partly considerably improving the accuracy of the measurements. BIFROST results provided evidence for the dominating GIA signal in Fennoscandia confirming tide gauge measurements and levelling survey results, and constraining Earth's large-scale subsurface structure (Milne et al. 2001). They also pointed to improvements in ice history models (Lidberg et al. 2007) and limitations in the strategy for GNSS analysis (Lidberg et al. 2010).

The most recent results were presented in Kierulf et al. (2021). The 3D velocity field is provided with and without plate motions, and with corrections for elastic deformation due to global atmospheric and non-tidal ocean loading, contemporary ice mass and hydrological changes as well as results from a well-fitting GIA model, all accompanied with uncertainties. The 3D velocity field is therefore applicable for different types of geoscientific investigations.

In the meantime, the international BIFROST team has initiated the next re-processing applying three different analysis software for potentially more than 800 GNSS stations in northern and parts of central Europe. Many stations will have observation time spans of more than 20 years. The next 3D velocity field will ultimately serve as backbone for new land uplift and 3D deformation models of the Nordic and Baltic areas, and will help to further constrain the 3D subsurface structure of the Earth.

References

Kierulf, H.P., Steffen, H., Barletta, V.R., Lidberg, M., Johansson, J., Kristiansen, O. & Tarasov, L., 2021: A GNSS velocity field for geophysical applications in Fennoscandia. *Journal of Geodynamics 146*, 101845.

Lidberg, M., Johansson, J., Scherneck, H.G. & Davis, J., 2007: An improved and extended GPS derived velocity field for the glacial isostatic adjustment in Fennoscandia. *Journal of Geodesy 81*, 213–230.

Lidberg, M., Johansson, J.M., Scherneck, H.G. & Milne, G.A., 2010: Recent results based on continuous GPS observations of the GIA process in fennoscandia from BIFROST. *Journal of Geodynamics 50*, 8–18.
Milne, G., Davis, J., Mitrovica, J., Scherneck, H.G., Johansson, J., Vermeer, M. & Koivula, H., 2001: Space-Geodetic constraints on glacial isostatic adjustments in Fennoscandia. *Science 291*, 2381–2385.
Scherneck, H.-G., Johansson, J.M., Mitrovica, J.X. & Davis, J.L., 1998: The BIFROST project: GPS determined 3D displacement rates in Fennoscandia from 800 days of continuous observations in the SWEPOS network. *Tectonophysics 294*, 305–322.

NKG2022GIA – A new, forthcoming product for northern Europe of the Nordic Geodetic Commission

Holger Steffen[a], Rebekka Steffen[a,b], Pingping Huang[c], Valentina R. Barletta[d], Maaria Nordman[e,f], Matthew J.R. Simpson[g], Lev Tarasov[h], Vents Zuševic[i]

[a]Geodetic Infrastruture, Lantmäteriet, Gävle, Sweden, holger.steffen@lm.se, rebekka.steffen@lm.se; [b]Department of Earth and Environmental Sciences, Dalhousie University, Halifax, Canada; [c]School of Engineering, Newcastle University, United Kingdom, Pingping.Huang@newcastle.ac.uk; [d]Geodesy and Earth observation, DTU Space, Lyngby, Denmark, vrba@space.dtu.dk; [e]Department of Built Environment, Aalto University, Espoo, Finland, maaria.nordman@aalto.fi; [f]Finnish Geospatial research Institute, National Land Survey of Finland, Espoo, Finland; [g]Geodetic Institute, Norwegian Mapping Authority, Hønefoss, Norway, Matthew.Simpson@kartverket.no; [h]Department of Physics and Physical Oceanography, Memorial Universityy, St. John's, Canada, lev@mun.ca; [i]Latvian Geospatial Information Agency, Riga, Latvia, vents.zusevics@lgia.gov.lv;

Summary. The Nordic Geodetic Commission (NKG) has a long history and tradition in providing geodetic data and geophysical models for northern Europe. Official land uplift and 3D deformation models were published in recent years. There are currently efforts toward an official NKG model of glacial isostatic adjustment (GIA) called NKG2022GIA. The new product applies the latest advances in GIA and ice history modelling. Model output includes GIA-induced deformations and related sea-level changes as well as geoid, gravity, rotation and stress changes. All quantities come along with uncertainties.

GIA is the dominant deformation process in northern Europe, which can be observed with several geodetic methods. This process causes among other things a significant land uplift of about 1 cm/year in the northern Gulf of Bothnia. As such, GIA affects the establishment and maintenance of reliable geodetic and gravimetric reference networks in north-European countries. Hence, adequate corrections based on dedicated GIA models are a necessity in supporting a high level of accuracy in positioning.

NKG is an association of Nordic and Baltic geodesists and specialists that are active in the field of geodesy and related disciplines. A part of NKG's mission is the creation and implementation of high-quality geodetic products and services. Latest products are the geoid model NKG2015 (Ågren et al. 2016), the official land uplift model NKG2016LU (Vestøl et al. 2019), the intraplate velocity model NKG_RF17vel (Häkli et al.2019) and the postglacial gravity change model NKG2016LU_gdot (Olsson et al. 2019).

Currently, there is ongoing work within NKG together with international scientists to develop a GIA model, called NKG2022GIA, for northern Europe that complements above-named observation-based models. It is thought as reference for GIA-induced vertical and horizontal motion, gravity, geoid, rotation and stress change and shall also provide topographic changes of the last c. 20,000 years. It will also include uncertainty estimates for each field.

Following former investigations, the GIA model is based on a combination of an ice and an earth model, solving the sea-level equation and rotational feedback. The selected reference ice model, GLAC, for Fennoscandia, the Barents/Kara seas and the British Isles is provided by Lev Tarasov and co-workers. The earth model will be a newly developed 3D spherical, compressible finite element model. Different rheologies and 3D subsurface structures will be tested.

References

Ågren, J., Strykowski, G., BilkerKoivula, M., Omang, O., Märdla, S., Forsberg, R., Ellmann, A., Oja, T., Liepins, I., Parseliunas, E., Kaminskis, J., Sjöberg, L.E. & Valsson, G., 2016: The NKG2015 gravimetric geoid model for the Nordic-Baltic region. 1st Joint Commission 2 and IGFS Meeting International Symposium on Gravity, Geoid and Height Systems, Thessaloniki, Greece.

Häkli, P., Lidberg, M., Jivall, L., Steffen, H., Kierulf, H., Ågren, J., Vestøl, O., Lahtinen, S., Steffen, R. & Tarasov, L., 2019: New horizontal intraplate velocity model for Nordic and Baltic countries. *Proceedings of the 81th FIG Working Week "Geospatial information for a smarter life and environmental resilience", Hanoi, Vietnam.*

Olsson, P.-A., Breili, K., Ophaug, V., Steffen, H., Bilker-Koivula, M., Nielsen, E., Oja, T. & Timmen, L., 2019: Postglacial gravity change in Fennoscandia – three decades of repeated absolute gravity observations. *Geophysical Journal International 217(2)*, 1141–1156:
Vestøl, O., Ågren, J., Steffen, H., Kierulf, H.P. & Tarasov, L., 2019: NKG2016LU – a new land uplift model for Fennoscandia and the Baltic Region. *Journal of Geodesy 93(9)*, 1759–1779.

EuVeM2022: A 3D GNSS velocity field for Europe

Rebekka Steffen[a], Ambrus Kenyeres[b], Holger Steffen[a], Martin Lidberg[a]

[a]Department of Geodetic Infrastructure, Lanmtäteriet, Gävle, Sweden, rebekka.steffen@lm.se, holger.steffen@lm.se, martin.lidberg@lm.se; [b]Kozmikus Geodéziai Obszervatórium, Hungary, ambrus.kenyeres@lechnerkozpont.hu

Summary. Strain maps contain information about deformation zones within the upper crust. While the strain maps are provided as a gridded dataset, unevenly distributed GNSS (global navigation satellite system) velocities are used to obtain the strain. Thus, an interpolation is required. Here, we will present a new GNSS velocity model for Europe based on an improved interpolation technique (least-squares collocation). We will apply the new velocity model to obtain a new strain map for Europe and compare it to the European Seismic Risk Model (ESRM20; Crowley et al. 2021).

Strain rates are an important factor to find areas that are under stress. Higher strain rates are usually observed along plate boundaries, while lower strain rates are found in intraplate regions. The increased availability of velocity solutions from GNSS for entire Europe allows a 2D strain rate to be estimated at high resolution. Thus, regions of high and low strain become clearly visible. However, GNSS stations are not evenly distributed and interpolations are required to obtain a velocity model for the entire continent.

A working group within EUREF, a European sub-commission within the International Association of Geodesy commission on Reference Frames, is working towards the development of a velocity model for entire Europe. However, the irregular and partly sparse distribution of GNSS stations makes it difficult to obtain a complete picture of the horizontal and vertical deformation for Europe. The solution for this problem is to use an interpolation. However, most well-known interpolation techniques (e.g. triangulation, spline interpolation) have the disadvantage that the entire signal is used while every signal always includes noise due to unknown errors or local effects. Additionally, those interpolation techniques can only be applied to one component at a time. The least-square collocation solves both problems of dividing the dataset into a signal and noise component and applying different datasets simultaneously. In addition, a recent extension to the least-squares collocation allows also the usage of the correlation between the horizontal velocity components (Steffen et al., 2022).

Here, we will show results of applying a combined least-square collocation for the example of Europe using a velocity field solution by the EUREF Permanent Network Densification (EPND2150; Kenyeres et al., 2019). This velocity field is obtained by the combination of weekly position SINEX solutions generated by 28 EPND Analysis Centres. More details on EPND can be found on the www.epnd.sgo-penc.hu website. The homogenized and quality-checked velocity field is then interpolated via a least-square collocation using a fixed scale length of 150 km. In addition, the effect of known plate boundaries is considered during the interpolation to avoid a smoothing of nearby velocities on different tectonic plates. We also apply a moving variance approach to avoid effects of non-stationarity, which arise due to the variable station densities. The interpolated velocity model, EuVeM2022 (European Velocity Model 2022, Fig. 1), is then used to estimate a 2D strain rate covering most of Europe. We will highlight the situation in intraplate areas with very low strain rates but dense GNSS networks, and compare the strain rate and velocity maps to the newly released ERSM20 (Crowley et al., 2021) and ESHM20 (European Seismic Hazard Model; Danciu et al., 2021). The final dataset (vertical and horizontal velocities) will be freely available and provided in different formats and reference frames to ease application for users with different scientific background.

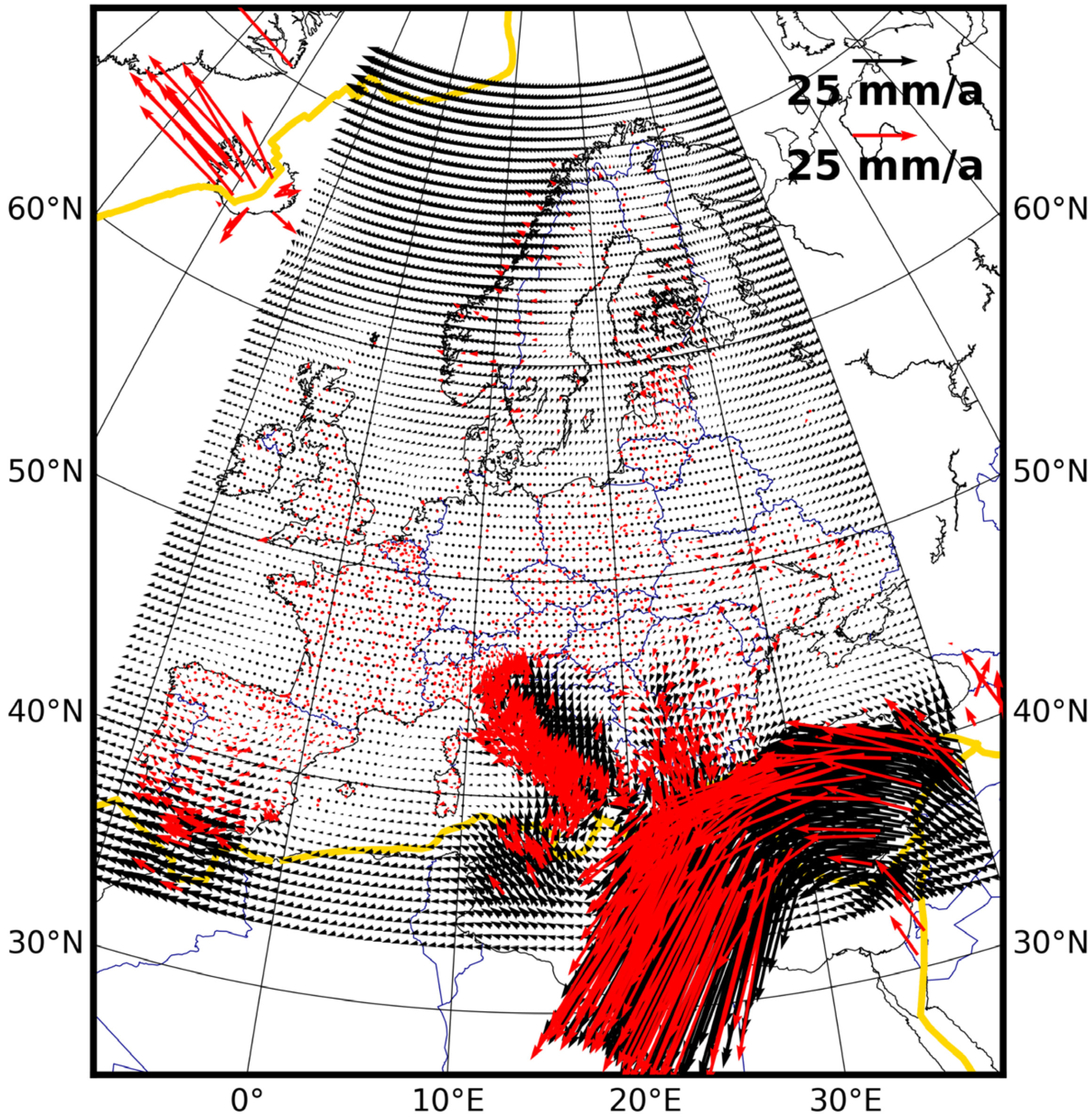

Figure 1:European Velocity Model 2022 (EuVeM2022) obtained using a least-squares collocation (HV-LSC-ex) and the GNSS velocity solution EPND2150 (www.epnd.sgo-penc.hu). Black arrows show the interpolated GNSS velocities on a 0.5° grid, red arrows represent the input GNSS velocities from EPND2150, and yellow lines mark the plate boundaries.

References

Crowley H., Dabbeek J., Despotaki V., Rodrigues D., Martins L., Silva V., Romao X., Pereira N., Weatherill G. & Danciu L., 2021: European Seismic Risk Model (ESRM20). *EFEHR Technical Report 002 V1.0.0*, doi:10.7414/EUC-EFEHR-TR002-ESRM20.

Danciu L., Nandan S., Reyes C., Basili R., Weatherill G., Beauval C., Rovida A., Vilanova S., Sesetyan K., Bard P-Y., Cotton F., Wiemer S., Giardini D., 2021: The 2020 update of the European Seismic Hazard Model: Model Overview. *EFEHR Technical Report 001 v1.0.0*, doi:10.12686/a15.

Kenyeres, A., Bellet, J.G., Bruyninx, C., Caporali, A., De Doncker, F., Droscak, B., Duret, A., Franke, P., Georgiev, I., Bingley, R., Huisman, L., Jivall, L., Khoda, O., Kollo, K., Kurt, A.I., Lahtinen, S., Legrand, J., Magyar, B., Mesmaker, D., Morozova, K., Nagl, J., Ozdemir, S., Papanikolaouo, X., Parseulinas, E., Stangl, G., Tangen, O.B., Valdes, M., Ryczywolski, M., Zurutuza, J., Weber, M., 2019: Regional integration of long-term national dense GNSS network solutions. *GPS Solutions 23*, 122, doi:10.1007/s10291-019-0902-7.

Steffen, R., Legrand, J., Ågren, J., Steffen, H. & Lidberg, M., 2022: HV-LSC-ex2: Velocity field interpolation using extended least-squares collocation. *Journal of Geodesy 96*, 15, doi:10.1007/s00190-022-01601-4.

Thematic Session 8
Marine geosciences

Session Chairs:
Martin Jakobsson (martin.jakobsson@geo.su.se)
Lovisa Zillén Snowball (Lovisa.zillen.snowball@sgu.se)

Medieval versus recent environmental conditions in the Baltic Proper, what was different a thousand years ago?

Elinor Andrén[a], Falkje van Wirdum[a], Lena Norbäck Ivarsson[a], Mikael Lönn[b], Matthias Moros[c], Thomas Andrén[a]

[a]School of Natural Sciences, Technology and Environmental Studies, Södertörn University, Huddinge, Sweden, elinor.andren@sh.se; [b]Department of Electrical Engineering, Mathematics, and Science, University of Gävle, Gävle, Sweden, mikael.lonn@hig.se; [c]The Leibniz Institute for Baltic Sea Research, Rostock, Germany, matthias.moros@io-warnemuende.de

Summary. A sediment core from the western Gotland Basin, northwestern Baltic Proper, covering the last 1200 years, was investigated for past changes in climate and the environment using diatoms as a proxy. The aim was to compare the environmental conditions reconstructed during Medieval times with settings occurring the last century under influence of environmental stressors like eutrophication and climate change.

Our data shows that more marine conditions than today prevailed during Medieval times, reaching a salinity of at least 8 in the surface waters compared to present-day about 6.5 (Andrén et al. 2020). The higher salinity made it possible for *Pseudosolenia calcar-avis*, an autumn blooming warm water diatom which forms massive algal mats in stratified waters, to thrive. This effectively enhanced the vertical export of organic carbon to the sediment and contributed to form extensive areas of benthic hypoxia. Both higher salinity and higher temperatures (stronger thermal stratification) during the Medieval Climate Anomaly (MCA; 950–1250 C.E.) were probably favourable to the vast production of *P. calcar-avis* in the Baltic Proper. Accordingly, our data support that a warm and dry climate induced the extensive hypoxic areas in the open Baltic Sea during the MCA.

A more efficient coastal filter and higher retention capacity in coastal wetlands could explain why intensified land-use during Medieval times did not result in higher nutrient discharge in the open Baltic Sea. Instead we suggest that massive flux of diatom "shade flora" promoted by warm and dry climate (higher salinity and thermal stratification) reinforced by cyanobacterial blooms and nitrogen fixation increased carbon sequestration to the sediments by diatoms due to extended length of the growing season, which made it possible to get high primary productivity and hypoxia during the MCA despite oligotrophic conditions.

The diatom data indicates decreased salinity, weaker stratification and low primary production during the Little ice Age (LIA; 1400–1700 C.E.), which resulted in a low organic content, homogeneous sediments and well oxygenated bottoms. The first signs of human-induced eutrophication are recorded about 1940 visible as a shift in diatom composition, increased primary production as well as carbon content, and benthic hypoxia. Impact of climate change is visible in the diatom composition data starting about 1975 C.E. and becoming more pronounced 2000 C.E. The less marine conditions in the area during present-day most probably prevent re-appearance and an expansion of *P. calcar-avis* from the southern Baltic Sea. However, other large diatom taxa that thrive in stratified waters during autumn blooms (*Coscinodiscus granii* and *Actinocyclus octonarius* including varieties) have increased the last two decades, interpreted as being the result of the documented global warming.

References

Andrén, E., van Wirdum, F., Norbäck Ivarsson, L., Lönn, M, Moros, M., & Andrén, T. 2020: Medieval versus recent environmental conditions in the Baltic Proper, what was different a thousand years ago? Palaeogeography, Palaeoclimatology, Palaeoecology 555, 109878. https://doi.org/10.1016/j.palaeo.2020.109878

Radiocarbon dating of coastal Northwestern Baltic proper Late Holocene sediments – pitfalls and possibilities

Thomas Andrén[a], Lena Norbäck Ivarsson[b], Elinor Andrén[c]

[a]School of Natural Science, Technology and Environmental Studies; Södertörn university, Huddinge, Sweden, thomas.andren@sh.se, [b]School of Natural Science, Technology and Environmental Studies; Södertörn university, Huddinge, Sweden, lena.norbäck.ivarsson@sh.se, [c]School of Natural Science, Technology and Environmental Studies; Södertörn university, Huddinge, Sweden, elinor.andren@sh.se

Summary. By using the mean difference between terrestrial macrofossil samples and bulk sediment samples, 1045±450 ^{14}C years, as $R(t)_{bulk}$ it has been possible to calibrate the bulk sediment samples with reasonable reliable ages compared to corresponding macrofossil ages, however with mean probability intervals of 501±72 years. We suggest that the northwestern Baltic proper local marine reservoir age may be in the order of c. 370 ^{14}C years. Our results clearly show the importance of considering the local geological conditions in the vicinity of the sampling site. The local geological conditions should be considered already during the design of marine geological investigation, especially in coastal areas.

The radiocarbon dating method was presented by Libby (1952) based on his finding of the cosmogenic radionuclide ^{14}C and he was later awarded the Nobel Prize in chemistry 1960 for his discovery. Dating with ^{14}C which have a half-life of 5730 years have become a commonly used method for establishing geochronological timescales covering the latest c. 50 000 years.

All fossils terrestrial organisms have achieved their ^{14}C directly from the atmosphere meaning that they were in balance with the global atmospheric ^{14}C content when they died making them perfect for dating with the ^{14}C method. Marine organisms take up their carbon from the world oceans water and in this case the $^{14}CO_2$ have been incorporated in the ocean water in the form of dissolved $H_2{}^{14}CO_3$ and $H_2{}^{14}CO_2$ which have been differently distributed globally due to altering mixing rates of the oceans.

The Baltic Sea is a semi enclosed brackish waterbody with a salinity too low for pelagic foraminifers. A strong salinity stratification creates a stable halocline which prevents vertical water mixing leading to hypoxic or anoxic bottom conditions in the deeper basins. Such seafloor conditions are not suitable for any benthic fauna and hence the sediments from below the permanent halocline at c. 60–80 water depth is usually barren of any datable fossils. This scarceness of datable macrofossil in the sediments from the open Baltic Sea have led to that bulk sediment samples have been used to constructing radiocarbon chronologies (e.g. Sohlenius et al., 1996; Andrén et al., 2000a; van Wirdum et al., 2019).

The carbon sources for Baltic Sea bulk sediment samples are not simple and straightforward. Primary productivity is governed by the input of nutrients from the catchment area which have varied over time and hence have the amount of contemporary carbon in the sediment also varied over time. This carbon is mixed with carbon from weathering products which in many areas around the Baltic Sea derives from calcareous bedrock. Finally, the fact that the Baltic Basin has been exposed to glaciations leading to an ongoing isostatic rebound resulting in that sediments containing old carbon of unknown age will be exposed to wave action and redeposited and mixed with younger sediments. We must accept that bulk sediment samples will have an unknown and varying reservoir age over time referred to as $R(t)_{bulk}$ (Lougheed et al., 2017). This makes calendar age determination of Baltic Sea bulk sediment samples less precise and there have been several attempts to determine $R(t)_{bulk}$ in the past (e.g. Andrén et al, 2000a; Hedenström & Possnert, 2001; Lougheed et al., 2012; Rössler et al., 2011).

Here we present the results from 57 radiocarbon dated samples of sediments and macrofossils, both terrestrial and marine from 9 sites along the Swedish east coast of the northwestern Baltic proper. We have dated macrofossils and bulk sediment samples from the corresponding stratigraphic interval in 17 cases, 9 terrestrial macrofossils/sediment and 8 marine macrofossils/sediment couples.

The software CLAM version 2.2 (Blaauw, 2010) was used for calendar years determination. A customized calibration curve based on the Marine13 calibration dataset (Reimer et al., 2013) and a deviation (ΔR) of –135 ± 40 from the Marine13 reservoir age was used for the marine fossil samples. The chosen ΔR is a mean based on the values for ΔR for clams, both suspension and deposit feeders, in three study sites relatively close to the sites investigated within the present study as reported in the Marine Reservoir Correction Database (http://calib.org/marine/), Map No 1710, 1717 and 1718 (Lougheed et al., 2013). Samples derived from terrestrial macro fossils were calibrated using the IntCal13 calibration dataset (Reimer et al., 2013).

As we also had the opportunity to date bulk sediment samples at the same level as the macrofossil samples this allow us to investigate the age discrepancy between different types of dated material. The recorded difference between terrestrial macrofossil samples and bulk sediment samples ranging from approximately 710 ^{14}C years to 2025 ^{14}C years with a mean difference of 1045±450 ^{14}C years is in good agreement with previously reported estimates of bulk sediment R from open Baltic Sea sediment cores (e.g. Hedenström & Possnert, 2001; Rössler et al., 2011; Lougheed et al., 2017). The span of the difference between the ^{14}C ages of marine fossils and the bulk sediment samples is smaller, 550 ^{14}C years to 1220 ^{14}C years with a mean difference of 673±228 ^{14}C years, which probably is a result of the marine reservoir effect as the marine organisms have taken the carbon from the seawater.

The mean difference of 1045±450 ^{14}C years for the terrestrial macrofossils and bulk sediment samples and 673±228 ^{14}C years for the marine macrofossil and sediment samples gives a difference between the two of 372 ^{14}C years, and this could be considered the effect of marine organisms taking up old carbon from the sea water and can therefore be regarded as an estimate of the local marine reservoir age.

References

Andrén, E., Andrén, T. and Kunzendorf, H. 2000a. Holocene history of the Baltic Sea as a background for assessing records of human impact in the sediments of the Gotland Basin. *The Holocene* 10, 687-702.

Blaauw, M., 2010. Methods and code for 'classical' age-modelling of radiocarbon sequences. *Quaternary Geochronology* 5: 512-518

Hedenström, A. and Possnert, G., 2001. Reservoir ages in Baltic Sea sedimentFa case study of an isolation sequence from the Litorina Sea stage. *Quaternary Science Reviews* 20, 1779–1785

Libby, W.F. 1952. Radiocarbon Dating. University of Chicago Press, 124pp.

Lougheed, B. C., H. L. Filipsson, and I. Snowball., 2013: Large spatial variations in coastal 14C reservoir age - a case study from the Baltic Sea. *Climate of the Past* 9: 1015-1028

Lougheed, B. C., S. P. Obrochta, C. Lenz, A. Mellstr€om, B. Metcalfe, R. Muscheler, M. Reinholdsson, I. Snowball, and L. Zillén (2017), Bulk sediment ^{14}C dating in an estuarine environment—How accurate can it be?, *Paleoceanography*, 32, doi:10.1002/2016PA002960.

Lougheed, B.C., Snowball, I., Moros, M., Kabel, K., Muscheler, R., Virtasalo, J.J. and Wacker, L. 2012. Using an independent geochronology based on palaeomagnetic secular variation (PSV) and atmospheric Pb deposition to date Baltic Sea sediments and infer 14C reservoir age. *Quaternary Science Reviews* 42: 43-58.

Reimer, P.J., Bard, E., Bayliss, A., Beck, J.W., Blackwell, P.G., Bronk Ramsey, C., Buck, C.E., Edwards, R.L., Friedrich, M., Grootes, P.M., Guilderson, T.P., Haflidason, H., Hajdas, I., Hatté, C., Heaton, T.J., Hoffmann, D.L., Hogg, A.G., Hughen, K.A., Kaiser, K.F., Kromer, B., Manning, S.W., Niu, M., Reimer, R.W., Richards, D.A., Scott, E.M., Southon, J.R., Turney, C.S.M., van der Plicht, J., 2013. IntCal13 and Marine13 radiocarbon age calibration curves, 0-50,000 years cal BP. *Radiocarbon* 55: 1869-1887.

Rössler, D.,Moros, M. & Lemke,W. 2011. The Littorina transgression in the southwestern Baltic Sea: new insights based on proxy methods and radiocarbon dating of sediment cores. *Boreas* 40: 231–241.

Sohlenius, G., Sternbeck, J., Andrén E. and Westman, P. 1996. Holocene history of the Baltic Sea as recorded in a sediment core from the Gotland Deep. *Marine Geology* 134, 183-201.

van Wirdum, F, Andrén, E, Wienholz, D, Kotthoff, U, Moros, M, Fanget, A-S, Seidenkrantz, M-S and Andrén, T., 2019: Middle to Late Holocene Variations in Salinity and Primary Productivity in the Central Baltic Sea: A Multiproxy Study from the Landsort Deep. *Frontiers in Marine Science* 6:51. doi: 10.3389/fmars.2019.00051

Diatoms from the late Holocene of the western Chukchi Sea, Arctic Ocean: environmental signals and palaeoceanography

Erik Browaldh[a], Helen K. Coxall[a], Matt O'Regan[a], Elinor Andrén[b]

[a]Department of Geological Sciences, Stockholm University, Stockholm, Sweden, erik.browaldh@gmail.com, helen.coxall@geo.su.se, mattoregan@geo.su.se, ;[b]School of Natural Science, Technology and Environmental Studies Södertörn University, Huddinge, Sweden, elinor.andren@sh.se

Summary. Increased inflow of Pacific Water (PW) to the Arctic Ocean is associated with reduced sea ice in the western Arctic, yet variability in PW inflow during the Holocene remains poorly defined. We explore this question using diatom assemblages from a late Holocene sediment core. Our results find diatom fluctuations in some key groups indicative of PW and sea ice that mirror existing proxy data suggesting increased PW inflow.

The 8.3 m-long SWERUS-L2-2-PC1 (2PC) core retrieved from the marginal ice zone in the Chukchi Sea, Arctic Ocean is well positioned to monitor marine and climate conditions in the region back through the late Holocene. Importantly its position should trace variability in inflow of Bering Sea Water (BSW) and Pacific Water (PW) through Herald Canyon. Furthermore, the high sedimentation rate (200 cm/kyr) of Core 2PC, allowing production of two independent age models (radiocarbon, palaeomagnetism and tephra constraints), and a richness of well-preserved siliceous microfossils, make 2PC an outstanding record for using diatom assemblages to gain insights into ocean-climate change back to 4250 years BP at high resolution.

Existing research on 2PC using benthic foraminifera Mg/Ca to constrain past changes in bottom water temperature (BWT) in Herold Canyon finds a clear pattern of BWT variability involving ~500–1000 yr fluctuations (–2.4 to 1 °C) that has been interpreted as indicating variability in PW inflow (Barrientos et al., in review). Times of warmer BWTs are interpreted as signalling increased PW inflow. This is important with regards understanding the role of Pacific Ocean forcings in driving variability in sea ice extent both in the Chukchi Sea and wider central Arctic Ocean. However, it is unclear if the inferred benthic BWT signal really is derived from the Pacific, or if other processes are involved that could modify BWT in Herold Canyon. Diatoms are sensitive indicators of ocean conditions. It is proposed that the distinctive environmental preferences of marine diatoms, having a variety of specialisms, e.g. to high-nutrients of the Pacific waters and/or sea ice conditions of the Chukchi Sea, and other factors, could help with this question. Here we present diatom assemblage analysis though the late Holocene 2PC record that can be compared to the benthic Mg/Ca data set. Existing understanding of diatom ecological indicator assemblages and species groups, or 'eco-groups', is fundamental to the approach.

The results reveal well preserved and diverse diatom assemblages throughout the 2PC section with 126 taxa from 56 genera identified. We find distinctive changes in assemblages down core that, for some groups, bear a striking similarity to the benthic Mg/Ca BWT reconstruction. Importantly, the results show millennial scale changes in the abundance of cryophilic, planktic and neritic species that can be related to changes in the source of surface water inflows to Herold Canyon, from BSW to PW. Times of warmer BWT from the Mg/Ca data correlate with increased abundance of warm water- and tychoplanktic species. A higher frequencey of *Thalassionema nitzschoides, Shionodiscus oestrupii* and *Thalassiosira simonsenii* dwelling in Pacific waters, are linked to warmer BWT where small signals of these species is suggested with more PW species. A link between warm water and tychoplanktic species, and the BWT was observed. 2PC assemblages were contrasted with other locations within Chukchi-, Laptev- and East Siberian seas, and the north Pacific Ocean. We conclude, that diatom assemblages and their inferred eco-groups from 2PC, support the hypotheses that Pacific water inflow to the Chukchi Sea has varied over late Holocene, with varying dimensions of ice-formation monitored from Herald Canyon.

Reference

Barrientos, N., Coxall, H. K., Lear, L. H., Pearce, P., Muschitiello, F., O'Regan, S., M., de Boer, A., Koshurnikov, A., and Jakobsson, M., in revision, Late Holocene variability in Arctic Ocean Pacific Water inflow through the Bering Strait: Geology.

Sediment carbon mineralization in the Ryder and Petermann fjords records increased productivity in northern Greenland fjords

Volker Brüchert[a], Jonas Fredriksson[a], Sebastian Brolin[a], Matt O'Regan[a], Adam Ulfsbo[b], Christian Stranne[a], Martin Jakobsson[a]

[a]Department of Geological Sciences, Stockholm University, Stockholm, Sweden, volker.bruchert@geo.su.se, jonas.fredriksson@geo.su.se, sebastian.brolin@gmail.com; matt.oregan@geo.su.se, martin.jakobsson@geo.su.se, christian.stranne@geo.su.se [b]Department of Marine Sciences, University of Gothenburg, Gothenburg, Sweden, adam.ulfsbo@marine.gu.se;

Summary. Porewater geochemical data and carbon mineralization rates in sediments of the Ryder and Petermann fjords were used to assess changes in benthic pelagic coupling related to ongoing environmental changes in these fjords. High carbon mineralization rates in the top 10 cm of sediment contrast with low rates below this depth and indicate abrupt recent increases in carbon export to these more than 800 m- deep sediments. These changes are likely related to recent ongoing hydrological and oceanographic changes that changed both nutrient and light availability and primary productivity in these fjords.

Subglacial runoff plays an important role for coastal marine ecosystems and future coastal Arctic ocean nutrient budgets. The Greenland icesheet has lost about 3600 Gigatons since 1990, and up to 40 percent of this mass may have been transported to the north by marine-terminating outlet glaciers such as the Ryder and Petermann fjords in northern Greenland (van den Broeke et al., 2017). Subglacial discharge of meltwater into the fjords is an important component of the mass loss (Hill et al., 2018). Marine fjord sediment of northern Greenland and the Lincoln Sea record recent recession of fjord sea ice and substantial increases in light availability. This study uses the porewater carbon and nutrient geochemistry and direct rate measurements of carbon mineralization to assess the effects of changing export productivity and nutrient levels on the benthic-pelagic coupling response. We present data on nutrient concentrations, dissolved inorganic carbon, sediment oxygen uptake, and bacterial sulfate reduction rates in surface and long sediment cores of these deep fjords to understand carbon and nutrient cycling in northern Greenland fjord sediments collected during the Ryder expedition 2019 with the icebreaker Oden. These are the first data on benthic nutrient and carbon mineralization rates reported for the Ryder and Petermann fjord systems and provide important new constraints on the spatial extent of potential future melting-associated fertilization processes on the northern Greenland coast. Sediments inside the silled fjords, in perched basins, and close to the glacial tongue had oxygen uptake rates that were up to nine times higher when compared to sediments in the adjacent, near-perennially ice-covered Lincoln Sea. The high oxygen uptake rates and increased DIC levels are indicative of substantial photic zone carbon export production rates – untypically high for sediments deposited in depths of more than 800 m water depth in Arctic sediment (Bourgeois et al., 2017). The magnitude of these O_2 uptake rates and the shallow oxygen penetration depths are comparable to sediment from perennial ice-free productive continental margin deposits from temperate latitudes of the north Atlantic continental margin, and the North and Baltic Seas. Most noteably, the high carbon mineralization rates were restricted to the topmost 10 cm and likely reflect environmental changes over the last decades of sediment deposition. Deeper-buried sediments below 10 cm depth show orders of magnitude low carbon mineralization. This abrupt drop in carbon mineralization cannot be reconciled with the conventional decrease in organic carbon reactivity due to progressive microbial degradation of organic matter commonly observed with increasing burial depth in continental margin sediment (Arndt et al., 2013). Instead, the change suggests a fundamental regime shift from a low-light, low-organic carbon and low-nutrient regime to a regime with more ice-free conditions, higher nutrient levels, and higher primary productivity. We conclude that these changes reflect ongoing oceanographic and hydrological changes in the fjord system that affect the stability of the marine-terminating glacier and lead to a fundamental reorganization of nutrient and carbon cycling in these fjord systems.

References

Arndt, S., Jørgensen, B.B., LaRowe, D.E., Middelburg, J.J., Pancost, R.D., and Regnier, P. (2013). Quantifying the degradation of organic matter in marine sediments: A review and synthesis. *Earth-Science Reviews* 123(0)**,** 53-86. doi: http://dx.doi.org/10.1016/j.earscirev.2013.02.008.

Bourgeois, S., Archambault, P., and Witte, U. (2017). Organic matter remineralization in marine sediments: A Pan-Arctic synthesis. *Global Biogeochemical Cycles* 31(1)**,** 190-213. doi: 10.1002/2016GB005378.

Hill, E. A., Carr, J. R., Stokes, C. R. & Gudmundsson, G. H. Dynamic changes in outlet glaciers in northern Greenland from 1948 to 2015. *The Cryosphere* **12**, 3243-3263, doi:10.5194/tc-12-3243-2018 (2018)

van den Broeke, M. *et al.* Greenland Ice Sheet Surface Mass Loss: Recent Developments in Observation and Modeling. *Current Climate Change Reports* **3**, 345-356, doi:10.1007/s40641-017-0084-8 (2017)

Peat as a potential total alkalinity source to the Baltic Sea through submarine groundwater

Nai-Chen Chen[a], Magnus Mörth[b], Wei-Li Hong[c], Christian Stranne[d], Matt O'Regan[e], Richard Gyllencreutz[f], Martin Jakobsson[g]

[a]Department of Geological Sciences, Stockholm University, Stockholm, Sweden, nai-chen.chen@geo.su.se; [b]Department of Geological Sciences, Stockholm University, Stockholm, Sweden, magnus.morth@su.se; [c]Department of Geological Sciences and Baltic Sea Center, Stockholm University, Stockholm, Sweden, wei-li.hong@geo.su.se; [d]Department of Geological Sciences and Baltic Sea Center, Stockholm University, Stockholm, Sweden, christian.stranne@geo.su.se; [e]Department of Geological Sciences, Stockholm University, Stockholm, Sweden, matt.oregan@geo.su.se; [f]Department of Geological Sciences, Stockholm University, Stockholm, Sweden, richard.gyllencreutz@geo.su.se; [g]Department of Geological Sciences, Stockholm University, Stockholm, Sweden, martin.jakobsson@geo.su.se

Summary. We use a geochemical approach to observe existence of submarine groundwater discharge and the dissolved substances it transports to assess the potential of submarine groundwater discharge as a total alkalinity supplier to the Baltic Sea.

Submarine groundwater discharge (SGD) is a process that can transport terrestrial dissolved chemical substances into coastal waters, and thereby potentially increase total alkalinity (TA) in the ocean and impact the coastal ecosystem and the ability of ocean to absorb atmospheric carbon dioxide (Lecher and Mackey, 2018). By considering inflow of rivers, microbial reactions, as well as carbonate dissolution/precipitation, it has been suggested that SGD could be an important TA source in the Baltic Sea (Brenner et al., 2016; Gustafsson et al., 2019). However, only a few studies in the southern Baltic Sea have discussed the impact of peat on TA budget (Kreuzburg et al., 2020; Racasa et al., 2021), and almost no survey has been conducted on the central Swedish Baltic Sea coast. In addition, the quantities of water and solutes transported by submarine groundwater have not been well investigated and quantified along the Swedish coast. To investigate this question, run-off water, groundwater, as well as terrestrial and marine sediment cores were collected from Fifång Island and surroundings waters in southern Stockholm Archipelago, where widely distributed submarine terraces have been discovered and hypothesized to be related to SGD (Jakobsson et la., 2020). The marine cores were taken at submarine terraces formed in glacial clay while the terrestrial core, comprised of peat overlying glacial clay, was retrieved at coast in a small bay of Fifång Island. Here we present the preliminary results from chemical analyses. The values of water isotopes of porewaters decrease with depth and are more negative than those of Baltic Sea water. In addtion, they fall on a mixing line between Baltic seawater and local precipitation, suggesting the infiltration of groundwater into the marine environments (Fig. 1). Chloride concentration shows decreasing trend in the terrestrial core, which is consistent with the results of water isotopes. However, chloride concentration increases in the marine sediment cores with depth below seafloor, suggesting the influence of a preserved paleo-seawater at depth. Compared to Baltic Sea water and Fifång run-off, TA is enriched in groundwater and all porewaters, and even can reach 20 mM in the terrestrial core. Such an enrichment in porewater may be related to a reducing environment as well as groundwater transportation. Collectively, our results imply that groundwater has the potential to export peat degradation and weathering products and further increase TA in the coastal waters in the Southern Stockholm Archipelago.

Reference

Brenner, H., Braeckman, U., Le Guitton, M., and Meysman, F. J. R., 2016: The impact of sedimentary alkalinity release on the water column CO_2 system in the North Sea, Biogeosciences, 13, 841– 863, https://doi.org/10.5194/bg-13-841-2016.

Dählmann, A. & De Lange, G. J., 2003: Fluid–sediment interactions at Eastern Mediterranean mud volcanoes: a stable isotope study from ODP Leg 160. Earth Planetary Science Letters, 212(3), 377–391, https://doi.org/10.1016/S0012-821X(03)00227-9.

Gustafsson, E., Hagens, M., Sun, X., Reed, D. C., Humborg, C., Slomp, C. P., & Gustafsson, B. G., 2019: Sedimentary alkalinity generation and long-term alkalinity development in the Baltic Sea. Biogeosciences, 16(2), 437– 456, https://doi.org/10.5194/bg-16-437-2019.

Jakobsson, M., O'Regan, M., Morth, C. M., Stranne, C., Weidner, E., Hansson, J., Gyllencreutz, R., Humborg, C., Elfwing, T., Norkko, A., Norkko, J., Nilsson, B., and Sjöström, A., 2020: Potential links between Baltic Sea submarine terraces and groundwater seeping. Earth surface dynamics, 8(1), 1–15, https://doi.org/10.5194/esurf-8-1-2020.

Kreuzburg, M., Rezanezhad, F., Milojevic, T., Voss, M., Gosch, L., Liebner, S., Van Cappellen, P., Rehder, G., 2020: Carbon release and transformation from coastal peat deposits controlled by submarine groundwater discharge: a column experiment study. Limnology and Oceanography, 65(5), 1116–1135, https://doi.org/10.1002/lno.11438.

Racasa, E. D., Lennartz, B., Toro, M., & Janssen, M., 2021: Submarine Groundwater Discharge From Non-Tidal Coastal Peatlands Along the Baltic Sea. Frontiers in Earth Science, 625, https://doi.org/10.3389/feart.2021.665802.

Lecher, A. L., & Mackey, K. R., 2018: Synthesizing the effects of submarine groundwater discharge on marine biota. Hydrology, 5(4), 60, https://doi.org/10.3390/hydrology5040060.

Paulsson, O., & Widerlund, A., 2020: Pit lake oxygen and hydrogen isotopic composition in subarctic Sweden: A comparison to the local meteoric water line. Applied Geochemistry, 118, 104611, https://doi.org/10.1016/j.apgeochem.2020.104611.

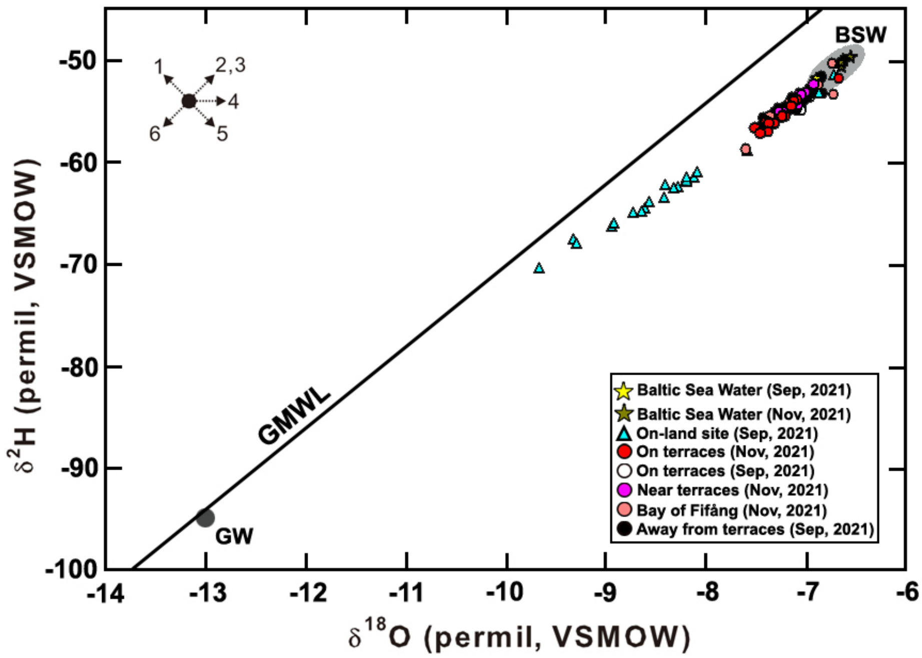

Figure 1. Plots of $\delta^{18}O$ versus $\delta^{2}H$ values. Data follow a mixing line from Baltic Sea water toward the Global Meteoric Water Line (GMWL; $\delta^{2}H = 8 \times \delta^{18}O + 10$). Areas denote with "BSW" and "GW" marked the ranges of isotopic compositions for the Baltic Sea water and groundwater from northern Sweden (Paulsson & Widerlund, 2020), respectively; Arrows marked with numbers represent processes potentially occurring at source depth, and their directions denote the trends associated with the processes (Dählmann & De Lange): 1: volcanic ash alteration at temperatures lower than 300 °C; 2: volcanic ash alteration at temperatures higher than 300 °C; 3: gas hydrate dissociation; 4: biogenic opal recrystallization; 5: clay mineral dehydration; 6: meteoric water input.

Sensitive drone mapping of methane emissions from anthropogenic fibrous sediments

Julie Falise[a,b], Erik Sahlée[a], Sarah E. Josefsson[c], Daniel Sopher[c], Panagiotis Stagianos[a], Alizée P. Lehoux[a]

[a]Department of Earth Sciences, Natural Resources and Sustainable Development, Uppsala University, Villavägen 16, SE-75136 Uppsala, Sweden; [b]Energetic and Environmental department, INSA de Lyon, Villeurbanne, France; [c]Geological Survey of Sweden, Box 670, 75128 Uppsala, Sweden

Summary. Old pulp and paper mills emitted a large quantity of fibers before regulation on wastewater rejections was implemented. These rejections formed banks of fibrous sediments, so-called *fiberbanks*, which are a threat to the aquatic environment because they are highly contaminated. In addition, biogenic degradation of the fiberbanks has a high potential to produce greenhouse gases, especially CH_4 and CO_2. In this study, we present a detection and measurement tool composed of a drone equipped with a methane sensor which allows good and fast estimates of the methane emissions from fiberbanks.

Pulp and paper production have historically been a major source of aquatic pollution due to the release of insufficiently treated wastewater containing high levels of fibrous material and contaminants (Ali & Sreekrishnan 2001). This fibrous material has often deposited in shallow coastal areas or lakes where it has accumulated and formed banks of sedimented fibers, called “fiberbanks”. Fibers have also spread further away from the factories and mixed with natural sediment, forming thin layers of “fiber-rich sediments”. Furthermore, as pulp and paper industries use different technologies to create paper, depending on the outcome expected, there exist several types of fiberbanks with different types of fibrous material. Fiberbanks are heavily polluted with persistent organic pollutants and metals (Apler et al. 2020, Dahlberg et al. 2020). Fibrous sediments have been found in various locations world-wide including Sweden, Finland, and Canada. The Geological Survey of Sweden (SGU) has been surveying fibrous-contaminated sites since 2010.

Lehoux et al. (2021) showed that a large amount of gas is produced in the fiberbanks (based on laboratory measurements only), and unpublished additional laboratory experiments also showed gas production and release from fiber-rich sediments. The gas is emitted from the sediments in two different ways, diffusion (gas diluted in the water transfers to the atmosphere at the surface) or locally with ebullition (bubbles). Gas is released into sediment pores as a by-product of biodegradation and when the gas concentration in the sediment pore water reaches oversaturation, gas bubbles start to form. Using a drone above the water to measure the quantity of gas emitted by the sediments allows detecting both ways of emission directly in the field and comparing with laboratory data.

In this study, the total methane emissions are compared to the fiberbank volumes at two well-characterized sites for calibration. These sites are both located in the Ångermanälven river estuary in Sweden and have been surveyed with different methods, including hydroacoustic measurements and sediment sampling in an SGU survey (Apler et al. 2014) and the Treasure project (FORMAS), and with the probe Flu-Mu (FIBREM project, VINNOVA), allowing a good estimation of the fiberbanks volumes.

The drone is equipped with a fast response, high precision methane gas analyser (Aeris Strato sensor) connected to the drone power output. Also, a lightweight anemometer is mounted on top of the drone to measure the wind speed, on top of a 40 cm long stick. The air, for methane measurements, is sampled at the same height above the drone to avoid as much disturbance generated by the propellers as possible. There exist different methods to determine the surface flux, such as the kriged mass balance approach as presented in Mays et al. (2009) and adapted in both Allen et al. (2015) and Gålfalk et al. (2021). The principle is to measure the CH_4 mole fraction simultaneous as the wind speed across some flux planes of the fiberbank, capturing the full emission plume. Predefined grids aiming to cover the all surface is set, in order to quantify both vertical and horizontal variations, like an imaginary box above the fiberbanks. CH_4 mapping is made by flying in a pattern previously defined on the drone controller, while sampling geotagged CH_4 concentrations at high frequency. The gas concentration measurements added with the wind speed values allow to determine the total surface flux.

Correlations between the methane release and the site specificities such as the type of fibrous sediment (fiberbanks vs fiber-rich, and fibrous vs coarse wood chips between both sites), the sediment volume and the water depth, are being studied. The results are compared with laboratory measurements of methane emission from fiberbanks (published in Lehoux et al. 2021), in order to evaluate the influence of field constraints (such as the water depth and chemical conditions) and refine the evaluation of the total potential emission of methane from Swedish fibrous sediments.

The estimation of methane fluxes from the two key sites Väja and Sandviken and correlations to the fibrous sediment properties aims to serve as a calibration for further detection and quantification of fibrous sediments over Sweden, and ultimately in other countries.

References

Ali, M., & Sreekrishnan, T. R. (2001). Aquatic toxicity from pulp and paper mill effluents: a review. Advances in environmental research, 5(2), 175-196.

Allen, G.; Pitt, J., Hollingsworth, P., Mead I., Kabbabe, K., Roberths, G., Percival, C., (2015) Measuring Landfill Methane Emissions using Unmanned Aerial Systems: Field Trial and Operational Guidance; Report SC140015/R. Environment Agency: Bristol

Apler, A., Snowball, I., Josefsson, S., 2020. Dispersal of cellulose fibers and metals from contaminated sediments of industrial origin in an estuary. Environ. Pollut. 266, 115182–115190. https://doi.org/10.1016/j.envpol.2020.115182.

Dahlberg, A.-K., Apler, A., Vogel, L., Wiberg, K., Josefsson, S., 2020. Persistent organic pollutants in wood fiber-contaminated sediments from the Baltic Sea. Journal of Soils and Sediments 20, 2471–2483. https://doi.org/10.1007/s11368-020-02610-6.

Gålfalk M., Påledal S. N., Bastviken D. (2021) Sensitive Drone Mapping of Methane Emissions without the Need for Supplementary Ground-Based Measurements, ACS Earth Space Chem. 2021, 5, 2668−2676

Lehoux, A. P., Isidorova, A., Collin, F., Koestel, J., Snowball, I., & Dahlberg, A. K. (2021). Extreme gas production in anthropogenic fibrous sediments: An overlooked biogenic source of greenhouse gas emissions. Science of the Total Environment, 781, 146772.

Mays, K. L., Shepson, P. B., Stirm, B. H., Karion, A., Sweeney, C., and Gurney, K.R. (2009) Aircraft-based measurements of the carbon footprint of Indianapolis. Environmental Science & Technology, 43 (20), 7816-7823

Biogeophysical characterization of the offshore reefs in the Baltic Sea for conservation and management

Francis Freire, Gustav Kågestan, Finn Baumgartner, Lovisa Zillen Snowball

Geological Survey of Sweden, Uppsala, Sweden, francis.freire@sgu.se

As part of its mandate, the Geological Survey of Sweden was given the task of conducting biogeophysical characterization of the areas within Swedens' territorial waters for protection and management. Found southeast of Sweden are the two large, ecologically important and economically strategic offshore reefs, Hoburgs and Norramidsjö Bank. These banks were declared as part of Sweden's contribution to the Natura-2000 protected area sites, a series of protected areas throughout Europe.

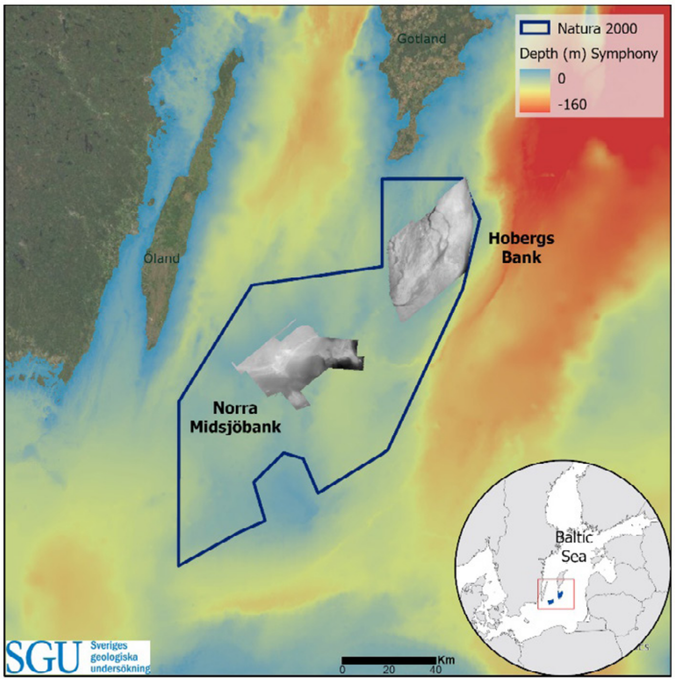

Figure 1. Norra Midsjöbank and Hobergs Bank form an integral part of Sweden's contribution to the Natura 2000 marine protected area.

The offshore banks were surveyed from 2016 to 2018 using newly developed approach to gather and analyse the biophysical and geological conditions of the banks. An integrated, 24-hr field data acquisition routine was established that allowed geophysical sampling to be undertaken during the night, and the data collected, was in-turn used as the basis for the geological and biological sampling during the day. The resulting data, together with other ancilliary and historical data were used as predictors that was fed into the machine learning algorithm to produce various substrate and habitat models.

Surveyed in 2016–17, the Hoburgs Bank study surveyed a total area of >1,300 km^2 with geophysical results revealing seafloor features of glacial origin such as ribbed moraines, glacial lineations, subglacial channels, and scarps left behind by past glacial activities. Hoburgs Bank has a relatively large flat (low rugosity) shallow area, covering ~39% of total survey area, with the depth ranging from mostly 13–50 m that were classified belonging to mostly mixed hard substrate cover, i.e. large fractions mixed with sand or coarse sediments. Underwater videos and images show these areas to be mostly covered by blue mussel and/or macroalgae beds, that serve as critical habitat for the species-rich invertebrates and fish communities. Norra Midsjöbank is another shallow reef found 30 km soutwest from Hoburgs Bank and was surveyed in 2018. Results from the Norra Midsjö Bank survey show the same extensive shallow reefs with hard substrate found in Hoburgs Bank, but smaller in area. The rest of the study area was mostly composed of soft sediment fractions of sand and silt that indicate these as sites for sand deposition. The smaller area of hard substrate cover means that marine productivity was less compared to that of Hoburgs Bank because of lower settlement-site availability for sessile organisms. Found close to the boundary between the hard substrate area and the larger and more extensive sandy areas in the southern part are sinous-shaped grounding zone wedges extending from east to west, which was probably shaped by retreating glacial ice margins. The extensive sandy areas observed on the southern part tend to be highly dynamic as evidenced by the presence of sand ridges.

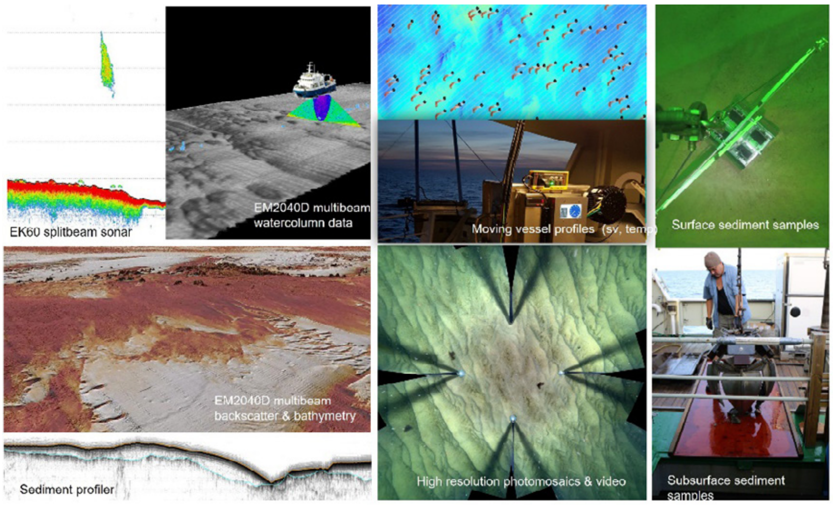

Figure 2. Field collection methods.

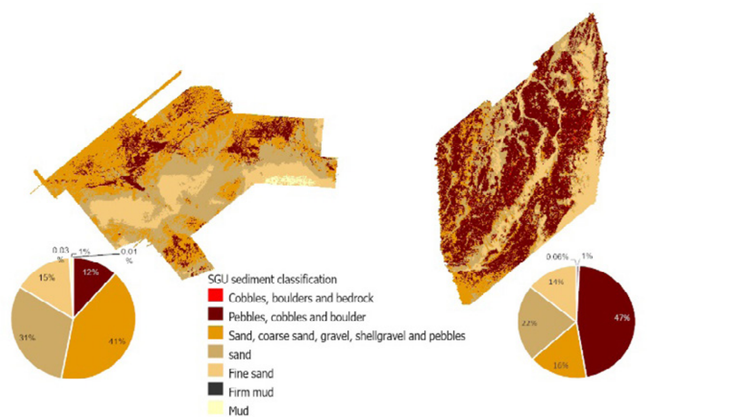

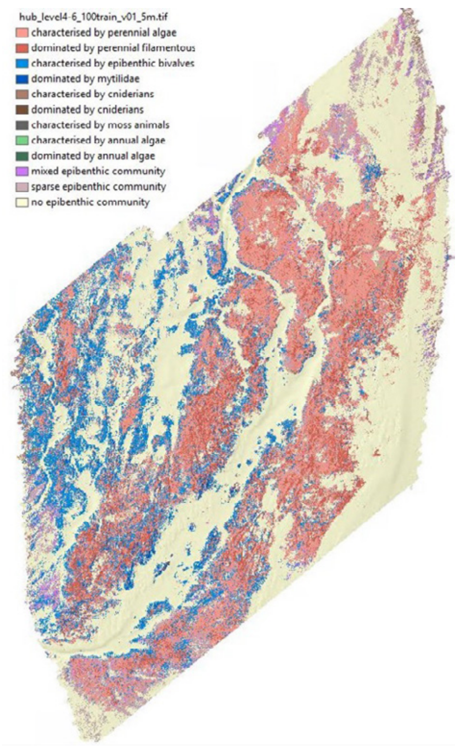

Figure 3. Some samples of the high-resolution (@5m) sediment (top) and habitat (side) map outputs of the project. These are available to the general public via a SGU web download service (below).

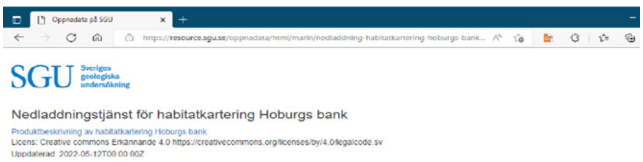

High-resolution, full-coverage habitat and sediment maps for both areas were produced from the results of the geophysical and biological sampling using machine learning algorithms. These map products, now available to the general public, serve as tools for various agencies and institutions in the protection and management of these critically important offshore resource.

References

Kågesten, G., Baumgartner, F., & Freire, F. (2020). High-resolution benthic habitat mapping of Hoburgs bank , Baltic Sea. Uppsala. https://resource.sgu.se/dokument/publikation/sgurapport/sgurapport202034rapport/s2034- rapport.pdf

Kågesten, G., Fiorentino, D., Baumgartner, F., & Zillén, L. (2019). How do continuous highresolution models of patchy seabed habitats enhance classification schemes? Geosciences (Switzerland), 9(5). https://doi.org/10.3390/geosciences9050237

Sub-bottom profile survey of the Ikka Fjord, South Western Greenland – mapping the "soil" of the ikaite column garden

Richard Gyllencreutz[a], Paul Seaman[b], Gabrielle J. Stockmann[c], Erik Sturkell[d], Bengt Liljebladh[d]

[a]Department of Geological Sciences & [b]Bolin Centre for Climate Research, Stockholm university, Stockholm, Sweden, richard.gyllencreutz@geo.su.se; [b]Independent scientist, Kinross, Scotland, United Kingdom, seaman_paul@yahoo.com; [c]Institute of Earth Sciences, University of Iceland, Reykjavik, Iceland, gabrielle@hi.is; [d]Department of Earth Sciences, University of Gothenburg, Gothenburg, Sweden, beli@gvc.gu.se

Summary. Sub-bottom profiling of the Ikka Fjord in SW Greenland revealed up to 13 m thick acoustically laminated sediments in the deep basins, and <2 m thick sediments in shallower areas, with no apparent relationship to the ikaite column distribution. Lack of penetration and upwards-bent reflectors under columns indicates a carbonate-related velocity pull-up effect. Similar features without columns, at various sediment depths, may thus represent broken-down columns and indicates previous episodes of column growth, interrupted by warmer sea water temperatures causing the former columns to disintegrate.

The Ikka Fjord in southwestern Greenland hosts a world-unique "garden" of stalagmite-like columns protruding from the seafloor. The columns are composed of the mineral ikaite, forming at low temperatures (<6°C) from solutions supersaturated with calcium carbonates (Stockmann et al. 2018a,b; Tollefsen et al. 2018) when the formation of anhydrous calcium carbonate minerals is inhibited by e.g. Mg^{2+} (Tollefsen et al. 2018). Ikaite will break down to less hydrated forms of calcium carbonate when exposed to higher temperatures (>6 °C), and the ikaite crystal framework has been shown to collapse into calcite powder within hours when exposed to ambient laboratory conditions of ~20 °C (Buchardt et al. 2001, Hansen et al. 2011). The present model of column formation suggests that they grow from ground water which has percolated through the carbonatite bedrock of the Grønnedal-Íka igneous complex before seeping out through fractures in the bedrock and interacting with the sea water (Buchardt et al. 2001; Stockmann et al. 2018a). Because the ground water density is lower than the sea water's, the ground water floats upwards and precipitates ikaite around the outflow in a chimney-like structure. This has resulted in the formation of at least 938 columns, ranging in height from 0.5 to 20 m above the sea floor, identified by multibeam sonar mapping (Seaman et al. 2022). The columns are confined to a restricted area in the inner part of the Ikka Fjord. Our previous multibeam mapping of the columns showed that column clusters in many cases align with observed fault lineations (Seaman et al. 2022), which supports ground water outflow as a responsible mechanism. However, little is known about the sediment thickness, stratigraphy, composition and distribution in the Ikka Fjord, or how any remnants of previously broken-down ikaite columns are manifested.

In August 2021, we collected acoustic profiles using a Kongsberg EA640 sub-bottom profiler, with 0.512 ms long chirp pulses ranging 13–17 kHz, at a ping rate of ~17 pings/s. Positioning was supplied by a Hemisphere 101 GPS with SBAS correction (~1 m horizontal accuracy), mounted directly above the sub-bottom transducer. The sub-bottom profiler was towed at c. 3.5 kts speed at c. 0.2 m depth in a styrofoam towfish from the port side ~10 m behind an open boat with an outboard engine, taking care to keep the towfish away from any propeller turbulence. Surveying was done with ~75 m line spacing, with 5 lines along and 24 across the fjord.

Our results show that coarse river sediments, acoustically characterized by hummocky surface and almost no penetration, occupy the inner ~500 m of the fjord and limit the water depth to a few metres. The <29 m deep inner basins show up to 13 m thick acoustically laminated soft sediment deposits (Figure 1). Shallower areas show <2 m thick sediments. The ikaite column distribution shows no apparent relationship with sediment thickness. Under the columns, the acoustic penetration is lost, and the surrounding acoustic reflectors are bent upwards. This is interpreted as a velocity pull-up effect caused by the carbonate in the columns. We also observe similar features in areas without columns, at various depths in the sediments. We suggest that these features represent carbonate sediments from broken-down columns. If correct, this indicates that there have been previous episodes of column growth, interrupted by warmer sea water temperatures causing the former columns to disintegrate. This hypothesis should be tested by coring of the inner Ikka Fjord.

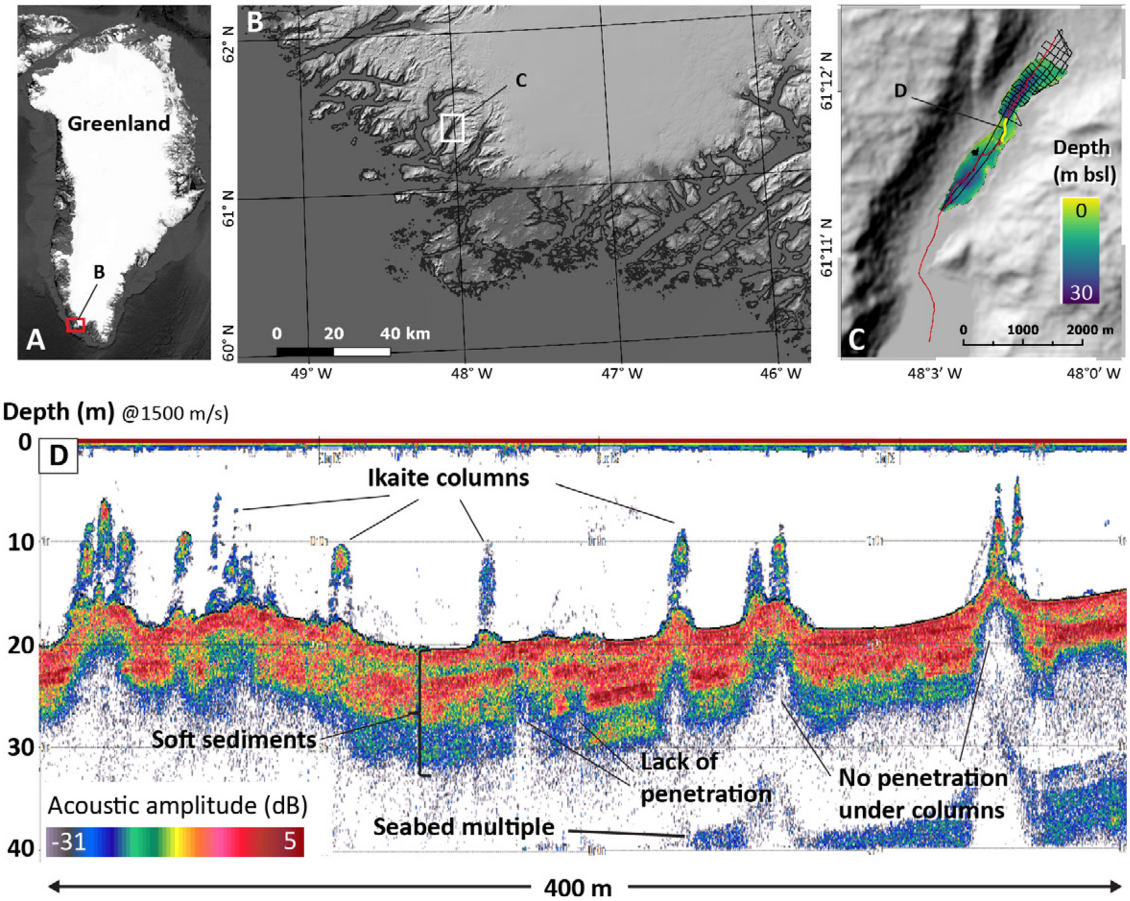

Figure 1. A) Location of the fieldwork area in Greenland, B) location of the Ikka Fjord, C) multibeam bathymetry and track chart of the sub-bottom profiles, where the yellow line indicates the shown profile (D), D) part of profile 3, showing prominent ikaite columns and up to 13 m of acoustically laminated sediments at c. 20 m water depth. There is no penetration under the columns, which is interpreted as velocity pull-up effect by the carbonate. Similar features without columns above indicate carbonate from former, broken-down columns. Background DEM: hill shaded 30 m resolution digital elevation model GIMPDEM v. 1.1 (Howat et al. 2014).

References

Buchardt, B., Israelsson, C., Seaman, P., Stockmann, G., 2001. Ikaite tufa towers in Ikka Fjord, Southwest Greenland: their formation by mixing of seawater and alkaline spring water. J. Sediment. Res. 71, 176–189.

Hansen, M.O., Buchardt, B., Kühl, M., Elberling, B., 2011. The fate of the submarine ikaite tufa columns in Southwest Greenland under changing climate conditions. J. Sediment. Res. 81, 553–561.

Howat, I.M., Negrete, A., Smith, B.E., 2014, The Greenland Ice Mapping Project (GIMP) land classification and surface elevation datasets, The Cryosphere, 8, 1509-1518, DOI:10.5194/tc-8-1509-2014

Seaman, P., Gyllencreutz, R., Sturkell, E., Stockmann, G. J., Geirsson, H., 2022. Surveying the ikaite ($CaCO_3 \cdot 6H_2O$) tufa columns in Ikka Fjord, SW Greenland. Marine Geology 444, 23 pp. DOI: 10.1016/j.margeo.2021.106710

Stockmann et al., 2018a: The role of a Calcite inhibitor (phosphate) and Temperature for ikaite precipitation in Ikka Fjord, Southwest Greenland. Applied Geochemistry 89, 11-22. DOI: 10.1016/j.apgeochem.2017.11.005.

Stockmann et al., 2018b: Carbon mineral storage in seawater: Ikaite ($CaCO_3 \cdot 6H_2O$) columns in Greenland. Energy Procedia 146, 59-67, DOI:10.1016/j.egypro.2018.07.009.

Tollefsen et al., 2018. Chemical controls on ikaite formation. Mineralogical Magazine 82(5), 1119-1129, DOI: 10.1180/mgm.2018.110.

Time scales of offshore freshened groundwater from Norwegian Sea, Barents Sea, and Chukchi Sea

Wei-Li Hong[a,b], Ji-Hoon Kim[c], Sophie ten Hietbrink[a], Arunima Sen[d], Aivo Lepland[e], Beata Szymczycha[f], Seyed Reza Saghravani[f], Jochen Knies[e]

[a]Department of Geological Sciences, Stockholm University, Stockholm, Sweden; [b]Baltic Sea Centre, Stockholm University, Stockholm, Sweden; [c]Marine Geology & Energy Division, Korea Institute of Geoscience and Mineral Resources (KIGAM), Daejeon, South Korea; [d]The University Centre in Svalbard, Longyearbyen, Norway; [e]Geological Survey of Norway, Trondheim, Norway; [f]Institute of Oceanology of Polish Academy of Sciences, Sopot, Poland.

Summary. The offshore freshened groundwater (OFG) has been identified from several locations along the continental slopes and shelves of the Arctic region. While the cryosphere-driven offshore groundwater circulation has been put forward to explain these observations, the time scales are poorly constrained. We summarize our recent findings from the Norwegian Sea, the Barents Sea, and the Chukchi Sea (Fig. 1), where the time scales of the OFG events were constrained either through C-14 and U-Th ages, or numerical modeling of the pore fluid profiles.

Methods

The occurance of OFG is confirmed through the analyses of pore fluid, including the concentrations of various solutes and the water isotopes ($\delta^{18}O$ and $\delta^{2}H$). To better constrain the time scales of groundwater emplacement, we determine the C-14 ages of the dissolved inorganic carbon (DIC) and compare them with the U-Th ages derived from the seafloor crusts from a groundwater seepage site from Eastern Norwegian Sea (c. 800 meters below sea level; Hong et al., 2019). Numerical modeling of the pore fluid chloride concentration profiles from Svalbard fjords (c. 40 to 260 meters below sea level; Kim et al., 2022) and Chukchi Sea shelf (c. 100 meters below sea level; Kim et al., 2021) help constrain the OFG events from these two regions.

Conclusions

We demonstrate how glacial-interglacial dynamics have promoted submarine groundwater circulation more than 100 km offshore at these locations. The seepage of groundwater from the East Norwegian Sea has been active at least since the Last Glacial Maximum and is thought to be driven by the changes in ice sheet extent (Fig. 2). No active seepage of OFG from both Svalbard fjords and Chukchi Sea shelf sediments is currently observed; rather, the freshened groundwater serves as a passive fluid source with diffusion as the primary transport mode for the geochemical signals observed. Melting of submarine permafrost during the past centuries to millenniums is the mostly like source of meteoric water from both regions (Fig. 3). We conclude that the presence of OFG from these regions serves as a sign of fluctuated cryosphere over the past millenniums.

References

Hong, W.L., Lepland, A., Himmler, T., Kim, J.H., Chand, S., Sahy, D., Solomon, E.A., Rae, J.W., Martma, T., Nam, S.I. and Knies, J., 2019. Discharge of meteoric water in the eastern Norwegian Sea since the last glacial period. *Geophysical Research Letters*, *46*(14), pp.8194-8204.

Kim, J.H., Ryu, J.S., Hong, W.L., Jang, K., Joo, Y.J., Lemarchand, D., Hur, J., Park, M.H., Chen, M., Kang, M.H. and Park, S., 2022. Assessing the impact of freshwater discharge on the fluid chemistry in the Svalbard fjords. *Science of The Total Environment*, p.155516.

Kim, J.H., Hong, W.L., Torres, M.E., Ryu, J.S., Kang, M.H., Han, D., Nam, S.I., Hur, J., Koh, D.C., Niessen, F. and Lee, D.H., 2021. A pulse of meteoric subsurface fluid discharging into the Chukchi Sea during the Early Holocene Thermal Maximum (EHTM). *Geochemistry, Geophysics, Geosystems*, *22*(8), p.e2021GC009750.

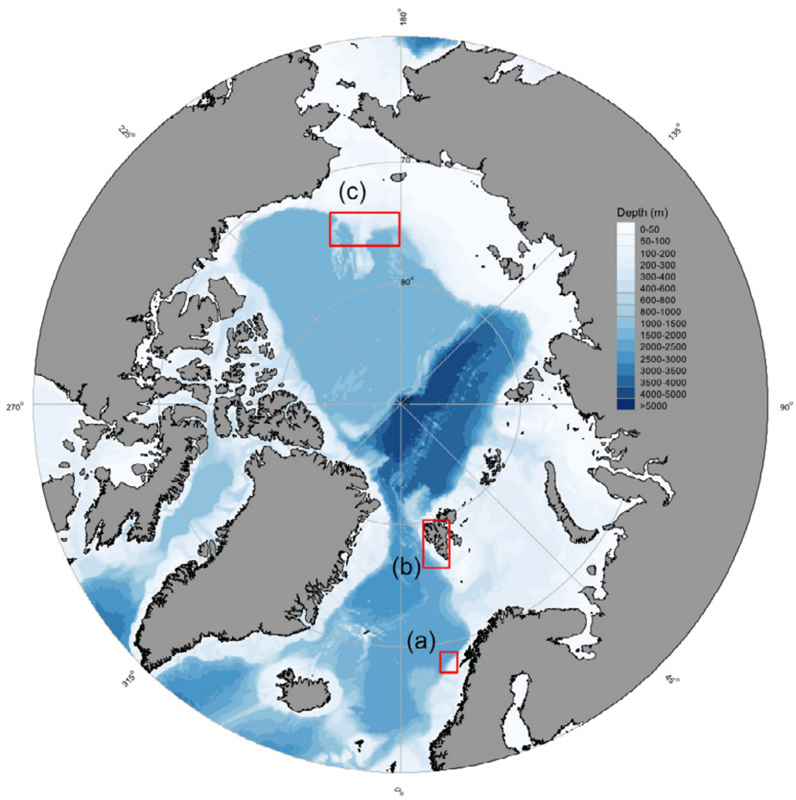

Figure 1. A pan-Arctic basemap showing the three regions where OFG was identified. (a) Lofoten-Vesterålen margin, eastern Norwegian Sea (Hong et al., 2019). (b) Svalbard fjords, Barents Sea (Kim et al., 2022). (c) Chukchi Sea shelf (Kim et al., 2021). The pan-Arctic land shapes are from *Natural Earth Data*. The pan-Arctic bathymetry is from *GEBCO One Minute Grid*.

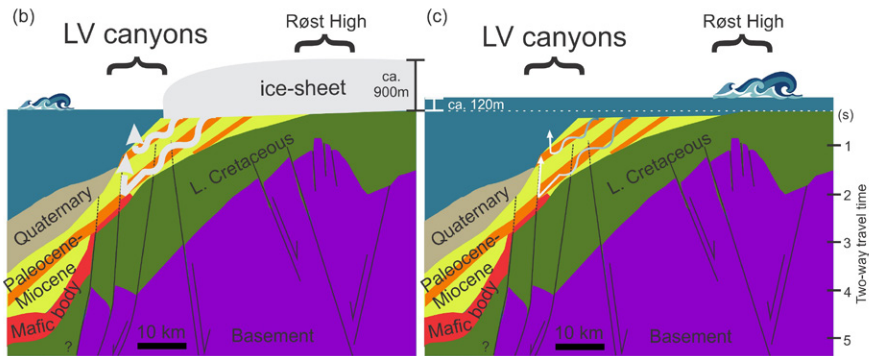

Figure 2. The proposed flow path for the freshwater component submarine groundwater discharge (fSGD; white arrows) as a result of glacial-interglacial dynamics from the eastern Norwegian Sea (from Hong et al., 2019).

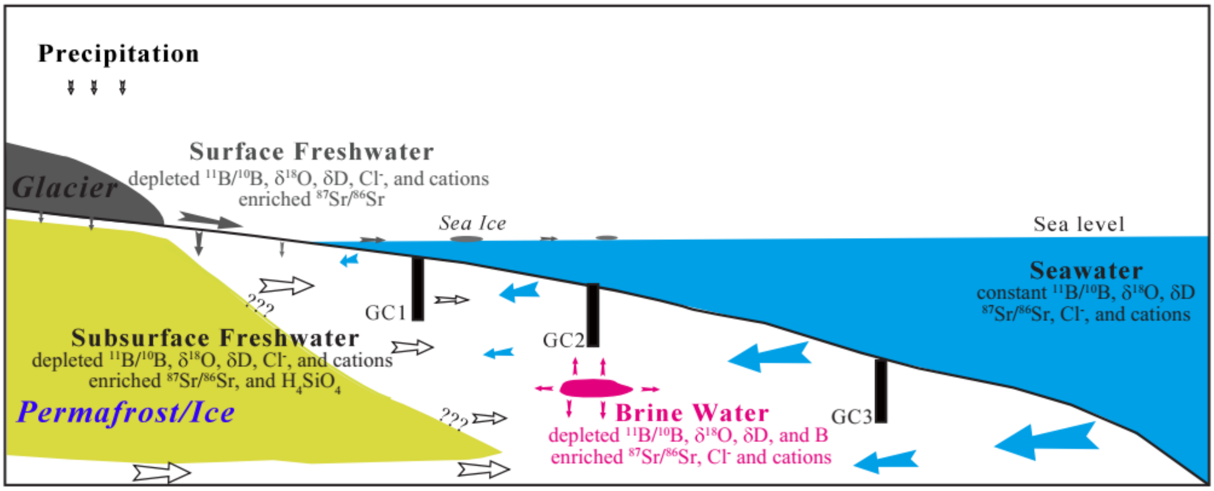

Figure 3. A conceptual model illustrating the hydrological processes, chemical reactions, and characteristics of each fluid source at Isfjord interacting with the hydrospherecryosphere-lithosphere (from Kim et al., 2022).

Exploring planktonic foraminifer evolution in response to environmental restructuring across the K-Pg using deep learning

Allison Y. Hsiang

Department of Geological Sciences, Stockholm University, Stockholm, Sweden, allison.hsiang@geo.su.se

Summary. The K-Pg mass extinction event resulted in the loss of >90% of planktonic foraminifer species and a significant restructuring of the ocean ecosystem, severely disrupting the biological pump. Here, I will describe current efforts to build a high-resolution morphological record of planktonic foraminifera across the K-Pg boundary using high-throughput imaging, automation, and deep learning. This record will be correlated against biogeochemical records in order to understand the interplay between large-scale community evolution in foraminifera and the collapse and recovery of the biological pump.

Background

The Chicxulub bolide impact that occurred at 66 Ma famously resulted in the extinction of the non-avian dinosaurs and is known as the Cretaceous-Paleogene (K-Pg) mass extinction event. Marine environments also suffered high losses, with planktonic foraminifera species diversity dropping by more than 90% at this time (Smit 1982). Modern planktonic foraminifera are estimated to contribute 23–56% of global oceanic carbonate export and 32–80% of total deep-marine calcite (Schiebel 2002). As such, planktonic foraminifera comprise a key component of the global carbon cycle, and the extinction of the majority of species at the K-Pg boundary was a significant contributor to the collapse of the biological pump at this time. Given the rapid timescale and global consequences of the environmental perturbation at the K-Pg boundary, it serves as an important case study of how the ocean ecosystem responds to dramatic environmental change, with application to modern concerns about the effect of anthropogenic climate change on our oceans.

Disruption of the biological pump at the K-Pg boundary led to high instability in ocean carbon cycling and a global drop in carbonate sedimentation and organic matter flux (D’Hondt 2005). Recent work suggests that this instability lasted for ~1.8 Myr, with the marine biotic community recovering after this time period (Alvarez et al. 2019). These results are corroborated by $\partial^{13}C$ values measured from planktonic and benthic foraminifera, which suggest that carbon export recovery began ~300 kyr after the boundary and returned to pre-extinction values by 1.77 Myr into the Danian (Birch et al. 2012). However, although the function of the biological pump was restored soon after the boundary, this recovery occurred independent of the recovery of diversity levels in marine plankton communities. Indeed, species richness remained low and did not reach pre-extinction levels until ~10 Myr after the mass extinction event (Alvarez et al. 2019).

The morphology of the calcium carbonate tests of planktonic foraminifera is linked to environmental conditions and ecological stress. Grigoratou et al. (2019) used trait-based ecological modelling to show that temperature is the dominant factor that drives calcification dynamics in foraminifera. Body size is also correlated with sea-surface temperatures and is a key trait that affects the ecology of planktonic foraminifer communities (e.g. Schmidt et al. 2004). In the wake of the K-Pg mass extinction, there is a strong dwarfing signal in planktonic foraminifera communities, with smaller species retaining higher levels of diversity and survivorship (Darling et al. 2009).

Deep learning and automation: Powerful tools for geobiology

In light of the importance of understanding the K-Pg mass extinction and the strong correlation between planktonic foraminifer morphology and environmental factors, a high-resolution, detailed morphological record of planktonic foraminifer communities across the K-Pg would be a vital dataset for decoding the interactions between biological and ecological processes and the physical environment. However, generating such a dataset using traditional manual methods would require a herculean amount of effort, limiting its scale and resolution. By applying methods developed in the field of computer vision, we can greatly decrease the amount of time and labor required to generate the large datasets necessary to quantify morphological evolution on a community level across large stretches of geological time. High-throughput imaging and automated object identification/segmentation is possible with modern microscopy equipment and deep learning algorithms that can remove the need for human workers to pick, arrange, identify, and measure individual specimens (Hsiang et al. 2017). For instance, a supervised machine learning model built using convolutional neural networks can identify ~25,000 planktonic foraminifer individuals in about 10 minutes with higher-than-human accuracy, a task which may take a team of taxonomists several months to achieve (Hsiang et al. 2019).

Here, these automation methods are applied to the task of generating a high-resolution record of planktonic foraminifer morphology on a community level across the K-Pg boundary (Figure 1). This record will stretch from 0.5 Myr before the boundary to 2 Myr after, effectively covering the period of pre-extinction diversity and environmental conditions, through the extinction event, and until biological pump function has recovered. This record will then be compared to biogeochemical and climatic records in order to develop morphological correlates of environmental perturbation and explore how community structure affects and interacts with the function of the biological pump, with the end goal of developing planktonic foraminifer morphology and community structure as a measurable proxy for ocean ecosystem health.

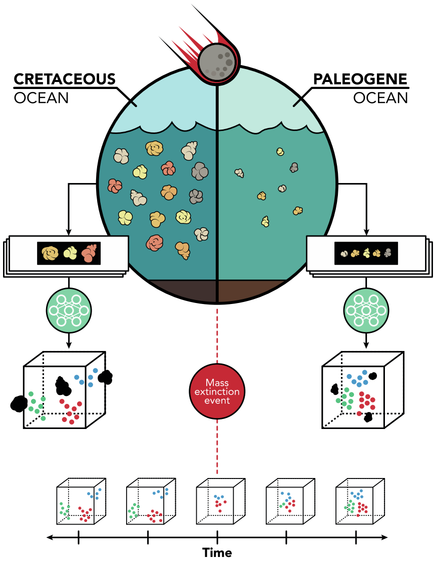

Figure 1. Pipeline for using high-throughput imaging and deep learning to reconstruct a high-resolution morphological record of planktonic foraminifera across the K-Pg boundary. Automation methods (e.g. deep learning algorithms) will be used to quantify body size and morphospace occupation at regular time intervals from 0.5 Myr before the mass extinction event to 2 Myr after.

References

Alvarez, S.A., et al., 2019: Diversity decoupled from ecosystem function and resilience during mass extinction recovery. *Nature* 574, 242–245.

Birch, H.A., et al., 2016: Partial collapse of the marine carbon pump after the Cretaceous Paleogene boundary. *Geology* 44:287–290.

Darling, K.F., et al., 2009: Surviving mass extinction by bridging the benthic/planktic divide. *PNAS* 406:12629–12633.

D'Hondt, S., 2005: Consequences of the Cretaceous/Paleogene mass extinction for marine ecosystems. *Annual Review of Ecology, Evolution, and Systematics* 36, 295–317.

Grigoratou, M., et al., 2019: A trait-based modelling approach to planktonic foraminifera ecology. *Biogeosciences* 16, 1469–1492.

Hsiang, A.Y., et al., 2017: AutoMorph: Accelerating morphometrics with automated 2D and 3D image processing and shape extraction. *Methods in Ecology and Evolution* 9(3):605–612.

Hsiang, A.Y., et al., 2019: Endless Forams: >34,000 Modern planktonic foraminiferal images for taxonomic training and auomated species recognition using convolution neural networks. *Paleoceanography and Paleoclimatology* 34(7), 1157–1177.

Schiebel, R., 2002: Planktonic foraminiferal sedimentation and the marine calcite budget. *Global Biogeochemical Cycles* 16(4), 13-1–13-21.

Schmidt, D., 2004: Size distribution of Holocene planktic foraminifer assemblages: Biogeography, ecology and adaptation. *Marine Micropaleontology* 50, 319–338.

Smit, J., 1982: Extinction and evolution of planktonic foraminifera at the Cretaceous/Tertiary boundary after a major impact. In: Silver, L.T. and Schultz, P.H., eds., *Geological implications of impacts of large asteroids and comets on the Earth: Geological Scoeity of America Special Paper* 190, 329–352.

North Greenland Earth-Ocean-Ecosystem Observatory (GEOEO)

Martin Jakobsson[a], Nina Kirchner[b], GEOEO-members

[a]Department of Geological Sciences, Stockholm University, Stockholm, Sweden, martin.jakobsson@geo.su.se;
[b]Department of Physical Geography, Stockholm University, Stockholm, Sweden, nina.kirchner@natgeo.su.se

Summary. The North Greenland Earth-Ocean-Ecosystem Observatory (GEOEO) is a Research Theme developed by a consortium of scientists for the Swedish Polar Research Secretariat's call for proposals within their Polar Process 2021. GEOEO is one of two Research Themes adopted. It addresses scientific questions focused on understanding the marine cryosphere's dynamic history and response to future climate change, including implications for marine and terrestrial ecosystems in North Greenland and adjacent Arctic Ocean. GEOEO is centred around the North of Greenland 2024 expedition with icebreaker (IB) Oden.

GEOEO

The more than three times greater warming the Arctic experienced over the last two decades compared to the rest of the Earth, has had huge implications for the marine cryosphere, the marine and terrestrial ecosystems of the region, and global climate. We define the "marine cryosphere" as glaciers and ice sheets in contact with the ocean, sea ice, gas hydrates and subsea permafrost (Fig. 1). GEOEO is focused on studying the marine cryosphere's history, dynamics and response to future climate change in North Greenland and the adjacent Lincoln Sea of the Arctic Ocean, where the marine realm is among the least known on Earth. The Theme also includes research questions on the marine and terrestrial ecosystems, specifically how these ecosystems interact with the cryosphere, and how they may be affected by a continued climate warming. Northern Greenland has fjords where outlet glaciers drains the Greenland Ice Sheet, still unvisited by vessels and therefore uncharted and unsampled. The 2019 *IPCC Special Report on the Ocean and Cryosphere in a Changing Climate* (SROCC) (Pörtner et al., 2020) emphasizes that the mass loss from calving and submarine melt of Greenland's marine outlet glaciers constitutes one of the largest uncertainties in predictions of future global sea-level rise. GEOEO will assess the future contribution to global sea-level rise from the North Greenland Ice Sheet.

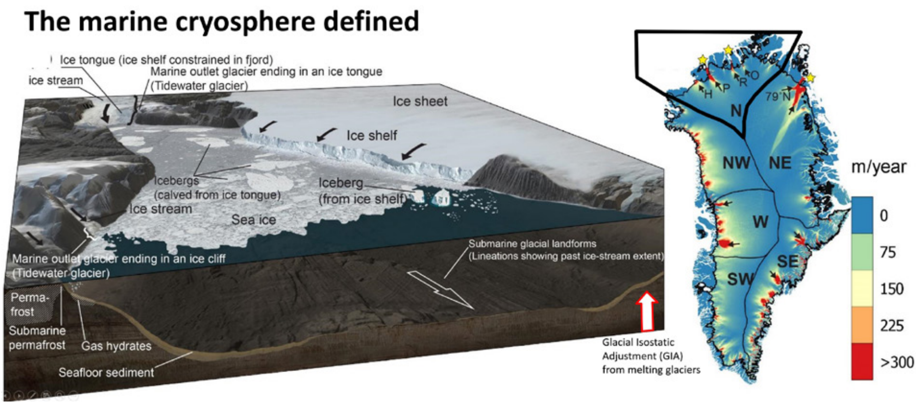

Figure 1. Visualization showing the components of the "marine cryosphere" in focus for GEOEO: marine outlet glaciers ending in floating ice tongues/ ice shelves or grounded ice cliffs, icebergs, ice sheets with their base suppressed below sea level and sea ice. The Greenland Ice Sheet is shown to the right with its ice velocity distribution in meter per year from the MEaSUREs project. Ice streams draining the ice sheet toward the ocean are seen by higher velocities. The Greenland Ice Sheet is divided into drainage sectors defined by ice-catchment areas (SW=South West, W=West, NW=North West, N=North, NE=North East, SE=South East). The larger marine outlet glaciers of the North Sector marked by black arrows are: H=Humboldt Glacier; P=Petermann Glacier; R=Ryder Glacier; O=C.H. Ostenfeld Glacier. The yellow stars mark the few remaining larger ice tongues; two exist in the North Sector in focus for GEOEO. 79°N=79° North Glacier.

The *North of Greenland 2024* expedition builds on two successful expeditions with IB Oden: *Petermann 2015* (e.g. Hogan et al., 2020; Jakobsson et al., 2018; Jennings et al., 2020; Reilly et al., 2019) and *Ryder 2019* (e.g. Holmes et al., 2021; Jakobsson et al., 2020; Jennings et al., 2022; O'Regan et al., 2021; Stranne et al., 2021) (Fig. 2). We aim to continue surveying areas north of Sherard Osborn Fjord, where the C.H Ostenfeldt Glacier drains into the unsurveyed Victoria Fjord. During year 2024 our collaborating partners within the Norwegian led *GoNorth*-project plan an expedition with FF Kronprins Haakon. This permits the two ships to complete the first synoptic transect, extending west of Svalbard (FF Kronprins Haakon), across the Fram Strait to Morris Jesup Rise, to north-western Greenland (IB Oden). Heat transport by warmer Atlantic water will be one of the key targets for this transect.

Under our proposed GEOEO Theme, we have brought together Swedish research groups from Stockholm University, University of Gothenburg, Uppsala University, Linnaeus University and Swedish Museum of Natural History to work with groups from the Geological Survey of Denmark and Greenland, Aarhus University, University of Oslo, University of Tromsø, University of Bergen, University of New Hampshire and US Geological Survey. We envision the IB *Oden* expedition to be a Swedish-US-Danish-Norwegian collaborative enterprise.

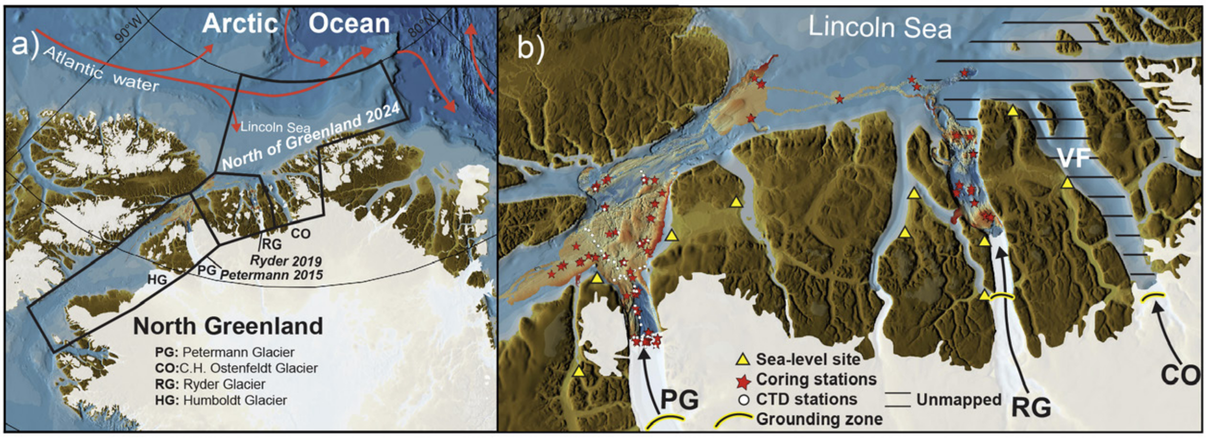

Figure 2. a) Map showing the data collected during the Petermann 2015 and Ryder 2019 expeditions, and the target area of the GEOEO North of Greenland 2024 Expedition. b) Close up showing the coverage of the multibeam bathymetry, coring/oceanographic stations and land sites for various kinds of studies, including sea-level. The region of Victoria Fjord (VF) is completely unmapped as indicated by line hatching. The bathymetry in this fjord is a product of the mass conservation algorithm applied in the Bedmachine V3 compilation (Morlighem et al., 2017), where the grounding line depths of outlet glaciers are extrapolated out into the fjord. This will not capture any depth features in the fjord, such as a shallow sill, which constitute critical information for sea-level rise predictions.

References

Hogan, K. A., et al., 2020: Glacial sedimentation, fluxes and erosion rates associated with ice retreat in Petermann Fjord and Nares Strait, north-west Greenland. *The Cryosphere 14*(1), 261-286, doi:10.5194/tc-14-261-2020.

Holmes, F. A., N. Kirchner, A. Prakash, C. Stranne, S. Dijkstra, and M. Jakobsson, 2021: Calving at Ryder Glacier, Northern Greenland *126*(4), e2020JF005872, doi:https://doi.org/10.1029/2020JF005872.

Jakobsson, M., et al., 2018: The Holocene retreat dynamics and stability of Petermann Glacier in northwest Greenland. *Nature Communications 9*(1), 2104, doi:10.1038/s41467-018-04573-2.

Jakobsson, M., et al., 2020: Ryder Glacier in northwest Greenland is shielded from warm Atlantic water by a bathymetric sill. *Communications Earth & Environment 1*(1), 45, doi:10.1038/s43247-020-00043-0.

Jennings, A., J. Andrews, B. Reilly, M. Walczak, M. Jakobsson, A. Mix, J. Stoner, K. W. Nicholls, and M. Cheseby, 2020: Modern foraminiferal assemblages in northern Nares Strait, Petermann Fjord, and beneath Petermann ice tongue, NW Greenland. *Arctic, Antarctic, and Alpine Research 52*(1), 491-511, doi:10.1080/15230430.2020.1806986.

Jennings, A., et al., 2022: Modern and early holocene ice shelf sediment facies from Petermann Fjord and northern Nares Strait, northwest Greenland. *Quaternary Science Reviews 283*, 107460, doi:https://doi.org/10.1016/j.quascirev.2022.107460.

Morlighem, M., et al., 2017: BedMachine v3: Complete Bed Topography and Ocean Bathymetry Mapping of Greenland From Multibeam Echo Sounding Combined With Mass Conservation. *Geophysical Research Letters 44*(21), 11,051-011,061, doi:10.1002/2017GL074954.

O'Regan, M., et al., 2021: The Holocene dynamics of Ryder Glacier and ice tongue in north Greenland. *The Cryosphere 15*, 4073-4097, doi:10.5194/tc-15-4073-2021.

Pörtner, H.-O., et al. (2020), IPCC Special Report on the Ocean and Cryosphere in a Changing Climate*Rep.*

Reilly, B. T., et al., 2019: Holocene break-up and reestablishment of the Petermann Ice Tongue, Northwest Greenland. *Quaternary Science Reviews 218*, 322-342, doi:10.1016/j.quascirev.2019.06.023.

Stranne, C., et al., 2021: The climate sensitivity of northern Greenland fjords is amplified through sea-ice damming. *Communications Earth & Environment 2*(1), 70, doi:10.1038/s43247-021-00140-8.

Response of the ocean circulation and ice shelf basal melt rates at Petermann Fjord to a year-round mobile sea ice cover in the Nares Strait

Abhay Prakash[a,b], Qin Zhou[c], Tore Hattermann[d,e], Nina Kirchner[a,b]

[a]Department of Physical Geography, Stockholm University, Stockholm, Sweden, abhay.prakash@natgeo.su.se; [b]Bolin Centre for Climate Research, Stockholm University, Stockholm, Sweden; [c]Akvaplan-niva, Tromsø, Norway; [d]Norwegian Polar Institute, Tromsø, Norway; [e]Department of Physics and Technology, University of Tromsø, Tromsø, Norway

Summary. Recent anomalous collapses of ice arches in the Nares Strait point towards the onset of year round mobile ice cover; a likely scenario under the CMIP5 future warming projections. Petermann, a large outlet glacier located downstream of the Robeson Channel is sensitive to seasonal shifts in the local sea ice cover. We use a 3-D numerical ocean-sea ice-ice shelf setup to prescribe a set of surface forcings modulated by the varying sea ice cover regimes in the Nares Strait. We present the seasonal changes in circulation and melt rates at Petermann, driven by the transitions in the Nares Strait ice cover that range from landfast and thick to mobile and thin.

The reported increase in GrIS mass loss rate over the last two decades is about 8 times higher than the Antarctic Ice Sheet mass loss rate (Chen et al. 2017). Draining the Northwest sector, and 4% of the total GrIS area (Rignot & Kanagaratnam 2006), Petermann glacier is one of the 5 remaining Greenland glaciers that still has a floating ice shelf (Münchow et al. 2016). It discharges ~12 Gt/yr of ice (Rignot & Steffen 2008) across its ~20 km wide grounding line (GL) into the Petermann fjord that is ~90 km long. The glacier mass imbalance is largely dictated by the interaction between the ice shelf and ocean, where channelized basal melting accounts for 80% of the mass loss (Münchow et al. 2014). Modelling of Petermann ice shelf-ocean interactions using an idealized ice shelf geometry demonstrated the significance of the seasonal cycle of sea-ice dynamics in the Nares Strait to the stability of the ice shelf (Shroyer et al. 2017). Here, changes in the ocean dynamics driven by the transition from a winter fast to a summer mobile sea ice state resulted in increased modelled basal melt rates. Recent observations have pointed towards the possible onset of an arch free Nares Strait (Moore et al. 2021); a likely scenario under the CMIP5 future warming projections (Koenigk et al. 2007, Wang & Overland 2012). From a sea ice dynamics perspective, under this new regime, ice cover in the Nares Strait will shift from a summer mobile to a year-round mobile state. Based on the mechanisms described in Shroyer et al. 2017, it can be argued that persistence of this year round mobile ice in the Nares Strait will most likely lengthen the duration of enhanced basal melting, impacting the long term stability of the Petermann Glacier Ice Shelf (PGIS). In this study, we present results regarding the implications of such a shift in the sea ice cover regime in the Nares Strait on the ocean circulation and ice shelf basal melt rates at Petermann Fjord. We use a nested high-resolution (200 m) unstructured grid 3-D ocean-sea ice-ice shelf setup (Prakash et al. 2022) which includes an improved representation of the sub ice shelf topography, a realistic ice shelf geometry and a new sea ice module (Ice Nudge), using which, ice conditions can be prescribed as external surface forcing parameters which allows us to simulate the PGIS basal melt sensitivity to differing Nares Strait ice cover regimes.

References

Chen, X., Zhang, X., Church, J. et al., 2017: The increasing rate of global mean sea-level rise during 1993–2014. *Nature Clim Change* 7, 492–495. https://doi.org/10.1038/nclimate3325

Koenigk, T., Mikolajewicz, U., Haak, H. & Jungclaus, J., 2007: Arctic freshwater export in the 20th and 21st centuries. *J. Geophys. Res.*, 112, G04S41, doi:10.1029/2006JG000274

Moore, G.W.K., Howell, S.E.L., Brady, M. et al., 2021: Anomalous collapses of Nares Strait ice arches leads to enhanced export of Arctic sea ice. *Nat Commun* 12, 1. https://doi.org/10.1038/s41467-020-20314-w

Münchow, A., Padman, L. & Fricker, H.A., 2014: Interannual changes of the floating ice shelf of Petermann Gletscher, North Greenland, from 2000 to 2012. *J. Glaciol.* 60(221), 489–499 (doi: 10.3189/2014JoG13J135)

Münchow, A., Padman, L., Washam, P. & Nicholls, K.W., 2016: The ice shelf of Petermann Gletscher, North Greenland, and its connection to the Arctic and Atlantic Oceans. *Oceanography* 29(4):84–95, https://doi.org/10.5670/oceanog.2016.101.

Prakash, A., Zhou, Q., Hattermann, T., Bao, W., Graversen, R. & Kirchner, N., 2022: A nested high-resolution unstructured grid 3-D ocean-sea ice-ice shelf setup for numerical investigations of the Petermann ice shelf and fjord. *MethodsX*, Volume 9, 101668, ISSN 2215-0161, https://doi.org/10.1016/j.mex.2022.101668.

Rignot, E. & Kanagaratnam, P., 2006: Changes in the velocity structure of the Greenland Ice Sheet. *Science* 311 (80). (101126/science.1121381), 986–990

Rignot, E. & Steffen, K., 2008: Channelized bottom melting and stability of floating ice shelves. *Geophys. Res. Lett.* 35(2) (doi:10.1029/2007GL031765)

Shroyer, E. L., Padman, L., Samelson, R.M., Münchow, A. & Stearns, L.A., 2017: Seasonal control of Petermann Gletscher ice-shelf melt by the ocean's response to sea-ice cover in Nares Strait. *J. Glaciol.*, 63(238), 324– 330, doi:10.1017/jog.2016.140

Wang, M. & Overland, J.E., 2012: A sea ice free summer Arctic within 30 years: an update from CMIP5 models. *Geophys. Res. Lett.* 39 (18), doi: 10.1029/2012GL052868

Mid-Pleistocene to Holocene calcareous nannofossil taxonomy and biochronology in the central Arctic Ocean

Mohammad J. Razmjooei[a], Matt O'Regan[a], Jorijntje Henderiks[b], Karl-Heinz Baumann[c]

[a]Department of Geological Sciences, Stockholm University, Stockholm, Sweden, mohammad.razmjooei@geo.su.se; matt.oregan@geo.su.se; [b]Department of Earth Sciences, Uppsala University, Uppsala SE-752 36, Sweden; [c]Geosciences, University of Bremen, PO Box 330440, 28334 Bremen, Germany

Summary. A half-century of research (since the 1970s) indicates that accurate dating of sediments in the Arctic Ocean is not straightforward due to puzzling magnetic polarity patterns, lack or scarcity of microfossils, and discontinuous oxygen isotope records in Arctic marine sediments. Our biostratigraphy studies show some intervals containing calcareous nannofossils with two valuable bio-zonational markers, including *Emiliania huxleyi* and *Pseudoemiliania lacunosa*, that could be used for providing an age model of the upper Quaternary sediments of the central Arctic ocean.

Recently two important bio-horizons of calcareous nannofossils, including the first occurrence of *Emiliania huxleyi* (291 kyr, Raffi et al., 2006) and the last occurrence of *Pseudoemiliania lacunosa* (436 kyr, Raffi et al., 1977) were reported for the first time in the central Arctic (LRG12-3PC, O'Regan et al., 2020). In order to study the taxonomic composition and abundance of calcareous nannofossil taxa and expand on the results provided by O'Regan et al. (2020), a high-resolution stratigraphic analysis of upper Quaternary sediments has been undertaken on three cores from the Lomonosov Ridge (LRG12-7PC, LRG12-9PC, and AO16-5-PC1) and one core from the Makarov Basin (AO16-8GC) in the central part of the Arctic Ocean. Although our studies confirm the presence of the two bio-events across the central Arctic, the extremely low abundances and variable preservation can make it very difficult to confidently resolve their stratigraphic position. Through detailed sampling and cross-verification using LM and SEM imaging, a new stratigraphic framework in support of key bio-events is emerging. This would significantly change the geochronological framework for central Arctic Ocean sediments – implying that what were identified as sub-stages (inter-stadials) within Marine Isotope Stage 5 are actually separate interglacials. The presence and absence pattern of nannofossil markers in the studied cores follows the nannofossil zones NN19, NN20, and NN21 of standard biozonation of Martini (1971) and would place the Mid-Pleistocene to Holocene in the upper 2–3 meters of the cores.

References

Martini, E., 1971. Standard Tertiary and Quaternary calcareous nannoplankton zonation. In: Farinacci, A. (Ed.), Proceedings of the II Planktonic Conference, Roma, 1970. Edizioni Tecnoscienza, Roma, 739-785.

O'Regan, M., Backman, J., Fornaciari, E., Jakobsson, M. and West, G., 2020. Calcareous nannofossils anchor chronologies for Arctic Ocean sediments back to 500 ka. Geology, 48(11), 1115-1119.

Raffi, I., Backman, J., Fornaciari, E., Pälike, H., Rio, D., Lourens, L. and Hilgen, F., 2006. A review of calcareous nannofossil astrobiochronology encompassing the past 25 million years. Quaternary Science Reviews, 25(23-24), pp.3113-3137.

Paleoceanography of the eastern equatorial Pacific since the late Miocene inferred from bulk sediment properties

Daniele Reghellin[a], Helen K. Coxall[b], Gerald R. Dickens[c], Jan Backman[d]

[a]Department of Pure and Applied Sciences (DiSPeA), University of Urbino Carlo Bo, Urbino, Italy, daniele.reghellin@uniurb.it; [b]Department of Geological Sciences, Stockholm University, Stockholm, Sweden, helen.coxall@geo.su.se; [c]Department of Geology, Trinity College, Dublin, Ireland, dickensg@tcd.ie; [d]Department of Geological Sciences, Stockholm University, Stockholm, Sweden, backman@geo.su.se

Summary. The paleoceanography of the eastern equatorial Pacific (EEP) since the late Miocene is of major interest in current research. However, a common view on its evolution is missing, with several and often contrasting scenarios being proposed. Here we present bulk sediment property records measured in sediments deposited at multiple location across the EEP, which provide information on surface water conditions and temperature. Our results indicate major changes in the EEP oceanography over this time interval, both in terms of productivity and temperature gradients.

The oceanography of the EEP since the late Miocene (~8 Ma) has long interested the paleoceanographic community. Its steep gradients in biological production, sea surface temperature (SST) and ocean-atmosphere CO_2 fluxes related to wind-driven equatorial upwelling, play a central role in regulating global climate (Fielder & Lavin 2017). The latter underwent major changes over the last 8 Ma, including the late Miocene climate cooling and the mid-Piacenzian warm period, the last period of sustained global warmth with similar atmospheric CO_2 concentration compared to present-day (Haywood et al. 2020; Berends et al. 2019. Deciphering EEP paleoceanography under global climate change is thus important for understanding how this ocean area works in the present global warming scenario.

The evolution of EEP ocean conditions since the late Miocene is still debated. Paleoceanographic reconstructions of this ocean area are challenging because i) most of the EEP seafloor lies below the lysocline (Farrell et al. 1995; Lyle et al. 2008), with carbonate dissolution impacting various sedimentary records (Pälike et al. 2012), and ii) of the extreme changes in ocean conditions over semi-decadal time scales, which are registered as major changes in sediment properties over decimeter-scale depth intervals. As a result, different proxy records have led to contrasting oceanographic scenarios.

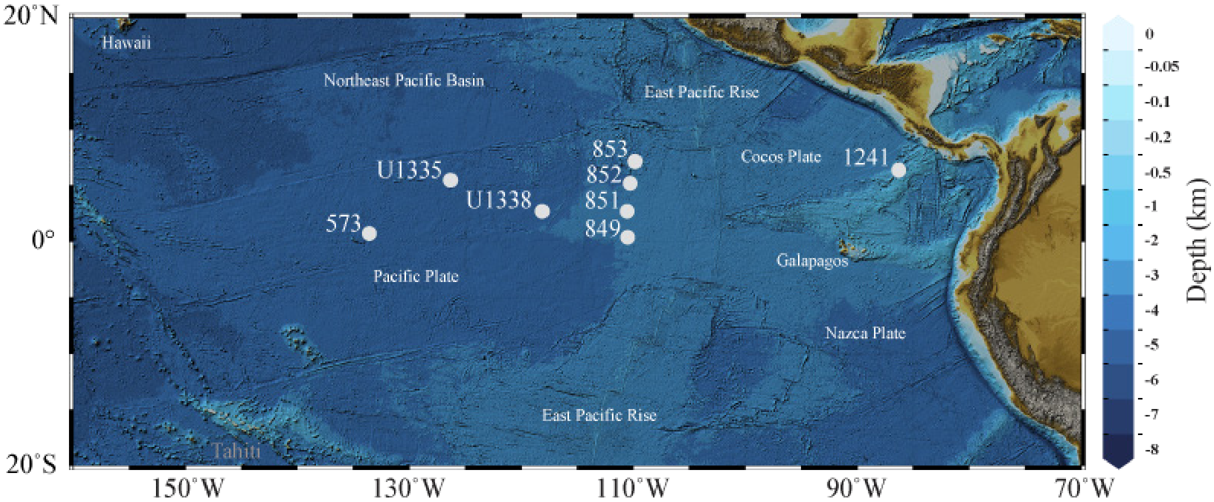

Figure 1. Bathymetry of the eastern equatorial Pacific Ocean (EEP) with location of the drilling sites considered in this study. The map is from GEBCO Compilation Group (2019).

To better depict the ocean evolution of the EEP we present a series of proxy records, including sedimentation rates, carbonate content, carbon and oxygen stable isotopes ($\delta^{13}C$ and $\delta^{18}O$), measured in sediments from multiple ocean drilling sites across the region. These signals mainly reflect surface ocean conditions, which are crucial to decipher EEP paleoceanography (Shackleton & Hall, 1995; Reghellin et al. 2015; 2020).

Our results show a remarkable coherence of bulk $\delta^{13}C$ records at sites separated by thousands of kilometres, and suggest EEP-wide changes in surface water $\delta^{13}C$ since the late Miocene. This is surprising considering the extreme surface water variance within the EEP. Higher sedimentation rates and low bulk $\delta^{18}O$ at sites located on the Equator indicate lower SST along the Equator during the late Miocene and the early Pliocene. During this time interval, the equatorial upwelling circulation was stronger, supporting a higher biological production and a greater ocean-atmosphere CO_2 flux compared to present day. In this time interval the geometry of the upwelling belt seems different from its current.

References

Berends, C.J., De Boer, B., Dolan, A.M., Hill, D.J., & Van De Wal, R.S.W., 2019: Modelling ice sheet evolution and atmospheric CO_2 during the Late Pliocene. *Climate of the Past 15*, 1603–1619. https://doi.org/10.5194/cp-15-1603-2019

Farrell, J.W., Murray, D.W., McKenna, V.S., and Ravelo, A.C., 1995: Upper ocean temperature and nutrient contrasts inferred from Pleistocene planktonic foraminifer $\delta^{18}O$ and $\delta^{13}C$ in the eastern equatorial Pacific. *In* Pisias, N.G., Mayer, L.A., Janecek, T.R., Palmer-Julson, A., and van Andel, T.H. (Eds.), *Proc. ODP, Sci. Results 138*, College Station, TX (Ocean Drilling Program), 289–319. doi:10.2973/odp.proc.sr.138.115.1995

Fiedler, P. & Lavín, F.M., 2017: Oceanographic conditions of the eastern tropical Pacific. *In* P. W. Glynn, D. Manzello, & I. Enochs (Eds.), Coral Reefs of the eastern Tropical Pacific. *Coral Reefs of the World 8*, 59–83. https://doi.org/10.1007/978-94-017-7499-4_3

GEBCO Compilation Group, 2019. doi: 10.5285/836f016a-33be-6ddc-e053-6c86abc0788e.

Haywood, A.M., Tindall, J.C., Dowsett, H.J., Dolan, A.M., Foley, K.M., et al., 2020: The Pliocene Model Intercomparison Project Phase 2: large-scale climate features and climate sensitivity. *Climate of the Past 16*, 2095–2123.

Lyle, M., Barron, J., Bralower, T.J., Huber, M., Olivarez Lyle, A., Ravelo, A.C., Rea, D.K., & Wilson, P.A., 2008: Pacific Ocean and Cenozoic evolution of climate. *Reviews of Geophysics 46*, RG2002. doi:10.1029/2005RG000190

Pälike, H., Lyle, M.W., Nishi, H., Raffi, I., Ridgwell, A., et al., 2012: A Cenozoic record of the equatorial Pacific carbonate compensation depth. *Nature 488*, 609–615.

Reghellin, D., Coxall, H.K., Dickens, G.R., Galeotti, S., & Backman, J., 2022: The late Miocene-early Pliocene biogenic bloom in the eastern equatorial Pacific: New insights from Integrated Ocean Drilling Program Site U1335. *Paleoceanography and Paleoclimatology 37*, e2021PA004313. https://doi. org/10.1029/2021PA004313

Reghellin, D., Dickens, G.R., Coxall, H.K., & Backman, J., 2020, Understanding bulk sediment stable isotope records in the eastern equatorial Pacific, from seven million years ago to present day. *Paleoceanography and Paleoclimatology 35*, e2019PA003586. https://doi.org/10.1029/2019PA003586

Shackleton, N.J., & Hall, M.A., 1995: Stable isotope records in bulk sediments (Leg 138). *In* Pisias, N.G., Mayer, L.A., Janecek, T.R., Palmer-Julson, A., and van Andel, T.H. (Eds.), *Proc. ODP, Sci. Results 138,* College Station, TX (Ocean Drilling Program), 797–805. doi:10.2973/odp.proc.sr.138.150.1995

Marine Geology and Holocene Paleoceanography of the Southern Quark, Baltic Sea

Anton Wagner[a], Martin Jakobsson[a], Christian Stranne[a], Matt O'Regan[a]

[a]Department of Geological Sciences, Stockholm University, Stockholm, Sweden, antwag1@gmail.com

Summary. The Southern Quark constitutes the narrowest passage between the Swedish mainland and Åland Archipelago. Here we use marine geophysical mapping data and sediment cores, acquired with Stockholm University's Research Vessel (RV) *Electra*, to address the Holocene paleoceanography of the Southern Quark and its broader implications for the development of the Baltic Sea. Eroded channels in the seafloor and sediment drift deposits formed synchronously around 3-4 kyr BP, suggesting a dramatic paleoceanographic change during the transition from the Littorina to Post Littorina stages of the Baltic Sea.

The Understen-Märket trench is located in the Southern Quark and is the only deep-water connection between the Baltic Propper and the Gulf of Bothnia (Hietala et al., 2007). Bathymetric mapping reveals a number of eroded channels and drift deposits exists on the seafloor, indicating that the area is heavily affected by current activity (Figure 1). Bottom current behavior in the area is not thoroughly understood, but generally in the Baltic Basin, there are southward flowing fresh surface waters compensated by denser northward flowing more saline bottom waters (Ambjoern and Gidhagen, 1979). The dominant direction of flow for bottom waters in the Southern Quark is northward. Northward speeds often exceed the threshold required to erode fine material on the seafloor (Ehlin et al., 1977; Palosuo, 1964; SMHI, 2021). Using geophysical data and marine sediment cores, this study shows that current eroded channels and drift deposits in the Understen-Märket trench were initially formed in the late Holocene between 3–4 kyr BP, during the transition from the Littorina to the Post Littorina stages of the Baltic Sea. Application of the sortable silt (SS) proxy for current sorting show three distinct regimes that closely match the assigned lithologic units (LU) based on core descriptions. Downcore grain size analysis of three marine sediment cores reveals a gradual boundary to sandy sediments that caps two of the cores recovered from an eroded channel. The third core was recovered from the drift deposit which mostly consists of silt. The progressive coarsening suggests that the current activity has increased during the late Holocene. A simplified model is presented that shows how moderate (20–50 m) shallowing of the sill, which has occurred in response to isostatic rebound between 8 and 4 kyr BP (Jilbert et al., 2015), could have generated the higher current speeds seen today. However, this could be explored using more advanced paleo-circulation models.

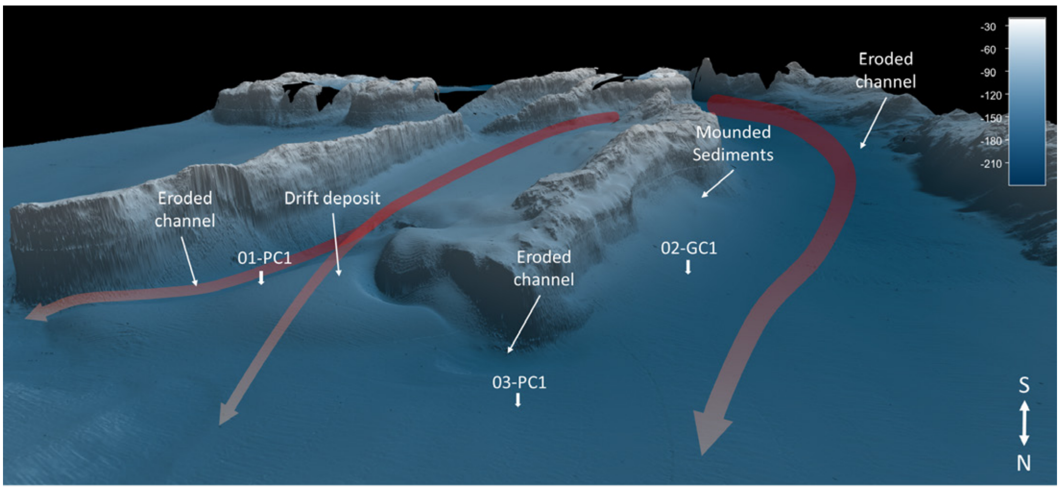

Figure 1. 3D-view of the bathymetry looking south of the survey area with a 3x depth exaggeration with core location and current created features marked out. Red graded arrows show the approximate bottom current direction with deep red representing a relative stronger current that the lighter red. Depth (m) scale in the top right corner. Shading with light source SW of the area.

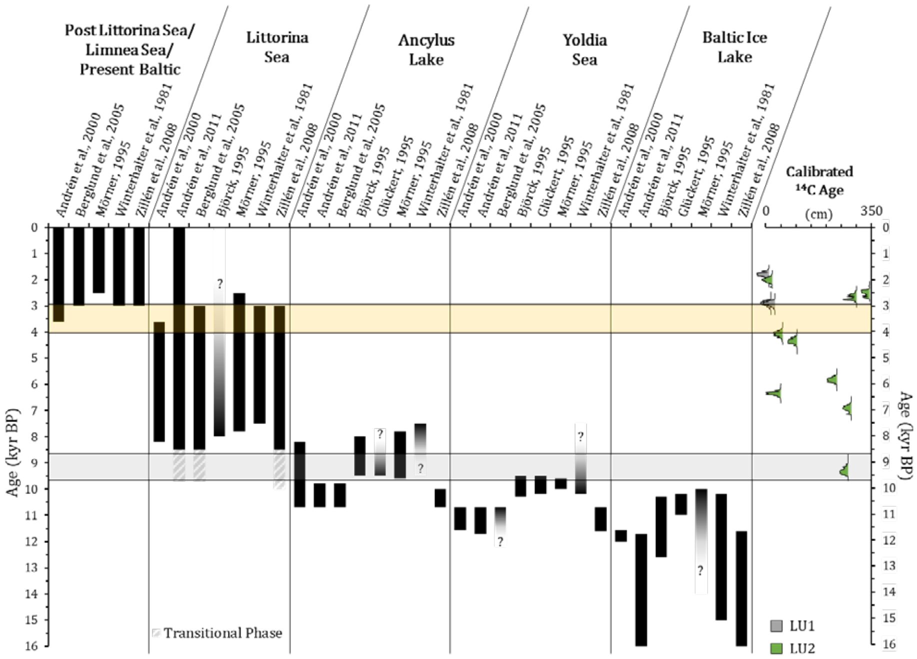

Figure 2. Timings of the Baltic Sea stages since the last deglaciation according to several authors (Andrén et al., 2000, 2011; Berglund et al., 2005; Björck, 1995; Glückert, 1995; Mörner, 1995; Winterhalter et al., 1981; Zillén et al., 2008; and references therein), With calibrated ^{14}C dates on the far right.. Faded vertical bars with question mark indicate a specified start point and unspecified end point (or vice versa) by that author. Striped, grey bars indicate an explicit transitional phase between two sea stages. Yellow horizontal bar marks the approximate age of a shift in water transfer to allow for the deposition of sediment found in 01-PC1. Grey horizontal bar indicates the age of the deepest sample collected from 03-PC1 and shows that it roughly lines up with estimated timings of the Ancylus Lake stage.

References

Ambjoern, C., Gidhagen, L., 1979. Water and material transports between the Gulf of Bothnia and the Baltic proper [current speed, current direction, water temperature, salinity, oxygen, total phosphorus, total nitrogen]. Hydrology & Oceanography, RHO 78.

Andrén, E., Andrén, T., Kunzendorf, H., 2000. Holocene history of the Baltic Sea as a background for assessing records of human impact in the sediments of the Gotland Basin. The Holocene 10, 687–702. https://doi.org/10.1191/09596830094944

Andrén, T., Björck, S., Andrén, E., Conley, D., Zillén, L., Anjar, J., 2011. The Development of the Baltic Sea Basin During the Last 130 ka, in: Harff, J., Björck, S., Hoth, P. (Eds.), The Baltic Sea Basin, Central and Eastern European Development Studies (CEEDES). Springer Berlin Heidelberg, Berlin, Heidelberg, pp. 75–97. https://doi.org/10.1007/978-3-642-17220-5_4

Berglund, B.E., Sandgren, P., Barnekow, L., Hannon, G., Jiang, H., Skog, G., Yu, S.-Y., 2005. Early Holocene history of the Baltic Sea, as reflected in coastal sediments in Blekinge, southeastern Sweden. Quaternary International 130, 111–139.

Björck, S., 1995. A review of the history of the Baltic Sea, 13.0-8.0 ka BP. Quaternary International 27, 19–40. https://doi.org/10.1016/1040-6182(94)00057-C

Ehlin, U., Ambjörn, C., Элин, У., Амбьёрн, C., 1977. Water Transport through the Åland Sea / Перемещение воды в Аландском море. Ambio Special Report 117–125.

Glückert, G., 1995. The Baltic Ice Lake in south Finland and its outlets. Quaternary International 27, 47–51. https://doi.org/10.1016/1040-6182(94)00059-E

Hietala, R., Lundberg, P., Nilsson, J.A.U., 2007. A note on the deep-water inflow to the Bothnian Sea. Journal of Marine Systems 68, 255–264. https://doi.org/10.1016/j.jmarsys.2006.12.004

Jilbert, T., Conley, D.J., Gustafsson, B.G., Funkey, C.P., Slomp, C.P., 2015. Glacio-isostatic control on hypoxia in a high-latitude shelf basin. Geology 43, 427–430. https://doi.org/10.1130/G36454.1

Mörner, N.-A., 1995. The Baltic Ice Lake-Yoldia Sea transition. Quaternary International 27, 95–98. https://doi.org/10.1016/1040-6182(94)00065-D

Palosuo, E., 1964. A Description of the Seasonal Variations of water Exchange Between the Baltic Proper and the Gulf of Bothnia. Publication of the Institute for Marine Research 1–32.

SMHI, 2021. SMHI mooring station “Södra Kvarken”, financed by the Swedish Agency for Marine and Water Management.

Winterhalter, B., Flodén, T., Ignatius, H., Axberg, S., Niemistö, L., 1981. Chapter 1 Geology of the Baltic Sea, in: Voipio, A. (Ed.), Elsevier Oceanography Series, The Baltic Sea. Elsevier, pp. 1–121. https://doi.org/10.1016/S0422-9894(08)70138-7

Zillén, L., Conley, D.J., Andrén, T., Andrén, E., Björck, S., 2008. Past occurrences of hypoxia in the Baltic Sea and the role of climate variability, environmental change and human impact. Earth-Science Reviews 91, 77–92. https://doi.org/10.1016/j.earscirev.2008.10.001

Thematic Session 9
Sedimentology & palaeontology

Session Chairs:
Lars Holmer (lars.holmer@pal.uu.se)
Mikael Calner (mikael.calner@geol.lu.se)

Organic macromolecules and Ca-phosphate components in Cambrian small shelly fossils: characterization and diagenesis

Oluwatoosin B.A. Agbaje[a,b,c], Simon C. George[b], Zhifei Zhang[d], Glenn A. Brock[c,d], Lars E. Holmer[a,d]

[a]Department of Earth Sciences, Palaeobiology, Uppsala University, Uppsala, Sweden, toosin.agbaje@mq.edu.au, toosin91014@gmail.com; lars.holmer@pal.uu.se; [b]Department of Earth and Environmental Sciences, Macquarie University, Sydney, Australia, simon.george@mq.edu.au; [c]Department of Biological Sciences, Macquarie University, Sydney, Australia, glenn.brock@mq.edu.au; [d]State Key Laboratory of Continental Dynamics, Shaanxi Key Laboratory of Early Life & Environments, Department of Geology, Northwest University, Xi'an, China, elizf@nwu.edu.cn

Summary. There are few studies using the synchronous analysis of the organophosphatic small shelly fossils (SSFs), despite their potential importance for understanding the Cambrian explosion. The nature of organic biopolymers in the shells of many SSFs is still unknown. Here, shell matrices in SSFs within lower Cambrian carbonate strata across the Arrowie Basin in South Australia were characterized. The findings were compared with the SSFs from other localities in Europe. This work provides excellent potential for large-scale screening of fossilised organic remains in biominerals.

Thousands of small shelly fossils (SSFs) occur within lower Cambrian carbonate strata across the Arrowie Basin in South Australia (Larsson et al. 2014; Betts et al. 2016). However, there are few studies using the synchronous analysis of the organic-inorganic hybrid component of these organophosphatic biominerals, despite their potential importance for understanding the Cambrian explosion. The nature of organic biopolymers in the shells of many SSFs is still unknown. Here, sclerites from the tannuolinid tommotiid *Micrina etheridgei*, the camenellan tommotiid *Dailyatia macroptera*, and one of the oldest known brachiopods from East Gondwana, *Askepasma toddense*, have been studied using micro-Raman spectroscopy, Fourier transform infrared spectroscopy (FTIR), and field-emission-gun and Phenol XL desktop scanning electron microscopes. These SSF taxa are palaeontologically important since they represent basal lophotrochozoan marine invertebrates and, because they secrete diagenetically stable, well preserved and readily identifiable biominerals. This study reveals for the first time the inorganic-organic hybrid composite components of these organophosphatic samples. FTIR spectra show the characteristic infrared absorption peaks for the amide I and III moieties of collagen matrix and/or glycosaminoglycan, comparable to the organic components of recently-alive (modern) linguliform brachiopod shells. A ~1060 cm^{-1} peak from Raman spectra is assigned to proteoglycan, although the peak overlaps with the collagen matrix and components of phosphate groups. A Raman peak at ~1003 cm^{-1} is assigned to phenylalanine and thus overlaps with the HPO_4^{2-} ion. Energy disperse X-ray spectra show a sulphur peak, which is attributed to the presence of proteoglycan, which is glycosaminoglycan associated with a core protein. Shell matrices of the described assemblages are also compared with the SSFs from other localities in Europe such as Sweden, France, and Belgium. This work provides excellent potential for large-scale screening of fossilised organic remains that are important sources of biological and evolutionary information with long-term potential for phylogenetic exploration.

References

Betts, M.J., Paterson, J.R., Jago, J.B., Jacquet, S.M., Skovsted, C.B., Topper, T.P. & Brock, G.A., 2016: A new lower Cambrian shelly fossil biostratigraphy for South Australia. *Gondwana Research 36, 176-208*.

Larsson, C.M., Skovsted, C.B., Brock, G.A., Balthasar, U., Topper, T.P. & Holmer, L.E., 2014: *Paterimitra pyramidalis* from South Australia: scleritome, shell structure and evolution of a lower Cambrian stem group brachiopod. *Palaeontology 57(2), 417-446*.

Record of the end-Triassic mass extinction in shallow marine carbonates: the Lorüns section (Austria)

Linus Brakebusch, Sylvain Richoz

Department of Geology, Lund University, Lund, Sweden, linusaage@gmail.com

Summary. The End-Triassic mass extinction is one of the big five mass extinctions during the Phanerozoic, and is believed to be triggered by cataclysmic magmatic activity. Here, we investigate the Rhaetian/Hettangian shallow marine carbonate section of the Lorüns Quarry, Austria, with petrographic and geochemical analyses (trace elements, carbon isotope) to reconstruct palaeoenvironmental conditions. In order to determine if the climatic signal recorded at Lorüns is regional or global, the results are compared with time-equivalent shallow-water deposits from the Arab Emirates.

The Earth has experienced five known major mass extinctions during the Phanerozoic. The End-Triassic Extinction (ETE) (~201 Ma years ago; Korte et al. 2019) involved a series of climate and environmental changes as well as faunal extinction of both marine and terrestrial taxa (Todaro et al. 2018). As for now, the most likely cause for the ETE was the massive eruptions of the Central Atlantic Magmatic Province (CAMP), linked to the break-up of the Pangea supercontinent. As a consequence of the eruptions, large amounts of greenhouse gases were released into the atmosphere. If the ultimate cause is known, the chain of events leading to mass-extinction is still under debate. The most cited hypotheses are cooling, warming, strong regression, acidification of the ocean due to the increased CO_2 or poisoning through mercury or metallic ions (Hautmann 2012; Kaiho et al. 2022). Most of the well-known marine records are from deeper marine sediments. The strong regression eroded most of the shallow sections which are moreover difficult to date. The Lorüns section from the Austrian Alps is an exception.

This section covers the Late Triassic Kössen Formation, the “Schattwald beds” with the extinction level and the Triassic-Jurassic boundary interval, and the Early Jurassic “Lorüns oolite” (Felber et al. 2015). This allows investigations on both the time interval before, during and after the extinction. Oolites are also a peculiar window in the seawater chemistry during the aftermath of the extinction. Thirty-six thin sections were produced, spread out over the entire Lorüns section, for analysing the lithologies and their fossil content. The Kössen Formation at Lorüns is dominated by wackestone with a rich fossil diversity. The “Schattwald beds” show significant siliciclastic input, especially in the lower parts of the section, and shift into a coarsening-upward section going from mudstone to packstone. The “Lorüns Oolite” shows regular shifts between more ooid-dominated grainstone/packstone and oncoid-dominated packstone. All coated grains display a strong micritisation in the “Lorüns Oolite”.

Here, we will also show the results of LA-ICP-MS analyses on ooids and oncoids. This allows us to constrain the palaeoenvironmental conditions during their deposition. We will also show the carbon isotope geochemistry of the section, which we use to assess variations in the carbon cycle. Our results from Lorüns are compared with shallow water sections from the Arab Emirates, to evaluate if the climatic signal recorded at Lorüns was regional or global.

References

Felber, R., Weissert, H.J., Furrer, H. & Bontognali, T.R.R., 2015: The Triassic-Jurassic Boundary in the shallow-water marine carbonates from the western Northern Calcareous Alps (Austria). *Swiss Journal of Geosciences 108*, 213-224.

Hautmann, M., 2012: *Extinction: End-Triassic Mass extinction.* In: eLS. John Wiley & Sons, Ltd: Chichester, 1-10.

Kaiho, K., Tanaka, D., Richoz, S., Jones, D.S., Saito, R., Kameyama, D., Ikeda, M., Takahashi, S., Aftabuzzam, Md. & Fujibayashi, M., 2022: Volcanic temperature changes modulated volatile release and climate fluctuations at the end-Triassic mass extinction. *Earth and Planetary Science Letters 579*, 1-12.

Korte, C., Ruhl, M., Pálfy, J., Ullmann, C.V. & Hesselbo, S.P., 2019: Chemostratigraphy across the Triassic-Jurassic Boundary. In: *Chemostratigraphy Across Major Chronological Boundaries, Geophysical Monograph 240*, John Wiley & Sons, Inc., 185-210.

Todaro, S., Rigo, M., Randazzo, V. & Di Stefano, P., 2018: The end-Triassic mass extinction: A new correlation between extinction events and ^{13}C fluctuations from a Triassic-Jurassic peritidal succession in western Sicily. *Sedimentary Geology 368*, 105-113.

Evolution in real time: when fossils tell you what happened when

Graham E. Budd[a], Richard P. Mann[b]

[a]Department of Earth Sciences, Palaeobiology Programme, Uppsala University, Uppsala, Sweden, graham.budd@pal.uu.se; [b]School of Mathematics, University of Leeds, Leeds, UK, r.p.mann@leeds.ac.uk

Summary. Molecular clocks often greatly over-estimate the age of origins of groups relative to the fossil record. However, certain radiations can be quite well dated by the fossil record, and this allows to examine the reasons for the mismatch. One of the most important of these is the calibration to prior conversion when trees are node-calibrated. In addition, mass extinctions may also exert significant disturbing effects. We explore the implications of some of these problems, and point to ways in which the information from the fossil record could be better used in dating the origins of major clades.

Being able to estimate when major groups of organisms evolved is of supreme importance in macroevolutionary and geobiological studies. From an evolutionary perspective, such estimates can inform the tempo and mode of evolution; from a geological perspective, the interaction between environment and organisms. For example, the arrival of major clades in the fossil record can be correlated with a vast swathe of correlated geological changes (Davies et al. 2019), including secular shifts in sediment production rates, erosion, architecture of rivers and many geochemical changes. It is thus somewhat surprising to learn that the actual time of origin of many major clades is a highly controversial topic. During the Cambrian (c. 539–487 Ma), there was a vast proliferation of fossils from animal clades; as is the case for angiosperms in the Early Cretaceous (143–100.5 Ma), and in the Palaeogene (66–23 Ma) for birds and placental mammals. These are all classical examples of major evolutionary radiations or "explosions". Furthermore, at least some have been considered to map out the phylogeny of the group in question (Coiro et al. 2019; Budd & Mann 2020). However, on the basis of molecular clock analyses (Lee & Ho 2016), it has become routine to consider each of these events to be artefactual, and that each group is actually considerably older than its fossil record – sometimes by hundreds of millions of years. Two important examples are the analysis by Dos Reis et al. (2015) of the origin of bilaterians which placed them between 688–595 Ma, even though the oldest credible bilaterian evidence is from trace fossils younger than 560 Ma (Budd & Jensen 2000); and estimates of the origin of the crown-group placental mammals placed them at 77–83 Ma (Alvarez-Carretero et al. 2021), with the the oldest recognised fossils all being younger than the K/Pg boundary at 66 Ma. It is, furthermore, striking that molecular clock predictions are rarely, if ever, borne out by subsequent fossil discoveries; and their proponents thus argue that the gap can be explained by groups emerging and staying in isolated places for many millions of years, or that their earliest members were small, hard to preserve or of low diversity/abundance – the so-called "phylogenetic fuse" concept (Howard et al. 2022). We take a different approach here, using a combined statistical, palaeontological and developmental approach, in order to understand better: why clocks behave as they do; what our rational expectations of early fossil records should be; and what those records are actually like. In general, node calibrations of trees, one common method of generating age priors for Bayesian inference of molecular clocks, suffer from several important problems, notably the issue of conversion of the calibration to the prior; the behaviour of many closely-spaced nodes, and the disturbing influence of mass extinctions. In addition, close matching of the posterior estimates to those of the priors suggests that the actual "molecular" part of molecular clocks is not in general strongly influencing the results. As a result, we argue that the evidence from the fossil record should not be overturned by molecular clock results without very careful examination of how the molecular clock posterior estimates emerge. In addition, we will look forward to more realistic modelling of the early fossil record of clades, with the view to creating more empirical calibrations of the origins of major groups.

References

Álvarez-Carretero, S., Tamuri, A.U., Battini, M., Nascimento, F.F., Carlisle, E., Asher, R.J., Yang, Z., Donoghue, P.C.J. & dos Reis, R., 2022: A species-level timeline of mammal evolution integrating phylogenomic data.
Nature 602, 263–267.
Budd, G.E. & Jensen, S., 2000: A critical reappraisal of the fossil record of the bilaterian phyla. *Biological Reviews 75*, 253–295.
Budd, G.E. & Mann, R.P., 2020: Survival and selection biases in early animal evolution and a source of systematic overestimation in molecular clocks. *Interface Focus 10, 20190110*.
Coiro, M., Doyle, J.A. & Hilton, J., 2019: How deep is the conflict between molecular and fossil evidence on the age of angiosperms? *New Phytologist 223*, 83–99.
Davies, N., Shillito, A., Slater, B., Liu, A. & McMahon, W., 2020: Evolutionary synchrony of Earth's biosphere and sedimentary-stratigraphic record. *Earth Science Reviews 201*, 102979.
Dos Reis, M., Thawornwattana, Y., Angelis, K., Telford, M.J., Donoghue, P.C.J. & Yang, Z., 2015: Uncertainty in the Timing of Origin of Animals and the Limits of Precision in Molecular Timescales. *Current Biology 25*, 2939–2950.
Howard, R.J., Giacomelli, M., Lozano-Fernandez, J., Edgecombe, G.D., Fleming, J.F., Kristensen, R.M., Ma, X., Olesen, J., Sorensen, M.V., Thomsen, P.F..Wills, M.A., Donoghue, P.C.J. & Pisani, D., 2022: The Ediacaran origin of Ecdysozoa; integrating fossil and phylogenomic data. *Journal of the Geological Society of London* 10.1144/jgs2021–107.
Lee, M.S.Y. & Ho, S.Y.W., 2016: Molecular Clocks. *Current Biology 26*, R399-402.

Recent advances in the Cambrian Series 2 of Antarctica: Palaeontological Systematics and Stratigraphy

Thomas M. Claybourn[a], Marrissa J. Betts[b], Lars E. Holmer[c], Christian B. Skovsted[d], Glenn A. Brock[a]

[a]Department of Biological Sciences, Macquarie University, Sydney, Australia, claybourntom@icloud.com, glenn.brock@mq.edu.au; [b]School of Environmental and Rural Science, University of New England, Armidale, Australia, marissa.betts@une.edu.au; [c]Department of Earth Sciences, Palaeobiology, Uppsala University, Uppsala, Sweden, lars.holmer@pal.uu.se; [d]Department of Palaeobiology, Swedish Museum of Natural History, Stockholm, Sweden, christian.skovsted@nrm.se.

Summary. Recently collected material from the Holyoake Range and Churchill Mountains of the Transantarctic Mountains of East Antarctica has yielded a diverse assemblage of fossils from rocks of the Byrd Group, allowing for the fossiliferous Shackleton Limestone and Holyoake Formation to be dated to the Cambrian Series 2, Stages 3–4 based on bio- and chemostratigraphic data. Correlation was aided by the better-constrained biostratigraphy of South Australia, which was conjoined to East Antarctica as part of East Gondwana in the Cambrian Period.

Recently collected rocks from the Transantarctic Mountains (Holyoake Range and Churchill mountains) were sampled for fossils and stable carbon isotopes. These collections were made to bio- and chemostratigraphically constrain the age of the sedimentary Byrd Group of rocks which had previously been recognised as 'lower Cambrian'. Study of the regional stratigraphy of the Cambrian Terrenuevian Series and Series 2 has been key in recent times in order to try to solve the issues with the remaining unnamed stratigraphic division of the Cambrian Period. The key units for dating the Byrd Group are the fossil-bearing Shackleton Limestone and the Holyoake Formation. The Shackleton Limestone consists of lower units of sandstone and limestone whereas the fossiliferous upper beds include well-developed archaeocyath-cyanobacterial bioherms. The uppermost bioherms and overlying Holyoake Formation contained the bulk of fossil material recovered. The Holyoake formation is a deeper-water formation that represents a marine transgression of the shallow-water bioherms of the Shackleton Limestone (Squire & Wilson, 2005).

The history of geology and palaeontology in Antarctica has been sporadic, advancing at times of interest in Antarctic exploration during much of the 20th century. The late 20th and 21st centuries saw a greater focus on scientific research in Antarctica, including an international effort including researchers from Uppsala University and The Natural History Museum in Sweden and Macquarie University in Australia in the Austral summer of 2010–11.

Systematics

Phosphatic fossil material was acid-etched from the carbonates of the Shackleton Limestone and Holyoake Formation, revealing a diverse assemblage of fossils, including brachiopods, molluscs, tommotiids, hyoliths, sponges, chancelloriids, bradoriids and other Cambrian problematica. Of these the brachiopods, molluscs and tommotiids were selected for further systematic treatment (Claybourn et al., 2019, 2020, 2021). The molluscan fauna recovered were of phosphatic steinkern (internal moulds) material almost entirely from a highly phospahtised horizon between the Shackleton Limestone and the overlying Holyoake Formation. This window yielded 12 mollusc that were described (Claybourn et al., 2019). Of these 12 only three: *Pojetaia runnegari*, *Davidonia rostrata* and *Xinjispira simplex* had sufficient morphological details to only be assigned to species, hindering biostratigraphic correlation. Other material included indeterminate members of genera: *Davidonia*, *Stenotheca*, *Yochelsionella, Anabarella*, *Anuliconus*, *Xianfengella* and *Pelagiella*. The brachiopod fauna consisted of material that is either primarily phosphatic or replaced, conserving many more morphological features allowing for better constrained taxonomy including the species: *Eohadrotreta zhenbaensis*, *Cordatia erinae, Schizopholis yorkensis* and *Plicarmus wildi* from the Shackleton Limestone and *Schizopholis yorkensis* from the Holyoake Formation (Claybourn et al., 2020). Other specimens recovered include *Eodicellomus* sp. and *Eoobolus* sp. The camenellan tommotiids from the collected sections were less abundant than hoped (Claybourn et al., 2021) as tommotiids have been used recently to advance a biozonal scheme for the palaeobiogeographically related province of South Australia (Betts et al., 2016, 2017). The sparce new material was studied alongside material collected from a previous expedition (Evans and Rowell, 1990), which also included material from the Shackleton Limestone of the Churchill Mountains, Holyoake Range and the poorly understood Schneider Hills limestone of the Argentina Range. Material studied from the Shackleton Limestone yielded fossils of the genus *Dailyatia,* including *D. decobruta*, *D. braddocki* and *D.* cf. *odyssei,* as well as fragments of the problematic tommotiid *Shetlandia multiplicata* and an indeterminate kennardiid. From the material from the Schneider Hills limestone a new species, *Dailyatia icari* was described.

Stratigraphy

The newly described fossil material was used to correlate and constrain the biostratigraphy of the Byrd Group. Fossil molluscs of the lower Cambrian have historically been hard to correlate due to their long stratigraphic records, but some correlation between molluscs of the Shackleton Limestone to the fossil biozones established for the lower Cambrian of South Australia, including the *Dailyatia odyssei* small shelly fossil Zone and the *Pararaia janeae* trilobite Zone. Many of the mollusc fossils range also into the lower Terreneuvian, Stage 2 strata of South Australia. The brachiopods proved a more useful point of comparison, the species *E. zhenbaensis* also found in Series 2 Stages 3–4 rocks of South China, the genus occurring in Cambrian Series 2 rocks around Gondwana. *Cordatia erinae* is also known only from the upper part of the *Dailyatia odyssei* Zone and *Pararaia janae* Zone of South Australia (Betts et al., 2017, 2018, 2019)

Chemostratigraphic data was also collected, and a sharp positive $\delta^{13}C$ excursion that is present in a section in the Churchill Mountains (section CM2) can be correlated to the global positive Cambrian Arthropod Radiation Excursion (CARE). A negative $\delta^{13}C$ excursion is also present at the base of the HRA section, which is interpreted to correlate to negative $\delta^{13}C$ excursion after the CARE positive excursion. The remaining HRA section has $\delta^{13}C$ values that trend positive, similar to those found globally after the CARE and before the Mingxinsi Carbon Isotope Excursion (MICE).

References

Betts, M.J., Paterson, J.R., Jago, J.B., Jacquet, S.M., Skovsted, C.B., Topper, T.P. & Brock, G.A., 2016: A new lower Cambrian shelly fossil biostratigraphy for South Australia. *Gondwana Research 36*, 176-208.

Betts, M.J., Paterson, J.R., Jago, J.B., Jacquet, S.M., Skovsted, C.B., Topper, T.P. & Brock, G.A., 2017: Global correlation of the early Cambrian of South Australia: Shelly fauna of the Dailyatia odyssei Zone. *Gondwana Research 36,* 240–279.

Betts, M.J., Paterson, J.R., Jacquet, S.M., Andrew, A.S., Hall, P.A., Jago, J.B., Jagodzinski, E.A., Preiss, W.V., Crowley, J.L., Brougham, T. & Mathewson, C.P., 2018: Early Cambrian chronostratigraphy and geochronology of South Australia. *Earth-Science Reviews 185*, 498-543.

Claybourn, T.M., Jacquet, S.M., Skovsted, C.B., Topper, T.P., Holmer, L.E. & Brock, G.A., 2019: Mollusks from the upper Shackleton Limestone (Cambrian Series 2), Central Transantarctic Mountains, East Antarctica. *Journal of Paleontology 93*, 437-459.

Claybourn, T.M., Skovsted, C.B., Holmer, L.E., Pan, B., Myrow, P.M., Topper, T.P. & Brock, G.A., 2020: Brachiopods from the Byrd Group (Cambrian Series 2, Stage 4) Central Transantarctic Mountains, East Antarctica: Biostratigraphy, phylogeny and systematics. *Papers in Palaeontology 6*, 349–383.

Claybourn, T., Skovsted, C., Betts, M.J., Holmer, L.E., Bassett-Butt, L. & Brock, G.A., 2021: Camenellan tommotiids from the Cambrian Series 2 of East Antarctica: Biostratigraphy, palaeobiogeography, and systematics. *Acta Palaeontologica Polonica 66*, 207–229.

Evans, K.R. & Rowell, A.J., 1990: Small Shelly Fossils from Antarctica: An Early Cambrian Faunal Connection with Australia. *Journal of Paleontology 64*, 692–700.

Squire, R.J. & Wilson, C.J.L., 2005: Interaction between collisional orogenesis and convergent margin processes: evolution of the Cambrian proto-Pacific margin of East Gondwana. *Journal of the Geological Society 162*, 749–761.

The phylogeny and ecological diversification of early Cambrian hyoliths from South China

Fan Liu[a], Christian B. Skovsted[a,b], Timothy P. Topper[a,b], Zhifei Zhang[a]

[a]State Key Laboratory of Continental Dynamics, Shaanxi Key Laboratory of Early Life and Environments and Department of Geology, Northwest University, Xi'an 710069, China; e-mail:liufan@nwu.edu.cn, elizf@nwu.edu.cn;
[b]Department of Palaeobiology, Swedish Museum of Natural History, Box 50007, SE-104 05 Stockholm, Sweden; e-mail: Christian.Skovsted@nrm.se, timothy.topper@nrm.se

Summary. Hyolitha, is an extinct invertebrate group from the early Cambrian to the end of Permian. As one of the most dominant benthic animals in the Cambrian explosion, Hyoliths are enigmatic marine animals with a lot of controversy on biological affinity, life mode, etc. Recently, new evidence is mainly from the early Cambrian Konservat Lagerstätten of South China to reveal the phylogeny and ecological diversification of hyoliths.

For the shell, the new hyoliths family Paramicrocornidae showing a hyolithid morphology but lacking the helens (Liu et al., in press), was assigned as the intermediate stage in the evolution between Orthothecida and Hyolithida. It indicated the development of helens (Skovsted et al., 2020) and the evolutionary pattern of hyoliths shell structures. From the perspective of anatomy, old orthothecid *Triplicatella* preserved a fan-shaped feeding apparatus with the spiral-loop folded gut, as a benthic deposit feeder (Liu et al., 2020, 2021a). On the contrary, the later hyolithid preserved elongate tentacles, U-shaped gut, and helens as the filter feeders (Moysiuk et al., 2017; Liu et al., 2021b).

Based on the information on skeleton morphology and anatomy, the phylogenetic tree was built to reveal a presumptive evolutionary model of hyoliths (Liu et al., in press). The hyoliths are derived from orthothecid ancestors, and the evolutionary polarity from simple to complex on skeletons shows the development of inner structures on the opercula (Li et al., 2020), followed by the evolution of hyolithid with helens. The feeding habits are reflected in the different morphology of hyoliths that orthothecids as deposit feeders (Liu et al., 2020), the Paramicrocornidae was considered with the detritus feeding habit (Sun et al., 2018), and the typical hyolithids supported by helens using the filter-feeding strategy (Moysiuk et al., 2017; Liu et al., 2021b). Thus, the life habit of hyolith evolution show the change from active deposit-feeding to passive suspension/filter feeding.

References

Li, L.Y., Skovsted, C. B., Yun, H., Betts, M. J., & Zhang, X. 2020: New insight into the soft anatomy and shell microstructures of early Cambrian orthothecids (Hyolitha). *Proceedings of the Royal Society B 287(1933)*, 20201467.

Liu, F., Skovsted, C. B., Topper, T. P., Zhang, Z., & Shu, D. 2020: Are hyoliths Palaeozoic lophophorates?. *National Science Review 7(2)*, 453-469.

Liu, F., Skovsted, C. B., Topper, T. P., & Zhang, Z. 2021a: Revision of Triplicatella (Orthothecida, Hyolitha) with preserved digestive tracts from the early Cambrian Chengjiang Lagerstätte, South China. *Historical Biology 33(9)*, 1857-1871.

Liu, F., Skovsted, C. B., Topper, T. P., & Zhang, Z. 2021b: Soft part preservation in hyolithids from the lower Cambrian (Stage 4) Guanshan Biota of South China and its implications. *Palaeogeography, Palaeoclimatology, Palaeoecology*, *562*, 110079.

Liu, F., Skovsted, C. B., Topper, T. P., & Zhang, Z. Hyolithid-like hyoliths without helens from the early Cambrian of South China, and their implications for the evolution of hyoliths. *In press*

Moysiuk, J., Smith, M. R., & Caron, J. B. 2017: Hyoliths are Palaeozoic lophophorates. *Nature 541*(7637), 394-397.

Skovsted, C. B., Mus, M. M., Zhang, Z., Pan, B., Li, L., Liu, F., ... & Zhang, Z. 2020: On the origin of hyolith helens. *Palaeogeography, Palaeoclimatology, Palaeoecology 555*, 109848.

Sun, H. J., Zhao, F. C., Wen, R. Q., Zeng, H., & Peng, J. 2018: Feeding strategy and locomotion of Cambrian hyolithides. *Palaeoworld 27*(3), 334-342.

The Hirnantian Stage and the Hirnantian Isotope Carbon Excursion (HICE) in the Gotland (Sweden) subsurface

Niklas Gunnarsson[a], Mikael Calner[b], Rongchang Wu[c], Christian M.Ø. Rasmussen[d], Oliver Lehnert[e], Mikael Erlström[f], Peter Dahlqvist[g]

[a]Department of Geology, Lund University, Lund, Sweden, ni0112gu-s@student.lu.se; [b]Department of Geology, Lund University, Lund, Sweden, mikael.calner@geol.lu.se; [c]Nanjing Institute of Geology and Palaeontology, Chinese Academy of Sciences, Nanjing, China, rcwu@nigpas.ac.cn; [d]Globe Institute, University of Copenhagen, c.macorum@sund.ku.dk, [e]GeoZentrum Nordbayern, Friedrich-Alexander University Erlangen-Nurnberg, Erlangen, Germany, oliver.lehnert@fau.de; [f]Geological Survey of Sweden, Lund, Sweden, mikael.erlstrom@sgu.se; [g]Geological Survey of Sweden, Lund, Sweden, peter.dahlqvist@sgu.se

Summary. We provide a stratigraphic assessment of the Upper Ordovician through lowermost Silurian of the Stora Sutarve drillcore from southernmost Gotland. Based on the combined information from lithological characteristics and carbon isotope chemostratigraphy we document a sedimentary succession tentatively ranging from the Kinnekulle K-bentonite near the Sandbian-Katian stage boundary to the earliest Silurian Motala Formation. Of particular importance is the identification of the Hirnantian Isotope Carbon Excursion (HICE) that relates to the latest Ordovician glaciation and associated mass extinction.

The Hirnantian of the Stora Sutarve core

The Stora Sutarve drillcore was drilled near Hamra on southernmost Gotland (coordinates Sweref 99 N 6320673 E 699981) by the Geological Survey of Sweden in 2018. Coring was stopped at 564.95 m below the surface in the Cambrian Faludden Sandstone and the core thus includes the entire Ordovician and most of the Silurian succession of the Baltoscandian Basin.

In this project we study the environmental changes across the Ordovician-Silurian transition, including the end-Ordovician glaciation and the Late Ordovician Mass Extinction (LOME). Key for identification of this interval is identification of the Hirnantian Isotope Carbon Excursion (HICE). This anomaly is known from many tens of localities globally and represents an exceptional geochemichal marker for correlations of even thin packages of sedimentary strata between regions and continents. In the Stora Sutarve core the HICE is associated with the 2-m-thick Loka Formation; that is, similar to the situation in the south-central Swedish mainland (e.g. Bergström et al., 2011, 2012), which is developed as a partly laminated grainstone with abundant lithoclasts and sparse ooids, clearly signalling a substantial shallowing of the depositional environment. The ideal tripartite signature of HICE with a rising limb of increasing $\delta^{13}C_{carb}$ values, a peak and plateau, and a falling limb back to baseline values is not fully preserved: Our analysis reveals stable $\delta^{13}C_{carb}$ baseline values near 1‰ in the uppermost Jonstorp Formation. They start to rise closely below the base of the Loka Formation, with the most rapid rate of increase in the basal Loka Formation, and reach peak values of 3.5‰ still in its lower half. This is followed by a plateau in the upper half of the Loka Formation, with $\delta^{13}C_{carb}$ values mostly around 2.5‰, and a subsequent abrupt change back to baseline values at the top of the Loka Formation. This abrupt change in $\delta^{13}C_{carb}$ is also associated with an unconformity in the core. A preliminary study of the brachiopod fauna associated with the succession supports a Hirnantian age and further provides palaeoecological insights into the deposistional environment. The most dominant taxa include specimens of *Hindella*? sp. and *Brevilamnulella*? sp., both occuring abundantly in coquinas. Previous studies of Baltoscandian Hirnantian sequences suggest that coquinas of *Hindella* tend to predate those of *Brevilamnulella* with the latter being constrained to the uppermost Hirnantian (Kröger et al., 2015; Calner et al., 2021). This is not corroborated by the current study, which finds *Brevilamnulella*? sp. roughly 30 cm into the Hirnantian sequence – just above an initial, conspicuously laminated facies, whereafter it occurs repeatedly and interchangably with *Hindella*? sp. The coquinas suggest storm-influenced deposition at ~60–67 cm above the base of the Hirnantian, which was abrubtly interrupted by much more calm conditions indicated by large strophomenoid brachiopods, adapted to a muddier facies. Towards the top of the succession the storm-related coquinas reappear.

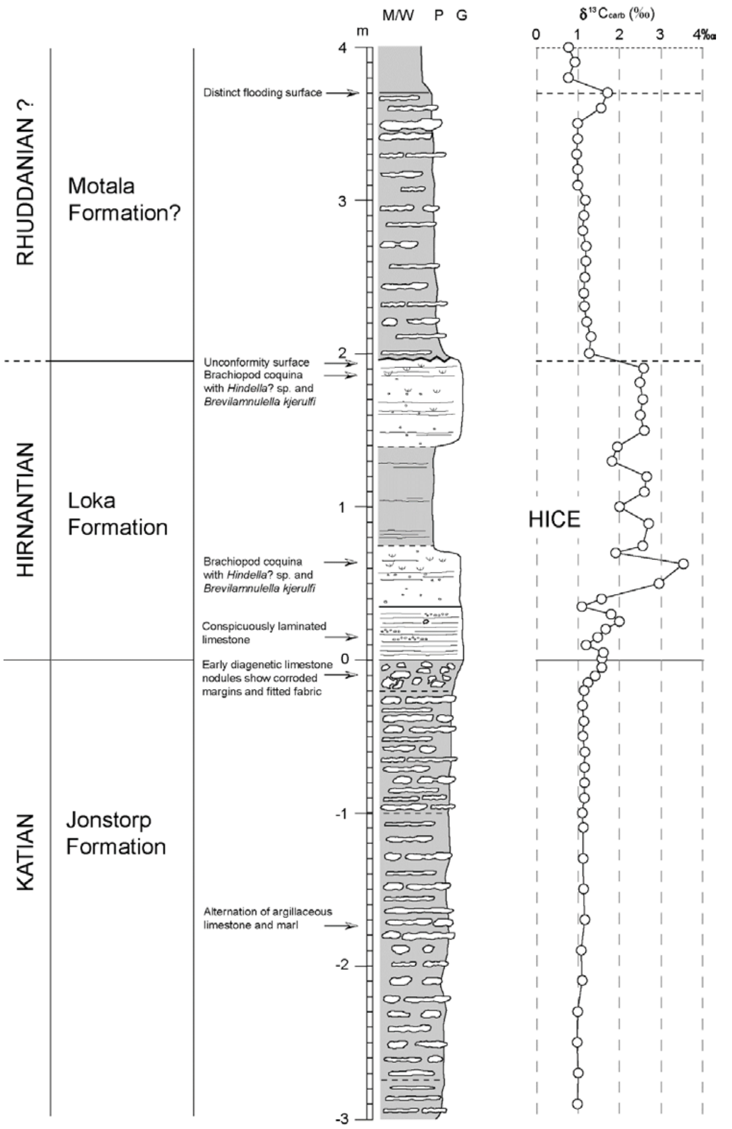

Fig. Log profile of the Ordovician-Silurian transition, including the Hirnantian Stage and HICE, in the Stora Sutarve core. Note the change from argillaceous limestone-marl alternations of the Jonstorp Formation to laminated, predominantly bioclastic limestone with abundant brachiopods in the Loka Formation. Also note the unconformity on top of the Loka Formation and transition into more argillaceous strata. The low and stable carbon isotope values of the upper part suggest a Silurian age and we tentatively assign these strata to the Motala Formation, pending more data.

References

Bergström, S., Calner, M., Lehnert, O. & Noor, A., 2011: A new upper Middle Ordovician–Lower Silurian drillcore standard succession from Borenshult in Östergötland, southern Sweden: 1. Stratigraphical review with regional comparisons. *GFF 133*, 149 - 171.

Bergström, S.M., Lehnert, O., Calner, M. & Joachimski, M., 2012: A new Upper Ordovician-Lower Silurian drillcore standard succession from Borenshult in Östergötland, southern Sweden: 2. Significance of $\delta^{13}C$ chemostratigraphy. *GFF 134*, 39-63.

Calner M., Bockelie, J.F., Rasmussen, C.M.Ø., Calner, H., Lehnert, O. & Joachimski, M.M., 2021: Carbon isotope chemostratigraphy and sea-level history of the Hirnantian Stage (uppermost Ordovician) in the Oslo–Asker district, Norway. *Geological Magazine 158*, 1977-2008.

Kröger, B., Ebbestad, J.O.R., Lehnert, O., Ullman, C.V., Korte, C., Frei, R., Rasmussen, C.M.Ø., 2015: Subaerial speleothems and deep karst in central Sweden linked to Hirnantian glaciations. *Journal of the Geological Society (London) 172*, 349-356.

Life habits of Ordovician infaunal lingulids – A Baltic perspective

Lars E. Holmer[a], Zhifei Zhang[b], Yue Liang[b]

[a]Department of Earth Sciences, Palaeobiology, Uppsala University, Uppsala, Sweden, lars.holmer@pal.uu.se;
[b]Shaanxi Key laboratory of Early Life and Environments, State Key Laboratory of Continental Dynamics and Department of Geology, Northwest University, Xi'an, China, elizf@nwu.edu.cn

Summary. In the Ordovician of Estonia infaunal lingulids are not uncommonly preserved in assumed vertical life positions, some of which are within deep vase-shaped trace fossils from the Uhaku and Vormsi stage. Well-documented records of lingulid brachiopods preserved in life position have previously been described from Ordovician and younger deposits, but the Estonian records are the first known in situ occurrence of lingulids from within Ordovician vase-shaped trace fossils. The lingulids probably settled within an existing trace.

Life habits of living and fossil lingulids

It has been commonly assumed that almost all fossil lingulids had an active infaunal burrowing life habit more or less identical to that of their living representatives (e.g. Yuagan et al. 1993). However, new detailed studies of the exceptionally preserved epifaunal lingulids in the early Cambrian Chengjiang and middle Cambrian Burgess Shale have brought this interpretation into question; soft-tissue morphology of lingulids suggest that all known linguliform brachiopods in Chengjiang and Burgess Shale had epifaunal lifestyles (e.g. Stolk et al. 2010; Wang et al. 2014).

The U-shaped burrows of living lingulids is produced "shell-down", with the pedicle trailing behind the shell, and this mode of life has been documented as far back as the Triassic (Zonneveld & Pemberton 2003); however, Savazzi (1986) pointed out that the orientation sculptures of many Palaeozoic lingulids indicate a burrowing process with the pedicle oriented downward in the sediment, with the shell trailing behind.

Life habits of lingulids in the Ordovician of Estonia

Lingulids (assigned to *Pseudolingula* in a wide sense) occur in assumed vertical life positions in the carbonate rocks of Uhaku and Vormsi stages. The lingulids occur within systems of deep vase-shaped trace fossils, broadly similar to *Gastrochaenolites*.

The *Gastrochaenolites*-like trace fossils from the Uhaku Stage are strongly phosphatized, whereas the Vormsi Stage traces are less well defined. Well-documented records of lingulid brachiopods preserved in life position have previously been described from Ordovician and younger deposits, but these are the first known in situ occurrence of lingulids from within *Gastrochaenolites*-like trace fossils.

There is no evidence indicating that the lingulids were responsible for producing the vase-shaped trace fossil, and they most likely settled within an existing trace, produced by another organism. If active burrowing was at all involved, it was most likely performed with the pedicle oriented downward (see Savazzi 1986) into the soft sediment filling the pre-existing depressions.

Lingulids preserved inside pre-existing organic borings have previously only been documented from the Late Ordovician and Silurian, where they occur within *Trypanites*-like borings occurring within tabulate corals and stromatoporoids (e.g. Tapanila & Holmer 2006).

References

Savazzi, E., 1986: Burrowing sculptures and life habits in Paleozoic lingulacean brachiopods. *Paleobiology 12*, 46-63.

Stolk, S.P., Holmer, L.E. & Caron, J.B., 2010: First record of the brachiopod *Lingulella waptaensis* with pedicle from the Middle Cambrian Burgess Shale. *Acta Zoologica 91*, 150–162.

Tapanila, L. & Holmer, L.E., 2006: Endosymbiosis in Ordovician-Silurian Corals and Stromatoporoids: A New Lingulid and Its Trace from Eastern Canada. *Journal of Paleontology 80*, 50-759.

Wang, H., Zhang, Z. & Holmer, L.E., 2014: Oldest glosselline linguliform brachiopod with soft parts from the Lower Cambrian of Yunnan, Southern China. *GFF 136*, 539-547

Yugan, J., Xianguang, H. & Huayu, W., 1993: Lower Cambrian Pediculate Lingulids from Yunnan, China. *Journal of Paleontology 67*, 788-798.

Zonneveld, J.-P. & Pemberton, S.G., 2003: Ichnotaxonomy and Behavioral Implications of Lingulide-Derived Trace Fossils from the Lower and Middle Triassic of Western Canada. *Ichnos 10*, 25-39.

Distinguishing borings and burrows in intraclasts: evidence from the Cambrian (Furongian) of North China

Yazhou Hu[a], Yue Liang[a,b], Zhifei Zhang[a]

[a]State Key Laboratory of Continental Dynamics, Shaanxi Key laboratory of Early Life & Environments, Department of Geology, Northwest University, Xi'an, PR China, elizf@nwe.edu.cn; huyz_nwu@163.com; yueliang_nwu@outlook.com; [b]Department of Earth Sciences, Palaeobiology, Uppsala University, Uppsala, Sweden

Hardgrounds represent synsedimentary cemented stratigraphic beds that form at or near the seafloor. They are concentrated at particular intervals in the geological record, and their presence has been closely linked to key climatic and evolutionary events. Borings represent a key line of evidence for investigations of hardground development and record the development of bioerosion. The unequivocal identification of borings is done through identification of crosscutting relationship between the proposed boring and a hard substrate, such as lithoclasts and/or shells, whereas morphological criteria can be used when dealing with a homogeneous substrate, such as micritic hardgrounds. Bioeroded hardgrounds and burrow with micrite halo are subject to fracturing and reworking, resulting in flat-pebble conglomerates (FPC) with accumulations of intraclasts, in which the recognition of borings and burrows with halo can be challenging. Using trace fossils from FPC and preserved *in-situ* in late Cambrian carbonates of North China, we establish a set of criteria for distinguishing borings from burrows in FPC. Features such as relative size, number of trace fossils per intraclast, cross-cutting relationship with the hosting pebble, and pyrite or glauconite encrustation can all be invoked to aid recognition of borings. Reworked burrows (i.e. ichnoclasts) occurring in FPC vary in abundance, making up 5.79~52.23% of the total volume of the pebbles or clasts in this study and the value vary from 5.68~70.70% (mean value = 32.43%) when some other burrows with halo from other researches are included. But Borings making up of 2.15~6.38% of the whole pebble or clast and the value is 0.05~17.88% (with mean value = 3.06%) when borings from later deposits are counted. Student's t-test show significant difference between the relative volume of burrows and borings in the pebble. Number of boring per clast or pebble ranges from 2~10 but most pebbles with burrows are only occupied by one burrow that is also with significant difference. Trace fossils that penetrate pyrite or glauconite encrustation are assigned to borings but trace fossils encrustated by pyrite or glauconite encrustation maybe not borings. Our results suggest caution is necessary, particularly as synsedimentary deformation of burrows common in late Cambrian FPC can create structures that resemble borings.

Seals, whales, and the Cenozoic decline of nautiloid cephalopods

Steffen Kiel[a], James L. Goedert[b], Cheng-Hsiu Tsai[c,d]

[a]Swedish Museum of Natural History, Department of Paleobiology, Stockholm, Sweden, steffen.kiel@nrm.se; [b]Burke Museum of Natural History and Culture, University of Washington, Seattle, Washington, USA, jamesgoedert@outlook.com; [c]Department of Life Science and Institute of Ecology and Evolutionary Biology, National Taiwan University, and [d]Museum of Zoology, National Taiwan University, Taipei, Taiwan, whaletsai@ntu.edu.tw.

Summary. We hypothesize that the present-day restriction of the iconic 'Living Fossil' Nautilus to the deep Indo-West Pacific Ocean is predator-driven. The radiation of pinnipeds (seals and walruses) from the Oligocene onward resulted in the local extinction of nautiloids in areas where pinnipeds appeared, eventually restricting nautilids to the deep-water refuge they inhabit today.

Results and interpretations

Nautiloid and pinnipeds have non-overlapping distributions in the present-day ocean (Figure 1). The Cenozoic distribution patterns of pinnipeds and nautilids from the Oligocene onward show the local extinction of nautiloids in the areas where pinnipeds appeared, eventually resulting in the present-day restriction of *Nautilus* and *Allonautilus* to the central Indo-West Pacific Ocean. In addition, the development of oxygen minimum zones (OMZs) due to enhanced ocean circulation in the Oligocene prevented nautiloids to escape predation by retreating to deeper waters, resulting in their disappearance especially from the west coast of the Americas. The demise of the nautiloid *Aturia* due to predation pressure was less immediate, probably because it avoided predation by fast swimming rather than retreating to greater depths. Ultimately, however, this might have resulted in *Aturia*'s end-Miocene extinction, because its adaptations to fast swimming prevented it from retreating to depths that allowed *Nautilus* to escape the ever-increasing predation pressure.

A major role of odontocetes in the demise of nautiloids is not apparent, except for a few brevirostrine Oligocene taxa from the North American Atlantic and Pacific coasts, which appeared in these areas at the same time as nautilids disappeared. The appearance of toothed mysticetes coincides with the local extinction of nautilids only in areas where brevirostrine odontocetes have been found; in the other areas it coincides with a notable size decrease among nautilids.

Our study emphasizes the prominent role of nektonic vertebrates in the evolution of cephalopods. A potential implication of our observations is that the broader disparity of cranial morphologies among early odontocetes and toothed mysticetes might have resulted from niche partitioning that exploited a broader diversity of prey, including those nautiloids that during Eocene and Oligocene times still inhabited a broader range of habitats than living *Nautilus*.

Figure 1. Present-day distribution of nautiloids (red) and pinnipeds (blue).

Brachiopods from the Latham Shale Lagerstätte (Cambrian Series 2, Stage 4) and Cadiz Formation (Miaolingian, Wuliuan), California

Yue Liang[a,b], Lars E. Holmer[a,b], Xiaolin Duan[a], Zhifei Zhang[a]

[a]State Key Laboratory of Continental Dynamics, Shaanxi Key laboratory of Early Life & Environments, Department of Geology, Northwest University, Xi'an, 710069, P. R. China; [b]Department of Earth Sciences, Paleobiology, Uppsala University, Uppsala, Sweden

A moderately diverse assemblage of brachiopods from the Latham Shale Lagerstätte (Cambrian Series 2, upper Stage 4) and the upper Cadiz Formation (Miaolingian, Wuliuan), California, is described in detail for the first time. The fauna includes both linguliform (*Hadrotreta primaea*, *Paterina prospectensis*, *Dictyonina pannula* and *Mickwitzia occidens*) and rhynchonelliform (*Nisusia fulleri* and *Wimanella highlandensis*) brachiopods, together with olenellid trilobite and hyolithids. The Latham Shale differs from other Cambrian Konservat-Lagerstätten (notably Cambrian Series 2 Chengjiang and Guanshan Lagerstätte, eastern Yunnan), in that the brachiopod shell valves in many cases are still preserved with their original mineralization. Moreover, the excellently preserved shale-hosted valves even include cases with exquisitely preserved epithelial cell moulds, otherwise only seen in acid-etched material from carbonate rocks. The pitted ornamentation in the paterinate *Dictyonina pannula* closely resembles those described from Ordovician linguliforms. The unusual preservation of *Nisusia fulleri* provides important clues for ancestral composition of the brachiopod shell. The two articulated rhynchonelliform species probably represent the oldest records of this group from the west Laurentia. The fauna may also represent the earliest onset of the Palaeozoic Evolutionary Fauna mostly consisting of rhynchonelliform and linguliform brachiopods in west Laurentia.

References

Liang, Y., Holmer, L.E., Hu, Y.Z., & Zhang, Z. F., 2020a, First report of brachiopods with soft parts from the Lower Cambrian Latham Shale (series 2, stage 4), California. *Science Bulletin 65*, p. 1505–1586.

Liang, Y., Holmer, L.E., Skovsted, C.B., Duan, X.L., & Zhang, Z.F., 2020b, Shell structure, ornamentation and affinity of the problematic early Cambrian brachiopod *Heliomedusa orienta*. *Lethaia 53*, p. 574–587.

Morphological evolution and ecological exaptation of the "living fossil" lingulid brachiopods across mass extinctions

Yue Liang[a,b], Luke C. Strotz[a], Timothy P. Topper[a], Lars E. Holmer[a,b], Yanlong Chen[a], Ruisen Fang[a], Yazhou Hu[a], Zhifei Zhang[a]

[a]State Key Laboratory of Continental Dynamics, Shaanxi Key laboratory of Early Life & Environments, Department of Geology, Northwest University, Xi'an, P.R. China; [b]Department of Earth Sciences, Paleobiology, Uppsala University, Uppsala, Sweden

Morphology usually serves as an effective proxy for functional ecology, and evaluating morphological, anatomical and ecological changes, permits a deeper understanding of the nature of diversification and macroevolution. Lingulid (Order Lingulida) brachiopods are diverse and abundant during the early Palaeozoic, but decrease in diversity over time, with only a few genera of linguloids and discinoids present in modern marine ecosystems. The dynamics that drove this decline remain uncertain and it has not been determined if there is an associated impact on morphological and ecological diversity. Here we apply geometric morphometrics to reconstruct global morphospace occupation for lingulid brachiopods through the Phanerozoic, with results showing that almost all of the total morphospace was occupied by the Early Ordovician. At this time of peak diversity, linguloids with sub-rectangular shell shape possessed all the evolutionary features necessary for an infaunal lifestyle, as evidenced by the rearrangement of mantle canals and the reduction of pseudointerarea, but infaunal forms remained rare. The end Ordovician mass extinction has a differential effect on linguloids, disproportionally wiping out those forms with a rounded shell shape. Forms with sub-rectangular shells survived both the end Ordovician mass extinction and the Permian-Triassic mass extinction leaving a fauna predominantly composed of infaunal forms.

Applying fossil herbivores ecometrics to reconstruct Neogene ecoregions in East Asia

Liping Liu

Department of Paleobiology, Swedish Natural History Museum, Stockholm, Sweden, e-mail: liping.liu@nrm.se; and Department of Geoscience, University of Helsinki, Helsinki, Finland, e-mail: liping.liu@helsinki.fi

Summary. We apply a data mining method called redescription to analyze Neogene ecoregions in East Asia via mammal fossil dental traits (ecometrics). The redescription method had been tested by modern data and successfully captured the most prominent modern ecoregions in East Asia, one of the most zoogeographic complex regions in the world. Its complex ecoregions were driven not only by global climate change but also by local climate change linked to uplifting of Tibet Plateau. Therefore, emergencies of ecoregions in this area are crucial to understand both climate changes and topographic change of Tibet Plateau. Our analysis indicates the new method is very powerful and promising to investigate geological ecoregions. Our result does not support an early Miocene uplifting Tibet Plateau, it happened more likely in the Late Miocene. Modern ecoregions in Asia should also emerge after the Late Miocene.

East Asia is one of the most zoogeographical complex regions in the world and hosts the Earth's most important biodiversity. Except for a latitude divergence between North (Palearctic biomes) and South (Oriental biomes), a west and east divergence is also prominent and links directly to uplifting of the world's largest and highest Tibetan Plateau. Furthermore, three hotspots (Indo_Burma, Western Ghats and Sri Lanka, South Central China) are located around the Plateau. Because of the elusive uplifting history of Tibet Plateau and poorly fossiliferous/fossil dating in South of East Asia, the history of hotspots and ecoregions in East Asia are still unclear.

A new data mining method called redescription (hybrid of cluster and regression) has been tested to be powerful and is able to capture modern ecoregions and give boundary conditions for both faunal feature and local climate context (Galbrun et al., 2021). In order to apply data mining analysis, each herbivore species is scored and transferred into 11 dental traits based on its tooth morphology. A fauna community can thus be described digitally by mean values of the 11 dental traits of all herbivores that cohabitate in the fauna. Using the redescription method, modern herbivore dental traits and perspective climate variables in East Asia are analyzed and 20 most accurate ecometrics redescriptions are obtained. The 20 redescriptions are clustered into 5 ecoregions. The five captured ecoregions are Tibetan Plateau, East China, India inland, Southeast Asia and isolated mangroves patches in South East Asia. The recognized ecoregions correspond well to the distribution of plant relicts found in these regions. Among these ecoregions, the modern Tibet Plateau ecoregion is characterized by two unique ecometrics redescriptions. Redescription R2.1 requires high longitudinal loph count (LOP) and no thickened enamel (ETH), which relates to the absence of suids and primate. The relevant climate prescribes low temperatures in the warmest quarter (T~WarmQ) and low annual precipitation (PTotY). Redescription R1.2 requires high obtuse lophs (OL), indicating generalist herbivory, and low structural fortification (SF), which manage to survive in seasonal environments that lack humid woodlands, as well as low thickened enamel (ETH) in R2.1. The climate requires a low mean annual temperature (T~Y) and high seasonality of the temperature. Since the two descriptions don't exist in other ecoregions in East Asia, we can apply it to investigate when the two redescriptions emerged in fossil data, in other word, to investigate when a prominent Tibet Plateau uplifted and a unique ecoregion appeared.

We apply fossil herbivores to reconstruct Neogene ecoregions in East Asia and compare the estimated climate conditions by climate modeling with modern climate. We divide Neogene into five periods: Early Miocene, Middle Miocene, Early Late Miocene, Late Miocene and Pliocene to cover the most prominent climate changes. Our aim is to investigate how biodiversity is impacted by the climate changes during the Neogene.

We download fossil records from NOW database of fossil mammals (The NOW Community, 2022) . We obtain 167 localities and 488 fossil herbivores species to run redescription data mining. Our result indicates that there is no signal of Tibet ecoregion in any regions of East Asia before the Late Miocene. Therefore, an early Miocene uplifting of Tibet is not supported by our studying. The redescriptions for modern Tibet emerged in Late Miocene in Tibet and North China, indicate Tibet ecoregion originated from the Palearctic realm and finally evolved into a unique Plateau fauna in Tibet. Although our fossil records are not good enough to recognize the three modern hotspots around Tibet Plateau, a late uplifting of Tibet Plateau suggests a Late Neogene emergence of these hotspots in East Asia.

References

Galbrun et al., 2021. Redescription mining for analyzing local limiting conditions: A case study on the biogeography of large mammals in China and southern Asia. Ecological Informatics, 63 (101314).

The NOW community. New and Old worlds database of fossil mammals (now). Licensed under CC BY 4.o, 2020. See http://www.helsinki.fi/science/now/.

Early Miocene predator-prey interaction on the SE Eurasian shelf revealed by trace fossils at Yehliu Promontory, Taiwan

Ludvig Löwemark

Department of Geosciences, National Taiwan University, Taipei, Taiwan, ludvig@ntu.edu.tw

Summary. Because trace fossils represent the fossilized behaviour of living organisms, they can provide information about what the organisms were doing, and how they interacted with each other. In the Miocene sandstones of NE Taiwan, spectacular trace fossils record both how vertebrates, such as stingrays, fed on invertebrates hiding in the sand, but also how invertebrates, such as huge ambush-predatory worms, snapped fish out of the water column and dragged the still living prey down into their burrows.

Trace fossils of the early Miocene Taliao Formation, NE Taiwan

The Miocene sandstones of the Taliao Formation were deposited in a shallow marine environment on the south-eastern passive margin of the Eurasian continent. In these sandstones, now uplifted and exposed along the NE Coast of Taiwan because of the Late Miocene-Pliocene collision with the Philippine Sea Plate, trace fossils that record the interaction between the inhabitants of the ocean and the sea floor have been recorded. Trace fossils from fully marine settings rarely record the activities of vertebrates, but at Yehliu Geopark, two different behaviours representing predator-prey interaction were recently described. The first trace fossil, *Piscichnus waitemata*, record how ancient stingrays located and flushed out crustaceans and worms from their burrows deep in the sediment on the sea floor (Löwemark 2015). Modern stingrays and many other elasmobranchs use electrosensory organs to locate prey based on the weak electric currents emitted by the animal's nervous system. At Yehliu, abundant circular, sediment-filled bowl-shaped depressions mark the sites of the stingrays' attacks on the endobenthic fauna. The fact that the stingrays managed to precisely locate their prey, despite them hiding in the sediment at depths of more than 10 cm, provides the first independent fossil evidence for the use of electrosensory organs used for hunting.

The second trace fossil is the first know trace fossil (*Pennichnus formosae* igen. nov. isp. nov.) of ambush-predatory worms similar to the modern Bobbit worms (Pan et al. 2021). These trace fossils consist of large L-shaped burrow with a diameter of 2–3 cm and a total length of more than 2 m. In the upper reaches of the L-shaped burrow, feather-like structures indicate the disturbance of the sediment surrounding the burrow opening at the paleo-sea floor. These feather-like structures represent a set of cone-in-cone collapse funnels that formed when the predatory work dragged its prey down into the burrow before consuming it. Modern Bobbit worms hide in their burrows with only the antennae sticking out on the sea floor. When a fish gets too close, the worm explodes out of the burrow opening, snapping its powerful jaws into the prey, and then quickly retreats into the burrow.

The two trace fossils, *Piscichnus Waitemata* and *Pennichnus formosae*, thus represent rare examples of predatory behaviours involving vertebrates and invertebrates.

References

Löwemark, L., 2015: Evidence for targeted elasmobranch predation on thalassinidean shrimp in the Miocene Taliao sandstone formation, NE Taiwan. *Lethaia 48*, 227-234.

Pan, Y.-Y., Nara, M., Löwemark, L., Miguez-Salas, O., Gunnarson, B., Iizuka, Y., Chen, T.-T., Dashtgard, S.E., 2021: The 20-million-year old lair of an ambush-predatory worm preserved in northeast Taiwan. *Scientific Reports 11*, 1174. https://doi.org/10.1038/s41598-020-79311-0.

Stratigraphy of the Beacon Supergroup in Victoria Land (northern Transantarctic Mountains, East Antarctica)

Thomas Mörs[a], Jan Unverfärth[b], Benjamin Bomfleur[b]

[a]Department of Palaeobiology, Swedish Museum of Natural History, Stockholm, Sweden, thomas.moers@nrm.se;
[b]Institute of Geology and Palaeontology, University of Münster, Germany, jan.unverfaerth@gmx.net, bbomfleur@uni-muenster.de;

Summary. Geological and palaeontological fieldwork in the northern Transantarctic Mountains (Ricker Hills, Eisenhower, Deep Freeze and Mesa ranges, Helliwell Hills) during the GANOVEX XI and XIII expeditions resulted in 1) an updated stratigraphy of the Beacon Supergroup in Victoria Land, 2) closing the stratigraphic gap between southern and northern Victoria Land in the Prince Albert Mountains, 3) first fossil vertebrate and invertebrate records from North Victoria Land, and 4) new localities with fossil wood, leaf compression fossils, and organic-rich mudstones.

Introduction

The remote mountain ranges of the northern Transantarctic Mountains in Victoria Land hold some of the least-explored outcrop areas of the Transantarctic Basin. Based on recent international fieldwork during GANOVEX XI (2015/2016) and XIII (2018/19) expeditions, we here report about comprehensive emendations to the regional stratigraphy. The results enable more detailed correlation of the Palaeozoic–Mesozoic successions throughout East Antarctica and into Tasmania.

Prince Albert Mountains and Mesa Range

In the southern Prince Albert Mountains (Hollingsworth Glacier area, northern South Victoria Land), organic-rich, fossiliferous mudstones document Late Triassic strata in the Morris Basin of the Ricker Hills. Early Jurassic sedimentary, mixed epiclastic-volcaniclastic deposits exposed at McLea Nunatak provide evidence for widespread synchronicity of silicic volcanic episodes preceding Ferrar magmatism (Unverfärth et al. 2020; Figure 1).

In the Eisenhower Range (northern Prince Albert Mountains, North Victoria Land), previously unvisited high-altitude outcrops have revealed silicified peat deposits and organic-rich mudstones with abundant plant fossils providing further support for a Late Triassic age, in agreement with previous fossil finds from nearby Timber Peak.

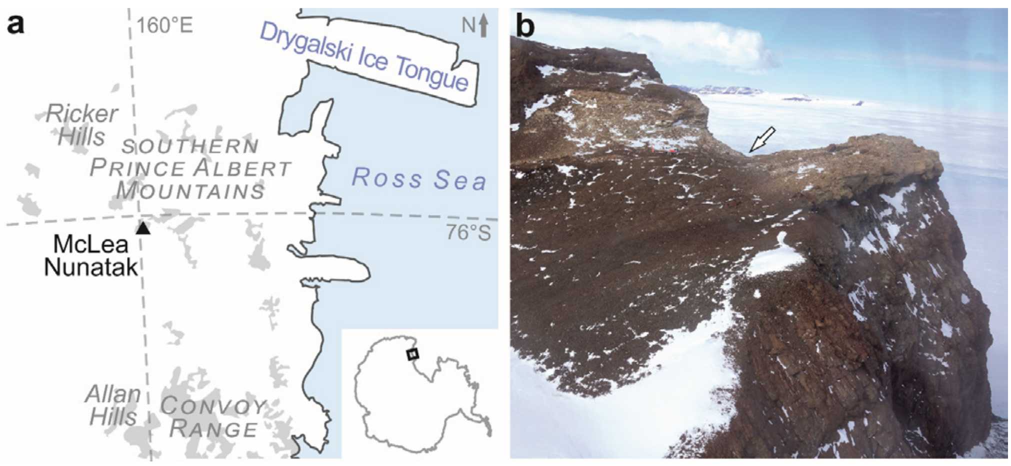

Fig. 1. a. Map showing the position of McLea Nunatak in the southern Prince Albert Mountains, East Antarctica. b. Field image of McLea Nunatak showing the raft of sedimentary deposits between Ferrar sills (arrow indicates the exposed basal part of the section). Modified from Unverfärth et al. (2020).

In the Mesa Range (Campbell Glacier area, North Victoria Land), new discoveries of Early Jurassic Exposure Hill deposits in the Diversions Hills expose in-situ trees.

Helliwell Hills

The Helliwell Hills (Rennick Glacier area, North Victoria Land) extend from Boggs Valley, a large dry valley, across Mount Van der Hoeven northwards to Dziura Nunatak and into unnamed nunataks and valley floors east. Permian sedimentary deposits of the Takrouna Formation have been described earlier from Boggs Valley. The recent geological and palaeontological investigations, including petrographic, geochemical and palynostratigraphic analyses reveal a stack of three previously unknown sedimentary units in the Helliwell Hills: the Lower Triassic Van der Hoeven Formation (115+ m thick), the Middle to Upper Triassic Helliwell Formation (235 m thick), and the uppermost Triassic–Lower Jurassic Section Peak Formation (c. 14 m) (Bomfleur et al. 2020). The new Van der Hoeven Fm. consists mainly of quartzose sandstone and non-carbonaceous mudstone rich in continental trace fossils, whereas the new Helliwell Fm. consists of coal-bearing overbank deposits and volcaniclastic sandstone with typical plant fossils of the Gondwanan *Dicroidium* flora, and silicified peat (Bomfleur et al. 2020). Greenish-weathered, fine-grained sandstone and mudstone layers of the Helliwell Fm. have also produced the first evidence of a Triassic terrestrial vertebrate in North Victoria Land (Mörs et al. 2019).

One section in the Helliwell Hills exposes the Permian-Triassic boundary (Takrouna Fm./Van der Hoeven Fm.), which promises to allow detailed reconstructions of high-latitude dynamics across the critical end-Permian mass extinction interval.

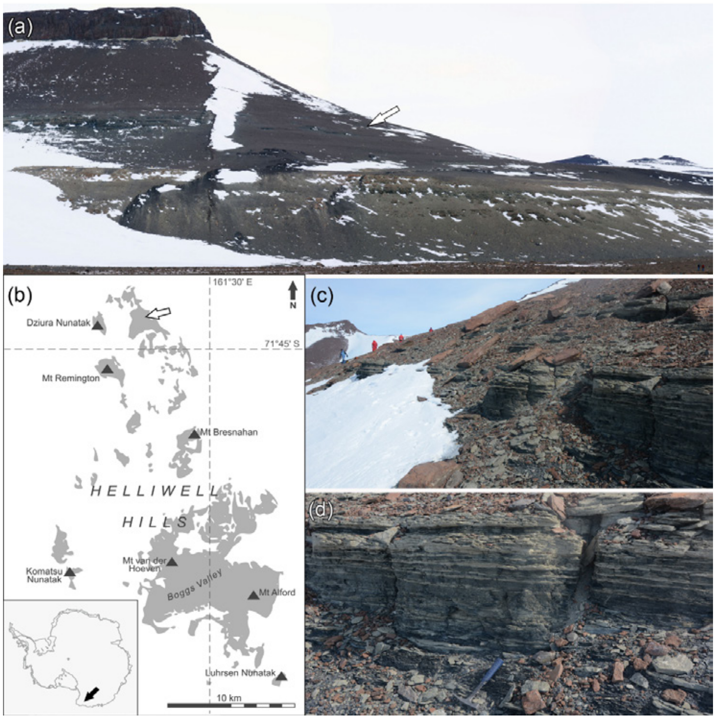

Fig 2. a. Location of the fossil locality in the northern Helliwell Hills (white arrow). b. Map with the fossil locality at the Helliwell Hills Camp (white arrow). c. Fossil locality. d. Greenish-weathered, fine-grained sandstone and mudstone layers, hammer for scale (from Mörs et al. 2019).

References

Bomfleur, B., Mörs, T., Unverfärth, J., Liu, F., Läufer, A., Castillo, P., Oh, C., Park, T.-Y., Woo, J. & Crispini, L., 2020: Uncharted Permian to Jurassic continental deposits in the far north of Victoria Land, East Antarctica. *Journal of the Geological Society 178 (1),* jgs2020-062. https://doi.org/10.1144/jgs2020-062.

Mörs, T., Niedzwiedzki, G., Crispini, L., Läufer, A. & Bomfleur, B., 2019: First evidence of a tetrapod footprint from the Triassic of northern Victoria Land, Antarctica. *Polar Research 38*, 3438. https://doi.org/10.33265/polar.v38.3438.

Unverfärth, J., Mörs, T., Bomfleur, B., 2020: Palynological evidence supporting widespread synchronicity of Early Jurassic silicic volcanism throughout the Transantarctic Basin. *Antarctic Science 32 (5),* 396–397. http://dx.doi.org/10.1017/S0954102020000346.

A new species of the microfossil genus Kuqaia; a possible water flea egg from the Jurassic of Sweden

Jungang Peng[a,b], Sam M. Slater[b], Vivi Vajda[b]

[a]State Key Laboratory of Palaeobiology and Stratigraphy, Nanjing Institute of Geology and Palaeontology and Center for Excellence in Life and Paleoenvironment, Chinese Academy of Sciences, Nanjing, China; [b]Department of Palaeobiology, Swedish Museum of Natural History, Stockholm, Sweden, jgpeng@nigpas.ac.cn, Sam.Slater@nrm.se, Vivi.Vajda@nrm.se

Summary. *Kuqaia* is a microfossil genus (a palynomorph) of unknown biological affinity, characterized by a bilateral symmetrical, ornamented shell with caudal spine. Here we present a new type of *Kuqaia*, based on an exceptionally preserved specimen from the Kävlinge BH-928 drill core, southern Sweden. Following a review of the distribution of *Kuqaia*, we highlight its utility in Jurassic biostratigraphy. The new type of *Kuqaia* has some morphological similarities with water flea (*Daphnia*) resting eggs, although a lack of key diagnostic features means that the affinity of *Kuqaia* remains uncertain.

The microfossil genus *Kuqaia* has been documented from Jurassic strata of several Chinese sedimentary basins, the North Sea, and now Sweden. Its distribution therefore covers much of Laurasia, but notably, it has not been recorded from Gondwana, suggesting that *Kuqaia* was confined to Laurasia.

The specimens studied here were collected from the interval, 57.00–39.60 m, of the Kävlinge BH-928 drill core from southwestern Sweden. Nine specimens, stored in the Norling foraminifera collection (Norling 1968) of the Department of Palaeobiology, Swedish Museum of Natural History, were examined and described, using reflected light, transmitted light and scanning electron microscopy.

Based on the Swedish material we show that *Kuqaia* is a useful stratigraphic marker for the Lower Jurassic to lower Middle Jurassic in Laurasia, with its first appearance in the Hettangian, and its last appearance is tentatively dated as early Bajocian based on North Sea material.

The new, well-preserved specimen displays morphological similarities to some water flea (*Daphnia*) resting eggs, although the affinity remains unclear due to a lack of conclusive evidence. Nevertheless, the occurrence of *Kuqaia* in only non-marine deposits suggests a terrestrial or freshwater origin.

References

Norling, E., 1968: On Liassic nodosariid Foraminifera and their wall structures. *Sveriges geologiska undersökning, Series C623, Årsbok 61*, 1–75.

The emergence of pelagic calcification in the Upper Triassic and its influence on seawater chemistry

Sylvain Richoz[a], Isaline Demangel[a], Zsófia Kovács[b]

[a]Department of Geology, University of Lund, Lund, Sweden, sylvain.richoz@geol.lu.se, isaline.demangel@geol.lu.se; [b]Department of Earth sciences, Graz University, Graz, Austria, kov.zsofia0108@gmail.com

Summary. We studied the emergence of pelagic calcification in the Upper Triassic to verify if the calcareous nannoplankton had, at an early stage of their evolution, such an important influence on seawater chemistry as today. We investigated 15 sections of different paleolatitudes for their nannofossil assemblages, mineralogical and elemental composition, $^{87}Sr/^{86}Sr$, $\delta^{44/40}Ca$ and $\delta^{13}C_{carb}$ isotopic ratios. The coccolithophorids show slow temporal diversification, nannoplankton reaches rock-forming abundance only during the upper Rhaetian and an influence on the seawater chemistry only during the Jurassic.

Calcareous nannoplankton is the most productive calcifying organism nowadays and has a tremendous influence on the climate and the seawater chemistry, as a biological pump and as a regulator of surface ocean alkalinity. Modelling studies neglected this group as a potential influencer before the Jurassic (*i.e.* Ridgwell et al. 2005), while first quantitative paleontological studies suggested that already before the Triassic-Jurassic boundary, calcareous nannofossils reached rock-forming abundance and influenced the oceanic system (Preto et al. 2013). This contradiction and the rare quantitative abundance data of the calcareous nannofossils in the Late Triassic indicated that further investigations were required to verify the hypothesis that the development of the calcareous nannoplankton had a significant influence on the seawater chemistry already in the Late Triassic i.e. at an early stage of their evolution. We investigated therefore quantitatively the calcareous nannofossil assemblages by light and scanning electron microscope in six Austrian and one Romanian sections (25°N), one section from Turkey (palaeo-equator), six sections from Oman (20°S) and one in Australia (30°S) (Demangel 2022). In parallel, geochemical analyses were performed first with trace elements concentration to evaluate the impact of diagenesis on the preservation of the sediments and calcareous nannofossils but also to trace changes in weathering rate during the Late Triassic. Second, isotopic measurements were performed for strontium, calcium, carbon and oxygen to better constrain the environmental conditions during the early evolution of the calcareous nannofossils (Kovàcs 2021).

The nannolith *Prinsiosphaera triassica* dominates the assemblage but is still a minor component of the rock during the Norian. It increases slightly in abundance in the lower Rhaetian, followed by a small-scale short-term increase during the middle Rhaetian and reaches rock-forming abundance only in the upper Rhaetian (Demangel et al. 2020; Demagel 2022). The abundance of *P. triassica* is affected by the occurrence of a second nannolith, *Eoconusphaera hallstattensis*, in the lower Rhaetian (Demangel et al. 2021). The coccolithophorids are present in low abundance, increasing slightly in the middle Rhaetian. After the first record of coccoliths in the middle Norian (Alaunian), the oldest *Crucirhabdus minutus* and *Archaeozygodiscus koessenensis* were observed in the upper Norian (Sevatian) and the FOD of *Crucirhabdus primulus* was recorded in the lower Rhaetian (Demangel et al. 2020). These observations suggest a rather slow temporal diversification of the first coccolithophorids with ~ 4 million years for three species.

The isotopic proxies revealed important palaeoenvironmental changes. The $^{87}Sr/^{86}Sr$ and $\delta^{44/40}Ca$ isotopic investigations highlighted the possible role of carbonate and evaporite dissolution on the chemical composition of the seawater due to a major sea-level fall just after the Norian-Rhaetian boundary (Kovács et al. 2020; Kovács 2021). On the contrary, the longer-term $^{87}Sr/^{86}Sr$ and $\delta^{13}C$ isotopic trends are compatible with the incipient break-up of the Pangea supercontinent. The emplacement of the Central Atlantic Magmatic Province clearly left its imprint on all the investigated isotopic systems. However, interestingly the Sr isotopic composition was not directly affected by the volcanisms, but by the consequent enhanced silicate weathering. In the preceding interval, no evidence was found for another significant volcanic event. This finding is in contradiction with several previous Norian-Rhaetian boundary carbon isotopic studies (Kovàcs, 2021).

By the comparison of the calcareous nannofossil abundance and isotopic composition results, no clear correlations were observed. Carbon and calcium isotopic composition could be theoretically influenced by the increasing proportion of calcareous nannofossils in the sediments. Therefore, in lack of correlation, it can be said that their importance in global geochemical cycles remained limited in the Late Triassic and they contributed to shifting the major carbonate production from the shallow seas to the open marine realm only during the Jurassic.

References

Demangel, I., 2022: The emergence of pelagic calcification and its influence on seawater chemistry in the Upper Triassic. *Unpublished Ph.D. Thesis, 236 p. Graz University*.

Demangel, I., Kovacs, Z., Richoz, S., Gardin, S., Krystyn, L., Baldermann, A. & Piller, W. E., 2020: Development of early calcareous nannoplankton in the Northern Calcareous Alps (Austria) in the Late Triassic. *Global and Planetary Change 193, 103254*.

Demangel, I., Howe, R., Gardin, S. & Richoz, S., 2021: *Eoconusphaera hallstattensis*, new species, and review of the Rhaetian genus *Eoconusphaera*. *Journal of Nannoplankton Research*, *39 (1), 77 – 87*.

Kovács, Z., 2021: Multi-proxy characterization of the influence of the rising pelagic calcification on seawater chemistry. *Unpublished Ph.D.hesis, 294 p. Graz University.*

Kovács, Z., Demangel, I., Richoz, S., Hippler, D., Baldermann, A. & Krystyn, L., 2020: New constraints on the evolution of $^{87}Sr/^{86}Sr$ of seawater during the Upper Triassic. *Global and Planetary Change 192, 103255.*

Preto, N., Agnini, C., Rigo, M., Sprovieri, M. & Westphal, H., 2013: The calcareous nannofossil *Prinsiosphaera* achieved rock-forming abundances in the latest Triassic of Tethys: consequences for the $\delta^{13}C$ of bulk carbonate. *Biogeoscinces 10, 6053–6068.*

Ridgwell, A., 2005: A mid-Mesozoic revolution in the regulation of ocean chemistry. *Marine Geology 217, 339–357*.

Correlation of Cretaceous deposits along the Dniester river (Ukraine) by palynological and lithological methods

Olena A. Shevchuk[a,b], Oleksandr I. Shevchuk[c]

[a]Department of Stratigraphy and Paleontology of Mesozoic sediments, Institute of Geological Sciences of the National Academy of Sciences of Ukraine, Kyiv, Ukraine; [b]Center for Paleogenetics, Stockholm University, and Departament of Paleobiology, Swedish Museum of Natural History, Stockholm, Sweden, hshevchuk@ukr.net; [c]Department of Environmental Safety, labor safety and fire safety (HSE) PJSC «Ukrnafta», Kyiv, Ukraine, alexo33@ukr.net

Summary. Rocks of Cenomanian and Turonian age, which are exposed on the right bank of the Dniester, Ukraine, are correlated with deposits of similar age in the left bank based on palynological (dinocysts and spore-pollen complexes) and lithological methods. The Dniester Pumped Storage Power Plant (PSP station) was built on this site, located on the right bank of the river between two dams of the Dniester Hydroelectric Power Plant (HPP station), and it is the Cretaceous and Neogene deposits that serve as the retaining walls of these fortifications.

The object of our study is the Cretaceous deposits of four outcrops located on the right bank of the Dniester River. Two dams of the Dniester HPP and the Dniester PSP were built along this section of the river. Construction of the Dniester Pumped Storage Power Plant is underway, a project that will give Europe its largest and most powerful hydroelectric facility.

Previously, we investigated sections of Cretaceous deposits on the left bank of the Dniester river (Shevchuk & Klimenko 2011; Ivanik et al. 2012; Shevchuk 2016, 2020). Many remains of fossil fauna and flora were documented here, which made it possible to stratify these deposits in detail (Gavrilishin et al. 1991). To date, rocks on the right bank of the Dniester river have not been studied by means of biostratigraphic and lithological methods.

Cretaceous deposits in this area are overlain by Neogene deposits. We have previously studied these Neogene deposits, stratified them in detail and attributed them to the Tortonian-Sarmatian age (Ivanik et al. 2021). All these places are united by the fact that something is built into these dense limestones of the Neogene age. These include the cave St. Nicholas Monastery (also known as the Halytska wall), the Dniester Pumped Storage Power Station, the Dniester Hydroelectric Power Station, quarries in the center of Sokyryany; the latter are mines for the extraction of white building stone. Cretaceous deposits lie on the Silurian and in some places on Ediacaran deposits. Phosphorites are often found in the studied Cenomanian deposits and underlying Ediacaran (Shekhunova et al. 2016).

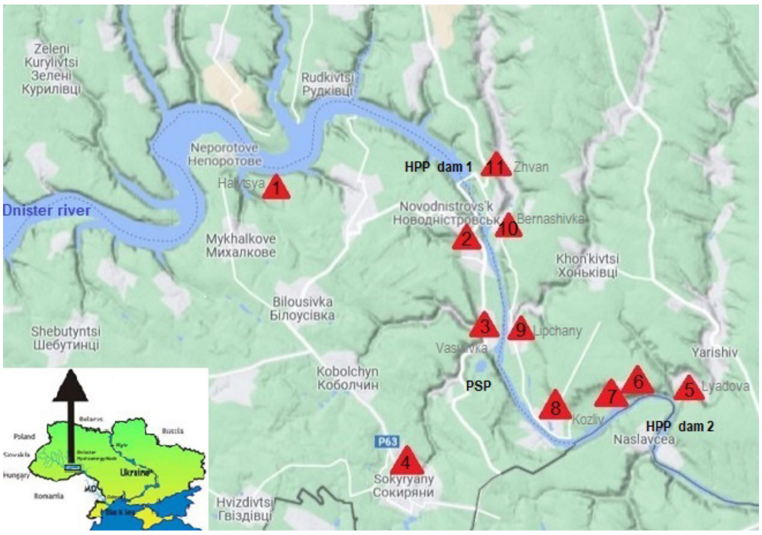

Fig. 1. Map of the study area. Outcrops of the the right bank of the Dnister district of Chernivtsi region: 1) outcrop near the village of Halytsya (Halytska wall); 2) the outskirts of the village of Novodnistrovsk including the wall of the Dniester HPP, dam №1; 3) outcrop under the Dniester PSP near the village of Vasylivka; 4) a series of outcrops in the town Sokyryany under the quarry mines; left bank of Mohyliv-Podilskyi district of Vinnytsia region: 5) outcrop under the wall on the territory of Lyadovsky monastery; 6-7) two outcrops between the villages of Kozliv and Nahoriany - near the dam №2 of the Dniester HPP; 8) outcrop near the village of Kozliv; 9) outcrop near the village Lipchany; 10) outcrop near the village of Bernashivka; 11) outcrop near the village Zhvan.

Outcrops exposing Cretaceous rocks of the Dniester district are of particular interest to stratigraphers-paleontologists as they contain a diverse complex of fossil biota. This includes brachiopods, gastropods, foraminifera, microspongiofauna and others. Also in the samples of these rocks there are organic remains of plant origin (spores and pollen of higher plants, wood remains, remains of green and dinophytic algae and others). Different systematic composition of fossil organisms distinguishes Cenomanian complex from Turonian.

Cenomanian spore-pollen complex established in these sections is characterized by the participation of spores of ferns - up to 25%, pollen of gymnosperms - 50% and angiosperms - up to 25%. There are spores of the family Polypodiaceae. Spores of *Gleicheniidites* sp., *Plisifera delicata*, *Cyathidites* sp., *Phlebopteris* sp., *Cicatricosisporites* sp., *Ophioglossum cenomanicus*, *Lygodiumsporites* sp. are rarely observed. The pollen part of the complex is dominated by pollen of the gymnosperm family Pinaceae and Podocarpaceae. There are genus of relatively small size: *Pinuspollenites* spp. and *Cedripites* spp. Pollen *Liliacidites* sp. dominates among angiosperms and pollen identified by artificial classification: *Tricolpopolenites* sp. and *Clavatipollenites* sp. Dinocyst: *Diconodinium cristatum*, *Spiniferites ramosus*, *Chlamydophorella nyei*, *Cleistosphaeridium* sp., *Odontochitina costata*, *Cribroperidinium cooksonae*, *Cribroperidinium intricatum*, *Oligosphaeridium* spp., *Callaiosphaeridium* sp., *Coronifera oceanica*, *Epelidosphaeridia spinosa*, *Litosphaeridium siphoniphorum*.

Turonian spore-pollen complex. Spores - up to 17% (Polypodiaceae, Gleicheniaceae, Schizaeaceae, Matoniaceae, *Leiotriletes* sp., *Staplinisporites caminus*, *Taurocusporites reduncus*. Gymnosperm pollen - 55% (Pinaceae, Cupressaceae, Ginkgocycadaceae, Araucariaceae). Angiosperm pollen - up to 33% (*Tricolpites* spp., *Tricolpites reticulatus*, *Tricolpopolenites* sp., *Tricolpoporopollenites* sp., *Liliacidides* sp., *Liliacidides variegates*. The first appearance of the pollen *Proteacidites magnus*. Dinocysts: *Florentinia mantelli*, *Spiniferites* spp., *Cauveridinium membraniphorum*.

The Cenomanian and Turonian deposits, which are exposed on the right bank of the Dniester, are well correlated with the similar age deposits of the left bank and adjacent territories. The lithological composition of rocks of the Mesozoic on the right bank of the Dniester river is more homogeneous and is characterized mainly by limestones of various origins.

References

Gavrilishin, V.I., Pasternak, S.I., Rozumeyko, S.V., 1991: Stratigraphic subdivisions of Cretaceous deposits of the platform part of western Ukraine. *Prepring of the Academy of Sciences of the Ukrainian SSR. Institute of Geology and Geochemistry of Fossil Fuels*. № 91-I. Lviv, 59. [in Russian]

Gozhik, P.F. et al., 2013: Stratigraphy of the Upper Proterozoic and Phanerozoic of Ukraine. Vol. 1. Stratigraphy of the Upper Prote-rozoic, Paleozoic and Mesozoic of Ukraine. Chief editor P.F. Gozhik. IGN NAS of Ukraine. Kyiv. *Logos* 637. [In Ukrainian].

Ivanik, M.M., Shevchuk, O.A., Klimenko, Yu.V., 2012: Sections Naddnestrianschiny (near the river Dniester) as neostratotyps Albian - Turonian sediments andf theirs paleontological described. *Tectonics end Stratigraphic*. Kyiv, 87-95. [in Ukrainian]

Ivanik O., Shevchuk, O., Vasylenko, S., 2021: Lithological and stratigraphic criteria for the development of geohazards within the Dniester river basin. *XV International Scientific Conference "Monitoring of geological processes and ecological condition of the environment" Institute of Geology of Taras Shevchenko National University of Kyiv*. Mon-21-106. [in English]

Shekhunova, S.B., Stadnichenko, S.M., Paliy, V.M., Permyakov, V.V., 2016: Nanotextures of Vendian and Alb-Cenomanian Phosphates of the Transnistria. *Collection of Scientific Works of the Institute of Geological Sciences of the NAS of Ukraine 9*. Kyiv. 190-201. [in Ukrainian]

Shevchuk, O.A., 2016: New data to the Zonal scale of the biostratigraphic subdivisions of the Albian - Campanian of the western regions of the platform Ukraine. *Materials of the Paleontological Society of the National Academy of Sciences of Ukraine*. Kyiv. 55-57. [in Ukrainian]

Shevchuk, O.A., 2020: Stratigraphy of the Middle Jurassic - Cretaceous of Ukraine on microfossils. *Abstract of the dissertation for the degree of Doctor of Geological sciences. Institute of Geological Sciences. National Academy of Sciences of Ukraine. Specialty – general and regional geology*. Kyiv. 44. [in Ukrainian]

Shevchuk, O.A., Klimenko, Yu.V., 2011: New data to the paleontological characteristics of the Alb-Turonian sediments of the Dniester region. *Problems of Stratigraphy and Correlation of Phanerozoic Deposits of Ukraine. Materials of the XXXIII session of the Paleontologist. Society of NAS of Ukraine*. Kyiv. 46-48. [in Ukrainian]

Tracking the Ediacaran–Cambrian transition using small carbonaceous fossils (SCFs): a newly emerging record from Baltica

Ben J. Slater

Department of Earth Sciences, Uppsala University, Uppsala, Sweden, ben.slater@geo.uu.se

Summary. The Ediacaran–Cambrian transition represents an inflection point in Earth history. At this time, animal-derived skeletal parts become common as fossils, heralding the dawn of the Phanerozoic fossil record as we know it. Yet most organisms (extant and extinct) lack mineralized skeletons. Consequently, our view of this key evolutionary radiation is heavily biased toward taxa that produced shells. On Baltica, Ediacaran–Cambrian strata have recently been shown to host a wealth of microscopic fragmentary remains of non-mineralized 'soft bodied' animals, with the potential to circumvent this bias.

Small Carbonaceous Fossils (SCFs)

The rapid expansion in diversity of metazoan-derived skeletal hard-parts observed in early Cambrian strata is the most dramatic signal in the fossil record (Brasier 1985, Bengtson et al. 1990, Cloud & Drake 1968, Davies et al. 2020). Rare Konservat-Lagerstätten sites, however, reveal that fossils of organisms possessing mineralized hard-parts represent only a minor fraction of the total diversity, which instead largely comprised unmineralized forms. An alternate, but largely overlooked source of data on otherwise taphonomically invisible unmineralized taxa comes from the developing record of 'small carbonaceous fossils' (SCFs) (Butterfield & Harvey 2012). SCFs comprise a polyphyletic assortment of fragmentary cuticular remains sourced from animals, algae and protists. Though fragmentary, SCFs can preserve phylogenetically informative morphological structures, and are beginning to reveal new aspects of Cambrian diversity from time-windows and areas which lack Burgess Shale-type Lagerstätten. For instance, a rich diversity of SCFs has recently been documented from the Cambrian palaeocontinent Laurentia (e.g., Harvey & Butterfield 2008, Harvey et al. 2012, Slater et al. 2018b, Wallet et al. 2021). Nevertheless, a widespread regional unconformity and localised tectonism has meant that in most places accross Laurentia, sediments from the earliest part of the Cambrian and late Ediacaran are missing or thermally altered, precluding the preservation of SCFs. On Baltica – the palaeocontinent roughly corresponding to modern day Scandinavia, Finland, and most of Eastern Europe – there is a relatively complete succession of Ediacaran–Cambrian strata preserved. Moreover, the comparatively quiescent tectonic history of Baltica has meant that these siliciclastic deposits are perfect for the preservation of SCFs, owing to their exceptionally low levels of thermal alteration. Investigations of target sediments across Baltica have yielded a multitude of SCFs (Figure 1) including unmineralized Cambrian metazoans previously unknown from Baltica (e.g. *Wiwaxia*), and even rare instances of 'Ediacaran survivors' – distinct taxa that have been found to range across the Ediacaran–Cambrian boundary (Slater et al. 2020). By combining these records and findings from across Baltica, a detailed new picture of this major biotic transition emerges: early Cambrian (stages 3–4) SCF assemblages preserve a rich assortment of animal fragments, sourced from a diverse array of metazoans, including iconic taxa known elsewhere exclusively from Burgess Shale-type Lagerstätten deposits (Slater et al. 2017, Guilbaud et al. 2018, Kesidis et al. 2019). Older strata of Terreneuvian age instead typically host a much lower diversity of metazoan remains among SCFs, and also exhibit a greater regional homogeneity among the fauna across Baltica (Slater et al. 2018a, Slater & Willman 2019). Prior to the Cambrian, Late Ediacaran SCF assemblages from Baltica preserve an abundance of algal and cyanobacterial microbial mat-forming structures, and significantly, include rare fragments of metazoans (Slater et al. 2020, Willman & Slater 2021). Though this taphonomic mode comprises mostly unmineralized taxa, the overall signal of diversification nevertheless broadly mirrors that of the classical Cambrian radiation of 'shelly' fossils. With their capacity to capture entirely unmineralized and otherwise unfossilisable aspects of diversity, SCFs clearly constitute a novel resource for tracking macroevolutionary patterns over the Proterozoic–Phanerozoic biotic transition.

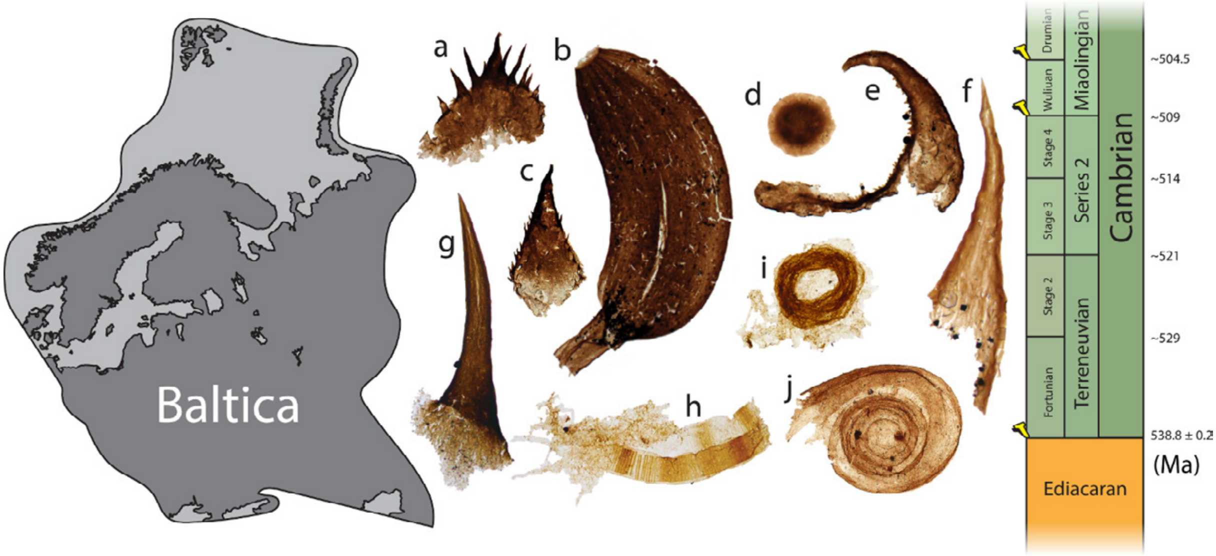

Figure 1. Example assortment of Ediacaran–Cambrian SCFs from the palaeocontinent Baltica. A–E, Cambrian Stage 3–4; F–G, earliest Cambrian Terreneuvian; H–J, late Ediacaran. All SCFs less than 1 milimetre in size.

References

Bengtson, S., Conway Morris, S. & Cooper, B.J. 1990. Early Cambrian fossils from South Australia. *Memoirs of the Association of Australasian Palaeontologists 9*, 1–364.

Brasier, M.D., 1985. Evolutionary and geological events across the Precambrian–Cambrian boundary. *Geology Today 1*, 141–146.

Butterfield, N.J. & Harvey, T.H.P., 2012. Small carbonaceous fossils (SCFs): a new measure of early Paleozoic paleobiology. *Geology 40*, 71–74.

Cloud, P.E. & Drake, E.T., 1968. Pre-Metazoan evolution and the origins of the Metazoa. *Evolution and Environment*, 1–72.

Davies, N.S., Shillito, A.P., Slater, B.J., Liu, A.G. & McMahon, W.J., 2020. Evolutionary synchrony of Earth's biosphere and sedimentary-stratigraphic record. *Earth-Science Reviews 201*, p.102979.

Guilbaud, R., Slater, B.J., Poulton, S.W., Harvey, T.H., Brocks, J.J., Nettersheim, B.J. & Butterfield, N.J., 2018. Oxygen minimum zones in the early Cambrian ocean. *Geochemical Perspectives Letters 6*, 33–38.

Harvey, T.H. & Butterfield, N.J., 2008. Sophisticated particle-feeding in a large early Cambrian crustacean. *Nature 452*, 868–871.

Harvey, T.H., Vélez, M.I., & Butterfield, N.J., 2012. Exceptionally preserved crustaceans from western Canada reveal a cryptic Cambrian radiation. *Proceedings of the National Academy of Sciences 109*, 1589–1594.

Kesidis, G., Slater, B.J., Jensen, S. & Budd, G.E., 2019. Caught in the act: priapulid burrowers in early Cambrian substrates. *Proceedings of the Royal Society B 286*, p.20182505.

Slater, B.J., Harvey, T.H. & Butterfield, N.J., 2018a. Small carbonaceous fossils (SCFs) from the Terreneuvian (lower Cambrian) of Baltica. *Palaeontology 61*, 417–439.

Slater, B.J., Harvey, T.H., Bekker, A. & Butterfield, N.J., 2020. *Cochleatina*: an enigmatic Ediacaran–Cambrian survivor among small carbonaceous fossils (SCFs). *Palaeontology 63*, 733–752.

Slater, B.J., Harvey, T.H., Guilbaud, R. & Butterfield, N.J., 2017. A cryptic record of Burgess Shale-type diversity from the early Cambrian of Baltica. *Palaeontology 60*, 117–140.

Slater, B.J. & Willman, S., 2019. Early Cambrian small carbonaceous fossils (SCFs) from an impact crater in western Finland. *Lethaia 52*, 570–582.

Slater, B.J., Willman, S., Budd, G.E. & Peel, J.S., 2018b. Widespread preservation of small carbonaceous fossils (SCFs) in the early Cambrian of North Greenland. *Geology 46*, 107–110.

Wallet, E., Slater, B.J., Willman, S. & Peel, J.S., 2021. Small carbonaceous fossils (SCFs) from North Greenland: New light on metazoan diversity in early Cambrian shelf environments. *Papers in Palaeontology 7*, 1403–1433.

Willman, S. & Slater, B.J., 2021. Late Ediacaran organic microfossils from Finland. *Geological Magazine 158*, 2231–2244.

Cryptic imprint fossils of nannoplankton reveal hidden records through intervals of past global warming

Sam M. Slater[a], Paul Bown[b], Richard J. Twitchett[c], Silvia Danise[d], Vivi Vajda[a]

[a]Department of Palaeobiology, Swedish Museum of Natural History, Stockholm, Sweden, sam.slater@nrm.se, vivi.vajda@nrm.se; [b]Department of Earth Sciences, University College London, London, p.bown@ucl.ac.uk; [c]The Natural History Museum, London, UK, r.twitchett@nhm.ac.uk; [d]Dipartimento di Scienze della Terra, Università degli Studi di Firenze, Firenze, Italy, silvia.danise@unifi.it

Summary. Several global warming intervals in the geological record are associated with substantial declines in calcium carbonate ($CaCO_3$) and nannofossil abundance. These signals have been interpreted as crises of calcareous nannoplankton, whereby ocean acidification and related factors compromised biocalcification. Here we present a cryptic style of fossil preservation – imprints of nannoplankton on organic matter, preserved in abundance throughout these warming intervals. Our findings indicate that the original $CaCO_3$ nannofossils dissolved during diagenesis, leaving behind only their “ghost” imprints.

Calcareous nannofossils – the calcium carbonate ($CaCO_3$) fossil remains of minute calcifying marine nannoplankton – are often highly abundant in rocks younger than ~200 million years old. Through several global warming intervals in the geological record, however, substantial declines in nannofossil abundance and $CaCO_3$ have been observed. These signals have been interpreted as biocalcification crises, whereby ocean acidification and/or related factors compromised biogenic $CaCO_3$ production in marine calcifying organisms, including nannoplankton. Since nannoplankton are the most productive marine calcifiers, and future responses of calcifying organisms to climate change and ocean acidification rely heavily on the nannofossil record, it is important to understand the causes behind these observed nannofossil abundance and $CaCO_3$ declines. Here we present an almost entirely overlooked mode of fossilisation – imprints of nannoplankton, or “ghost” nannofossils, preserved in abundance throughout three inferred biocalcification crisis intervals. These inferred crises are associated with three distinct oceanic anoxic events (OAEs) in the Jurassic and Cretaceous: the Toarcian-OAE (~183 million years ago [Ma]), OAE1a (~120 Ma) and OAE2 (~94 Ma). Imprints were recorded from a global array of sites (UK, Germany, Japan and New Zealand) for the T-OAE, and from Sweden and Italy for OAE1a and OAE2, respectively. The imprints occur on the surfaces of particles of organic matter, including on pollen, spores, marine organic-walled plankton and amorphous organic matter, and are particularly well preserved and abundant within the black shales that characterise the OAEs. The occurrence of these imprints without their $CaCO_3$ casts suggests that during diagenesis, acidic pore waters within the sediments dissolved the $CaCO_3$, distorting the $CaCO_3$-dependent nannofossil record. Our findings indicate no evidence for nannoplankton biocalcification crises during the examined OAEs, and instead suggest that nannoplankton communities were more resilient than the traditional $CaCO_3$ fossil record would suggest. The imprints further reveal evidence for high nannoplankton productivity and blooms during the OAEs, suggesting that nannoplankton, as well as other types of algae, contributed to the development of oxygen-starved marine dead zones on the seafloor, which became widespread throughout these global warming events.

Fresh look at Early Cambrian Brachiopod shell Micro-structures in sections by Ion-milling

Bao-peng Song, Yazhou Hu, Zhifei Zhang

State Key Laboratory of Continental Dynamics, Shaanxi Key Laboratory of Early Life and Environment, and Department of Geology, Northwest University, Xi'an 710069, China; baopeng.nwu@foxmail.com (B.S.); huyz_nwu@163.com (Y.H.); elizf@nwu.edu.cn (Z.Z.)

Summary. The origin of biomineralized skeletons has been a hotly debated topic for tens decades. During the Cambrian explosion, a variety of mineralized skeletons with exquisite organization of multiple layers firstly appeared in many metazoans. Although there have been considerable achievements in understanding of Cambrian explosion, the origin of mineralized multi-layered microstructure in distinct metazoans still remains unsolved. Here, we present the first examples of ion-milling on three-dimensionally preserved phosphatic acrotretoid brachiopod shell valves and other small shelly fossils recovered from the lower Cambrian Shuijingtuo Formation (Series 2, Stage 3) in the Xiaoyangba section, Zhenba County, South Shaanxi Province of China.

Ion-milling tests provide us a perfect and new perspective on internal micro-textual structures of shell valves from the early Cambrian brachiopods. As seen in fragmented valves, the shell valve of acrotretoids is mainly composed of secondary columnar layers concentrically arranged in a pattern of conveyor-belts. On an adult dorsal valve, up to 20 conveyor-belt layers can be distinguished. Each layer is comprised of columnar structures sandwiched by two laminar layers. The diameter of column means generally 1.5~5 μm, and the length varies from 5 μm to 25 μm across different growth lines of the shell valves. Secondary electronic Microphography (SEM) imaging shows that the columns, seen in fractured natural section, is composed of apatite particles about 150 nm wide and 700 nm long, with high contrast in morphology and obvious boundary between grains. The morphological contrast in the SEM images of the polished ion-milling surface is, by contrast, considerably low and the columnar shape is rather unclear. Nevertheless, the smooth ion-milling surface greatly improves the electron channel contrast (ECC) of BSE and the micro-orientation accuracy of EBSD. In addition, the intralaminar and interlaminar columnar structures is encased distinctly by phosphatized materials, which are most probably thought as counterparts of the original organic sheets/membranes. Compared to the acid-etched natural fractured sections, the original biomineralization of micro-structures and the phosphatized structures resulted from post-mortem diagenesis, which disappeared in the acid etching treatment, could be recognized in ion-milling sections, which provides new material information on the microstructure of shell valves in phosphatic-shelled brachiopods from the lower Cambrian. Therefore, the sections by means of ion-milling are providing new insights into the mineralization that took place under the control of organic sheets/membrane and well-defined fabrics and textures of mineralized skeletons, e.g. shells and tubes.

Ion-milled samples show that the polishing is pretty fine, without obvious physical damage and particle embedding when compared to those after mechanical polishing treatments. And the cutting height (2 μm per move) can be accurately controlled by computer so as to obtain the desired location of the fossil profile. Compared with FIB, ion-milling has a larger polishing surface (~5 cm^2) and can be applied to both small skeletal fossil and macro-fossils. Therefore, it's a perfect tool for SEM sample preparation, which provides convenience for showing SEM sample internal structure and analysis of sample characteristics, also a powerful approach in research of microscopic textures and fabrics of skeletons and shells with more or less biomineralization.

Bradoriids from the late early Cambrian of Norway and Sweden

Michael Streng[a], Magne Høyberget[b], Jan Ove R. Ebbestad[c]

[a]Department of Earth Sciences, Uppsala University, Uppsala, Sweden, michael.streng@geo.uu.se; [b]Rennesveien, Mandal, Norway, a-rostr@online.no; [c]Museum of Evolution, Uppsala University, Uppsala, Sweden, jan-ove.ebbestad@em.uu.se.

Summary. A new bradoriid fauna comprising seven taxa is introduced from the early Cambrian Skyberg Member of the Ringstrand Formation of the Mjøsa area in Norway. The fauna is compared to coeval specimens described from Sweden (Wiman 1903), which have been restudied for this study. Both faunas comprise the same, or similar, genera of the families Bradoriidae, Beyrichonidae, Hipponicharionidae, and Svealutidae. Reevaluation of Wiman's specimens revealed the presence of five distinct taxa rather than nine. The faunas from Norway and Sweden are similar to contemporaneous faunas of Avalonia and West Gondwana.

The Mjøsa fauna

All specimens from the Mjøsa area originate from a single locality and stratigraphic unit, the mudrocks of the Skyberg Member as exposed near the farm of the same name (Fig. 1A). The Skyberg Member is the youngest member of the Ringstrand Formation and belongs to the *Kingaspidoides lunatus-Chelediscus acifer* Biozone (Cambrian Stage 4) representing the youngest zone of the early Cambrian in Scandinavia (Fig. 1B). Seven bradoriid taxa belonging to six genera have been distinguished in the

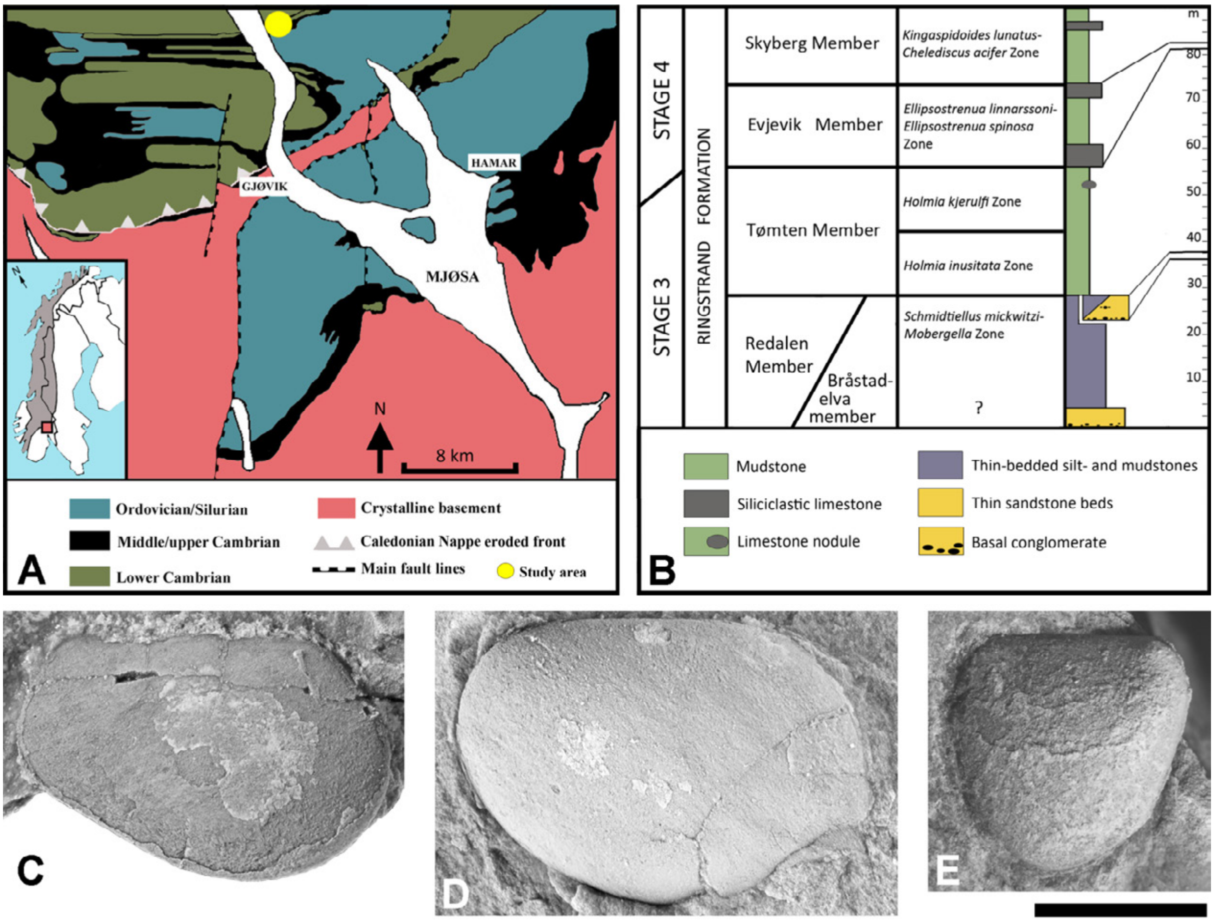

Fig. 1: A, Location of the Mjøsa area in southern Norway and its general geology; study area marked by yellow circle. B, Stratigraphy and biozonation of the Ringstrand Formation. C–E, Specimens of *Indiana* spp. (C, D) and *Beyrichona* sp. (E). Scale bar 2 mm for C–E.

Skyberg Member, with most taxa represented only by one or two specimens. The fauna comprises the genera *Indiana* and *Indota* of the Family Bradoriidae, simple beyrichonids (genus *Beyrichona*; Fig. 1E), the cosmopolitan svealutid *Liangshanella*, and the hipponicharionids *Neokunmingella* and *Albrunnicola*. Within *Indiana* two distinct species appear to be present (Fig. 1C, 1D), one of which is new whereas the other one is close to *Indiana ovoides* (Kautsky) known from a coeval level in central Lapland, Sweden (see Streng & Geyer, 2019).

The Wiman fauna

In 1903, Wiman described nine species of bradoriids from several erratic boulders collected in northern Uppland, Sweden, and on several islands in the Bothnian Sea area (Limön, Eggegrund, and Åland). Based on rare co-occurring olenellid trilobites, Wiman's material is generally considered to be of late early Cambrian in age (Nielsen & Schovsbo, 2011), coeval or slightly younger than the Skyberg material. As most of Wiman's specimens haven't be looked at in detail since their original description, they have been re-investigated to enable a meaningful comparison with the Skyberg material. It turned out that specimens described under a single taxon not necessarily represent all the very same taxon. In contrast, several specimens described as distinct species or even genera are here interpreted to represent a single species. Thus, the genus *Sellula* with its type species *Sellula fallax*, known only by a single specimen, represents a partly compressed specimen of *Beyrichona gevalensis*, a species also described by Wiman (1903) from rocks with the same lithology as those containing *S. fallax*. As a result, instead of nine species, Wiman's bradoriid fauna is here considered to comprise only five species belonging to the genera *Indiana*, *Beyrichona*, *Liangshanella* and *Wimanicharion*.

Comparison

Revision of Wiman's specimens revealed a distinct taxonomic similarity on family and genus level between the Swedish occurrences and the Skyberg fauna. Both faunas share the genera *Indiana*, *Beyrichona*, and *Liangshanella* plus both comprise rather similar hipponicharionids. Surprisingly, on species level only the svealutid *Liangshanella* might be directly comparable between the faunas. Faunas with an equivalent or similar composition have also been described from contemporaneous units of Avalonia (Siveter & Williams 1997; Williams & Siveter 1998) and West Gondwana (Streng & Geyer 2019).

References

Nielsen, A. T. & Schovsbo, N. H., 2011: The Lower Cambrian of Scandinavia: Depositional environment, sequence stratigraphy and palaeogeography. *Earth-Science Reviews 107*, 207–310.

Siveter, D. J. & Williams, M., 1997: Cambrian bradoriid and phosphatocopid arthropods of North America. *Special Papers in Palaeontology 57*, 1–69.

Streng, M. & Geyer, G., 2019: Middle Cambrian Bradoriida (Arthropoda) from the Franconian Forest, Germany, with a review of the bradoriids described from West Gondwana and a revision of material from Baltica. *PalZ 93*, 567–591.

Williams, M. & Siveter, D. J., 1998: British Cambrian and Tremadoc bradoriid and phosphatocopid arthropods. *Monograph of the Palaeontographical Society of London 152*, 1–49.

Wiman, C., 1903: Studien über das Nordbaltische Silurgebiet. I. Olenellussandstein, Obolussandstein und Ceratopygeschiefer. *Bulletin of the Geological Institution of the University of Upsala 6*, 12–76.

New discoveries of Small Shelly Fossils from the early Cambrian (Stage 4) of the Swedish Caledonides, Lappland

Timothy P. Topper[a,b], Stephen McLoughlin[a], Ove Johansson[a], Fan Liu[b], Vivi Vajda[a]

[a]Department of Palaeobiology, Swedish Museum of Natural History, Box 50007, SE-10405 Stockholm, Sweden, e-mails; timothy.topper@nrm.se; Steve.Mcloughlin@nrm.se; Ove.Johansson@nrm.se; Vivi.Vajda@nrm.se; [b]State Key Laboratory of Continental Dynamics, Shaanxi Key Laboratory of Early Life and Environments and Department of Geology, Northwest University, Xi'an, 710069, China, e-mails; timothy.topper@nwu.edu.cn; liufan@nwu.edu.cn.

Summary. New fossil discoveries are reported from early Cambrian strata in northern Swedish Lappland, including a fauna of Small Shelly Fossils (SSF) and new occurrences of brachiopods and trilobites. The moderately diverse SSF fauna is the first of its kind reported from the Swedish Caledonides. These discoveries markedly increase the known diversity of the palaeobiota from the early Cambrian in northern Lappland and provide new insights into the biostratigraphy and palaeoenvironment of the lower Cambrian in Scandinavia and the palaeobiogeograpy of Cambrian faunas in general.

After the break-up of Rodinia in the late Proterozoic, the palaeocontinent Baltica was situated in the Southern Hemisphere and was moving northwards. During the first half of the Cambrian, Baltica was situated at middle to high southern latitudes (c. 35–60°) with modern Scandinavia along its northern margin (Meert, 2013). The Cambrian oceans witnessed the first major radiation of metazoan life – the so called 'Cambrian Radiation' when all the major extant phyla of animals evolved during a short period of time from the terminal Ediacaran through the first four stages of the Cambrian. Rich fossil faunas of early Cambrian (Terreneuvian and Series 2) are known from most Cambrian palaeocontinents, but the fossil record of Baltica remains comparatively poorly understood and described faunas are predominantly restricted to trilobites. As a result, our understanding of the Cambrian marine ecosystems of Baltica remains incomplete until other components of the fauna are documented.

The so-called Small Shelly Fossils (SSFs) include a great diversity of typically very small, skeletal fossils representing a wide range of invertebrates that are commonly extracted from carbonates using weak acids (Bengtson, 2004). Although such fossil assemblages occur throughout the Phanerozoic (Freeman et al., 2019), the term SSFs, as commonly defined, is restricted to assemblages from the Cambrian where they include examples of the oldest known representatives of many fossil and extant animal clades (Matthews & Missarzhevsky, 1975; Bengtson, 2004). This informal group incorporates early members of well-known animal clades, such as Mollusca, Brachiopoda and Porifera (Bengtson et al. 1990), and also many problematic fossils that, historically, have been difficult to place in modern animal groups, although they now appear to belong the stem groups of modern lineages (Skovsted et al. 2008). The oldest SSF assemblages stem from the terminal Ediacaran (Grant 1990), but the Cambrian witnessed a remarkable, successive increase in taxonomic diversity and morphological disparity of SSFs from the Terreneuvian through to Cambrian Stage 4 (Kouchinsky et al., 2012). Thus, the fossil record of SSFs in the Ediacaran–Cambrian significantly reflects the dramatic changes in the Earth's biota around the beginning of the Phanerozoic.

Historically, SSF assemblages have been studied extensively from early Cambrian carbonate successions in Siberia, South China, Australia, Mongolia and Laurentia (see Topper et al., 2022 for review). From the palaeocontinent of Baltica, early works on brachiopods and some other fossils that fit under the SSF umbrella were published as early as the late nineteenth century (Moberg 1892). However, in recent times, only a few studies targeting individual fossil taxa have been published (Bengtson 1968). Instead, much attention has been devoted to coeval trilobite faunas, this is particularly true for the autochthonous Cambrian sequences that crop out along the eastern margins of the Caledonian mountains in northern Scandinavia (see Høyberget et al. 2019 for details).

Here we report a new fauna of Small Shelly Fossils and brachiopods (Fig. 1) from Cambrian outcrops in northern Sweden that includes the first record of the tommotiid *Lapworthella schodakensis* and

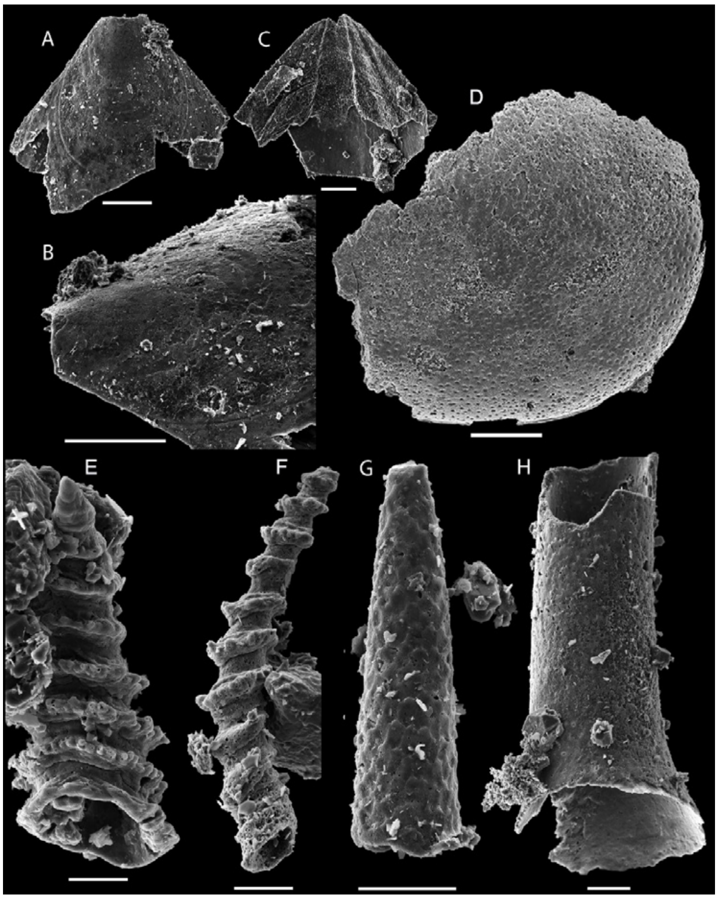

Fig. 1. Small shelly fossils from the Cambrian of northern Sweden. A-C, *Eoobolus* cf. *priscus*, scale bars 200 mm. *D, Bradoria* sp., scale bar 500 mm. *E-F, Lapworthella shodackensis*, scale bars 50 mm. G-H, *Mongolitubulus spinosus*, scale bar 100 mm.

the bradoriid spine *Mongolitubulus spinosus* from Baltica, together with fragmentary specimens of *Bradoria* sp. and remains of one additional bradoriid arthropod, a protoconodont and a helcionelloid mollusc. In addition, the limestone bed yields abundant specimens of the brachiopods *Botsfordia* cf. *caelata*, *Eoobolus* cf. *priscus* and orthothecid hyoliths. The biostratigraphic and palaeobiogeographic implications of the fossil fauna are also discussed.

References

Bengtson, S., 1968: The problematic genus *Mobergella* from the Lower Cambrian of the Baltic area. *Lethaia 1*, 325–351.

Bengtson, S., Morris, S.C., Cooper, B., Jell, P.A. & Runnegar, B., 1990: Early Cambrian fossils from South Australia. *Memoir of the Association of Australasian Palaeontologists 9*, 1–364.

Bengtson, S., 2004: Early skeletal fossils. *The Paleontological Society Papers 10*, 67–78.

Freeman, R.L., Dattilo, B.F. & Brett, C.E., 2019: An integrated stratinomic model for the genesis and concentration of "small shelly fossil"-style phosphatic microsteinkerns in not-so-exceptional conditions. *Palaeogeography, Palaeoclimatology, Palaeoecology 535*, 109344.

Grant, S.W., 1990: Shell structure and distribution of *Cloudina*, a potential index fossil for the terminal Proterozoic. *American Journal of Science 290*, 261.

Høyberget, M., Ebbestad, J.O.R. & Funke, B., 2019: Re-evaluation of the stratigraphically important olenellid trilobite *Holmia* cf. *mobergi* from the Cambrian Series 2, Stage 3 and its implications for the lower Cambrian stratigraphy in the Mjøsa area, Norway. *Norwegian Journal of Geology 99*, 1–30

Kouchinsky, A., Bengtson, S., Runnegar, B., Skovsted, C., Steiner, M. & Vendrasco, M., 2012: Chronology of early Cambrian biomineralization. *Geological Magazine 149*, 221–251.

Matthews, S.C. & Missarzhevsky, V.V., 1975. Small shelly fossils of late Precambrian and early Cambrian age: a review of recent work. *Journal of the Geological Society 131*, 289–304.

Meert, J.G., 2013: Ediacaran–Early Ordovician paleomagnetism of Baltica: A review. *Gondwana Research 25*, 159-169.

Moberg, J.C., 1892: Om en nyupptäckt fauna i block af kambrisk sandsten, insamlade av Dr. N.O. Holst. *Geologiska Föreningens i Stockholm Förhandlingar 14*, 103–120.

Skovsted, C.B., Brock, G.A., Paterson, J.R., Holmer, L.E. & Budd, G.E., 2008: The scleritome of *Eccentrotheca* from the Lower Cambrian of South Australia: Lophophorate affinities and implications for tommotiid phylogeny. *Geology 36*, 171–174.

The lophophore configurations in early Cambrian (Series 2) brachiopods and their phylogenetic implications

Zhifei Zhang[a], Xinyi Ren[a], Yue Liang[a,b], Lars E. Holmer[a,b]

[a]State Key Laboratory of Continental Dynamics, Shaanxi Key laboratory of Early Life & Environments, Department of Geology, Northwest University, Xi'an, 710069, P. R. China [b]Department of Earth Sciences, Paleobiology, Uppsala University, Uppsala, Sweden

More than a decade of collaborations led by the Professors Lars Holmer in UU and Zhifei Zhang in NWU resulted in the production of over 50 international peer-reviewed papers and a number of exchanged PhD and postdoctoral researchers, which mostly focused on brachiopods and their lophotrochozoan relatives. Notably, an increasing number of brachiopods are discovered in the Cambrian Konservat-Lagerstätten, yet extraordinarily preserved non-mineralized shell interior soft tissue and organs, including lophophores or digestive tracts, are exclusively restricted to the celebrated fauna, such as Chengjiang and Guanshan Lagerstätten in East Yunnan of China, and known so far for only a very fraction of genera and species. For the first time we conducted a micro X-Ray Fluorescence (µXRF) investigation on the Series 2 brachiopods from eastern Yunnan of China, and present the first evidence on the lophophore imprints, well revealed by using µXRF scanning of shell valves of Cambrian brachiopods from the Families Botsfordiidae, Acrothelidae and Neobolidae, and Acrotretidae within Subphylum Linguliformea of Brachiopoda. All the lophophores are impressed as more or less coiled ridges and preserved with high concentrations of Fe (iron oxide) in the internal moulds of certain heavily mineralized shell valves with circular or subcircular contours. Apparently, the lophophores are spirolophs, showing great similarities to those known from the fossil and Recent lingulids. In conjunction with the fossil lophophores described earlier from the Chengjiang fauna, the paper presents a more complete picture of the suspension-feeding organizations of lophophores in nearly all the Cambrian brachiopods among 13 Families within 6 Orders within 2 subphyla of Linguliformea and Rhynchonelliformea. Accordingly, the new discoveries of spirolophs in different taxa of Cambrian brachiopods provide further fossil support for the idea that a spirolophe is the most basal and common lophophore state among brachiopods. By contrast, all the Cambrian brachiopod lophophores differ distinctly from the tuft-like arrangement of tentacles in hyolithids, suggesting that hyoliths are more likely to be basal members of the lophotrochozoans rather than lophophorates closely linked with the Phylum Brachiopoda.

References

Zhang, Z.F., Strotz, L.C. & Topper, T.P. et al., 2020a: An encrusting kleptoparasite-host interaction from the early Cambrian. *Nature Communications 11*, 1-7.

Zhang, Z.F., Holmer, L.E. & Liang, Y. et al., 2020b: The oldest 'Lingulellotreta' (Lingulata, Brachiopoda) from China and its phylogenetic significance: integrating new material from the Cambrian Stage 3–4 Lagerstätten in eastern Yunnan, South China. *Journal of Systematic Palaeontology 18*, 945–973.

Zhang, Z.F. & Holmer, L.E., 2013: Exceptionally preserved brachiopods from the Chengjiang Lagerstätte (Yunnan, China): Perspectives on the Cambrian explosion of metazoans. *Science Foundation in China 21*, 66-80.

Thematic Session 10
Petrology & mineralogy

Session Chairs:
Jenny Andersson (jenny.andersson@sgu.se)
Ulf B. Andersson (ulf.b.andersson@lkab.com)
Hannes Mattsson (hannes.mattsson@geo.uu.se)
Dan Holtstam (dan.holtstam@nrm.se)

Uranium mineralizations in Kiirunavaara, Sweden

Ulf B. Andersson[a], Diego Segovia Menard[b,c], Jarosław Majka[b]

[a]Luossavaara-Kiirunavaara AB, Research & Development, TG, FK9, SE-981 86 Kiruna, Sweden, ulf.b.andersson@lkab.com; [b]Institute of Earth Sciences, Uppsala University, Villavägen 16, 752 36 Uppsala, Sweden; [c]Luossavaara-Kiirunavaara AB, EXG, FK9, SE-981 86 Kiruna, Sweden;

Summary. The presence of U and Rn in mine water and air has prompted a search for its origin. Samples with elevated U contents were identified and observed to consist of hydrothermally altered, sulphate-rich country rocks to the ore, containing U minerals. Uraninite samples have mostly unaltered compositions and dominantly show chemical ages of 1.88–1.76 Ga. Other U minerals, partly unknown, do not show reliable ages. The paragenesis suggests that these U-bearing veins are soluble in water circulating in the rock, transporting U into the mine infrastructure.

Background

In recent years elevated contents of U and Rn in the mine waters and air in the LKAB Kiirunavaara mine have become an increasing concern. Because the origin of the U has been unknown, this study was undertaken to search for the source/s in the rock mass. After scrutinizing the drill core geochemical database, a number of rocks with elevated U contents (up to c. 100 ppm) were identified and sampled for thin section preparation, petrographic examination and mineral analysis.

Results

All samples were found in the foot or hanging wall rocks, and most in relative proximity to the iron ore. The U-enriched samples are of two main types: i) altered quartzofeldspatic metavolcanic rocks, often rich in mica/chlorite, titanite, allanite, some sulphides, more or less rich in sulphates (anhydrite/gypsum) and carbonates in the groundmass or in small veins (Fig. 1A), ii) larger veins (dm scale) dominated by rather coarse anhydrite/gypsum and titanite, with rutile, Fe-oxides, quartz, carbonates, and some feldspar, mica, allanite, epidote and sulphides. The former type generally shows textural evidence for hydrothermal fluid flow by anastomosing oriented mica seams and small veins of sulphates, while the latter appear to be larger equivalents of sulphate-dominated veins.

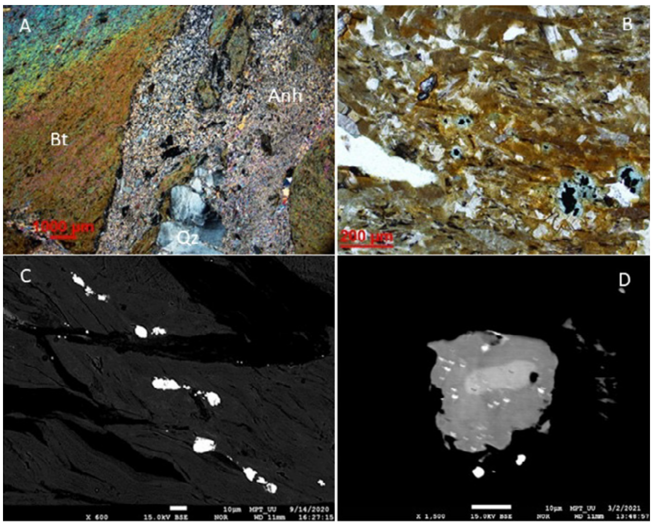

In the former type, ubiquitous uraninite have been found, typically as small grains (up to a few tens of mm) included within masses of biotite/chlorite (Figs. 1B, C), often associated with allanite. In the second type, uraninite is uncommon and replaced by brannerite, thorite, and at least two unknown U minerals (Fig. 1D) associated with the titanite, rutile, quartz etc.

Figure 1. A. Biotite-rich rhyodacite penetrated by a fine-grained vein of mostly anhydrite (sample 87115A). Crossed nicols. B. Biotite-rich area (sample 19076) showing uraninite with green radiation haloes. Parallel nicols. C. BSE photo of uraninite in mica mass (sample 87115A). D. BSE photo of inhomogeneous, unknown U-mineral (sample 19024A).

The uraninite samples show UO_2 contents of 64–72 wt% with totals between 91 and 98%. ThO_2 contents are low: 0–3.0%, while PbO contents are high: 15.7–20.5%, except for one. The sums of REE_2O_3 are in the range 4.0–10.7%. CaO is below 1.6 and FeO below 3.1%, while all other elements are below 1%. These are compositions overlapping well with data from the literature (e.g. Alexandre et al. 2016). Based on charge balance calculations the $U^{6+}/(U^{6+} + U^{4+})$ ratios are in the range 0.16–0.47. UO_2 and ThO_2 contents of the associated titanite and allanite are very low (all below 0.2%).

Brannerite encountered in one sample has c. 45% UO_2 and c. 27% TiO_2, and a sum c. 100%, similarly high REE_2O_3 contents as uraninite, and several % of ThO_2, PbO, CaO and FeO. Thorite, found in one sample, has c. 70% ThO_2, 17–19% SiO_2, c. 2% UO_2 and low contents of other elements. Two U minerals with unusual compositions were encountered. One show 27–39% UO_2, 37–40% TiO_2, 1.9–3.5% CaO, 1.3–3.4% FeO, 1.6–4.9% SiO_2, 6.2–18.9% REE_2O_3, and a few % of PbO and ThO_2, with totals of 93.5–98.3%. The other one is SiO_2-rich (19–20%), with 20–21% UO_2, 32–34% TiO_2, 4.6–4.8% CaO, 2.2–4.5% FeO, 3.0–3.2 Al_2O_3, 2.2–2.4% ThO_2, very low PbO, 8.4–9.1% REE_2O_3, and totals of 95–97%. We have not been able to fit these to any known U minerals.

Discussion and conclusions

The U minerals in Kiirunavaara are associated with mica-rich zones and anhydrite-rich veins in the country rocks to the iron ore, formed by sulphur/sulphate-rich (partly also carbonate) hydrothermal activity at some stage after crystallization of the silicate rocks.

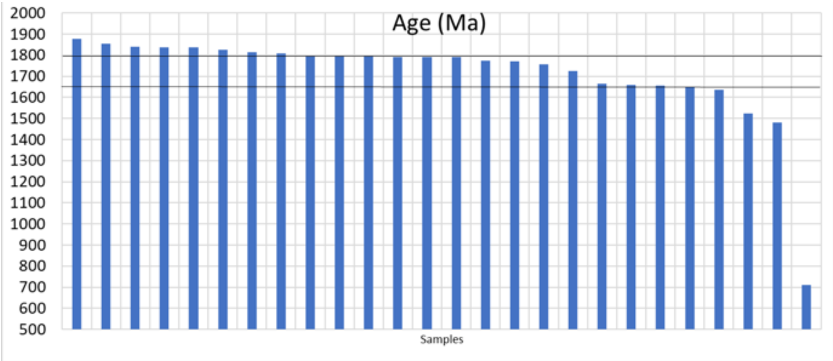

Figure 2. Chemical ages (after Montel et al. 1996) calculated for the Kiirunavaara uraninites. Most centre around 1800 Ma, some close to 1650 Ma, and a few younger that presumably lost Pb.

Calculation of U-Th-Pb chemical ages (Montel et al. 1996) of the uraninite samples, assuming that all Pb is radiogenic, yield ages of 1482–1877 Ma, except one at 709 Ma (Fig. 2), where most of the data are in the range 1.76–1.88 Ga, centring around 1.80 Ga. Younger ages may represent Pb loss or later events of uraninite growth, but the majority of data suggest that the main event/s of hydrothermal uraninite precipitation occurred in early–late Svecofennian time (1.88–1.76 Ga). The other U minerals all show calculated ages of 660 Ma or younger, probably reflecting Pb loss rather than real events. As a comparison, a province rich in uraninite, formed at c. 1.75 Ga, has been identified about 250 km south of Kiruna (e.g. Adamek & Wilson 1979).

There are indistinct chemical correlations between decreasing UO_2 and PbO and increasing $CaO+FeO+SiO_2+Al_2O_3$, but no correlation of the latter with calculated age, as would be expected from alteration of uraninite (e.g. Alexandre & Kyser 2005). This, together with a rough correlation of decreasing UO_2 with increasing $Y_2O_3+ThO_2$ seem to suggest that most of the chemical variations are primary and not due to alteration of uraninite.

In conclusion, U mineralizations in Kiirunavaara are associated with sulphur/sulphate-rich hydrothermal fluids, penetrating the rocks and precipitating uraninite somewhere in the time span 1.88-1.76 Ga, possibly also partly later. The mineral chemistry of uraninite is dominantly primary unaltered, but it contains some amount of U^{6+}. Brannerite, thorite and some unknown U minerals also formed locally. The association of the U minerals with easy soluble sulphates and carbonates can explain the elevated contents of U and Rn in mine air and water, as brittle fracturing in the rock mass preferentially may occur in such weak zones and thus channelize water in the rock mass.

References

Adamek, P. &Wilson, M., 1979: The evolution of a uranium province in northern Sweden. Phil. Trans. R. Soc. Lond. A 291, 355–368.

Alexandre, P. & Kyser, T., 2005: Effects of cationic substitutions and alteration in uraninite, and implications for the dating of uranium deposits. The Canadian Mineralogist, 43(3), 1005–1017.

Alexandre, P., Kyser, K., Layton-Matthews, D., Joy, B. & Uvarova, Y., 2015: Chemical compositions of natural uraninite. The Canadian Mineralogist, 53(4), 595–622.

Montel, J.-M., Foret, S., Verschambre, M., Nicollet, C. & Provost, A., 1996: Electron microprobe dating of monazite. Chem. Geol. 131, 37–53.

Records of crustal assimilation in Neoproterozoic metaigneous rocks from Southwest Svalbard

Abigail K. Barker[a], Karolina Gołuchowska[b], Maciej Manecki[b], Jarosław Majka[a,b], Karolina Kośmińska[b], Robert M. Ellam[c], Jakub Bazarnik[d], Karol Faehnrich[e]

[a]Department of Earth Sciences, Uppsala university, Uppsala, Sweden, abigail.barker@geo.uu.se [b]AGH University of Science and Technology, Faculty of Geology, Geophysics and Environmental Protection, Kraków, Poland, [c]Scottish Universities Environmental Research Centre, East Kilbride, UK, [c]Polish Geological Institute, Kraków, Poland, [e]Department of Earth Sciences, Dartmouth College, Hanover, USA

Summary. Late Neoproterozoic lavas, dykes and tuffs are found in SW Svalbard, they were metamorphosed under greenschist facies conditions during the Caledonidian orogeny. We aim to determine the role of magma-crust interaction and identify the crustal assimilants involved in the genesis of these metaigneous rocks. Enrichment in trace elements and Sr-Nd isotopes traces assimilation with pelitic assemblages as well as lower crustal granulites and amphibolites. We observe spatial variations in the extent and compositions of crustal assimilants.

Late Neoproterozoic metavolcanic rocks and associated feeder dykes are exposed in Southwest Spitsbergen, Svalbard. The primary magmas traversed the continental crust to the sites of eruption and subvolcanic intrusion. The continental crust was approximately 40 km thick at the time of the magmatic activity and the stratigraphy reveals lower crustal granulites and amphibolites overlain by an upper metasedimentary crust. We set out to investigate the magmatic processes and signs of magma-crust interaction preserved in the metaigneous rocks. We employed trace element geochemistry and Sr-Nd isotopes to fingerprint magma-crust interaction.

The metaigneous rock suite includes basaltic lavas, dolerite dykes and felsic tuff. The lavas, dykes and tuffs are metamorphosed under greenschist facies conditions during the Caledonian orogeny. The primary magmatic compositions are dominantly preserved over variations in the geochemistry caused by metamorphism. They show elevated LILE and LREE compositions and have $^{87}Sr/^{86}Sr_{(635\ Ma)}$ of 0.7040 to 0.7305 and $^{143}Nd/^{144}Nd_{(635\ Ma)}$ of 0.5115 to 0.5125. The concentrations of several trace elements such as Ba, Rb, La increase with corresponding decrease in $^{143}Nd/^{144}Nd_{(635\ Ma)}$ (Figure 1).

We observe two geochemical trends between the parental magma source and enriched crustal sources. One trend extends to low $^{143}Nd/^{144}Nd_{(635\ Ma)}$ at low to intermediate $^{87}Sr/^{86}Sr_{(635\ Ma)}$ and the second trend is towards very high $^{87}Sr/^{86}Sr_{(635\ Ma)}$ at intermediate to high $^{143}Nd/^{144}Nd_{(635\ Ma)}$ (Figure 1). These trends are associated with assimilation of lower crustal granulites or amphibolites and upper crustal pelites respectively. In the northern part of the study area assimilation of carbonate assemblages is apparent. The patterns of assimilation vary spatially, with degrees of crustal assimilation increasing from North to South corresponding to a shift in the upper crustal assimilants from mixed carbonate-pelite lithologies to dominantly pelites. The lower crust to upper crust boundary and the presence of impermeable pelitic layers in the upper crust force ascending magmas to stall and assimilate the surrounding country rocks.

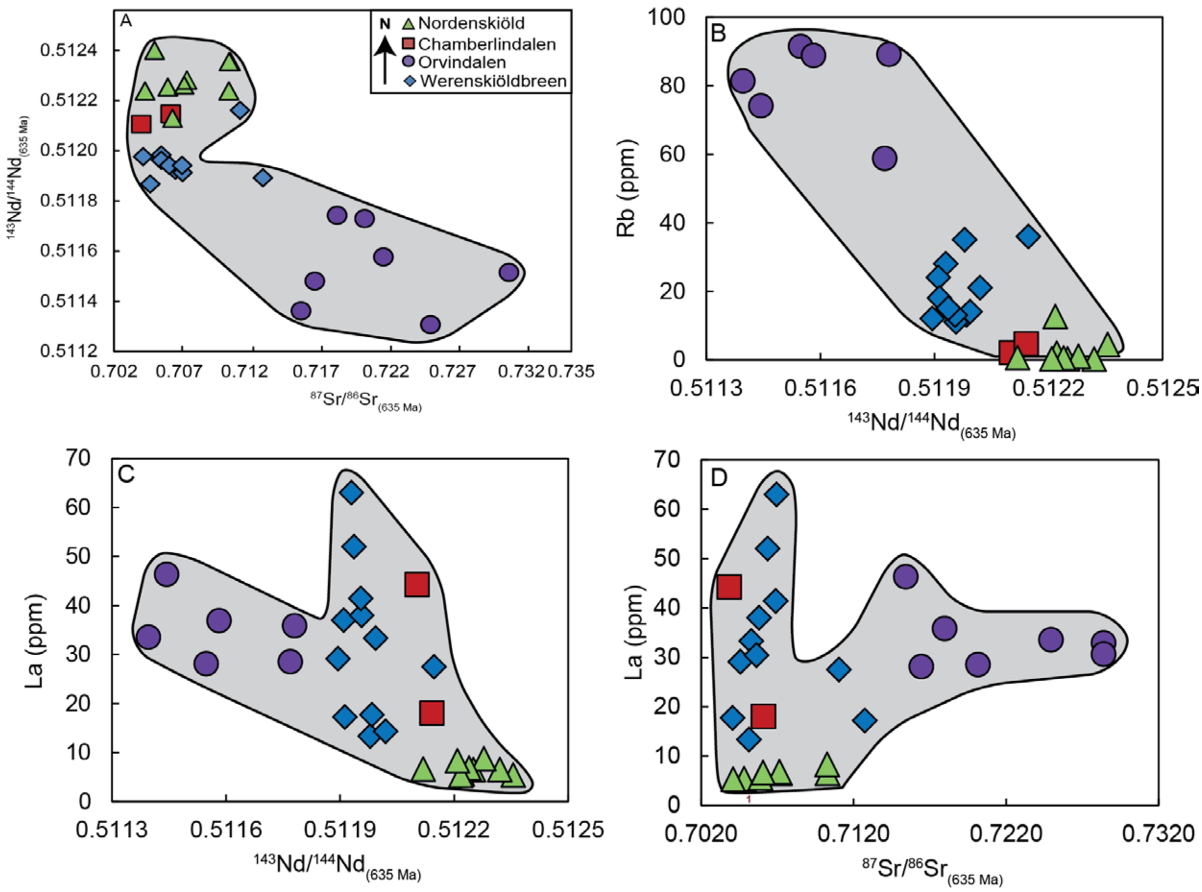

Figure 1. Geochemistry of metaigneous rocks from Svalbard. (A) Sr-Nd isotopes, (B) Increasing Rb concentration with decreasing Nd isotopes, (C) La concentration versus Nd isotopes, and (D) La concentration versus St isotopes. Data from Gołuchowska et al. 2022.

References

Gołuchowska, K., Barker, A.K., Manecki, M., Majka, J. Kośmińska, K., Ellam R., Bazarnik, J., Faehnrich, K., Czerny, J., 2022: The role of crustal contamination in magma evolution of Neoproterozoic metaigneous rocks from Southwest Svalbard. *Precambrian Research* 370, 106521.

Baggalútar from Hvalfjörður, Iceland: Mysterious spheroids of hydrothermally altered basaltic tephra

Emmie Djuse, Hannes B. Mattsson, Bjarne S.G. Almqvist

Department of Earth Sciences, Uppsala University, Uppsala, Sweden, emmie.djuse@hotmail.com

Summary. Enigmatic reddish-brown rock spheroids (*Icelandic*: baggalútar) of unknown origin can be found along beaches in Hvalfjörður, Iceland. Here we combine electron microprobe analyses with petrographic observations and measurements of magnetic susceptibility to characterize their primary and secondary mineral assemblages, as well as their internal textures. The results are compared to other geological spheroidal features found on Earth and Mars and their origin is discussed.

Well-rounded spheroids (baggalútar) can be found along the shorelines of Hvalfjörður in SW Iceland. They typically occur as either singles or doubles, but clusters of up to nine spheroids do occur (Fig. 1a). Internally they consist of two main components: an extremely fine-grained groundmass with randomly oriented crystals less than 15 µm in size, and zeolites that infill voids (Fig. 1b–c).

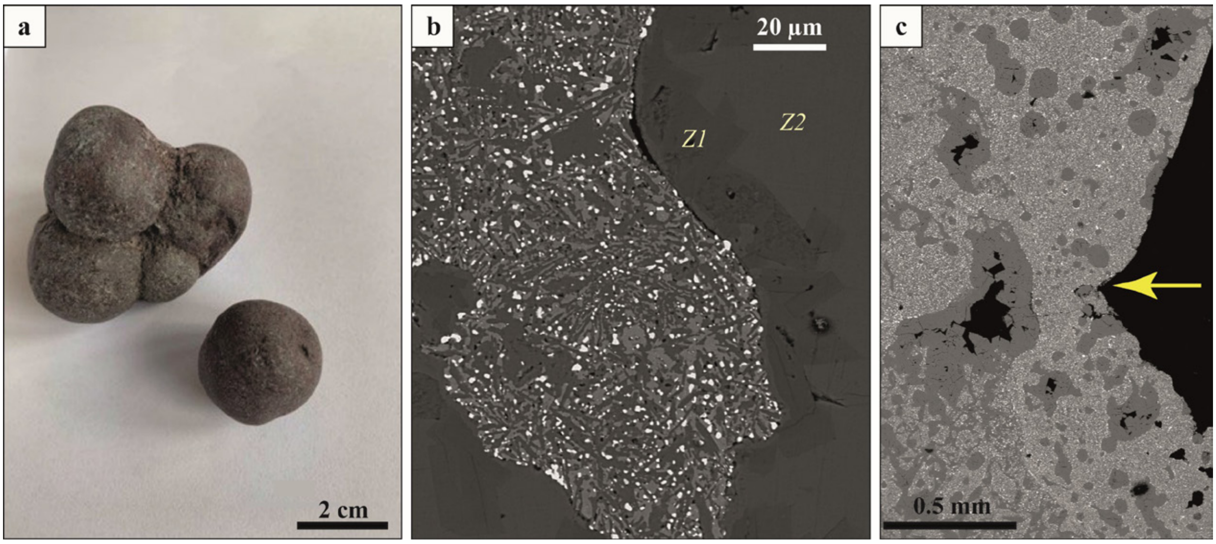

Fig. 1. Characteristic features for baggalútar. (a) Photograph showing baggalútar in hand specimens. (b) Close-up backscatter image showing randomly oriented minerals in the groundmass and infill of different zeolites in voids (*Z1* and *Z2*). (c) Backscatter image showing the area where two spheroids meet (indicated by arrow).

Microprobe analyses of the groundmass shows that it is predominantly composed of augitic clinopyroxene, Ti-magnetite and Ti-hematite (or possibly minute exsolution lamellae of ilmenite in magnetite too small to detect using the microprobe) together with subordinate amounts of plagioclase (An_{60}–An_{50}). In many places, the original plagioclase have been replaced by secondary zeolites. The Curie temperatures of ~470 °C and ~320 °C, together with the observed mineral chemistry, point towards FeTi-bearing oxides as ferromagnetic phases. The presence of a Mg-rich mineral (olivine?) and a P-rich mineral (apatite?) is indicated by area analyses using EDS, but if present these crystals were too small to be analyzed using the electron microprobe. The mineral assemblage of the groundmass is thus consistent with what could be expected in a relatively evolved tholeiitic basalt, similar to the 2.6 to 5.3 Ma rocks that dominate the exposed stratigraphy in the Hvafjörður area (Jóhannesson 2014).

The secondary minerals infilling voids and cavities are identified by microprobe analyses as thomsonite, stilbite, analcime, and chabazite ± apatite. XRD-spectra of additional samples indicate that heulandite-Ca and mesolite are present in some samples.

Whole-rock analyses show limited variation of the major elements between individual samples, which supports the petrographic observations that baggalútar are composed of basaltic tephra together with Si-poor zeolites in broadly similar ratios.

In nature there are many potential processes that can result in spheroidal shapes. The most simple explanation would be that the form reflects mechanical abrasion as a result of rolling on the beaches were they are found. This does not, however, explain the clusters of spheroids that occur (Fig. 1a). The marine environment suggest that they could be FeMn-nodules formed by hydrothermal processes on the ocean floor (Calvert 1978), that were washed up on the beaches during storms. However, such an origin can quickly be ruled out based on their bulk chemistry (moderate Fe- and Mn-contents, with very low Mn/Fe-ratios), basaltic mineralogy and the absence of concentric internal textures (Fig. 1c). An interesting alternative explanation is that baggalútar could be analoguous to the so-called “Moqui marbles” that form spheroidal concretions in the Navajo Sandstone in Utah (USA). Those spheroids have been interpreted to form by inundation of Fe-rich waters into quartz-rich sand, precipitating hematite interstitially between grains that results in spheroidal concretions (occuring alone or in clusters, Chan et al. 2000). Similar spheroidal structures were also found on the surface of Mars by the Opportunity rover in 2004 (commonly referred to as “Martian blueberries”). The “Martian blueberries” have been interpreted to form in a similar way as the “Moqui marbles”, but in a basaltic sediment rather than a quartz-rich sand (e.g. Chan et al. 2004). This could potentially explain the shape and bulk-rock composition of baggalútar from Hvalfjörður. However, measurements of temperature-dependent magnetic susceptibility show that no, or at least very little hematite, is present in our samples and therefore this specific process can also be excluded. A final explanation could be that baggalútar represent accretionary lapilli formed in a phreatomagmatic volcanic eruption involving external water. This could explain the basaltic mineralogy and the bulk chemistry, as well as the rapid crystallization (i.e. quench textures, Fig. 1b). However, accretionary lapilli typically have concentric internal textures which is at odds with what we observe in our samples. It also cannot explain why the internal textures are continuous across the contect where two spheroids meet (Fig. 1c).

Although the exact process that results in the spheroidal shapes of baggalútar remain undetermined, their internal textures strongly indicate that the final shape is caused by external factors. Finding an outcrop where they occur *in-situ* would greatly help to better understand their formation. The mineralogical and geochemical evidence show strong similarities to the other rocks found in the Hvalfjörður area, suggesting that they are probably derived from a local source. The zeolite assemblage observed in our samples is consistent with that previously described as the “mesolite zone” in Hvalfjörður (Weisenberger & Selbekk 2008). Thus, if we assume that the baggalútar we investigated are locally derived, their source should be located somewhere between 50 and 300 m above the sea level (Weisenberger & Selbekk 2008). Any attempts to find outcrops with baggalútar *in-situ* should therefore be focused on volcaniclastic beds occurring within this interval.

References

Calvert, S.E., 1978: Geochemistry of oceanic ferromanganese deposits. *Philosophical Transactions of the Royal Society of London, Series A, 249*, 43-73.

Chan, M.A., Parry, W.T. & Bowman, J.R,, 2000: Diagenetic hematite and manganese oxides and fault-related fluid flow in Jurassic sandstones, Southwestern Utah. *AAPG Bulletin 84*, 1281-1310.

Chan, M.A., Beitler, B., Parry, W.T., Ormö, J. & Komatsu, G., 2004: A possible terrestrial analogue for haematite concretions on Mars. *Nature 429*, 731-734.

Jóhannesson, H., 2014: Geological map 1:600 000. *Mál og Menning, Reykjavik*.

Weisenberger, T. & Selbekk, R.S., 2008: Multi-stage zeolite facies mineralization in the Hvalfjördur area, Iceland. *International Journal of Earth Sciences 98*, 985-999.

From the mantle to the surface: A petrological travel log recorded by melilititic lapilli in the Sälskär breccia (Alnö alkaline complex)

Vincent Gustafsson, Hannes B. Mattsson

Department of Earth Sciences, Uppsala University, Uppsala, Sweden, vincent.gustafsson.0466@student.uu.se

Summary. Primitive magmas can provide important details about the mantle from which they are derived. Here, we report petrographic observations and new mineral chemistry analyses of the Sälskär breccia at Alnö. The results are consistent with low-degree melting of a volatile-rich, metasomatized, mantle source (indicated by phlogopite and magmatic calcite). During ascent the melilititic magma entrained mantle debris and traveled rapidly through the crust. Pyroclast textures indicate an explosive eruption, and formation of a diatreme, within the uppermost 1.5 km of the paleosurface.

The Alnö alkaline complex is located approximately 10 km NE of Sundsvall in central Sweden. The intrusive complex has a roughly circular outline with a radius of about 2.5 kilometers. The rocks are mostly plutonic belonging the ijolite-meltegeite-urtite series, pyroxenites, nepheline-syenites and sövites together with a variety of alnöite dykes (von Eckermann 1948).

Petrographically, the Sälskär breccia consist of three main components (Fig. 1): (*i*) vesiculated melilititic lapilli, ranging in size from < 2 mm to 20 mm, displaying fluidal shapes and often have a central core consisting of olivine or phlogopite crystals, (*ii*) angular to subrounded clasts of sövite, ranging in size from a few mm to >30 cm, (*iii*) a carbonate-dominated matrix with randomly dipersed minerals from the the melilitite and the sövites as well as other xenolitic material (including mantle debris).

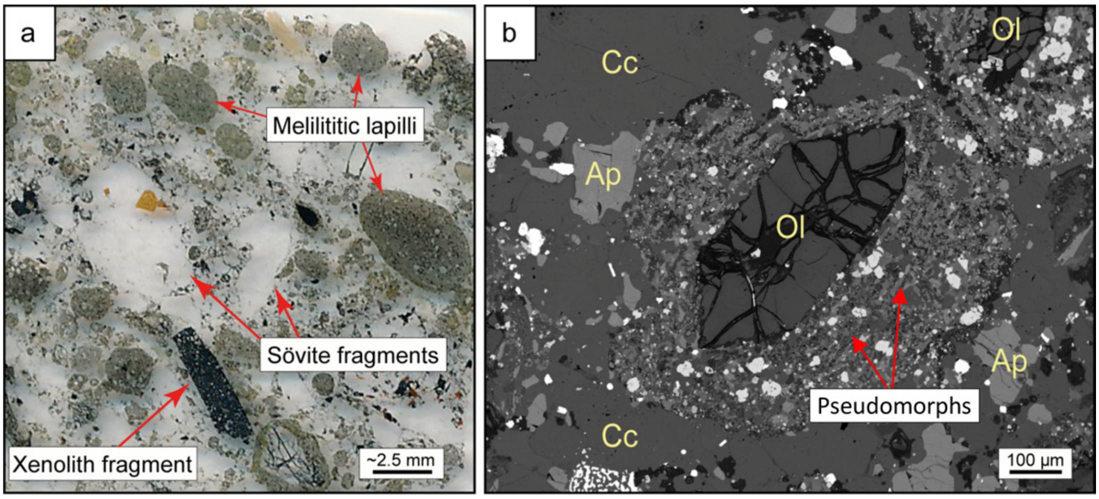

Fig. 1. Petrography of the Sälskär breccia. (a) Scan of thin section showing rounded melilititic lapilli and sövite fragments in a carbonate-dominated matrix. (b) Backscatter image showing a pelletal lapillus cored by an euhedral olivine crystal.

The juvenile melilititic lapilli have larger crystals of olivine and/or phlogopite together with occasional larger crystals of diopside and/or Ti-magnetite. The same minerals are also present in the groundmass together with Cr-spinel, monticellite, perovskite, apatite and calcite. In addition to this, pseudomorphs after an originally lath-shaped mineral (melilite?) are common. These laths are frequently preferentially aligned following the overall shape of the lapilli (Fig. 1b), indicating a fluidal origin for the pyroclasts.

Olivines range in composition from Fo_{97} to Fo_{77}, with most being ~Fo_{85}. The more primitive olivines ($Fo_{>90}$) in the lapilli generally have anhedral to subhedral shapes and are overgrown by a rim of more evolved composition (~Fo_{85}), whereas the population that clusters around Fo_{85} typically show euhdral shapes with minor normal zonation. The anhedral, high-Fo, olivines are interpreted to represent mantle-derived xenocrysts based on their shape and composition, whereas the euhedral olivines with normal zonation are intepreted to be in equilibrium in the melilititic magma.

Clinopyroxene and phlogopite also show primitive compositions with X_{Mg} ranging between 0.93–0.64 and 0.96–0.81 respectively. Early crystallizing Cr-spinel (28.4 to 17.7 wt% Cr_2O_3) have overgrowths of Ti-magnetite rims (1.6 to 13.8 wt% TiO_2), and late-crystallizing phlogopite are enriched in BaO and TiO_2. Such an evolution is consistent with countinuous crystallization within the system itself.

The presence of perovskite in the lapilli indicates a low silica-activity in the magma (Carmichael et al. 1970), which support the interpretation that the lath-shaped pseudomorphs are likely to represent melilite and not feldspar. Furthermore, phlogopite and primary euhdral calcite crystals indicate that the the magma was rich in volatiles (primarily CO_2, but also H_2O), which is in line with the vesiculated nature of some of the lapilli (Fig. 1) and with experimental data (Brooker et al. 2001).

The melilititic compotent of the Sälskär breccia is thus similar with primitive olivine melilitites reported elsewhere, and consitent with being formed by small degrees of melting of a metasomatized mantle source (e.g. Mattsson et al. 2013). Following magma formation within the mantle, the ascent through the crust was probably very rapid as the melilitite show no evidence of extensive fractionation. Moreover, rapid ascent is essential to keep mantle debris, such as that found in the carbonate-dominated matrix, entrained with an ascending magma (Sparks et al. 2006).

Spheroidal pelletal lapilli have been interpreted for form due to fluidization within a diatreme in explosive volcanic eruptions that involves low-viscosity magmas (Gernon et al. 2012). The petrography of the Sälskär breccia, with abundant pelletal lapilli (Fig. 1), exhibit a striking resemblance to that observed in kimberlites and olivine meliltitites elsewhere (e.g. Berghuijs & Mattsson 2013). We therefore interpret the Sälskär breccia to be remnants of the central parts of a diatreme, with the observed pelletal lapilli pointing to a maximum depth of <1.5 km from the surface at the time of the eruption.

References

Berghuijs, J.F. & Mattsson, H.B., 2013: Magma ascent, fragmentation and depositional characteristics of "dry" maar volcanoes: Similarities with vent-facies kimberlite deposits. *Journal of Volcanology and Geothermal Research 252*, 53–72.

Brooker, R., Kohn, S.C., Holloway, J.R. & McMillan, P., 2001: Structural controls on the solubility of CO_2 in silicate melts. *Chemical Geology 174*, 225-239.

Carmichael, I.S.E., Nicholls, J. & Smoth, A.L., 1970: Silica activity in igneous rocks. *American Mineralogist 55*, 246–263.

Gernon, T.M., Brown, R.J., Tait, M.A. & Hincks, T.K., 2012: The origin of pelletal lapilli in explosive kimberlite eruptions. *Nature Communications 3*, 832.

Mattsson, H.B., Nandedkar, R.H. & Ulmer, P., 2013: Petrogenesis of the melilititic and nephelinitic rock suites in the Lake Natron–Engaruka monogenetic volcanic field, northern Tanzania. *Lithos 179*, 175–192.

Sparks, R.S.J., Baker, L., Brown, R.J., Field, M., Schumacher, Stripp, J. & Walters, A., 2006: Dynamical constraints on kimberlite volcanism. *Journal of Volcanology and Geothermal Research 155*, 18–48.

Von Eckermann, H., 1948: The alkaline district of Alnö island. *Sveriges Geologiska Undersökning, Ca 36*, 232 p.

An ununusal mineral assemblage of Pb silicates

Dan Holtstam, Andreas Karlsson

Department of Geosciences, Swedish Museum of Natural History, Stockhom, Sweden, dan.holtstam@nrm.se

Summary. Rare assemblages of Pb silicates, from skarn in the Långban and Pajsbergs mines, Värmland, Sweden, have been investigated. Minerals observed are alamosite, barysilite, jagoite, joesmithite, melanotekite, nasonite and yangite, together with common metamorphic skarn components like andradite, diopside, hematite and quartz. Jagoite likely formed from primary melanotekite and quartz under the influence of a fluid with high Cl activity. Jagoite is prone to hydrothermal alteration, producing unidentified phases in the system CaO–PbO–SiO_2–H_2O–(±Cl_2).

Introduction

Lead silicates form a prolific category of compounds, occuring in both natural mineral assemblages (skarns) and in anthropogenic formations (e.g. metallurgical slags). The diversity is underpinned by the behaviour of the Pb^{2+} ion, with a stereoactive lone pair of electrons, and its influence on the structural arrangement of the tetrahedral SiO_4 units (Siidra et al. 2014). Pb as an environmental pollutant can be immobilized in silicate matrices, but the element may also be released during hydrothermal or supergene alteration of such compounds.

As minerals, Pb silicates are very rare globally, restricted to a few ore deposits, like Långban in Sweden (Holtstam & Langhof 1999), Franklin, New Jersey and the Kombat mine, Namibia. We have investigated museum samples not studied in detail before, from the Långban and Pajsberg Mn-Fe deposits, Filipstad, Värmland. The Långban material stems from an ocurrence in the *Canberra* stope at 220 m depth of the mine. Selected samples have been investigated under the scanning electron microscope fitted with an energy dispersion micro-analyzer, and with X-ray powder diffraction.

Table 1. Lead silicates found in the present study.

Alamosite (Aam)	$PbSiO_3$	Melanotekite (Mtk)	$Pb_2Fe_2[Si_2O_7]O_2$
Barysilite (Bsl)	$Pb_8Mn[Si_2O_7]_3$	Nasonite (Nso)	$Pb_6Ca_4[Si_2O_7]_3Cl_2$
Jagoite (Jg)	$Pb_{11}Fe_5Si_{12}O_{41}Cl_3$	Unknown (Uk)	$Pb_2Ca_3Si_5Cl_2O_{14}(OH)_6$ (?)
Joesmithite (Joe)	$PbCa_2(Mg_3Fe_2)[Si_6Be_2]O_{22}(OH)_2$	'Wickenburgite-like' (Wbul)	$Pb_3(Mn,Ca)Al_2Si_{10}O_{27}\cdot 4H_2O$
'Margarosanite-like' (Mgal)	$PbCa_2Si_3O_8(OH)_2$ (?)	Yangite (Ygi)	$PbMnSi_3O_8\cdot H_2O$

Preliminary results

The mineral assemblage is a highly heterogeneous skarn, with andradite, diopside, hematite, quartz, plus the lead silicates alamosite, barysilite, jagoite, joesmithite, melanotekite, nasonite and yangite, of which most approach their nominal chemical compositions (see Table 1). A wickenburgite-like mineral, which may represent an Mn-rich analogue of it, is present. A Pb-Ca silicate (with similar cation proportions as margarosanite) as well as an unkown Pb-Ca-Cl silicate – both formed via breakdown of jagoite – have also been observed. Other minerals ocurring in minor or trace amounts are: baryte, native lead, aegirine, fluorapophyllite-(K), calcite, talc, serpentine, albite, fluorapatite and phosphohedyphane. Långban is the second recorded locality of yangite (Fig.1, left), which is previously only known from its type specimen (Kombat). The refined triclinic unit-cell parameters of yangite from Långban is a = 9.597(2) Å, b = 7.281(2) Å, c = 7.968(2) Å, α = 106.03(1)°, 118.14(1)°, γ = 109.85(1)° and V = 392.7(1) Å^3, in good agreement with original data (Downs et al. 2016).

Discussion

The minerals of the skarn infered to be primary are melanotekite, barysilite, andradite, hematite, quartz and diopside. At some point, chlorine has been added to the system and formation of jagoite and nasonite has occurred, at the expense of the above minerals. Jagoite may be obtain directly from melanotekite and quartz via:

$$\underset{Mtk}{11\ Pb_2Fe_2Si_2O_9} + 2\ SiO_2 + 6\ HCl \rightarrow \underset{Jg}{2\ Pb_{11}Fe_5Si_{12}O_{41}Cl_3} + 6\ Fe_2O_3 + 3\ H_2O$$

However, there is no sharp boundary between the peak-metamorphic assemblage and later recrystallization products, since euhedral, poikiloblastic andradite contain jagoite inclusions (Fig. 1, right).

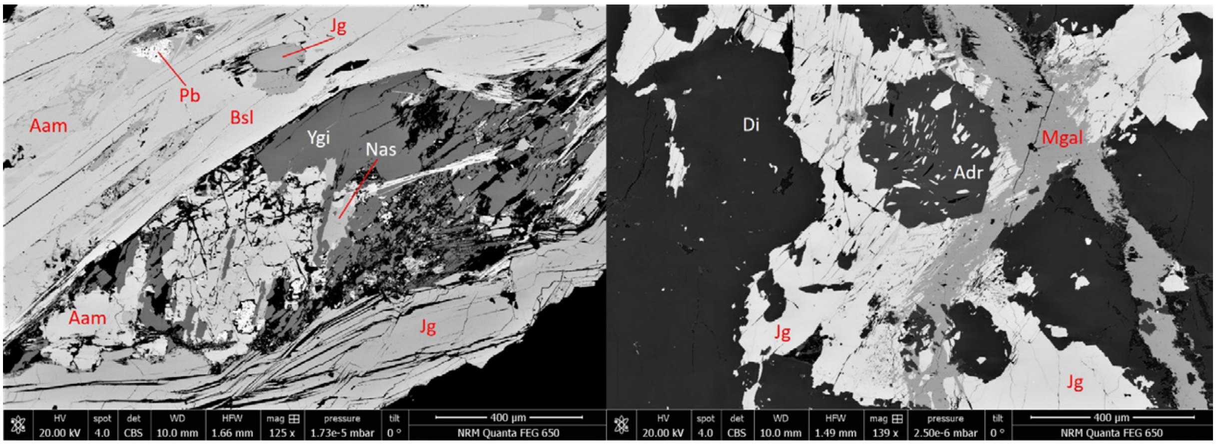

Fig. 1. Back-scattered electron images of polished sections from Långban. Mineral symbols from Table 1. Adr = andradite, Di = diopside, Pb = native lead.

Hydrothermal alteration of the above lead silicates, involving fluids bearing Ca^{2+} and SiO_2 (aq), likely has produced late-stage mineral formation. Our observations suggest alteration of jagoite according to reactions like (cf. Fig. 1, right):

$$\underset{Jg}{Pb_{11}Fe_5Si_{12}O_{41}Cl_3} + 22\ Ca^{2+} + 21\ SiO_2 + 27\ H_2O \rightarrow \underset{Mgal}{11\ PbCa_2Si_3O_8(OH)_2} + 5\ Fe^{3+} + 3\ Cl^- + 32\ H^+$$

The unknown Pb-Ca-Cl-O-H silicate may have formed in a similar kind of reaction with the addition of extra Cl. The presence of zeolitic H_2O in the secondary formed Pb silicates cannot be excluded. Barysilite may have been converted by:

$$\underset{Bsl}{Pb_8Mn[Si_2O_7]_3} + 4\ SiO_2 + H_2O = \underset{Ala}{7\ PbSiO_3} + \underset{Ygi}{PbMnSi_3O_8 \cdot H_2O}$$

(supported by the fact that alamosite is far more common than yangite in these assemblages). The wickenburgite-like mineral may also be a product of a hydrothermal alteration process. From the suggested reactions, it seems as most of Pb is retained in silicate minerals; however, the mechanisms of formation and paragenetical relations of native lead and phosphohedyphane are not clear.

References

Downs, R.T., Pinch, W.W., Thompson, R.M., Evans, S.H. & Megaw, L., 2016: Yangite, $PbMnSi_3O_8 \cdot H_2O$, a new mineral species with double wollastonite silicate chains, from the Kombat mine, Namibia. *American Mineralogist 101*, 2539–2543.

Holtstam, D. & Langhof, J., 1999: *Långban: the mines, their minerals, geology and explorers*. Raster Förlag. 215 pp.

Siidra, O.I., Zenko, D.S. & Krivovichev, S.V., 2014: Structural complexity of lead silicates: Crystal structure of $Pb_{21}[Si_7O_{22}]_2[Si_4O_{13}]$ and its comparison to hyttsjöite. *American Mineralogist 99*, 817–823.

The mineralogy and geochronology of an arfvedsonite-bearing monzonite at Balltorp in western Sweden

Andreas Karlsson[a], Thomas Zack[b]

[a]Department of Geosciences, Swedish Museum of Natural History, Stockholm, Sweden, andreas.karlsson@nrm.se;
[b]Department of Earth Sciences, University of Gothenburg, Göteborg, Sweden, thomas.zack@gu.se

Summary. Mineralogical investigation of a monzonite at Balltorp in western Sweden reveal that the major constituents are albite, microcline, arfvedsonite, aegirine and zircon. In addition, the two rare minerals astrophyllite and chevkinite-(Ce) were identified. U-Pb ages in zircon show that the rock crystallized at ~1330 Ma and was subsequently overprinted at the peak of the Sweconorwegian orogeny at ~1035 Ma. Rb-Sr analyses of microcline yield an age of 890 Ma and indicate that the area was hot for ca 140 Ma years.

Introduction and mineralogy

The Balltorp monzonite was first recognized by Lundegård (1953) as a "red-gray to red, predominantly acidic, alkali-rich gneiss" in which he described a feldspar and "alkali-hornblende" bearing rock south-west of Mölndal. On the basis of this and the U and Th flight maps the rock was targeted for Be-exploration in the 1980's but only slightly elevated Be-concentrations were found (Holmquist 1989). However, the most noteworthy results are highly elevated Zr and REE concentrations.

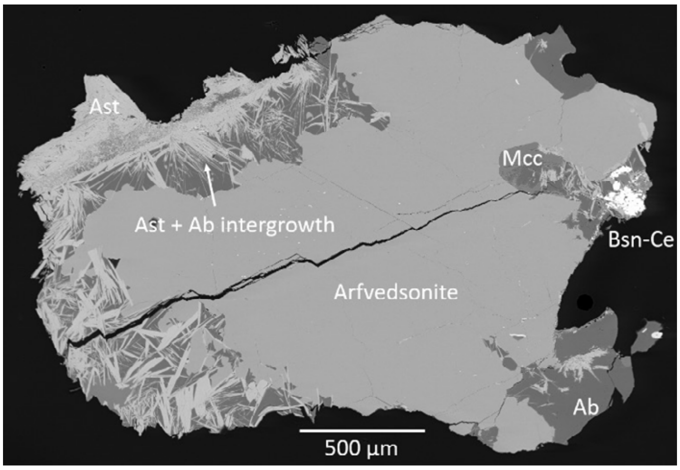

Fig. 1. SEM-BSE image of a fine intergrowth of albite (Ab) and astrophyllite (Ast) replacing arfvedsonite (Arf), primary microcline (Mcc) and secondary Bastnäsite-(Ce) (Bsn-Ce) also shown.

The main mineralogy is dominated by albite, microcline, arfvedsonite, fluorite and zircon, other minerals that are common in the Balltorp monzonite is monazite-(Ce), chevkinite-(Ce), ilmenite, aegirine, astrophyllite and minor bastnäsite-(Ce) see Fig. 1. Balltorp represents the first recorded Swedish locality for the quite rare silicate astrophyllite ($K_2NaFe^{2+}{}_7Ti_2Si_8O_{26}(OH)_4F$). Astrophyllite usually occurs in silica-undersatured rocks such as the Larvik Plutonic Complex (Norway), the Pilanesberg alkaline complex (South Africa) or the Khibiny alkaline massif (Kola, Russia). However, quartz occurs in subordinate amounts and is interpreted as texturally late. The rock grades from foliated medium-grained to unfoliated and very coarse-grained, the coarser type is comparatively richer in arfvedsonite. Most of the minerals are close to their ideal composition, however the fluorite is very Y-rich (6–7 wt%) while the ilmenite usually exhibit a significant pyrophanite component.

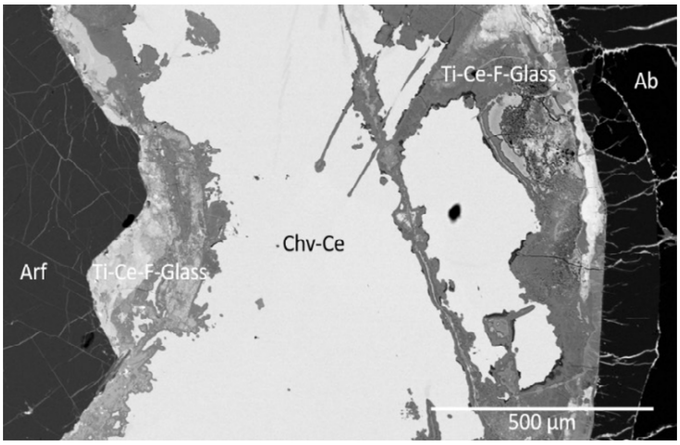

Fig. 2. SEM-BSE image of chevkinite-(Ce)(Chv-Ce) broken down to a Ti-Ce-F-rich glass in contact with the rock-forming silicates, the bright minerals lining the cleavage planes and fractures are mostly consisting of bastnäsite-(Ce).

Another peculiar mineral adding to the complexity of the Balltorp monzonite is chevkinite-(Ce), $Ce_4(Ti,Fe^{2+},Fe^{3+})_5(Si_2O_7)_2O_8$. It is usually metamict and have a broad glassy rim (normally enriched in Ce, Ti and F) surrounding more intact chevikinite-(Ce) cores (see Fig. 2). Chevkinte-(Ce) is not too uncommon in evolved and silica-undersatured rocks and is usually at least partly metamict (Macdonald et al. 2019). Another common secondary feature is small specks of bastnäsite-(Ce), thorite or euxenite-(Y) that has formed in the cleavage planes in arfvedsonite, microcline, albite and aegirine, or as inclusions in chevkinite-(Ce), or as fracture-coatings of the main silicates. Astrophyllite tend to form fanlike aggregates of up to a few mm in size which consists of numerous small individual crystals of a few µm each usually intergrown with albite. This texture is interpreted as a replacement of arfvedsonite, aegirine or ilmenite (see Fig. 1). The formation of secondary astrophyllite could be explained by the breakdown of the main silicates and fluorite, and the metamictization of chevikinite-(Ce). The subsequent release of Ti and F to the fluid, could facilitate astrophyllite crystallization.

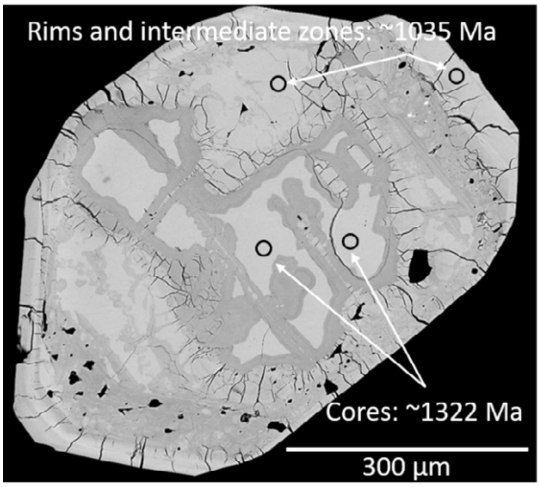

Fig. 3. Typical zircon from Balltorp. The inner homogenous cores yield ages of ~1322 Ma and the different cores yield ages of ~1035 Ma. Black rings represent 20 µm LA-ICP-MS/MS spots.

Zircon and monazite-(Ce) are unusually large and range from 200 µm to a few mm across. Furthermore, zircon displays an intricate zonation pattern (see Fig. 3), while the monazites have a simpler zonation pattern.

Geochronology and discussion

Ongoing geochronological investigation with the aid of *in situ* LA-ICP-MS/MS of the U-Pb systematics in zircon reveal a few small relict cores in some zircons. These zones are internally homogenous but display an embayed and corroded contact towards the other parts of the zircon. The preserved cores yield a concordant age at 1322±10 Ma. Other styles of zircon cores, intermediate zones and rims, all with different textures give a concordant Sweconorwegian age at 1035±8 Ma. The majority of the zircon domains give Sweconorwegian ages, in comparison to other rocks of Kungsbacka bimodal suite, wherein only very fine rims yield this age (see Hegardt et al. 2007). Additionally, *in situ* single spot Rb-Sr dating microcline using the protocols established by Rösel & Zack (in press) yielded an age of 898±6 Ma. For further details on Rb-Sr systematics, see Zack & Karlsson (this conference).

Zircon core ages reveal that the Balltorp monzonite is coeval with rocks of the Kungsbacka bimodal suite, which consists of both granitic and gabbroic intrusive magmas. Fluid-assisted recrystallization during the Sweconorwegian has reset most of the zircons at Balltorp and this event is contemporaneous with migmatiziation in the country rocks in the area (Hegardt et al. 2007). The microcline Rb-Sr data indicate that the Sweconorwegian orogeny was still quite hot ~140 million years after the peak metamorphism. Additionally, these new observations reveal that there were intrusive rocks with an alkaline to peralkaline character associated to the anorogenic magmatism at around 1330 Ma in the Western Segment.

References

Holmqvist, A., 1989: Be-F-Nb-REE-Sn-Ta-Th-U-Zr-mineraliserad granit i Västsverige. *In: Sveriges Geologiska AB,Division Prospektering, PRAP-Rapport 89026*; Geological Survey of Sweden: Uppsala, Sweden, 1989.

Macdonald, R., Bagiński, B., Belkin, H. E., & Stachowicz, M. 2019: Composition, paragenesis, and alteration of the chevkinite group of minerals. *American Mineralogist 104*(3), 348-369.

Lundegårdh, P.H., 1953: Petrology of the Mölndal-Styrsö-Vallda region in the vicinity of Gothenburg. *Sveriges Geologiska Undersökning C531*, 58 pp.

Hegardt, E. A., Cornell, D. H., Hellström, F. A., & Lundqvist, I., 2007: Emplacement ages of the mid-Proterozoic Kungsbacka bimodal suite, SW Sweden. *GFF 129*(3), 227-234.

Rösel, D., & Zack, T. in press: LA-ICP-MS/MS Single-Spot Rb-Sr Dating. *Geostandards and Geoanalytical Research*.

Zack, T., & Karlsson, A. 2022: Extreme initial $^{87}Sr/^{86}Sr$ ratios through metamorphic overprinting: an example from Balltorp (western Sweden). *This conference.*

The saga of the high and ultra-high pressure gneisses of the Seve Nappe Complex in Jämtland, Scandinavian Caledonides

Iwona Klonowska

Faculty of Geology, Geophysics and Environmental Protection, AGH University of Science and Technology, Kraków, Poland, klonowska@agh.edu.pl

Summary. In the last decade, the petrological and geochronological studies of the Seve Nappe Complex contributed to a better understanding of the subduction-collision processes in the Scandinavian Caledonides. Detailed investigations of the gneisses hosting high and ultra-high pressure eclogites and peridotites helped to constrain the metamorphic history of this unit. Below is a summary of the metamorphic processes recorded by the Seve gneisses.

Mineralogical and petrological studies of the high and ultra-high pressure (HP-UHP) metamorphic rocks provide evidence of subduction of the continental rocks to mantle depths (e.g. Gilotti 2013). In the Scandinavian Caledonides the deep continental subduction is recorded in the rocks from the Western Gneiss Region in southwestern Norway (e.g. Smith 1984, March et al. 2022) and its possible equivalent farther north in the Lofoten Islands (Froitzheim et al. 2016), the Tromsø Nappe in northern Norway (e.g. Janák et al. 2013a) and the Seve Nappe Complex (SNC) in Sweden (e.g. Gee et al. 2020 and references therein). These units, thus, together with the units bearing ophiolitic sequences, are the best targets for unraveling the processes occurring during the closure of the Iapetus Ocean and Baltica-Laurentia collision. The summary of the ~100 My-long subduction-contraction processes leading to the formation of the Scandinavian Caledonides is given by Majka (2022) in this abstract volume.

The research focus on the metamorphism in the SNC in Jämtland was primarily put on the self-evident HP rocks, i.e. eclogites and garnet peridotites that are interspersed within the continental crustal rocks, including gneisses, mica schists and quartzites and which occur in the northern part of Jämtland (e.g. van Roermund & Bakker 1983). Later studies have shown that the garnet peridotites and associated eclogite-pyroxenite dykes have reached UHP conditions (e.g. Brueckner et al. 2004, Janák et al. 2013b). The timing of the HP-UHP metamorphism is here estimated to c. 460–450 Ma (e.g. Brueckner and van Roermund 2007, Fassmer et al. 2017). In contrast, in west-central Jämtland neither eclogites nor garnet peridotites have been found so far, but possible retro-eclogites are present as garnet-clinopyroxene-plagioclase rocks. Paragneisses, often migmatized, dominate the SNC in this region. Detailed petrological and mineralogical studies by e.g. Ghosh et al. (1979) and Arnbom (1980) of the SNC paragneisses at Åreskutan suggested only amphibolite to lower granulite facies metamorphism of these rocks. Migmatization (peak temperature metamorphism) has been dated to ~440 Ma by e.g. Claesson (1982, 1987), which has been later confirmed by Ladenberger et al. (2014) and Majka et al. (2012). For the first time, the latter study showed evidence for an older higher grade event recorded in these gneisses, dated to c. 455 ± 11 Ma. Further investigations resulted in discoveries of microdiamond, the UHP index mineral, first at the Tväråklumparna Mt. (Majka et al. 2014) and later at the Åreskutan Mt. (Klonowska et al. 2017). The evidence of the UHP metamorphism in the latter has been supported by thermodynamic modelling (Klonowska et al. 2017) and, most recently, by re-homogenization experiments of the melt inclusions in garnets (Słupski et al. 2022, this abstract volume). The experiments show that the crustal melting occurred at 900 °C and 4.5 GPa. Dating of zircon in the diamond-bearing gneisses from the Tväråklumparna Mt. revealed that the deep subduction event is older than anticipated. The zircon overgrowths with eclogite facies chemical patterns yielded an age of ~483 Ma and the second zircon overgrowth with granulite facies signature yielded an age of ~439 Ma (Walczak et al. 2022). These results provide evidence for a protracted evolution of SNC in Jämtland, perhaps recording two subduction events, which agrees with the 'dunk-tectonic' model proposed by Brueckner & van Roermund (2004) and Brueckner (2006) for the Scandinavian Caledonides.

References

Arnbom, J.O., 1980: Metamorphism of the Seve Nappes at Åreskutan, Swedish Caledonides. *Geologiska Föreningens i Stockholm Förhandlingar 102*, 359-371.

Brueckner, H.K., 2006: Dunk, dunkless and re-dunk tectonics: a model for metamorphism, lack of metamorphism, and repeated metamorphism of HP/UHP terranes. *International Geology Review 48*, 978–995.

Brueckner, H.K., van Roermund, H.L.M. & Pearson, N., 2004: An Archean to Paleozoic evolution for a garnet peridotite lens with sub-Baltic Shield affinity within the Seve Nappe Complex of Jämtland, Sweden, Central Scandinavian Caledonides. *Journal of Petrology 45*, 415–437.

Brueckner, H.K. & van Roermund, H.L.M., 2004: Dunk tectonics: a multiple subduction/eduction model for the evolution of the Scandinavian Caledonides. *Tectonics 23*, TC2004.

Brueckner, H.K. & Van Roermund, H.L.M., 2007: Concurrent HP metamorphism on both margins of Iapetus: Ordovician ages for eclogites and garnet pyroxenites from the Seve Nappe Complex, Swedish Caledonides. *Journal of the Geological Society 164*, 117–128.

Claesson, S., 1982: Caledonian metamorphism of Proterozoic Seve rocks on Mt. Åreskutan, southern Swedish Caledonides. *Geologiska Föreningens i Stockholm Förhandlingar 103*, 291–304.

Claesson, S. 1987: Isotopic evidence for the Precambrian provenance and Caledonian metamorphism of high-grade paragneisses from the Seve Nappes, Scandinavian Caledonides. I. Conventional U– Pb zircon and Sm–Nd whole rock data. *Contributions to Mineralogy and Petrology 97*, 196–204.

Fassmer, K., Klonowska, I., Walczak, K., et al. 2017: Middle Ordovician subduction of continental crust in the Scandinavian Caledonides: an example from Tjeliken , Seve Nappe Complex, Sweden. *Contributions to Mineralalogy and Petrology 172*, 1–21.

Froitzheim, N., Miladinova, I., Janák, M., Kullerud, K., et al. 2016: Devonian subduction and syncollisional exhumation of continental crust in Lofoten, Norway. *Geology 44*, 223-226.

Gee, D.G., Klonowska, I., Andréasson, P.-G. & Stephens, M.B., 2020: Middle thrust sheets in the Caledonide orogen, Sweden: The outer margin of Baltica, the continent-ocean transition zone and late Cambrian-Ordovician subduction-accretion. In: Stephens, M.B., Weihed, J.B. (eds) Sweden: Lithotectonic Framework, Tectonic Evolution and Mineral Resources, *Geological Society, London, Memoirs,* pp. 517–548.

Ghosh, S.K., Roy, A.B. & Troëng, B., 1979: Superposed folding and metamorphism in the Seve nappe around Åreskutan in the Swedish Caledonides. *Geologiska Föreningens i Stockholm Förhandlingar 101*, 85–103.

Gilotti, J.A., 2013: The Realm of Ultrahigh-Pressure Metamorphism. *Elements 9*, 255-260.

Janák, M., Van Roermund, H., Majka, J. & Gee, D.G., 2013b: UHP metamorphism recorded by kyanite-bearing eclogite in the Seve Nappe Complex of northern Jämtland, Swedish Caledonides. *Gondwana Research 23*, 865–879.

Janák, M., Ravna, E.J.K., Kullerud, K., Yoshida, K., Milovský, R. & Hirajima, T., 2013a: Discovery of diamond in the Tromsø Nappe, Scandinavian Caledonides (N. Norway). *Journal of Metamorphic Geology 31*, 691–703.

Klonowska, I., Janák, M., Majka, J., et al. 2017: Microdiamond on Åreskutan confirms regional UHP metamorphism in the Seve Nappe Complex of the Scandinavian Caledonides. *Journal of Metamorphic Geology 35*, 541–564.

Ladenberger, A., Be'eri-Shevin, Y., Claesson, S., Gee, D.G., Majka, J. & Romanova, I.V., 2014: Tectonometamorphic evolution of the Åreskutan Nappe – Caledonian history revealed by SIMS U-Pb zircon geochronology. In: Corfu, F., Gasser, D. & Chew, M. (eds) New Perspectives on the Caledonides of Scandinavia and Related Areas. *Geological Society, London, Special Publication 390*, 337-368.

Majka, J., 2022: Subduction of a Baltica margin followed by Baltica-Laurentia collision during the Cambrian to Devonian as part of the assembly of Pangaea. *This abstract volume*.

Majka, J., Be'eri-Shlevin, Y., Gee, D.G., Ladenberger, A., Claesson, S., Konečný, P. & Klonowska, I., 2012: Multiple monazite growth in the Åreskutan migmatites: evidence for a polymetamorphic Late Ordovician to Late Silurian evolution in the Seve Nappe Complex of the west-central Jämtland, Sweden. *Journal of Geosciences 57*, 3-23.

March, S., Hand, M., Tamblyn, R., et al. 2022: A diachronous record of metamorphism in metapelites of the Western Gneiss Region, Norway. *Journal of Metamorphic Geology*, https://doi.org/10.1111/jmg.12660

Słupski, P., et al. 2022: Former melt inclusions in garnet from UHP gneisses of the Seve Nappe Complex (Scandinavian Caledonides). 150 year anniversary meeting of the Geological Society of Sweden. *This Abstact volume*.

Smith, D.C., 1984: Coesite in clinopyroxene in the Caledonides and its implications for geodynamics. *Nature 310*, 641–644.

van Roermund, H.L.M. & Bakker, E., 1983: Structure and metamorphism of the Tången—Inviken area, Seve Nappes, Central Scandinavian Caledonides. *Geologiska Föreningen i Stockholm Förhandlingar, 105*, 301–319.

Walczak, K., Barnes, C.J., Majka, J., Gee, D.G. & Klonowska, I. 2022: Zircon age depth-profiling sheds light on the early Caledonian evolution of the Seve Nappe Complex in west-central Jämtland. *Geoscience Frontiers 13*, 101112.

Rutile petrochronology: fundamentals and applications

Ellen Kooijman[a], Matthijs A. Smit[b]

[a]Department of Geosciences, Swedish Museum of Natural History, Stockholm, Sweden, ellen.kooijman@nrm.se;
[b]Department of Earth, Ocean and Atmospheric Sciences, University of British Columbia, Vancouver, Canada, msmit@eoas.ubc.ca

Summary. Petrochronology is a rapidly growing branch of geoscience, which focusses on linking time with specific rock-forming processes and their physical conditions. Using analytical aspects in petrology, geochemistry and geochronology, this technique allows detailed linkage of a petrogenetic process to time. This combination leads to a better understanding of petrogenetic processes than petrology or geochronology alone. Rutile has provided a new avenue in the field of petrochronology. In this contribution, we investigate the fundamentals of rutile petrochronology and explore its application in a number of case studies representing different geological settings.

Introduction

Rutile (TiO_2) is a common accessory mineral in metamorphic rocks and also occurs in Ti-rich igneous rocks, mantle xenoliths, meteorites, and as a detrital mineral in clastic sediments. Rutile provides a myriad of opportunities for studying the history of such rocks, because it 1) provides a reliable single-mineral thermometer – the Zr-in-rutile thermometer (e.g. Zack et al. 2004, Tomkins et al. 2007) – which retains temperature information even up to ultra-high temperature conditions; 2) is a main host of high field strength elements (HFSE), which can be used to constrain crust-mantle differentiation and subduction-zone metamorphism (e.g. Rudnick et al. 2000); 3) exhibits high U/Pb, thus enabling U-Pb dating. The utility of rutile U-Pb dating in thermochronology has greatly increased due to improved constraints on the closure temperature (T_c) for Pb diffusion. This temperature is in the range of 500–650 °C (e.g. Cherniak 2000, Kooijman et al. 2010) making rutile U-Pb thermochronlogy complementary to high-T U-Pb chronology using zircon and monazite, as well as to low-T thermochronology using phases such as apatite. Rutile chronology thus can be used to investigate and date a range of processes from igneous eruptions to the cooling history of metamorphic terranes. In this presentation, we show the versatility of rutile in the study of petrological and tectonic processes and highlight new approaches towards further expanding the rutile analytical toolkit.

Rutile as a new approach to date volcanic eruptions

The intermediate-T closure temperature lies well below most solidus temperatures, meaning that rutile U-Pb dates could be used to date volcanic eruptions. Although rutile is typically not present in lavas, the mineral does occur in xenolith cargo derived from the middle crust down into the mantle. We have used rutile in xenoliths to successfully date volcanic eruptions in different settings. The first case study was done using crustal xenoliths hosted by Miocene carbonatites and alkali basalts in the Dunkeldik magmatic field, Pamir, Tajikistan. The xenoliths derive from c. 90 km depth within the thickened orogenic crust and comprise a diverse set of lithologies, including eclogites and high-pressure granulites. The eruption age was previously determined to be c. 11 Ma based on Ar-Ar dating (Hacker et al. 2005). In-situ U-Pb dating by laser ablation multi-collector inductively-coupled plasma mass spectrometry (LA-MC-ICP-MS) on rutile in ten xenolith samples yielded a consistent age of 11.17 ± 0.06 Ma. In a second case study, we dated rutile inclusions in diamond from the Mir kimberlite pipe, Siberia. Rutile U-Pb dating through secondary ionization mass spectrometry yielded a uniform U-Pb concordia age of 376 ± 7 Ma. Matrix rutile within the eclogitic paragenesis that contains the diamonds yielded c. 366 Ma – slightly younger than the inclusion ages. Differences in trace-element concentrations between matrix and inclusion rutile indicates that both originated in chemically different environments, and that rutile likely predates diamond formation. Radiogenic Pb accumulated only after entrapment in diamond (for inclusions) or eruptive quenching (for matrix rutile). Rutile petrochronology thus provides one of the very few approaches that can provide petrological and age constraints on diamond formation and kimberlite eruption.

Thermal histories of metamorphic terranes

Rutile petrochronology provides a prime research avenue in tectonics research. Conventionally, this involved the analysis of many grains, either through bulk-grain analysis or in-situ through LA-ICP-MS. Analytical advances now allow U/Pb age profiles to be resolved in single rutile grains (e.g. Kooijman et al. 2010). Diffusion forward modelling can be used to constrain thermal histories of metamorphic terranes (e.g. Harrison & Zeitler, 2005). Here, we explore this avenue for rutile through two case studies. The first example is set in the Western Gneiss Complex of Norway (WGC), which is an archetypal continental (ultra)high-pressure (UHP) terrane. Rutile petrochronology was previously used by Cutts et al. (2019) across the WGC to constrain peak T, the timing of midcrustal cooling, and governing exhumation processes, including flexural rebound, slab flattening and exhumation through removal of an overlying plateau. High spatial-resolution U-Pb age transect analysis by LA-MC-ICP-MS was done on a single grain from a UHP eclogite. An age gradient of over 30 Myr was found over a radial distance of c. 200 µm. When coupled with peak-T estimates from Zr-in-rutile in the same grain, diffusion forward modelling allowed the thermal history during this time to be resolved. A similar approach was done on a slowly cooled granulite from the Saglek Block (SB), Nain Province, Labrador, Canada, which is a terrane from a fundamentally different time and tectonic setting as the WGC; the SB is an Archean craton within the Canadian Shield, with a history dating back to c. 3.8 Ga. Rutile within the granulite provided an age range of 140 Myr over a c. 50 µm radial distance. In both cases, age heterogeneity could be resolved at a precision of 1.5–2.0% (2 s.d.) and spatial resolution of ~14 µm. The thermal histories resolved from the WGC and SB rutile grains match those established for the two terranes through $^{40}Ar/^{39}Ar$ thermochronology. The examples demonstrate that rutile yields reliable and precise temperature and age information that can be combined to resolve full thermal histories from single crystals. The major advantages compared to conventional thermochronology are that the thermal histories obtained from rutile 1) show continuous time resolution for cooling through a temperature range of c. 300 °C, rather than a single blocking temperature, and 2) could be obtained by the analysis of a single grain, which takes hours, rather than weeks, of analytical time.

Conclusion

Through its trace-element and age signatures, rutile can be utilized to investigate a diverse range of geological processes. Rutile in xenoliths can, for instance, be used to date volcanic eruptions, which is particularly useful in the case of mafic and ultramafic magmas that are K-poor and do not produce conventional chronometric minerals such as zircon. Rutile allows precise time-resolved cooling histories of crustal terranes, specifically in the intermediate-T regime that is most relevant to studying exhumation processes. These are among the many features that makes rutile petrochronology one of the most promising new approaches in lithosphere research.

References

Cherniak, 2000: Pb diffusion in rutile. *Contrib. Mineral. Petrol. 139*, 198–207.

Cutts, J.A., Smit, M.A., Kooijman, E. & Schmitt, M., 2019: Two-stage cooling and exhumation of deeply subducted continents. *Tectonics 38*, 863–877.

Hacker, B.R., Luffi, P., Lutkov, V., Minaev, V., Ratschbacher, L., Plank, T., Ducea, M., Patiño-Douce, A., McWilliams, M. & Metcalf, J. 2005: Near-ultrahigh pressure processing of continental crust: Miocene crustal xenoliths from the Pamir. *J. Petrol. 46*, 1661–1687.

Harrison, T.M. & Zeitler, P.K., 2005: Fundamentals of noble gas thermochronometry. *Rev. Mineral. Geochem. 58*, 123–149.

Kooijman, E., Mezger, K. & Berndt, J., 2010: Constraints on the U-Pb systematics of metamorphic rutile from in situ LA-ICP-MS analysis. *Earth Planet. Sci. Lett. 293*, 321-330.

Rudnick, R.L., Barth, M., Horn, I., McDonough, W.F., 2000: Rutile-bearing refractory eclogites: missing link between continents and depleted mantle. *Science 287*, 278–281.

Schmitt, A.K., Zack, T., Kooijman, E., Logvinova, A.M. & Sobolev, N.V., 2019: U-Pb ages of rare rutile inclusions in diamond indicate entrapment synchronous with kimberlite formation. *Lithos 350-351*, 105251.

Tomkins, H.S., Powell, R. & Ellis, D.J., 2007: The pressure dependence of the zirconium-in-rutile thermometer. *J. Metamorph. Geol. 25*, 703–713.

Zack, T., Moraes, R. & Kronz, A., 2004: *Contrib. Mineral. Petrol. 148*, 471–488.

Stability of metamorphic index minerals in 'magnesium-altered' volcanic rocks from Bergslagen, Sweden

Alexander Lewerentz

Department of Mineral Resources, Geological Survey of Sweden, Lund, Sweden, alexander.lewerentz@sgu.se

Summary. 'Magnesium-altered' volcanic rocks are found throughout Bergslagen and often exhibit index minerals formed by regional metamorphism during the Svecokarelian orogeny. The prograde sequence of index minerals in 'magnesium-altered' volcanic rocks differs from the classic Barrovian sequence, such as that the stabilisation of garnet precedes biotite. Further work on 'magnesium-altered' volcanic rocks, and different styles of alterations, has the potential to significantly improve our understanding of the evolution of metamorphic conditions during the Svecokarelian orogeny.

Introduction

The geology of the Bergslagen lithotectonic unit in central Sweden is dominated by c. 1.91–1.89 Ga volcanic rocks with subordinate carbonate horizons and mafic intrusions, as well as related iron oxide and sulphide mineralisations (Stephens & Jansson 2020). The volcanic stratigraphy is intruded by c. 1.91–1.87 Ga granitoids. The area records two metamorphic events related to the Svecokarelian orogeny, at c. 1.86 Ga and c. 1.84–1.80 Ga, during which syn-orogenic granitoids were emplaced. Several generations of ser- to post-orogenic granitoids are also found in the area, as well as several generations of post-orogenic dolerites.

Different styles of regional hydrothermal alteration affected the volcanic succession prior to Svecokarelian regional metamorphism; Na alteration, K alteration, Ca±Mg±Fe 'skarn' alteration, and Mg±Fe±K±Si 'magnesium' alteration (Stephens & Jansson 2020). The 'magnesium alteration' resulted in destruction of feldspars and replacement by phyllosilicates (Stephens & Jansson 2020), which upon regional metamorphism favoured the growth of index minerals such as chlorite, biotite, garnet, andalusite, sillimanite, and cordierite (Trägårdh 1991). These index minerals coincide with those of the classic Barrovian sequence and have been used as indicators and estimators of metamorphic grade. But are these 'magnesium-altered' volcanic rocks comparable to the metapelites of the Barrovian sequence?

Previous assessments mainly use general petrogenetic grids and does not consider that mineral stability is affected by bulk rock composition. Here, I use bulk rock composition-specific phase equilibria calculations to revisit the 'magnesium-altered' rocks reported by Trägårdh (1991) and further investigate their importance for the understanding of metamorphic P-T conditions during the Svecokarelian orogeny.

Discussion

Index mineral stability in the least-altered volcanic rocks of Trägårdh (1991) is rather monotonic; biotite is stable over the entire investigated P-T window and makes a poor indicator of metamorphic grade (Fig. 1a). Chlorite and cordierite are good indicators for low and high metamorphic temperatures, respectively; however, they bracket most of the greenschist and amphibolite facies.

In comparison, the stability of chlorite and garnet in the 'magnesium-altered' rocks is expanded at the cost of biotite stability, and cordierite stability is slightly expanded towards temperatures as low as c. 500°C (Fig. 1b). Four isograds are thereby outlined; chlorite, garnet, biotite, and cordierite, and the appearance of these index minerals constitute useful indicators of increasing metamorphic grade. Because of the low-temperature stability of garnet, the garnet isograd precedes the biotite isograd which contrasts to the classic Barrovian sequence of index minerals.

Chlorite and biotite are as index minerals generally associated with greenschist facies metamorphism, and likewise garnet with amphibolite facies metamorphism. The high-T stability of chlorite and low-T stability of garnet (Fig. 1b), respectively, may lead to either over- or underestimation of the metamorphic grade of 'magnesium-altered' metavolcanic rocks if only using the index minerals as indicators of metamorphic grade and not taking bulk rock compositions into account. The wider implication being, in a worst-case scenario, misinterpretation of the regional metamorphic evolution.

Although only the 'magnesium' style of alteration is investigated here, it is reasonable to assume that the other main styles of alteration (K, Na, and 'skarn') affect index mineral stability differently. Further studies of phase equilibria in altered volcanic rocks from several locations throughout Bergslagen has the potential to significantly increase our understanding of the metamorphic P-T regimes during the Svecokarelian orogeny.

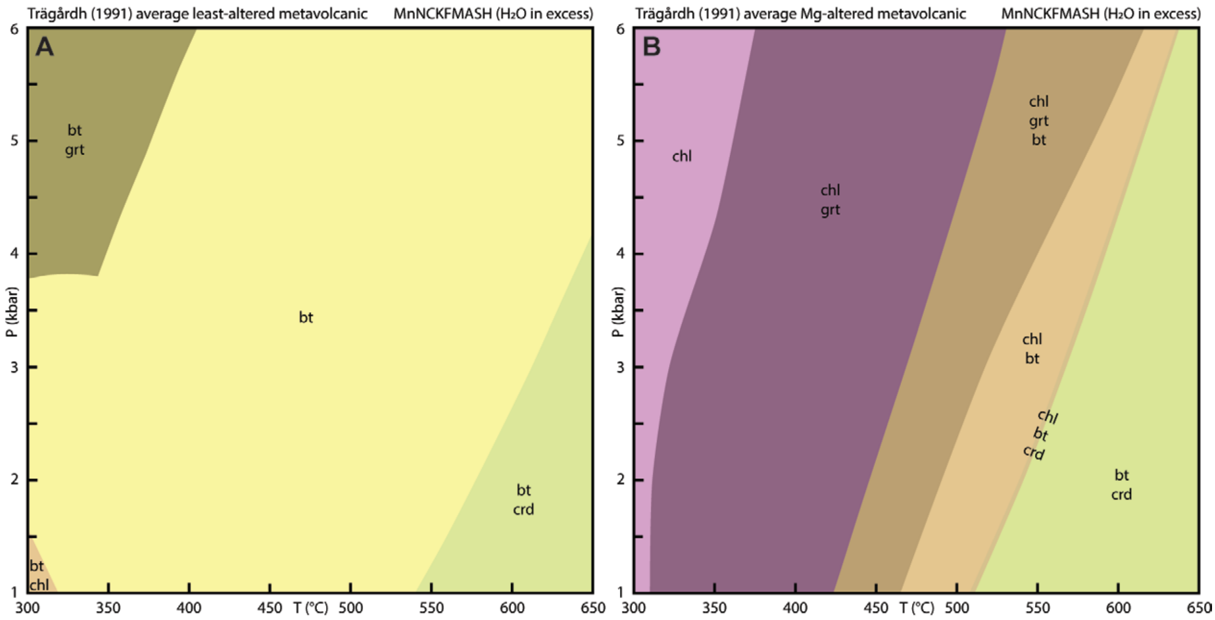

Fig. 1. Stability of index minerals in the $MnO-Na_2O-CaO-K_2O-MgO-Al_2O_3-SiO_2-H_2O$ system for bulk rock compositions equivalent of the (A) average least-altered and (B) average 'magnesium-altered' metavolcanic rocks as reported by Trägårdh (1991). Constructed using Perple_X 6.6.7 (Connolly 2009) with ds6.22 (Holland & Powell 2011).

References

Connolly, J.A.D., 2009: The geodynamic equation of state: What and how. *Geochemistry, Geophysics, Geosystems 10*, Q10014.

Holland, T. J. B. & Powell, R., 2011: An improved and extended internally consistent thermodynamic dataset for phases of petrological interest, involving a new equation of state for solids. *Journal of Metamorphic Geology* 29, 333–383.

Stephens, M.B. & Jansson, N.F., 2020: Chapter 6, Paleoproterozoic (1.9–1.8 Ga) syn-orogenic magmatism, sedimentation and mineralization in the Bergslagen lithotectonic unit, Svecokarelian orogen. In M.B. Stephens & J. Bergman Weihed (eds.): Sweden: lithotectonic framework, tectonic evolution and mineral resources. *Geological Society of London Memoirs 50*, 105–206.

Trägårdh, J., 1991: Metamorphism of magnesium-altered felsic volcanic rocks from Bergslagen, central Sweden. A transition from Mg-chlorite- to cordierite-rich rocks. *Ore Geology Reviews 6*, 485-497.

Traces of a volcano in southeastern Sweden – geology, geophysics and geochemistry

Joakim Mansfeld[a], Erik Sturkell[b], Richard Gyllencreutz[a]

[a]Department of Geological Sciences, Stockholm University, Stockholm, Sweden, joakim.mansfeld@geo.su.se, richard.gyllencreutz@geo.su.se; [b]Department of Earth Sciences, University of Gothenburg, Göteborg, Sweden, erik.sturkell@gvc.gu.se

Summary. For 18 years an area with a varied assemblage of magmatic rocks, from ultramafic to felsic, south of Virserum in central Småland, was studied as part of a course in geophysical field methods. In addition four batchelor/master projects, including an age determination (Johansson 1999) have been based in the area. A large number of samples have also been collected for petrographic analyses and whole-rock geochemistry. By combining the petrological observations, ground-based geophysics and geochemistry we suggest that the rock units form a volcanic system within the Transscandinavian Igneous Belt.

The central volcano of Tönshult

South of Virserum in eastern Småland, where calc-alkaline rocks of the Oskarshamn-Jönköping Belt are replaced by units of the Transscandinavian Igneous Belt (Fig. 1) a c. 15 km long belt of volcanic rocks, mainly porphyritic ryolites to rhyodacites, but also non-porphyritic rhyolites and thin basaltic layers occur.

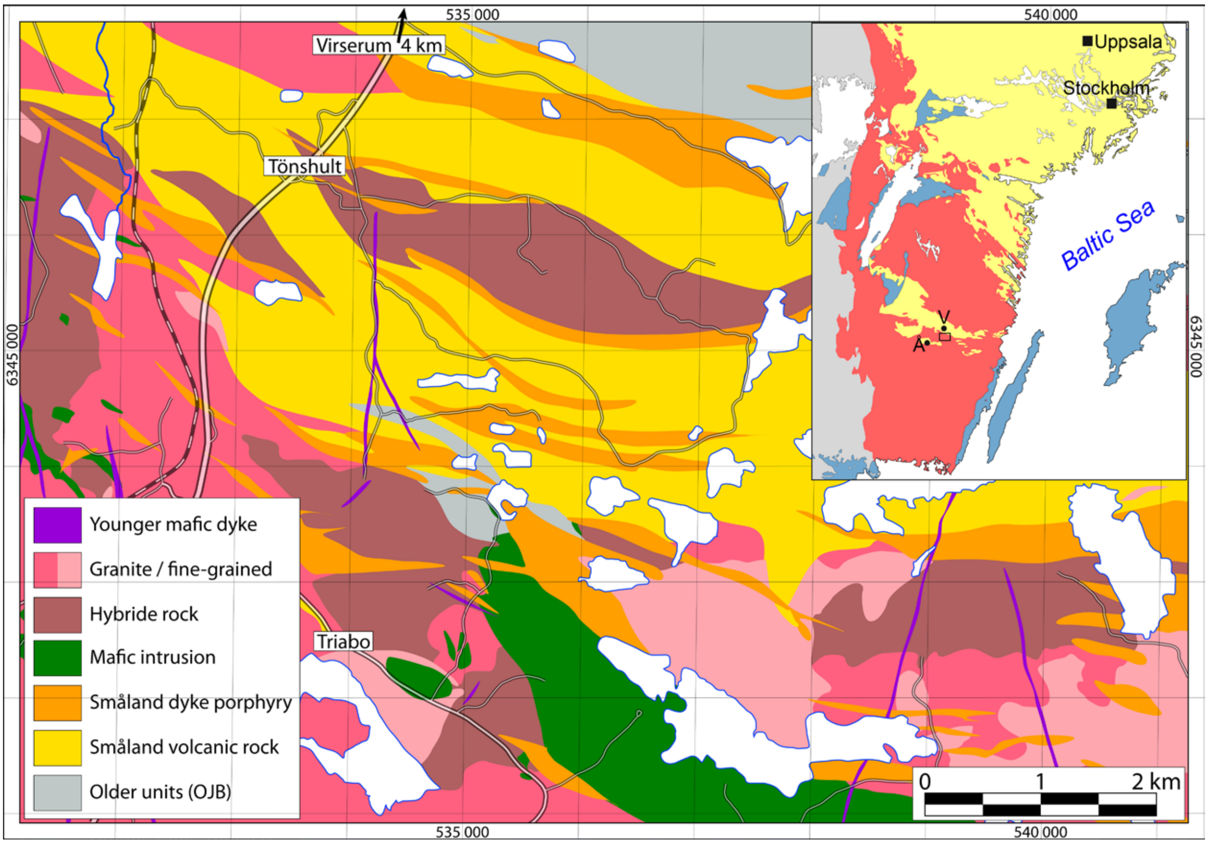

Fig. 1. Simplified geological map of the bedrock south of Virserum. Numbers in the frame are SweRef 99 coordinates. Inset map shows the Transscandinavian igneous Belt (red), Svecofennian Domain (yellow), units of the Southwest Scandinavian Domain (grey) and younger sedimentary units (blue). Small square shows location of the main map, V = Virserum, Å = Åseda.

The area has been affected by a shear zone (the Tönshult shear zone; Mansfeld & Sturkell 1996), but locally the rocks are well preserved and show flow banding, ignimbritic textures and pumice fragments (Fig. 2). To the south the volcanic units are gradually replaced by fine-grained leucocratic granites, sometimes with lensoid mafic enclaves, and very fine-grained phenocrysts-rich rocks that sometimes form meter-wide crosscutting dykes (Småland dyke porphyries). The latter rock type is also found within the volcanic units. Even further to the south the rocks are replaced by medium to coarse-grained intrusive rocks, mostly granites (Växjö granite), but also intermediate, mafic and more seldom ultramafic units.

Fig. 2. Felsic volcanic rock showing ignimbritic texture and a relict flattened pumice fragment. c. 2 km NE of the Tönshult farm.

The volcanic and fine-grained granite units comprise a large low-magnetic area (–500 nT or more), which also coincides with the Tönshult shear zone (Mansfeld & Sturkell 1996). The coarse-grained granitoids and mafic intrusions in contrast show positive anomalies (+1000, and up to +2000 nT for the mafic intrusion). Younger north-south orientated mafic dykes that probably belongs to the c. 1.0 Ga Blekinge-Dala diabases are also evident in the magnetic map.

The gravity survey of the area, which includes more than 3000 measurements, show a general regional trend with increasing gravity towards the south, which is in agreement with a regional positive anomaly centered c. 15 km east of Åseda. At a local scale gravity shows positive anomalies coinciding with the mafic intrusive bodies and a negative trough coinciding with the Tönshult shear zone.

Whole rock geochemistry yields a continuous spectrum of compositions, from 40 to 78 wt% SiO_2, with a variation between 0.1 and 36 wt% MgO, and between 0.2 and 6.3 wt% K_2O. The data suggests two major trends where a majority of the samples form a high-K calc-alkaline trend, whereas a smaller group seems to show a shoshonitic trend.

Our interpretation of the rock units and the geophysical anomalies is that they represent a small central volcano system, where the very fine-grained to aphanitic units represents eruption products such as lavas, pyroclastic flows and ashes. The coarse porphyritic dykes and units represents feeder dikes or local magma pods within the volcano. Fine-grained granites, with or without structures, represent shallow magma chambers, where dragged-out lenses of mafic enclaves in the mainly felsic rocks formed as pulses of mafic intrusions into the magma chamber. At deeper levels the volcanic plumbing system is seen as intrusive rocks, both granitic and gabbroic, which sometimes show evidence of extensive magma mixing and formation of monzonitic hybride rocks, all probably driven by a deep-seated mafic intrusion.

References

Johansson, S., 1999: Fältrelationer och U/Pb zirkonålder på en variant av småländs gångporfyr vid Axebosjön, SO om Virserum, Småland. *Unpubl. master thesis, Department of Geology and Geochemistry, Stockholm University*, 30 p.

Mansfeld, J. & Sturkell, E.F.F., 1996: Geological and geophysical investigation of a major shear zone in southeastern Sweden. *GFF 118 Jubilee issue*, A18–19.

The Alnö alkaline complex: an older, more eroded, Swedish equivalent to the Oldoinyo Lengai volcano?

Hannes B. Mattsson

Department of Earth Sciences, Uppsala University, Uppsala, Sweden, hannes.mattsson@geo.uu.se;

Summary. Magmas from the Alnö alkaline complex in central Sweden and those from the world's only active carbonatite volcano (Oldoinyo Lengai, Tanzania) show strong petrological, mineralogical and volcanological similarities. Here the similaritites, and differences, are discussed and potential future research directions are outlined.

The ~580 Ma Alnö alkaline complex in central Sweden measures ~2.5 km across and is comprised of intrusive and hypabyssal rocks with compositions spanning from the ijolite-series to more evolved syenites and phonolites together with pyroxenites and calciocarbonatites (von Eckermann 1948). Mafic dikes, and to a lesser extent also maar-diatremes, of olivine melilititic compositions (alnöites) also occur in, and surrounding, the central intrusive complex.

The world's only active carbonatite volcano, Oldoinyo Lengai (OL), is located in the East African Rift System in northern Tanzania. The edifice rises 2000 m above the rift floor and is predominantly composed of nephelinitic to phonolitic lavas and pyroclastics, together with minor amounts of natrocarbonatitic lavas (<<5 vol.%; Klaudius and Keller 2006). Surrounding the central volcano are more than 250 small monogenetic volcanic vents and maar-diatreme volcanoes of olivine melilititic composition, with a subordinate number of nephelinitic and basanitic landforms (Mattsson et al. 2013).

In terms of their whole-rock compositions, silicate rocks from Alnö and OL overlap and forms two distinct groups (Fig. 1). One group of highly evolved magmas with alkali contents >10 wt% that is represented by evolved nephelinites to phonolites and different types of syenites. Within this evolved group the alkali content correlates positively with SiO_2. The second group of silicate magmas, with alkali contents of <8 wt%, is represented by more primitive nephelinites, olivine melilitites, basanites, pyroxenites and other cumulate rocks. This group show considerable scatter in the TAS plot, but there is a general trend that the alkalis are negatively correlated with SiO_2 for both Alnö and OL (Fig. 1), albeit with consistently lower SiO_2 for any given alkali content in the Alnö rocks.

The composition of the carbonatites differs significantly between Alnö and OL. Notably, the extrusive natrocarbonatites that are characteristic for Oldoinyo Lengai (with Na_2O+K_2O = >40 wt%) are absent at Alnö. Instead, the Alnö carbonatites are predominantly calciocarbonatites, with low alkali content. This does not exclude that alkali-rich carbonatites may have existed at some point also at Alnö. Alteration of primary natrocarbonatites is a rapid process that results in whole-rock compositions similar to calciocarbonatites (Fig. 1). However, altered natrocarbonatites at OL typically show characteristic replacement textures in thin section (Keller & Zaitsev 2006), which have not been observed at Alnö. At OL fractional crystallization of a broadly calciocarbonatitic mineral assemblage have been shown to be able to produce natrocarbonatites (Weidendorfer et al. 2017). Thus, the calciocarbonatites at Alnö could potentially represent residua from such a crystallization process, and that any fractionated alkali-rich carbonatites have since then been removed by erosion.

Petrographically, olivine melilititic maar-diatreme volcanoes at Alnö (i.e. the Sälskär and Hovid breccias) are virtually indistinguishable from the olivine melilitites surrounding OL. Both consist of juvenile spheroidal lapilli and ash (rich in olivine and phlogopite) that occur together with xenolithic fragments (country rock and mantle debris), set in a fine-grained matrix composed of the same two main components. This points to similar eruptive behavior of the magmas at the two locations, and shows a strong resemblance to kimberlite-type volcanism.

The current erosion level at Alnö has been estimated to represent ~2 km depth (von Eckermann 1948). Given time, it is likely that erosion will expose a similar geology at OL as that exposed at Alnö today.

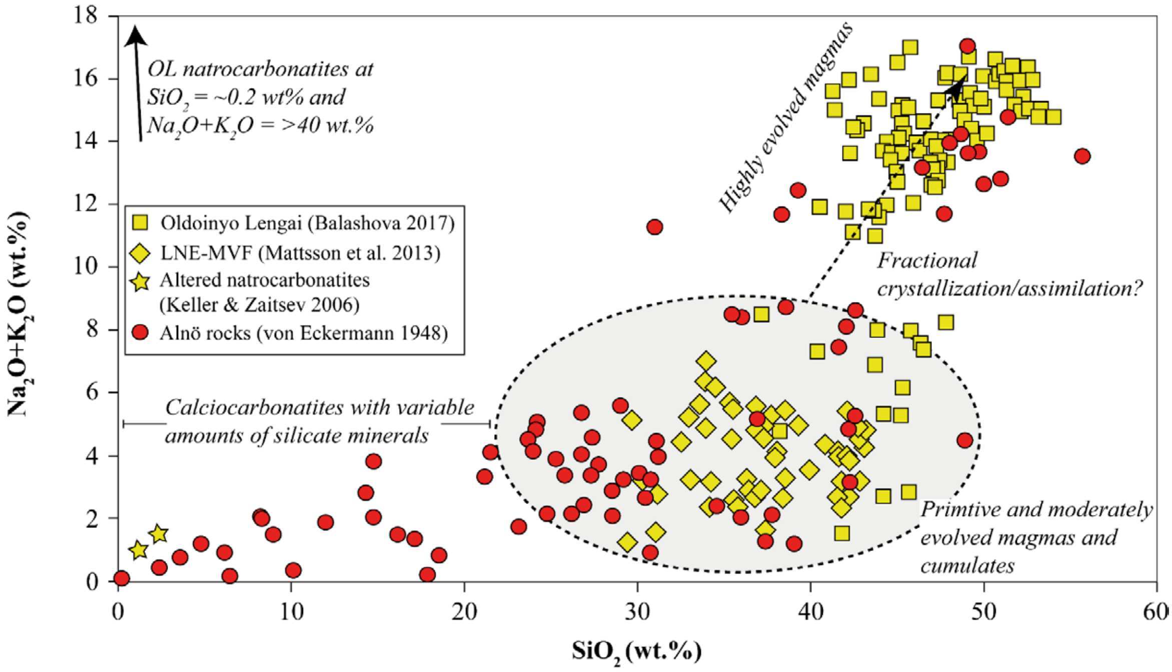

Fig. 1. Plot showing total alkalis vs. silica for rocks from Alnö alkaline-carbonatite complex (red circles) in comparison with those from Oldoinyo Lengai volcano (yellow symbols).

That is, a central complex dominated by intrusive rocks belonging to the ijolite-series coexisting with various types of syenites and calciocarbonatites (sövites). After erosion only dikes and the deepest levels of diatreme structures will remain of the small monogenetic landforms (olivine melilitites) that surrounds the volcano.

Despite the many similarities between the Alnö and OL rock suites, there are still some questions that remain open (especially for Alnö). The association of carbonatites and ijolite-series rocks, nephelinitic to phonolitic rocks and olivine melilitites is common around the world, indicating a possible genetic link between these types of magmas (Woolley & Kjarsgaard 2008). However, we do not know exactly how the more primitive group of silicate rocks are related to the more evolved group and through which process(es). The primitive silicate magmas have received surprisingly limited attention in the literature as the main research focus have traditionally been placed on the more exotic carbonatites. However, understanding the relationship between primary mantle-derived magmas at these locations, and their crustal evolution, may hold the key to a better understanding of how carbonatites form and how economically important elements (such as the REE) are redistributed by magmatic processes within the Earth's crust.

References

Balashova, A., 2017: Magma evolution and tephrostratigraphy of the Gregory Rift, northern Tanzania. *PhD-thesis, ETH Zürich*, 184 p.

Keller, J. & Zaitsev, A.N., 2006: Calciocarbonatite dykes at Oldoinyo Lengai, Tanzania: the fate of natrocarbonatite. *The Canadian Mineralogist 44*, 857–876

Klaudius, J. & Keller, J., 2006: Peralkaline silicate lavas at Oldoinyo Lengai (Tanzania). *Lithos 91*, 173–190.

Mattsson, H.B., Nandedkar, R. & Ulmer, P., 2013: Petrogenesis of the melilititic and nephelinitic rock suites in the Lake Natron–Engaruka monogenetic volcanic field, northern Tanzania. *Lithos 179*, 175–192.

von Eckermann, H., 1948: The alkaline district of Alnö island. *Sveriges Geologiska Undersökning, Ca 36*, 232 p.

Weidendorfer, D., Schmidt, M.W. & Mattsson, H.B., 2017: A common origin of carbonatite magmas. *Geology 45*, 507–510.

Woolley, A. & Kjarsgaard, B.A., 2008: Paragenetic types of carbonatite as indicated by the diversity and relative abundances of associated silicate rocks: Evidence from a global database. *Geochmica et Cosmochimica Acta 46*, 741–752.

Preliminary report on a moderately fractionated rare-element pegmatite at Långåsen, Arlanda, Sweden

Per Nysten

Geological Survey of Sweden, Uppsala, per.nysten@sgu.se;

Summary. At Arlanda airport granitic pegmatite dykes, varying from simple ceramic to highly fractionated types, have been identified.The Norrskogen dyke at runway no. 3 is the chemically most evolved. Here additional data are presented on a moderately complex dyke from the Långåsen quarry situated just to the east of runway no. 3. A possible genetic link to the Vallentuna granite massif situated east of Långåsen is briefly discussed.

During a project initiated last year with the aim to identify toxic elements (e.g. As) in the bedrock in the Arlanda–Rosersberg, area especially pegmatite dykes were investigated as possible source rocks for As-bearing minerals. Arsenic hosted by arsenopyrite is identified from the well documented Norrskogen dyke as compact pods up to 10 × 10 cm in size. During a visit to the Långåsen quarry (March 2021) presently operated by NCC, several 1–2 m wide steeply dipping, light grey pegmatite bodies were found. Most of these carried local concentrations of schorl and muscovite together with grey microcline. At the northernmost part of the quarry (SWEREF coordinates 6614717/667419), boulders from a freshly blasted pegmatite seen in the quarry wall 25–30 m north of the boulders were present (Figure 1). The quarry wall containing the dyke was not accessible due to the sharply angular and large boulders covering the quarry floor. The orientation of this dyke was estimated to 310/60. As seen from the boulders the pegmatite was in sharp contact with a foliated grey granodiorite/tonalite of Uppsala type, which is the main commodity quarried by NCC.

Figure 1. The exposed dyke at the northern part of the Långåsen quarry.

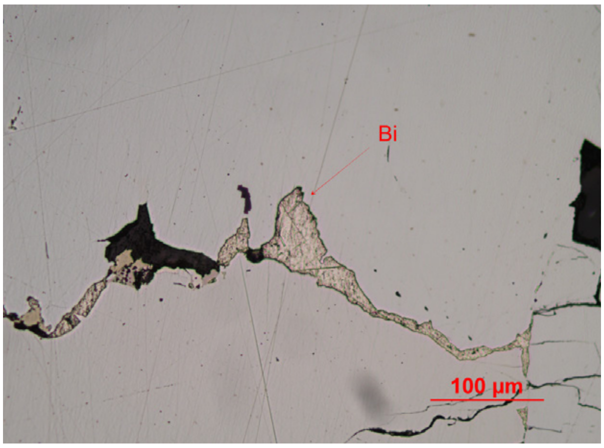

Figure 2. Fracture-filling of native bismuth in arsenopyrite, polished section in reflected, polarized light.

During a visit a month later, the exposed dyke was already removed, but boulders could still be sampled. At this time, I also examined the top surface of the remaining unblasted parts were granite dykes cutting the granodiorite/tonalite were seen. This granite is light grey, even-grained and with a grainsize of 1–3 mm. It contains conspicous concentrations of garnet in 1 cm large areas, a phenomenon also mentioned by Stålhös, (1972). It is estimated to belong to the 1.8 Ga Vallentuna granite massif occurring 1 km SE of Långåsen.

The pegmatite investigated consists of light grey microcline + plagioclase, grey quartz, biotite and minor muscovite. Accessory phases are light yellow euhedral beryl up to a few cm in length, bluish green apatite, red garnet, schorl and probably thucolite (bitumen) as small (< 1mm) black grains disseminated within the feldspar matrix. Thucolite also occupy fracture zones. Very thin, small bladed columbite *(sensu lato)* is locally identified with a hand lens and also seen in polished sections.

The pegmatite is richly mineralized with sulphides, where arsenopyrite constitute a major part as euhedral, striated, light grey, metallic crystals and anhedral grains up to 1 cm in size. The identity of arsenopyrite has been verified by a Bruker hand-held XRF instrument. Locally pyrrhotite, and to some extent also pyrite, and traces of sphalerite and chalcopyrite, have been found. Native bismuth occupy fractures in arsenopyrite (Figure 2) and also form concentrations of rounded inclusions (maximum 50 µm) in both arsenopyrite and pyrite. Complex heterogeneous oxides are also seen in polished sections.

Following the classification by Černý (1991), the pegmatite at Långåsen belongs to the rare element class of granitic pegmatites of the lithium-cesium-tanatalum (LCT, beryl subtype) family. It may be regarded as moderately fractionated as apatite is the only phosphate present. The fertile source granites are regarded by Černý as syn- to late orogenic (e.g. the Vallentuna–Stockholm type). Pegmatites of this type, although mostly devoid of visible arsenopyrite/löllingite, are common in the Arlanda area. Beryl, schorl, apatite, muscovite and garnet are locally common. The beryl crystals are locally also chemically altered into secondary bertrandite as euhedral crystals within hexagonally shaped voids after beryl (e.g. at the entrance to the Långåsen quarry). At the time of construction for runway no. 3 at Arlanda during the years 1994–1997, a vertical, ca 1 m wide pegmatite, very rich in slender beryl crystals, was exposed. These crystals were up to two cm wide and several dm long, locally tectonized and broken with secondary quartz filling the fractures. A typical feature of these crystals is the occurrence of dark brown anhedral zircon, a few mm in size, within the beryl. This dyke was situated between the Norrskogen and Långåsen dykes. Beryl crystals have also been noted within pegmatites intruding metasedimentary rocks at the Laggatorp quarry just north of runway no. 2. Beryl was also common in the mineralogically complex and highly fractionated Norrskogen dyke (now hidden under runway no. 3). Thus a mineralogical pattern may be discerned in the pegmatite field at Arlanda with simple ceramic types close to the contact of the Vallentuna massif, with moderately fractionated dykes at a distance (e.g. Långåsen), and the chemically most complex type somewhat further away (Norrskogen).

Acknowledgement: This project is financed by BeFo (Stiftelsen bergteknisk forskning).

References

Černý, P., 1991: Rare-element pegmatites. Part 1: Anatomy and evolution of pegmatite deposits. *Geoscience Canada 18*, 49–67.

Nysten, P. & Jonsson, E., 1998: Mineralogy of a late Svecofennian Granitic Pegmatite,Norrskogen,Uppland,Sweden. 17th General meeting of the international Mineralogical Association, Toronto,Canada A150.

Stålhös, G., 1972: Beskrivning till berggrundskartbladen Uppsala SV och SO. *Sveriges Geologiska Undersökning Af 105 – 106.* 165 s.

Schallerite from Harstigen

Per Nysten[a], Andreas Karlsson[b]

[a]Svedbovägen 44, Vänge, Sweden, per.nysten@gmail.com; [b]Enheten för Geovetenskap, Naturhistoriska Riksmuseet, Stockholm, Sweden, andreas.karlsson@nrm.se

Summary. The rare mineral schallerite $(Mn^{2+}, Fe^{2+})_{16}Si_{12}As_3^{3+}O_{36}(OH)_{17}$ has been identified as euhedral crystals within calcite-filled pods in an iron-rich skarn at Harstigen based on EDS data and physical characteristics.

Schallerite is a rare arsenosilicate with a phyllosilicate structure first described from Franklin by Gage et al. (1925). It was restudied by Bauer and Berman (1928) who showed a chemical relationship with friedelite and that the arsenic is trivalent in the structure. This mineral has been the focus of extensive studies by several authors discussing the substitution mechanism between As and Si + Cl and OH. Dunn et al. (1981) provided additional data relating schallerite to friedelite, pyrosmalite-(Fe), nelenite, mcGillite, and pyrosmalite-(Mn). The crystal structure of schallerite was described by Kato and Watanabe (1992). Schallerite is also known from Kodnitztal, Austria.

Schallerite at Harstigen was initially found at the dump by Rudolf who sent material for XRD investigation to Müller in September 1991 (Nysten 1995). Additional material was found in a few specimens by Nysten during the early 2000 and was subsequently investigated by Lorin using EDS. This material may be described as small brownish yellow to orange, poorly developed platy crystals growing on ferro-actinolite needles associated with tiny brown garnets in calcite-filled vugs. Arsenic was detected but the quality of the EDS analysis prompted Nysten to put a question mark of the identity of schallerite from Harstigen (Nysten unpublished data).

Recent collecting at the dump by Nysten during 2020 and 2021 has uncovered new excellent material for study. The small but heavily overgrown dump close to the eastern part of the mine contained *inter alia* rich boulders of rhodonite but also a small specimen of dark green Fe-skarn with a calcite-filled vug. Etching of this by HCl revealed a brownish yellow to beige-coloured rosette, a few millimeters in size of intergrown schallerite crystals. Further collecting efforts at the northernmost part of the dump revealed several large Fe-skarn boulders brecciated by calcite richly mineralized by schallerite. Sharp single hexagonal crystals and crystal groups of schallerite were found emplanted on the walls of calcite-filled vugs and as floaters within calcite. These crystal aggregates may reach up to three or four millimeters and the single crystals are mostly of sub-millimeter size and very thin. Associated minerals consist of very dark green to black ferro-actinolite and dark short prismatic diopside. Chemical data obtained of schallerite from a large euhedral crystal shows chemical heterogeneity in the form of a slight zonation with higher SiO_2 and Cl + a lower As_2O_3 towards the rim indicating a solid solution towards friedelite or pyrosmalite-(Mn) (Fig. 1). The same phenomena is also mentioned by Dunn (1995) for schallerite from Franklin, furthermore the schallerite from Harstigen partly shows resorption of the crystal edges comparable to the material from Franklin.

An empirical chemical formula of the schallerite core from Harstigen (n = 22) based on 53 O and OH may be given as $(Mn^{2+}_{12.60}Fe^{2+}_{3.18}Ca_{0.10}Mg_{0.01})_{\Sigma=15.89}\,Si_{11.88}As^{3+}_{3.12}O_{36}(OH_{16.31}Cl_{0.35})$.

Genetical considerations

The Harstigen deposit is well known for its content of rare mineral species containing both manganese and arsenic including manganese skarn minerals (e.g. rhodonite) and arsenates occurring as pods and veinlets (*e.g.* hedyphane) within skarn silicates, and also as euhedral crystals within open cavities (e.g. brandtite). In total some 120+ species are known from this very small iron and manganese mine (only a few hundred metric tons of Fe- and Mn-ore was extracted). Genetically Harstigen may be regarded as being of Långban type. Among the Mn-silicates known at Harstigen prior to the discovery of schal-

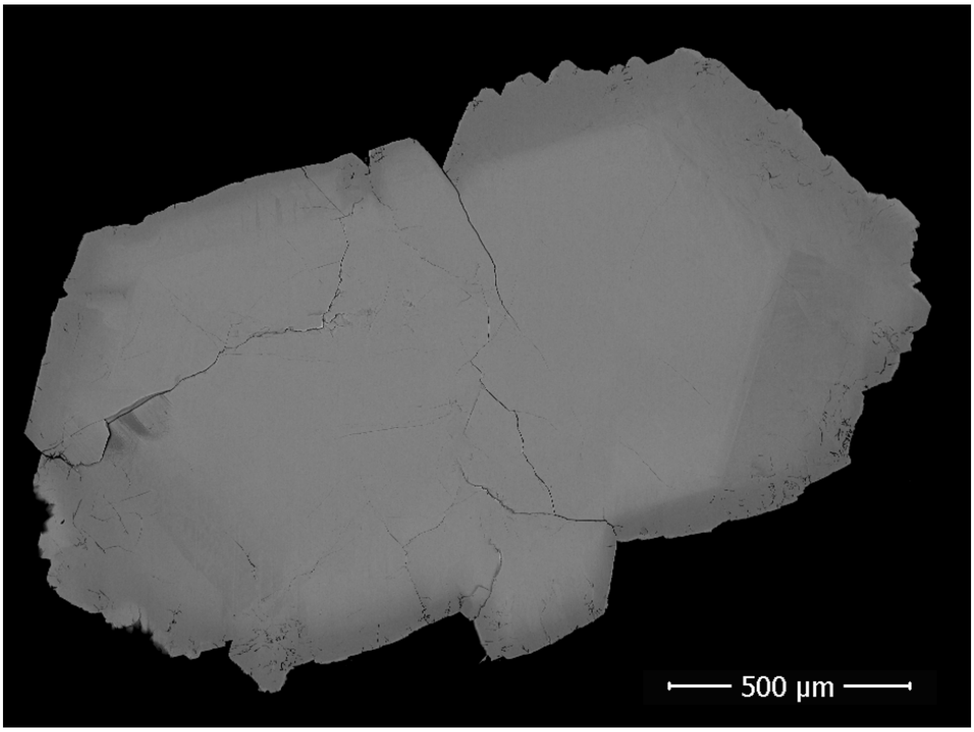

Figure 1. SEM BSE image of a chemically zoned euhedral schallerite crystal.

lerite, the structurally related mineral friedelite may be mentioned. Friedelite occurs as pink euhedral crystals and intergrown crystal groups in a paragenetic setting similar to schallerite. Friedelite is implanted on walls of calcite-filled pods and cracks within tremolite skarn accompanied by bementite and magnetite. According to a pXRD investigation, the Cl-bearing mineral pyrosmalite-(Mn) has also been identified from Harstigen. Furthermore, hematolite containing both As^{3+} and As^{5+} occurs as a late mineral within alteration zones in hausmannite. Thus, the elements necessary for the formation of schallerite as a late stage mineral, are present at the deposit. The paragenetic setting indicates that schallerite formed later than the iron skarn matrix, probably simultaneous with the calcite, which is infilling the vugs in the skarn.

References

Bauer, L. H. & Berman, H., 1928: Friedelite, schallerite, and related minerals. *American Mineralogist 13*, 341-348.

Dunn, P. J. 1995: Franklin and Sterlin Hill, New Jersey: the world´s most magnificient mineral deposits, Part Four Phyllosilicates – layer silicates. *The Franklin-Ogdensburg Mineralogical Society*, p. 463-505.

Gage, R.L., Larsen, E.S. & Vassar, H.E., 1925: Schallerite, a new arseno-silicate mineral from Franklin Furnace, New Jersey. *American Mineralogist 10*, 9-11.

Kato, T. & Watanabe, I., 1992: The crystal structure of schallerite and friedelite. *Yamagashi University, College of Arts Bulletin 26*, 51-63.

Nysten, P., 1995: The Harstigen mine, a compilation. Långbansällskapet Skrifter och rapporter 1, 47 p.

Euhedral low-temperature phosphate minerals from the Leveäniemi open cut, Norrbotten county, Sweden

Per Nysten[a], Ulf B. Andersson[b], Torbjörn Lorin[c], Andreas Forsberg[d]

[a] Svedbovägen 44, 755 76 Vänge, Sweden, per.nysten@gmail.com; [b] Luossavaara-Kiirunavaara AB, Research & Development, TG, FK9, 981 86 Kiruna, Sweden; [c] Kofallsvägen 42, 71830 Frövi; [d] Hasselqvistvägen 12, 121 46 Johanneshov, Sweden

Summary. Euhedrally developed phosphate minerals have been identified from the Leveäniemi open cut, Norrbotten County, Sweden. Fifteen different, mainly hydrous, phosphates occur in vugs or open fractures, as a result of low-*T* hydrothermal (c. 100°C) redistribution of phosphorus.

Introduction

At Leveäniemi, iron ore is presently mined by LKAB. The ore mainly consists of apatite-bearing magnetite ore, partly oxidized to hematite (martitization). During this oxidation, the primary apatite has been transformed into an exotic assemblage of secondary Fe-Ca-Al-phosphates, forming euhedral crystals in drusy parts of the martite ore. The size and quality of these phosphate specimens renders Leveäniemi world class status for such a mineralization (cf. e.g. Bjällerud 1989). A large fold structure exists in which several large and small irregular ore bodies occur surrounded by an ore breccia (Parák & Espersen 1965; Frietsch 1966). The main ore body is up to 150 m wide and exists down to at least 500 m depth. In calcite-bearing parts skarn minerals occur. The surroundings consist of strongly altered volcanic and sedimentary rocks intruded by the Lina granite and pegmatites. An exposed body of martite ore in the northern part carries most of the rich phosphate mineralization.

The phosphates

Fifteen, mainly hydrous phosphates have been identified using powder X-ray diffraction (XRD), electron microscopy (with energy-dispersion X-ray analysis), and ore microscopy. Here the different minerals are described in more detail.

Cacoxenite $Fe^{3+}{}_{24}AlO_6(PO_4)_{17}(OH)_{12} \cdot nH_2O$. Locally cacoxenite forms straw yellow to golden, strongly shiny radiating aggregates of thin needles up to 5 mm in cross-section. Cacoxenite occurs on a core of beraunite or intergrown with this phosphate.

Crandallite $CaAl_3(PO_4)(PO_3OH)(OH)_6$. Crandallite is uncommon at Leveäniemi, forming beige trigonal crystal aggregates up to 5 mm in size.

Ferroberaunite, $FeFe^{3+}{}_5(PO_4)_4(OH)_5 \cdot 6H_2O$, is common in vugs as needles and stubby crystals forming dark green spherical aggregates up to 5 mm in cross-section associated with strengite. The colour of these aggregates changes from a greenish black interior to an outer greyish green. A Mössbauer investigation gives 18% ferrous iron in good agreement with the theoretical formula.

Ferrostrunzite, $Fe^{2+}Fe^{3+}{}_2(PO_4)_2(OH)_2 \cdot 6H_2O$, is rare at Leveäniemi, forming pale brown translucent needles or radiating aggregates, filling vugs in martite ore. The ratio ferrous to ferric iron matching the theoretical formula was confirmed by Mössbauer spectroscopy.

Fluellite, $Al_2(PO_4)F_2(OH) \cdot 7H_2O$, is a rare mineral but present locally as transparent to white, prismatic bipyramidal crystals, a few mm in size occurring in vugs at Leveäniemi, Fluellite also forms white compact masses, which may reach several cm, filling druses in the martite ore.

Fluorapatite $Ca_5(PO_4)_3(OH,F,Cl)$: Secondary apatite is common in the martite ore as white to beige colloform aggregates in druses. An evidence for the very late formation of this mineral is diverging fluorapatite needles emplanted on mitridatite.

Kidwellite, $NaFe_3{+}9(PO_4)_6(OH)_{10} \cdot 5H_2O$, forms moss-green to yellowish green, finely crystalline mats, and crystal aggregates, emplanted on walls of druses.

Mitridatite, $Ca_2Fe_3^{3+}O_2(PO_4)_3 \cdot 3H_2O$, is an inconspicuous mineral forming small, dark brown to olive green spheres, or crusts, on other phosphates. It is one of the youngest minerals found in vugs.

Montgomeryite, $Ca_4MgAl_4(PO_4)_6(OH)_4 \cdot 12H_2O$, is colourless to weakly beige, with a pearly lustre, forming rose-like crystal sprays of bladed crystals. It occurs isolated or with other phosphates being one of the latest minerals in vugs. Paravauxite and montgomeryite occurs on mitridatite,

Paravauxite, $Fe^{2+}Al_2(PO_4)_2(OH)_2 \cdot 8H_2O$, forms well-developed, weakly diverging crystal aggregates in vugs. It displays vitreous, to weakly greasy lustre and associated minerals are montgomeryite, Al-strengite, beraunite, mitridatite and rockbridgeite.

Rockbridgeite, $(Fe^{2+},Mn^{2+})Fe^{3+}{}_4(PO_4)_3(OH)$, and beraunite may be difficult to separate visually from each other, as both forms dark green spherical aggregates with a vitreous lustre and a fibrous texture. However, both minerals, co-existing on one specimen, have been verified by XRD.

Strengite, $Fe^{3+}PO_4 \cdot 2H_2O$, is typical of Leveäniemi, forming spherical aggregates of radially intergrown, wine-red to purple crystals. It forms colourful combinations with other phosphates. In cross-section concentric shells with different chemical composition may be seen (Al – Fe^{3+} substitution) with transformation from strengite to variscite.

Figure 1. Strengite, 3 mm on goethite.

Tinticite, $Fe^{3+}{}_4(PO_4)_3(OH)_3 \cdot 5H_2O$, forms light greenish yellow to dark yellow crystals implanted directly on goethite or associated with strengite and beraunite. XRD investigation on tinticite shows admixed dufrenite, beraunit and kidwellite.

Variscite, $AlPO_4 \cdot 2H_2O$, occurs in light blue colloform habitus.

Wavellite, $Al_3(PO_4)_2(OH,F)_3 \cdot 5H_2O$. This Al-rich phosphate occurs in lesser amounts associated with beraunite forming radial, yellowish white aggregates with a vitreous to silky lustre.

Conditions of formation

All these phosphates are secondary formed from circulating, low-*T* hydrothermal solutions as they contain water in the crystal structure. A conspicuous feature is that they often form spherical aggregates consisting of several layers with different composition, growing onto each other. Among the earliest formed minerals, following goethite in vugs, are ferroberaunite and rockbridgeite. The younger phases tend to be H_2O-richer: wavellite, cacoxenite, strengite, and paravauxite. The source of P is most probably the primary fluorapatite and the phosphates described here have all formed in conjunction with, or slightly after oxidation, of the original magnetite ore. Other typical late-formed minerals here are zeolites and scapolite adjacent to the ore body. The zeolites have formed at low T (50–120 °C) together with clay minerals (Rieger 2016), at temperatures similar to those inferred for the present kind of phosphates (Dill et al. 2009). Zeolites from Malmberget have been dated to 1740–1620 Ma (Romer 1996) and clays from the same locality gave c. 900 Ma (Gilg et al. 2017). This suggests that the phosphates at Leveäniemi may have formed during several events during a long period.

References

Bjällerud, C.G., 1989: Phosphate minerals from the Leveäniemi iron mine, Svappavaara, Sweden. *The Mineralogical Record 20*, 343–346.

Dill, H.G., Weber, B. & Kaufhold, S., 2009: The origin of siderite-goethite-phosphate mineralization in the karst-related faultbound iron ore deposit Auerbach, Germany, a clue to the timing of hypogene and supergene Fe-Al phosphates in NE Bavaria. *Neues Jahrbuch für Minaralogie – Abhandlungen 186,* 283–307.

Frietsch, R., 1966: Berggrund och malmer i Svappavaarafältet. *Sveriges geologiska undersökning C 604,* 282 s.

Gilg, H.A., Rieger, P., Wampler, J.M. & Andersson, U.B., (2017): Origin of clays in Kiruna-type iron ore deposits, Sweden. *Clay Mineral Soc., Ann. Meeting, Edmonton, Canada, June 2-8 2017,* Conf. Abs. p. 22.

Parak, T. & Espersen, J., 1965: Leveäniemi järnmalmsfyndighet. Rapport rörande resultaten av de under åren 1957–1964 av Sveriges geologiska undersökning utförda arbetena. Prospekteringsrapport *Brap 854,* 1–153.

Rieger, P., 2016: Low-temperature alteration in the iron ore deposits of Norrbotten, Sweden. *Master´s thesis, Ludwig-Maximilianuniversitetet, München,* 100 p.

Romer, R.L., 1996: U-Pb systematics of stilbite-bearing low-temperature mineral assemblages from the Malmberget iron ore, northern Sweden. *Geochimica et Cosmochimica Acta 60,* 1951-1961.

Overview of Palaeo-Mesoproterozoic anorogenic granites in the Baltic Sea region

Evgenia Salin[a], Krister Sundblad[b], Richard Gyllencreutz[c]

[a]Department of Geography and Geology, University of Turku, Turku, Finland, evgenia.salin@utu.fi; [b]Lokomotivmannagatan 5:15, FIN-20100 Åbo, Finland, sundblad.krister@gmail.com; [c]Department of Geological Sciences, Stockholm University, Stockholm, Sweden, richard.gyllencreutz@geo.su.

Summary. Three groups of granite-dominated anorogenic plutons can be distinguished in Fennoscandia. The first group (e.g. Wiborg) consists of A-type rapakivi granite-anorthosite-gabbro complexes and is associated with mafic dykes and clastic sedimentary basins. The granites in the second group (e.g. Mazury) are geochemically and texturally similar to the rapakivi granites, but lack association with mafic dykes and sedimentary basins. The third group (e.g. Götemar) is characterized by both I- and A-type signatures, but neither mafic dykes, nor sedimentary basins exist and rapakivi textures are rare.

Compressional tectonics, predominating in northern Europe in the early Palaeoproterozoic, culminated with the Svecokarelian orogeny, which led to the formation of the proto-continent Baltica at 1.8 Ga and extensive magmatic activity within theTransscandinavian Igneous Belt (TIB). A shift towards extensional tectonic regimes was noted already in the final TIB phases (Ahl et al. 1999) and became the most important tectonic regime for more than 200 m.y. (c. 1.71–1.49 Ga), expressed in a widespread anorogenic granitic magmatism. Three distinct groups of granite-dominated anorogenic plutons can be distinguished in Fennoscandia.

The most well-known of them is group 1, the rapakivi granite-anorthosite-gabbro complexes, which intruded into the up to 55 km thick Palaeoproterozoic metamorphosed Svecofennian crust in central Sweden and southern Finland (and locally Archaean crust in the Ladoga region) during the Palaeo- to Mesoproterozoic (e.g. Ahl et al. 1997). The earliest expression of this anorogenic igneous activity was already at 1.70–1.67 Ga when the Dala suite formed as the final phase of the TIB. It was soon followed by proper rapakivi magmatism, which resulted in the emplacement of large batholiths (e.g. Wiborg, Åland and Riga, the latter probably extending to northern Gotland) and smaller plutons (e.g. Vehma, Nordingrå and Strömsbro) between 1.65 and 1.50 Ga (Fig. 1). The granites in these batholiths often show rapakivi texture, expressed by K-feldspar phenocrysts rimmed by plagioclase (wiborgite), and are characterized by metaluminous to marginally peraluminous compositions with high Fe/Mg, K/Na, Ga/Al, Zr and F, low CaO and Sr, and a distinct negative Eu anomaly. These geochemical trends, supported by temporal and spatial association of the rapakivi granites with mafic dykes and clastic sedimentary basins deposited within back-arc basins, indicate that the rapakivi batholiths are related to intra-continental extension.

Two slightly younger granite groups (2 and 3) occur southwest of the Svecofennian Domain and were emplaced into the Transscandinavian Igneous Belt (or the Polish-Lithuanian megadomain, which may represent a granulite facies variety of the TIB). These granitic plutons lack association to mafic dykes and sedimentary basins, suggesting major differences in tectonic conditions compared to group 1.

The major 1.53–1.50 Ga Mazury granite-anorthosite complex (often referred to as the anorthosite-mangerite-charnockite-granitoid suite) is one of the granite associations in this setting and forms group 2. The granitoids are characterized by monzodioritic to granitic compositions, high Zr, Ce and Y contents, a low Nb content and a gentle REE trend with a slight mostly negative Eu anomaly.

The third group comprises relatively small (<20 km) 1.51–1.44 Ga granitic plutons (e.g. Götemar, Figeholm, Blå Jungfrun and Karlshamn, Bornholm and Grötlingbo as well as Geluva and Kabeliai in Lithuania). Other, recently recognized plutons, belonging to this group include Emsfors and Rockneby on mainland Sweden, the 1442 ± 7 Ma Kvinnsgröta pluton (Öland) and the 1471 ± 7 Ma Hamra pluton (Gotland); Salin et al. (2020). It is worth to note that according to the TIB nomenclature suggested by

Salin et al. (2019), the oldest (≈1.49 Ga) plutons (Grötlingbo and Kabeliai) were emplaced into TIB 0 units, while the 1.45–1.44 Ga plutons intruded either into TIB 1a units or close to the border between TIB 1b and 1c (Karlshamn-Eringsboda and Kvinnsgröta). The small plutons in the TIB are characterized by metaluminous compositions, lower Fe/Mg and K/Na ratios, as well as rather gentle REE trends, with a slightly negative Eu anomalies, typical for I-type granites.However, they have high Zr, Nb, Ce contents and Ga/Al ratios showing A-type affinities, similar to the rapakivi granites. Rapakivi textures are not observed except on Bornholm.

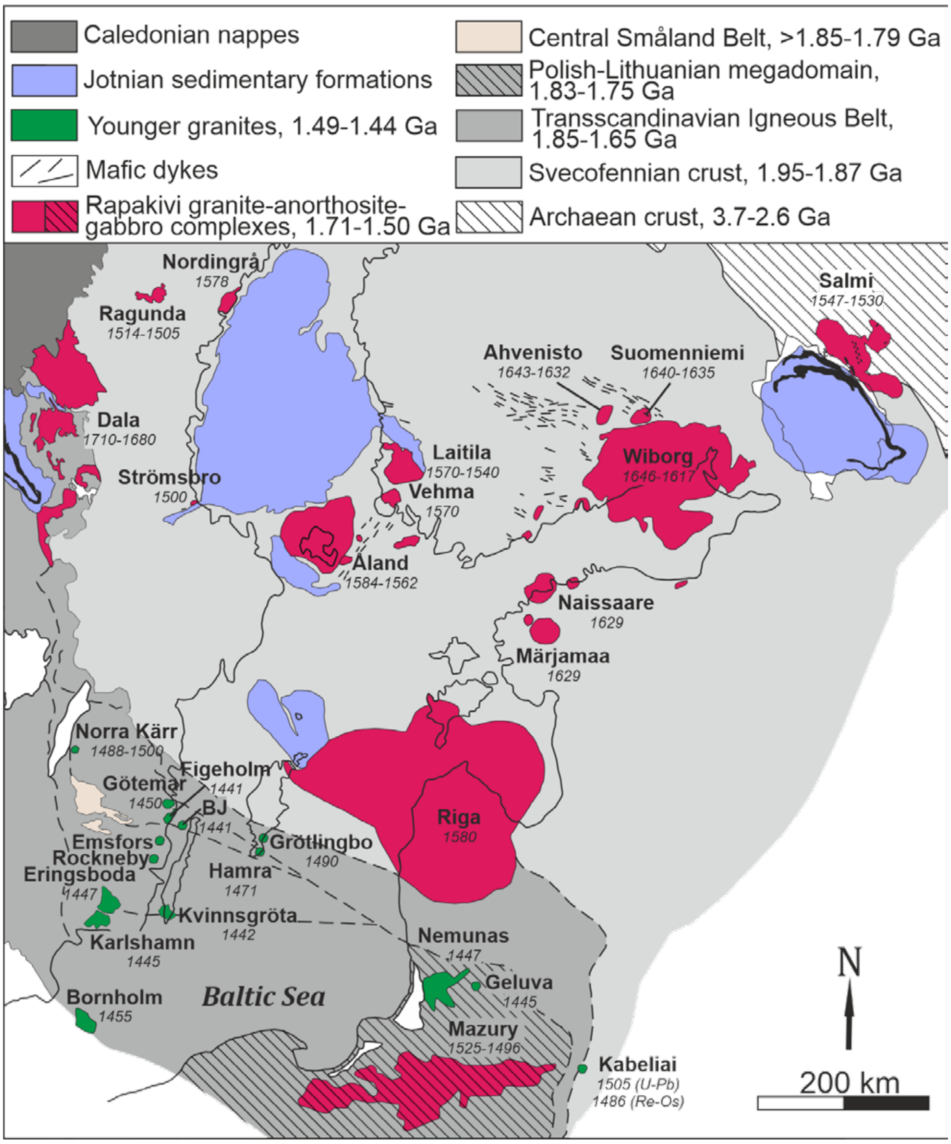

Figure 1. Palaeo- to Mesoproterozoic anorogenic granites and associated igneous and sedimentary formations in the Baltic Sea region (modified after Ahl et al. 1997 and Wybraniec 1999). BJ – Blå Jungfrun.

References

Ahl, M., Andersson, U.B., Lundqvist, T. & Sundblad, K. (Eds.), 1997: Rapakivi granites and related rocks in central Sweden. *Sveriges geologiska undersökning Ca 87*, 99 pp.

Ahl, M., Sundblad, K. & Schöberg, H., 1999: Geology, geochemistry, age and geotectonic evolution of the Dala granitoids, central Sweden. *Precambrian Research* 95, 147-166.

Salin, E., Sundblad, K., Woodard, J. & O'Brien, H., 2019: The extension of the Transscandinavian Igneous Belt into the Baltic Sea region. *Precambrian Research* 328, 287-308.

Salin, E., Sundblad, K. & Woodard, J., 2020: Distribution, age, geochemistry and origin of "anorogenic" granites in the Baltic Sea region. *NGF Abstracts and Proceedings 1*, 189-190.

Sundblad, K., Salin, E., Claesson, S., Gyllencreutz, R. & Billström, K., 2021: The Precambrian of Gotland, a key for understanding the Proterozoic evolution in southern Fennoscandia. *Precambrian Research* 363, 106321.

Wybraniec, S., 1999: Transformation and visualization of potential field data. *Panstw. Inst. Geol. Spec. Pap. I*, 1-88.

Alkaline igneous rocks in Sweden: An overview

Axel S.L. Sjöqvist[a], Hannes B. Mattsson[b]

[a]Department of Earth Sciences, University of Gothenburg, Göteborg, Sweden, axel.sjoqvist@gu.se;
[b]Department of Earth Sciences, Uppsala University, Uppsala, Sweden, hannes.mattsson@geo.uu.se;

Summary. Alkaline igneous rocks are complex and volumetrically subordinate in comparison with the dominantly subalkaline igneous rocks in the Earth's crust. Therefore their importance as records of geodynamic processes and as resources of raw materials is sometimes underestimated. Here, we present a brief compilation of the occurrences of alkaline igneous rocks in Sweden that we are aware of. More information about the state of knowledge for each locality is available on the poster. We encourage meeting participants to make new additions to this list.

Definition

According to modern petrological classification, alkaline igneous rocks are defined by their silica-undersaturated and/or peralkaline nature (Le Maitre 2002). Carbonatites, which are igneous rocks that contain more than 50% modal carbonate, are also often included (Mitchell 2005).

Silica undersaturation is indicated by the presence of feldspathoids, such as nepheline and leucite, as well as forsterite in the absence of orthopyroxene, either in the mode or in the norm. Less common but significant silica-undersaturated minerals include melilite and perovskite.

Peralkalinity is defined by the molar excess of alkali elements sodium and potassium relative to aluminium. The presence of alkali-rich minerals devoid of aluminium, such as aegirine, arfvedsonite, and riebeckite, is indicative of peralkalinity in an igneous rock.

Examples of rocks that are commonly misperceived as alkaline igneous rocks include calc-alkaline lamprophyre, alkali-feldspar granite, and some rocks in the alkaline magma series such as trachyte.

Significance

Alkaline igneous rocks are rare geological "anomalies" produced under specific geodynamic conditions. As such, they can be important pieces of the puzzle in the construction of regional lithotectonic frameworks. Some varieties, such as kimberlite, olivine melilitite, and nephelinite, may contain mantle xenoliths. Globally, alkaline igneous rocks host significant resources of critical raw materials, such as phosphorous, niobium, and rare-earth elements.

Almunge alkaline complex (1.88 Ga), Uppsala county

Probably the oldest locality of alkaline rocks in Sweden. The complex contains umptekite and nepheline syenite (*canadite*), which were metamorphosed. There is a lack of detailed modern petrological studies.

Rapakivi complexes (c. 1.5 Ga), Jämtland, Västernorrland, Gävleborg, and Dalarna counties

Locally peralkaline granite is known in the Ragunda, Mullnäset, Nordsjö, and Strömsund complexes in Jämtland–Ångermanland, as well as the Noran granite in Dalarna.

Norra Kärr alkaline complex (1.49 Ga), Gränna, Jönköping county

Small occurrence of agpaitic rocks, which during the last decade has gained fame as the fourth largest heavy-rare-earth element deposit in the world. The complex consists of metamorphic fine-grained peralkaline nepheline syenite (*grennaite*) and other nepheline syenites (*lakarpite*, *kaxtorpite*).

Balltorp granite (1.31 Ga), Mölndal, Västra Götaland county

Locally peralkaline metamorphic A-type granite of the Kungsbacka Bimodal Suite, possibly a variety of Kärra granite also known as "RA granite".

Central Scandinavian Dolerite Group (1.27–1.25 Ga), Västerbotten, Jämtland, Västernorrland, Gävleborg, and Dalarna counties

Alkali to transitional (ne-normative) basaltic sills and dykes that occur widely in central Sweden.

Vårgårda quartz-monzonite (1.22 Ga), Västra Götaland county

Metamorphic quartz-monzonite, which locally contains aegirine-augite, riebeckite, and fayalite.

Kalix alkaline ultramafic dykes (1.14 Ga), Norrbotten county

Narrow dykes composed of beforsite, silico-carbonatite, and lamprophyre occurring most prominently as a swarm in the coastal area near Kalix.

Alnö carbonatite complex (0.58 Ga), Västernorrland county

This classic locality of alkaline igneous rocks has been extensively studied, including pioneering work on carbonatite petrology. The complex contains sövite and varieties of variably-fenitised nepheline syenite and nephelinite as well as alnöite dykes. Glacial erratic boulders on the southern coast of Åvikebukten indicate the presence of an additional alkaline centre on the seafloor. Potentially coeval, less studied, alkaline rocks include ultramafic diatremes c. 50 km north and northwest from Alnö.

Prästrun & Åkersjön (unknown age), Krokom, Jämtland county

Metamorphic nepheline syenite and carbonatite in the Caledonian Seve nappe, locally rich in betafite.

Särna alkaline complex and tinguaite dyke swarms (0.29 Ga), Dalarna county

Poorly-exposed complex that contains nepheline syenite and cancrinite syenite of variable composition and texture. Tinguaite dykes occur in conjunction with the central complex, but also in discrete swarms c. 25 and 50 km east of the Särna alkaline centre.

Torpa Klint and Kullen lamprophyres (Permo-Carboniferous), Skåne county

Camptonite–alkali basalt and spessartite dykes.

Skåne alkaline volcanism (c. 0.18 Ga), Skåne county

More than 100 basanitic and melanephelinitic volcanic necks from a 30 by 40 km volcanic field, some of which contain mantle xenoliths.

Other localities

One minor spinel glimmerite dyke of unclear origin has been documented near Västervik, Kalmar county.

The Permian plateau dolerite sills in Västra Götaland county have not been extensively studied in modern times. Their composition is transitional to alkali basalt. A coeval swarm of north-south trending dykes in Skagerrak consists of ultramafic lamprophyre, dolerite, and rhomb porphyry. These are at least temporally associated with alkaline rocks in the Permian Oslo Rift and in Skåne.

References

Le Maitre, R.W. (ed), 2002: *Igneous Rocks: A Classification and Glossary of Terms*, Cambridge University Press.
Mitchell, R.H., 2005: Carbonatites and carbonatites and carbonatites. *The Canadian Mineralogist 43*, 2049–2068.

Petrography of arsenic-bearing metasupracrustal rocks in the Arlanda area

Klara Skoog[a], Jenny Andersson[a,b], Jarosław Majka[a,c]

[a]Department of Earth Sciences, University of Uppsala, Uppsala, Sweden, klara.skoog@hotmail.com, jaroslaw.majka@geo.uu.se; [b]Geological Survey of Sweden, Uppsala, Sweden, jenny.andersson@sgu.se; [c]AGH University of Science and Technology, Kraków, Poland;

Summary. Elevated concentations of As occur in the bedrock at Arlanda. New petrographic information obtained by optical and electron microscopy shows that the As minerals arsenopyrite (FeAsS) and löllingite ($FeAs_2$) occur in metamorphic rocks of presumably sedimentary origin. Up to 1 cm large grains of arsenopyrite have also been detected in pegmatite injecting both metaintrusive and metasedimentary rocks. Calculated pressure-temperature (*P*-*T*) estimates suggest *P* of 3.0–5.5 kbar and *T* of 490–640 °C, corresponding to lower amphibolite facies metamorphism.

In the Arlanda area there is risk for leaching of arsenic (As) from the bedrock to surface- and groundwater during processing of aggregates in quarries and during construction and tunnelling. Tubed wells penetrating the bedrock in the region have high concentrations of As and in many wells the concentrations are too high for potable water (Thunholm et al. 2009). It is a construction intensive area but construction projects have encountered problems with high background levels of As in the bedrock (e.g. Bidros, 2014). Elevated concentrations of As appear to occur in metasedimentary rock units, but may also occur in other rock types (Thunholm et al. 2009). It is, for example also present in pegmatite and pegmatite granite (Nysten, this volume). Understanding of the occurrence of As in different rock types, metamorphic mineral parageneses and tectonic structures is a prerequisite for prediction of As-enrichments in the bedrock and necessary to avoid risk for health and the environment during construction work.

Methods

This project aims to determine the metamorphic conditions in a part of the Arlanda area where the levels of As in the bedrock in places exceed 100 ppm. Field work, optical- and electron microscopy, including both energy- and wavelength dispersive-X-ray spectroscopy have been performed to pin down mineralogy, mineral chemistry and textural relations of metamorphic assemblages and occurrence of As-bearing minerals. These data are used for modelling of pressure and temperature (*P*-*T*) and oxidation conditions during metamorphic recrystallization of these rocks, the latter an important factor controlling the mobility of As in the crust.

Results

Twelve localities have been examined and three of these were selected for detailed petrographic studies. (I) A meta-igneous, presumably subvolcanic rock of andesitic to dacitic composition with mafic enclaves and sporadic occurrence of ca 1 cm large garnet crystals (locality 4). It is composed of plagioclase + biotite + quartz + K-feldspar with accessory apatite, pyrrhotite, fluorite, pyrite, zircon, rutile, ilmenite and chalcopyrite. (II) A garnet-rich mica schist with garnet occurring both as <1 cm, purple, euhedral crystals and ~1 cm, more pinkish and inclusion-rich crystals (Figure 1A, locality 5). The fine-grained garnet occurs in a rock type with the assemblage plagioclase + biotite + quartz + ilmenite + garnet + grunerite. Accessory minerals are pyrrhotite, pyrite, chlorite, apatite, chalcopyrite and calcite. Garnet has both euhedral and anhedral crystal shapes (Figure 1B). Grunerite is the dominating amphibole, but ferro-hornblende or ferro-tschermakite was observed as a texturally older phase within some grunerite crystals, suggesting that the rock is polymetamorphic. The rock with coarse garnet has the mineral assemblage garnet + biotite + plagioclase + quartz + ilmenite, with accessory chlorite, apatite, rutile, pyrite and monazite-(Ce). The sample also contains arsenopyrite and löllingite (Figure 1C), primarily in the matrix close to garnet. Most löllingite crystals are anhedral, while arsenopyrite is more euhedral in shape. (III) A fine-grained, grey, homogenous, supracrustal rock with the mineral assemblage quartz + plagioclase + biotite + muscovite (locality 8:2). The sample has a few occurrences of near euhedral crystals of a tourmaline-group mineral (Figure 1D). The presence of a boron-rich mineral may indicate a marine sedimentary rock protolith (Henry & Dutrow 1992). In this sample cobalt- and nickel-bearing löllingite occur in contact with biotite.

Geothermobarometry coupled with phase equilibrium modelling indicate P of 3.0–5.5 kbar and T of 490–640 °C, corresponding to lower amphibolite-facies metamorphism. The P-T-estimates predominantly plot in the sillimanite stability field. These results agree with previous work in the region (Sjöström & Bergman 1998).

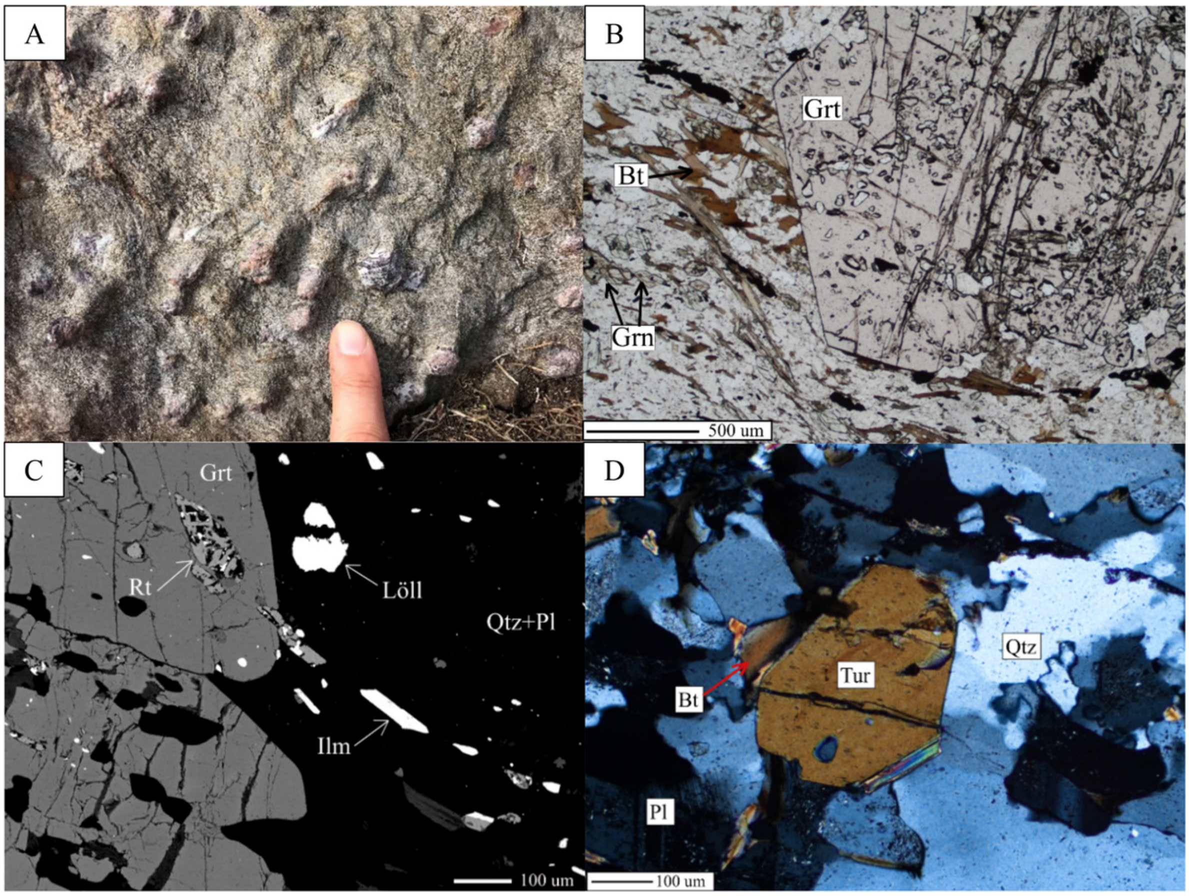

Figure 1. A) Coarse garnet crystals in mica schist (locality 5). B) Fine grained euhedral section of a garnet crystal in mica schist; optical microscope, plane polarized image (locality 5). C) Löllingite crystal close to garnet in mica schist, backscattered electron image (locality 5). D) Euhedral tourmaline crystal in a presumably metasedimentary rock; optical microscope, cross polarized image (locality 8).

References

Bidros, S., 2013: *Encounters with natural arsenic in production and its management*. (2013;76). KTH. Bachelor's Programme in Construction Engineering and Design.

Henry, D.J. & Dutrow, B.L., 1992: Tourmaline in a low-grade clastic metasedimentary rock: an example of the petrogenetic potential of tourmaline. *Contributions to Mineralogy and Petrology 112* (2–3): 203–218

Nysten, P., 2022: Preliminary report on a moderately fractionated rare-element pegmatite at Långåsen, Arlanda, Sweden. Extended Abstract Volume, The Geological Society 150 years Jubilee meeting in Uppsala 17-19th of August 2022.

Sjöström, H. & Bergman, S., 1998: *Svecofennian Metamorphic and Tectonic Evolution of East Central Sweden*: *Research report of a project entitled*; *Svekeofennisk metamorf och tektonisk utveckling I östra mellansverige*. Uppsala: Geological Survey of Sweden.

Thunholm, B., Johansson, O. & Söderholm, H., 2009: *Vattenkvalitet i bergborrade brunnar i Sigtuna kommun*. (2009:9). Uppsala: Geological Survey of Sweden.

Former melt inclusions in garnet from UHP gneisses of the Seve Nappe Complex, Scandinavian Caledonides

Paweł Słupski[a], Bernardo Cesare[a], Omar Bartoli[a], Jarosław Majka[b,c], Iwona Klonowska[c], Laurent Remusat[d]

[a]Department of Geosciences, University of Padua, Padua, Italy, pawelmichal.slupski@studenti.unipd.it, bernardo.cesare@unipd.it, omar.bartoli@unipd.it; [b]Department of Earth Sciences, Uppsala University, Uppsala, Sweden, jaroslaw.majka@geo.uu.se; [c]Faculty of Geology, Geophysics and Environmental Protection, AGH University of Science and Technology, Kraków, Poland, klonowska@agh.edu.pl; [d]Institut de Mineralogie, Physique des Materiaux et Cosmochimie, Museum National d'Historie Naturelle, 75231 Paris, France, laurent.remusat@mnhn.fr

Summary. This work applies melt inclusion studies to an ultra-high pressure metamorphic environment by investigating petrology of nanogranitoids. Diamond-bearing migmatitic paragneisses from the Seve Nappe Complex are composed of Kfs+Grt+Qz+Pl+Bt+Wm+Ky+Sil+Ru. Clusters of nanogranitoids and multiphase inclusions are present in garnet porphyroblasts. Nanogranitoids were experimentally remelted at different UHP conditions. The best homogenization was acquired at 900 °C and 4.5 GPa. Homogenous glass was analysed revealing the chemical composition and content of volatiles in the anatectic melt.

Ultrahigh pressure (UHP) metamorphism has been recently reported in gneisses from the Seve Nappe Complex (SNC) of the Scandinavian Caledonides (Klonowska et al. 2017, Majka et al. 2014). This study is focused on crystallized former melt inclusions – so-called *nanogranitoids* – and the information they preserve about anatectic processes occurring during ultradeep subduction. Nanogranitoids are small, usually less than 20 µm, fully crystallized droplets of anatectic melt entrapped in peritectic phases like garnet (Bartoli et al. 2016, Cesare et al. 2015). Paragneisses from the Åreskutan Mountain representing the SNC are part of the outermost Baltica margin, which has been subducted, metamorphosed and melted during the closure of the Iapetus Ocean causing the collision between Baltica and Laurentia in Early Devonian (Gee et al. 2013).

The mineral assemblage of the paragneiss is K-feldspar, garnet, quartz, plagioclase, biotite, white mica, kyanite, sillimanite and rutile. Garnet occur as porphyroblasts or aggregates of coalesced crystals up to 3 mm in diameter and they are randomly spread in the matrix. Clusters of inclusions are present in most garnets (Fig. 1a) and are mostly composed of small multiphase inclusions (MPI), less than 5 µm in size. MPI represent former fluid inclusions (Tacchettto et al. 2019) and consist of various carbonates, (such as calcite, siderite, and magnesite), biotite, pyrophyllite, ± quartz, graphite, rutile, corundum, and a residual fluid made of CO_2, CH_4 and N_2. Within the clusters MPI occur with relatively larger (5–20 µm) and rarer nanogranitoid inclusions (Fig. 1b), composed of quartz, biotite, K-feldspar, plagioclase and rarely carbonates. The presence of microdiamonds coexisting with nanogranitoids and MPI in the clusters was confirmed by Raman spectroscopy (Fig. 1c).

Initial estimation of temperature during the metamorphic peak was done with the use of Zr-in-Rutile thermometry. The concentration of zirconium in rutile was measured by electron microprobe and subsequently recalculated into temperature according to the formula calibrated for high-pressure conditions proposed by Kohn (2020). The highest obtained temperature is 873 °C ± 20 °C, which is consistent with earlier estimations by Klonowska et al. (2017) for the metamorphic peak temperature. Seven re-homogenization experiments at different P-T conditions were conducted in a multi-anvil apparatus to remelt nanogranitoids and determine the composition of the anatectic melt. The best homogenization was acquired at 900 °C and 4.5 GPa. The entrapped melt is mostly rhyolitic to trachytic in composition, with a systematic high alkali content (~10 wt% N_2O+K_2O). The H_2O and CO_2 content of the remelted nanogranitoids analysed by NanoSIMS is respectively ~ 5 wt% and 2000–5000 ppm. The chemical composition of reconstructed anatectic melt from paragneisses of SNC is consistent with experimental studies of UHP melts derived from metapelites presented by Schmidt (2015).

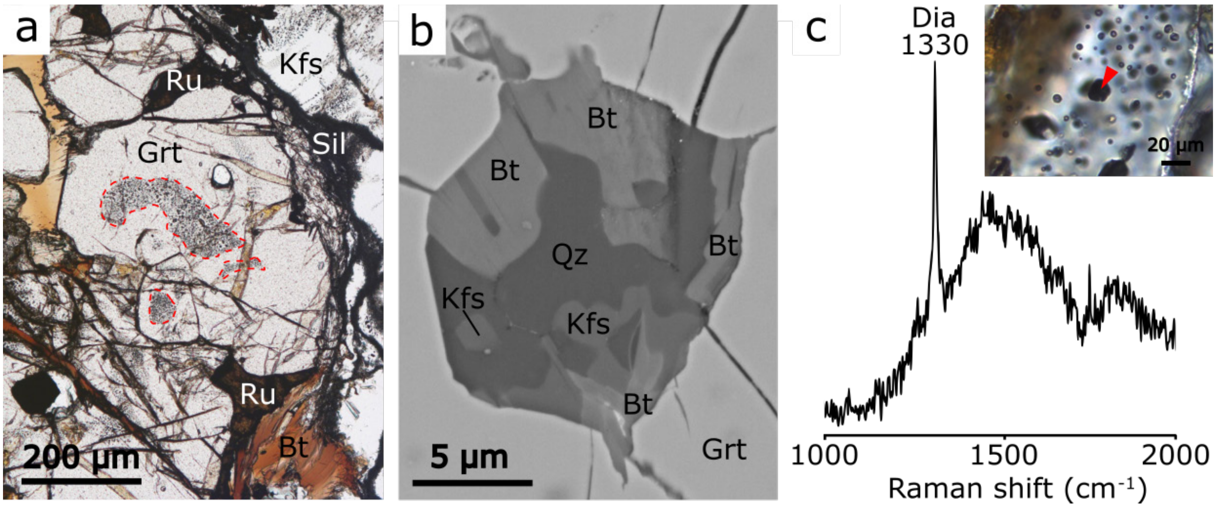

Figure 1. a. Photomicrograph of garnet, dashed red line indicates inclusion clusters, b. Backscattered electron image of nanogranitoid from Åreskutan, c. Fragment of Raman spectra showing diagnostic diamond peak and photomicrograph of inclusion cluster with marked analytical point. Abbreviations: Bt – biotite, Dia – diamond, Grt – garnet, Kfs – K-feldspar, Ru – rutile, Sil – sillimanite, Qz – quartz.

References

Bartoli O., Acosta-Vigil A., Ferrero S., Cesare B., 2016: Granitoid magmas preserved as melt inclusions in high-grade metamorphic rocks. *American Mineralogist 101*, 1543-1559

Cesare B., Acosta-Vigil A., Bartoil O., Ferrero S., 2015: What can we learn from melt incluisons in migmatites and granulites? *Lithos 239*, 186-216

Gee, D.G., Jan_ak, M., Majka, J., Robinson, P. & van Roermund, H., 2013. Subduction along and within the Baltoscandian margin during closing of the Iapetus Ocean and Baltica-Laurentia collision. Lithosphere 5, 169-178

Kohn M. J., 2020: A refined zirconium-in-rutile thermometer. *American Mineralogist 105*, 963-971

Klonowska, I., Janak M., Majka J., Froitzheim N., Klonowska I., Manecki M., Sasinkova V., and Yoshida K., 2017: Microdiamond on Areskutan confirms regional UHP metamorphism in the Seve Nappe Complex of the Scandinavian Caledonides. *Journal of Metamorphic Geology 35*, 541-564

Majka J., Rosen Å., Janak M., Majka J., Petrik I., Froitzheim N., Gee D., G., Sasinkova V., 2017: Microdiamond discovered in the in the Seve Nappe (Scandinavian Caledonides) and its exhumation by the "vacuum-cleaner" mechanism. *Geology 42*, 1107-1110

Schmidt M. W., 2015: Melting of pelitic sediments at subarc depths: 2. Melt chemistry, viscosities and a parameterization of melt composition. *Chemical Geology 404*, 168-182

Tacchetto T., Bartoli O., Cesare B., Berkesi M., Aradi L. E., Dumond G., Szabo C., 2019: Multiphase inclusions in peritectic garnet from granulites of the Athabasca granulite terrane (Canada): Evidence of carbon recycling during Neoarchean crustal melting. *Chemical Geology 508*, 197-209

Mary, Mary, quite contrary, how does your garnet grow? – Lessons from garnet trace-element mapping and Lu-Hf (micro-)chronometry

Matthijs A. Smit[a], Lorraine Tual[a,b], Ellen Kooijman[c]

[a]Department of Earth, Ocean and Atmospheric Sciences, University of British Columbia, Vancouver, Canada, msmit@eoas.ubc.ca, [b]Geological Survey of Canada, Ottawa, Canada, [c]Department of Geosciences, Naturhistoriska Riksmuseet, Stockholm, Sweden.

Summary. This presentation will provide an overview of the process of metamorphic garnet growth. To answer the question of the paraphrased nursery in the title, we have, for the past years, investigated garnet petrogenesis in metamorphic rocks across a range of compositions and tectonic settings. Our approach involved integrating novel trace-element mapping techniques with Lu-Hf (micro-) chronology applied to individual garnet grains or zones therein. The analyses provided new insights into the cause and meaning of garnet trace-element zoning, specifically REE, and the general style and duration of garnet growth in metamorphic systems.

Few things are more self-evident than saying that garnet is of great importance to solid-Earth sciences; garnet – in some chemical variety – is stable across most of continental crust and the upper mantle. It occurs as igneous phase in skarns and peraluminous pegmatites and granites, as metasomatic phase in rodingites and serpentinites, as rock-forming mineral in mantle peridotites and eclogites, and of course as metamorphic mineral in crustal rocks across the range of compositions and metamorphic facies. In general, but particularly in metamorphic rocks, garnet records and retains a unique record of sub- and supra-solidus reactions, and the pressure (P) and temperature (T) conditions at which these occur (Spear, 1993). The Fe and O isotope systematics of garnet can be used to track redox conditions and fluid sources (Gerrits et al., 2019; Bovay et al., 2021). To complete the utterly versatile toolbox, garnet typically exhibits high Sm/Nd and Lu/Hf values, enabling direct dating through the ^{147}Sm-^{143}Nd and ^{176}Lu-^{176}Hf chronometers (Griffin & Brueckner, 1980; Duchene et al., 1997). The latter in particular is among the most robust mineral chronometers available, with garnet grains smaller than 0.1 mm perfectly retaining age information even through extreme metamorphic cycles lasting for hundreds of millions of years and involving ultrahigh temperatures (Scherer et al., 2000; Smit et al., 2013).

With an odd 500 papers per year mentioning garnet, or using this mineral in some way or form, surely we know how this phase grows. Or do we? How long does it take for grains to grow a decent size and is this faster or slower than the pace at which rocks are buried and heated? What do compositions actually reflect: changes in mineral assemblages and P-T conditions, or changes in growth rate? Both? Neither? Where in the history of a metamorphic rock does garnet usually come into the story? What is the meaning of REE compositions and zoning, and to what extent do these (still) reflect equilibrium with other minerals, including phases that are commonly used to *indirectly* date garnet growth via REE petrochronology (e.g. zircon and monazite)?

During the past years, we have performed a series of studies on garnet from various settings, including blueschists, low- and high-grade metapelites, and mafic to felsic granulites. In each of these studies, we integrated novel techniques in trace-element mapping by LA-ICPMS with high-precision Lu-Hf chronometry on single grains, or even individual zones within grains. The mapping of trace elements, and REE in particular, shows the peculiar interplay between the supply and demand of the chemical ingredients for growth and demonstrates the strong control of growth rate on finite zoning development. The maps furthermore provide new insight into uptake mechanisms for REE, which provides clues as to why these elements rehomogenize far less effectively by volume diffusion than diffusion experiments predict.

Comparison between REE and age records of garnet and coexisting monazite and zircon in high-grade rocks shows that basic expectations and requirements for petrochronology broadly apply. It is clear, though, that one-to-one linkages between a dated zircon or monazite, and coexisting garnet through individual REE signatures of single grains may not always be reliable. Extreme REE zoning is common in garnet, also in garnet formed at very high temperatures (>750 °C), meaning that the REE composition of the matrix with which zircon and monazite equilibrate fluctuates strongly as garnet grains grow. It is this fluctuation that nevertheless becomes captured by the REE systematics of the accesory mineral record as a whole. Often, it therefore is the magnitude of the range in REE concentrations observed for a given time, rather than individual compositions in that range, that inform on garnet stability.

Coupling the new mapping capabilities with Lu-Hf (micro-)chronology – the dating of individual growth zones isolated using micro-sampling techniques, in our case laser cutting – provides a cutting edge approach (literally) to look beyond the grain-scale. The first application of Lu-Hf chronometry using laser-cutting-microsampling was done on blueschists, with the explicit goal to determine the duration and pace of the garnet growth and associated H_2O-releasing reactions within the shallow part of subduction zones. The analysis revealed an intriguing record of ultrafast, yet pulsed growth, leading to the complete transformation of prime mineral assemblages within less than a million years. Similar time scales appear involved in the growth of garnet in metapelitic rocks undergoing Barrovian metamorphism in collisional orogens.

The new studies confirm that, although (or because?) garnet reactions may be overstepped, grains can grow exceedingly fast. Growth histories, or pulses therein, may last far shorter than any change in P-T conditions caused by the tectonic burial or exhumation of rocks. The sharp REE zoning observed in those cases is similar to the zoning observed in garnet from more extreme metamorphic grades, including the ultrahigh-temperature granulite facies. It is thus possible that the major-element zoning, which is generally smooth in high-grade garnet and taken as a record of steady long-term growth during changing P-T conditions and tectonics, may in fact mask the actual style of garnet growth: fast, pulsed, and only possible during the brief episodes when grain boundaries are not entirely dry.

References

Bovay, T., Rubatto, D. & Lanari, P., 2021: Pervasive fluid-rock interaction in subducted oceanic crust revealed by oxygen isotope zoning in garnet. *Contributions to Mineralogy and Petrology 176*, 55.

Duchêne, S., Blichert-Toft, J., Luais, B., Télouk, P., Lardeaux, J.-M., & Albarède, F., 1997: The Lu–Hf dating of garnets an the ages of the Alpine high-pressure metamorphism. *Nature 387*, 586–589.

Gerrits, A.R., Inglis, E.C., Dragovic, B., Starr, P.S., Baxter, E.F. & Burton, K.V., 2019: Release of oxidizing fluids in subduction zones recorded by iron isotope zonation in garnet. *Nature Geoscience 12*, 1029–1033.

Griffin, W.L. & Brueckner, H.K., 1980: Caledonian Sm–Nd ages and a crustal origin for Norwegian eclogites. *Nature 285*, 319–321.

Scherer, E.E., Cameron, K.L. & Blichert-Toft, J., 2000, Lu–Hf garnet geochronology: Closure temperature relative to the Sm–Nd system and the effects of trace mineral inclusions. *Geochimica et Cosmochimica Acta 64*, 3413–3432.

Smit, M.A., Scherer, E.E. & Mezger, K., 2013: Lu–Hf and Sm–Nd garnet geochronology: Chronometric closure and implications for dating petrological processes. *Earth and Planetary Science Letters 381*, 222–233.

Spear, F.S., 1993: Metamorphic phase equilibria and pressure-temperature-time paths. *Mineralogical Society of America Monographs 1*, 799 p.

Major disturbance of the TIB 1 evolution in SE Sweden, caused by the arrival of exotic crust to the SW margin of Baltica at c. 1795 Ma

Krister Sundblad[a], Evgenia Salin[b]

[a]Lokomotivmannagatan 5:15, FIN-20100 Åbo, Finland, sundblad.krister@gmail.com;
[b]Department of Geography and Geology, University of Turku, Finland, e-mail evgenia.salin@utu.fi;

Summary. TIB 1 formed in two cycles (TIB 1a and 1b), each with an incipient shallow-marine basement-cover stage, first followed by an early and secondly by a main batholith stage (with abundant terrestrial volcanics). TIB 1a started at 1813 Ma with volcanoclastic deposition on the Västervik quartzites, followed by the two batholith stages but the TIB 1 evolution was dramatically disturbed when exotic crust arrived to and collided with TIB 1a at 1795 Ma. TIB 1b started with sedimentation and shallow-marine volcanism on top of the exotic crust before being intruded by 1786–1769 Ma TIB 1b batholith stages.

Introduction

The Transscandinavian Igneous Belt (TIB) is a Palaeoproterozoic plutonic-volcanic unit that formed along the SW margin of the proto-continent Baltica from 1860 to 1650 Ma. Based on geochronology, it is commonly divided into three igneous phases; TIB 0 (1860–1830 Ma), TIB 1 (1815–1760 Ma) and TIB 2 (1710–1650 Ma), but it was also demonstrated by Salin et al. (2019) that TIB 1 can be further subdivided into the 1815–1796 Ma TIB 1a (Vimmerby Batholith), the 1796–1760 Ma TIB 1b (Växjö Batholith) and the 1770–1750 Ma TIB 1c (Blekinge region) generations.

This contribution shows that even further subdivisions can be made within TIB 1 a-b by making use of the geochronology database of the Geological Survey of Sweden (SGU) and by combining that information with new geological observations and new geochemical data. Inspiration has also come from many GFF and SGU sources, not the least the pioneer work of Stolpe (1892) and modern contributions like Appelquist et al. (2009) and Bjärnborg et al. (2015). With deepest respect to all previous contributors, a completely new view of the evolution of TIB 1 will be presented here.

TIB 0 and TIB 1a

Shortly after the cratonization of Baltica, the first TIB phase (TIB 0) formed along the SW margin of this continent, when it intruded into the metamorphosed 1.89 Ga Svecofennian crust in the Bergslagen region and the 1.87 Ga Västervik quartzites closer to the Baltic Sea.

The first expressions of the igneous activity within TIB 1a (Vimmerby batholith) followed the within-continent pattern of TIB 0. The onset was at 1813 Ma at Stormandebo where a suite of basaltic to rhyolitic volcanic rocks and volcaniclastic strata formed as the *Incipient TIB 1a stage* on the eroded basement of the Västervik quartzites. The shallow-marine Stormandebo strata (and their basement) were intruded by the 1812 Ma Tjällmo and 1808 Ma Sjögestad granitoids as the *Early batholith stage* before 1802–1796 Ma granitoids and abundant rhyolitic subaerial volcanic rocks were emplaced in the Tranås-Vimmerby region as the *Main batholith stage*, southwest of the continental margin.

Arrival of allochthonous metamorphic crust; a major break between TIB 1a and TIB 1b

The igneous evolution of TIB 1 was severely interrupted at c. 1795 Ma when exotic metamorphosed crustal units arrived from distant offshore positions to the Baltica continental margin (which now had moved to the SW border of TIB 1a). Three distinct exotic fragments can be identified, representing (from east to west) increasing metamorphic grade, transport distances and probably also ages: 1.83–1.82 Ga tonalites in the Eksjö-Bäckaby region, the primitive 1.85 Ga oceanic arc at Fröderyd (Salin et al., 2021), and migmatitic orthogneisses of unknown ages in the Malmbäck and Stockaryd regions. The latter unit was probably derived from a separate and previously unknown continent.

TIB 1b

Shortly after the arrival of the allochthonous crustal fragments to Baltica, they were covered by rapidly accumulating autochthonous epiclastic, poorly sorted sediments and volcanic strata. These successions have kept a very low metamorphic grade and constitute the *Incipient stage* of TIB 1b. The sediments are best known in the Malmbäck and Vetlanda areas and include arkoses and conglomerates, with a wide range of detrital components (quartz, feldspars, amphibole, garnet and even biotite) indicating very short transport distances from the source rocks (probably TIB 1a and the exotic basement rocks) and deposition in very shallow water, probably in a beach setting. Volcanic rocks occur in the Malmbäck, Nömmen and Vetlanda-Ädelfors regions where they are associated with the c. 1792 Ma Kleva Ni-Cu gabbro and separated from the TIB 1a granitoids by a major shear zone. They range in composition from basalts to rhyolites and show a high-K, calc-alkaline trend, suggesting a similar continent-continent setting as the alkaline Aeolian Arc in the Tyrrhenian basin (Giordano et al., 2017). In such a perspective, a new door has now opened to a previously unknown room in the house of Fennoscandian geology.

The allochthonous basement complex, with its cover of autochthonous low-metamorphic supracrustal rocks, is here defined as the Central Småland Belt. The entire process in creating the Central Småland Belt (i.e. docking of exotic metamorphic terranes to Baltica, and subsequent deposition of supracrustal cover rocks) must have been completed within a very short time period (probably not more than a few millions of years) at c. 1795 Ma.

The Central Småland Belt forms two discontinuous basins along the SW margin of TIB 1a. One of them can be followed from Eksjö via Vetlanda and Holm (S of Virserum) to Oskarshamn (with northwards facing stratigraphy) and the second in an arc-shaped structure from Malmbäck via Stockaryd and Hörnebo to Mönsterås (with southwards facing stratigraphy).

The Central Småland Belt was intruded by the 1786 Ma TIB 1b granitoids at Sävsjö (*Early batholith stage*). Even if the metamorphic grade of the Vetlanda sediments generally is very low, the heat from the Sävsjö granite caused locally a hornfels-related andalusite-garnet assemblage (SW of Vetlanda town) and a Cu-Mo skarn ore (Sunnerskog) in the Vetlanda sediments. Subsequent magmatism, S of the Central Småland Belt, formed the *Main batholith stage* of TIB 1b; the 1769 Ma Växjö granitoids and associated 1780 Ma terrestrial rhyolites (with polymetallic sulphide ores; Sundblad, 1997).

Acknowledgements. Mats Stolpe (1833–1918) was one of the founding members of the Geological Society of Sweden in 1871. His map sheet (1892) includes the most important key areas in this contribution (Malmbäck, Nömmen, Stockaryd, Fröderyd and the western parts of the Vetlanda region). Stolpe was the first geologist ever to make observations on every single outcrop in this vast area (c. 2500 km2), where the only means of transportation was by walking or by using horses. Stolpes map is still, after 130 years, the best source of information for many details concerning the local bedrock in Central Småland. Ulf Söderlund (Lund) and Dick Claeson (SGU, Uppsala) inspired us (more than they can imagine) to initiate this work in late 2021. Our ideas benefitted also from discussions with Lars Persson (Uppsala), Kennert Röshoff and Elisabet Alm (Stockholm).

Selected references

Appelquist, K., Eliasson, T., Bergström, U. & Rimša, A., 2009. The Palaeoproterozoic Malmbäck Formation in S Sweden: age composition and tectonic setting. *GFF* 131, 229-243.

Bjärnborg, K., Scherstén, A., Söderlund, U. & Maier, W.D., 2015. Geochronology and geochemical evidence for a magmatic arc setting for the Ni-Cu-mineralised 1.79 Ga Kleva gabbro-diorite intrusive complex, southeast Sweden. *GFF* 137, 83-101.

Giordano, R., Caggianelli, A., Sulpizio, R., Balestrieri, M.L., Maiorano, P. & Solari, L., 2017. Magmatic and geodynamic significance of two volcaniclastic deposits in the Oligo-Miocene successions of the Southern Apennines (Italy). *Italian Journal of Geosciences* 136, 157-170.

Salin, E., Sundblad, K., Woodard, J. & O'Brien, H., 2019. The extension of the Transscandinavian Igneous Belt into the Baltic Sea region. *Precambrian Research* 328, 287-308.

Salin, E., Sundblad, K. & Lahaye, Y., 2021. A 1.85 Ga volcanic arc offshore the proto-continent Fennoscandia in southern Sweden. *Precambrian Research* 356, 106-134.

Stolpe, M., 1892. Kartbladet Nydala med beskrifning. *Sveriges Geologiska Undersökning* Ab 14.

Sundblad, K., 1997. Syngenetic Pb-Zn-Cu sulphide mineralization in 1.8 Ga subaerial volcanic rocks, southeastern Sweden. *GFF* 119, 103-108.

Magma mixing and replenishment beneath Laurens Peninsula, Heard Island

Ransom U. Telson[a], Abigail K. Barker[a], Jane Barling[b]

[a]Department of Earth Sciences, Uppsala University, Uppsala, Sweden, ransom.telson95@gmail.com,
[b]Department of Earth Sciences, University of Oxford, Oxford, UK

Summary. Magmatic processes beneath the Laurens Peninsula, Heard Island, are investigated by crystal size distribution (CSD). Three samples are analysed that range from mafic to felsic compositions. The CSD's of clinopyroxene and titanomagnetite/ilmenite crystals all display curved profiles indicating open system magma storage. Magma replenishment has led to coarsening of phenocrysts and assimilation of smaller crystals into melt. Microcrysts nucleated during eruption processes like degassing and decompressing, creating steep CSD slopes.

The Kerguelen Plateau is an oceanic plateau located in the central region of the Indian Ocean. The volcanism is attributed to a hotspot beneath the plateau named the Kerguelen plume, thereby making it an analogy for magmatism on Iceland. Heard Island is in the centre of the Kerguelen Plateau. It is approximately 372 km^2 and modern volcanism has been periodic since about 1 Ma (Barling et al., 1994). The Laurens Peninsula extends northwest from the main part of Heard Island, at its centre lies Mt Dixon volcano (715 m.a.s.l.). The rocks belonging to this series of lavas are typically moderately porphyritic basanites (Leitchenkov et al. 2018). This study aims to investigate magmatic processes occurring beneath the Laurens Peninsula by crystal size distribution (CSD). We used machine learning and image segmentation to distinguish crystals.

A phonolite sample contains subhedral-anhedral clinopyroxene phenocrysts with rare normal zoning, typically ranging from 0.5–1.5 mm, suspended in a fine-grained (approximately <0.03 mm) plagioclase rich groundmass. This phonolite has occasional amphibole crystals that are breaking down and being replaced by clinopyroxene and titanomagnetite/ilmenite microcrysts (Fig. 1a). The phonolite also contains rare plagioclase with patchy zoning (Fig. 1b). Subhedral titanomagnetite/ilmenite (0.1–0.5 mm) also occur associated with large clinopyroxene phenocrysts. The CSDs for both clinopyroxene and titanomagnetite/ilmenite are concave upwards (Fig. 2).

A tephriphonolite sample contains euhedral-subhedral clinopyroxene phenocrysts, typically 0.5–3 mm in size, with oscillatory zoning and simple twinning. Subhedral olivine were found with grain sizes of about 0.5–1.5 mm. Unique to this sample were large plagioclase crystals which measured up to 2 mm but did not contain patchy zoning. The subhedral titanomagnetite/ilmenite crystals were approximately 0.5–1.5 mm and commonly found near rims or included in other crystals (Fig. 1c). The groundmass was composed of plagioclase, iron-oxides and some olivine and pyroxene that grew up to approximately <0.5 mm. The CSDs for both clinopyroxene and titanomagnetite/ilmenite are concave upwards (Fig. 2).

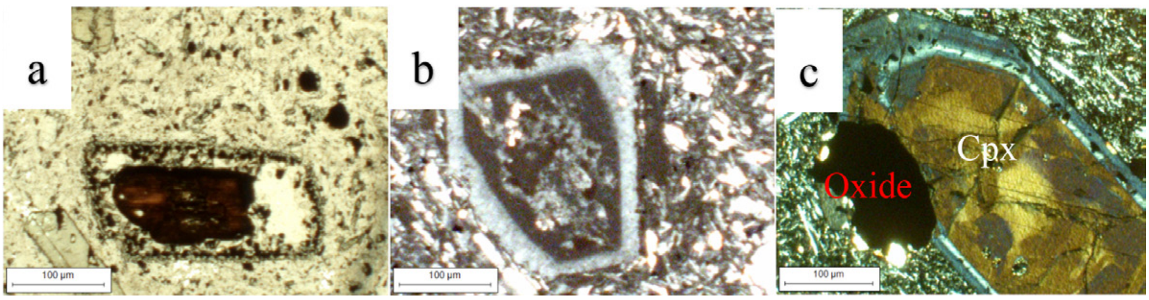

Figure 1. Disintegrating amphibole (a), patchy zoning in plagioclase (b), example from the tephrite of the oxide growing on the rims of other crystals, typical in all samples. Also showing clinopyroxene with un-zoned cores (c).

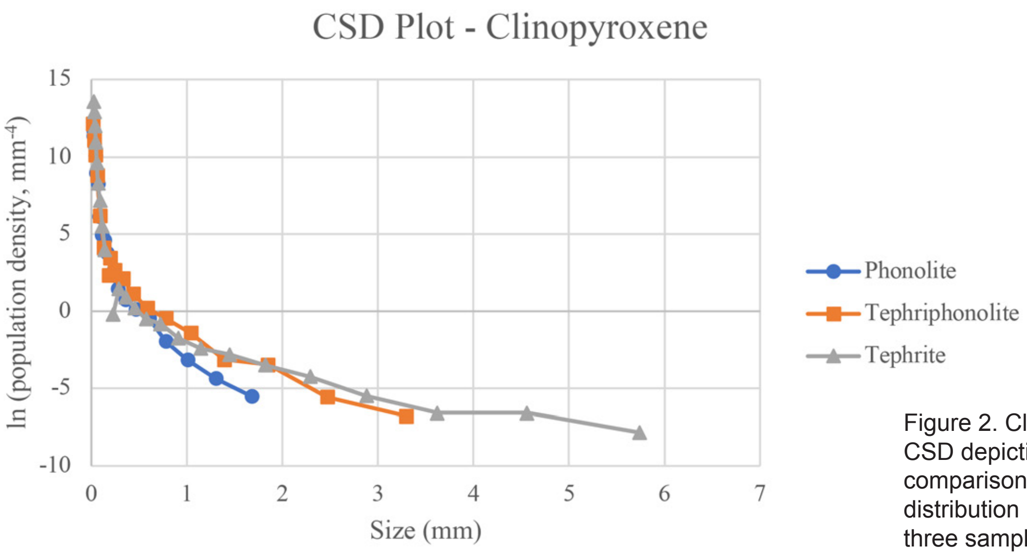

Figure 2. Clinopyroxene CSD depicting the comparison of size distribution between the three samples.

The tephrite sample contains euhedral clinopyroxene phenocrysts around 1.0–4,0 mm with oscillatory zoning around un-zoned cores (Fig 1c). Euhedral-subhedral olivine were commonly 1.0–2.0 mm with no zonation. Subhedral titanomagnetite/ilmenite approximately 0.5–1.5 mm in size was common. The groundmass was fine-grained at approximately <0.3 mm and contained plagioclase, pyroxene, and iron-oxides. The CSDs for both clinopyroxene and titanomagnetite/ilmenite are concave upwards (Fig. 2).

The slopes of both clinopyroxene and titanomagnetite/ilmenite CSD show concave up shapes, which suggests the magmas beneath the Laurens Peninsula have experienced mixing (Marsh 1998). The plot clearly depicts two separate populations of crystals which have crystallized under different conditions. The smaller crystals show a steep slope with a high nucleation density (Fig. 2). The larger phenocrysts record a shallower slope with larger longer residence time and lower nucleation density (Fig. 2). This type of shape is typical of magmas which have undergone replenishment (Marsh 1998). During replenishment, crystals above a critical size coarsen, while crystals below it assimilate into melt (Marsh 1998). This coarsening event is what is plotted by the phenocrysts in Fig. 2. The microcrysts probably nucleated during eruption due to processes such as degassing and decompression in relatively cooler environments, giving them the steep slope with high nucleation density (Higgins & Roberge 2007). The kinks in the plots are evidence of fractionation and accumulation processes that might have occurred as the magma ascended towards the surface (Higgins & Roberge 2007). Although this study does not provide evidence for or against three component mixing, a previous geochemical study concluded that the variations in ratios of incompatible elements and isotopic composition suggest binary magma mixing (Barling *et al.* 1994). Large crystals in the tephrite indicate that it had the longest residence time, followed by the tephriphonolite and finally the phonolite (Fig. 2). If replenishment was indeed the mechanism of mixing, then volcanism may well be active beneath the Laurens Peninsula, but currently in a hiatus and replenishing.

References

Barling J, Goldstein SL, Nicholls IA. 1994. Geochemistry of Heard Island (Southern Indian Ocean): Characterization of an Enriched Mantle Component and Implications for Enrichment of the Sub-Indian Ocean Mantle. Journal of Petrology 35: 1017–1053.

Higgins MD, Roberge J. 2007. Three magmatic components in the 1973 eruption of Eldfell volcano, Iceland: Evidence from plagioclase crystal size distribution (CSD) and geochemistry. Journal of Volcanology and Geothermal Research 161: 247–260.

Marsh B. 1998. On the Interpretation of Crystal Size Distributions in Magmatic Systems. Journal of Petrology, doi 10.1093/petroj/39.4.553.

Leitchenkov GL, Dubinin EP, Grokholsky AL, Agranov GD. 2018. Formation and Evolution of Microcontinents of the Kerguelen Plateau, Southern Indian Ocean. Geotectonics 52: 499–515.

Thematic Session 11
Quaternary geology

Session Chairs:
Mark Johnson (mark@gvc.gu.se)
Ian Snowball (ian.snowball@geo.uu.se)

Ice sheet and North Sea drainage drive dust source variability recorded in late Quaternary loess deposits at Pegwell Bay, SE England

Yunus Baykal[a], Thomas Stevens[a], Mark Bateman[b], Daniele Sechi[c], Katharina Pfaff[d], Adriano Banak[e], Haobo Zhang[f], Junsheng Nie[f]

[a]Department of Earth Sciences, Uppsala University, Uppsala, Sweden, yunus.baykal@geo.uu.se; [b]Department of Geography, University of Sheffield, Sheffield, UK; [c]Department of Architecture, Design and Planning, University of Sassari, Alghero, Italy; [d]Department of Geology and Geological Engineering, Colorado School of Mines, Golden, USA; [e]Department of Geology, Croatian Geological Survey, Zagreb, Croatia,[f]College of Earth and Environmental Sciences, Lanzhou University, Lanzhou, China

Summary. Loess deposits in NW Europe record past atmospheric dust emission from regions close to the former Eurasian Ice Sheet. Luminescence dating of loess at Pegwell Bay, SE England showed that dust accumulated rapidly during the late last glacial, possibly linked to British-Irish Ice Sheet (BIIS) dynamics. Here we undertake a multi-method provenance study of loess at Pegwell Bay to test the role of the BIIS and proglacial drainage dynamics in driving high latitude dust emission and loess accumulation in SE England.

Atmospheric dust is a major component of the Earth's climate system both driving and responding to climate change (Knippertz, 2014). Loess deposits along the European loess belt potentially record past changes in atmospheric dust activity. In particular, loess deposits from NW Europe may serve as valuable archives of dust emission from regions close to the former Eurasian Ice Sheet. Recently, detailed luminescence dating of loess at Pegwell Bay, SE England showed that dust deposition occurred rapidly during the late last glacial, with two phases of enhanced accumulation potentially linked to British-Irish Ice Sheet (BIIS) dynamics and associated glaciofluvial drainage activity (Stevens et al., 2020). However, uncertainties over the sources and origins of this loess limit constraint of the precise causes of this dust deposition variability.

Traditionally, loess deposits in SE England have been attributed to northern ice sheet derived sediments exposed in the North Sea basin (Lill & Smalley, 1978). Evidence from heavy mineral studies of loess and tills in England has been presented to support both BIIS and FIS derived sources for the loess (Madgett & Catt, 1978; Eden, 1980). In contrast, Smalley et al. (2009) argued for an Alpine provenance of loess in SE England involving sediment transport via the last glacial Rhine. Moreover, local derivation of loess from the underlying shallow marine Thanet Fm. has been suggested by numerous authors at the SE England Pegwell Bay site (Pitcher et al., 1954; Milodowski et al., 2015). As such, multiple source scenarios for loess in SE England seem plausible at present.

New chronological data from Stevens et al. (2020) allows re-evaluation of these scenarios in the context of the relatively well constrained North Sea ice history. Loess at Pegwell Bay accumulated rapidly during the late last glacial when the British-Irish (BIIS) and Fennoscandian Ice Sheet (FIS) had coalesced. Moreover, two phases of strongly enhanced deposition rates were detected, coincident with advances and retreats of the nearby North Sea Lobe (NSL), and associated glaciofluvial drainage activity in the southern North Sea basin. By extension, these findings suggest a genetic linkage between ice sheet derived detritus in the North Sea basin and loess in SE England. Here we study the sources of this episodically deposited loess at Pegwell Bay using multiple provenance techniques. We analysed detrital zircon U-Pb ages, heavy mineral spectra and bulk Nd isotopes from the loess as well as potential source samples in the North Sea region. Moreover, we use SEM imagery of detrital quartz grain morphology to yield insight into the mechanisms involved during sediment generation and transport.

Our results indicate that the provenance of loess deposited during the first accumulation phase at Pegwell Bay (25–23.5 ka) is consistent with a combination of protosources in Britain, Continental Europe and possibly Scandinavia, while loess deposited during the second accumulation phase (20–

19 ka) seems entirely derived from British basement. This difference in loess sources between the two accumulation phases implies that dust accumulation and provenance is not solely controlled by NSL dynamics, although overall it plays a major role at least in SE England. Indeed, fluctuations of the NSL extent interacted with North Sea drainage of the coalesced FIS and BIIS as well as river input from Continental Europe. During repeated advances, the NSL blocked drainage flow in the ice marginal spillway and potentially caused formation of the proglacial lake Dogger in the central North Sea. As such, sediment particles originating from protosource terranes in Britain, Scandinavia and Continental Europe are potentially released during NSL retreats and associated Dogger lake outburst floods into the southern North Sea and, by extension, deposited as loess in SE England. Our findings contribute to the understanding of sediment transport pathways in the last glacial North Sea basin while highlighting the importance of abrupt ice sheet dynamics and their drainage in controlling atmospheric dust emission from high latitude regions.

References

Eden, D.N., 1980: The loess of North-East Essex, England. *Boreas 9*, 165–177.

Knippertz, P., 2014: Mineral Dust.

Lill, G.O. & Smalley, I.J., 1978: Distribution of loess in Britain. *Proceedings of the Geologists' Association 89*, 57–65.

Madgett, P.A. & Catt, J.A., 1978: Petrography, Stratigraphy and Weathering of Late Pleistocene Tills in East Yorkshire, Lincolnshire and North Norfolk. *Proceedings of the Yorkshire Geological Society 42*, 55–108.

Milodowski, A.E., Northmore, K.J., Kemp, S.J., Entwisle, D.C., Gunn, D.A., Jackson, P.D., Boardman, D.I., Zoumpakis, A., Rogers, C.D.F., Dixon, N., Jefferson, I., Smalley, I.J. & Clarke, M., 2015: The mineralogy and fabric of 'Brickearths' in Kent, UK and their relationship to engineering behaviour. *Bulletin of Engineering Geology and the Environment 74*, 1187–1211.

Pitcher, W.S., Shearman, D.J. & Pugh, D.C., 1954: The Loess of Pegwell Bay, Kent, and its Associated Frost Soils. *Geological Magazine 91,* 308–315.

Smalley, I., Hara-dhand, K.O., Wint, J., Machalett, B., Jary, Z.& Jefferson, I., 2009: Rivers and loess : The significance of long river transportation in the complex event-sequence approach to loess deposit formation. *Quaternary International 198*, 7–18.

Stevens, T., Sechi, D., Bradák, B., Orbe, R., Baykal, Y., Cossu, G., Tziavaras, C., Andreucci, S. & Pascucci, V., 2020: Abrupt last glacial dust fall over southeast England associated with dynamics of the British-Irish ice sheet. *Quaternary Science Reviews 250*.

The Deglaciation of the Kebnekaise region, Northern Sweden

Calum .J. Edward[a], Robin Blomdin[b], Gunhild Rosqvist[c]

[a]Department of Earth Sciences, Uppsala University, Uppsala, Sweden, calum.edward@geo.uu.se; [b]Department of Geography, Norwegian University of Science and Technology, Trondheim, Norway, robin.blomdin@ntnu.no; [c]Department of Physical geography, Stockholm University, Stockholm, Sweden, ninis.rosqvist@natgeo.su.se.

Summary. Palaeoglaciological reconstructions are critical tools for indicating the future behaviour of modern ice bodies. We present the first geomorphological map for the Kebnekasie region since Melander (1975), and a comprehensive landform classification, produced through LiDAR analysis and ground truthing. In reconstructing the retreating ice from the glacial geomorphology, we apply a glacial inversion model, a conceptual framework composed of a set of assumptions regarding landforms' genetic properties (Kleman et al. 2006), and conclude with indication to the ice sheet's local deglaciation pattern.

Glacial geomorphology reveals local pattern of Scandinavian Ice Sheet deglaciation

The recent availability of the 2m-resolution Swedish LiDAR based terrain model provides the opportunity to map glacial landforms and landscapes over large areas with greater accuracy than was previously possible through satellite images or aerial photographs. In combination with field observation-based ground-truthing, we employ this LiDAR resource to map the geomorphology of the Kebnekaise region of the northern Swedish mountains to produce a landform-driven reconstruction of the deglaciation of the remnant Scandinavian Ice Sheet during its final stage of retreat.

We present a comprehensive landform classification for the delineation and interpretation of the Kebnekaise region's (see figure) complex 'palimpsest' landscape, according to the relative age and formative conditions of the landform assemblages comprised. We pay particular attention to the segregation of glacial (e.g. ice-marginal moraines, drumlinoids), deglacial (e.g. eskers, lateral meltwater channels, ice-dammed lake shorelines) and 'relict' (i.e. pre-glacial palaeosurfaces) landform assemblages, in order to differentiate those formed during the final deglaciation. We present the reconstruction of the final deglaciation in a series of landform-inferred time slices, providing a high-resolution visualisation of the ice sheet's local retreat pattern, and glacial lake evolution.

The mapping process yielded the identification of landforms in detail hitherto undocumented in the region, including the recognition of evidence for ice-dammed lakes that had not previously been described, facilitating an investigation into the deglaciation final ice remnant location and pattern of retreat, giving indication to the nature of the basal thermal regime, and topographic response. We give an evaluation of the use of the Swedish LiDAR database as a means of efficiently and accurately mapping previously-glaciated landscapes and test our deglaciation reconstruction against formerly produced regional reconstructions.

We draw the following conclusions:

- Our mapping provides an updated analysis of the region's late Quaternary geomorphology, successive to that of Melander (1975), and forms the foundation for a landform-inferred reconstruction of the deglaciation of the remnant Fennoscandian Ice Sheet during its final retreat.
- We present the identification of previously undescribed ice-dammed lakes present during the final deglaciation, the presence of which serves as a key inference to the proposal of a more easterly final retreat, due to the required ice-damming in the east, which would not be possible with a mountain-located final ice remnant.
- We support, therefore, a final ice remnant location to the east of the Sarek mountains, reflective of that proposed by Regnéll et al. (2019).

- High-resolution LiDAR data proves an effective tool in allowing the high-resolution identification and classification of landforms within the study area and has facilitated the description of landforms that have not been described to such a high level of detail in previous research.
- The combination of LiDAR-based mapping and field observation is effective, and good correlation between the verification of remotely observed landforms by ground-truthing, and vice versa, has been evident.

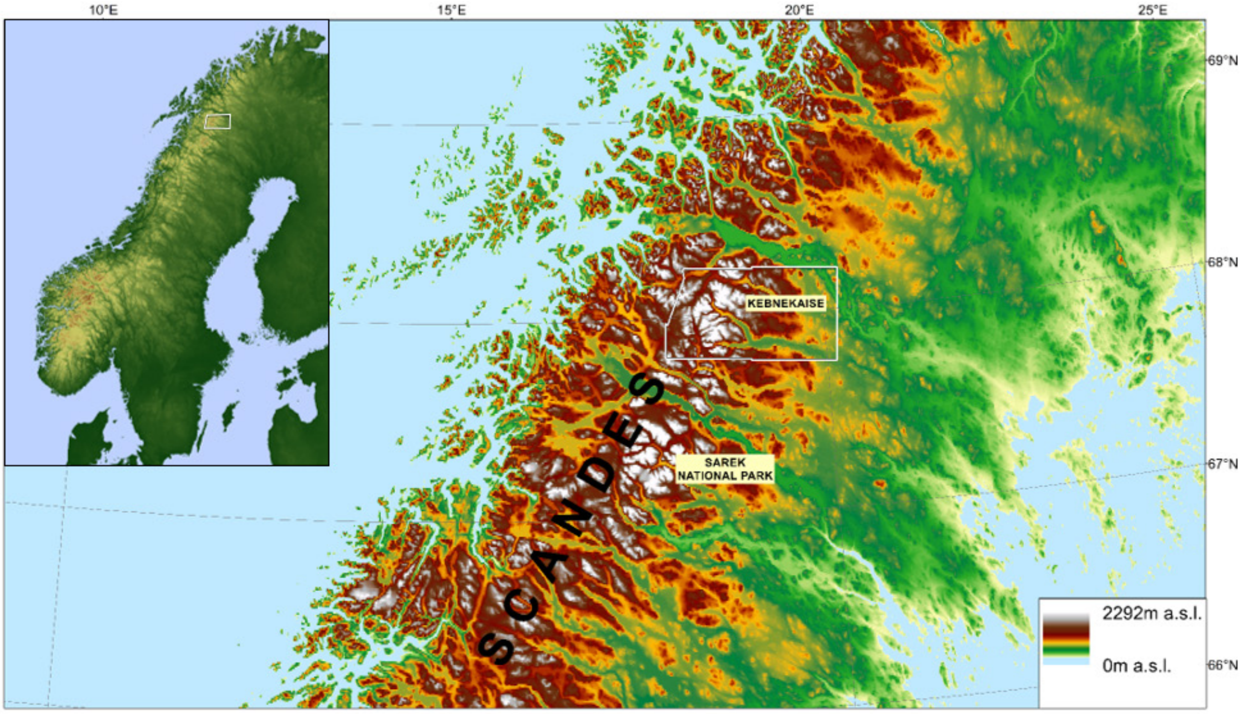

Map showing study area (white border) within Scandinavia and the northern Scandes.

References

Melander, 0., 1975a: The geomorphological map 29 I Kebnekaise - Description and assessment of nature value. *Statens Naturvårdsverk, PM 540*, 77.

Kleman, J., Hättestrand, C., Stroeven, A.P., Jansson, K.N., De Angelis, H., Borgström, I., 2006. Reconstruction of palaeo-ice sheets - inversion of their glacial geomorphological record. In: Knight, P.G. (Ed.), *Glacier Science and Environmental Change. Blackwell Publishing*, *Malden, Ma, USA*, pp. 192-198.

Regnéll, C., Mangerud, J. and Svendsen, J.I., 2019. Tracing the last remnants of the Scandinavian Ice Sheet: Ice-dammed lakes and a catastrophic outburst flood in northern 75 Sweden. *Quaternary Science Reviews*, *221*, 105862. doi: 10.1016/j.quascirev.2019.105862.

New insights to the Weichselian interstadial records of northern Sweden based on OSL-dating, pollen records and isotope analysis

Martina Hättestrand[a], Helena Alexanderson[b,c], Elin Norström[a,f], Mimmi A. Lindqvist[c], Thorbjörg Sigfúsdóttir[b,d], Christos Katrantsiotis[e], Rienk H. Smittenberg[f]

[a]Department of Physical Geography, Stockholm University, Stockholm, Sweden, martina.hattestrand@geo.su.se; elin.norstrom@natgeo.su.se, [b]Department of Geology, Lund University, Lund, Sweden, helena.alexanderson@geol.lu.se, [c]Department of Geosciences, The Arctic University of Norway, Tromsø, Norway, mimmilindq@gmail.com, [d]Present address: Icelandic Meteorological Office, Reykjavik, Iceland, thorbjorgsi@vedur.is, [e]Environmental Archaeology Laboratory, Department of Historical, Philosophical and Religious Studies, Umeå University, Umeå, Sweden, christos.katrantsiotis@umu.se, [f]Department of Geological Sciences, Stockholm University, Stockholm, Sweden, rienk.smittenberg@geo.su.se

Summary. OSL-dating shows that the dead ice landscape of the Veiki moraines in northern Sweden was formed during MIS 3, giving evidence of an intermediate-sized ice sheet in Scandinavia at this time. Through comparisons with other data on glacial history and climate we suggest that the ice sheet advance prior to Veiki moraine formation occurred during Greenland stadials 16.1–15.1 (56.5–54.2 ka) and that final melting of the ice within the landscape took place during GI-14 (54.2–48.3 ka). Pollen, macrofossils and leaf wax stable isotope data give additional information about the interstadial conditions.

In parts of northern Sweden, a relict pre-Late Weichselian landscape has been preserved due to frozen-bed conditions of the last ice sheet covering the area. Characteristic of this landscape is the Veiki moraine, a type of ice-walled lake plains formed during melting of stagnant ice, and eskers and drumlins showing ice flow from the NW. Earlier studies have shown that the preserved landforms are from the Weichselian glacial period. However, which stadial/interstadial phase they belong to has been debated.

We have studied sedimentary records from the relict landscape with the aim to date the glacial history and improve earlier studies of Weichselian interstadial climate and vegetation. Methods used are

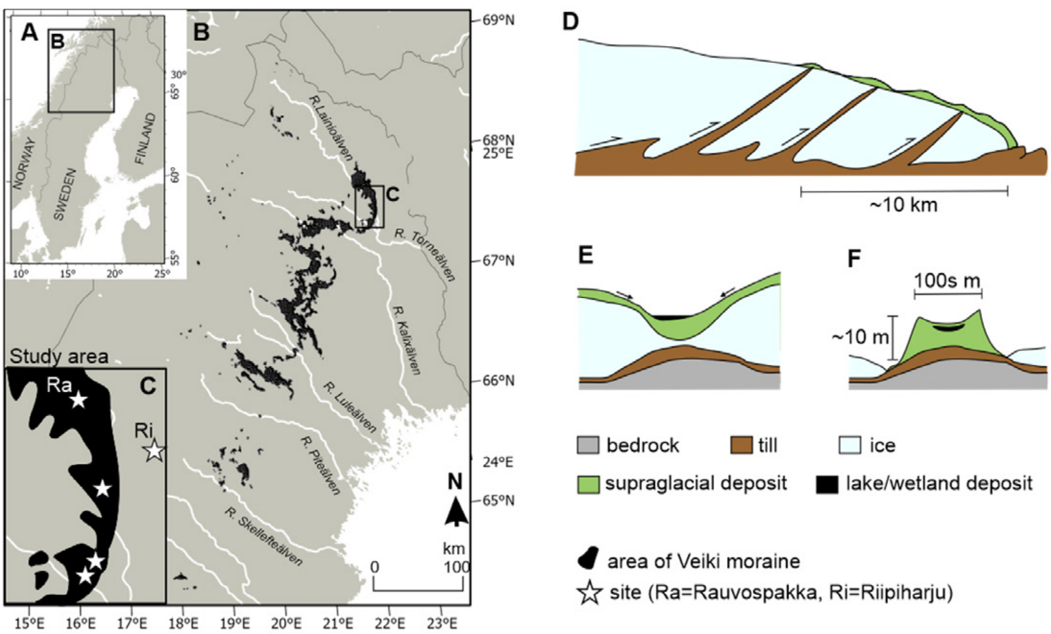

Distribution of Veiki moraine in northern Sweden (from Hättestrand (1998)), the study area (C) and sites used for dating (stars). Analysis of pollen and stable isotopes of leaf waxes has been performed on interstadial sediments from Rauvospakka (Ra) and Riipiharju (Ri). Rauvospakka is a Veiki moraine plateau, while Riipiharju is a kettle hole within a NW-SE oriented esker, 6 km east of the eastern limit of the Veiki moraine distribution. Principle sketches of Veiki moraine formation due to melting of a debris covered stagnant ice (D-F).

OSL-dating, radiocarbon dating, pollen analysis, macro fossil identification and stable isotope analysis of leaf waxes.

Our OSL-dates of the Veiki landscape give ages of 56–39 ka and show that it was formed during MIS 3. Since the landscape was formed due to down wasting of debris-covered ice at the easternmost margin of an ice sheet, the ages are evidence of a phase with an intermediate-sized ice sheet in Scandinavia. Through linking our results with the Greenland ice core record of warm and cold phases during MIS 4 and 3 and with other records of ice sheet history, we discuss the possibility to assign more exact ages for the ice sheet events in the area.

We suggest that there was an extensive ice retreat of the Fennoscandian ice sheet during GI-16.1 (58.0–56.5 ka) leading to an intermediate-sized ice sheet with its margins west of the Veiki moraine zone in central northern Sweden. The period 56.5–54.2 ka, when three relatively short lived stadials occurred, could have been the phase when the ice sheet advanced into the area resulting in the debris covered ice lobes that later melted and resulted in the Veiki landscape (Fig.). The long GI-14 interstadial (54.2–48.3 ka) lasted almost 9000 years and during this long interstadial it is likely that all ice within the Veiki landscape melted off.

During melting of the stagnant ice, depressions formed in the debris covered ice surface. The depressions were infilled by diamict sediments and sometimes lakes and mires were also present. When melting of the ice continued, lakes and mires in the depressions were often infilled by diamict debris. After all ice had melted off, the former depressions were standing out as plateaus with rim ridges, the so called Veiki plateaus. Pollen and macro fossil evidence from peat within a Veiki plateau at Rauvospakka indicate warm climatic conditions during melting of the stagnant ice.

At Riipiharju, a kettle hole formed in a pre-Late Weichselian esker 6 km east of the Veiki landscape, a 10 m long sequence of Weichselian interstadial sediments is present. Previous pollen studies indicate large climatic shifts from warm to cold and back to warm again when the sediments were deposited. It was suggested that the cold phase could match with a period of ice sheet advance west of the site leading up to the formation of the Veiki moraine. Initial attempts to date the interstadial sequence indicate MIS 3 ages for the sediment.

The stable hydrogen isotopic composition preserved in fossil leaf waxes (δ^2H_{wax}, δD) directly reflect that of the source water of the vegetation. Since the water isotopes are linked to large scale climate circulation patterns in the North Atlantic, δ^2H_{wax} can indirectly inform about these past climatic variations. We analysed δ^2H_{wax} both from Riipiharju and Rauvospakka. The clear climatic shift from cold to warm conditions reflected in the pollen signal in the upper part of the Riipiharju interstadial sequence is also reflected as a change in the isotope data. For Rauvospakka the isotope data indicate more climatic variability than inferred by the pollen data.

References

Alexanderson, H., Hättestrand, M. & Buylaert, J. P. 2011: New dates from the Riipiharju interstadial site, northernmost Sweden. *In* Johansson, P., Lunkka, J. P. & Sarala, P. (eds.): *INQUA Peribaltic Working Group Meeting and Excursion.* Geological Survey of Finland, Northern Finland.

Hättestrand, C. 1998: *The glacial geomorphology of central and northern Sweden*. Geological Survey of Sweden Ca 85, 47 pp.

Hättestrand, M. 2008: *Vegetation and climate during Weichselian ice free intervals in northern Sweden*. PhD thesis, Stockholm University. 35 pp. http://urn.kb.se/resolve?urn=urn:nbn:se:su:diva-8222.

Hättestrand, M. & Robertsson, A.-M. 2010: Weichselian interstadials at Riipiharju, northern Sweden – interpretation of vegetation and climate from fossil and modern pollen records. *Boreas 39*, 296-311.

Lagerbäck, R. 1988b: The Veiki moraines in northern Sweden - widespread evidence of an Early Weichselian deglaciation. *Boreas 17*, 469-486.

Lindqvist, M. A. 2020: *Kortejärvi Veiki moraine plateau - a key to the glacial history of northern Sweden*. MSc thesis, UiT the Arctic University of Norway. 109 pp. https://hdl.handle.net/10037/18227.

Sigfúsdóttir, T. 2013: *A sedimentological and stratigraphical study of Veiki moraine in northernmost Sweden*. MSc thesis, Lund University. 27 pp. http://lup.lub.lu.se/student-papers/record/3911959.

Geomorphology and sedimentology at the outlet of the final drainage of the Baltic Ice Lake and a conceptual model

Mark D. Johnson[a], Christian Öhrling[b]

[a]Department of Earth Sciences, University of Gothenburg, Gothenburg, Sweden, markj@gvc.gu.se ;
[b] Geological Survey of Sweden, Uppsala, Sweden, christian.ohrling@sgu.se

Summary. The final drainage of the Baltic Ice Lake at Billingen,11.6 cal. ka BP, is one of the central events in Swedish Quaternary history and has been studied for over 100 years. Based on past research, a new geomorphological map, and new sedimentological information, we present a concpetual model for the drainage event. The drainage started subglacially as indicated by cobbly sediment on Mt. Billingen and the Timmersdala ridge, and implies remnant ice in Lången, which quickly broke up. Drainage water traveled 7 km acorss Klyftamon, leaving boulder bars and bared bedrock, before entering deeper waters.

The Baltic Ice Lake (BIL) existed as soon as the retreating Scandinavian Ice Sheet (SIS) exposed the southern Baltic basin (Björck 1995). When the retreating SIS ice margin neared the northern tip of Billingen, a lower outlet became available and the drainage occurred. The BIL dropped c. 25 m (from 150 to 125 m asl) in elevation releasing over 7000 km^3 of water to the North Sea (Strömberg 1992, Jakobsson et al 2007).

The fact of the drainage and the location of the drainage have been known for over 100 years (e.g. Munthe 1910). Evidence for the drainage has accumulated and has long been accepted (e.g. Johansson 1926, Lundqvist et al. 1931, Björck & Digerfeldt 1984, Strömberg 1992, Påsse & Pile 2016). However, the ice sheet itself left few clear traces of its precise position at the time of drainage. Here, we offer a conceptual model and a map of the position of the ice when the drainage began. Additionally, with the advent of LiDAR, it is now possible to map the Klyftamon boulder bars produced during the drainage more precisely (although these were mapped accurately by Johansson (1926) and Lundqvist et al (1931)). We also present new sedimentological data (grain size, grain composition, facies analysis) on the drainage deposits at Timmersdala and on Klyftamon.

Drainage began when the ice margin position was as shown in the figure. The shoreline sediment of Lundqvist et al. (1931) at Garparör (G in figure), which they mapped 'with reservation', we interpret to represent a cobble-boulder lag formed in an ice tunnel, as also suggested by Strömberg (1992) and Påsse and Pile (2016). This gravel body lies in line with the eroded, bare bedrock at the northern tip of Billingen (around St. Stolan (S)), and the ridge at Timmersdala (T), and thus outlines the path of the initial subglacial drainage.

Timmersdala ridge is derived of sediment eroded from Billingen, and its westward-dipping, uncollapsed internal structure indicates it was formed on solid ground in an ice tunnel. This requires remnant ice in the Lången valley. All previous workers that worked on the drainage problem (with the exception of Johansson (1926)), concluded that remnant ice must have been present in the Lången valley when the drainage started.

The initial drainage water exited the ice west from Timmersdala onto Klyftamon and produced the bars at Hornsberg (H) as well as the previously unmapped fluvial surface and bars on the west side of the Lången valley at Sparresäter (Sp). We interpret Sp to be a small outwash plain with a distal, ice-contact slope built up against remnant ice in Lången. However, these initial features are small in scale compared to those in the southern trough.

Once the drainage had begun, the increasing meltwater flow and head difference would have rapidly lifted, melted, and structurally broken-up the ice tongue, similar to what is seen in the majority of ice-dammed-lake drainage events described elsewhere (e.g. Walder and Costa, 1996).

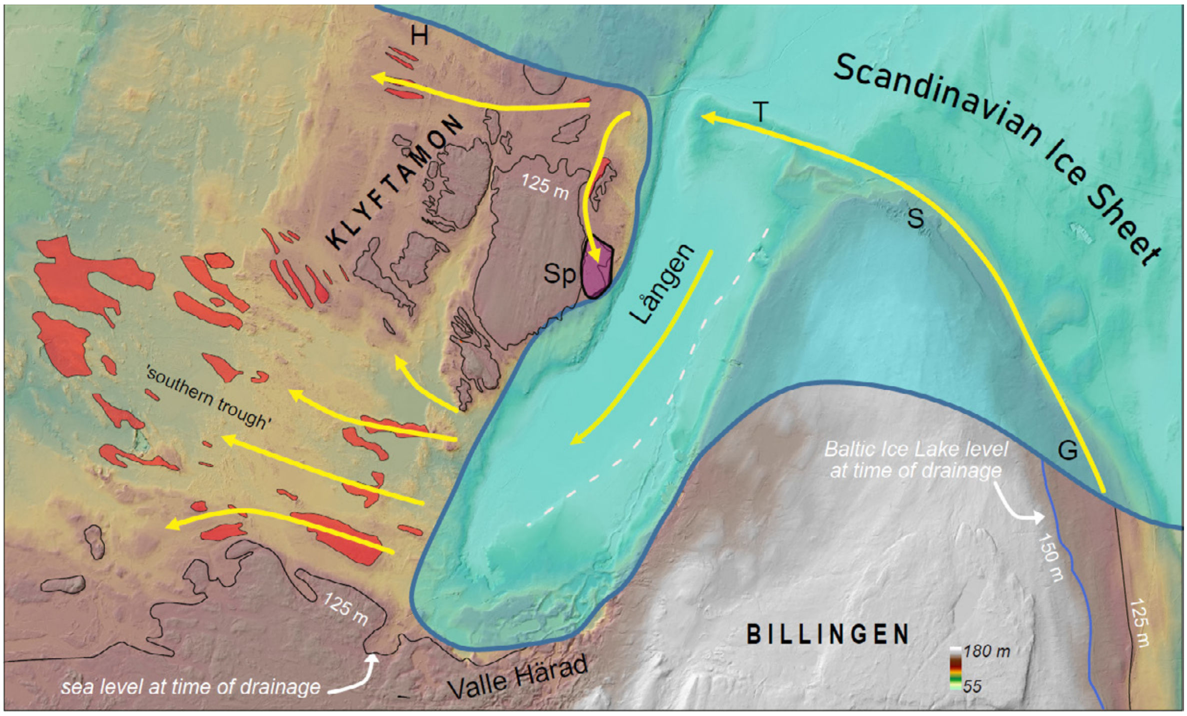

Figure showing Billingen, Klyftamon and the suggested shape of the Scandinavian Ice Sheet margin. G, H, S, Sp and T explained in text. Orange polygons = boulder bars; Yellow arrows = generalized drainage flow paths; white dashed line = subglacial erosional scarp in Lången

As the ice lifted, it allowed drainage water to flow subglacially from Billingen to the southern trough, which was a lower and much wider outlet. The subglacial flow produced the scarp in the figure.

The vast majority of the drainage water flowed through the southern trough essentially as a 'river' producing boulder bars of various types from sediment-charged bedload. The maximum grain size diminishes east to west from over 1 meter to less than 0.5 m. Much if not most of the bar sediment comes from the erosion of till on Klyftamon. Cambrian clasts are also present in the bars, and their amount decreases also to the west. Cambrian clasts came to the southern outlet either directly from subglacial drainage water or from melting ice bergs that 'jammed' the outlet. Erosional 'cut banks' in the southern trough indicate the elevation of the flood waters to be around 126 m. Little sedimentologic evidence is apparent west of Klyftamon because deposits are blanketed with marine clay (Johnson et al, 2010).

References

Björck, S. 1995: A review of the history of the Baltic Sea, 13.0-8.0 ka BP. *Quaternary international*, *27*, 19-40.

Björck, S. & Digerfeldt, G. 1984: Climatic changes at Pleistocene/Holocene boundary in the Middle Swedish end moraine zone, mainly inferred from stratigraphic indications. In *Climatic changes on a yearly to millennial basis* 37-56. Springer, Dordrecht.

Jakobsson, M., Björck, S., Alm, G., Andrén, T., Lindeberg, G., & Svensson, N. O. 2007: Reconstructing the Younger Dryas ice dammed lake in the Baltic Basin: Bathymetry, area and volume. *Global and Planetary Change 57,* 355-370.

Johansson, S. 1926: Baltiska issjöns tappning. *Geologiska Föreningen i Stockholm Förhandlingar 48*, 186-263.

Johnson, M. D., Ståhl, Y., Larsson, O. & Seger, S. 2010: New exposures of Baltic ice lake drainage sediments, Götene, Sweden. *GFF 132*, 1-12.

Lundqvist, G., Högbom, A. & Westergård, A. H. 1931: *Beskrivning till kartbladet Lugnås*, Sveriges Geologiska Undersökning Ser. Aa, No. 172, 185 p.

Munthe, H. 1910: Studies in the Late-Quaternary history of southern Sweden. *Geologiska Föreningen i Stockholm Förhandlingar 32*, 1197-1293.

Påsse, T. & Pile, O. 2016: *Beskrivning till jordartskartorna 8D Skara NV, NO, SV och SO och 9D Mariestad SV*. Sveriges geologiska undersökning. 132 p.

Walder, J. S. & Costa, J. E. 1996: Outburst floods from glacier-dammed lakes: The effect of mode of lake drainage on flood magnitude. *Earth Surface Processes and Landforms 21*, 701-723.

Strömberg, B., 1992: The final stage of the Baltic Ice Lake. *Sveriges Geologiska Undersökning Ca 81*, 347–353.

Glacial geomorphology of the Swedish east coast – adding pieces to solve the 'Gävle problem'

Christian Öhrling

Geological Survey of Sweden, Gothenburg, Sweden, christian.ohrling@sgu.se

Summary. Mapping of glacial geomorphology, Stockholm to Sundsvall, adds clues to the deglaciation of eastern Sweden. Re-interpretations of previously presented geological evidence and significant new data are presented.

The course of events during deglaciation of eastern Sweden and the Bothnian Sea has been debated for a long time. Mapping and analysis of glacial geomorphology provides essential information for understanding the behaviour of the Scandinavian Ice Sheet (SIS) during deglaciation shedding light on how ice moved and how it eroded, transported, and deposited sediment. New mapping was conducted on LiDAR derived elevation models in a GIS environment.

In general, variations in orientations of striations in a given area have been interpreted variously as readvancing ice, ice-stream activity or as different ice-sheet configuration. It is known that the ice-flow direction is generally oriented perpendicular to the ice margin (e.g. Chamberlin 1883, De Geer 1897). Based on striations and varve measurements, Strömberg (1981) showed several deep calving bays in the study area. For this study, the striation orientation W and E extremes are clearly corelated to melt-water drainage paths; the striations tend to turn towards large eskers, large lakes or the Baltic. Where calving bays occurred, the striations have a converging pattern into the bay. However, further up ice, the striation pattern is splaying indicating more of a lobe shape. This change shows the transition from terrestrial to marine deglaciation, previously reported by Halden (1936).

Defining what is an end moraine has also been a problem in the area. Sandegren (1929), G. Lundqvist and L. von Post (in Lundqvist 1943), among others concluded that the large till ridges in the Gävle region oriented NNV-SSE and which have a distinct western scarp and an almost flat eastern side, are end moraines (Lundqvist 1943). G. Lundqvist later changed his mind and joined Caldenius (1939) opinion that the ridges are some type of drumlin. Sandegren (1949) mapped more end moraines, but G. Lundqvist (1951) interpreted them as radial moraines (drumlins). (Wennberg 1949) interpreted the strange ridges to have been formed where the ice sheet had conflicting ice-flow directions, a landform not previously reported. In this study these ridges are interpreted to have formd by subglacial meltwater erosion, and they follow the direction of the subglacial drainage system (Fig.1). Several other reported end moraines in the area, which appears in many of SGUs descriptions of geological maps, are in LiDAR clearly revealed as subglacial fluvial ridges/channels. Some features are murtoos or landorms related to murtoo formation.

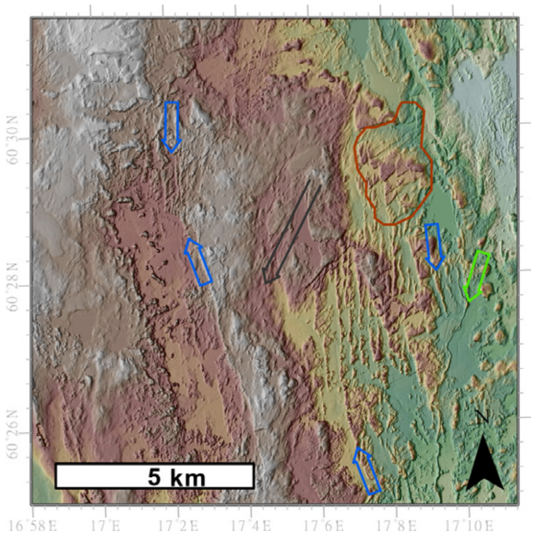

Fig.1: Examples of the previously misinterpreted fluvial scarps (blue), murtoos (red). Green arrows mark an esker and grey the ice-flow direction.

Disturbed sediments of different sorts are commonly shown in sedimentological studies, from more or less flat locations, in the area. Lagerbäck and Sundh (unpublished) reported normal graded bedding, turbidites and folded varves, which were attributed to paleoseismicity (Svantesson 1999). Agrell & Mikko (2003) described folded layers of silt which they also attributed to paleoseismicity. Sandegren (1929) interpreted disturbances as glacial tectonic deformation caused by a readvancing ice sheet. Gerhard De Geer (1919) described diamict sediments superposing glacial varves, often in flat locations, and post glacial in age as determined from the varves. De Geer's idea was that icebergs had brought the diamict and instead of sediment rain out, the icebergs sunk to the bottom with the ungraded diamicton intact before the iceberg had fully melted. In this study, revisits to several old sites by using : LiDAR show that the areas are replete with traces of grounding icebergs. The graded bedding previously reported can have been from iceberg rain-out, and deformaions from iceberg activity. Iceberg scouring was shown to be widespread by Öhrling et al. (2019; Fig.2). This adds an important piece to the puzzle of SIS history. While the varve chronology from terrestrial areas displays a uniform ice-margin retreat, the Bothnian Sea record presents an ice streaming behaviour (e.g. Greenwood et al., 2017). Calving at the ice-stream margin, or even break up, can explain the abundant iceberg features.

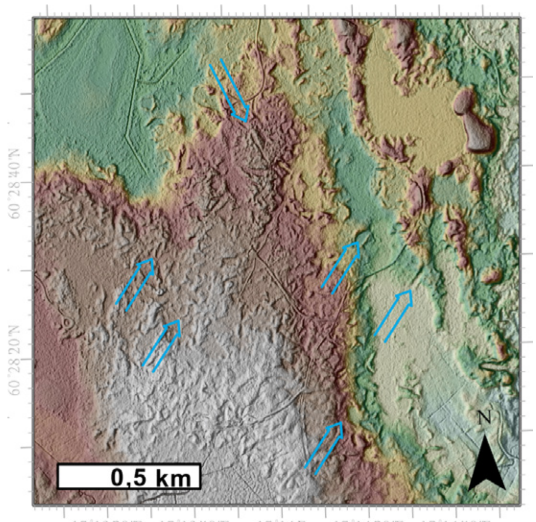

Figure 2: Example of a landscape bombarded by icebergs.

In physical planning it is important to know where sediments have melted out from icebergs, as it must be considered that stability sensitive sediments might be found underlying the iceberg diamicton. The widespread evidence of massive meltwater, subglacially, channelized into corridors, helps geologists to understand and predict the properties of the surficial deposits.

References

Agrell, H. & Mikko, H., 2003: Beskrivning till jordartskartan 12H Söderfors SV. *Sveriges Geologiska Undersökning Ae 154*.

Caldenius, C., 1939: Den förmodade israndsoscillationen i Gävlotrakten. *Geologiska Föreningen i Stockholm Förhandlingar 61*(1), 112–122.

Chamberlin, T. C., 1883: Terminal moraines of the second glacial epoch. *US Geological Survey 3rd Ann. Rept*, 291–402.

De Geer, G., 1897: Stockholmstraktens geologi. *Stockholm Sveriges Huvudstad 1*, 1-27.

De Geer, G., 1919: Om moränmaterial i sekundärt läge. *Geologiska Föreningen i Stockholm Förhandlingar 41*(2), 193–201.

Greenwood, S. L., Clason, C. C., Nyberg, J., Jakobsson, M., & Holmlund, P., 2017: The Bothnian Sea ice stream: early Holocene retreat dynamics of the south-central Fennoscandian Ice Sheet. *Boreas 46*(2), 346–362.

Halden, B. E., 1936: Isavsmältning och strandförskjutningar i siljansdalen. *GFF 58*(1), 19–89.

Lundqvist, G., 1943: Norrlands jordarter. *Sveriges Geologiska Undersökning C 457*.

Öhrling, C., Peterson, G., Sohlenius, G., & Mikko, H., 2019: Iceberg scouring in terrestrial eastern Sweden and implications for deglacial history. *20th Congress of the International Union for Quaternary Research (INQUA)*.

Sandegren, R., 1929: Om isrecessionen i Gefletrakten och den senkvartära geokronologien. *Geologiska Föreningen i Stockholm Förhandlingar 51*(4), 573–579.

Sandegren, R., 1949: Beskrivning till kartbladet Untra. *Sveriges Geologiska Undersökning Aa 191*.

Strömberg, B., 1981: Calving Bays , Striae and Moraines at Gysinge-Hedesunda , Central Sweden. *Geografiska Annaler 63*(3), 149–154.

Svantesson, S.-I., 1999: Beskrivning till jordartskartan 11H Enköping NV. *Sveriges Geologiska Undersökning Ae* 131.

Wennberg, G., 1949: Differentialrörelser i inlandsisen. *Sista istiden i Danmark, Skåne och Östersjön* 1. C. Blom.

The glacial landscape of central Jämtland, Sweden; societal and scientific implications of a new map

Gustaf Peterson Becher[a], Robin Blomdin[a,b], Bradley W. Goodfellow[a], Jonas Ising[a], Henrik Mikko[a], Christina Nysten[a], Christian Öhrling[a], Gunnel Ransed[a], Carl Regnéll[a,c], Colby Smith[a]

[a]Department of Quaternary Geology for Physical Planning, Geological Survey of Sweden, Uppsala, Sweden, gustaf.peterson.becher@sgu.se ; [b]Department of Geography, Norwegian University of Science and Technology, Trondheim, Norway ; [c]Department of Geological Sciences, Stockholm University, Stockholm, Sweden

Summary. The central part of the former Scandinavian Ice Sheet was located over Jämtland and has left a complex landform and stratigraphic archive, which has been studied by geologists for more than a century. This archive shows numerous glacial configurations based on cross-cutting glacial landforms, sub-till sediments, and subglacial till sequences, which presents challenges for land use because, for example, risk indicators for earth mass movements may be obscured.

Societal and scientific implications of new mapping in Jämtland

Jämtland covers a large part of central Sweden (Fig. 1) and was initially mapped for surface deposits and landforms by the Geological Survey of Sweden (SGU) during the 1960s (Lundqvist 1969). However, societal use of geologic information has changed over the past decades, most notably the need for digitalisation, which has also driven a demand for higher spatial detail, and for society relevant derivates of geologic data (Fig. 2) (Hill et al. 2020).

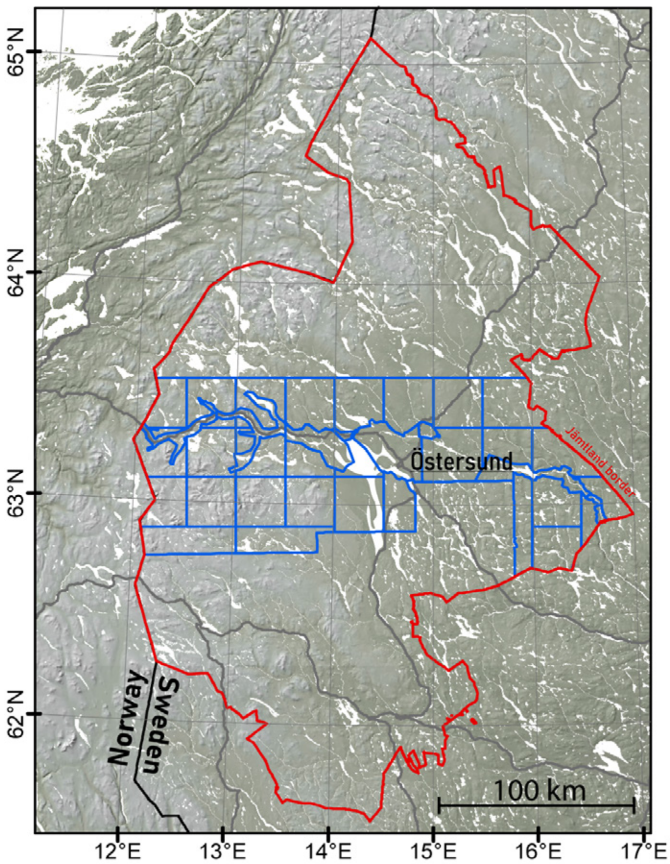

Figure 1. Overview map. Red = Jämtland county as well as the extent of the geomorphological mapping, Blue = Surface deposits maps in database or in production.

Regional authorities in Jämtland, including land-use planners, highlight a lack of high-resolution data that informs geohazard assessment, groundwater resources, and urban infrastructure development. SGU has therefore recently undertaken detailed mapping of the Quaternary landforms and sediments of Jämtland. To map such a large area effectively and efficiently, we have combined several strategies. We generate our digital Quaternary surface deposits maps from observations of surface characteristics, vegetation, and landforms observable on LiDAR-derived elevation models and aerial orthophotography. We then 'ground truth' these observations against field data collected during the 1960s mapping campaigns and from our own field campaigns. Our fieldwork is focused on field control (quality check) and collection of new geological observations and conceptual understanding (e.g. stratigraphy), rather than providing the initial data to support mapping.

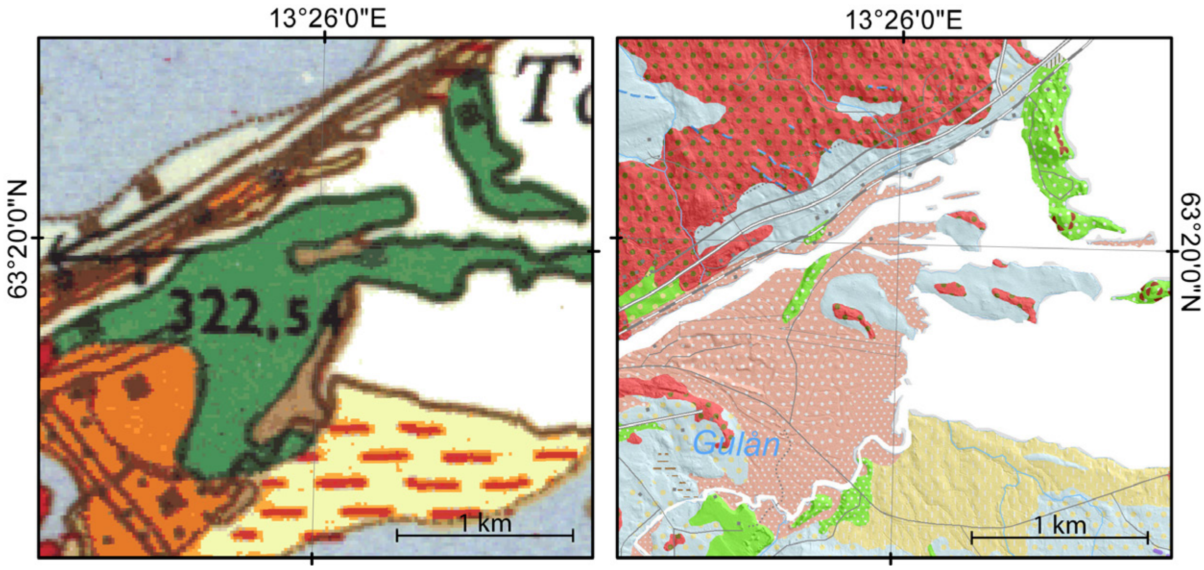

Figure 2. Comparison of old (left) and new (right) maps in an area west of Järpen.

During 2020 and 2021, we have published new maps covering more than 10 000 km^2 of Quaternary surface deposit maps (Fig. 1) and 50 000 km^2 of Quaternary geomorphology (Fig. 1) (Blomdin et al. 2021). Our mapping has generated important new findings including:

1. Glacial landforms indicate large temporal and spatial variations in ice-flow directions during the Weichselian. We have divided these landforms into chronological groups based on their stratigraphic relations, including a likely new group of glacial lineations formed by an east-flowing mountain centred ice sheet (Blomdin et al. 2021).
2. During mapping, several observations of multiple tills have been recorded from west central Jämtland. The till fabrics agree well with the landform record and are possibly explained by local variations in ice-flow pattern.
3. The sediment stratigraphy contains units that may initiate mud and coarse-debris flows and should therefore be further assessed from a geohazard perspective.
4. During deglaciation the ice sheet retreated eastward, onto the piedmont, which dammed large lakes against the mountains. Our mapping has notably increased the detail of ice-dammed lake extents, enabling reconstruction of the final ice-sheet retreat (Regnéll et al. 2021).

In conclusion, our mapping has generated results that motivate further scientific investigation to help us better understand past and modern ice sheet dynamics. Moreover, our maps and data now support better decision-making regarding appropriate land use, particularly in a mountainous region undergoing rapid climate warming.

References

Blomdin, R., Peterson Becher, G., Smith, C. A., Regnell, C., Öhrling, C., Goodfellow, B. W., & Mikko, H. 2021: Beskrivning till geomorfologiska kartan Jämtlands län. *Sveriges Geologiska Undersökning, Serie K*, *705*.

Hill, P. R., Lebel, D., Hitzman, M., Smelror, M., & Thorleifson, H. 2020: The changing role of geological surveys: Introduction. *Geological Society Special Publication*, *499*(1), 1–15.

Lundqvist, J. 1969: Beskrivning till jordartskarta över Jämtlands län. *Sveriges Geologiska Undersökning, Serie Ca*, *45*.

Regnéll, C., Blomdin, R., Goodfellow, B. W., Greenwood, S. L., Gyllencreutz, R., Mangerud, J., Mikko, H., Peterson Becher, G., Regnéll, J., Svendsen, J. I., & Öhrling, C. 2021: Ice-dammed lakes of Scandinavia - a key to the pattern and chronology of the final decay of the Scandinavian Ice Sheet. *EGU General Assembly*, EGU21-3827.

The geomorphological imprint and implications of a 'new' ice margin in central Sweden

Gustaf Peterson Becher, Henrik Mikko, Colby A. Smith, Christian Öhrling, Gunnel Ransed, Bradley W. Goodfellow

Department of Quaternary Geology for Physical Planning, Geological Survey of Sweden, Uppsala, Sweden, gustaf.peterson.becher@sgu.se

Summary. We have found a zone of dead-ice depressions in association with ice-marginal landforms in north central Sweden. Based on the apperance of these landforms we interpret them to have been formed at the ice. margin of an ice-sheet. Furthermore, based on the landforms overall pattern and it topographic conenction to known MIS 3 ice marginal landforms, and the abundance of interstadial localities in it's surroundings we hypothesize that this suite of landforms was formed during a standstill or re-advance during an overall retreat from an MIS 4 ice-sheet.

A better understanding of the extent of pre-Late Weichselian ice sheets is important for vali-dating numerical ice-sheet models. Moreover, a knowledge of older ice-sheet extents is an important key in developing geological frameworks for the subsurface. Several localities in central and northern Sweden show interstadial sediments with assumed early Marine Isotope Stage (MIS) 3 ages (e.g. Lundqvist & Miller 1992, Wohlfarth et al. 2011, Möller et al. 2013 Lagerbäck 2007) (Figure 1). These sediments and landforms were preserved during periods of frozen-bed conditions (e.g. Lagerbäck 1988, Kleman 1992). In the far north of Sweden, the ice margin of an MIS 3 ice sheet is assumed to be the Veiki moraine (i.e. ice walled lake plains) zone in the interior of Norrbotten (Lagerbäck 1988, Hättestrand & Robertsson 2010, Sigfúsdóttir 2013) (Figure 1). Recently, a moraine in the southern part of the Swedish mountains (Figure 1) have been, based on OSL, interpreted to have been formed during the MIS 3 (Kleman et al. 2020) interstadial and as such be contemporaneous with the Veiki moraine zone to the north. However, there has been no evidence presented of any MIS 3 ice margin between these localities, a distance of almost 600 km. We have mapped a suite of landforms that we interpret as ice-marginal and that we hypothesize is the continuation of the MIS 3 ice margin, connecting the Veiki moraines in the north with the Idre moraine in the south (Figure 1). The mapped ice margin is only in a few places visible as clear end moraines but is more often seen as a series of landforms indicative of an ice-marginal dead-ice environment such as dead-ice depressions (Figure 2) but to some extent also Veiki moraines and pro-glacial channels. The overall geometry of the hypothesized ice margin shows a series of lobate structures. Moreover, cross-cutting relationships suggest that at least segments of the interpreted ice margin have been overridden by a late-Weichselian ice sheet (MIS 2).

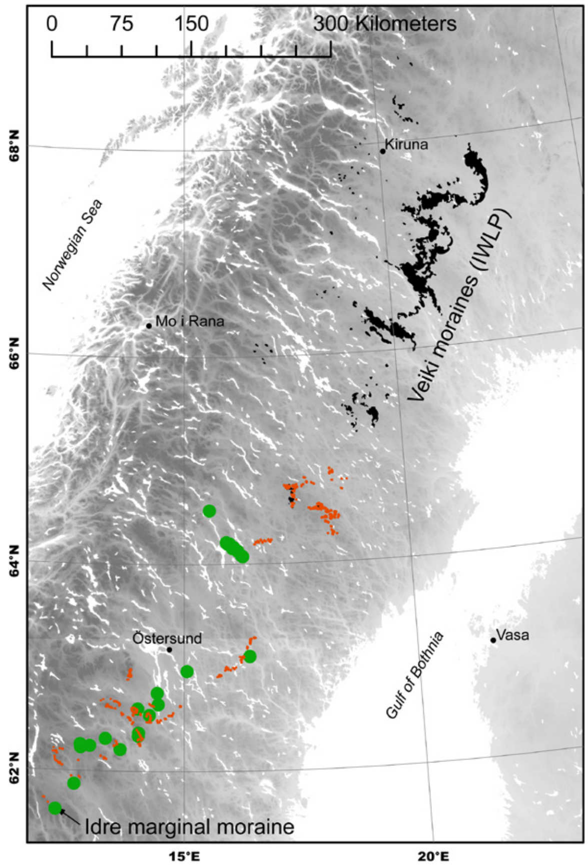

Figure 1.Overview map. Red = mapped dead-ice depressions, Green = Interstadial localities, Black = Veiki moraines (IWLP).

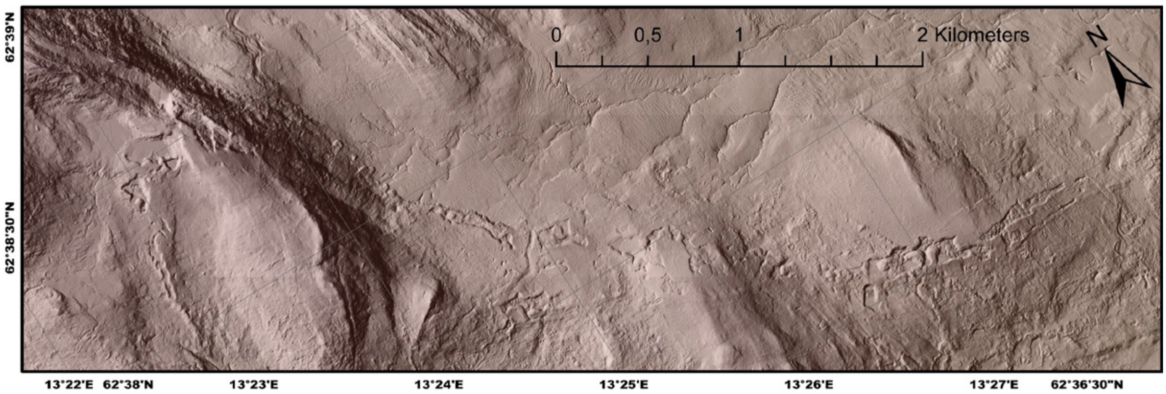

Figure 2. Example of a suite of lobate dead-ice depression from. Proposed ice-flow from the north.

Dead-ice depressions as well as Veiki moraines are generally attributed to stagnant ice-margins (Johnson & Clayton 2003). However, the proposed ice-margin is in places associated with push moraines and crevasse-squeeze ridges, suggesting, in places, an active ice-margin. Based on the presence of dead-ice depressions, active and stagnant ice-marginal features we suggest the following model of formation. Step 1) The MIS 4 ice-sheet retreats into the mountains during early MIS 3. The ice margin was stagnant and left ice-blocks behind. Step 2) At some point parts of the ice-margin advanced a short distance, overriding the ice-blocks and covering them with till. Moreover, this advance created crevasse-squeeze ridges, push-moraines, and produced supraglacial material leading to Veiki-moraine formation. Step 3) The ice-margin once again started to retreat, and left a zone of dead-ice depressions, Veiki moraines, and other ice-marginal landforms. Although there are no direct attempts to date the proposed end-moraine itself there are an abundance of stratigraphic sites with interstadial strata, in places dated to MIS 3 (e.g. Alexanderson et al. 2010, Wohlfarth et al. 2011, Möller et al. 2013) in the vicinity of the suggested ice-margin (Figure 1). Based on the interstadial stratigraphies nearby the proposed ice-margin, cross-cutting relationships, and the morphological connection to ice-marginal landforms with known ages, we hypothesize that this suite of landforms was formed during the early MIS 3. To test this hypothesis future research will include dating of potential interstadial strata within the dead-ice depression using optically stimulated luminescence and radiocarbon dating as well as cosmogenic dating of boulders on moraine ridges.

References

Alexanderson, H., Johnsen, T., & Murray, A. S., 2010: Re-dating the Pilgrimstad Interstadial with OSL: A warmer climate and a smaller ice sheet during the Swedish Middle Weichselian (MIS 3)? *Boreas*, *39*(2), 367–376.

Hättestrand, M., & Robertsson, A. M., 2010: Weichselian interstadials at Riipiharju, Northern Sweden - interpretation of vegetation and climate from fossil and modern pollen records. *Boreas*, *39*(2), 296–311.

Johnson, M. D., & Clayton, L., 2003: Supraglacial landsystems in lowland terrain. In D. J. A. Evans (Ed.), *Glacial Landsystems* (pp. 228–258). Arnold.

Kleman, J., Hättestrand, M., Borgström, I., Preusser, F., & Fabel, D., 2020: The Idre marginal moraine – An anchorpoint for Middle and Late Weichselian ice sheet chronology. *Quaternary Science Advances*, *2*.

Kleman, J., 1992: The Palimpsest Glacial Landscape in Northwestern Sweden. Late Weichselian Deglaciation Landforms and Traces of Older West-Centered Ice Sheets. *Geografiska Annaler*, *74 A*(4), 305–325.

Lagerbäck, R., 1988: The Veiki moraines in northern Sweden - widespread evidence of an Early Weichselian deglaciation. *Boreas*, *17*(4), 469–486.

Lundqvist, J., & Miller, U., 1992: Weichselian stratigraphy and glaciations in the Tåsjö-Hoting area, central Sweden. *Geological Survey of Sweden*, *C 826*, 1–35.

Möller, P., Anjar, J., & Murray, A. S., 2013: An OSL-dated sediment sequence at Idre, west-central Sweden, indicates ice-free conditions in MIS 3. *Boreas*, *42*(1), 25–42.

Sigfúsdóttir, T., 2013: A sedimentological and stratigraphical study of Veiki moraine in northernmost Sweden. *Dissertations in Geology at Lund University*, *354*, 42.

Wohlfarth, B., Alexanderson, H., Ampel, L., Bennike, O., Engels, S., Johnsen, T. F., Lundqvist, J., & Reimer, P., 2011: Pilgrimstad revisited - a multi-proxy reconstruction of Early/Middle Weichselian climate and environment at a key site in central Sweden. *Boreas*, *40*(2), 211–230.

Shore displacement along the planned high-speed railway Ostlänken, in eastern south-central Sweden

Anna Plikk[a], Jan Risberg[b], Jonas Bergman[c]

[a]The Archaeologists, National Historical Museums, Sweden, anna.plikk@arkeologerna.com; [b]Department of Physical Geography, Stockholm University, Stockholm, Sweden, jan.risberg@geo.su.se; [a]The Archaeologists, National Historical Museums, Sweden, jonas.bergman@arkeologerna.com

Summary. We present an ongoing shore displacement study from eastern south-central Sweden. The study is part of a palaeoecological program to support the archaeological investigations along the first phase of the planned high-speed railway line between Stockholm and Linköping and includes 23 sites situated between 127 and 2.5 m asl and covers a time span of 11 600 years.

A high-speed railway line is planned in order to reduce the travelling time between Stockholm and Gothenburg/Malmö. A first phase involves the part between Södertälje in Stockholm County and Linköping in Östergötland County. This stretch also passes through Södermanland County. As part of a palaeoecological program to support the archaeological investigations along the railway, shore displacement studies have been initiated.

Previous shore displacement curves from the area are in most cases based on either bulk sediment dating and/or pollen dating (Fromm 1976, Persson 1979, Risberg 1991, Hedenström & Risberg 1999). The main aim of this project is to produce new data on shore displacement based on modern radiocarbon dating using terrestrial macrofossils. Isolation events are based on variations in water content/loss on ignition and diatom analyses.

The investigated area stretches over approximately 130 km in a NE–SW extension. To record differences in shore displacement, the area has been divided into four subsections where basins within 10 to15 km apart have been used to construct four different shore displacement curves. The basins are situated between 127 m asl and 3.5 m asl in Östergötland and 50 and 2.5 m asl in Södermanland.

So far, seven basins from Södermanland and sixteen basins from Östergötland County have been investigated and dated. The preliminary results indicate that the shore displacement curves from Södermanland are similar to a recent shore displacement curve from the Södertörn peninsula (eastern part of Södermanland County) (Risberg et al. 2006). In Östergötland however there is a significant difference from previous curves and from the, by archaeologists much used, shore displacement model published by the Swedish Geological Survey (Påsse & Daniels 2015), with differences of up to around 800 years or 5–10 m in height.

The oldest isolation in the study is dated to the early Holocene, c. 11 600 ka BP. The Littorina transgression is recorded as a stillstand culminating around 7800-7500 ka BP, and the Ancylus transgression seems to be recorded in Östergötland.

The results will be of significance for archaeologists working in the area when studying positions of settlements, transportation routes and possibilities for food exploitation, but may also be used to further improve shore displacement models within the Baltic Sea region.

References

Bergman, J., Plikk, A. & Risberg, J., 2021: Paleoekologisk rekognoscering utmed Ostlänken i Södermanlands län. *Arkeologerna Rapport 2021:170*, 1-38.

Fromm, E., 1976: Description to the Quaternary map Linköping NO. *Sveriges geologiska undersökning Ae 19*, 1-77.

Hedenström, A. & Risberg, J., 1999: Early Holocene shore-displacement in southern central Sweden as recorded in elevated isolated basins. *Boreas 28*, 490-504.

Persson, C., 1979: Shore displacement during Ancylus time in Rejmyra area, south central Sweden. *Sveriges geologiska undersökning C 755*, 1-23.

Påsse, T. & Daniels, J., 2015: Past shore-level and sea-level displacements. *Sveriges geologiska undersökning, Rapporter och meddelanden 137*, 1-33.

Risberg, J., 1991: Palaeoenvironment and sea-level changes during the early Holocene on the Södertörn peninsula, Södermanland, eastern Sweden. *Stockholm University, Department of Quaternary Research Report 20,* 1-27.

Risberg, J., Berntsson, A. & Kaislahti Tillman, P., 2006: Strandförskjutning under mesolitikum på centrala Södertörn, östra Mellansverige. Kvartärgeologiska undersökningar längs väg 73, Överfors – Västnora. *Rapporter från Arkeologikonsult 2006:2037*, 1-57.

Revised Middle and Late Pleistocene interglacial and interstadial records in Finland reveal a long palaeoecological record

Matti E. Räsänen

Vapparintie 732, 20960 Turku, Finland, matti.rasanen@professori.fi

Summary. The Middle to Late Pleistocene palaeoenvironmental record from the eastern sector of Scandinavian ice sheet in Sweden and Finland is composed of numerous isolated localities. The reconstruction of the glacial-interglacial history has engaged researchers more than a century. In Finland, most of the records have been interpreted to represent Weichselian glacial cycle. Now the stratigraphical record in central and southern Finland has been reviewed (Räsänen et al. 2021). The results show, that a big part of the record extends further back in time and is more complete than previously published.

Material and methods

Ostrobothnia and southern Finland has historically had a central role in the recostruction of the Scandinavian glacial history due to the high amounts of documented subtill organic deposits in the area. Recently a major revision of the Quaternary stratigraphy of the documented key localities in has been performed. The investigation has been done by applying an integrated sequence stratigraphic analysis of the existing litho- and biostratigraphic data.

Results and conclusions

In the revised key locality stratigraphies, litho- and biofacies trends together with their bounding discontinuities repeatedly indicate the same type of development within the glacial sequences and their different systems tracts. A major finding was that large part of the organic deposits originally interpreted as i*n situ* deposits were composed of reworked organic materials. The regionally repetitive stratigraphies reveal a proglacial subaquatic glaciofluvial redepositional process of organic matter which was common in the study area during the Late Saalian but has been poorly described until now. Similar type of recent analogies of erosion and entrainment of subglacial preglacial organics are described by Kohler et al. (2017) at the retreating Greenland ice margins.

One of the reviewed depositional record at Hietaniemi may contain reworked Middle Pleistocene Holsteinian Interglacial (≈MIS 11, 424–374 ka ago) organic material, and the redeposited organic matter at a number of other well known localities, like Oulainen (Forsström 1982, Donner 1983), Harrinkangas (Gibbard 1989) and Horonkylä (Nenonen 1995) are attributed to the Middle Pleistocene sc. Röpersdorf-Schöningen Interglacial (≈MIS 7, 243–191 ka ago). During this possible Röpersdorf-Schöningen Interglacial, the Gulf of Bothnia hosted larger alkaline and smaller dystrophic lakes surrounded by boreal pine forests in a continental climate with warmer summers and colder winters than today. The Eemian (≈MIS 5e, 131–119 ka) sea coastal records show detailed evidence of the widespread intermixing of continental fresh and marine waters. During the Early Weichselian Brörup Interstadial (≈MIS 5c 109–96 ka), central and southern Finland seem to have supported open birch forest tundra, later invaded by spruce; not boreal pine forest as earlier thought (Donner 1983). The early birch vegetation faced a tundra phase which may be the Montaigu cooling event c. 103 ka ago. The revised palaeoenvironmental interpretation shows that the development in Fennoscandia during the four discussed warmer intervals is well in line with the central European vegetational development. No indisputable Middle Weichselian (≈MIS 3, 57–29 ka) sedimentary record seems to have been recorded in the studied area.

Fig. 1. Map of the research localities that have records from different interglacials and interstadials. The map shows the revised and closer-discussed localities within the Ostrobothnian research area (grey ellipsoid) together with the other referred localities in NW Europe. The thick grey W-E zone shows the approximate position of the inferred possible northern limit of boreal Pinus forest in the Late Brörup (fig. from Räsänen et al. 2021).

References

Donner, J., 1983. The identification of Eemian interglacial and Weichselian interstadial deposits in Finland: *Ann. Acad. Sci. Fennicæ Ser. A III Geol.-Geogr.* 136, 38.

Forsström, L., 1982. The Oulainen Interglacial in Ostrobothnia, Western Finland. *Acta Universitatis Ouluensis, Ser. A Scientiae Rerum Naturalium*. No. 136 Geologica No. 4, 123.

Gibbard, P., Forman, S., Salomaa, R., Alhonen, P., Jungner, H., Peglar, S., Suksi, J., Vuorinen, A., 1989. Late Pleistocene stratigraphy at Harrinkangas, Kauhajoki, western Finland. *Ann. Acad. Sci. Fennicæ Ser. A III Geolog.-Geogr.* 150, 36.

Kohler, T. J., Žárský, J. D., Yde, J. C., Lamarche-Gagnon, G., Hawkings, J. R., Tedstone, A. J., Wadham, J. L., Box, J. E., Beaton, A. D., Stibal, M. 2017. Carbon Dating Reveals a Seasonal Progression in the Source of Particulate Organic Carbon Exported from the Greenland Ice Sheet.” *Geophys. Res. Lett*. 44, 6209–6217.

Nenonen, K., 1995. Pleistocene Stratigraphy and Reference Sections in Southern and Western Finland. Geological Survey of Finland, Kuopio.

Räsänen, M.E., Auri, J., Ovaskainen, J., 2021. Revised Middle and Late Pleistocene interglacial and interstadial records from the glaciated eastern Fennoscandia. *Quat. Sci. Rev*. 251, 106716. https://doi.org/10.1016/j.quascirev.2020.106716.

150 years of ice-dammed lake research in the Scandinavian Mountains and the way forward

Carl Regnéll[a,b], Sarah L. Greenwood[a,b], Richard Gyllencreutz[a,b]

[a]Department of Geological Sciences, Stockholm University, Stockholm, Sweden, carl.regnell@geo.su.se.
[b]Bolin Centre for Climate Research, Stockholm University, Stockholm, Sweden

Summary. The study of ice-dammed lakes, formed along the Scandinavian mountains during the demise of the last ice sheet, has historically formed a classic discipline in Swedish Quaternary research. Ever since their discovery, ice-dammed lakes have been at the centre of the debate when reconstructing the last deglaciation. However, interpretations of the lakes have changed back and forth throughout their 150-year research history and their marks in the mountains still hold a wealth of palaeoglaciological information, also important for the predicted future behaviours of modern ice sheets.

Ice-dammed lakes and their palaeoglaciological significance

Hardly any traces of the Ice Age are as spectacular and have attracted such attention as the ice-dammed lake shorelines, often located high up on mountain slopes and visible as horizontal lines at long distances (Hoppe 1983, p. 34). Here, we present the rich history of ice-dammed lake research in the Scandinavian Mountains, their importance for understanding ice sheet decay, how interpretations have changed through the years, recent developments and promising new ways ahead.

The study of ice-dammed lakes along the Scandinavian mountain range is a classic discipline in Swedish Quaternary research. As early as 1734 CE, ancient shorelines located high above the valley floors were described from the central mountain range by Carl von Linné. His observations, however, escaped the geological community and it was not until 150 years ago, in the very first volume of GFF (Geologiska Föreningen i Stockholm Förhandlingar), that A. E. Törnebohm first addressed such shorelines in a geoscientific publication (Törnebohm 1872). Törnebohm described horizontal terraces at high elevations on valley sides west and southwest of lake Femunden, Norway, and noted that these closely resembled an illustration he had seen of the "Parallel Roads" of Glen Roy, Scotland. His conclusion was that these, like the "Roads", must be abandoned shorelines, formed in ice-dammed lakes. However, it took another decade before research on the subject really took off, following reports of other ice-dammed lake shorelines along the mountains in 1885 (Hansen 1885, Högbom 1885, Svenonius 1885). These initial studies started a period of intense research on ice-dammed lakes all along the mountain range, from Østerdalen and Härjedalen in the south to Torneträsk in the north.

The main interest in ice-dammed lakes was driven by their value for reconstructing the retreat of the last Scandinavian Ice Sheet. Mapping the extent of different ice-dammed lakes and their requisite ice-damming positions enables the pattern of ice margin retreat to be traced, and the relative age of ice-marginal positions determined using cross-cutting relations. The conclusion was that, even though it likely acted as nucleation centre, the mountain range did not host the final vestiges of the ice sheet. Instead, extensive glacial lakes were dammed between the eastward retreating ice sheet and the water divide within the mountains to the west (e.g. Gavelin & Högbom 1910).

Towards the middle of the 20th century, divergent opinions arose concerning the nature and extent of the ice-dammed lakes (e.g. Lundqvist 1942, Holdar 1957). In the northern part of the mountains, mapping of glacial striae, drumlins and glaciofluvial deposits led Holdar (1957) and Hoppe (1959) to conclude that the ice sheet instead had retreated back into the high mountain areas. While it is now understood that these landforms are older, preserved during cold-based deglaciation (e.g. Rodhe 1988), retreat towards the highest parts of the mountain range is still proposed in more recent studies (e.g. Stroeven et al. 2016). In the southern part of the mountain range, in Jämtland, the absence of glacio-lacustrine sediments and presence of ribbed (Rogen) moraines, led J. Lundqvist to propose that many of the previously reconstructed ice-dammed lakes were, in fact, not open lakes but instead valleys were largely filled with stagnant "dead-ice", with small water bodies trapped around the margins (e.g. Lundqvist 1973). This latter view remained unchallenged for about half a century.

In recent years, LiDAR (Light Detection and Ranging) based digital terrain models have revealed the Scandinavian landscape at an unprecedented resolution (Johnson et al. 2015). Shorelines and other landforms relating to ice-dammed lakes are evident over larger areas and in greater numbers than previously known (e.g. Regnéll et al. 2019). Furthermore, recent mapping efforts by the Geological Surveys in both Norway and Sweden have revealed streamlined bedforms, eskers, De Geer moraines and iceberg imprints, confirming active ice-sheet retreat in open ice-dammed lakes (Høgaas & Longva 2019, Blomdin et al. 2021, Öhrling et al. 2021). The current view of the deglaciation is, therefore, shifting away from the "dead-ice school of thought" of the 60s-70s and back to the conceptual ideas and original reconstructions of more than 100 years ago, this time based on a wealth of new high-resolution data as compared to the limited observations available around the turn of the 20th century.

The availability of nationwide LiDAR coverage now, for the first time, enables us to trace the filling, coalescence and drainage of the full suite of ice-dammed lakes along the Scandinavian mountains, and determine their requisite and evolving ice sheet margin positions and thicknesses, while a concerted dating campaign will resolve their chronology. This endeavour is addressed within the framework of a recently started research project based at Stockholm University, funded by the Swedish Research Council. Not only does our work revisit a classic problem in Swedish Quaternary geology, it is timely and urgent in improving projections for the future behaviour of the Greenland ice sheet. With extreme rates of surface melt and margin retreat inward of the rugged coastal topography, proglacial lake-damming is set to become more extensive. Swathes of the terminal setting of the ice sheet will change from land-terminating to lake-terminating, with poorly understood – and little considered – consequences for ice margin behaviour and the future health and stability of the ice sheet. By reconstructing the extents and timing of ice-dammed lakes and investigating their effect on the demise of the Scandinavian Ice Sheet we aim to greatly improve our understanding of its final decay as well as inform the boundary conditions for ice–climate models, highlighting the relative importance of processes that should be (or are unnecessarily) parameterised in such models.

References

Blomdin, R., Peterson Becher, G., Smith, C.A., Regnéll, C., Öhrling, C., Goodfellow, B.W. & Mikko, H., 2021: Beskrivning till geomorfologiska kartan: Jämtlands län. Sveriges geologiska undersökning k 705, 1-54.

Gavelin, A. & Högbom, A.G., 1910: Norra Sveriges issjöar: en sammanställning af hittills gjorda undersökningar. Sveriges geologiska undersökning. Serie Ca, Avhandlingar och uppsatser 7. Norstedt, Stockholm, 1-115.

Hansen, A.M., 1885: Om seter eller strandlinjer i større høider over havet. Archiv for Mathematik og Naturvidenskab 10, 329-352.

Høgaas, F., & Longva, O., 2019: The late-glacial ice-dammed lake Nedre Glomsjø in Mid-Norway: an open lake system succeeding an actively retreating ice sheet. Norwegian Journal of Geology, 98(4), 1–15.

Holdar, C. G. (1957). Deglaciationsförloppet i Torneträsk-området efter senaste nedisningsperioden, med vissa tillbakablickar och regionala jämförelser. Geologiska Föreningen i Stockholm Förhandlingar, 79(3), 291–528.

Hoppe, G., 1983: Fjällens terrängformer. Statens Naturvårdsverk, Stockholm, 1- 60.

Högbom, A.G., 1885: Glaciala och petrografiska iakttagelser i Jemtlands län. Sveriges geologiska undersökning C 70, 1-42.

Johnson, M. D., Fredin, O., Ojala, A. E. K. & Peterson, G., 2015: Unraveling Scandinavian geomorphology: the LiDAR revolution. GFF, 137(4), 245–251.

Lundqvist, G., 1942: Var äro issjöarnas sediment?. Geologiska Föreningen i Stockholm Förhandlingar, 64(2), 160–162.

Lundqvist, J., 1973: Isavsmältningens förlopp i Jämtlands län. Sveriges Geologiska Undersökning Serie C, 681, 1–187.

Öhrling, C., Mikko, H., Peterson Becher, G., & Regnéll, C., 2021: Meteorite crater re-interpreted as iceberg pit in west-central Sweden. GFF, 143(1), 84–91.

Regnéll, C., Mangerud, J., & Svendsen, J. I., 2019: Tracing the last remnants of the Scandinavian Ice Sheet: Ice-dammed lakes and a catastrophic outburst flood in northern Sweden. Quaternary Science Reviews, 221, 105862.

Rodhe, L., 1988: Glaciofluvial channels formed prior to the last deglaciation: examples from Swedish Lapland. Boreas, 17(4), 511–516.

Svenonius, F., 1885: In: Minutes of Meeting 10 April 1885. Geologiska Föreningen I Stockholms Förhandlingar, 7, 605-609.

Törnebohm, A. E., 1872: Om flyttblock och terrasser vid Rendals-Sölen i Norge. Geologiska Föreningens i Stockholm Förhandlingar 1(6), 106–109.

Lake Odensjön – an annually laminated sediment record from southern Sweden

Ethan Silvester, Hanna Hertzman, Karl Ljung, Dan Hammarlund

Department of Geology. Lund Universty, Lund, Sweden, ethan.silvester@geol.lu.se

Summary. The origin of the peculiar Lake Odensjön on the Söderåsen Horst in Skåne, southern Sweden, has been debated. Glacial over-deepening of a fracture zone in the gneiss bedrock ridge is a plausible explanation. Its sediment succession is known to extend to the Bølling Interstadial of the Late Weichselian but the Holocene sediments have not been studied in detail. As revealed by a freeze-core sediment sequence sampled from the deepest, central part of the lake, at least the uppermost part consists of annually laminated sediments, providing opportunities for highly resolved environmental reconstructions.

Lake Odensjön occupies the most prominent of a series of deeply incised canyons on the Söderåsen Horst (Fig. 1), which have been interpreted as shaped partly by circque glaciers (Rapp 1982, 1984). Berglund & Rapp (1988) investigated the lithostratigraphy and pollen assemblages of the Late Weichselian sections of two piston cores obtained from the lake. The upper, 4.8-m thick unit of the sediment sequence from 18.7 m depth, which was beyond the scope of their study, was described as dark green fine detritus gyttja. Using the equipment described by Renberg & Hansson (2010), we retrieved an 89-cm long freeze core in January 2016, which revealed more details and probably a different character of the most recent sediments in the deepest, central part of the lake (Fig. 2).

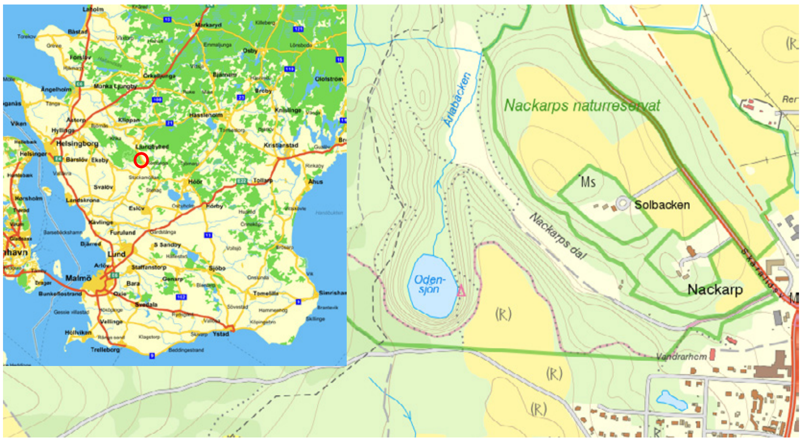

Figure 1. Location and topographic setting of Lake Odensjön, NW of the village of Röstånga in the province of Skåne, southernmost Sweden. The lake, which is situated in a canyon valley incised into the gneiss horst of Söderåsen, measures approximately 160 by 130 m and has a maximum depth of about 20 m.

Figure 2. Photograph of the sediment sequence from 19.9 m water depth in the central part of Lake Odensjön obtained with a freeze corer in January 2016. The total length of the sequence is 89 cm, spanning the last c. 450 years as estimated by varve counting and confirmed by radocarbon dating.

The uppermost 27-cm part of the sediments exhibits a series of several mm thick whitish to yellowish brown laminations, sharply contrasting against darker and usually thicker layers. Frequent small-scale unconformities and other irregularities occur, probably related to the incorporation of large amounts of well-preserved leaves, predominantly from beech (*Fagus sylvatica*) but also from oak (*Quercus robur*) and hornbeam (*Carpinus betula*). Below 27 cm follows a unit of faintly laminated dark brown gyttja with a substantially lower content of macroscopic plant remains, which in turn rests on a type of sediment that broadly resembles the most recent unit but with thinner, although clearly visible laminations. The thinner laminations in the lower part can be attributed to increasing compaction with sediment depth. Repeated attempts at counting the laminations throughout the core, involving interpolation within the dark brown unit, yielded sums in the range of 400−450 (Hertzman 2021).

To test the hypothesis that the laminations represent annual varves, we applied two independent dating techniques to the upper part of the sequence. Radioisotope analysis using gamma spectroscopy determined the base of the upper, clearly laminated section to around AD1940 based on ^{210}Pb, while ^{137}Cs data provided additional dating control at 17−23 cm depth (Fig. 3). Analysis of total Pb content using X-ray fluorescence established the peak in air-bourne Pb pollution related to maximum use of leaded petrol in the mid 1970ies as commonly observed in Swedish lake sediments (Brännvall et al. 1999) at about 20 cm depth, in excellent agreement with the radioisotope data and the rather precise counting of laminations in this section. In addition, macroscopic plant remains from three levels in the lower part of the core yielded ages in the range of 296−534 cal. BP (mid intercepts AD1601−1488) based on radiocarbon dating, in general agreement with the lamina counting.

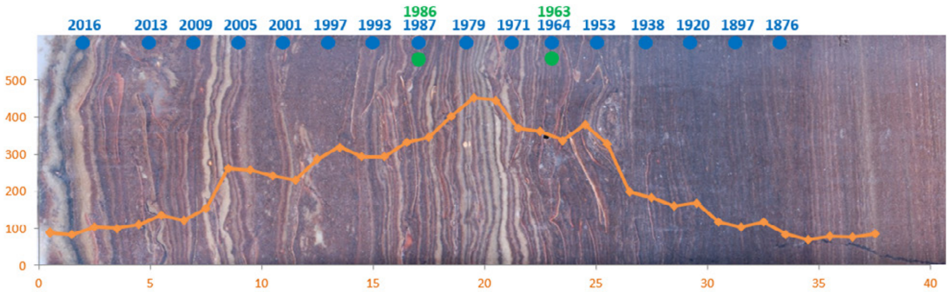

Figure 3. Blow-up photograph of the upper 40-cm part of the sediment sequence (cf. Fig. 2). Distinct laminations are clearly visible and countable to a depth of about 27 cm, and their annual character (varves) is confirmed independantly by radioisotope dating and pollution Pb variations. Blue dots represent samples analysed for ^{210}Pb, yielding age estimates by constant-rate-of-supply age modelling. Green dots indicate peaks in ^{137}Cs content, representing the Chernobyl nuclear accident and the maximum fallout from nuclear weapons testing, respectively. The orange graph shows total Pb content variations in the sediments as estimated by X-ray fluorescence analysis of discrete freeze-dried samples (expressed as XRF counts on the Y axis), exhibiting a distinct peak around 20 cm, which reflects maximum air-bourne pollution from leaded petrol in the mid 1970ies.

We conclude that the laminations observed in the recent sediments of Lake Odensjön represent annually deposited varves (Zolitschka et al. 2015), most likely as a result of oxygen deficit in the deepest part of the lake during an extended period of the year. The character of the varves is currently under investigation through diatom analysis and geochemistry. The sediment sequence has also been studied by pollen and plant macrofossil analyses for reconstruction of past changes in land use around the lake (Damber 2020), a study that forms the basis for a presentation by M. Rundgren in another session of this conference. In addition, we are currently in the process of evaluating the possibility of identifying the potential effects of sulphur emissions from large volcanic eruptions during historical time, such as Laki 1783−84 and Tambora 1815−16, on the lake ecosystem based on detailed biostratigraphic and geochemical analyses of the varved sediments of Lake Odensjön.

References

Berglund, B.E. & Rapp, A., 1988: Geomorphology, climate and vegetation in North-West Scania, Sweden, during the Late Weichselian. *Geographica Polonica 55*, 13–35.

Brännvall, M.-L., Bindler, R. & Renberg, I., 1999: The Medieval metal industry was the cradle of modern large-scale atmospheric lead pollution in northern Europe. *Environmental Science and Technology 33*, 4391−4395.

Damber, M. 2020: A palaeoecological study of the establishment of beech forest in Söderåsen National Park, southern Sweden. *Dissertations in Geology at Lund University, Master's thesis, 608*, 42 pp.

Hertzman, H. 2021. Odensjön – A new laminated (varved) lake sediment record from southern Sweden. *Dissertations in Geology at Lund University, Master's thesis, 611,* 26 pp.

Renberg, I. & Hansson, H., 2010: Freeze corer No. 3 for lake sediments. *Journal of Paleolimnology 44*, 731–736.

Rapp, A., 1982: Odensjön, Skäralid och Klövahallar. Ett nytt tolkningsförsök. *Svensk Geografisk Årsbok 58*, 131–142.

Rapp, A., 1984: Nivation hollows and glacial cirques in Söderåsen, Scania, South Sweden. *Geografiska Annaler 66A*, 11–28.

Zolitschka, B., Francus, P., Ojala, A.E.K. & Schimmelmann, A. 2015: Varves in lake sediments – a review. *Quaternary Science Reviews 117*, 1-41.

Bogs as archives of atmospheric mineral dust – overview and examples from southern Sweden

Jenny K. Sjöström[a,b], Malin E. Kylander[a,b], Eleonor E.E.S. Ryberg[a,b], Antonio Martínez Cortizas[c], Richard Bindler[d]

[a]Department of Geologial Sciences, Stockholm University, Stockholm, Sweden, jenny.sjostrom@geo.su.se; [b]Bolin Centre for Climate Research, Stockholm, Sweden; [c]CRETUS, EcoPast (GI-1553), Universidad de Santiago de Compostela, Santiago de Compostela, Spain; [d]Department of Ecology and Environmental Science, Umeå University, Umeå, Sweden.

Summary. Bogs have a long history of being used as paleoenvironmental archives. During the last three decades bogs have also been recognized as archives of past atmospheric mineral dust deposition (paleodust). Here, we provide an overview of the field of peat paleodust studies, commonly applied analytical procedures and examples of peat paleodust reconstructions from southern Sweden. Paleodust deposition is reconstructed through geochemical analysis of peat sequences, aiming to obtain information on concentrations of lithogenic elements (e.g. Ti, Sc, Al, REE), which can be used to reconstruct paleodust deposition rates, infer mineral composition, provenance, and to explore particle grain sizes. Recently, the effect of mineral dust deposition on peatland dynamics have been explored, showing that mineral dust contains important nutrients that fertilize the bog, affecting plant composition, microbial activity, and peat accumulation rates. In three Swedish bogs (Store Mosse, Draftinge Mosse and Davidsmosse), a majority of mineral dust events was coupled to increased peat (and carbon) accumulation rates, while during some events, mineral deposition contributed to decreased accumulation rates, indicating that a threshold affect may have been reached. A few differences between the three bogs were also observed, such as the magnitude of recorded changes, indicating that local factors (e.g. size of the bog, successional stage, mineral composition, hydrology), may also affect how individual bogs respond to the same forcing mechanism. Future studies could include plant macrofossil analysis, particle size analysis, spectroscopic analysis, as well as peat mineral weathering studies, to further increase our knowledge on the interaction between mineral dust and bog ecosystems.

Bogs and atmospheric mineral dust

Atmospheric mineral dust plays a dynamic role in the climate system acting both as a forcing and a feedback mechanism interacting with the Earth's climate system by affecting incoming solar radiation, atmospheric chemistry, and by bringing nutrients to marine and terrestrial ecosystems (Knippertz and Stuut, 2014; Albani et al., 2015). Terrestrial paleodust archives that can be utilized as paleodust archives include loess, lakes and ombrotrophic (rain-fed) bogs. Bogs have a long history of being used as a natural archive for paleoenvironmental variability, with early studies using pollen and plant macrofossils to reconstruct vegetation and hydrological changes already a century ago (e.g. Sernander, 1894; Von Post, 1916). Since then, the field has developed with an increasing number of proxies, dating techniques and statistical approaches. The peat paleodust field evolved from metal pollution studies (e.g. Aaby and Jacobsen, 1978) and the number of studies has since steadily increased. Peat paleodust deposition is reconstructed through down-core elemental analysis, where conservative lithogenic elements (e.g. Al, Ti, Sc or REE) are used to infer mineral deposition, composition and particle sizes (Steinmann and Shotyk, 1997; Shotyk et al., 2002; Kylander et al., 2013; Marx et al., 2018). Recently, spectroscopic analysis has also been applied to peat and paleodust studies (Martínez Cortizas et al., 2021)

Early peat paleodust studies related changes in paleodust deposition to large-scale atmospheric circulation changes, such as increased input of coarse particles during the Younger Dryas and enrichment of fine-grained, long-distance transported particles at the end of the African Humid Period (Shotyk et al., 2002). Later studies showed also that local and regional contexts (e.g. vegetation cover, mire successional stage) need to be considered (Martínez Cortizas et al., 2005; Silva-Sánchez et al., 2014; Sjöström et al., 2020). Lately, the effect of the deposited dust on bog dynamics has gained attention, showing that mineral dust may affect carbon accumulation, species composition and microbial activity (Kylander et al., 2018; Schillereff et al., 2021; Sjöström et al., 2022; Ryberg et al., 2022).

In the context of Scandinavia, paleodust deposition has been studied in three Swedish bogs. Two of them, Draftinge Mosse and Store Mosse, located 18 km apart, show similar patterns of mineral dust deposition as well as peat accumulation rates, but also some differences. The similarities indicate that mineral dust events are at least regionally reflected, while the differences indicate that local factors, (i.e. size of the bog) influence the recorded signals. The third bog, Davidsmosse, located c. 30 km from the west coast, recorded more episodic events compared to the more inland bogs. This suggests that bog location, and available mineral source areas, influence which type of aeolian event that is recorded. The Davidsmosse sequence was also coupled to analysis of local mineral sources which showed that the most likely sources of current-day mineral deposition are local glaciofluvial sediments (within 1.5 km distance), whereas more distant sources provided the bulk of the minerals during past dust events.

Future studies could benefit from including: a) grain size analysis, which would allow inferring wind strengths, b) combination of spectroscopic analysis with direct mineral observations (XRD, SEM), c) peat pore water analysis, and d) comparison of multiple peat paleodust records, from different climate zones, to further disentangle the role that different factors have on peat accumulation processes.

References

Aaby, B., and Jacobsen, J., 1978: Changes in biotic conditions and metal deposition in the last millenium as reflected in ombrotrophic peat in Draved Mose, Denmark.: *Dan. Geol. Årsbog*, 5, 5-43.

Albani, S. et al., 2015: Twelve thousand years of dust: the Holocene global dust cycle constrained by natural archives: *Climate of the Past*, 11, 869–903, doi:10.5194/cp-11-869-2015.

Knippertz, P., and Stuut, J.-B.W. (Eds.), 2014: *Mineral Dust: a Key Player in the Earth System*: Dordrecht, Springer Netherlands, doi:10.1007/978-94-017-8978-3.

Kylander, M.E. et al., 2018: Mineral dust as a driver of carbon accumulation in northern latitudes. *Scientific Reports*, 8, 6876, doi:10.1038/s41598-018-25162-9.

Kylander, M.E., Bindler, R., Cortizas, A.M., Gallagher, K., Mörth, C.-M., and Rauch, S., 2013: A novel geochemical approach to paleorecords of dust deposition and effective humidity: 8500 years of peat accumulation at Store Mosse (the "Great Bog") Sweden. *Quaternary Science Reviews*, 69, 69–82, doi:10.1016/j.quascirev.2013.02.010.

Martínez Cortizas, A., López-Merino, L., Silva-Sánchez, N., Sjöström, J.K., and Kylander, M.E., 2021: Investigating the Mineral Composition of Peat by Combining FTIR-ATR and Multivariate Analysis. *Minerals*, 11, 1084, doi:10.3390/min11101084.

Martínez Cortizas, A., Mighall, T., Pontevedra Pombal, X., Nóva Muñfoz, J.C., Peiteado Varelal, E., and Piñero Rebolol, R., 2005: Linking changes in atmospheric dust deposition, vegetation change and human activities in northwest Spain during the last 5300 years. *The Holocene*, 15, 698–706, doi:10.1191/0959683605hl834rp.

Marx, S.K., Kamber, B.S., McGowan, H.A., Petherick, L.M., McTainsh, G.H., Stromsoe, N., Hooper, J.N., and May, J.-H., 2018: Palaeo-dust records: A window to understanding past environments. *Global and Planetary Change*, 165, 13–43, doi:10.1016/j.gloplacha.2018.03.001.

Ryberg, E.E., Väliranta, M., Martinez-Cortizas, A., Ehrlén, J., Sjöström, J.K., and Kylander, M.E., 2022: Postglacial peatland vegetation succession in Store Mosse bog, south-central Sweden: An exploration of factors driving species change. *Boreas*, 12580, doi:10.1111/bor.12580.

Schillereff, D.N., Chiverrell, R.C., Sjöström, J.K., Kylander, M.E., Boyle, J.F., Davies, J.A.C., Toberman, H., and Tipping, E., 2021: Phosphorus supply affects the long-term functioning of mid-latitude ombrotrophic peatlands. *Communications Earth & Environment*, 2, 1-10, doi:https://doi.org/10.1038/s43247-021-00316-2.

Sernander, R., 1894: Studier öfver den Gotlandändska vegetationens utvecklingshistoria., in Uppsala. PhD thesis. *Uppsala University*, 1, 1-112.

Shotyk, W., Krachler, M., Martinez-Cortizas, A., Cheburkin, A.K., and Emons, H., 2002: A peat bog record of natural, pre-anthropogenic enrichments of trace elements in atmospheric aerosols since 12 370 14 C yr BP, and their variation with Holocene climate change. *Earth and Planetary Science Letters*, 199, 21–37, doi:10.1016/S0012-821X(02)00553-8.

Silva-Sánchez, N., Martínez Cortizas, A., and López-Merino, L., 2014: Linking forest cover, soil erosion and mire hydrology to late-Holocene human activity and climate in NW Spain. *The Holocene*, 24, 714–725, doi:10.1177/0959683614526934.

Sjöström, J.K., Bindler, R., Cortizas, A.M., Björck, S., Karlsson, A., Ellerton, D.T., and Kylander, M.E., 2022: Late Holocene peat paleodust deposition in south-western Sweden - exploring geochemical properties, local mineral sources and regional aeolian activity. *Chemical Geology*, 602, 1-14, doi:https://doi.org/10.1016/j.chemgeo.2022.120881.

Sjöström, J.K., Martínez Cortizas, A., Hansson, S.V., Silva Sánchez, N., Bindler, R., Rydberg, J., Mörth, C.-M., Ryberg, E.E.S., and Kylander, M.E., 2020: Paleodust deposition and peat accumulation rates – Bog size matters. *Chemical Geology*, 554, 1-14, doi:10.1016/j.chemgeo.2020.119795.

Steinmann, P., and Shotyk, W., 1997: Geochemistry, mineralogy, and geochemical mass balance on major elements in two peat bog profiles (Jura Mountains, Switzerland). *Chemical Geology*, 138, 25–53, doi:10.1016/S0009-2541(96)00171-4.

von Post, L., 1916: Om skogsträdpollen i sydsvenska torfmosselagerföljder. Geologiska föreningen i Stockholm, Förh. 38, 384-394.

Paleomagnetic inclination shallowing in Late-Glacial sediments recovered from the Baltic Sea Basin

Ian Snowball[a], E. Herrero-Bervera[b], Thomas Andrén[c]

[a]Department of Earth Sciences, Uppsala University, Sweden, ian.snowball@geo.uu.se; [b]Hawai'i Institute of Geophysics and Planetology, University of Hawai'i at Manoa, USA; herrero@soest.hawaii.edu; [c]School of Natural Sciences, Technology and Environmental Studies, Södertörn University, Sweden, thomas.andren@sh.se

Summary. Natural magnetic remanence carried by sediment depends not only on the geometry of the geomagnetic field at the time of recording but also on gravity and post-depositional sediment consolidation, both of which can cause so-called inclination shallowing. A paleomagnetic data set attained during IODP Expedition 347 (Baltic Sea Paleoenvironment) contains glacially influenced lithologic units characterised by inclinations that could – without independent evidence to the contrary – be interpreted as evidence of low latitude (equatorial) glaciers at sea level.

Background

The International Ocean Discovery Program (IODP) sampled 6 subbasins of the Baltic Sea Basin (BSB) during Expedition 347 – Baltic Sea Paleoenvironment (Andrén et al. 2015) which led to the recovery of ~1.6 km of core, containing primarily sediments that were deposited since the last retreat of the Scandinavian Ice Sheet (SIS). As routinely undertaken during IODP expeditions that use a mission specific platform (MSP) and an onshore science party (OSP), discrete paleomagnetic subsamples (a total of 1779) were taken from working halves of split cores and their natural remanent magnetization (NRM) measured before and after alternating field demagnetization at 5 mT (with the exception of pilot samples taken from each lithologic unit that were demagnetized up to a maximum of 100 mT).

It was noted during the OSP that inclinations trended towards shallower than geo-axial dipole model predictions (sites GADs range between 70 and 75°) with increasing depth below the seafloor at each site. Some subsamples had reversed directions that were ascribed to high energy sedimentary environments (Andrén et al. 2015). We compiled a paleomagnetic dataset based on the available OSP data, although we removed data from (i) the core-catchers, (ii) lithologic units identified as folded and/or disturbed and (iii) sections of cores known to be compromised by sediment expansion (Obrochta et al. 2017). The resulting compilation contains a total of 1423 paleomagnetic directions. We subsequently subdivided the compiled palaeomagnetic data into two distinct groups that were based on the expedition's sedimentologists' descriptions into "glacially influenced" (e.g. diamicton and varved clays) and "non-glacially influenced" (e.g. greenish black organic clays deposited in estuarine or marine environments). Due to the aims of the expedition different lithologic units were sampled at different resolution, which resulted in significantly more paleomagnetic data from the non-glacially influenced deposits.

Results

We present the inclinations of the two groups as histograms. The group of glacially influenced sediments is characterised by a roughly bimodal distribution with inclination peaks of about 5° and 45°, both of which are significantly lower than the range of GAD predictions for the sampled sites (70–75°). In contrast the non-glacially influenced sediments show a distinct main peak at 70–75°, in agreement with the GAD predictions, although there is a thin tail of data with low inclinations. Given the complex deglaciation of the BSB, with waxing and waning of the SIS, there is a distinct possibility that the rough method of subdividing the data set into two groups led to some misplacement of data, but the size of the data set is sufficient large to draw some conclusions.

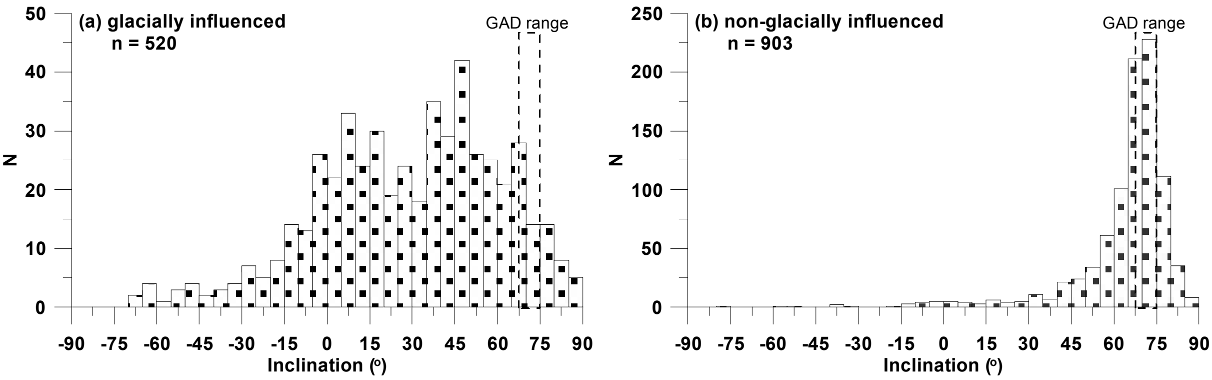

Histograms that show the range of paleomagnetic inclinations for (a) glacially influenced sediments and (b) non-glacially influenced sediments recovered during the onshore science party of IODP Expedition 347. The group of glacially influenced sediments is characterised by a broad, but roughly bimodal distribution of inclinations, with the vast majority lower than the range of GAD predictions. The group of non-glacially influenced sediments has a much narrower distribution, with a peak within the range of GAD predictions.

Conclusion

Our simple subdivision of the compiled paleomagnetic dataset obtained during IODP Expedition 347 elegantly illustrates the well-known problem of inclination shallowing in coarse-grained sediments, which is of concern for paleomagnetic studies of sedimentary rocks that aim to build apparent polar wander paths and reconstruct paleogeography (e.g. Vaes et al. 2021). Further (post OSP) measurements and sampling of fine-grained non-glacially influenced sediments from three of the IODP-347 sites (M0060, M0061 & M0062) were able to reconstruct paleomagnetic secular variation (Snowball et al. 2019, Herrero-Bervera et al. 2020). Without independent prior knowledge of the regional Quaternary geology, conversion of the paleomagnetic data obtained from the glacially influenced sediments in the BSB into a paleogeographic reconstruction could lead to the erroneous conclusion of evidence of glaciers located at sea level near the equator. Our investigation of the IODP Expedition 347 paleomagnetic data set shows the importance of sampling paleomagnetically suitable sedimentary rocks for paleogeographic studies, including those of Proterozoic and Neoproterozoic Snowball Earths (e.g. Evans 2006, Schmidt et al. 2009).

References

Andrén, T., Jøgensen, B.B., Cotterill, C., Green, S., & the Expedition 347 Scientists., 2015: Expedition 347 Summary. *Proceedings of the Integrated Ocean Drilling Program, Volume 347*, 1-66.

Evans, D.A.D., 2006: Proterozoic low orbital obliquity and axial-dipolar geomagnetic field from evaporite palaeolatitudes. *Nature 444*, 51-55.

Herrero-Bervera, E. & Snowball, I. 2020: Integrated high-resolution PSV, RPI and 14C study of IODP-347 Site M0060 (Anholt Loch, Baltic Sea) for the last c. 14 ka. In: Tema, E., Di Chiara, A. & Herrero-Bervera, E. (Eds.) *Geomagnetic Field Variations in the Past: New Data, Applications and Recent Advances*. Geological Society, London, Special Publications 497.

Obrochta, S.P., Andrén, T.A., Fazekas, S.F., Lougheed, B.C., Snowball, I., Yokoyama, Y., Miyairi, Y., Kondo, R., Kotilainen, A.T., Hyttinen, O. & Fehr, A., 2017: The undatables: Quantifying uncertainty in a highly expanded Late Glacial-Holocene sediment sequence recovered from the deepest Baltic Sea basin—IODP Site M0063. *Geochemistry, Geophysics, Geosystems 18*, 858-871.

Schmidt,P.W., Williams, G.E. & McWilliams, M.O. 2009: Palaeomagnetism and magnetic anisotropy of late Neoproterozoic strata, South Australia: Implications for the palaeolatitude of late Cryogenian glaciation, cap carbonate and the Ediacaran System. *Precambrian Research 174*, 35-52.

Snowball, I., Almqvist, B., Lougheed, B.C., Wiers, S., Obrochta, S. & Herrero-Bervera, E., 2019: Coring induced sediment fabrics at IODP Expedition 347 Sites M0061 and M0062 identified by anisotropy of magnetic susceptibility (AMS): criteria for accepting palaeomagnetic data. *Geophysical Journal International 217*, 1089-1107.

Vaes, B., Li, S., Langeries, C.G., & van Hinsbergen, D.J.J., 2021: Reliability of palaeomagnetic poles from sedimentary rocks. *Geophysical Journal International 255*, 1281-1303.

Age and distribution of aeolian sand dunes in Arctic Sweden

Thomas Stevens[a], Melanie Stammler[b], Salome Oehler[c], Thomas Kolb[c], Daniel Hölbling[d], Göran Possnert[e]

[a]Department of Earth Sciences, Uppsala University, Uppsala, Sweden, thomas.stevens@geo.uu.se; [b]Rheinische Friedrich-Wilhelms-Universität Bonn, Bonn, Germany, stammler@uni-bonn.de ; [c]Department of Physical Geography, Justus-Liebig-University Giessen, Germany, oehler.salome@gmail.com; thomas.r.kolb@geogr.uni-giessen.de; [d]Department of Geoinformatics - Z_GIS, University of Salzburg, Salzburg, Austria, Daniel.Hoelbling@plus.ac.at; [e]Department of Physics and Astronomy, Ion Physics, Uppsala University, Sweden, goran.possnert@physics.uu.se

Summary. Aeolian sand dunes in Arctic Sweden have great potential as archives of landscape change, wind direction, and Holocene environment. However, the precise nature of their distribution, form, age, and formation history remain unclear. Here we apply geographic object-based image analysis (GEOBIA) to reveal multiple new dune features, sediment sources, and the influence of wind direction on dune form. Furthermore, we undertake detailed luminescence and radiocarbon dating of dune age and reworking history, revealing multiple episodes of dune reactivation and stability through the Holocene.

Aeolian sand dunes are widespread in the Swedish Arctic and Subarctic. These cold climate, often vegetated dunes tend to be parabolic in type, and often form complex associations with landforms such as eskers and drumlins. Their formation, development, and preservation is forced by changes in wind, temperature, and moisture, and today many dunes exhibit blowouts and hollows, often caused by disturbance to vegetation. Extensive ground-based mapping has previously been conducted on dunes in Arctic Sweden (e.g. Bergqvist 1981) but due to the large, sometimes inaccessible areas these dunes are found in, such point mapping is likely to be incomplete.

Dunes in Arctic Fennoscanidia likely formed immediately following the last deglaciation (Lundqvist & Mejdahl 1995). However, analysis of dune stratigraphy in Arctic Finland reveals complex alternations of laminated to massive sands, palaeosols and charcoal layers, indicating complex histories of formation, stability and reworking (Clarke & Käyhkö 2007). Furthermore, radiocarbon and luminescence dating studies conducted on these Finnish dune sediments reveal multiple episodes of reactivation during the Holocene, as well as inconsistencies over the ages of dune cores (Clarke & Käyhkö 1997; Matthews & Seppälä 2014). The reactivation of Fennoscandian Arctic dunes may be related to climate or human-induced fires, which destabilize anchoring vegetation and facilitate dune movement. As well as recording these periodic disturbances, parabolic dunes can be used as indicators of prevalent sand-transporting wind directions during dune formation.

Previous work on Arctic Fennoscandian dunes has tended to focus on dunes in Finland, and recent research on dunes in Arctic Sweden is lacking. A first step in utilising these dunes to infer climate and landscape development is accurate, systematic and detailed mapping and characterisation. Here we use geographic object-based image analysis (GEOBIA), which permits the creation of reproducible parameter-based polygons from landforms through segmentation and classification of spatial data (Blaschke 2010; Fitzsimmons et al. 2020), to better define the of the occurrence of Arctic Swedish aeolian dunes. A digital elevation model (DEM) and its derivatives were segmented in a GEOBIA context, enabling the identification and mapping of aeolian dunes. Analysis of the GEOBIA-derived and expert-accepted polygons reveals multiple previously unmapped dune features, and reinforces the prevalence of parabolic dune types, sometimes with the coexistence of simple dunes with large coalesced systems. Mapped dune orientations and relationships to other geomorphological features allow identification of dominant glaciofluvial and fluvial disturbances of esker systems as dune sediment sources. Topographic control of wind direction is the dominant influence on dune orientation.

Furthermore, few detailed chronostratigraphic analyses have been conducted on Arctic Swedish dunes, and a detailed chronology of their formation, evolution and reworking is lacking. As such, we developed and tested a suitable quartz optically stimulated luminescence (OSL) dating protocol based on dunes at the sites of Vastakielinen and Jorggástat. Single aliquot regeneration (SAR) and double-SAR procedures (Murray and Wintle 2000) were tested using dose recovery and preheat plateau tests. Due to feldspar microinclusions within the quartz fraction, a double-SAR protocol was finally used for equivalent dose determination and the reliability of these doses tested using standard rejection criteria. Independent control of the determined ages was provided by ^{14}C dating of charcoal fragments recovered from charcoal layers within the dunes.

Most aliquots passed the acceptance criteria and resultant OSL ages from massive sand layers in the dunes (reworked sands) are in good agreement with corresponding ^{14}C ages from bracketing charcoal bands, suggesting that quartz OSL is well suited for the dating of aeolian sediments in this part of northern Sweden. However, weak quartz OSL signals in dune core stratified sands, likely deposited during original dune formation, precludes precise quartz OSL dating of initial dune formation. Overall, the results suggest that the two investigated dunes likely started forming immediately after deglaciation and were active for multiple millennia, even when vegetation had already established in the area. The Vastakielinen dune further shows evidence of renewed aeolian activity at 3.6±0.18 ka and 0.26±0.01 ka, with the latter episode traced back to a forest fire event at 145±112 cal yrs BP. At Jorggástat, only one reactivated massive sand horizon could be identified, which is constrained by the underlying ^{14}C age of 3549±84 cal yrs BP. However, evidence of mutiple charcoal bands in other dunes in Arctic Sweden suggests an even more extensive history of reworking may be preserved in these deposits.

References

Bergqvist, E., 1981: Svenska inlandsdyner: översikt och förslag till dynreservat. Uppsala.

Blaschke, T., 2010: Object based image analysis for remote sensing. *ISPRS Journal of Photogrammetry and Remote Sensing 65*, 2–16.

Clarke, M.L. & Käyhkö, J.A., 1997: Evidence of holocene aeolian activity in sand dunes from Lapland. *Quaternary Science Reviews 16,* 341–348.

Fitzsimmons, K.E. Nowatzki, M. Dave, A.K. and Harder, H., 2020: Intersections between wind regimes, topography and sediment supply: Perspectives from aeolian landforms in Central Asia. *Palaeogeography Palaeoclimatology Palaeoecology 540*, 109531.

Lundqvist, J. & Mejdahl, V., 1995: Luminescence dating of the deglaciation in Northern Sweden. *Science 28*, 193–197.

Matthews, J.A. & Seppälä, M., 2014: Holocene environmental change in subarctic aeolian dune fields: The chronology of sand dune re-activation events in relation to forest fires, palaeosol development and climatic variations in Finnish Lapland. *Holocene 24*, 149–164.

Murray, A.S. & Wintle, A.G., 2000: Application of the Single-Aliquot Regenerative-Dose Protocol to the 375°C Quartz TL Signal. *Radiation Measurements 32*, 579-583.

Loess deposits in central Sweden: age, formation and significance

Thomas Stevens[a], Daniele Sechi[b], Charilaos Tsiavaras[a], Ramona Schneider[a], Adriano Banak[c], Calum J. Edward[a], Stefano Andreucci[d], Martina Hättestrand[e], Vincenzo Pascucci[b]

[a]Department of Earth Sciences, Uppsala University, Uppsala, Sweden, thomas.stevens@geo.uu.se; Charilaos. Tziavaras.6555@student.uu.se; ramona.schneider@geo.uu.se; calum.edward@geo.uu.se; [b]Department of Architecture, Design and Planning, University of Sassari, Alghero, Italy, dasechi@uniss.it; pascucci@uniss.it; [c]Department for Geology, Croatian Geological Survey, Zagreb, Croatia, abanak@hgi-cgs.hr; [d]Dipartimento di Scienze Chimiche e Geologiche, Universita degli Studi di Cagliari, Monserrato, Italy, sandreucci@unica.it; [e]Department of Physical Geography, Stockholm University, Stockholm, Sweden, martina.hattestrand@geo.su.se

Summary. Loess deposits are excellent climate and landscape archives, widely found across mid latitude Europe. Thin (up to 1 m) loess deposits are also sporadically found in Sweden, but their distribution, age and formation are not well understood. Here we conduct detailed mapping, sedimentological analysis and luminescence dating of loess around Brattforsheden and Bonäsheden, and identify more extensive loess cover than previously shown. The loess deposits also yield luminescence ages extending into the mid to late Holocene, younger than expected based on sedimentologic and geomorphic associations.

Loess deposits are common over the mid-latitudes and contain excellent records of past climate, landscape change and coarse (>5 µm) dust activity. In contrast, loess is rarely reported in Fennoscandia, but has been previously suggested to occur sporadically in central Sweden (Hörner 1927, Hjulström et al. 1955, Agrell & Hultman 1971, Ekström & Hedeving 2021). Hörner (1927) first mapped what he suggested to be up to 1 m thick windblown loess deposits around the former glaciofluvial meltwater system at Brattforsheden. Hjulström et al. (1955) also mapped suspected loess deposits further north, just west of the Bonäsheden glaciofluvial delta system and aeolian dune field. These deposits share many sedimentary and geomorphic properties and associations to those at Brattforsheden. Possible loess deposits are also reported in southern Sweden, both at Svartedalen (Ekström & Hedeving 2021) and the southern Swedish uplands (Agrell & Hultman 1971). Again, both these deposits are located close to former glaciofluvial meltwater channels or deltas. However, numerous questions remain regarding the true distribution of loess in Sweden, the timing of loess deposition, its relationship to other geomorphic features or sedimentary deposits, and whether the deposits can be used to understand past wind directions.

Here we investigate possible loess deposits in Brattforsheden and west of Bonäsheden, where post glacial aeolian silt and sand dune activity has been documented previously (Hörner 1927, Hjulström et al. 1955). Based on detailed mapping, grain-size, SEM and quartz optically stimulated luminescence dating analyses, we confirm and extend the presence of windblown loess deposits at these sites. Our results imply loess deposits in Sweden may be more common than previly believed, but also demonstrate mixing and reworking in basal parts of many of these loess deposits. This may be a common feature of thin loess deposits close to former ice margins. Quartz luminescence is well suited for dating loess deposits at the sites, but ages from the mixed basal loess layers are older than expected, while ages from apparently undisturbed loess extend well into the Holocene, pointing to loess deposition to c. 5 ka. These reults contrast with the timing of main dune activity in these areas, which is dominantly constrained to the 1–3 ka post deglaciation (Bernhardson et al. 2019). Two hypotheses are proposed to explain this anomaly. One possibility is that loess deposits may record a more extended phase of periodic landscape destabilization and aeolian activity late into the Holocene in central Sweden. Alternatively, the luminescence ages from the loess may be underestimates of the true depositional age, potentially due to the effects of extensive soil formation and sediment reworking processes in these thin deposits. In any case, there is a clear topographic control on aeolian sedimentary facies, with loess covering high ground and dunes mantling valleys. Furthermore, loess deposits are only found to the south and southwest of likely glaciofluvial and dune source areas, implying transport from the north and east. This contrasts with evidence for NW winds from the morphology of close by sand dunes. This differenvce may be explained by the coarse silts being deposited at higher elevations and therefore via higher level winds, which may well have been affected by Ekman transport deflection (sensu Hjulström et al. 1955).

References

Agrell, H. & Hultman, R., 1971: Deposits of wind-blown silt in the north-eastern part of the southern Swedish uplands. *GFF 93*, 231-235.

Bernhardson, M. Alexanderson, H., Björck, S. & Adolphi, F. 2019: Sand drift events and surface winds in south-central Sweden: From the deglaciation to the present. *Quaternary Science Reviews 209*, 13–22.

Ekström, F. & Hedeving, A., 2021: Loess in southwestern Sweden: determining the genesis of the silt-rich layer rödfemman in Svartedalen nature reserve. *MSc thesis University of Gothenberg*, pp. 70.

Hjulström, F. Sundborg, Å. & Falk, Å., 1955: Problems concerning the deposits of windblown silt in Sweden. *Geografiska Annaler 1-2,* 86-117.

Hörner, N.G., 1927: Brattforsheden ett värmländskt randdeltekomplex och dess dyner. *SGU C342. 206 pp*. Geological Survey of Sweden, Uppsala

Late Quaternary tephrochronology of Sweden

Sefan Wastegård[a], Simon A. Larsson[a,b]

[a]Department of Physical Geography, Stockholm University, Stockholm, Sweden, stefan.wastegard@geo.su.se
[b]Geological Survey of Sweden, Uppsala, Sweden, e-mail: simon.larsson@sgu.se

Summary. Tephrochronology is based on the identification of volcanic ashes from explosive volcanic eruptions and their useage as isochrons in diverse palaeoclimate archives such as lake sediment, ice cores and marine cores. One of the first to use tephras as stratigraphical markers was the Icelander Sigurdur Thorarinsson in his thesis from Stockholm University College (Thorarinsson 1944) in which he coined the term tephrochronology for the establishment of an absolute geological chronology, based on measurements, correlations and dating of volcanic ash layers. Already in his thesis he outlined the prospect of finding ash from major Icelandic eruptions in peat bogs in Scandinavia, inspired by the fallout of tephra in Central Norway and Sweden from the eruption of Askja in March 1875. This abstract is a short summary of tephrochronological investigations in Sweden since the 1960s. Tephrochronology has today evolved as a powerful tool in the efforts to understand the behaviour of the climate system in the past considering its combined spatial and temporal advantages.

Tephra in Swedish peat bogs

The geology student Christer Persson met Thorarinsson during an excursion in Iceland in 1962 and a PhD project was set up at Stockholm University aiming at exploring the possibilities of finding tephra from Icelandic eruptions in bogs in Scandinavia and the Faroe Islands. Persson's work resulted in four papers, all published in Geologiska Föreningen i Stockholm Förhandlingar and the main results were summarised in his PhD thesis (Persson 1971). Geochemical analysis of the tephras was not possible at this time, but he made tentative correlations with known tephra layers in Iceland, among them Askja-1875, Hekla-3 (c. 3000 cal a BP) and Hekla-4 (c. 4260 cal a BP), using refractive indices of the glass, radiocarbon dating and pollen analyses. Persson's studies were confined to bogs in south-central Sweden, and especially in the counties of Dalarna and Värmland. Later on, during the 1990s and early 2000s Boygle (1998, 2004) and Borgmark & Wastegård (2008) revisited some of the bogs investigated by Persson and were able to confirm several of his results with geochemical analyses using the EMPA technique. An additional tephra from Hekla; Kebister or Hekla-S was found with high concentrations in many bogs (Boygle 1998), and was later dated at Fågelmossen in Värmland by wiggle-matching of radiocarbon dates to c. 3720 cal a BP (Wastegård et al. 2008). Hekla-3, Hekla-S and Hekla-4 have also been reported from annually varved lake sediment sequences in Värmland (Zillén et al. 2002).

Several bogs in central and northern Sweden have been investigated for tephras during the last ca 20 years (e.g. Bergman et al. 2004, Borgmark & Wastegård, 2008, Watson et al. 2016) and the tephra network for the Middle and Late Holocene (c. 8200 cal a BP-present) now comprises c. 10 geochemically confirmed layers, suggesting that ashfall events may have occurred in Sweden at least once every millennium during the Holocene. There is still a scarcity of tephra investigations of peat from south Sweden, and this part of Sweden can be considered a white spot for the middle to late tephrochonology of Sweden.

Tephra in Swedish records from the Last Glacial-Interglacial transition

The Last Glacial-Interglacial transition (LGIT; c. 14–8 ka BP), was a complex time period, but suitable for tephra-based studies and correlations (e.g. Lane et al. 2013, Larsson & Wastegård, 2022). Recent developments of tephra detection and extraction as well as improved analytical protocols for geochemical analyses of individual tephra shards has led to a rapid expansion of tephrochronology to distal sites, many thousands of kilometres from the volcanic sources. Although tentative records of the Laacher See Tephra and the Vedde Ash have been reported from Swedish records, geochemical identification of the Vedde Ash in Sweden was first reported from Lake Madtjärn in Dalsland by (Wastegård et al. 1998), followed by several other findings in Sweden in lake sediment as well as in uplifted marine clays (e.g. Schoning et al. 2001). Two significant new additions to the LGIT tephrochronological frameworks of NW Europe are the Hässeldalen (c. 11.4 ka BP) and Askja-S tephras (c. 10.8 ka BP) that were first decribed from two sites in Blekinge, SE Sweden by Davies et al. (2003). These two tephras have emerged as two of the most important isochrons for the the LGIT in NW Europe (Davies et al. 2012). The Hässeldalen Tephra (HDT) holds a key stratigraphic position for the climate development during the early Holocene and is being thought to mark the onset of the Preboreal Oscillation (e.g. Davies et al. 2003). HDT is widespread around the southern Baltic Sea basin and has been reported from at least six sites in south Sweden (e.g. Wohlfarth et al. 2018, Larsson & Wastegård, 2022).

Several sites in south Sweden have been investigated for the widespread Laacher See Tephra (LST; c. 13.0 ka BP) and the Saksunarvatn Ash (c. 10.2 ka BP), but it was not until recently that the LST was confirmed in a palaeo-lake sediment sequence at Körslättamossen in NW Skåne (Larsson & Wastegård 2018). The Saksunarvatn Ash still remains elusive in Sweden.

Several recent investigations have confirmed the potential of tephrochronology in Sweden, but some areas and time periods are still underinvestigated, such as Holocene peat records in south Sweden and interstadial deposits in central and north Sweden. Many research questions have been solved with the use of tephras, but there are several others that tephrochronology has a potential to provide answers to, such as the timing and synchronicity of events during the LGIT and the Holocene, changes in the marine reservoir age over time, errors in the Swedish glacial varve chronology and the age of interstadial deposits in northern Sweden.

References

Bergman, J., Wastegård, S., Hammarlund, D., Wohlfarth, B., Roberts, S.J., 2004: Holocene tephra horizons at Klocka Bog, west-central Sweden: Aspects of reproducibility in subarctic peat deposits. *Journal of Quaternary Science 19*, 241–249.

Borgmark, A., Wastegård, S., 2008: Regional and local patterns of peat humification in three raised peat bogs in Värmland, south-central Sweden. *GFF 130*, 161–176.

Boygle, J., 1998: A little goes a long way: Discovery of a new mid-Holocene tephra in Sweden. *Boreas 27*, 195–199.

Boygle, J., 2004: Towards a Holocene tephrochronology for Sweden: Geochemistry and correlation with the North Atlantic tephra stratigraphy. *Journal of Quaternary Science 19*, 103–109.

Davies, S.M., Abbott, P.M., Pearce, N.J.G., Wastegård, S., Blockley, S.P.E., 2012: Integrating the INTIMATE records using tephrochronology: Rising to the challenge. *Quaternary Science Reviews 36*, 11–27.

Davies, S.M., Wastegård, S., Wohlfarth, B., 2003: Extending the limits of the Borrobol Tephra to Scandinavia and detection of new early Holocene tephras. *Quaternary Research 59*, 345–352.

Lane, C.S., Brauer, A., Blockley, S.P.E., Dulski, P., 2013: Volcanic ash reveals time-transgressive abrupt climate change during the Younger Dryas. *Geology 41*, 1251–1254.

Larsson, S.A., Wastegård, S., 2022: A high-resolution Lateglacial–Early Holocene tephrostratigraphy from southernmost Sweden with comments on the Borrobol–Penifiler tephra complex. *Quaternary Geochronology 67*, 101239.

Larsson, S.A., Wastegård, S., 2018: The Laacher See Tephra discovered in southernmost Sweden. *Journal of Quaternary Science 33*, 477–481.

Persson, C., 1971: Tephrochronological investigation of peat deposits in Scandinavia and on the Faroe Islands, Geological Survey of Sweden C656.

Schoning, K., Klingberg, F., Wastegård, S., 2001. Marine conditions in central Sweden during the early Preboreal as inferred from a stable oxygen isotope gradient. *Journal of Quaternary Science 16,* 785-794.

Thorarinsson, S., 1944: Tefrokronologiska Studier På Island. Thjórsárdalur och dess förödelse. *Geografiska Annaler 26*, 1–217.

Wastegård, S., Björck, S., Possnert, G., Wohlfarth, B., 1998: Evidence for the occurrence of Vedde Ash in Sweden: radiocarbon and calendar age estimates. *Journal of Quaternary Science 13*, 271–274.

Wastegård, S., Rundgren, M., Schoning, K., Andersson, S., Björck, S., Borgmark, A., Possnert, G., 2008: Age, geochemistry and distribution of the mid-Holocene Hekla-S/Kebister tephra. *The Holocene 18*, 539–549.

Watson, E.J., Swindles, G.T., Lawson, I.T., Savov, I.P., 2016: Do peatlands or lakes provide the most comprehensive distal tephra records? *Quaternary Science Reviews 139*, 110–128.

Wohlfarth, B., Luoto, T.P., Muschitiello, F., Väliranta, M., Björck, S., Davies, S.M., Kylander, M., Ljung, K., Reimer, P.J., Smittenberg, R.H., 2018: Climate and environment in southwest Sweden 15.5–11.3 cal. ka BP. *Boreas 47*, 687–710.

Zillén, L.M., Wastegård, S., Snowball, I.F., 2002: Calendar year ages of three mid-Holocene tephra layers identified in varved lake sediments in west central Sweden. *Quaternary Science Reviews 21*, 1583–1591.

Thematic Session 12
Structural geology & tectonics

Session Chairs:
Tobias Bauer (tobias.bauer@ltu.se)
Karin Högdahl (karin.hogdahl@geo.uu.se)
Stefan Luth (stefan.luth@sgu.se)

Age and crustal affinity of Precambrian basement nappes and underlying basement in the east central Scandinavian Caledonides

Jenny Andersson[a,b], StefanClaesson[c], Ellen Kooijman[c]

[a]Department of Earth Sciences, University of Uppsala, Uppsala, Sweden, jenny.andersson@geo.uu.se; [b]Geological Survey of Sweden, Uppsala, Sweden, jenny.andersson@sgu.se; [c]Swedish Museum of Natural history, Stockholm, Sweden, ellen.kooijman@nrm.se; stefan.claesson@nrm.se

Summary. 1690 Ma to 1640 Ma U-Pb zircon ages and whole-rock geochemical data for igneous rocks in Precambrian crystalline basement thrust sheets and the deep underlying basement in the east central Scandinavian Caledonides demonstrate that these rocks represent an extended phase of Transscandinavian Igenous Belt (TIB) magmatism related to the Svecokarelian accretionary orogenic system. The new data contradicts the presence of 1660–1520 Ma Gothian crust in the Caledonides. Instead, the Caledonian nappes and the underlying basement include TIB rocks as young as 1650–1620 Ma not exposed in the Fennoscandian Shield.

Introduction and methodology

The Caledonian orogeny involved long distance south-eastward thrusting of nappe sheets onto to the Fennoscandian continent in Mid-Palaeozoic time. The Lower and Middle Allochthons include Precambrian crystalline basement rocks that are the unique remains of the pre-Caledonian continental margin. Understanding of the age, character and crustal affinity of these units is critical for reconstructions of the Precambrian active margins of Fennoscandia.

U-Pb zircon and whole-rock geochemical analyses have been performed on 24 samples of Precambrian crystalline basement rocks in the Lower and Middle Allochthons of the east-central Scandinavian Caledonides. The study also includes three samples from the presumably authochthonous Precambrian basement underlying the Caledonian nappe complex at depth, retrieved through the scientific drilling Collisional Orogeny Scandinavian Caledonides project (COSC-project, cf. Lorenz et al. 2022).

Results

Metaintrusive rocks in the Lower Allochthon are dated at between 1689±7 Ma and 1660±5 Ma (N=4). This includes undeformed granodiorite to quartzmonzonite east of lake Grundsjön in Härjedalen (Veman nappe), gneissic granite and metagabbro at Lake Ottsjön, and partly mylonitic monzonitic gneiss along the Vålån river in west central Jämtland. These rocks have igneous crystallization ages and whole-rock geochemical compositions identical to 1870–1660 Ma TIB rocks (TIB phases 0–3) in the Fennoscandian Shield east of the Caledonides.

Porphyritic rhyolitic to dacitic and trachytic rocks (Östberget porphyries), are the dominating lithology in the Lower Allochthon crystalline basement nappes in the east central Caledonides. They typically occur as undeformed and unmetamorphosed rocks with fine grained 1–2 mm large feldspar phenocrysts in an aphanitic matrix or as penetratively deformed, in places mylonitic rocks. Felsic porphyries in the Lower Allochthons of the Grong-Olden, Skardöra and Mullfjället antiforms (culminations) are dated at between 1670±6 Ma and 1662±4 Ma (N=7). Rhyolitic rocks at Östberget (Frösön) and Hoverberget tectonically overlying the Lower Allochthon Cambrian to Early Silurian supracrustal thrust sheets in the Caledonian nappe front are dated at 1668±4 Ma and 1654±7 Ma, respectively. Felsic porphyries in the presumably autochthonous basement underlying the Caledonian nappes, sampled in the COSC-2 drill core from the bore hole at the southern shore of Lake Liten, southeast of Järpen in Jämtland, was dated at 1651±4 Ma, 1660±4 Ma and 1654±4 Ma, at c. 1230 m, 1400 m, and 2250 m depths, respectively. The felsic porphyries in the Lower Allochthon and its underlying basement (the COSC-2 samples) have whole-rock geochemical compositions identical to volcanic rocks of the TIB in the adjacent Fennoscandian Shield.

Metaintrusive rocks in the lower thrust sheets of the Middle Allochthon (Offerdal Nappes) give the youngest intrusive protolith ages. Strongly deformed protomylonitic to mylonitic augen gneiss at Storlien, Jämtland (Skardöra antiform) and at the northern shore of Lake Anjan (Mullfjället antiform) are dated at between 1657±7 Ma and 1648±7 Ma (N=3). Augen gneisses in the Tännäs augen gneiss Nappe (Offerdal Nappe) sampled at the southern shore of lake Grundsjön [N=2, locality dated by Claesson (1980)] and at Svansjökläppen, close to the Norwegian border in Härjedalen, are dated at between 1651±3 Ma and 1643±4 Ma. The 1660–1640 Ma Middle Allochthon metaintrusive rocks have whole-rock geochemical compositions identical to the TIB rocks in the Fennoscandian Shield east of the Caledonides. They are, however, noticeably younger.

Cobbles of granitic gneiss in metatillites in the Offerdal Nappe at Tännäs, Härjedalen, were dated at between 1686±4 Ma and 1679±8 Ma (N=3). The source of the cobbles is thus older than metaintrusive rocks in the Middle Allochthon in this part of the Caledonides. Secondary zircon rims cross-cutting oscillatory-zoned igneous zircon in one of the samples were dated at 965±9 Ma. Reworked TIB rocks in the high-grade orthogneiss complex of the Eastern Segment in the Sveconorwegian Province, southern Fennoscandian Shield is a potential source rock.

A less than 1 km wide Precambrian thrust sheet just below the eastern contact to the Seve nappe complex of the upper Middle Allochthon in west central Jämtland was sampled at two localities. A weakly metamorphosed fine grained banded rock at Sölsved, just north of Lake Kallsjön, and a fine-grained quartz-feldspar rock with weak lithological banding and up to 10 meters wide amphibolite boudins at Skalberget south of Undersåker. These rocks contain zircon dated at between c. 2000 Ma and 950 Ma. Together with field appearance and geochemistry of these rocks it is concluded that they are Neoproterozoic metasedimentary rocks and not affiliated with the TIB.

Concluding discussion

This study shows that 1690–1640 Ma Precambrian igneous rocks and reworked equivalents in the east central Lower and Middle Caledonian allochthons have geochemical compositions equivalent to TIB rocks in the autochthonous basement east of the orogen. A TIB affinity for 1690–1620 Ma rocks in the Caledonides has previously been proposed for the crystalline Precambrian basement thrust sheets in the Grong-Olden culmination (Roberts et al. 1999), in the Western Gneiss Region and the southeasternmost Caledonian nappes; Hf-zircon data support a petrogenetic link (Lamminen et al. 2011). This crystalline basement thus represents a continuation of the Svecokarelian active continental margin and the accretionary orogenic system that formed the TIB rocks in the Fennoscandian shield, however, extending far more to the west and far more in time than previously thought, down to 1620 Ma.

The chemical and chronological data in this study support the suggestion by Lamminen et al. (2011) that the Gothian continental crust of the Idefjorden Terrane in the Sveconorwegian Province is absent in the Caledonides. If so, it has fundamental implications for the pre-Caledonian crustal architecture of Fennoscandia which must be accounted for in models of the tectonic build-up of the Sveconorwegian orogen.

References

Claesson, S., 1980: A Rb-Sr isotope study of granitoids and related mylonites in the Tännäs Augen Gneiss Nappe, southern Swedish Caledonides. *Geologiska Föreningen i Stockholm Förhandlingar, 102(4)*, 403-420.

Lamminen, J., Andersen, T., & Nystuen, J. P., 2011: Zircon U-Pb ages and Lu-Hf isotopes from basement rocks associated with Neoproterozoic sedimentary successions in the Sparagmite Region and adjacent areas, South Norway: the crustal architecture of western Baltica. *Norwegian Journal of Geology 91*, 35-55.

Lorenz, H., Rosberg, J. E., Juhlin, C., Klonowska, I., Lescoutre, R., et al., 2022: COSC-2–drilling the basal décollement and underlying margin of palaeocontinent Baltica in the Paleozoic Caledonide Orogen of Scandinavia. *Scientific Drilling, 30*, 43-57.

Roberts, D., Nissen, A. L., & Walker, N., 1999: U-Pb zircon age and geochemistry of the Blåfjellhatten granite, Grong-Olden Culmination, Central Norway. *Norsk Geologisk Tidsskrift, 79(3),* 161-168.

Stockholm's geology: granite taken for gneiss

Paul M. Evins

WSP, Stockholm, Sweden, paul.evins@wsp.com

Summary. Conventional descriptions of Stockholm's geology need to be updated with the following:
- A more detailed subdivision of the sedimentary and igneous gneisses that include their metamorphic history
- Recognition of various generations of "Stockholm granite"
- Description and classification of the multiple generations of brittle deformation that have affected the area
- Recognition of a brittle thrusting event

Ståhlös' geological map of Stockholm hasn't really changed for over half a century. It presents sedimentary gneiss (metagreywacke) with subordinate interfingerings of 1.92-1.87 Ga granitic gneiss and amphibolite which were later intruded by the 1.8 Ga Stockholm granite. The metamorphic and deformation events that have affected these rocks have not been systematically investigated within Stockholm, yet they have major implications for the chemical, mechanical and hydrogeological properties of Stockholm's bedrock. High grade metamorphism between 1.9 and 1.8 Ga created massive quantities of diatexite within the sedimentary gneiss which effectively divides the gneiss into units with low strength / high sulfide risk and high strength / low sulfide risk. Furthermore, significant portions of sedimentary gneiss on the map are actually intermediate orthogneisses grading into amphibolite. The younger Stockholm granite is also more complicated than previously thought showing multiple generations that intrude each other with sharp contacts. Several generations of post-1.8 Ga deformation events created mylonites that have been reactivated multiple times across the brittle-ductile transition. The steep mylonite zones have been known for decades. However, there are also shallow-dipping thrusts that have not been documented until now. These thrusts preferentially occur in the Stockholm granite and are often highly hydrogeologically transmissive. The discoveries presented above would benefit from more in-depth research and a new geological map of Stockholm.

References

Stålhös G., 1969: Stockholmstraktens berggrund. *SGU ser. Ba 24*.

Structures and metamorphism of Fjärdlång and Ornö, SE Stockholm archipelago

Karin Högdahl[a], Katarina P. Nilsson[b], Riccardo Callegari[a,c], Erik Jonsson[a,d], Håkan Sjöström[a], Åke Johansson[e], Stefan Claesson[e]

[a]Department of Earth Sciences, Uppsala University, Uppsala, Sweden, karin.hogdahl@geo.uu.se; [b]Svemin, Stockholm, Sweden; [c]AGH, University of Science and Technology, Karaków University, Karaków, Poland; [d]Department of Mineral Resources, Geological Survey of Sweden, Uppsala, Sweden; [e]Department of Earth Sciences, Swedish Museum of Natural History, Stockholm, Sweden

Summary. Fjärdlång and Ornö are located in the southern part of the Stockholm archipelago. Fjärdlång comprises low-grade metasupracrustal rocks of dominating volcaniclastic origin, with various preserved primary sedimentary structures, whereas Ornö is dominated by intrusive rocks. Three fold phases and two, possibly three metamorphic episodes have been identified. F1 are post-M1, asymmetric reclined folds and F2 are open, overturned NNE plunging folds formed after M2. At Ornö these structures are overprinted by the repeatedly active OBS established after M1 peak metamorphism and during early D2.

The islands of Fjärdlång and Ornö (Fig. 1A) are located in the southern part of the Stockholm archipelago, to the northeast of the relative well-studied Utö (Gavelin et al. 1976, Allen et al. 1996). While some studies have been conducted on Ornö, the character of the bedrock geology of Fjärdlång is virtually unknown; the island was only briefly investigated in the late 19th century as a part of a larger mapping campaign of the southern archipelago and the adjacent mainland (Holst 1882).

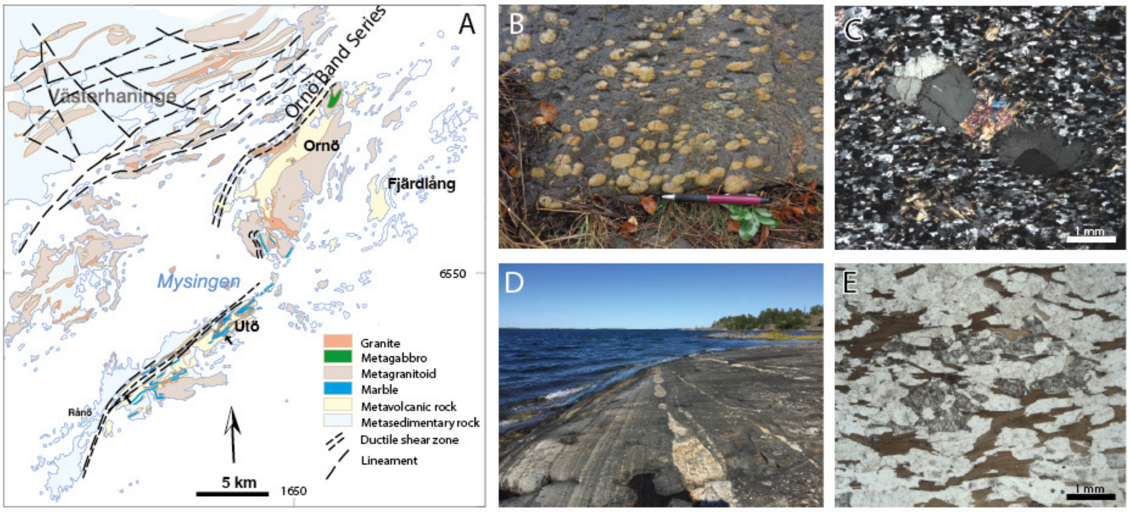

Figure 1. A) Simplified bedrock map over the southeast part of the Stockholm archipelago. Modified after Stephens et al. (2009) and coordinates in Sweref 99TM. B) Porphyroblastic pseudomorphs in a mica-rich layer consist of C) a fine-grained sillimanite-quartz assemblage with remnants of unstable muscovite. Crossed polarised light. D) Ornö Band Series (OBS) with late-stage dextrally deformed pegmatite dykes. E) Biotite, plagioclase and orthopyroxene arrested during early and high-T shear along OBS. Plane polarised light.

The bedrock of Fjärdlång is dominated by rather well-preserved reworked Svecofennian felsic metavolcanic sand- and siltstones, and minor amounts of polymict and monomict breccias and massive, weakly quartz-porphyric units with or without lithic clasts. Primary sedimentary structures such as cross bedding, graded bedding, ripples and parallel lamination are common. Two fold phases and associated fold interferences have been recognised. The first fold phase produced asymmetric, NW-SE trending, reclined F1-folds with a shallow-plunging fold axis and a penetrative S1-cleavage. The long limb of these folds are parallel to shear zones with top-to-the-NW kinematics. An early generation of migmatites have a gneissic S1 fabric and are tectonically emplaced on top of the lower grade rocks during D1. F1-folds are refolded by NNE-plunging, open and overturned F2-folds with steep easterly dipping axial surfaces. Higher order F2-folds define a large-scale W-synform fold that in turn is gently folded by a large-scale S-fold, mimicked by the outline of the island (Fig. 1A).

Granitic and pegmatitic veins and dykes are rather common and in less refractive units, patch or stromatic metatexites have formed, representing a second generation of migmatites. Coarse sillimanite has crystallised in stromatic neosome, cordierite is present in patch migmatites, and porphyroblastic pseudomorphs, that may be up to 3-4 cm (Fig. 1B), are abundant along S0 and S1 in some mica-rich layers. These pseudomorphs consist either of an intergrowth of sillimanite + quartz±muscovite (Fig. 1C) or coarse-grained muscovite surrounded by a sillimanite + feldspar + quartz assemblage generated by the muscovite breakdown reaction.The original porphyroblasts and the replacement assemblages were formed as a result of three separated metamorphic events and together with cross-cutting relationships of granitic veins, patch neosomes and hydrothermal alterations, the metamorphic evolution can be deciphered. The replacement assemblage suggests that the original blastic phase was andalusite or cordierite that most likely formed as a result of contact metamorphism (M1) prior to F1. Replacement by (subsequently) coarse-grained muscovite could be related to retrograde processes during fluid circulation and/or decompression. The sillimanite+quartz pseudomorph assemblage is formed by muscovite dehydration melting during peak metamorphic conditions (M2). Micro-scale features related to melt crystallisation can be found, like K-feldspar and quartz with lobate grain boundaries in the pseudomorphic rims. Regionally, hydrothermal alteration, including ubiquitous red staining of the rocks, incipient partial melting with generation of patch and stromatic metatexites could all be coupled to break-down of muscovite prior or syn-F2.

At Ornö, early Svecokarelian intrusive rocks are common, in contrast to Fjärdlång from which it is separated by a c. 3.5 km wide strait. Ornö is structurally dominated by deformation along the repeatedly active Ornö Band Series (OBS; Fig. 1D) that can be traced from northeast of Stockholm to south of Utö. At Ornö, the main deformation stage of the OBS is associated with its high-strain banded parts that run along the west coast in addition to local anastomosing deformation zones that occur throughout the island. These deformation zones pre-dates sparsely occurring migmatites. Tight to isoclinal intrafolial folds observed in metavolcanic rocks probably corresponds to F1 at Fjärdlång, and F2 to the NNE plunging, flattened M-folds running through the central part of Ornö. Early deformation along OBS occurred in granulite facies conditions given by syn-kinematic opx (Fig. 1E) and appears to be related to an early M2-D2 phase. The early shear zones have often opposite kinematics at the tapering edges of tectonic lenses, indicating a large portion of pure shear, and continued convergence caused F2-folding and subsequent flattening of these folds. F2-folds are mainly preserved within tectonic lenses. Late-stage ductile deformation is recorded by pegmatites and granitic dykes that truncate the high-T fabric and show dextral strike-slip shear. This deformation phase (D3) is related to large-scale S-folding of the OBS, double verging folds at Ornö and the S-fold shape of the Fjärdlång island. Even later, tens of meters wide retrograde zones are found along the coast of Ornö, and the metamorphic break between Fjärdlång and Ornö underscores the presence of an east-side-down fault between these islands.

Despite the metamorphic and structural differences at Fjärdlång and Ornö the relative timing can be unravelled. Early migmatites and crystallisation of porphyroblasts pre-dates D1 that in turn is followed by initiation of OBS, a second metamorphic event and subsequently F2-folding during D2. Later deformation (D3) folded the earlier OBS fabric at Ornö into S and Z folds, and caused the S-shape rotation of Fjärdlång.

References

Allen, R.L., Lundström, I., Ripa, M., Simeonov, A. & Christofferson, H., 1996: Facies analysis of a 1.9 Ga, continental margin, back-arc, felsic caldera province with diverse Zn–Pb–Ag–(Cu–Au) sulfide and Fe oxide deposits, Bergslagen region, Sweden. *Economic Geology 91*, 979–1008.

Gavelin, S., Lundström, I. & Norström, S., 1976: Svecofennian stratigraphy on Utö, Stockholm archipelago. *Sveriges geologiska undersökning ser. C 719,* 44 pp.

Holst, N.O., 1882: Beskrifning till karbladen "Dalarö" och "Utö". *Sveriges geologiska undersökning ser. Aa 80 & 81*, 46 pp.

Stephens, M.B., Ripa, M., Lundström, I., Persson, L., Bergman, T., Ahl, M., Wahlgren, C.-H., Persson P.-O. & Wickström, L., 2009: Synthesis of the bedrock geology in the Bergslagen region, Fennoscandian Shield, south-central Sweden. *Sveriges geologiska undersökning ser. Ba 58*, 259 pp.

Extensional faults crossing paths; does a graben always rid on the back of a horst?

Hemin Koyi[a,b], Fusheng Yu[c]

[a]The Hans Ramberg Tectonic Laboratory, Department of Earth Sciences, Uppsala University, Uppsala, Sweden
[b]Currently at the Department of Earth Sciences; Khalifa University, Abu Dhabi, United Arab Emirates; [c]State Key Lab of Petroleum Resources and Prospecting, China University of Petroleum, Changping, Beijing, China

Summary. Fault intersection may form complex structures which can be counter intuitive. It is known that when extensional faults intersect along their dips, a pair of graben and horst forms, where a horst is "burried" by a graben riding on its back. However, when normal faults intersect along strike, the graben-horst pair is visible in a mapview separated by a plunging intersection line between the two faults. This study uses modelling and a theoretical approach to explore the intersection of non-parallel faults in extensional regime and give some perspective of such intersection scenarios in a compressional regime where this issue is far less explored.

Introduction

Conjugate normal faults, develop at different scales (Horsfield 1980, Watterson et al. 1998, Kornsawan and Morley, 2002). It has been demonstrated that there is a simple geometrical relationship between area change and fault slip for different fault dips (Ferrill et al., 2000). When parallel in strike, conjugate normal faults intersect only along their dips. However, non-parallel normal faults (i.e. faults with different strikes) in the basement intersect along both their strike and dip during their upward propagation to cover units. This intersection results in formation of conjugate normal faults both in map view and profile (Yu and Koyi 2016, 2017). In this study, we use results of analogue models, theoretical approach and a natural example to illustrate the complex structural evolution of non-parallel faults.

Model results and interpretation

A series of sand-box of models were constructed where layers of sand were deposited on a basement horst bounded by two non-parallel normal faults. During extension of the models, movement along these two faults propagated to the sedimentary cover where a pair of graben and horst formed both in dip and horizontal sections (Fig. 1). During their upward propagation, the model "basement" faults may intersect within the cover sequences and form a graben above the basement horst (Fig. 1). Length and width of the graben increase with cover thickness. The strike and dip intersection points are controlled directly by the thickness of the cover sequences, dip and strike of the basement faults, and width of the basement horst. The intersection point migrates along the axis of the graben toward the wide end of the basement horst, when the cover sequence thickens. In contrast, it migrates toward the narrow end of the basement horst, where both fault dip and angle of strike difference increase. The intersection point moves upward with increasing width of the basement horst crest (Figs. 1 & 2).

Data from a sedimentary basin (Lufeng Sag of Pearl River Mouth Basin in the northern part of South China Sea), where conjugate non-parallel basement faults propagate and intersect in cover units will be shown to illustrate that modelling results are compatible with both theoretical geometric estimation and observations from a natural prototype. Seismic data and model results show that the intersection pattern developed in the Lufeng Sag is a result of propagation of basement faults into cover units during different extension stages of the basin. Theoretical analysis show that plunge of the intersection line between two non-parallel faults depend on both the angle bewteen the strikes of the two intersecting faults and their dips (Fig. 2).

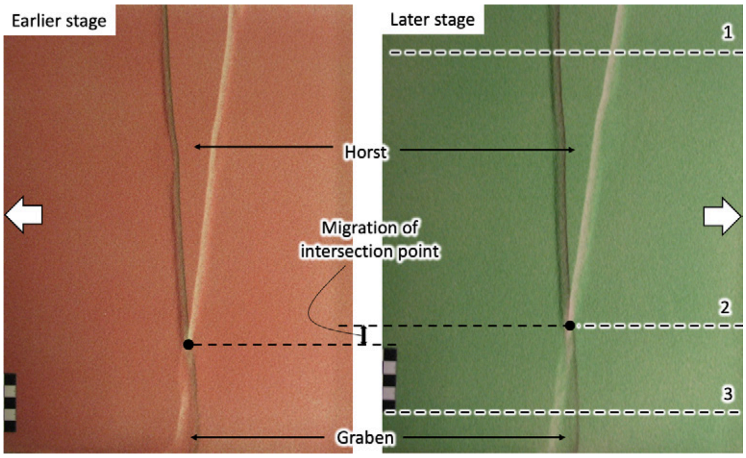

Figure 1. Top views of two subsequet stages of model extension showing migration of intersection point (black dot) between the two faults (f1 and f2) separting a graben from a horst. Thick white arrows show the direction of extension. Dashed black lines with white shade show the location of the three sections shown in Figure 2.

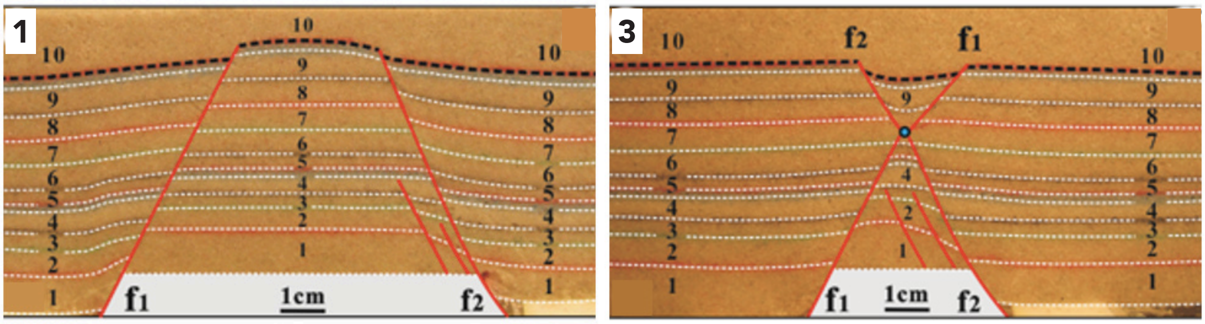

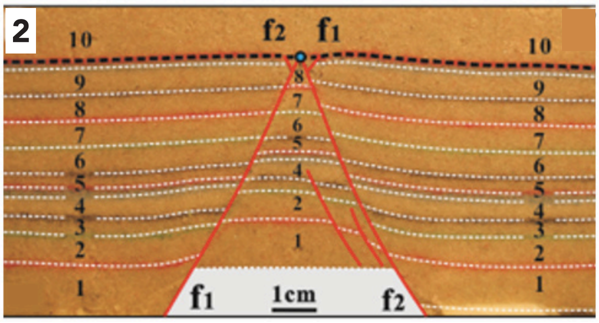

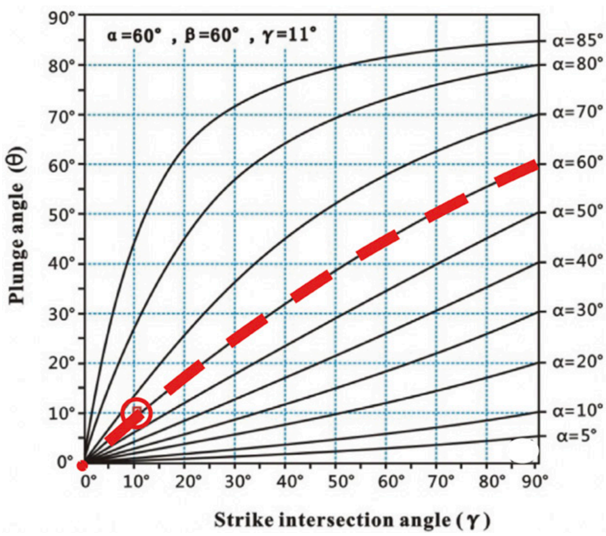

Figure 2. Three model sections (1, 2, and 3) illustrating the lateral variation of structures forming due to intersection of non-parallel extensional faults. Section1 shows only a horst; 2, shows the tip of the horst at the intersection of the two faults; and 3, shows a graben-horst pair. Lower right, theoretical plots showing the relationship between dips of two intersecting faults, the angle between their strikes, and plunge of their intersection line. Circle on the thick dashed line shows the match in plunge angle (c. 10 degrees) between model results and the theoretical calculations (Yu and Koyi, 2017).

References

Horsfield, W., 1980. Contemporaneous movement along crossing conjugate normal faults. Journal of Structural Geology 2, 305–310.

Ferrill, D.A., Morris, A.P., Stamatakos, J.A. & Sims, D.W., 2000. Crossing conjugate normal faults. American Associaiton of Petroleum Geologists Bulletin. 84, 1543–1559.

Karlsson, G.H. & Vikström, A.R., 2012: Title of paper comes here. Journal of Geology 15, 3–17.

Yu, F., Koyi, H. & Zhang, X., 2016. Intersection patterns of normal faults in the Lufeng Sag of Pearl River Mouth Basin, China: Insights from 4D physical simulations. . Journal of Structural Geology 93, 67-90.

Yu, F. & Koyi, H., 2017. Theoretical and experimental estimation of geometric relationship of non-parallel conjugate normal faults. Tectonophysics 703, 85-97.

1.47 Ga and 1.27–1.26 Ga dolerite sheets within the basement underneath the east-central Scandinavian Caledonides

Rodolphe Lescoutre[a], Ulf Söderlund[b], Jenny Andersson[a,c], Bjarne Almqvist[a]

[a]Department of Earth Sciences, University of Uppsala, Uppsala, Sweden, rodolphe.lescoutre@gmail.com, bjarne.almqvist@geo.uu.se, jenny.andersson@geo.uu.se; [b]Department of Geology, University of Lund, Lund, Sweden, ulf.soderlund@geol.lu.se; [c]Geological Survey of Sweden, Uppsala, Sweden, jenny.andersson@sgu.se

Summary. Drilling to 2276 meters depth in the Precambrian basement underneath the east-central Scandinavian Caledonides reveals that regional scale seismic reflections coincide with mafic dolerite sheets, which appear largely unaffected by ductile deformation. U-Pb baddeleyite geochronology shows that at least two generations of dolerite occur in the drill core with ages of 1.47 Ga at ~1879 meters depth and 1.27–1.26 Ga at 1665–1680 meters depth. Complementary geochemistry, petrography and geochronology is needed to further explore the timing, character and distribution of mafic magmatism at depth.

Introduction and objectives

In central Sweden, the crystalline basement in the Fennoscandian Shield east of the Caledonian orogen, has been intruded by several generations of dolerites including dolerites of Hallandian age (~1.47–1.44 Ga), the Central Scandinavian Dolerite Group (CSDG) (~1.27–1.25 Ga) and the Blekinge–Dalarna Dolerite suite (BDD) (~0.98–0.95 Ga; Söderlund et al. 2005; 2006). In central western Sweden, below the Caledonian nappes, the overall results from the Collisional Orogeny in the Scandinavian Caledonides (COSC) scientific drilling project allow us to identify a dense network of flat-lying mafic intrusions in the basement based on seismic interpretation and potential field modeling (Lescoutre et al. 2022; Lorenz et al. 2022). These intrusions were originally proposed to belong to the CSDG (Lescoutre et al. 2022), based on the geometry and the widespread occurrence of the 1.27–1.25 Ga dolerites in the autochthonous basement east of the Caledonides (Söderlund et al. 2006). However, detailed information about the composition, structure and crystallization age of these mafic intrusion remains to be investigated.

Methods

The Precambrian crystalline basement sections in the drill core from the COSC-2 borehole at Lake Liten, southeast of the village of Järpen in Jämtland, were examined at the core repository of the Geological Survey of Germany in Berlin. Texturally and petrographically different varieties of mafic rocks in the core were sampled for reconnaissance petrography, geochemical analyses and U-Pb ID-TIMS analyses on baddeleyite of four selected samples. Sampling targeted macroscopically unaltered sections with coarse dolerite, which was assessed to be the most likely variety to contain baddeleyite and/or zircon. The petrography of the samples was examined by optical microscopy in thin sections. The U-Pb ID-TIMS analyses were performed on a Thermo Triton thermal ionization mass spectrometer at the Museum of Natural History in Stockholm and the analytical procedures followed Söderlund & Johansson (2002) and Söderlund et al. (2010).

Results

The COSC-2 drill core covers a Precambrian basement section from 1220 to 2276 meters depth composed of 1.66–1.65 Ga felsic porphyry (Andersson et al. this volume) disrupted by a ~250 meters thick continuous section of gabbro and dolerite from 1590 to 1850 meters depth. Two samples of undeformed coarse gabbro with sub-ophitic texture and on average 0.5–2 cm long plagioclase laths were sampled at 1665 and 1684 meters depth. They are composed of clinopyroxene + plagioclase (variously altered) + ilmenite (commonly associated with fine grained Fe-Mg-rich alteration minerals) and accessory amounts of apatite, biotite and opaque minerals. A third sample of a coarse- to medium-grained gabbro with tabular feldspar and granophyric matrix domains dominated by clinopyroxene and plagioclase was selected in the same depth interval, at 1672 meters. U-Pb geochronology on baddeleyite from these three samples fall in the 1.27–1.26 Ga age range. In addition, a medium-grained dolerite with well-developed subophitic texture was sampled at 1879 meters depth. In thin sections the rock shows advanced alteration of both plagioclase and pyroxene. This rock is preliminarily dated to c. 1.47 Ga.

Concluding remarks

The U-Pb baddeleyite data show that the large-scale seismic reflections underneath the east central Caledonian nappes represent 1.47–1.46 Ga Hallandian and 1.27–1.25 Ga CSDG mafic intrusions. The occurrence of different intrusive generations is corroborated by comparison of the depth of the samples with the seismic reflection pattern of the COSC Composite Seismic Profile (Juhlin et al. 2016) at the location of the borehole. The CSDG corresponds to the prominent west-dipping parallel reflections of opposite polarity on the seismic profile, whilst the Hallandian dolerite seems to be imaged by a set of blurry, yet prominent, flat-lying reflections of unknown polarity (Lescoutre et al. 2022). Further geochronological investigations are needed to assess the proportion of CSDG and Hallandian dolerites, as well as a potential presence of younger intrusions (i.e. BDD). Another important topic to investigate, is if the emplacement of the CSDG may have been controlled by the older Hallandian dolerites. Finally, our preliminary results suggest that it may be difficult to discriminate between 1.47–1.46 Ga or 1.27–1.25 Ga mafic intrusions based on their seismic or mineralogical characteristics. Such observation raises the question as to what extent mafic rocks with surface exposures in Dalarna and Värmland correspond to the Hallandian event rather than being intrusions of the CSDG.

References

Andersson, J., Claesson, S., Koojiman, E., this volume: Age and crustal affinity of Precambrian basement nappes and underlying basement in the east central Scandinavian Caledonides. *Extended Abstract Volume, The Geological Society 150 years Jubilee meeting in Uppsala 17-19th of August 2022*.

Juhlin, C., Hedin, P., Gee, D. G., Lorenz, H., Kalscheuer, T., Yan, P., 2016: Seismic imaging in the eastern Scandinavian Caledonides: siting the 2.5 km deep COSC-2 borehole, central Sweden, *Solid Earth, 7*, 769–787.

Lescoutre, R., Almqvist, B., Koyi, H., Berthet, T., Hedin, P., Galland, O., Brahimi, S., Lorenz, H., Juhlin, C., 2022: Large-scale, flat-lying mafic intrusions in the Baltican crust and their influence on basement deformation during the Caledonian orogeny. *GSA Bulletin*; doi: https://doi.org/10.1130/B36202.1

Lorenz, H., Rosberg, J. E., Juhlin, C., Klonowska, I., Lescoutre, R., et al., 2022: COSC-2–drilling the basal décollement and underlying margin of palaeocontinent Baltica in the Paleozoic Caledonide Orogen of Scandinavia. *Scientific Drilling, 30*, 43-57.

Söderlund, U. & Johansson, L., 2002: A simple way to extract baddeleyite (ZrO2), *Geochemistry Geophysics Geosystems, 3(2)*, doi: 10.1029/2001GC000212.

Söderlund, U., Isachsen, C., Bylund, G., Heaman, L., Patchett. P.J., Vervoort, J.D. and Andersson, U.B., 2005: U-Pb baddeleyite ages and Hf, Nd isotope chemistry constraining repeated mafic magmatism in the Fennoscandian Shield from 1.6 to 0.9 Ga. *Contributions to Mineralogy and Petrology*, 150: 174-194.

Söderlund, U., Elming, S.-Å., Ernst, R. and Schissel D., 2006: The Central Scandinavian Dolerite Group – protracted hotspot activity or back-arc magmatism? Constraints from U-Pb baddeleyite geochronology and Hf isotopic data. *Precambrian Research, 150*: 136-152.

Söderlund, U., Hofmann, A., Klausen, M.B., Olsson, J.R., Ernst, R., Persson, P.-O., 2010: Towards a complete magmatic barcode for the Zimbabwe craton: Baddeleyite U-Pb dating of regional dolerite dyke swarms and sill complexes. *Precambrian Research, 183*: 388-398.

Structural data from XCT-XRF drill core scanning to constrain geological modelling in the Mavres Petres Zn-Pb mine, Greece

Stefan Luth[a], Mikael Bergqvist[b]

[a]Department of Mineral Resources, Geological Survey of Sweden, Uppsala, Sweden, stefan.luth@sgu.se
[b]Orexplore, Kista, Sweden, mikael.bergqvist@orexplore.com

Summary. We present the use of a novel drill core scanning method that combines X-ray Computed Tomography (XCT) and X-ray Fluorescence (XRF) to extract structural- and textural data directly after drilling. For this study 865 meters of oriented drill core from the Mavres Petres Pb-Zn deposit in northern Greece were scanned and digitally logged using the software Insight (by Orexplore). Structural fabrics were identified and measured from the rotatable 3D tomographic imagery and used for detailed geological modelling of the Zn-Pb ore bodies and adjacent rock units within the underground mine.

Introduction and methodology

Structural data extraction from drill core is a time-consuming task and can only be performed at the drilling site or core shed on oriented core using a variety of hand measuring tools such as core protractor, rat-trap and template, for instance. Here, we present an alternative approach for structural data extraction from drill core using combined XCT-XRF drill core scanning. Scanning 865 meters of oriented drill core from 8 holes in the underground Mavres Petres Zn-Pb mine was performed using the GeoCoreX10 instrument developed by Orexplore (e.g. Bergqvist et al. 2019; Luth et al. 2022). The instrument contains an X-ray source, a transmission detector and a spectrometer moving up and down while the drill core is rotating vertically. Scanning time was 3 to 4 meters per hour with an applied X-ray energy of 120 kVp producing 3D voxel images with a resolution of 200 µm per voxel side. The obtained XCT and XRF datasets – also including element and density data – were imported into Insight® software (https://orexplore.com) where orientations of planar and linear features were manually measured on the rotatable 3D imagery and exported for further structural analysis and 3D geological modelling (Fig. 1).

The Mavres Petres Mine

The actively producing Mavres Petres underground mine contains measured and indicated resources of 0.94 Mt at 9.5% Zn, 6.5% Pb and at 159 g/t Ag, and is one of a number of polymetallic (Zn-Pb-Ag-Au-Cu) carbonate-hosted sulfide orebodies that formed around 24 Ma within the Kassandra mining district (e.g. Siron et al. 2018). The deposit occurs along the Stratoni Fault Zone (SFZ) where fault-bounded marble hosts the replacement orebodies over a strike length of less than a 1 km and with a south-southwest plunging depth extent of more than 700 m. Replacement-style sulfides consist of pyrite, sphalerite and galena in varying proportions with accessory arsenopyrite, stibnite and minor boulangerite and chalcopyrite.

Results

Core photos and 3D tomographic imagery (XCT) from the main lithologies and ores are compiled in Fig. 1. The ore breccia and fault gouge contain Pb-Zn mineral assemblages and pyrite which all can be distinguished in XCT imagery from gangue minerals by their relatively high attenuations. The fault gouge and carbonaceous biotite schists contain carbonate, quartz and phyllosilicates, which in combination with ore minerals produce a high contrast in the XCT scans allowing for the identification of an S_1 schistosity which is locally folded and intersected by S_F. The latter developed solely within the SFZ and postdates mineralization. The orientation of S_F in drill core is predominantly 30–40° south to southwest dipping and correlates well with structural measurements from outcrops around Mavres Petres. The XCT scans of all 8 drillholes were used for a borehole correlation in where multiple layers of Pb-Zn mineralization were identified of which MZ2 and MG are the most significant. The main contact between the carbonaceous biotite schist and the marble can be traced among all holes, with the potential remaining of a more detailed correlation within these units. Both the borehole correlation and the structural measurements were used to refine the geological model of a relatively small volume in the underground Mavres Petres mine. We conclude that extracting structural data from XCT-XRF drill core scans is a rapid and accurate method that can easily replace measuring by hand in core sheds.

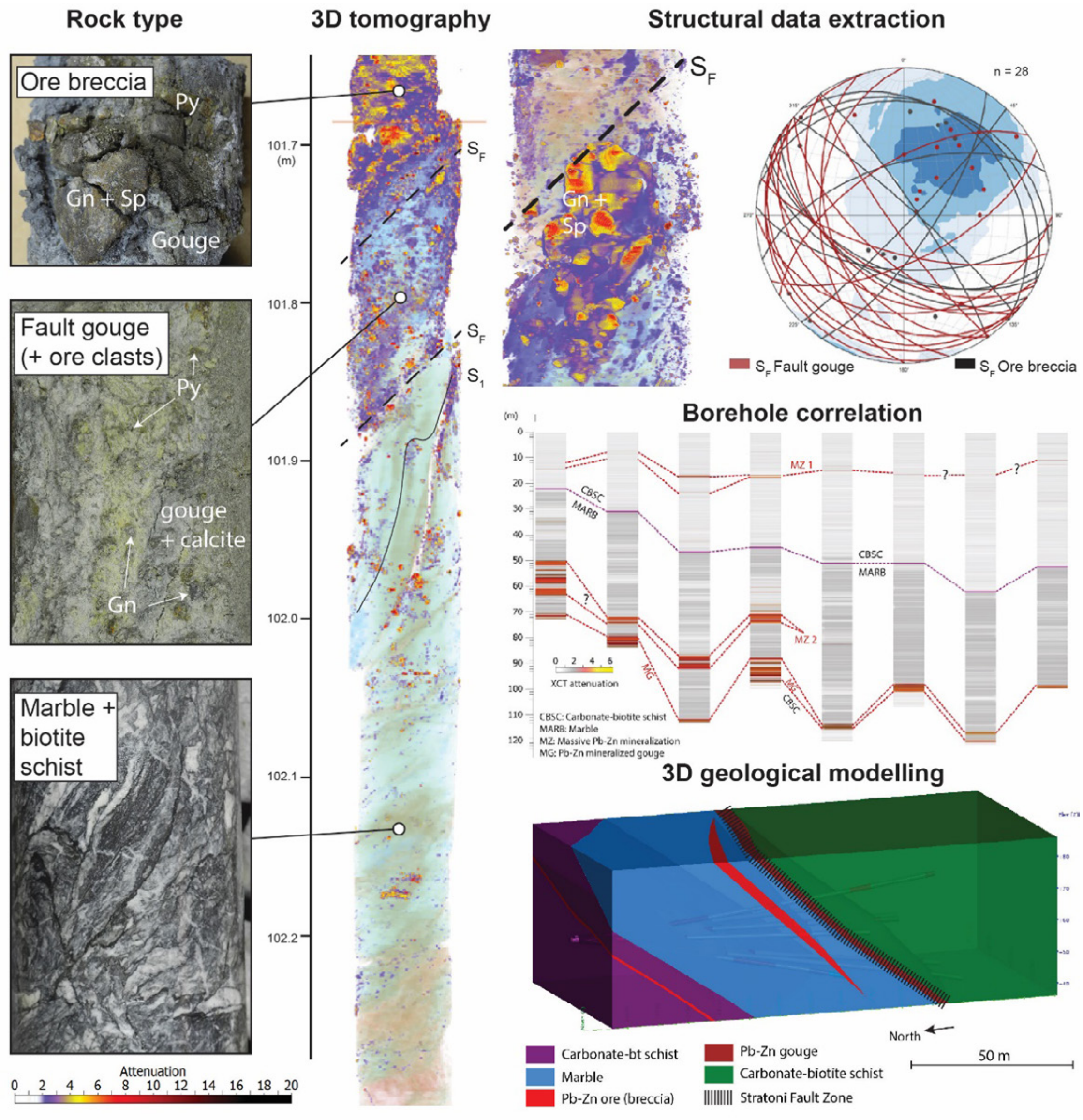

Figure 1. Rock characterization and structural data extraction from XCT-XRF drill core scanning to facilitate borehole correlation and 3D geological modelling in the Mavres Petres mine (see text for details). Gn: galena; Py: pyrite.

References

Bergqvist, M., Landström, E., Hansson, A. & Luth, S., 2019: Access to geological structures, density, minerals and textures through novel combination of 3D tomography, XRF and sample weight. *Australian Exploration Geoscience Conference (AEGC), Perth, 2019, Extended Abstracts,* v. 1, p. 1–3.

Luth, S., Sahlström, F., Bergqvist M., Hansson, A., Lynch, E-P., Sädbom, S., Jonsson, E., Andersson, S-S. & Arvanitidis, N., 2022: Combined X-Ray Computed Tomography and X-Ray Fluorescence Drill Core Scanning for 3-D Rock and Ore Characterization: Implications for the Lovisa Stratiform Zn-Pb Deposit and Its Structural Setting, Bergslagen, Sweden. Economic Geology doi: https://doi.org/10.5382/econgeo.4929.

Siron, C. R., Rhys, D., Thompson, J. F., Baker, T., Veligrakis, T., Camacho, A. & Dalampiras, L., 2018: Structural controls on porphyry Au-Cu and Au-rich polymetallic carbonate-hosted replacement deposits of the Kassandra mining district, northern Greece. *Economic Geology, 113(2)*, 309-345.

Melt transport in the Götemar granite pluton

Tobias Mattsson[a,b], William McCarthy[b], Tobias Schmiedel[c]

[a]Department of Geological Sciences, Stockholm University, Stockholm, Sweden, tobias.mattsson@geo.su.se; [b]School of Earth and Environmental Sciences, University of St Andrews, St Andrews, UK, wm37@st-andrews.ac.uk; [c]Department of Geoscience & Engineering, TU Delft, Delft, Netherlands, t.schmiedel@outlook.de

Summary. This contribution investigates how the architecture of remnant melt-transport networks relate to the emplacement structures of the circular Götemar granite pluton. Contact-parallel fine- and medium-grained granite sheets within the Götemar pluton indicate that the transport of melt within the pluton occurred in contact-parallel arcuate sheets reminiscent of ring-dykes. Magma flow within the sheets transitioned from vertical to horizontal along strike to from sub-horizontal sheets that migrated into a crystal mush toward the centre of the Götemar pluton.

Granitic melt is commonly hosted and sometimes generated in crystal-dominated magma mush systems through the evolution of interstitial melt. Studying the melt extraction and transportation processes within a magma mush helps us understand the precursors to volcanic eruptions. The existing petrological model predicts that a magma mush system grows vertically by the stacking of tabular melt-rich sills (Cashman et al. 2017). However, this model cannot be reconciled with observations of horizontally zoned granitic mush systems, which are thought to grow by lateral inflation (e.g. Machek et al. 2019). This study investigates how intra-plutonic melt-transport mechanisms operate during the growth of magma mush systems.

The 1.45 Ga Götemar pluton is located north of Oskarshamn and is one of several similar aged anorogenic intrusions in the area (Åhäll 2001; Wik et al. 2005). The pluton has a circular shape defined by concentric faults and consists of three major granite units, (i) a coarse-grained red granite, (ii) a medium-grained pale to red granite, and (iii) a fine-grained pale microgranite (Kresten & Chyssler 1976). The microgranite sheets occur all over the pluton with both sharp and gradational contacts and are the remnants of melt pockets in a crystal mush. Moreover, the coarse-grained granite records multiple stages of metasomatism and solid-state deformation caused by the successive intrusions of granite sheets (Friese et al. 2012).

Melt pocket distribution and the structure of the pluton were investigated with field mapping and Anisotropy of Magnetic Susceptibility (AMS). The Götemar pluton has a concentric internal structure. The pluton is dominantly composed of the coarse-grained granite in the southern and eastern part of the pluton and medium-grained granite in the north-western part of the pluton. The coarse-grained granite is intruded by multiple microgranitic and medium-grained granite sheets that strike parallel to the pluton contact (Figure 1). Contact-parallel sheets are also observed within the host rock close to the north-eastern contact of the pluton. The abundance and width of the sheets, which pinch out to the southeast, indicate that they were fed from the north and the west (Figure 1). The fringes of the larger sheets also commonly display sub-horizontal flow banding, which is an indication that the magma flow transitioned from vertical to sub horizontal as it migrated into the mush. The AMS fabric is overall concentric and shallowly-dipping microgranite sheets dip away from the centre of the pluton, which suggest that pluton emplacement involved inflation.

The concentric sheet distribution indicates that melt transport within the Götemar pluton occurred along multiple arcuate sheets similar to ring dykes. We interpret that magma propagated laterally into the centre of the pluton (i.e. the crystal mush) from the larger concentric sheets (10s of metres wide) through a network of smaller sub-horizontal sheets (>2 m wide). The Götemar pluton shows that melt transport in concentrically zoned granitic magma mush systems are governed by the internal structure of the pluton. The melt accumulation zones and transport networks in magma mush systems are therefore expected to differ depending on the emplacement mechanism of the system, which should be considered when monitoring a volcano.

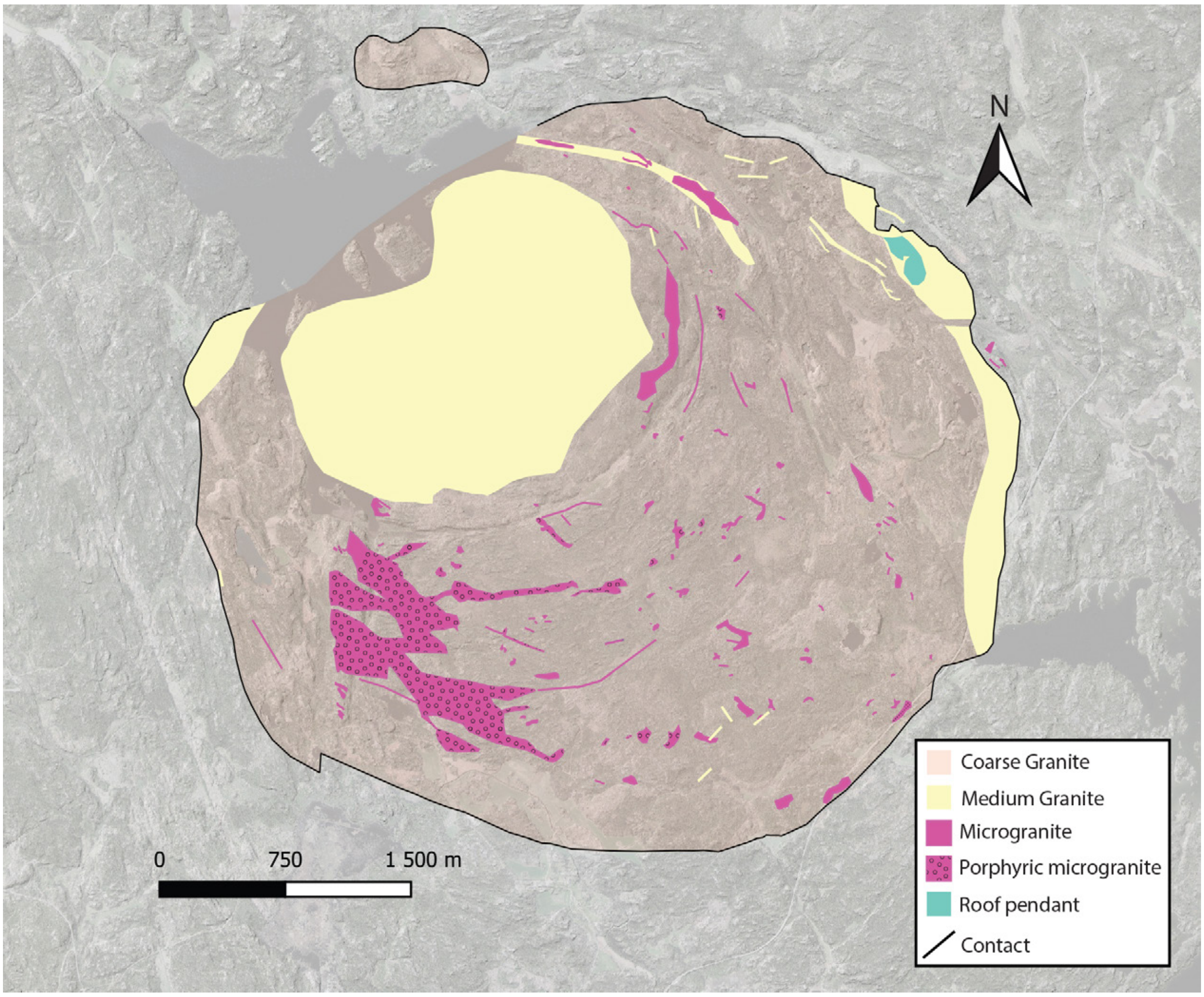

Figure 1. Map of the Götemar pluton with medium and fine-grained granite exposure variants overlaid on a satellite photo. Background photo: RGB-Orthophoto 0.25 m © Lantmäteriet (2017) and GSD-Elevation data, Grid 2+ © Lantmäteriet. Licence: FUK (Forskning, utbildning och kulturverksamhet).

References

Cashman, K. V., Sparks, R. S. J., & Blundy, J. D., 2017: Vertically extensive and unstable magmatic systems: A unified view of igneous processes. *Science*, *355*(6331), eaag3055, 1–9.

Friese, N., Vollbrecht, A., Tanner, D. C., Fahlbusch, W., & Weidemann, M., 2012: Multi-stage emplacement of the Götemar Pluton, SE Sweden: new evidence inferred from field observations and microfabric analysis, including cathodoluminescence microscopy. *International Journal of Earth Sciences*, *101*(5), 1149–1167.

Kresten, P., & Chyssler, J., 1976: The Götemar massif in south-eastern Sweden: A reconnaissance survey. *Geologiska Föreningen i Stockholm Förhandlingar*, *98*(2), 155–161.

Machek, M., Závada, P., Roxerová, Z., Petrovský, E., Špičák, A., & Kusbach, V., 2019: Crystal Mush Flow in Small Concentrically Expanded Pluton (Castle Crags Pluton; Klamath Mountains, CA, USA). *Geochemistry, Geophysics, Geosystems*, *20*(4), 1954–1974.

Wik, N.-G., Bergström, U., Bruun, Å., Claeson, D., Jelinek, C., Juhojunti, N., et al., 2005: *Beskrivning till regional berggrundskarta över Kalmar län, Ba66*. Östervåla: Sveriges Geologiska Undersökning, Serie Ba, 50 s.

Åhäll, K.-I., 2001: *Åldersbestämning av svårdaterade bergarter i sydöstra Sverige*. SKB, progress Rapport R-01-60, 28 p.

The Norrbotten Mega-Fault

Thorkild M. Rasmussen, Roshanak Vadoodi, Tobias E. Bauer

Lulea University of Technology, Luleå, Sweden, e-mail: thorkild.maack.rasmussen@ltu.se

Summary. The airborne magnetic data set acquired by SGU is one of the most important data sources for regional scale structural mapping. Despite these data have been publicly available for decades, the data reveal important information of hitherto unrecognized large-scale structures. This is exemplified by a recent discovery of the regional scale Norrbotten brittle strike-slip fault in northern Sweden with a length >250 km and apparent offset of 51.2 km. The fault extends northwards through Finland and possibly to the Caledonian Front in northern Norway. The discovery implies that geological maps need to be revised.

Results

The interpretation of the >250 km long Norrbotten Mega Fault was initiated by simple visual inspection of the total field magnetic anomaly map provided by SGU. Similarities in anomaly patterns between different areas suggested that the crust east of an approximately north striking line have moved roughly 50 km southwards relative to the western part. Figure 1 illustrates this observation. The areas marked A_w and A_e have similar anomaly pattern and also areas marked B_w and B_e are characterized by similar patterns. Application of a horizontal shift of roughly 50 km northward relative to the eastern block provides continuity of patterns across the proposed fault line. To validate and support the hypothesis of the fault, several other arguments and data are included. They are:

- Multi-variate classification of magnetic gradient tensor data
- The Bouguer gravity field and derived gradient data
- Inspection of airborne gamma-ray and VLF data
- Geological field observations and structural measurements
- Early Holocene faulting (Fig. 2) and present-day seismicity along the fault
- A joint three-dimensional classification of crustal scale magnetic susceptibility, density, and electrical conductivity models
- Partly continuity of geological units across the fault after application of shift to the mapped units

Identification of faults and in particular estimation of fault displacements is in the ideal case based on a visual matching of well-defined markers. A simple restoration of the anomaly pattern on one side of the fault provides the estimate of displacement provided that a match between one or preferentially several anomalies is obtained. The anomalies are in this manner used as a simple barcode in the matching procedure. The above-mentioned interpretation based on pattern recognition was therefore followed by visual inspection of short wavelength anomalies to quantify the displacement. An apparent horizontal displacement of 51.2 km is proposed for the discovered fault. In Sweden, the fault strikes N–S from Karesuando at the Swedish-Finnish border in the north to the Archaean-Proterozoic boundary marked by the Luleå-Jokkmokk Zone (c.f. Mellqvist et al., 1999).

A detailed geological follow-up study has so far not been possible, but in-situ observations are available from previous studies on Holocene faulting (Lagerbäck and Sundh, 2008) and a short field visit in 2021 (Fig. 2). The width of the zone tectonically influenced by the faulting is not investigated in detail yet.

The strikingly linear and straight character of the proposed fault implies a timing later than mapped ductile deformation events dated to 1.80–1.78 Ga (Bauer et al., 2022). We tentatively suggest the timing to coincide with the post-orogenic collapse at the latest stages of the Svecokarelian orogeny (approx. 1.76–1.70 Ga; Korja et al., 2006).

Provided that the interpretation of the >250 km long brittle, strike-slip fault is correct, the geological map of the Norrbotten region needs updating. The present geological map (Bergman et al., 2001, Fig. 3) does not have any indication of the proposed fault and the geological units that are adjacent and across the fault are at most places marked to be of similar type. The bedrock of the Norrbotten area is poorly exposed which is likely the main reason for the observed inconsistencies.

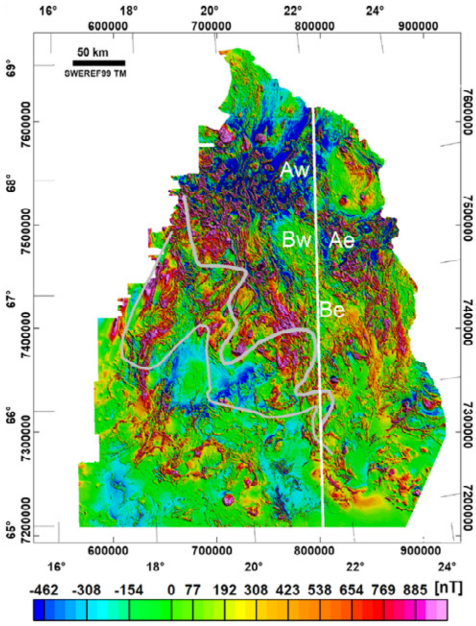

Fig. 1. (left). Total field magnetic anomaly, where white line marks position of proposed fault. The southern termination is so far not well defined. The two grey lines mark isolines of ε_{Nd} ratio of –3 (thick grey line) and ε_{Nd}=0 (thin grey line) used to define the Luleå-Jokkmokk Zone interpreted as the Archaean-Proterozoic Boundary (Öhlander et al., 1993).

Fig. 2. Photo (above left) of Lina granite intersected by the fault 3 km north of Kuoksu and interpreted as having been subjected to later Holocene faulting. Photo (above right) from Merasjärvi shows a possible damage zone. associated with the fault.

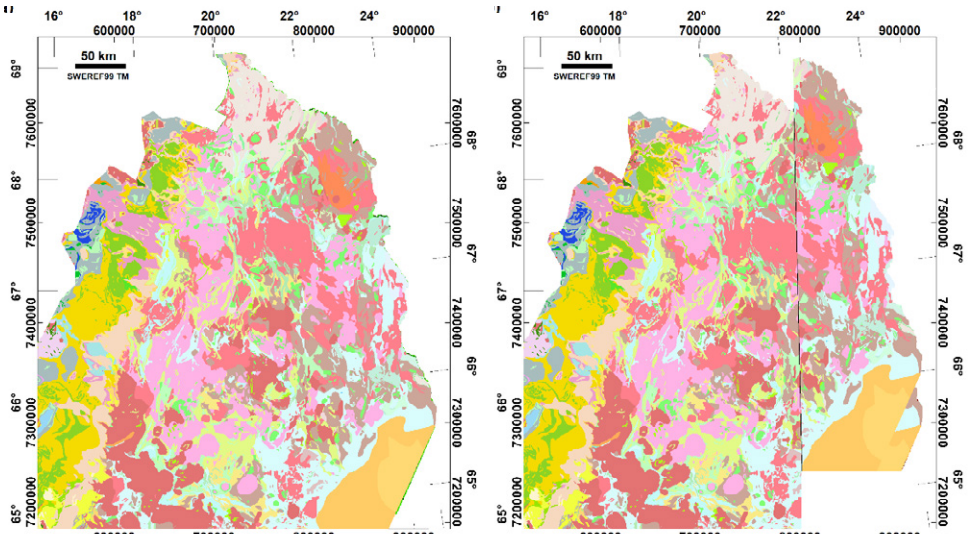

Fig. 3. Geological maps (Bergman et al. 2001) of northern Sweden without and with northward displacement of the eastern block.

References

Bauer, T. E., Lynch, E. P., Sarlus, Z., Drejing-Carroll, D., Martinsson, O., Metzger, N., & Wanhainen, C., 2022: Structural Controls on Iron Oxide Copper-Gold Mineralization and Related Alteration in a Paleoproterozoic Supracrustal Belt: Insights from the Nautanen Deformation Zone and Surroundings, Northern Sweden. *Economic Geology 117*, 327–359.

Bergman, S., Kübler, L., & Martinsson, O., 2001: Description of regional geological and geophysical maps of northern Norrbotten county (east of the Caledonian orogen). *Geological Survey of Sweden*.

Korja, A., Lahtinen, R., & Nironen, M., 2006: The Svecofennian orogen: a collage of microcontinents and island arcs. *Geological Society, London, Memoirs 32(1)*, 561–578.

Lagerbäck, R. & Sundh, S., 2008: Early Holocene faulting and paleoseismicity in northern Sweden. *Geological Survey of Sweden*, *Research Paper C 836*.

Öhlander, B., Skiöld, T., Elming, S. Å., Claesson, S., & Nisca, D. H. (1993). Delineation and character of the Archaean-Proterozoic boundary in northern Sweden. Precambrian Research, 64(1–4), 67–84. https://doi.org/10.1016/0301-9268(93)90069-E

Strain in analogue models revealed by AMS analyses – recent discoveries of the Hans-Ramberg-Tectonic Laboratory, Uppsala

Thorben Schöfisch[a], Hemin Koyi[a], Bjarne Almqvist[a], Stefan Luth[b]

[a]Department of Earth Sciences, Uppsala University, Uppsala, Sweden, thorben.schofisch@geo.uu.se;
[b]Geological Survey of Sweden (SGU), Uppsala, Sweden,

Summary. Analysing the anisotropy of magnetic susceptibility (AMS) in rock samples is commonly used to study deformation in rocks. We have tested the application of AMS as a strain indicator in analogue sandbox models by conducting a series of experiments simulating compressional tectonic regimes. The main outcome of these experiments are (i) the AMS signal corresponds to (relative) changes in strain, (ii) AMS depicts characteristic sets of magnetic fabric of developed structures in the models, and (iii) gradients in strain are revealed with the help of AMS.

Anisotropy of magnetic susceptibilty as strain indicator in analogue models

The anisotropy of magnetic susceptibility (AMS) provides valuable insights into the petrofabric of rocks (e.g. Parés 2015). From measurements of susceptibility of a rock sample it is possible to derive the magnetic susceptibility ellipsoid, with three main principal axes ($k_{max} \geq k_{int} \geq k_{min}$), a shape of anisotropy (Tj), and a corrected degree of anistropy (Pj). The magnetic fabric is described with the help of these parameters. Particularly valuable is that AMS reflects the bulk orientation of grains in the sample. Analysing and interpreting different grain orientations enables a link to different accomodation of deformation (i.e. penetrative strain, folding and thrusting). For example, penetrative strain develops a magnetic lineation (k_{max} clustering) perpendicular to the shortening direction and a vertical k_{min} orientation, which differs from a sedimentary fabric where a magnetic foliation (k_{max}-k_{int} girdle) is distributed horizontally around the primitve circle. With increasing deformation the “penetrative-strain” induced fabric becomes overprinted by a tectonic fabric, where k_{min} axes rotates to be become parallel with the shortening direction, resulting in a magnetic foliation parallel to the cleavage or thrust surface. Additionally, the degree of anisotropy (Pj) and the shape of anisotropy (Tj) are changing with increasing strain from an oblate shape towards a lower degree of anisotropy and presence of prolate shape fabric. Consequently, AMS developed as a usefull strain marker over the past 70 years and is mainly based on field studies (Parés 2015).

We, in the Hans-Ramberg-Tectonic Laboratory (HRTL) in Uppsala (Sweden), tested systematically, if similar changes in magnetic fabric can be observed in analogue models simulating fold-and-thrust belts (FTBs). For the model design we mixed sand with magnetite, which provides a strong magnetic signal, and shortened sandbox models in three series of experiments (Almqvist and Koyi 2018; Schöfisch et al. 2021; Schöfisch 2021). The pilot experiments of Almqvist and Koyi (2018) revealed changes in magnetic fabric from an undeformed foreland towards the deformed hinterland. In Schöfisch et al. (2021), the method was refined and layers of the sand-magnetite mixture were shortened above two adjcent décollements with different friction to also study the lateral strain distribution in FTBs. In this study, we provide an overview of magnetic fabric pattern in FTBs and relate these to different accomodation of deformation (Fig. 1). For example, in the hinterland above the high-friction décollement, thrust imbricates are stacked on top of each other and a “thrust-induced” fabric can be observed. In comparison, above the low-friction décollement, where a series of boxfolds developed with propagation of the deformation front far into the foreland, a mix between a “penetrative-strain” induced fabric and “thrust-induced” fabric is revealed (Fig. 1). Similar to Almqvist and Koyi (2018), Schöfisch et al. (2021) shows a decrease in degree of anisotropy from the foreland to the hinterland associated with a transition to a prolate fabric.

The third model series, which is summarized in Schöfisch (2021), shows the development of a thrust imbricate within a FTB with its associated magnetic fabric. In more detail, this study reveals a strain gradient within a thrust imbricate towards the thrusts and kinkzone that bound the imbricate. The strain gradient is illustrated by the change in inclination of the principal axes as well as in a decreasing degree of anisotropy. As such, those experiments clearly indicate the development of a "thrust-induced" fabric that has a magnetic foliation parallel to the thrust surface of a well developed thrust accomodating variable amounts of displacement. A complex kinkzone-fabric is indicated by a magnetic fabric resulting from an interplay between penetrative strain, folding and thrusting. Overall, this study shows the development of characteristic magnetic fabrics that all can be used to deduce the the strain distribution within thrust imbricates in 3D.

In conclusion, AMS is a useful tool to illustrate strain in analogue sandbox models that simulate compressional tectonic regimes. These new discoveries from the HRTL are described as pioneering work and provide a benchmark in the field of analogue modelling (Zwaan et al. 2022). Moreover, the models from the work from the HRTL validate hypotheses taken from field studies.

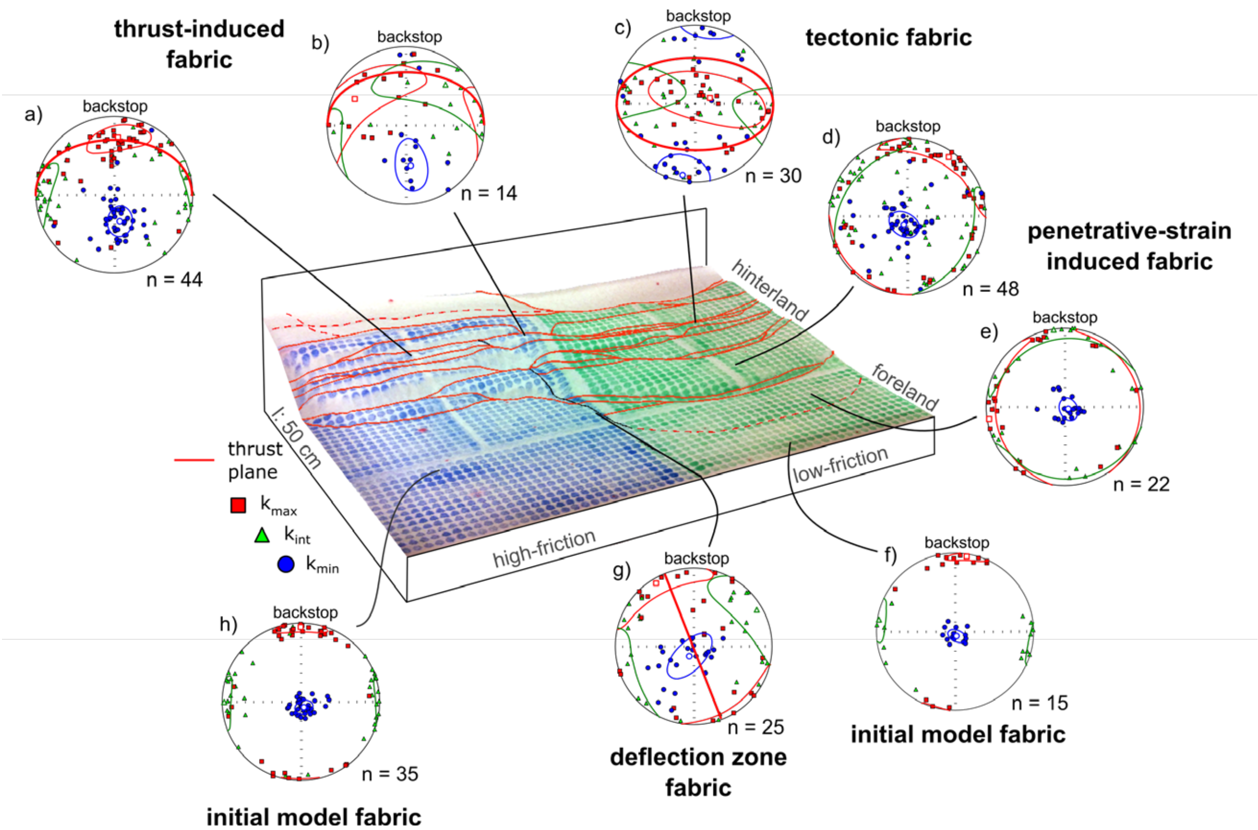

Fig. 1: Overview of characteristic magnetic fabrics within a sandbox model that was shortened above two adjacent different frictional décollements with a high-friction (blue colour on model surface) and low-friction (green colour on model surface). Characteristic magnetic fabrics are a thrust-induced and tectonic fabric in the hinterland (a, b, c), penetrative-strain induced fabric (d, e), and strike-slip fabric in the deflection zone (g). Plots (f, h) show data from the undeformed foreland and represent the initial model fabric. Each fabric is presented in equal-area projections with confidence ellipses and their mean (filled white symbols) (after Schöfisch 2021).

References

Almqvist, B. S. G., & Koyi, H., 2018: Bulk strain in orogenic wedges based on insights from magnetic fabrics in sandbox models. *Geology*, *46*(6), 483–486. https://doi.org/10.1130/G39998.1

Parés, J. M., 2015: Sixty years of anisotropy of magnetic susceptibility in deformed sedimentary rocks. *Frontiers in Earth Science*, *3*, 4. https://doi.org/10.3389/feart.2015.00004

Schöfisch, T., Koyi, H., & Almqvist, B., 2021: Influence of décollement friction on anisotropy of magnetic susceptibility in a fold-and-thrust belt model. *Journal of Structural Geology*, *144,* 104274. https://doi.org/10.1016/j.jsg.2020.104274

Schöfisch, T. 2021: Quantifying strain in analogue models simulating fold-and-thrust belts using magnetic fabric analysis (Licentiate dissertation). 42 pp. Uppsala University.

Zwaan, F., Schreurs, G., Buiter, S. J. H., Ferrer, O., Reitano, R., & Willingshofer, E., 2022: Analogue modelling of basin inversion: a review and future perspectives. *Solid Earth* (February), 1–84.

The effect of glacially induced stresses on the background stress regime – Insights from numerical models

Rebekka Steffen[a,b], Holger Steffen[a]

[a]Department of Geodetic Infrastructure, Lanmtäteriet, Gävle, Sweden, rebekka.steffen@lm.se, holger.steffen@lm.se; [b]Department of Earth and Environmental Sciences, Dalhousie University, Halifax, Canada

Summary. The build-up and melting of ice sheets affects the Earth on various scales in time and space. The generation of stresses due to the ice sheet build-up is one of them and which has led to the reactivation of several faults in northern Europe and eastern Canada (Steffen et al. 2021). Simple models show that these stresses can alter the existing stress regime and also allow the reactivation of non-optimally orientated faults. These stresses might create unstable conditions more than 10,000 years after the end of the deglaciation in a few locations.

The stresses induced by glacial loading are due to the flexure of the lithosphere, stresses migrating from the mantle into the lithosphere, and stresses due to the load itself. While the latter is only existing beneath the ice sheet itself and is zero when the ice sheet is not longer existing, the first two have different directions with respect to the location of the ice sheet and are also present after the ice sheet is gone. The combination of the three stress components is called glacially induced stresses and are in addition to the existing stress conditions within a region.

A finite-element model is created to simulate the glacially induced stresses during an entire glacial cycle for a simple circular ice sheet. We apply the finite-element software Abaqus (Dassault Systems 2021) for a 3D flat Earth (halfspace) to calculate the glacially induced stresses and the vertical deformation. The ice sheet is circular with a diameter of 2000 km at maximum glaciation (at 100,000 years) and advances and retreats with time in radius and height. The total height at glacial maximum is 2000 m at the ice-sheet centre. The ice sheet has a parabolic curve as in Wu et al. (2021) and Steffen & Steffen (2021). The ice sheet is build-up over 100,000 years and retreats over 10,000 years, with time steps of 1000 years. The model runs for an additional period of 50,000 years with 1000 years time steps as well. Glacially induced stresses are calculated for every time steps during the entire model run (0 to 160,000 years). The ice sheet is applied as pressure load on a simple Earth model, where material parameters vary with depth only (see Steffen & Steffen 2021, for a detailed model explanation).

The calculated glacially induced stresses are combined with background stress magnitudes, which are based on the assumption of a critically stressed crust and are depending on the stress ratio R (Etchecopar et al. 1981). Background stress magnitudes for all three stress regimes are calculated: thrust-faulting stress regime, strike-slip-faulting stress regime, and normal-faulting stress regime. The total stresses are analysed in time as well as at various location with respect to the ice sheet configuration. For low and high stress ratios a change in the stress regime is obtained. Of special importance is the change of a strike-slip-faulting stress regime to a thrust-faulting stress regime beneath the ice sheet centre during and after deglaciation. This could explain the reactivation of thrust/reverse faults in northern Europe despite a strike-slip-faulting stress regime is indicated by some focal mechanisms (Heidbach et al. 2016). In addition, the model results show that optimal fault orientations are not necessary and glacially induced stresses can be large enough to reactivate existing non-optimally orientated faults. Areas to the east and west of the ice sheet can become unstable even 10,000 years after the end of the deglaciation. Thus, the complete retreat of the ice sheet does not mean that stress levels are back to the values as before immediately. The time-dependent response of the mantle leads to changed stress conditions for several 10,000 years after the end of the deglaciation. We will present the main findings of this study and interpret them in relation to the location of glacially induced faults and the indications for glacially triggered earthquakes in northern Europe.

References

Dassault Systemes, 2021: Abaqus Unified FEA. Retrieved from https://www.3ds.com/products-services/simulia/products/abaqus/.

Etchecopar, A., Vasseur, G. & Daignieres, M., 1981: An inverse problem in microtectonics for the determination of stress tensors from fault striation analysis. *Journal of Structural Geology 3*, 51–65, doi:10.1016/0191-8141(81)90056-0.

Heidbach, O., Rajabi, M., Reiter, K., Ziegler, M. & Team, W., 2016: World stress map database release 2016. *GFZ Data Services*. doi:10.5880/WSM.2016.001.

Steffen, R. & Steffen, H., 2021: Reactivation of non-optimally orientated faults due to glacially induced stresses. *Tectonics 40*, doi:10.1029/2021TC006853.

Steffen, H., Olesen, O. & Sutinen, R., 2021: Glacially Triggered Faulting. . In Steffen, H., Olesen, O. & Sutinen, R. (Eds.), *Glacially-triggered faulting*, 3–19, Cambridge University Press. doi:10.1017/9781108779906.003.

Wu, P., Steffen, R., Steffen, H. & Lund, B., 2021: Glacial isostatic adjustment models for earthquake triggering. In In Steffen, H., Olesen, O. & Sutinen, R. (Eds.), *Glacially-triggered faulting*, 383–401, Cambridge University Press. doi:10.1017/9781108779906.029.

Centrifuge analogue modelling of transcrustal granite diapirs in the Moldanubian unit of the Variscan Bohemian Massif

Filip Tomek[a,b], Ondřej Krýza[c], Jakub Trubač[d], Steffi Burchart[e], Irena Olšanská[b], Hemin Koyi[e,f]

[a]Institute of Geology, Czech Academy of Sciences, Prague, Czech Republic, filip.tomek@natur.cuni.cz; [b]Institute of Geology and Paleontology, Faculty of Science, Charles University, Prague, Czech Republic; [c]Institute of Geophysics, Czech Academy of Sciences, Prague, Czech Republic, kryza@ig.cas.cz; [d]Institute of Geochemistry, Mineralogy, and Natural Resources, Faculty of Science, Charles University, Prague, Czech Republic, jakub.trubac@natur.cuni.cz; [e]Hans Ramberg Tectonic Laboratory, Department of Earth Sciences, Uppsala University, Uppsala, Sweden, hemin.koyi@geo.uu.se; [f]Department of Earth Sciences, Khalifa University, Abu Dhabi, United Arab Emirates

Summary. The extrapolation of magmatic intrusion field data into 3D models may leave us with sometimes contentious emplacement models. The centrifuge analogue modelling was used to model the granite-migmatite core-complex exhumation. We aim to simulate the emplacement mechanisms of the 329–327 Ma Pelhřimov complex (Bohemian Massif). The combinations of various materials along with the different geometries of the material setup revealed a geometrical-kinematic pattern of the material inversion consistent with the field geologic data of the Pelhřimov complex.

Introduction

The Variscan orogenic collapse was accompanied by voluminous post-orogenic S-type granite-dominated magmatic activity in the Bohemian Massif (Žák et al. 2014). Verner et al. (2014) and Žák et al. (2020) interpreted the ~NE–SW branch of the Moldanubian batholith and its migmatitic host (the Pelhřimov complex) as an exhumed core complex with a diapiric upwelling driven by extensional gravitational collapse. Detailed petrology and geochronology constrained the migmatitization at ~329 Ma and exhumation from ~21 km to ~9 km depth at a rate of 6–7 mm/year (Žák et al. 2011). Based on the 3D gravity modelling, seismic refractions and reflections, the emplacement was influenced by the existence of the underthrusted Brunovistulian microplate (indentor) beneath the lower to mid-crustal Moldanubian unit (Guy et al. 2010, Verner et al. 2014). The surface expression of this deep boundary is marked at the present-day erosional surface by the NNE-SSW striking Přibyslav mylonite zone. Due to limited exposure, field studies provide only a near-2D view on the internal architecture of otherwise 3D vertically-extensive transcrustal magmatic systems. The extrapolation of the surface data may leave us with sometimes unclear and contentious emplacement models. Careful field studies along with analogue modelling may help to fill the missing gap.

Centrifuge analogue modelling

The analogue modelling is limited by the scaling of the gravitational potentials of small-scale experiments in the laboratory to large-scale geological systems. Thus the vertical inversion of lighter and heavier rock analogues has to be supported by artificial gravity (centrifugal force) to allow realistic scaling together with reasonable time for the model run. To investigate the vertical extrusion of partially molten granitic and migmatitic masses which formed the Moldanubian batholith, we employed the centrifuge modelling at the Hans Ramberg Tectonic Laboratory, University of Uppsala, Sweden (Ramberg 1981). Our modelling strategy was to activate a predefined normal fault and initiate simultaneous material inversion extruding along the weakened fault zone. As such, we have simulated the granite-migmatite core complex exhumation and associated diapiric upwelling of partially molten lower to middle crust that occurred during the gravitational collapse and associated horizontal extension in the Bohemian Massif. In our first two models, a single diapiric-like structure was formed, through which magma (silicone) was transported upwards simultaneously as the host rock (plasticine) subsided. These two linked processes were enabled by the presence of a pre-existing steep fault in the models simulating the Přibyslav mylonite zone. The deformation pattern in the upwelling silicone marked by different colour layers revealed a gradient of vertical displacement and progressive folding; both in the extruded part and beneath the diapiric channel in the source region. Another important result is the presence of descending backflow streams in the feeding channel between the source layer and surface dome. The next four experiments included step-by-step improvement of the modelled domain to progressively reach a more complex geometrical setup which corresponds to assumed space relationships between Brunia microplate and Moldanubian unit. The upper crust, the middle crust, and melt were represented by coloured layers of plasticine (competent), silly putty (less competent), and silicone (least competent), respectively. The fault orientation was set as 110°/60° (i.e. a normal fault striking obliquely to the extension direction) to better simulate the mylonite zone. Three of these experiments resulted in a simple material inversion with lateral asymmetry of fault opening. We observed first-order (molten-partially molten crust) and second-order (partially molten-solid crust) divergent diapirism along the opened fault. The map view revealed two independent conduits with effusion of the lower upper crust to two opposite directions which correspond well to structural and map patterns of the Pelhřimov complex. The last model incorporated also the asymmetry to the lowermost layer. Here we simulated higher density Brunia (the competent plasticine indentor) at one side of the magma reservoir, while the opposite side represented the Moldanubian unit (less competent silly putty) which is characterized by the presence of the lower density rocks. We observed multiple localized melt effusions which were elongate in extension direction and rimmed by “anatectic” material from the middle layer of the model. Some secondary and small-scale diapirs were developed in the middle-lower level of the main conduit. We claim that these models successfully simulate the geometric-kinematic pattern of the material inversion which might have occurred during the formative stage of the Pelhřimov Complex and which is in good correspondence with the field data.

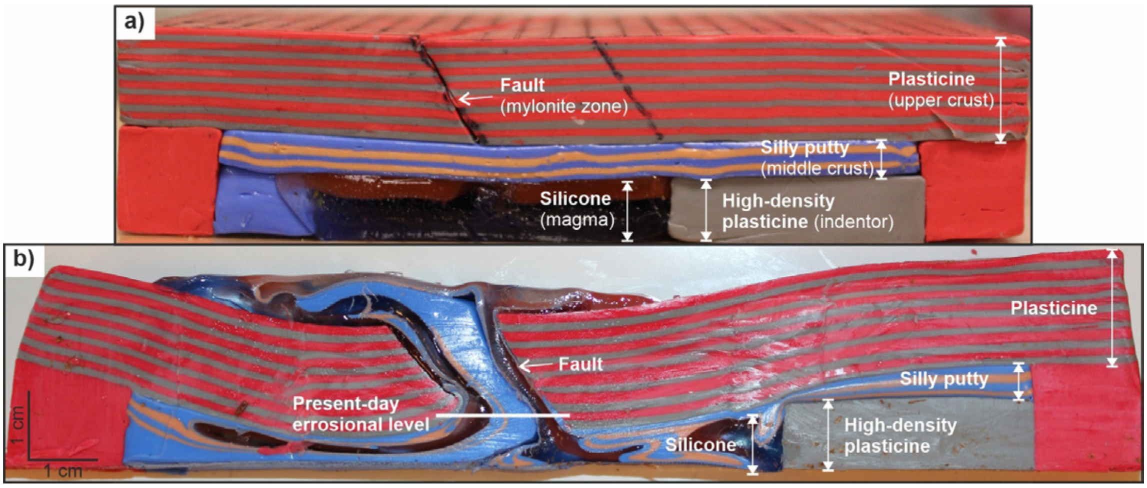

Figure 1. Representative section through model number No. 6 highlighting the diapiric upwelling of silicone and silly putty along the pre-defined fault a) before and b) after centrifuging.

References

Guy, A., Edel, J. B., Schulmann, K., Tomek, Č., & Lexa, O., 2011: A geophysical model of the Variscan orogenic root (Bohemian Massif): implications for modern collisional orogens. *Lithos 124*, 144–157.

Ramberg H., 1981: Gravity, deformation, and the Earth’s crust: in theory, experiments, and geological application. Academic Press, London, 452 p.

Verner, K., Žák, J., Šrámek, J., Paclíková, J., Zavřelová, A., Machek, M., Finger, F., & Johnson, K., 2014: Formation of elongated granite–migmatite domes as isostatic accommodation structures in collisional orogens. *Journal of Geodynamics 73*, 100–117.

Žák, J., Verner, K., Finger, F., Faryad, S. W., Chlupáčová, M., & Veselovský, F., 2011: The generation of voluminous S-type granites in the Moldanubian unit, Bohemian Massif, by rapid isothermal exhumation of the metapelitic middle crust. *Lithos 121*, 25–40.

Žák, J., Verner, K., Janoušek, V., Holub, F. V., Kachlík, V., Finger, F., Hajná, J., Tomek, F., Vondrovic, L., & Trubač, J., 2014: A plate-kinematic model for the assembly of the Bohemian Massif constrained by structural relationships around granitoid plutons. *Geological Society, London, Special Publications 405*, 169–196.

Žák, J., Verner, K., Ježek, J., & Trubač, J., 2019: Complex mid-crustal flow within a growing granite–migmatite dome: An example from the Variscan belt illustrated by the anisotropy of magnetic susceptibility and fabric modelling. *Geological Journal 54*, 3681–3699.

Author index

Sponsors

Gold

LULEÅ TEKNISKA UNIVERSITET

Stockholms universitet
Institutionen för geologiska vetenskaper
Institutionen för naturgeografi

UPPSALA UNIVERSITET

NEW BOLIDEN

Zinkgruvan Mining
a subsidiary of lundin mining

LKAB

Silver

NITRO CONSULT

GREENNA MINERAL

LOVISAGRUVAN

BERGS KRAFT SWEDEN

Geoveta

KAUNIS IRON

geopool
DISCOVERING TOGETHER

Bronze

ALICANTO MINERALS LIMITED

MINALYZE